Architectural Science and the Sun

THE POETICS AND PRAGMATICS OF SOLAR DESIGN

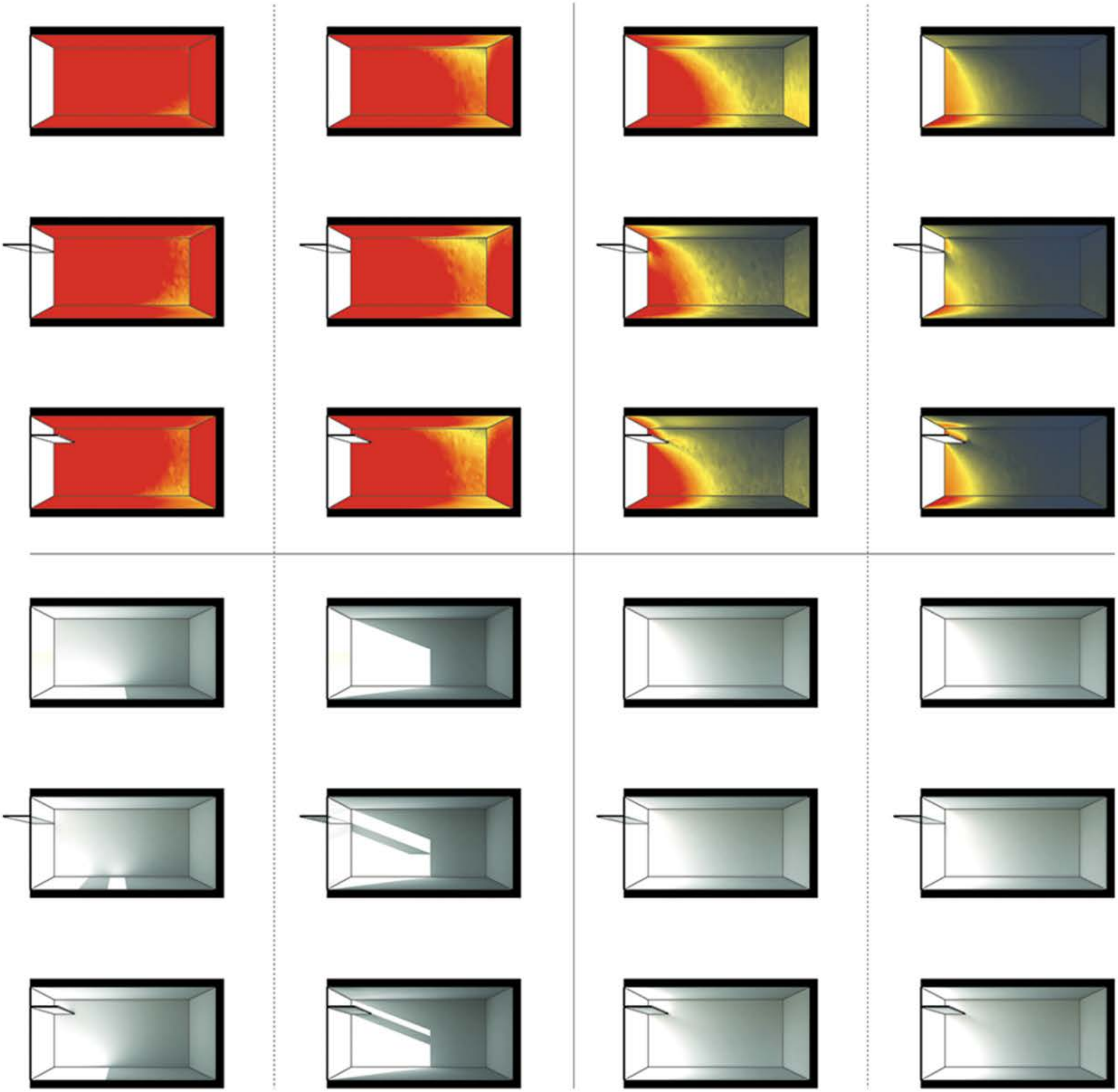

Matt Fajkus and Dason Whitsett

ROUTLEDGE

ARCHITECTURAL SCIENCE AND THE SUN

Architectural Science and the Sun synthesizes physics, climate, program, and perception to provide a foundation in the principles of architectural science related to the sun: solar geometry, solar analysis and design techniques, passive design principles, and daylighting. Part analytical handbook, part inspiration source for schematic design, the content comprises a critical component of effective sustainable design.

Beyond the purely technical aspects of these topics, *Architectural Science and the Sun* begins with the premise that great architecture goes beyond energy performance and the visual-aesthetic to engage all of the senses. Given that the stimuli to which our senses respond are physical phenomena such as light, heat, and sound, the designer must manipulate these parameters through the craft of building form and technology to create the desired qualitative experience. This book is designed to help the reader develop that skill.

Matt Fajkus is an Associate Professor at the University of Texas at Austin School of Architecture, USA, as well as Director of the UT Sustainable Design Program. He holds a Master of Architecture from the Harvard University Graduate School of Design, and is currently Principal Architect of Matt Fajkus Architecture, an AIA National Award-winning practice.

Dason Whitsett teaches in the Sustainable Design Program at the University of Texas at Austin School of Architecture, USA, and holds a Master of Science in Sustainable Design from the same institution. He is also Principal Architect for Kasita, an award-winning modern modular building manufacturer.

Taylor & Francis
Taylor & Francis Group
http://taylorandfrancis.com

ARCHITECTURAL SCIENCE AND THE SUN

The Poetics and Pragmatics of Solar Design

Matt Fajkus and Dason Whitsett

Routledge
Taylor & Francis Group
NEW YORK AND LONDON

First published 2018
by Routledge
711 Third Avenue, New York, NY 10017

and by Routledge
2 Park Square, Milton Park, Abingdon, Oxon, OX14 4RN

Routledge is an imprint of the Taylor & Francis Group, an informa business

Library of Congress Cataloging-in-Publication Data
Names: Fajkus, Matt, author. | Whitsett, Dason, author.
Title: Architectural science and the sun : the poetics and pragmatics of solar design / Matt Fajkus and Dason Whitsett.
Description: New York : Routledge, 2018. | Includes index.
Identifiers: LCCN 2017044154 (print) | LCCN 2017044516 (ebook) | ISBN 9781315708041 (Master) | ISBN 9781317481669 (ePub) | ISBN 9781317481652 (Mobi) | ISBN 9781317481676 (Web PDF) | ISBN 9781138899209 (hardback : alk. paper) | ISBN 9781138899216 (pbk. : alk. paper) | ISBN 9781315708041 (ebook)
Subjects: LCSH: Architecture and solar radiation.
Classification: LCC NA2542.S6 (ebook) | LCC NA2542.S6 F35 2018 (print) | DDC 720—dc23
LC record available at https://lccn.loc.gov/2017044154

ISBN: 978-1-138-89920-9 (hbk)
ISBN: 978-1-138-89921-6 (pbk)
ISBN: 978-1-315-70804-1 (ebk)

Typeset in Univers
by Apex CoVantage, LLC

CONTENTS

Preface vi
Acknowledgements viii

1 Introduction **1**

2 The Earth–Sun Relationship **11**

3 The Geocentric Model **39**

4 Climate and Solar Radiation **67**

5 The Sun and Form **98**

6 Received Shadows **123**

7 The Solar Microclimate **134**

8 Creating Shadows **152**

9 Fenestration and the Sun **181**

10 Light and Effect **207**

Appendix A: Mathematical Symbols 216
Appendix B: Equations List 219
Appendix C: Solar Tables 223
Appendix D: Sample Statistical Summary Radiation Files 264
Appendix E: Solar Protractor Components 270
Glossary 274
Index 285

PREFACE

This book explores the intersection of physics, climate, and perception in architecture. The primary task of this book will be to provide the designer with essential tools and knowledge to address the central architectural challenge of our time: combating climate change through the design of low-energy buildings. The text will cover principles of architectural science, the foundation of high-performance building design, including topics such as thermal comfort, solar geometry, building thermodynamics, passive design, and daylighting.

Energy-efficiency alone is an insufficient goal for the built environment, however. Building on the work of classics such as Lisa Heschong's *Thermal Delight in Architecture* and Juhanni Pallasmaa's *The Eyes of the Skin*, *Architectural Science and the Sun* starts from the premise that great architecture goes beyond energy performance and the visual-aesthetic to engage all of the senses. Much of the power of work by masters such as Glenn Murcutt, Peter Zumthor, and Sigurd Lewerentz, for example, results from their skill at designing fulfilling multi-sensory experiences. Given that the stimuli to which our senses respond are physical phenomena such as light, heat, and sound, the design team must manipulate these parameters through the craft of building form and technology to create the desired qualitative experience. This book will help the designer develop the skills to do so.

Part analytical handbook, part inspiration source for schematic design, this book aims to fill two gaps in the literature. First, while there are numerous books covering passive design strategies, these books generally do not provide adequate grounding in the fundamental principles governing the performance of such building techniques. The engineering literature, on the other hand, includes many texts on building physics, but the material tends to be presented in a highly technical manner inaccessible to the design community. This gap leaves many architects without the tools to properly evaluate the applicability of specific techniques to unique conditions and hinders sustainable design innovation. *Architectural Science and the Sun* will serve as a detailed reference on the principles of architectural science for the design community.

The book aims to fill a second niche by taking a specific and analytical approach to sensory phenomenology where other works on the topic have tended to be more general and conceptual. The objective is to connect the designer with the sensory experiences that physical phenomena create. The book facilitates integrated design by providing architects with the skills to translate back and forth between quantitative data and qualitative experience, thus serving designers whether working with an intuitive approach or applying the powerful simulation tools readily available today.

The book synthesizes physics, climate, program, and perception to create high-performance buildings that provide superlative experiences for their users. This book intends to serve design practitioners, academics, and architecture students as a guide for performing this synthesis. Part of the purpose is as a handbook, for which certain conventions are established and explained next.

NOTES ON THE USE OF THIS BOOK

Example Locations

Austin, Texas (latitude = ~30° N), was chosen as the location for many of the examples in this book. While it is true that the authors live in that city, approximately 50% of the world's population also lives between 20° and 40° N latitude.[1] So, a city right in the middle of that zone seems like a good choice to address a broad audience. That means there is an excellent chance that a large fraction of the readers of this book will be using the techniques described in a similar context. Austin has a hot-humid, moderately overcast climate. Some cases use two other cities at approximately the same latitude as examples of two extremes of cloud cover, and therefore solar radiation: Shanghai and Kuwait City. For examples at other latitudes, Caracas at approximately 10° N and London at 51° N are used in several cases.

Geometry Conventions

Coordinates are specified in space using a modified left-hand coordinate system. To model this system, place the outside edge of your left hand on the table. The index finger should point straight in front of you and indicates the positive *y*-axis (south). Bend your middle finger 90° so that it is pointing to the right for the positive *x*-axis (west). For the positive *z*-axis, point the thumb straight at the ceiling (zenith direction). Curling the index and middle fingers indicate positive rotation (clockwise) on the ground plane.

Spherical or angular coordinates follow the same system, with south being 0° of azimuth and positive rotation to the west of south in the clockwise direction. Azimuth angles greater than 180° are usually specified as negative, indicating rotation to the east of south or counter-clockwise. These conventions are typical for solar geometry calculations, but many other applications use different models. In particular, energy simulation, drawing, and building-information modeling software often use different conventions, so it is important to check the documentation for the particular application to make sure that you are following the proper convention.

Time Conventions

Unless noted otherwise, time is expressed using the *24-hour time* system, the time-keeping convention in which hours are numbered sequentially 1–24 rather than distinguishing between a.m./p.m. Although 24-hour time is the most commonly used convention worldwide, the United States still primarily relies on 12-hour time. However, 24-hour time eliminates the ambiguity of the 12-hour system. For example, 3:25 p.m. is 15:25 in 24-hour time.

Unless noted otherwise, time will be indicated in *apparent solar time* rather than clock or standard time. See Chapter 2 for an explanation of the differences in these systems.

Symbols

See Appendix A for a key to the mathematical symbols used throughout the book.

Equations

See Appendix B for a quick reference list of mathematical formulas used in the text.

NOTE

1 Matti Kummu and Olli Varis, "The World by Latitudes: A Global Analysis of Human Population, Development Level and Environment across the North South Axis over the Past Half Century," *Applied Geography* (2011): 495–507.

ACKNOWLEDGEMENTS

We are grateful for the support and assistance from numerous individuals in the extended adventure of creating this book. Dr. Barbara Brown-Wilson of the Center for Sustainable Development nurtured the idea in its earliest phases, and without her general support and the seed funding she secured for the project, the effort never would have gotten off the ground. Dr. Michael Oden also provided important early backing. Through Dean Fritz Steiner, the University of Texas at Austin DPAC funded a significant portion of the work. UT School of Architecture faculty Dr. Steven Moore and Ulrich Dangel were valuable sources of advice along the way. Francois Levy was an important sounding board on the publishing process.

Our research assistants provided invaluable work in research and production of many of the diagrams featured in the book as well as significant insight along the way. Gregory Arcangeli worked periodically over the course of several years and showed an unflagging devotion to the project. Jesefa Templo and Nic Allinder did excellent work finding elegant ways to express difficult concepts visually.

The project also benefitted from the generosity of several volunteers. Ekta Khuler, Juan Carlos Fornino, and Steven Mathai gave significant amounts of their time and played an important role in making this a reality.

Matt Fajkus:
My wonderful parents, Mel and Jean Fajkus, provided both encouragement as well as support with proofreading and general development of the text. I would like to also thank mentors who have inspired me along the way, including George Gintole, Max Levy, Julie Snow, Rafael Moneo, Sarah Whiting, and my former colleagues at Foster + Partners.

Dason Whitsett:
My incredible wife, Juliet, never wavered in her support of the cause or acceptance of me typing away late at night. My children, Kai, Fischer, and Sequoia, did not receive as much of my attention as they deserved while I was finishing this work. Mal and Janette Whitsett, my parents and the best writers I know, did a tremendous amount of proofreading at a moment's notice and improved the text in important ways. Without these contributions from my family, my work would not have been possible.

1 INTRODUCTION

LIGHT AND EXISTENCE: TRAJECTORY OF LIGHT AND FORM

> Our eyes are constructed to enable us to see forms in light . . . The key is light, and light illuminates shapes and shapes have an emotional power . . .
> I use light abundantly, as you may have suspected; Light for me is the fundamental basis of architecture. I compose with light.[1]
>
> —*Le Corbusier*

DEPENDENCE ON DAYLIGHT: GLOBAL SUSTAINABILITY

In the broadest sense of the term "sustainability," the sun is perhaps the most important ingredient to sustain life on Earth. The ability of design to adapt to the sun is critical to the very existence of any living being. Sun patterns and natural light have been a driving force in the development and prosperity of humankind. Our very understanding of the world around us is dictated by daily cycles and the specificities of our given climate, all animated by mysterious and awe-inspiring skies as the backdrop to our existence. The sun has been heralded for its many powers and meanings by the ancients (Figure 1.1), and even today we must appreciate the sun as the basis for all organic existence.

Light pervades our universe, literally and figuratively, yet it is often not at the forefront of architecture and spatial design thinking or everyday routines. As humans currently spend an average of 90% of their time indoors, natural light is often considered an indirect or supplemental asset, but not of primary importance to existence. Sunlight is not merely beneficial to humans; it is actually an absolute necessity.[2]

Thus, the design of spaces around us and how they embrace the sun is of paramount importance not only to our physical existence but also to our emotional and psychological well-being. Sunlight is elemental to vegetation and is just as important to the chemical balances of humans. A proper level of natural light is required to maintain physical health and to provide basic sustenance for all natural cycles on Earth.

Natural light has also been shown to have a direct connection to human health and productivity. Student performance is also connected to natural light, and is seen in test score differentials due to classroom light levels.[3] Conversely, clinical light therapy is recommended by doctors to overcome depression and other illnesses related to a lack of proper daylight exposure. Rather than reaching this point, it is far more preferable to be preventative by designing space that carefully considers the sun and daylight to enrich and balance the lives of occupants.

Figure 1.1
Arizona petrified-forest petroglyphs of Anasazi origin, c. 700–1300 A.D.
Marilyn Angel Wynn/Nativestock Pictures

HISTORICAL PERSPECTIVES ON LIGHT AND VISION

In order to appreciate our current comprehension of light, it is helpful to trace a trajectory of discovery from the past. Vision is one of the principal perceptual senses in humankind. It is understandable, then, that vision (and therefore light) has been pondered and considered by humankind since prehistoric times.

The story of light includes a history going back multiple millennia, in which humankind has struggled to understand it. Many ancient civilizations worshipped the sun or some type of sun deity, as Gary Waldman establishes and lays out a framework for.[4] The development of a global comprehension of light and vision has not been a linear nor consistent path, as it has spanned across geographical areas of concentration, and has had moments of steady progress and pauses along the way. Around 1400 B.C., Egyptian Pharaoh Akhenaton began the worship of a more complex sun deity that included a parsing of the individual rays of sunlight.[5] In this way of thinking, the light from the sun is seen as life-generative. The Amarna style of Egyptian art represents this idea, where separate rays are isolated with unique qualities in each (Figure 1.2).[6] Interestingly, this account of sun rays bears some similarities to our current understanding of light, with variation along the electromagnetic spectrum. Although there is evidence that simple optical instruments such as plane and curved mirrors and convex lenses were used by some early civilizations, it is the ancient Greek philosophers who are generally credited with the first secular and pragmatic speculations about the nature of light. The Greeks developed a series of philosophies on light and perception in quick succession, in relative terms. Their research and theoretical development went far beyond properties related to vision, including advancements in mathematics, psychology, and ethics.

From Pythagoras to Anaxagoras, progress was made in the definition of light and dark, as well as an improved understanding of darkness as the absence of light,

Figure 1.2

Solar rays depicted in the Amarna style of Egyptian art, 1370 B.C.

The Amarna art style of Egyptian art, 1370 B.C., depicting the worship of individual rays of sunlight, which is surprisingly consistent with wave theory which breaks light down into wavelengths along a spectrum.

Erich Lessing/Art Resource, NY

rather than as an entity in itself. In the 4th century B.C., Aristotle deeply explored ideas of sensory perception, and he attempted to break down the components of perception into their own respective realms, including the human biological sensory component, the medium through which light traveled, the object being seen, and the process of transmission between each element. He advocated a theory of intromission in which the eye received rays rather than directing them outward. Furthermore, Aristotle proposed a more holistic view of light and the circumstances in which it operates in a more specific and general sense.[7] The predominant way of understanding the universe at the time was the assumption that the Earth was at the center with the other celestial bodies orbiting around it. The assumption that the Earth is at the center of the orbits of celestial bodies is known as the *geocentric model*. Aristotle laid the foundations of modern science with his argument that theory should agree with observations. He advocated a geocentric model of the universe composed of concentric spheres centered around the Earth. In his conception, the sun's sphere was between Venus and Mars. This model was largely accepted even though the Greeks had recorded planetary phenomena with contradictions to this notion, which were unexplained by Aristotle.[8] Aristotle began to speculate that "vision" goes beyond what is literally seen, and that concepts can be understood, or "seen," without having been directly witnessed.

Aristotle brought a theory that light and heat and even gravitational forces are disseminated across the spaces between planets, and he therefore needed to account for how this occurred. He suggested that there was a medium that allowed for the transmission of light, and thus was the first to describe physical space in the way we currently understand it. Because the term "spatium" was used for "room" or "interval," but not as an abstract notion of a void with some mass and particulates, he was incorrect in his postulation that there existed a sort of "fire" emanating from objects within said physical space. Claudius Ptolemy, a Roman citizen of Egypt in the 1st century A.D., sought to improve the Aristotelian model of the universe so that it would better agree with empirical observations by adding extra loops known as epicycles to planetary orbits. Although Ptolemy's model matched observations better than Aristotle's, its predictive power was still poor. Nevertheless, it eventually became part of Roman Catholic Church doctrine and was accepted as the dominant view for over 1,500 years. There was then a large gap in time regarding development of vision theories; it was not until the 16th and 17th centuries that humankind's understanding of light began to progress once again. Thinkers such as Copernicus, Kepler, and Galileo refuted and reconstructed Aristotelian concepts in astronomy, geometry, and thus light—beginning a platform for contemporary scientific thought. Kepler made great strides in optics with his description of how the eye works, explaining how the eye manages the light rays that enter. Kepler's work brought together geometrical optics and intromission theories of vision, which had been started by Alhazen.[9]

The Heliocentric Perspective

Although the ancient Greek philosopher Aristarchus had proposed such a model over 1,800 years earlier, Nicolaus Copernicus is generally credited with developing the first detailed *heliocentric model* of the universe. Working in the 16th century, Copernicus threw out several key assumptions held by previous philosophers to devise a much more elegant model describing planetary motion. Most importantly, he put the sun at the center of the orbits of all the planets and explained apparent retrograde motion as the result of planets passing one another in their concentric orbits. Copernicus's model was a substantial improvement in terms of elegance, but still did not provide strong predictive power because he retained the assumption that planetary orbits were circular.

In the early 17th century, Galileo Galilei made observations using the telescope he invented, which provided strong support for the heliocentric model. He observed moons orbiting Jupiter and phases of Venus relative to the sun that would have been impossible under the Ptolemaic model. The Catholic Church punished Galileo for his views, which were considered to be in opposition to church doctrine, but, as a result of his observations, most astronomers had accepted the heliocentric viewpoint by the end of the 17th century.

It was Johannes Kepler, a contemporary of Galileo, who resolved the mathematics of the heliocentric model with his three laws of planetary motion. Most important among these was the recognition that the orbits of the planets were ellipses rather than circles. Using his model, astronomers could finally predict the locations of celestial bodies with accuracy. Willebrord Snell studied and developed theories involving refraction. Snell's Law explains the relationship between angles of incidence and refraction, thus bearing his name.[10]

Today, we understand our entire solar system to be an insignificant speck in our galaxy and our galaxy one of billions in the universe. Chapter 2 and Chapter 3 and the following will examine solar geometry, the geometry of the sun's position relative to a point on Earth. A solid working understanding of this material is essential to successful design. Chapter 2 frames the earth–sun relationship from a heliocentric perspective. Because we and our buildings are located on Earth, however, it is more convenient to work from a geocentric perspective in design. Chapter 3 covers the geocentric model useful to designers.

In the 17th century, Descartes, a French philosopher, developed a new concept of space that related to light perception and ultimately furthered the standing body of knowledge at the time (Figure 1.3). Descartes's system proposed the use of only matter and motion to explain perception. In the view of Descartes, space was filled with small masses of a material called the "ether" that could transmit forces by direct contact. Thus, the sun, a light-emitting body, could cause a ripple in the ether, and the conveyance through the ripple was thus light. This light would

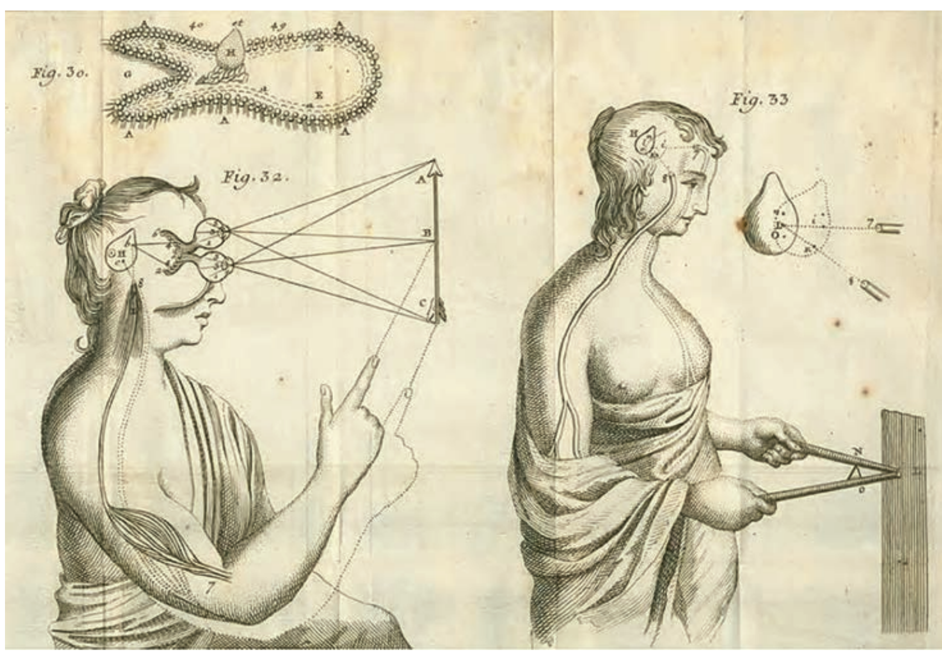

Figure 1.3

Descartes's Theory of Light and Perception

Diagrammatic representation of Rene Descartes's scientific research of light perception theory, using geometry and "ether" theory.

Public domain

be transmitted with immediacy and therefore would have unlimited speed. This "ether" could not be directly seen, yet it enabled the transfer of forces such as light and gravity. Descartes also had a unique perspective on color as it relates to the rotation of particles, theorizing that the speed of particle rotation determined the perceived color.[11] Although many of Descartes's ideas were unable to be supported by experimental evidence at the time, two of his ideas about light were supported in later theories: first, the notion of light as a ripple through the ether and, second, his thought that color may be determined by the speed of particle rotation.[12]

Arriving at Wave Theory

Near the end of the 17th century, there was no agreement on whether light was composed of particles or waves. A prominent advocate of corpuscular theory (or particle theory) was English scientist Isaac Newton. Newton described how he used a glass prism to show that white light must be composed of many different colored components, which the prism separated out according to their refractive capabilities. While Newton basically agreed with Descartes's idea of particles for the transmission of forces such as electricity, his theories suggested that light operated more similarly to the travel of sound waves as explained in theories of acoustics. Rather than casting broad assumptions, Newton proposed a myriad of theories and quantitative analyses. He attempted to understand the behavior of light using other principles of physics. As for his concept on light, Newton made it clear that he thought light to be the motion of some other substance through the ether, perhaps small particles or corpuscles, issuing from the luminous body.[13] Dutch physicist Christian Huygens was a proponent of wave theory and his theories were able to better explain some of the theories of Newton. Huygens' principle, involving secondary wave fronts, contributed to the later establishment of wave theory.

In the next 300 years, these ideas were advanced and wave theory was developed as an understanding of the electromagnetic spectrum, where visible light came to be understood as a small portion of the overall spectrum of wave frequencies transmitted through space. Quantum mechanics unveiled a new perspective as Max Plank's work of 1900 postulated that light's strength was proportional to its frequency and also demonstrated that light exists in discrete packets of energy called quanta. Albert Einstein's theory of the coefficients of emission and absorption set the table for theoretical physicists to later create a functional quantum theory of the scatter, refraction, and dispersion of light.[14] Einstein effectively extended Plank's theory by putting forward the idea that light frequency is related to behavior at the atomic level, and is connected to electron emission and incident radiation. Einstein's model suggested that light is composed of photons, or very small parcels of energy. Just as the notion of heat was registered in the infrared spectrum and differentiated from visible light, ultraviolet light was also better characterized. Likewise, the impact of ultraviolet (UV) rays on the body were further understood in the past century, where it became clear that too much UV exposure is harmful to human skin, while too much isolation or removal from natural daylight is also detrimental.

In actuality, light can behave according to a particle theory and a wave theory simultaneously, depending on the context and dimension. Frequently, light acts as a wave, or electromagnetic wave due to being composed of both electric and magnetic fields. Light waves have two primary attributes—wavelength and frequency—both of which are quantitative and scalable dimensions, and theoretically go on for infinity.

In essence, wave theory unites all forms of radiation and all kinds of matter and, as such, the universe can accurately be described as being composed of light.[15] Light is therefore a component of the electromagnetic spectrum. The photoelectric effect is described as the phenomena in which atoms of a material or substance emit electrons when struck by light.

The contemplation and study of light as it relates to vision and senses has carried forward to the present day, with more sophisticated theories and scientific advances continually being developed. In his book *The Eyes of the Skin: Architecture and the Senses*, Juhani Pallasmaa speaks of the dominance of the visual realm in today's culture and challenges it as the primary sense, particularly in architecture. Since the time of the Greeks, philosophical writings have been rich with visual metaphors; knowledge has become analogous with clear vision and light is regarded as the metaphor for truth.

While not discounting the importance of the sense of sight, Pallasmaa presents the idea that man's other sensory realms have been suppressed, leading to an impoverishment of our environment, causing a feeling of detachment and alienation. In the field of architecture, vision and light understandably play an important role, but Pallasmaa's writing supports a multi-sensory architecture that facilitates a sense of belonging and integration.[16] The positioning and design of structures and living spaces to allow the admittance of sunlight not only provides natural light for vision and modulation of light, but enables people to feel the warmth of the sun on their skin and reap the healthful benefits of sun exposure. Humans require sunlight for maximum health, both physically and mentally. In coordination with the sunlight, shadows and darkness are also essential. To quote Pallasmaa, "How much more mysterious and inviting is the street of an old town with its alternating realms of darkness and light than are the brightly and evenly lit streets of today!"[17]

The most relevant point made by Pallasmaa is that our senses have generally been deprived and repressed in our highly technological world. He feels that design should incorporate all senses, including the visual, in meaningful ways to better understand and appreciate our surroundings. As designers, we benefit from increasing our understanding of senses and the importance of crafting spaces to address a variety of elements, including light and its interconnected thermal factors that relate to the sense of touch.

FUTURISTIC UTOPIAN/DYSTOPIAN LIGHT VISIONS

Although change may be the only constant heading into the foreseeable future, light, particularly sunlight, can be certain to play an important role. Of all known natural phenomena, light is the longest-lasting. The sun, in scientific terms, is actually not permanent, but its lifespan is beyond our worldly comprehension. Therefore, because the star we refer to as the sun will last for billions more years, for the scale of mankind's history, it may be considered infinite.

A historical account of the role of daylight warrants a new perspective, and opens opportunities for innovative architectural design that incorporates time-tested solar design principles. Additionally, new analytical methods allow for calibrated design moves based on empirical modeling data that were either previously unavailable or at least not presented in a manner readily understood by architects. In other words, architecture will necessarily need to simultaneously respond to physical parameters as well as phenomenological considerations instead of leaning too far to either side to its own detriment.

Figure 1.4

The Walled City of Kowloon

The Walled City of Kowloon, unregulated by building codes for years as it fell in the cracks between Chinese and British rule.

Jodi Cobb/Getty Images

An example of ignoring solar principles in an actual development is the Kowloon Walled City in Hong Kong (Figure 1.4). Due to falling between the cracks of legislation between Chinese and British rule, the district was unzoned and unregulated for decades. What resulted was unmonitored growth, driven by consumptive desire, ignoring basic fundamental needs of natural light and natural ventilation. Most dense urban daylight codes require that tall buildings step back in plan, or taper in, at the higher levels. The buildings in the walled city actually expanded outward as they grew higher, to the point that they touched and allowed no natural light to the streets below. The virtual "city of darkness" was not only unfit for healthy living, it also mutated lifestyles and attracted immoral behavior.

Leung Ping Kwan writes of the Kowloon Walled City:

> Here, prostitutes installed themselves on one side of the street, while a priest preached and handed out powdered milk to the poor on the other; social workers gave guidance, while drug addicts squatted under the stairs getting high; what were children's games centers by day became strip show venues by night. It was a very complex place, difficult to generalize about, a place that seemed frightening but where most people continued to lead normal lives. A place just like the rest of Hong Kong.[18]

Robert Ludlum, the author of *The Bourne Supremacy* (1986), wrote:

> The Walled City of Kowloon has no visible wall around it, but it is as clearly defined as if there were one made of hard, high steel. It is instantly sensed by the congested open market that runs along the street in front of the row of dark run-down flats—shacks haphazardly perched on top of one another giving the impression that at any moment the entire blighted complex will collapse under its own weight, leaving nothing but rubble where elevated rubble had stood.[19]

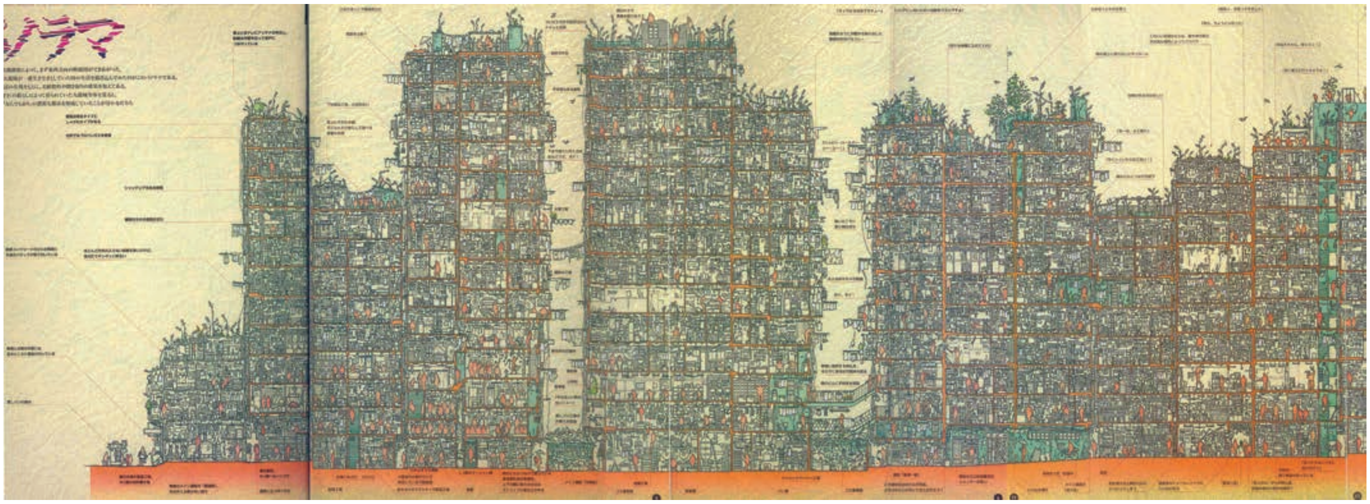

Figure 1.5

Diagrammatic Section of the Walled City of Kowloon

Diagrammatic section of Kowloon Walled City, representing the overdensification and lack of appropriate daylight/ventilation shafts.

Iwanami Shoten/Iwanami Shoten

Figure 1.6

A Scene from the Film *THX 1138*

Completely even diffuse light used as an incarceratory space in the film *THX 1138*.

American Zoetrope/Warner Bros/Alamy Images

Although it was torn down in the 1990s, the Walled City of Kowloon stood as a testament to the importance of solar consideration in dense urban developments. While density is better than sprawl in terms of energy consumption, it of course has its limits. The growth of the city was enabled by just enough construction technology to get into trouble, and a greed for more and more space, to the point where the value of the space greatly diminished for everyone. Nonetheless, the city was an incredible spectacle, particularly when viewed in section, considering the amazing density and programmatic diversity (Figure 1.5).

At the opposite end of the spectrum from the "city of darkness," one may consider the film *THX 1138* (Figure 1.6). In the film, the character THX 1138, portrayed by Robert Duvall, is sentenced to torture by placement in a completely bright, ambient diffused light setting, with no darkness or shadow. This lack of contrast drives him insane, as the homogeneity of light is as bothersome as the homogeneity of darkness. Without contrast, it is impossible to discern a horizon, surfaces, depth, and ultimately substance. Thus, the extreme of too much diffuse light is not an ideal environment either. Varied, modulated light is most desirable, and critical to consider at all scales of spatial design.

In the UK and in China, for example, daylight and sunlight codes require that each bedroom receive a minimum amount of daylight (view to the sky) and sunlight (direct solar penetration) each day. Thus, any newly constructed building must perform careful shadow studies to ensure it will not block too much daylight and sunlight from its neighbors. This "right to light," however, is negotiable, at least in London. The developer of a new tower can buy off the rights to daylight and sunlight from the owner of a neighboring residence that agrees with its fate to be severely overshadowed. This commodification of light is of particular interest, as land and property have historically been considered highly valuable assets. A fictional example of ultimate density is illustrated in the *Star Wars* series with the planet of Coruscant, which is so dense that the entire planet is a single "spherical" city, and there is no open space. Therefore, taking the "right to light" to its logical end, and imagining a city such as Coruscant, one might imagine a future where rights to light, and thus light itself, is more valuable than property. In this visage of the future, daylight and sunlight would attain the level of importance it had historically, but now in a more quantifiable and commercial manner. Nonetheless, humans will always need sunlight, even if only through indirect means, and the careful consideration of it is absolutely critical to the sustainability of humankind as we know it.

NOTES

1 Stanislaus von Moos, *Le Corbusier: Elements of a Synthesis* (Rotterdam: 010 Publishers, 2009), 122.
2 "Buildings and Their Impact on the Environment: A Statistical Summary," *Healthy Workplaces | Achieving Worker Health & Well-Being*, accessed October 31, 2014, http://healthyworkplaces.berkeley.edu/environmental-design/buildings-and-their-impact-on-the-environment-a-statistical-summary/.
3 Lindsay Baker, *A History of School Design and Its Indoor Environmental Standards, 1900 to Today* (National Clearinghouse for Educational Facilities, 2012), http://eric.ed.gov/?id=ED539480.
4 Gary Waldman, *Introduction to Light: The Physics of Light, Vision, and Color* (Englewood Cliffs, NJ: Prentice-Hall, 1983).
5 Ibid.
6 Cyril Aldred, *The Development of Ancient Egyptian Art from 3200 to 1315 B.C* (London: Tiranti, 1962), 27.
7 Aristotle and Jonathan Barnes, *The Complete Works of Aristotle: The Revised Oxford Translation* (Princeton, NJ: Princeton University Press, 1984).
8 Ibid.
9 Waldman, *Introduction to Light*, 7.
10 David C. Lindberg, *Studies in the History of Medieval Optics* (London: Variorum Reprints, 1983), 35.
11 Sir Edmund Whittaker, *A History of the Theories of Aether and Electricity—Vol. 1: The Classical Theories* (New York: Harper Torchbooks; The Science Library, 1960), 5.
12 Waldman, *Introduction to Light*, 6.
13 Whittaker, *A History of the Theories of Aether and Electricity—Vol. 1*, 19.
14 Ibid.
15 William Henry Bragg, *The Universe of Light: With Plates and Illustrations* (London: Scientific Book Guild, 1962).
16 Juhani Pallasmaa, *The Eyes of the Skin: Architecture and the Senses* (Chichester; Hoboken, NJ: Wiley-Academy; John Wiley & Sons, 2005), 7.
17 Ibid., 46.
18 Greg Girard and Ian Lambot, *City of Darkness Life in Kowloon Walled City* (Haslemere: Watermark, 2009).
19 Ibid.

2 THE EARTH–SUN RELATIONSHIP

SOLAR SYSTEM

Sun Characteristics

As stars go, the sun is quite ordinary; it is one of around 100 billion stars in our galaxy, the Milky Way, and one of perhaps between 10 sextillion (10^{23}) and 1 septillion (10^{24}) stars in the observable universe.[1] To put this number in perspective for those that have not seen the Charles and Ray Eames film *Powers of Ten*,[2] at a distance of 10^{23} meters from Earth, the Milky Way would appear as just a dot among other galaxies. This translates to a distance of 10 million light years.

Figure 2.1 shows several images of the varying surface activity on the sun. The mean sun-Earth distance is approximately 150,000,000 km, varying at any given time by an average of 1.7% due to the elliptical eccentricity of the earth's orbit. This distance is known as an astronomical unit and is the basis for measuring distances in the solar system. At a diameter of 1,390,000 km, the sun is so large that, even at this extraordinary distance from Earth, its angular diameter is still 0.53° (Figure 2.2). Because the sun is so far away and its angular diameter relatively small, we assume for the purposes of solar geometry calculations that it is a point source of light with all of its rays arriving at the surface of the Earth parallel to one another. Table 2.3 shows important distances in the solar system and on Earth in relation to one another.

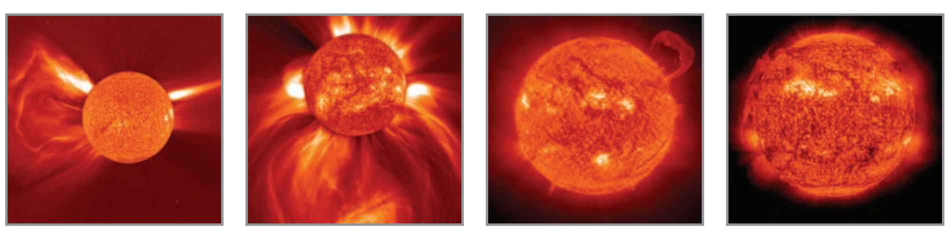

Figure 2.1

The Sun (Images)

Notable solar activity includes coronal ejections, which send billions of tons of matter into space in mere seconds. Sunspots are another well-known, but not entirely understood, solar phenomenon. Solar activity has direct effects on the Earth.

NASA/ESA

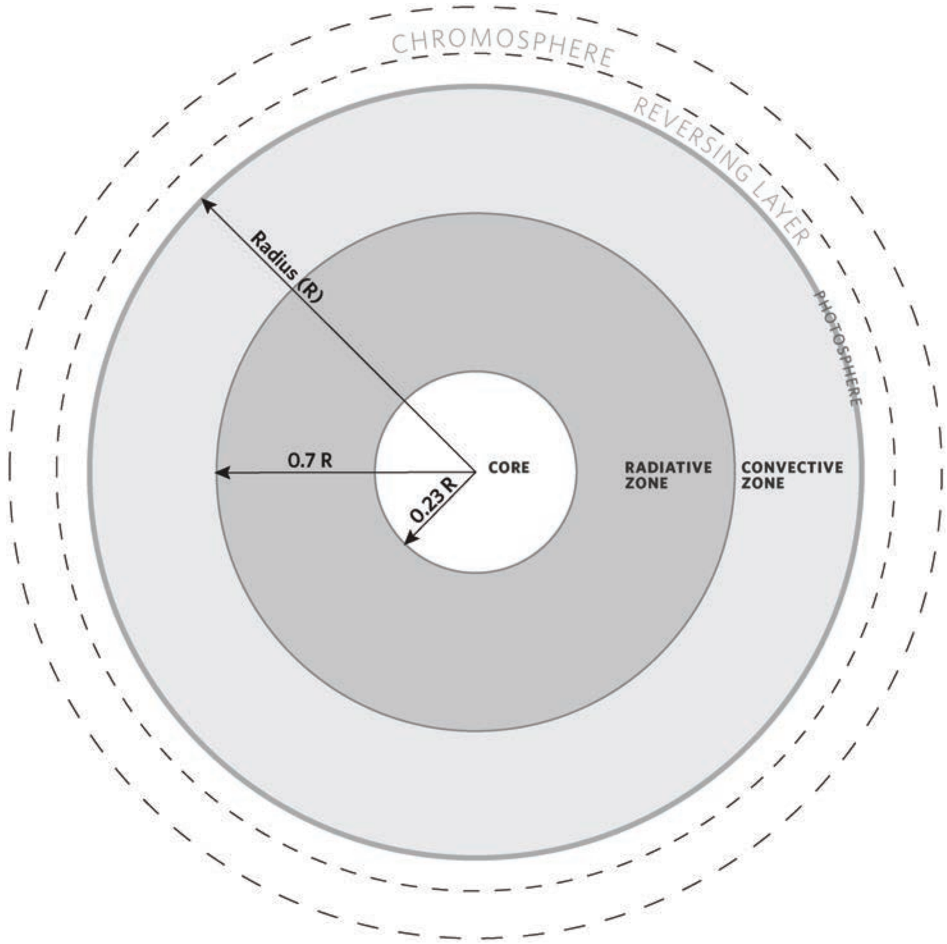

Figure 2.2

Structure of the Sun Diagram

The core of the sun contains 40% of the sun's mass in only 15% of its volume, and generates 90% of the sun's energy. The core has a mean temperature of roughly 8.40 x 106 K (~15 million °F), and a density of 105 kg/m^3—10 times more dense than lead.

From the center of the sun to the chromosphere, the temperature decreases proportionally as the distance from the core increases. The temperature of the convective zone is approximately 130,000 K. This layer is much less dense than the core (70 kg/m^3).

The chromosphere's temperature is 7000 K, hotter than that of the 5000 K photosphere. Surrounding the chromosphere is the corona. This layer has a negligible density, and a temperature that ranges from 1 million to 3 million K.

Greg Arcangeli

Planetary Orbits

Earth's Orbit

The Earth completes one full revolution around the sun in a solar year, 365.2425 days on average, necessitating adjustments such as leap days in the Gregorian calendar every four years and other adjustments over longer timeframes to maintain synchronicity between the standard calendar and the orbit of the Earth around the sun.

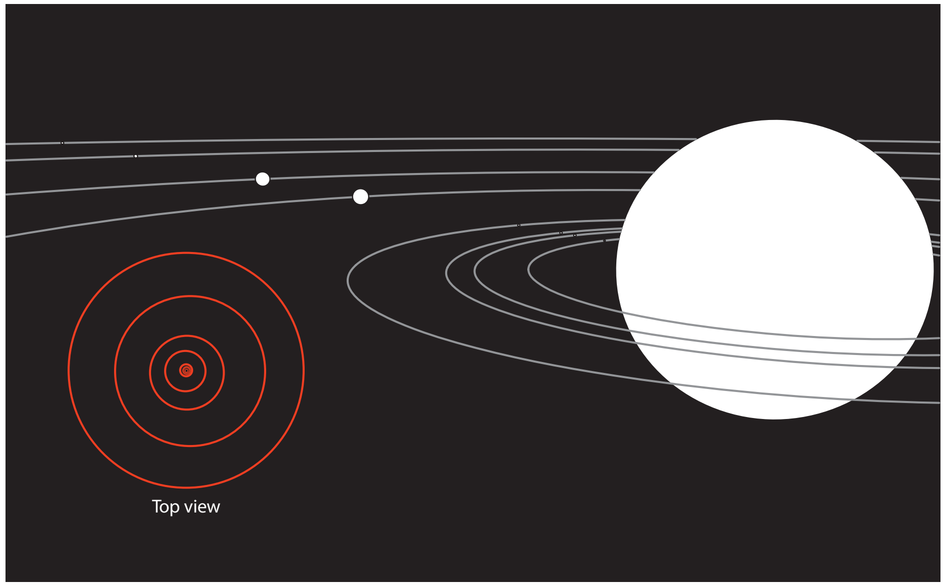

Figure 2.3

The Solar System

A note about scales—the "plan view," which shows the solar system from a position perpendicular to the plane of the orbits, displays the sun and planetary orbits in correct proportion to one another. The larger view is a distorted perspective of the solar system, but shows a reasonable approximation of the relative sizes of the sun and planets to one another.

Greg Arcangeli

Earth's orbit is a nearly circular ellipse with an eccentricity of 0.017, a value that varies over a cycle of thousands of years due to gravitational attractions of other celestial bodies. Because the eccentricity of Earth's elliptical orbit is small, for design purposes, it is treated as a circle (Figure 2.3).

Orbital Angle

The *orbital angle* (Γ) describes the position of Earth in its orbit at any time. In space, there are no obvious fixed landmarks, so some constant reference is necessary to measure the orbital angle against. The earth's rotational axis, which points in a constant direction during the earth's orbit around the sun, serves as this reference. The orbital angle is set by convention to 0° at the March equinox. As shown in Figure 2.4, on the June solstice (Γ=90°), the North Pole points toward the sun, whereas on the December solstice (Γ=270°), the North Pole points away from the sun.

Calendar dates are not readily used mathematically, so for the purpose of solar geometry calculations, these are converted to ordinal dates. The *ordinal date* (*n*) is the sequential numbered day of the year starting at 1 on January 1 and ending with 365 on December 31. Generally, solar geometry calculations for design purposes ignore the year number and are assumed to occur in a non-leap year. Table 2.1 or a spreadsheet can be used as a shortcut to convert calendar dates to ordinal dates.

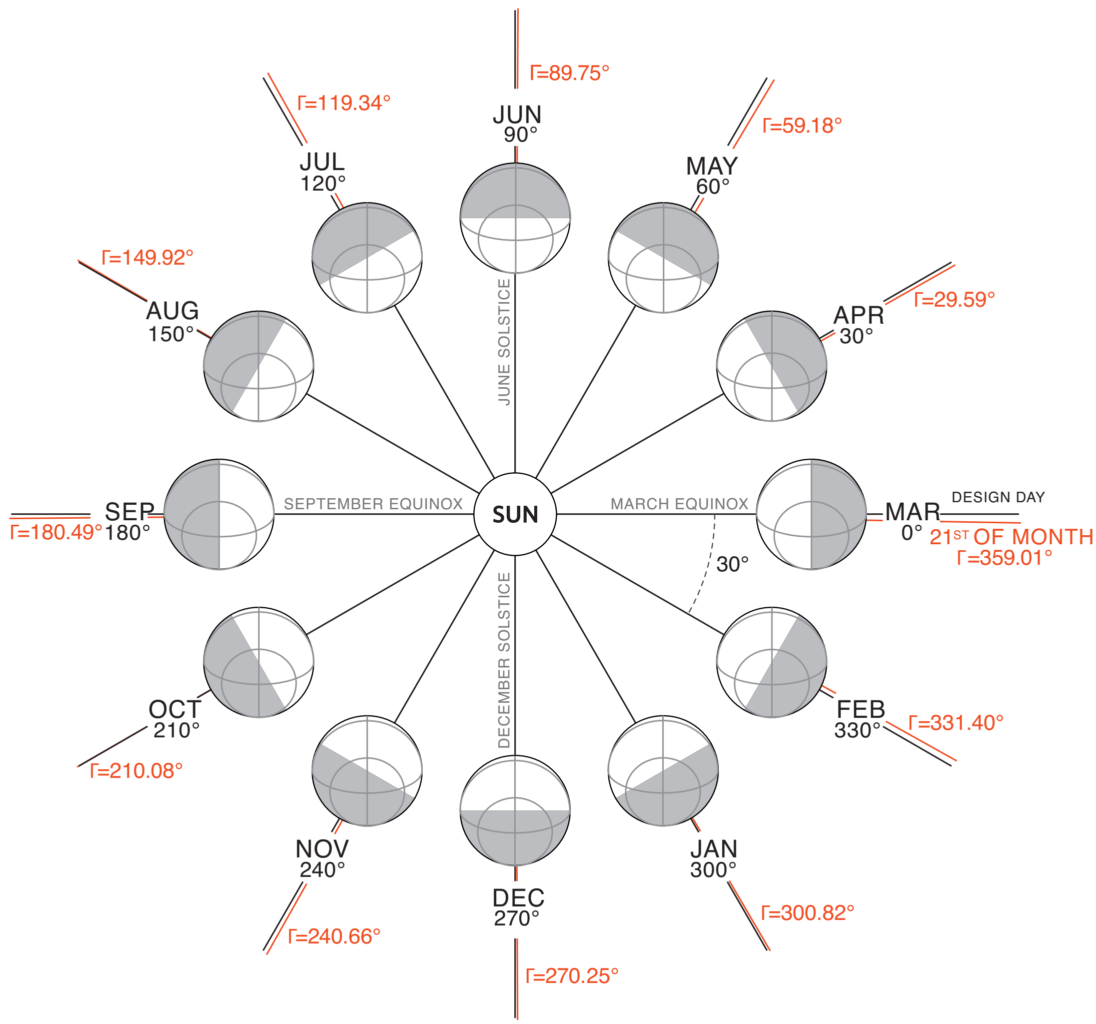

Figure 2.4

Orbital Position of the Earth throughout the Year

Greg Arcangeli

Table 2.1 Ordinal Dates for the 1st of Each Month

Date	*n*	*n (leap year)*
1/1	1	1
2/1	32	32
3/1	60	61
4/1	91	92
5/1	121	122
6/1	152	153
7/1	182	183
8/1	213	214
9/1	244	245
10/1	274	275
11/1	305	306
12/1	335	336

EXAMPLE 2.1 CONVERTING CALENDAR DATE TO ORDINAL DATE IN MICROSOFT EXCEL

To convert calendar dates to ordinal dates in a spreadsheet, first format the cell the calendar date will be entered into as "date" and select a month/day/year display format. Enter "1" into the cell. The date displayed is the base date in the spreadsheet, which in Microsoft Excel defaults to different dates for Mac and PC computer operating systems. It is advisable to use the January 1, 1900, date system to minimize translation problems. Spreadsheets also use an ordinal date system, but start with "1" on the base date just identified and count upward from there. To calculate a given ordinal date, enter the desired date into the formatted cell. The year is irrelevant, except that it should not be a leap year. Enter December 31 of the previous year into another "date" formatted cell. In a third cell, create a formula subtracting December 31 of the previous year from the desired date. Format this cell as a number and the difference displayed will be the ordinal date.

Equation 2.1 Orbital Angle

$$\Gamma = 360^\circ\left(\frac{n+284}{365}\right)$$

EXAMPLE 2.2 CALCULATING ORBITAL ANGLE

What is the orbital angle of the Earth on April 14?

First, convert the calendar date to its ordinal date:

April 14 is 13 days after April 1.

From Table 2.1, on April 1, n = 91

$n = 91 + 13 = 104$

Using Equation 2.1:

$$\Gamma = 360^\circ\left(\frac{n+284}{365}\right)$$

$$\Gamma = 360^\circ\left(\frac{91+284}{365}\right)$$

$$\Gamma = 382.68^\circ$$

$$382.68^\circ - 360^\circ = 22.68^\circ$$

The calculated orbital angle is greater than 360° for most dates; therefore, we subtract 360° to more readily interpret the results. In this example, the Earth has traveled an angular distance slightly less than 23° since the March equinox—approximately one quarter of its trip toward the June solstice.

Table 2.2 Design Day Data

		Design Days Based on 30° of Orbit				*21st of Each Month*			
	Day	*n*	*Γ*	*ET*	*δ*	*n*	*Γ*	*ET*	*δ*
Dec	12/20	354.75	270	2.29	−23.45	355	270.25	2.17	−23.45
Jan	1/20	20.17	300	−10.35	−20.31	21	300.82	−10.60	−20.14
Feb	2/19	50.58	330	−14.07	−11.73	52	331.40	−13.96	−11.23
Mar	3/22	81.00	0	−7.55	0.00	80	359.01	−7.86	−0.40
Apr	4/21	111.42	30	1.31	11.73	111	29.59	1.22	11.58
May	5/21	141.83	60	3.69	20.31	141	59.18	3.74	20.14
Jun	6/21	172.25	90	−1.38	23.45	172	89.75	−1.32	23.45
Jul	7/21	202.67	120	−6.40	20.31	202	119.34	−6.35	20.44
Aug	8/21	233.08	150	−3.55	11.73	233	149.92	−3.57	11.75
Sep	9/20	263.50	180	6.71	0.00	264	180.49	6.90	−0.20
Oct	10/20	293.92	210	15.50	−11.73	294	210.08	15.51	−11.75
Nov	11/20	324.33	240	14.00	−20.31	325	240.66	13.83	−20.44
Dec	12/20	354.72	270	2.29	−23.45	355	270.25	2.17	−23.45

Design Days/Months

A solar year is one full 360° revolution of the Earth around the sun. The solstices and equinoxes occur at 90° intervals in this rotation. It is convenient to specify one day of each month to use as representative of solar position at that time of year. Dividing 360° of the orbit by 12 months yields a progression of 30° of orbital angle per month. These representative days are known as ***design days***. Solar geometry is identical on the Jan/Nov, Feb/Oct, Mar/Sep, Apr/Aug, and May/Jul design days because they occur at orbital angles that are symmetrical around the solstices.

The solstices and equinoxes occur around the 21st day of their respective months, so by convention, design days are often taken as the 21st of each month. Because of variations in the number of days per month, and the fact that the orbital length of a day is not an integer value in degrees, using the 21st of each month results in slight asymmetry across design days. In practice, this does not pose significant problems, but may lead to minor confusion. Table 2.2 outlines the differences between using the 21st of each month compared to design days in increments of 30° of orbital angle. When this book refers to design days, they will be in increments of 30°/month from the March equinox.

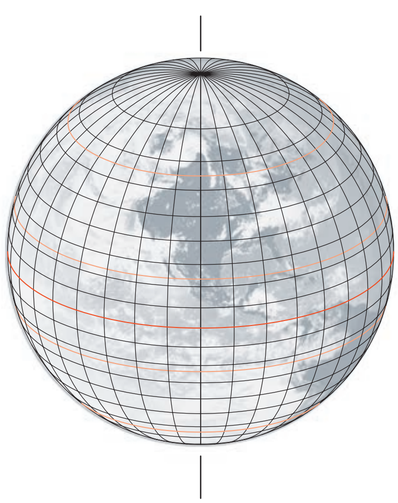

Figure 2.5
The Geodesic Grid
Greg Arcangeli

GEODESY

To allow the specification of precise locations on Earth, a coordinate system known as the ***geodesic grid*** has been established (Figure 2.5). Any point on this spherical grid may be described with unique coordinates of latitude and longitude.

This grid aligns with the axis on which the Earth rotates. The North and South Poles are those points on the surface of the Earth pierced by the imaginary line of the rotational axis. The plane perpendicular to the rotational axis through the center of the Earth is known as the ***equatorial plane***. The circle formed where this plane intersects the surface of the Earth is the ***equator***. The equator is a ***great circle***, which is a circle on a sphere whose plane intersects the sphere's center point. As such, a great circle traces the full circumference of the sphere. This is in contrast to ***minor circles***, which are circles on a sphere that do not lie in planes intersecting the sphere's center and have a diameter smaller than the full diameter of the sphere.

Latitude (*L*) is the measure of north-south position on Earth. Specifically, it is the absolute angular distance from the center of the equatorial plane to a point on the surface of the Earth. Latitude ranges from 0° at the equator to 90° at the North Pole and –90° at the South Pole. The imaginary lines that connect all points of the same latitude are known as ***parallels***. Except for the equator, parallels are minor circles. As shown in Figure 2.6, when viewed from the north or south, parallels appear to be concentric circles. When viewed from the equatorial plane, they are parallel lines. Because lines of latitude are parallel and separated by the same angular distance on the surface of the Earth, the distance between parallels is constant. The circumference of the Earth is approximately 40,008 km around the poles, resulting in a surface distance for each degree of latitude of approximately 111.3 km.

Longitude (***LON***) measures east-west position on Earth. Lines of longitude are known as ***meridians***. A meridian is an imaginary semi-circular line on the surface of the Earth starting at one pole, passing through a point of interest and ending at the other pole. Each meridian is a segment of a great circle, and all points on a meridian are at the same longitude. The meridian that passes through a place is known as its ***local meridian***. As shown in Figure 2.6, when viewed from the north or south, meridians appear to divide the Earth up into pie-shaped pieces. When viewed from the

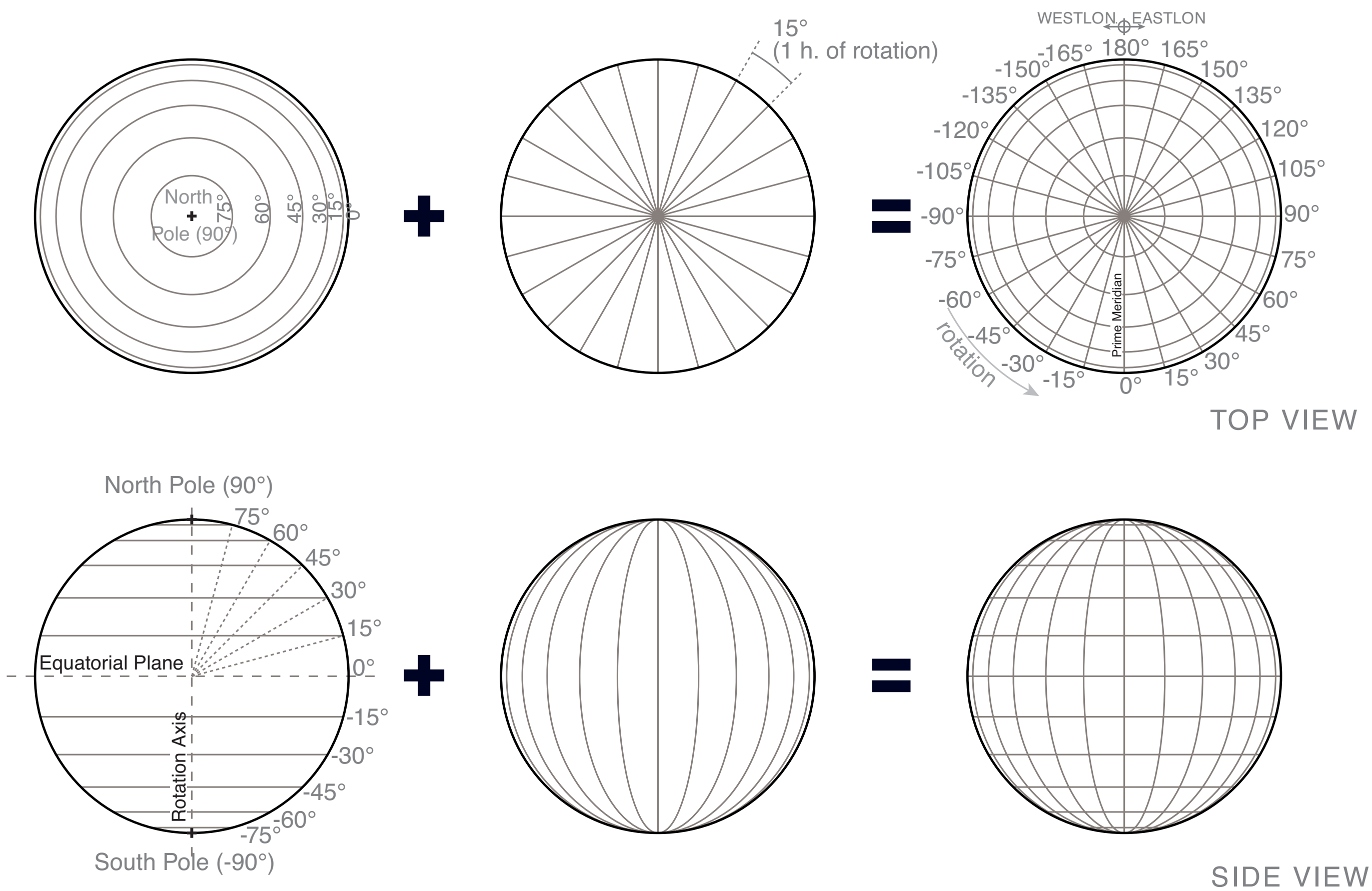

Figure 2.6

Latitude and Longitude Construction

Greg Arcangeli

equatorial plane, meridians appear as ellipses. Longitude, then, is the angular distance on the equatorial plane of a point's meridian from the ***prime meridian*** (0°), which runs just through the eastern part of London, England. Unlike latitude, for which there are obvious fixed reference points (the poles and equator), there is no geodesically rational starting point from which to measure the radial system of longitude.

Until the mid-18th century, individual countries used their own prime meridians for navigation. However, in 1884, the meridian passing through the Royal Observatory in Greenwich, England, was established as the internationally recognized prime meridian through a geopolitical process.

The lack of a celestial basis for longitude meant that in nautical navigation, mariners were able to determine latitude with a high degree of accuracy using the position of stars for hundreds of years before reliable methods of determining longitude were available. The solution was a highly accurate time-keeping device known as the marine chronometer that allowed sailors to calculate the difference between the time at the prime meridian and local solar time and thus determine their longitude. Today, global positioning systems have largely solved the challenges of determining east-west position at sea, but in the absence of GPS data, the marine chronometer is still the primary means for doing so.

Longitude is measured positive toward the east and negative to the west, ranging from 180° eastward to −180° westward, at the ***antimeridian***, which is the meridian opposite the prime meridian. Longitude may also be specified with an E or W modifier indicating east or west. For example, 97.7° W is the same as −97.7° longitude. Figure 2.7 diagrams the geometry of two cities on the same meridian. Because meridians are not parallel, there is no fixed surface distance between them. At the equator, the distance for each degree of longitude would be equal to that for latitude if the Earth were a perfect sphere, but it actually bulges slightly at the equator due to the centrifugal force generated by the earth's rotation on its axis. The earth's equatorial circumference of approximately 40,076 km results in a distance between meridians of approximately 111.3 km. As one moves north or south, meridians begin to converge until they intersect at the poles. Table 2.3 shows longitudinal distances at various points on the earth's surface.

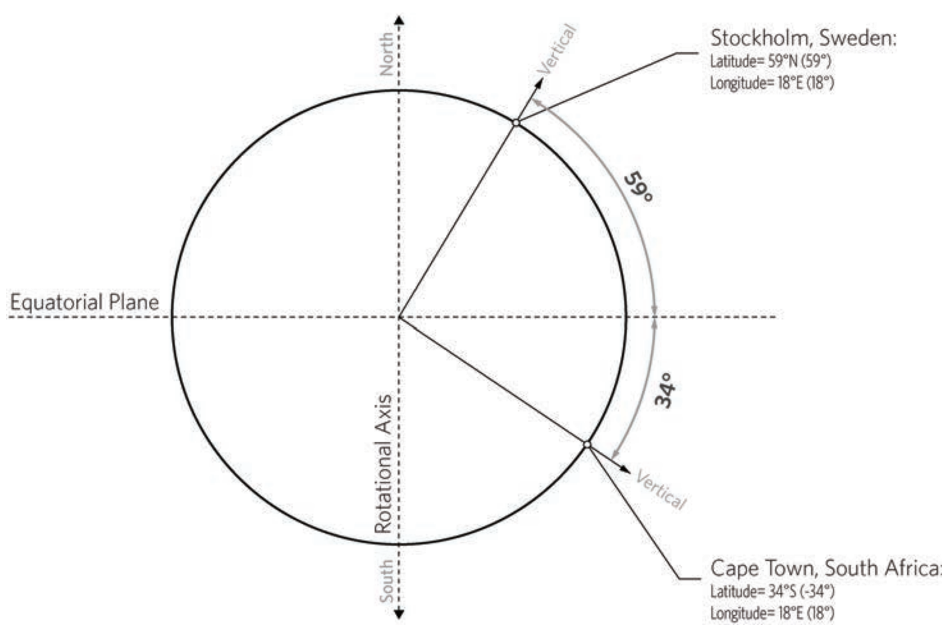

Figure 2.7

Latitude and Longitude Example

Greg Arcangeli

Table 2.3 Important Distances

	km	*miles*
Diameter of Sun	1.39×10^6	8.62×10^5
Earth/Sun		
Perihelion	1.48×10^8	9.17×10^7
Mean	1.50×10^8	9.29×10^7
Aphelion	1.53×10^8	9.48×10^7
Earth at Equator		
Circumference	40,075.02	24,901.46
Diameter	12,756.27	7,926.39
Earth at Prime Meridian		
Circumference	39,940.65	24,817.97
Diameter	12,713.50	7,899.81
1° of Latitude	111.32	69.17
1° of Longitude at Latitude		
0°	111.33	69.17
30°	96.62	59.9
60°	55.78	34.59
90°	0.00	0.00

Magnetic Declination

Another key issue in navigation as well as solar design is that of magnetic declination. The pole of the earth's magnetic field is not centered at the North Pole; therefore, a compass needle does not point toward true north, except in a few areas where true north and magnetic north happen to align. To further complicate the issue, the magnetic pole is in constant motion at a speed that varies over time. In recent years, it has moved at a rate of approximately 55 km/year to the north-northwest. In 2015, it was located at 86.27°N and 159.18°W in the Arctic Ocean north of Canada.[3]

Magnetic declination is the angle at any location between ***magnetic north*** and ***true north***. Magnetic declination varies considerably from place to place and also changes as the magnetic pole moves. Figure 2.8 shows contours of magnetic declination for North America in 2010 based on models from NOAA.[4] Table 2.4 lists the magnetic declination for some major cities worldwide. Positive magnetic declination indicates magnetic north is east of true north. If the magnetic declination is negative, magnetic north is west of true north. For compass readings to be useful, it is essential that they be adjusted for magnetic declination (Figure 2.9).

Locating True North

When embarking on a design, it is essential to locate true north. Sometimes, older surveys, plat maps, and other such documents indicate magnetic north of the era in which they were made as north on the map. Because the magnetic pole moves over time, and such maps do not necessarily specify whether they are based on true north, magnetic north, or other sources such as older maps, it can be difficult to determine their accuracy. This confusion can carry over to current surveys because north may be simply transposed from previous documents. To ensure that true north is indicated accurately, one should specify this to the surveyor.

There are other means of establishing true cardinal directions when a survey is not available. Using a compass and adjusting for magnetic declination can provide a

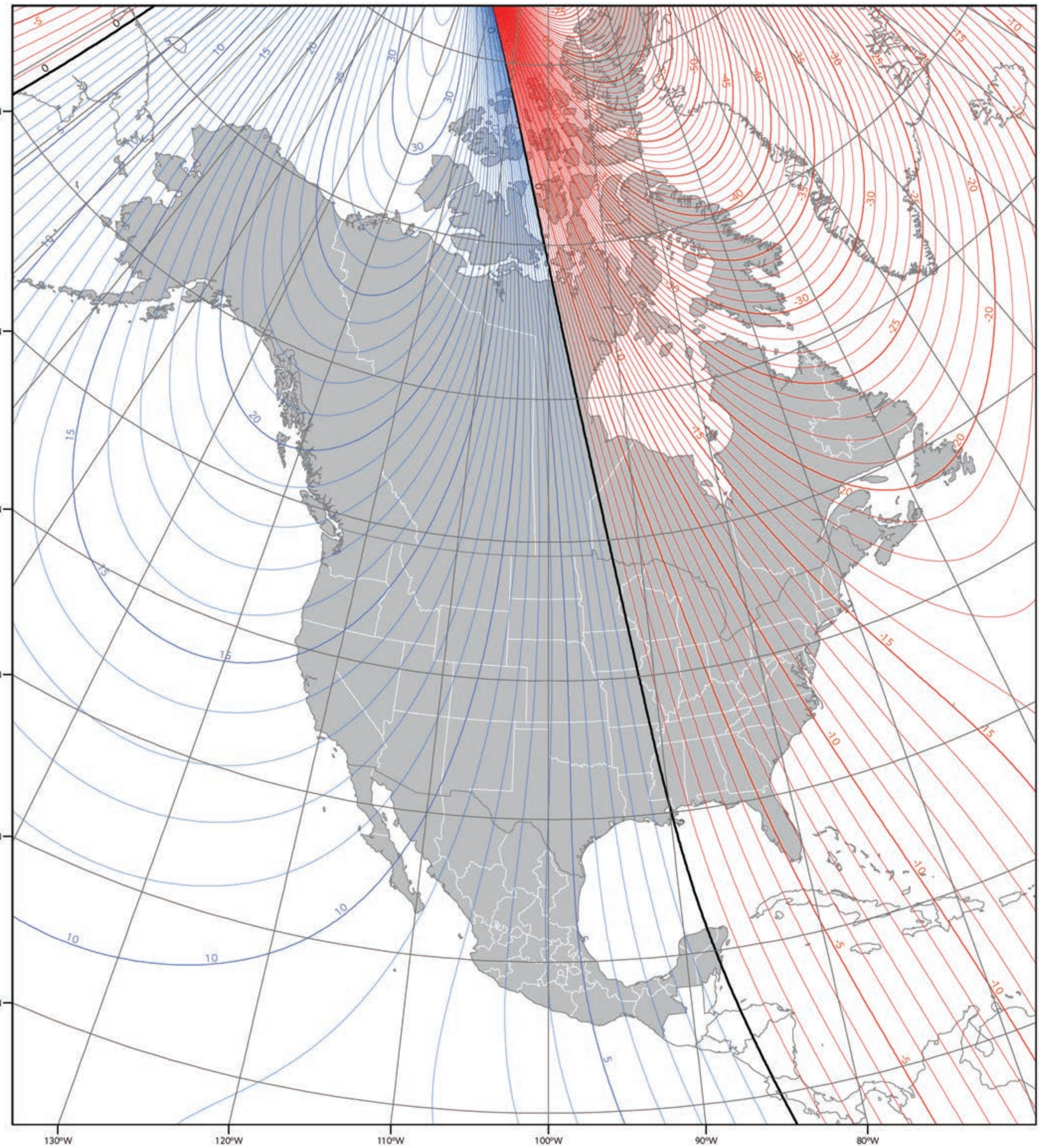

Figure 2.8

Magnetic Declination in North America, 2010

Greg Arcangeli

Table 2.4 Magnetic Declination for Major Cities, 2010

Country	*City*	*Declination*
Australia	Canberra	12° E
Austria	Vienna	2° E
Bangladesh	Dhaka	0°
Belgium	Brussels	1° W
Brazil	Brasilia	19° W
Canada	Ottawa	14° W
Chile	Santiago	5° E
China	Beijing	6° W
China	Hong Kong	2° W
Costa Rica	San Jose	0°
Cuba	Havana	3° W
Czech Republic	Prague	2° E
Denmark	Copenhagen	1° E
Egypt	Cairo	3° E
Finland	Helsinki	6° E
France	Paris	1° W
Germany	Berlin	1° E
Greece	Athens	3° E
Hungary	Budapest	4° E
India	New Delhi	1° E
Indonesia	Jakarta	1° E
Israel	Jerusalem	3° E
Thailand	Bangkok	0°
UAE	Abu Dhabi	1° E
United Kingdom	London	3° W
United States	Washington DC	10° W
United States	Juneau, AK	25° E
United States	Phoenix, AZ	12° E
United States	Little Rock, AK	2° E
United States	Sacramento, CA	16° E
United States	Denver, CO	10° E
United States	Atlanta, GA	4° W
United States	Honolulu, HI	10° E
United States	Boston, MA	16° W
United States	Jackson, MS	1° E
United States	Salt Lake City, UT	14° E

reasonable level of accuracy, but one must be careful when doing so in urban environments or near any sort of electrical equipment because compass bearings are affected by proximity to metal and electromagnetic interference. This issue extends to GPS devices that rely on magnetic compasses to provide direction readings when stationary. When in motion, some GPS devices can provide accurate directional information by calculating a bearing based on the vector between two coordinate points, but this may not be practical when investigating a building site. For design purposes, accuracy within 1° is generally sufficient, although greater accuracy is desirable. In this case, web-based map services can provide a readily available reference for true north. As direction sometimes varies slightly between the various map providers, it is a good idea to triangulate by checking several sources. These services generally do not provide a means of determining a compass bearing directly, so it may be

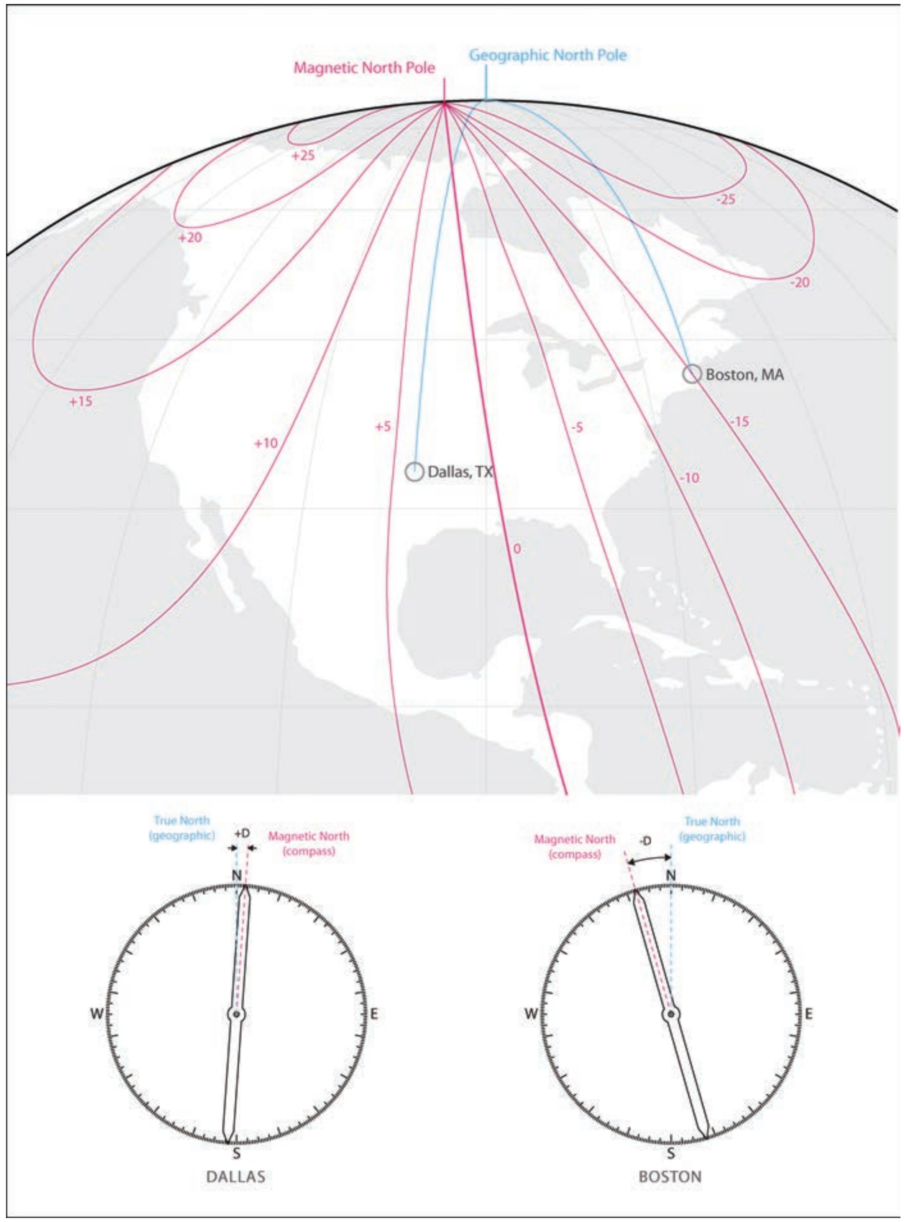

Figure 2.9

Adjusting for Magnetic Declination

Accounting for magnetic declination requires a compass reading and current declination for the location where the reading is taken. All good maps provide the declination correction, but because declination changes over time, it is important to use a current map.

Greg Arcangeli

necessary to export an image, import it into a vector-based drawing application, and trace over the image to measure the compass bearing of a line or object of interest.

Finally, there is the time-honored technique of finding the direction of the shortest shadow during the day. This requires marking the locations of the shadow of a vertical object (it needs to come to a relatively small point for accuracy) on a horizontal surface around the time of solar noon at short intervals. The shortest shadow will occur at solar noon and fall along the local meridian of the shadow-casting object. For an observer outside the tropics, the point will be in the direction of the closest pole. Within the tropics, the point will still always be on the north-south line, but the direction will reverse depending on the time of year. This method is less accurate when the sun is close to being overhead (summer and lower latitudes) because of the short length of the shadow.

GEOMETRY

The Earth orbits the sun on the ***ecliptic plane***, which passes through both the center of the Earth and the center of the sun, as shown in Figure 2.10. The Earth's axis of rotation is tilted relative to this plane. The resulting angular difference between the equatorial plane and the ecliptic plane is approximately 23.45° and is known as the ***obliquity of the ecliptic***. This is the same angle that occurs between the Earth's axis of rotation and the ecliptic pole—the line passing through the center of the Earth perpendicular to the ecliptic plane.

Precession and Nutation

We generally assume that the Earth's rotational axis points in one fixed direction but it actually changes gradually over a very long cycle. Imagine a spinning top just after it has been released. If it was a good spin, the top pivots rapidly around an axis that remains vertical as the top travels across the floor. As the rotation slows, the axis begins to wobble, tracing a wider and wider cone shape. The Earth experiences the same wobbling in its rotation, but over a dramatically longer time period. This axial wobble is known as *precession* and it occurs over approximately a 26,000-year cycle.

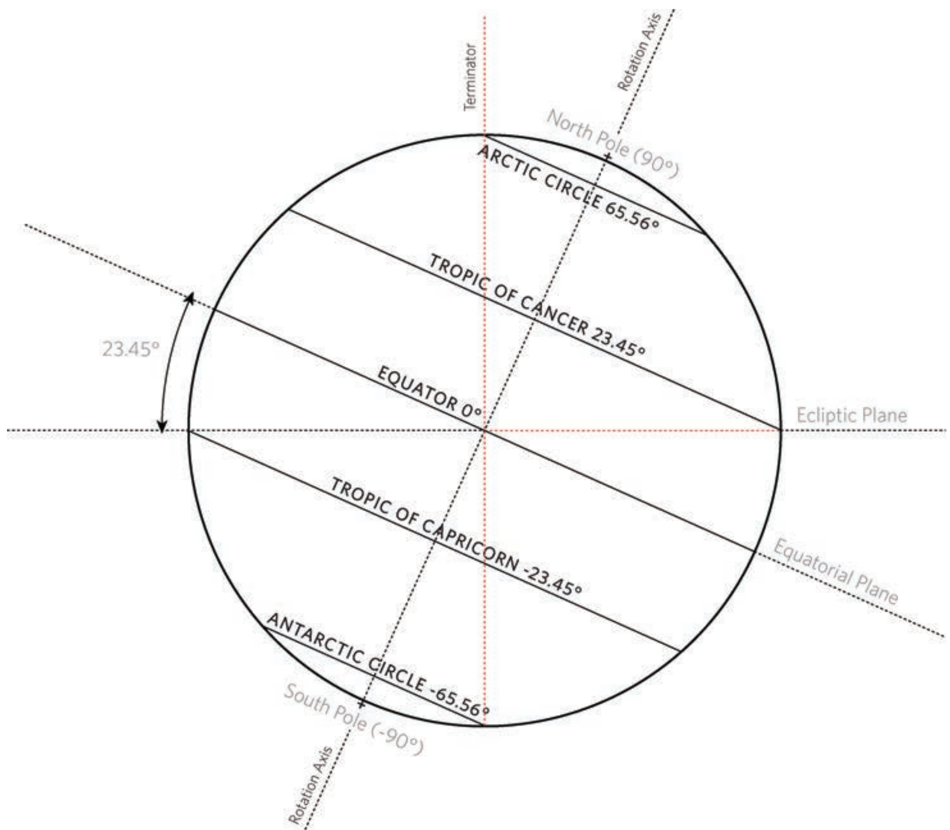

Figure 2.10
Geometry of the Earth and the ecliptic plane
Greg Arcangeli

Currently, the North Pole is pointing away from the sun at the same time the Earth passes closest to the sun in its orbit. In 13,000 years, the Earth's axis will be pointing in the opposite direction than it does today. Precession is the result of the gravitational pull of the moon and other celestial bodies on the Earth's equatorial bulge.

Today, the star Polaris is known as the ***North Star*** or Pole Star because the Earth's rotational axis points within 0.7° of its position, with the result that the star appears to stay nearly fixed in place while the rest of the stars rotate around it from our perspective on Earth. As such, the North Star is an enormously useful navigational tool. In the time of the ancient Greeks, prior to the last several thousand years of precession, the Earth's axis pointed at the star Thuban, which they considered the Pole Star.

Within the long cycle of precession, the Earth also rocks slightly on its axis over a period of 18.6 years, slightly changing the obliquity of the ecliptic. This phenomenon, known as ***nutation***, is the result of the gravitation pull of the moon on the Earth along its orbital path, which is inclined approximately 5° relative to the ecliptic plane. For design purposes, precession and nutation are not significant factors and may be ignored.

DAYS

Sunrise is always occurring on the side of the Earth that is rotating toward the sun along the great semi-circle tangent to the sun's rays at any moment. Sunset is underway on the opposite side of the Earth. The circle formed by these two arcs separates day from night and is known as the ***terminator***. See Figure 2.10 for a diagrammatic depiction of the terminator line.

While for simplicity of calculation we model the terminator as though it is a crisp line, in reality, day fades into night and vice-versa due to atmospheric diffraction of sunlight and the fact that the solar disc has width so a point near sunrise or sunset sees only part of the sun for some time (Figure 2.11).

For solar geometry purposes, sunrise is that moment when the center of the solar disc crests the horizon and begins to illuminate the reference location. Sunset occurs when the center of the sun drops below the horizon. Day is any time the center of the sun is above the horizon with respect to the reference location, while night is the time when the sun is not visible from that position. All latitudes along a local meridian will experience the same solar time, while times of sunrise and sunset vary along that meridian. Days for the points along this local meridian will be longest toward the summer pole and shortest at the winter pole.

Apparent Solar Time

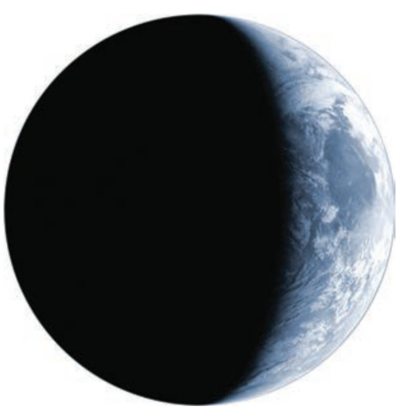

Figure 2.11
Image of the Day/Night Terminator
Greg Arcangeli

For millennia, man has used the sun to keep track of time. Ancients recognized that a vertical stick placed in the ground would cast a shadow that moved in a predictable pattern. Later, obelisks cast these shadows on a larger scale, and marks could be made on the ground indicating the path of the sun on various days. The longest shadow would indicate the winter solstice, while the shortest one indicated the summer solstice. Eventually, as these movements became better understood, sundials were created that could measure time of day and the date more precisely. The first sundial was probably constructed around 1500 BCE in Egypt.

The shadow-casting component of a sundial is known as the ***gnomon***. The movement of its shadow on the ground or sundial face indicates ***apparent solar time*** (*AST*), more commonly referred to simply as ***solar time***. At *solar noon*, the gnomon's shadow always falls along the due north-south line. Put more technically, solar time is the timekeeping convention where noon is defined as the time at which the sun ***transits*** (crosses) the local meridian. In solar time, sun positions in the morning and afternoon are symmetrical around the north-south axis. The current time at any location on Earth is a function of the Earth's position relative to the sun in its axial rotation. Apparent solar time varies from the time kept by clocks due to a number of factors, which are discussed in the following sections. Solar geometry calculations are based on solar time; conversion to the more familiar local (clock) time is straightforward, but for many design applications, solar time is more useful.

Hour Angle

Each hour, the Earth rotates 15° on its axis, turning a full 360° rotation in 24 hours. The Earth's position at any moment in this rotation is measured by the ***hour angle*** (H). The hour angle is taken relative to the meridian of the reference point on Earth, so every point along that meridian, regardless of latitude, will have the same hour angle and solar time. Locations to the east or west, however, will have different hour angles at the same instant. The hour angle is similar to longitude (it is identical to longitude at 12:00 apparent solar time on the prime meridian), but the longitude of a place is fixed while the hour angle changes constantly.

When the sun's position is normal to the local meridian at the ecliptic plane ($H = 0°$), it is solar noon along that meridian. Hour angle is negative in the morning and positive in the afternoon. When the hour angle is 0° (solar noon) at the prime meridian, it is 180° (solar midnight) on the antemeridian and vice-versa. Figure 2.12 shows how the hour angle is measured.

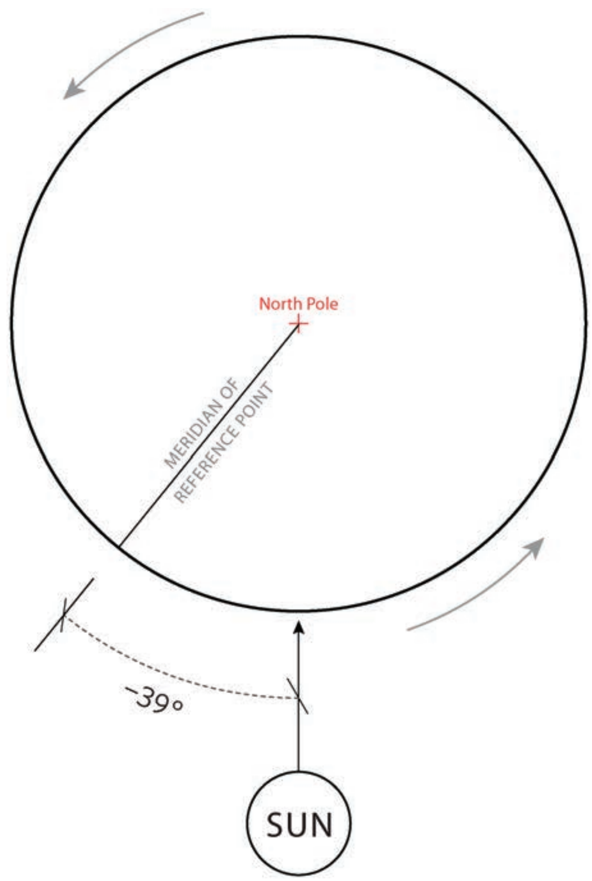

Figure 2.12

Hour Angle

The hour angle of −39° calculated in Example 2.3 is shown in this diagram. This angle corresponds to the solar time of 9:24, and it is apparent from the diagram that the sun is to the east of the reference meridian, as we would expect it to be in mid-morning.

Greg Arcangeli

Use Equation 2.2 to calculate the hour angle at a given solar time. Solve for *AST* to determine the solar time from a known hour angle.

Equation 2.2 Hour Angle

$$H = 15°(AST - 12.00\ \text{h})$$

EXAMPLE 2.3 HOUR ANGLE CALCULATION

Determine the hour angle at 9:24 apparent solar time.

Solution

1) Because hour angle is relative only to the reference location's view of the sun, it is not necessary to know longitude to calculate the hour angle. Start by converting the time to decimal hours.
$AST = 9{:}24 = 9.40$ h

2) Use Equation 2.2 to solve for the hour angle.

$$H = 15°(AST - 12.00)$$
$$H = 15°(9.40 - 12.00)$$
$$H = -39°$$

The hour angle is negative, indicating that the time is before solar noon.

Standard Time

As the only reliable time-keeping reference available, apparent solar time was the norm worldwide until the 19th century. The difference in solar time between locations at different longitudes was not a significant problem before long-distance communication and rapid transportation became available. Railroad schedules and the advent of the telegraph, however, made it essential that standardized time-keeping conventions be established.

In an effort to alleviate this confusion, in 1878, Sir Sanford Fleming proposed the establishment of ***time zones*** (*TZ*) within which there would be only one ***local standard time***. The Royal Observatory at Greenwich, England, was declared the basis for measurement of time, with the creation of Greenwich Mean Time (GMT). GMT has since been superseded by ***coordinated universal time*** (UTC) as the standard for time keeping. For most practical purposes, GMT and UTC are the same, but UTC should be used to avoid confusion. Each time zone is offset by a given increment ahead of or behind UTC. For example, UTC +5 indicates local standard time is 5 hours ahead of UTC 0 (formerly Greenwich Mean Time). The Earth rotates 15° on its axis each hour, turning a full 360° rotation in 24 hours. Therefore, to establish time zones with increments of one hour, reference meridians known as ***local standard meridians*** (*LSM*) occur every 15° of longitude in each direction from the prime meridian. The area from 7.5° west to 7.5° east of the local standard meridian theoretically falls into that one-hour time zone.

This idealized model poses some problems in practice, however, and political decisions have greatly altered the standard time zone map. A global map of time zones is shown in Figure 2.13, based on the map by the CIA.[5] Countries generally prefer

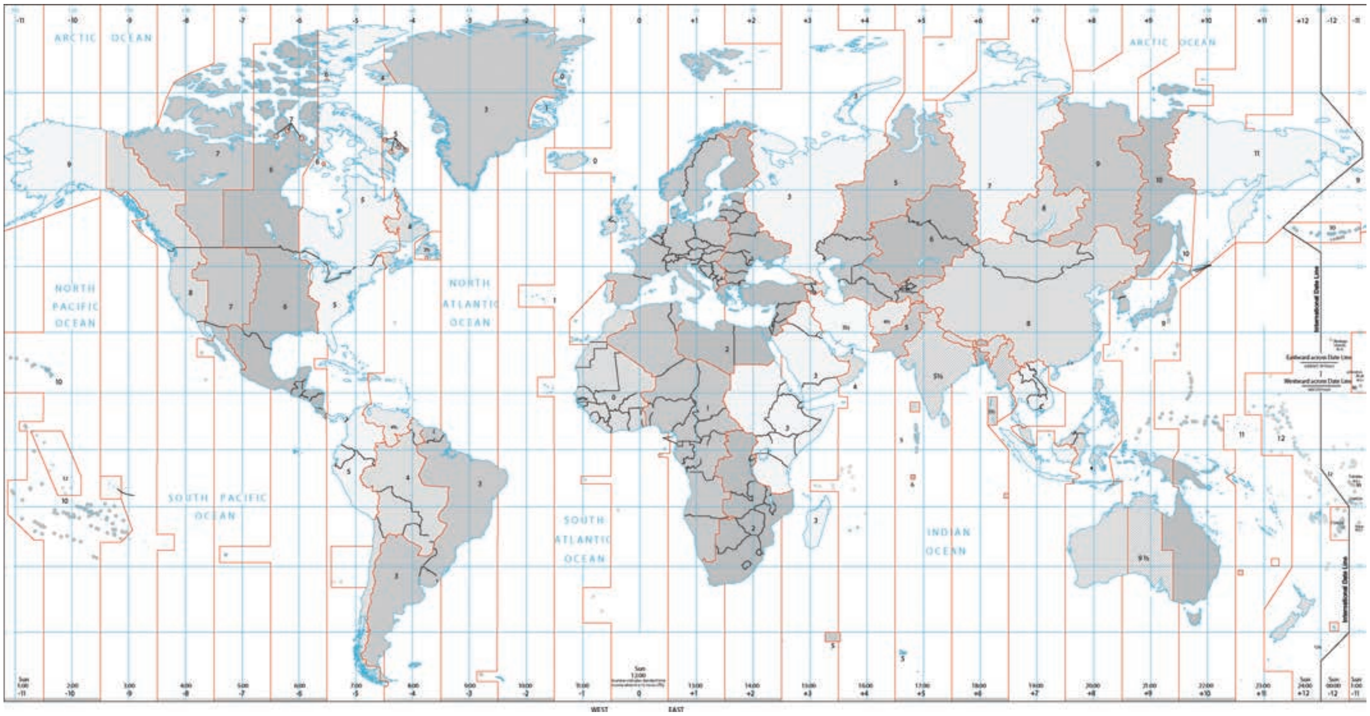

Figure 2.13
Global Time Zones
Greg Arcangeli

to limit the number of time zones within their borders. In much of the world, time zones have been drawn to follow national borders. Larger countries may have territory within several time zones. The lower 48 United States, for example, includes four time zones (UTC –5 to –8) that meander to follow state boundaries, Alaska and Hawaii fall in two more, and U.S. territories exist in several others. China on the other hand, based on its longitudinal breadth, should encompass five time zones, but the entire country operates on one (UTC +8).

Even more inconvenient than dealing with multiple time zones within a region is the problem of coping with different dates, as would occur in countries crossed by the antemeridian. To alleviate this difficulty, the ***International Date Line*** was established as the demarcation between one day and the next. This line jogs around multiple island groups and landmasses in the Pacific. The time zones in the South Pacific area are so gerrymandered that if one begins on the atolls of Tokelau, New Zealand (UTC −10), at 172° west longitude and travels due north just 520 km along the antemeridian to Hull Island, Kiribati (UTC +13), it is an hour earlier but the next day there. However, if one travels 520 km due south of Tokelau to Apia, Samoa (UTC −11), standard time is one hour earlier the same day. In fact, traversing this meridian from pole to pole, one encounters nine time changes, five unique time zones, and four date changes.

Because of the extent to which time zones have been adjusted based on political boundaries, local standard meridians are not necessarily located in the center of the standard time zone they correspond with, and in many locations apply to a range of longitudes much wider than their ideal 15° increment. Determine the local standard meridian for a given time zone using Equation 2.3.

Equation 2.3 Local Standard Meridian

$$LSM = 15° \ (TZ)$$

EXAMPLE 2.4 LOCAL STANDARD MERIDIAN

Determine the Local Standard Meridian for Austin, Texas.

Solution

Find the time zone for Austin, Texas, using Figure 2.13, or from numerous Internet resources.

TZ = UTC –6, also known as Central Standard Time (CST) in the United States. Use Equation 2.3 to solve for the local standard meridian.

$$LSM = 15°(TZ)$$
$$LSM = 15°(-6)$$
$$LSM = -90°$$

Austin's longitude is –97.74°, which places the city just outside the 7.5° range a time zone would ideally span on either side of the local standard meridian. Nevertheless, the Central Standard Time zone continues 690 km west of Austin to Hudspeth County, Texas, at approximately –105°. In Mexico, UTC –6 extends as far as –108° and in Canada, the same zone extends as far as –110°, 20° of longitude (1:20 of axial rotation) beyond the zone's *LSM*!

Because solar geometry calculations employ apparent solar time, it is frequently necessary to convert to or from ***local time***, the official time shown on clocks at a given location. To convert from solar time to local time, two or three adjustments must be made: a constant adjustment due to the position of the location in its time zone, a variable adjustment for the equation of time, and an adjustment for daylight saving time if it is in effect.

Longitude Time Adjustment

The ***longitude time adjustment*** (*LA*) concerns the longitudinal position of the reference location relative to its local standard meridian and is the first adjustment necessary for conversion between solar and standard time (Figure 2.14). Locations to the east of their local standard meridian will see sunrise earlier than the *LSM* and locations to the west will see sunrise later. The longitude time adjustment calculates how much earlier or later these events occur.

Equation 2.4 Longitude Time Adjustment

$$LA = \frac{LON - LSM}{15°}$$

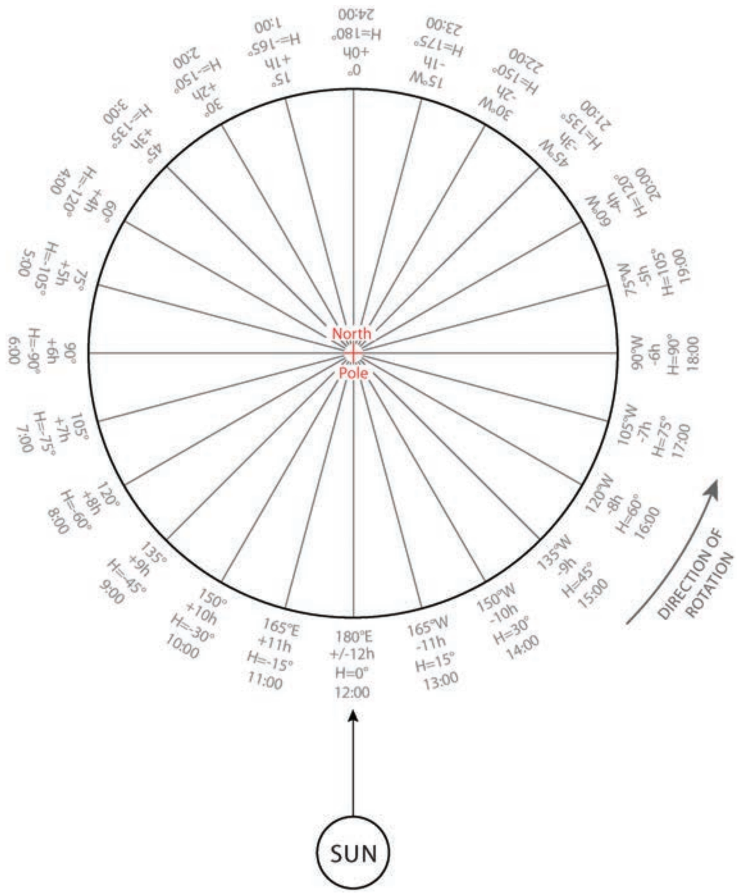

Figure 2.14

Relationship of Local Standard Meridians and Hour Angle

Solar noon at the anti-meridian is depicted in this diagram. At each local standard meridian, the local time offset, along with the current hour angle and current solar time, is shown. The diagram depicts just one moment in time; however, hour angle is changing constantly while longitude and the related time zone offset are fixed.

Greg Arcangeli

EXAMPLE 2.5 LONGITUDE TIME ADJUSTMENT

Calculate the time adjustment necessary based on the position of Austin, Texas, within its time zone.

Solution

$LON = -97.74°$

From Example 2.4, $LSM = -90.00°$
Use Equation 2.4 to calculate the required adjustment.

$$LA = \frac{LON - LSM}{15°}$$

$$LA = \frac{-97.74° - (-)90.00°}{15°}$$

LA = −0.52 hours = −30.96 mins

EXAMPLE 2.5 CONTINUED

Thus, Austin's meridian will rotate past the sun just over half an hour after the local standard meridian (−90.00°) at New Orleans, Louisiana, approximately 740 km to the east. Because time in a time zone is normalized to the *LSM*, on a day when solar noon occurs at 12:00 local standard time in New Orleans, it would occur at 12:31 in Austin. Because of factors discussed in the following section, solar noon will only occur at exactly 12:00 standard time on the local standard meridian several times per year.

Equation of Time

The ***equation of time*** (*ET*) is the second adjustment necessary to convert between solar and standard time. If one records the position of the shadow of a point at the same ***mean time*** (the time as measured by a highly accurate clock) each day for a year, or takes pictures of the sun's position superimposed upon one another at the same intervals, a distinctive elongated figure-eight shape will appear, as shown in Figure 2.16. This shape is known as an ***analemma*** and is the result of two factors: the varying speed of the Earth in its elliptical orbit around the sun, and the obliquity of the ecliptic.

These two factors cause clocks to variously run ahead of and behind solar time over the course of the year. The equation of time reaches its maximum with solar time ahead of clock time by over 16 minutes in early November and its minimum with solar time lagging approximately 14 minutes behind in mid-February. Figure 2.15 shows a graph of this variability.

To determine the equation of time adjustment for a given date, first use Equation 2.5a or 2.5b to calculate the ***calendar date orbital angle*** (*B*). This is similar to the solar orbital angle (Γ), but sets January 1 to 0° orbital rotation rather than the equinox. Equation 2.6 then gives the equation of time adjustment in minutes for the two factors described previously. Equations 2.5a and 2.6 are from Iqbal as cited in ASHRAE Fundamentals.[6] The term "calendar date orbital angle" has been coined in this text to distinguish it from the solar orbital angle.

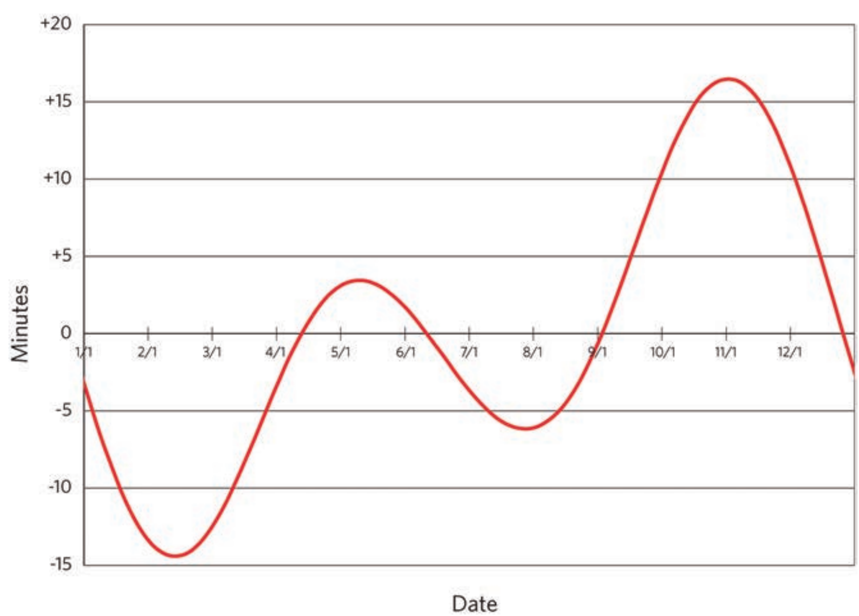

Figure 2.15

Equation of Time

Greg Arcangeli

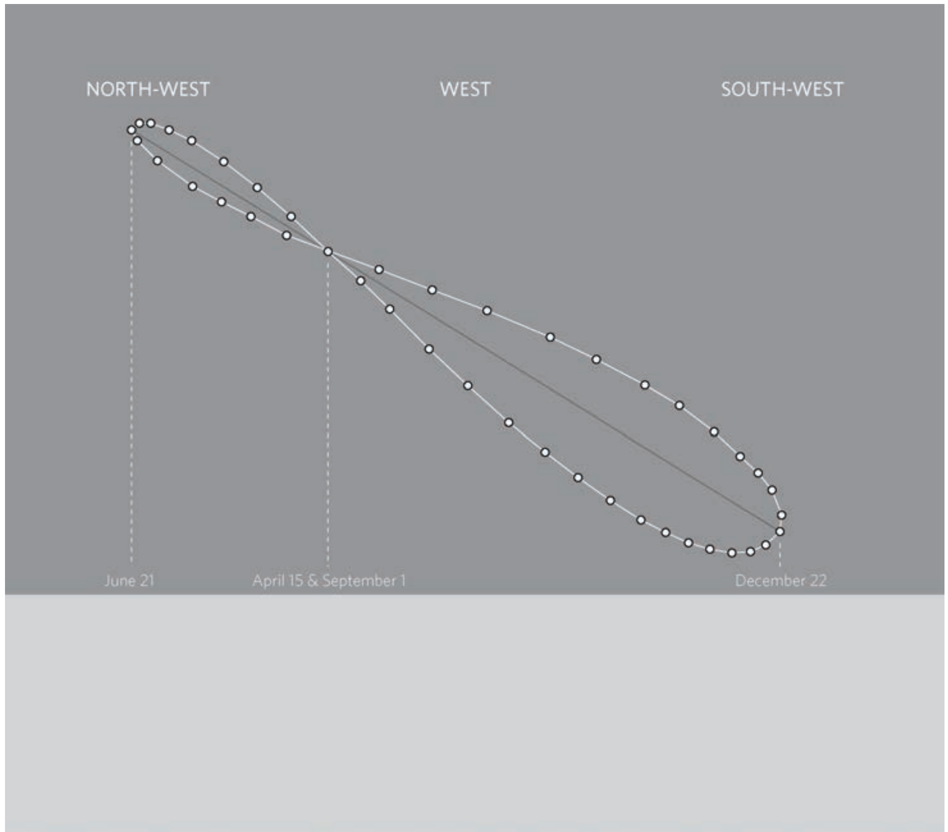

Figure 2.16
Analemma
Greg Arcangeli

To convert from local standard time to apparent solar time, *LA* and *ET* are added to *LST*. Note that the longitudinal adjustment is calculated in decimal hours, but the equation of time is in minutes, so the two must be converted to the same units. Equation 2.7 brings these quantities together, including the conversion to decimal hours.

Equation 2.5a Calendar Date Orbital Angle

$$B = 360°\left(\frac{n-1}{365}\right)$$

Equation 2.5b Calendar Date Orbital Angle from Solar Orbital Angle

$$B = \Gamma - 281.096$$

Equation 2.6 Equation of Time

$$ET = 2.2918\begin{bmatrix} 0.0075 + 0.1868\cos(B) - 3.2077\sin(B) \\ -1.4615\cos(2B) - 4.089\sin(2B) \end{bmatrix}$$

Equation 2.7 Apparent Solar Time Conversion from LST

$$AST = LST + \frac{ET}{60\,\text{min}} + LA$$

EXAMPLE 2.6 FIND APPARENT SOLAR TIME FROM LOCAL STANDARD TIME

What is the apparent solar time at 14:51 local standard time in Austin, Texas, on July 11?

Solution

1) Convert *LST* to decimal hours: 14:51 = 14.85.
2) Convert July 11 to an ordinal date using Table 2.1 or a spreadsheet configured to convert calendar dates to ordinal dates (see Example 2.1): $n = 192$.
3) Use Equations 2.5a or b and 2.6 to calculate the calendar date orbital angle and equation of time for this date, or estimate *ET* from Figure 2.15.

$$B = 360°\left(\frac{n-1}{365}\right)$$

$$B = 360°\left(\frac{192-1}{365}\right)$$

$$B = 188.38°$$

$$ET = 2.2918\begin{bmatrix} 0.0075 + 0.1868\cos(B) - 3.2077\sin(B) \\ -1.4615\cos(2B) - 4.089\sin(2B) \end{bmatrix}$$

$$ET = 2.2918\begin{pmatrix} 0.0075 + 0.1868\cos(188.38°) - 3.2077\sin(188.38°) \\ -1.4615\cos 2(188.38°) - 4.089\sin 2(188.38°) \end{pmatrix}$$

$$ET = -5.24\,\text{min}$$

So on this date, local standard time lags 5.24 minutes behind solar time due to the factors contributing to the equation of time.

4) Because the longitudinal time adjustment for Austin, Texas, was calculated in Example 2.5 (LA = 0.52 h), we can apply Equation 2.7 to calculate apparent solar time (*AST*).

$$AST = LST + \frac{ET}{60\,\text{min}} + LA$$

$$AST = 14.85 + \frac{-5.24\,\text{min}}{60} + (-0.52)$$

$$AST = 14.24\text{ h} = 14{:}14$$

Thus, solar time at this date and location is 37 minutes behind standard time. On July 11, in Austin, Texas, however, daylight saving time is in effect so clocks will not read local standard time. The following section discusses how to adjust for *DST*.

Daylight Saving Time

Many localities adjust clocks to ***daylight saving time*** (*DST*), where clocks are set one hour ahead in summer in an effort to take advantage of energy savings as the result of longer daylight hours. In the United States, all states except Hawaii and most of Arizona observe daylight saving time, but most U.S. territories do not. The European Union and quite a few other countries use daylight saving time as well, but many do not. As a general rule, countries in or near the tropics do not employ daylight saving time because day lengths do not change significantly enough during the year to make a substantial impact on energy use. Outside the tropics, countries are more likely to adopt daylight saving time.

Equation 2.8 Convert *DST* to *LST*

$$LST = DST - 1$$

See Table 2.5 for start and end dates of daylight saving time in the United States and European Union through 2025. Daylight saving time has a colorful and controversial history and its dates and usage are often modified in response to political or economic conditions, so it is a good idea to check current standards. As of 2011, daylight saving time begins in the United States at 2:00 on the second Sunday in March and ends at 2:00 on the first Sunday in November. Equation 2.8 may be used to convert between *LST* and *DST*.

Clock Time

To mitigate confusion about the proper time standard for any location and date, the current official time in any location is known as ***local time***. Local time is the same as local standard time, except when daylight saving time is in effect.

Table 2.5 Daylight Saving Time Start and End Dates

	United States		*European Union*	
	Begin	*End*	*Begin*	*End*
2011	Mar-13	Nov-06	Mar-27	Oct-30
2012	Mar-11	Nov-04	Mar-25	Oct-28
2013	Mar-10	Nov-03	Mar-31	Oct-27
2014	Mar-09	Nov-02	Mar-30	Oct-26
2015	Mar-08	Nov-01	Mar-29	Oct-25
2016	Mar-13	Nov-06	Mar-27	Oct-30
2017	Mar-12	Nov-05	Mar-26	Oct-29
2018	Mar-11	Nov-04	Mar-25	Oct-28
2019	Mar-10	Nov-03	Mar-31	Oct-27
2020	Mar-08	Nov-01	Mar-29	Oct-25
2021	Mar-14	Nov-07	Mar-28	Oct-31
2022	Mar-13	Nov-06	Mar-27	Oct-30
2023	Mar-12	Nov-05	Mar-26	Oct-29
2024	Mar-10	Nov-03	Mar-31	Oct-27
2025	Mar-09	Nov-02	Mar-30	Oct-26

EXAMPLE 2.7 LOCAL STANDARD TIME TO DAYLIGHT SAVING TIME

What is the daylight saving time at 14:51 local standard time in Austin, Texas, on July 11?

Solution

In Example 2.5, we determined that 14:51 = 14.85 in decimal hours.

Rearrange Equation 2.8 to solve for daylight saving time:

$$DST = LST + 1$$
$$DST = 14.85 + 1$$
$$DST = 15.85 = 15:51$$

EXAMPLE 2.8 APPARENT SOLAR TIME TO LOCAL TIME

What is the local time in Harare, Zimbabwe, on November 27 at 11:08 solar time?

Solution

1) See Example 2.6 for instructions for determining the following basic parameters:

Harare $LON = 31.05°$ UTC $= +2$ $n = 331$ $11{:}08 = 11.13$ h

2) Find the local standard meridian and longitudinal time adjustment.

$$LSM = 15°(TZ)$$
$$LSM = 15°(2)$$
$$LSM = 30°$$
$$LA = \frac{LON - LSM}{15°}$$
$$LA = \frac{31.05° - 30°}{15°}$$
$$LA = 0.07\,\text{h} = 4\,\text{min}$$

3) Use Equations 2.5a or b and 2.6 to calculate the calendar date orbital angle and equation of time for this date, or estimate *ET* from Figure 2.15.

$B = 325.48°$
$ET = 12.09$ min

4) Rearrange Equation 2.7 to solve for *LST*.

$$LST = AST - \frac{ET}{60\,\text{min}} - LA$$
$$LST = 11.13 - \frac{12.09}{60\,\text{min}} - 0.07$$
$$LST = 10.85 = 10:51$$

Harare does not observe daylight saving time, so local standard time is the local time.

Declination

While the tilt of the Earth's rotational axis is essentially fixed, its apparent tilt relative to the ray of the sun changes constantly as the Earth moves along its orbit. This changing relationship results in seasons and varying day lengths over the course of a year. Summer occurs when one's hemisphere is tilted toward the sun because the solar radiation arrives at that portion of the Earth's surface closer to perpendicular. During winter, one's hemisphere is tilted away from the sun and the same density of radiation is distributed over a larger area.

In astronomy, ***declination*** is one of two coordinates, along with right ascension, used in the equatorial coordinate system to describe the position of any celestial body. Declination corresponds with terrestrial latitude, measuring the angular distance of an object from the celestial equator, while ***right ascension*** corresponds to longitude, except that it is measured in hours, minutes, and seconds rather than degrees.

Solar declination (δ) is the angle of the solar ray relative to the Earth's equatorial plane on a given day. If the sun is to the north of the equator, declination is positive, while to the south is negative. Specifically, declination is measured as the angular distance between the Earth–sun line and the equatorial plane. Figure 2.17 depicts declination as well as orbital angle for each design day of the year. Solar declination on the June solstice is equal to the obliquity of the ecliptic at 23.45°. It is 0° at the equinoxes, and a minimum of −23.45° on the December solstice. For most architectural and engineering purposes, declination is assumed to be constant for the duration of each day, but in actuality it is constantly shifting.

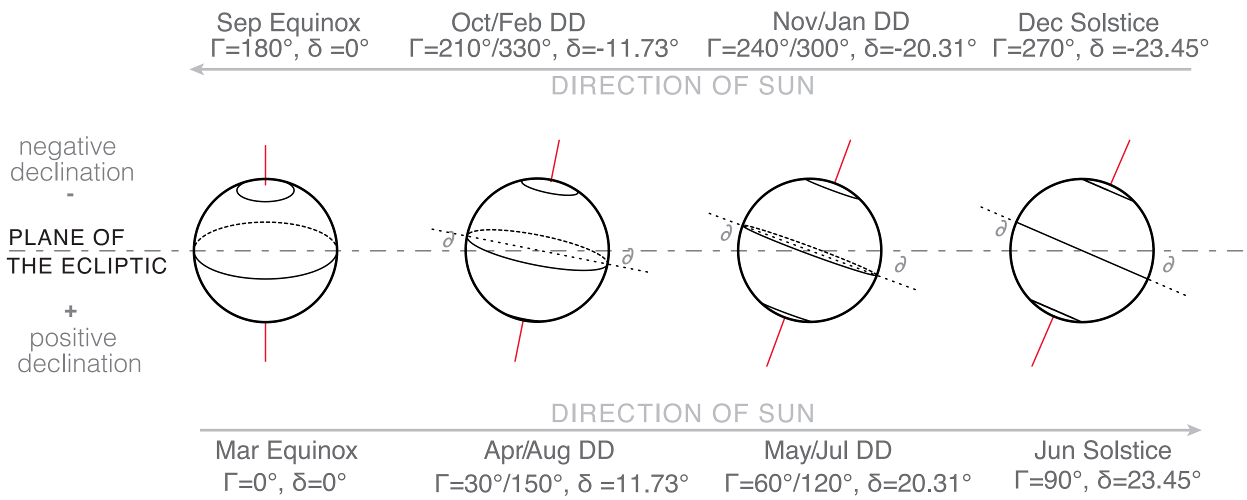

Figure 2.17
Declination at Key Dates
Greg Arcangeli

Using Equation 2.9, one may calculate solar declination with a degree of accuracy sufficient for most design applications. For a more precise formula, see Iqbal.[7] The terms in Equation 2.9 set declination to the appropriate maximum and minimum on the solstices. Refer to Table 2.2 for declination values on both the true solar design days and the 21st of each month.

Because the Earth's axis is perpendicular to the equatorial plane, solar declination also describes the apparent tilt of the Earth's rotational axis on a given date relative to the ecliptic pole, or a line perpendicular to the ecliptic plane. By apparent tilt, we mean the tilt as viewed perpendicular to the Earth–sun line. The apparent tilt of the Earth's rotational axis is often more convenient to use than the tilt of the equatorial plan when drawing the Earth's position relative to the sun in two dimensions.

Equation 2.9 Solar Declination

$$\delta = 23.45°\mathrm{T}$$

EXAMPLE 2.9 SOLAR DECLINATION

What is the solar declination on July 11?

Solution

1) From Example 2.6, $n = 192$ on July 11.
2) Use Equation 2.1 to find the orbital angle.

$$\Gamma = 360°\left(\frac{n+284}{365}\right)$$

$$\Gamma = 360°\left(\frac{192+284}{365}\right)$$

$$\Gamma = 469.48° = 109.48°$$

3) Use Equation 2.9 to determine the solar declination.

$$\delta = 23.45° \sin \Gamma$$

$$\delta = 23.45° \sin 109.48°$$

$$\delta = 22.11°$$

The solar declination is positive, indicating that the sun is to the north of the equatorial plane as we would expect on July 11.

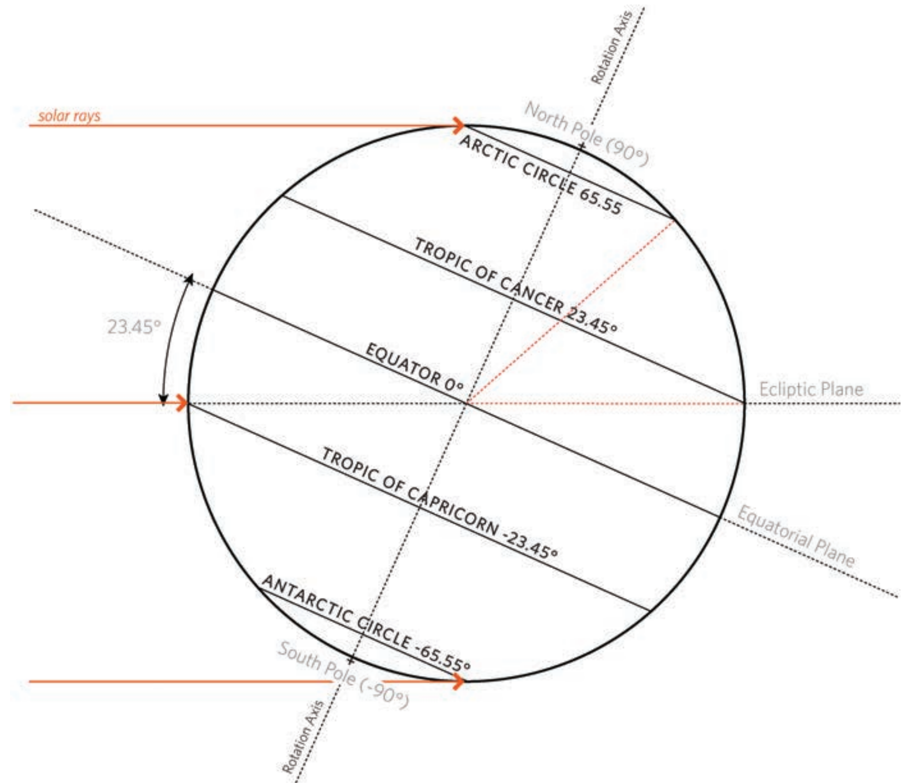

Figure 2.18
Special Latitudes
Greg Arcangeli

Certain parallels of latitude acquire a particular significance on the solstices as the sun reaches maximum and minimum declination relative to the Earth. As shown in Figure 2.18, on the June solstice, the northern hemisphere is tilted toward the sun. At this time, the solar ray is normal to the parallel of latitude known as the Tropic of Cancer, located at 23.45° N. It is tangent to two parallels of latitude: the Arctic and Antarctic Circles. At this time, the Arctic Circle is experiencing 24 hours of daylight while the Antarctic Circle experiences 24 hours of night. On the December solstice, the sun's rays are normal to the Tropic of Capricorn, 23.45° south, and again tangent at the two arctic circles, but with the Antarctic experiencing 24 hours of daylight.

Zenith Angle

The ***zenith*** is the direction directly overhead from any point on Earth, also known as vertical. As shown in Figure 2.19, the ***zenith angle*** (Z) is the angle of the sun or any vector down from the zenith. The zenith angle at solar noon (Z_{12}) on any day is a simple function of a site's latitude and declination. Use Equation 2.10 to calculate zenith angle.

Equation 2.10 Zenith Angle at Solar Noon

$$Z_{12} = L - \delta$$

Equation 2.11 Zenith Angle at Solar Noon on Equinox

$$Z_{12 = L}$$

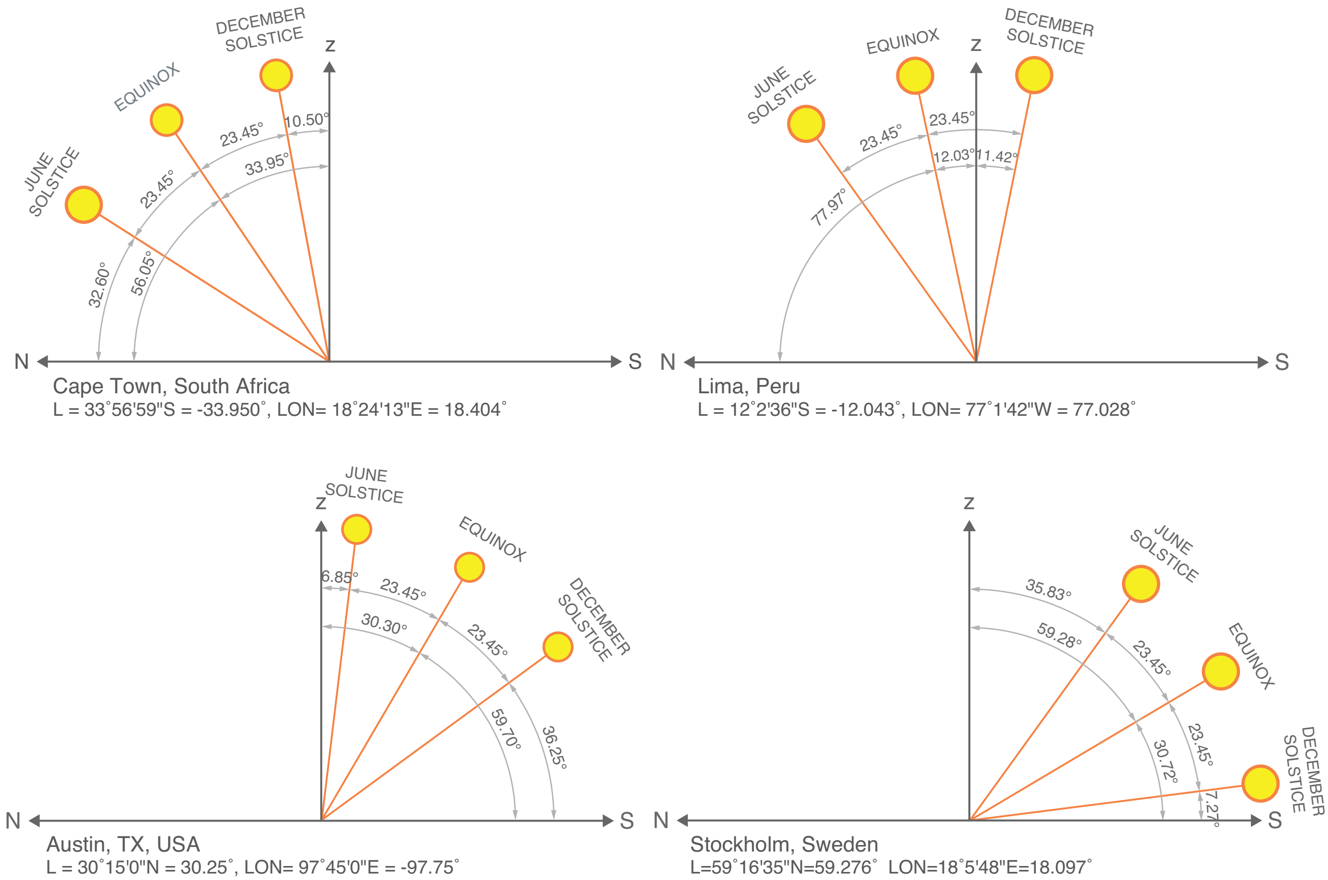

Figure 2.19

Zenith Angles at Solar Noon for Four Locations

Note how the relationships between the sun position on the solstices and equinoxes remain fixed and rotate as a unit from horizon to horizon. At high northern latitudes, the sun is close to the southern horizon at solar noon throughout the year. As one moves southward, it gets higher overhead, until it is directly overhead near the equator on the equinox. At southern latitudes, it tilts to the north.

Greg Arcangeli

Because solar declination is 0° on the equinoxes, and varies by an angle equal to the obliquity of the ecliptic, the variations of this equation for the solstices and equinoxes shown in Example 2.10 are worthwhile to commit to memory. Remembering these simple relationships, particularly the equinox version reiterated in Equation 2.11, will allow the reader to instantly visualize the sun's path throughout the year relative to any point on Earth knowing only the latitude. See the section on the solar path band in Chapter 3 for a discussion on how to do so.

EXAMPLE 2.10 ZENITH ANGLE

What is the solar zenith angle at solar noon in Austin, Texas (30.29° N), on the solstices, equinoxes, and July 11?

Solution

By definition, the June solstice is the point of maximum declination of 23.45°. We could also either calculate this value using Equation 2.9 or look it up in Table 2.2. Solar declination on the equinoxes is 0°, and the December solstice is –23.45°. On July 11, δ was found to be 22.11° in Example 2.9.

From Eq. 2.10:

$$Z_{12} = L - \delta$$

June solstice:

$$Z_{12} = L - 23.45°$$
$$Z_{12} = 30.29° - 23.45° = 6.84°$$

Equinoxes:

$$Z_{12} = L - 0°$$
$$Z_{12} = 30.29°$$

December solstice:

$$Z_{12} = L - (-)\ 23.45° = L + 23.45°$$
$$Z_{12} = 30.29° + 23.45° = 53.74°$$

July 11:

$$Z_{12} = 30.29° - 22.11°$$
$$Z_{12} = 8.18°$$

NOTES

1 "How Many Stars Are There in the Universe?," *European Space Agency*, accessed February 14, 2016, www.esa.int/Our_Activities/Space_Science/Herschel/How_many_stars_are_there_in_the_Universe.
2 Charles Eames and Ray Eames, *Powers of Ten*, 1977, https://en.wikipedia.org/w/index.php?title=Powers_of_Ten_(film)&oldid=707258428.
3 "Wandering of the Geomagnetic Poles," *National Oceanic and Atmospheric Administration, National Centers for Environmental Information*, accessed February 14, 2016, www.ngdc.noaa.gov/geomag/GeomagneticPoles.shtml.
4 National Oceanic and Atmospheric Administration, "US/UK World Magnetic Model: Epoch 2010.0, Main Field Declination (D)," January 2010, http://ngdc.noaa.gov/geomag/WMM/.
5 CIA, *Standard Time Zones of the World, Map* (Washington, DC: U.S. Central Intelligence Agency, 2010).
6 ASHRAE, *2009 ASHRAE Handbook: Fundamentals*, SI ed. (Atlanta, GA: American Society of Heating, Refrigerating and Air-Conditioning Engineers, Inc., 2009).
7 Muhammad Iqbal, *An Introduction to Solar Radiation* (Toronto: Academic Press, 1983).

3 THE GEOCENTRIC MODEL

Aristotle and Ptolemy's model placed the Earth at the center of the universe and was the dominant view for over a millennium. Ptolemy's version (almost) succeeded in solving the problem of retrograde motion of planets with the gymnastic trick of epicycles—small sub-orbits superimposed on the primary orbits of planets. The geocentric view of the solar system was finally dismantled by Copernicus, Galileo, and Kepler in the early Renaissance with the more elegant heliocentric model, which agreed much better with actual observations of planetary and stellar movement (Figure 3.1).

While the heliocentric model is the best description for the workings of our solar system, all motion is relative to the viewer's position in space. For design purposes, a sufficiently accurate model exists to predict the movement of celestial bodies as

Figure 3.1

Pinhole Photograph Illustrating the Changing Path of the Sun

A long-exposure pinhole photograph, which strikingly illustrates the changing path of the sun during a six-month cycle between the June and December solstices over the University of Texas at Austin Campus.

James Sherman

though the observer's position is fixed and everything else is moving around her. In fact, this is how the majority of our measurements are taken, so there must be a translation to the heliocentric point of view in order to place them in the context of the solar system, and perhaps even another translation to put them in the context of the universe as a whole. While these translations are useful for astronomers, we and our buildings are located on Earth, so employing a geocentric model is significantly more useful and practical for those interested in understanding how the sun will affect objects on Earth.

In fact, the model we use for solar geometry calculations is not truly a geocentric one because its reference point moves to the observer's location instead of being referenced to the center of the Earth. Szokolay[1] has pointed out this model might be better termed loco-centric because it is specific to the observer's location. Nevertheless, geocentric is the term most often applied and we will adopt it here.

SKY DOME CONCEPT

The sky dome is a theoretical construct, the understanding of which is key to visualizing the sun's relationship to any point on Earth. Each day, the sun follows a predictable path across the sky, appearing to orbit around the observer's position. Its path is an arc, rising from the east and setting to the west. On the equinoxes at any location, this arc is a semi-circle beginning due east at 6 a.m. and ending due west at 6 p.m., except at the poles where it becomes a circle skimming the horizon. On the June solstice in the northern hemisphere, the sun's arcing path begins north of east and west. The further north one travels, the further to the north this arc originates, until above the Arctic Circle, the arc becomes a circle orbiting in the sky above the horizon. On the December solstice, the reverse is true, with the arc starting and ending further to the south until one travels beyond the Antarctic Circle, where the sun follows a circular path overhead.

These movements may be modeled as occurring on the surface of an imaginary sphere with its center at the observer's position on Earth. The half of this sphere that is above the horizon (ignoring the Earth's curvature) is known as the *sky dome*. When using this model for analysis, generally only this exposed portion is relevant, but in discussing the geometry involved, this construct will also be referred to as the *sky sphere* where necessary to describe the complete path of the sun as it relates to a point on Earth.

The radius of the sky dome is not important; it can be imagined as infinitely large if convenient or the size of a pinhead when that is more useful. What is important is that the geometry of the sun's movement relative to the reference point at the dome's center is always the same and is always modeled as falling somewhere on the surface of that sphere. When the observer's point of reference moves, the sky dome moves along with him.

The beauty of this model is that, no matter where on Earth the observer is located, the relationship between the sun's position at any given date and time relative to any other date and time remains fixed. What changes is the position of those points relative to the observer's point in space. So, once one understands the geometry that describes that fixed set of relationships, one can almost instantly visualize the sun's path throughout the year for any point on Earth. This section begins with a discussion of those relationships. The solar position calculations presented in the following sections simply reflect this geometric model and provide an accurate method for pinpointing the sun's position at a particular date and time.

The sky dome is useful, not only as a tool to visualize the sun's position, but also as a way to begin to assess its relationship to one's physical surroundings at the reference point. By drawing a view of fixed objects such as buildings and trees around the reference point projected onto the sky dome, one can instantly see when the reference point will be in direct sun or shade throughout the entire year. This type of projection is known as a sky dome projection and will be discussed in Chapter 7.

Solar Path Band

When the sun's apparent movement is inscribed on the sky dome, it takes the characteristic form known as the ***solar path band***. As shown in Figure 3.2, it is usually depicted as a strip of spherical grid across the sky dome created by arcs representing the sun's path for design days, with crossing segments of arcs marking hours. The arcs forming this grid are known as ***date lines*** and ***hour lines*** rather than arcs because, when viewed from different angles or projections, they frequently take on other shapes. In truth, the path of the sun traces a spiral around the sky sphere between the solstices when declination reaches its maximum and minimum. From a design perspective, however, the offset due to this spiraling that occurs in the course of a single day is negligible. Therefore, we model the path of the sun on a given day as occurring on an arc instead of a segment of a spiral.

At the center of this band is the equinox date line. It is a ***great circle***, one that circumscribes the full diameter of the sky sphere. No matter where on Earth one is located, the sun-path arc intersects the horizon due east and west on the equinox.

The two extremes of the solar path band occur on the solstices. These are ***minor circles***, or circles on the surface of the sky sphere of a diameter less than the total diameter of the sphere. They run parallel to the equinox line and are offset from the equinox sun path by an angular distance equal to the apparent solar declination at the solstices (23.45°), which is also the obliquity of the ecliptic. As a result, the total angular width of the solar path band is equal to two times the obliquity of the ecliptic (46.90°).

All other date lines fall somewhere between these extremes and are also minor circles offset from the equinox line by the apparent solar declination for that date. Design days are most commonly represented, but the path for any date can be easily shown.

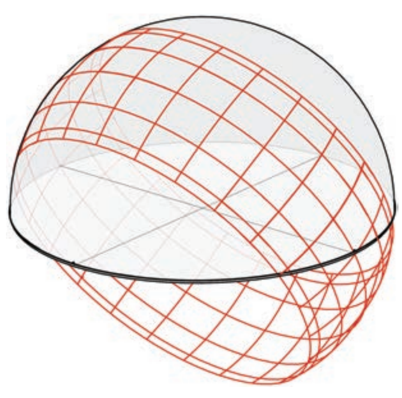

Figure 3.2
The Sky Dome
Dason Whitsett

Hour lines are segments of great circles that run perpendicular to the date lines. Because there are 24 hours in a day in which the Earth makes a 360° rotation, hours occur every 15° around the solar path band. Solar noon is always aligned with due north-south.

Moving the sky dome to a different latitude causes the entire solar path band to rotate around the dome on the east-west axis. In doing so, date and hour lines always maintain the same relationships to one another. Imagine the solar path band as an armature pivoting around the east-west axis. Remember from the previous discussion and Equation 2.11 that for any location, the zenith angle at solar noon on the equinox is equal to the latitude. For example, to position the solar path band on the sky dome for 30° N latitude, rotate the equinox date line 30° toward the south from vertical. In fact, this is precisely how the device known as a ***heliodon*** works. As shown in Figure 3.3, a heliodon is a design analysis device for testing building designs in terms of solar geometry. It has bright lights representing the sun that rotate on the design-day sun-path arcs and

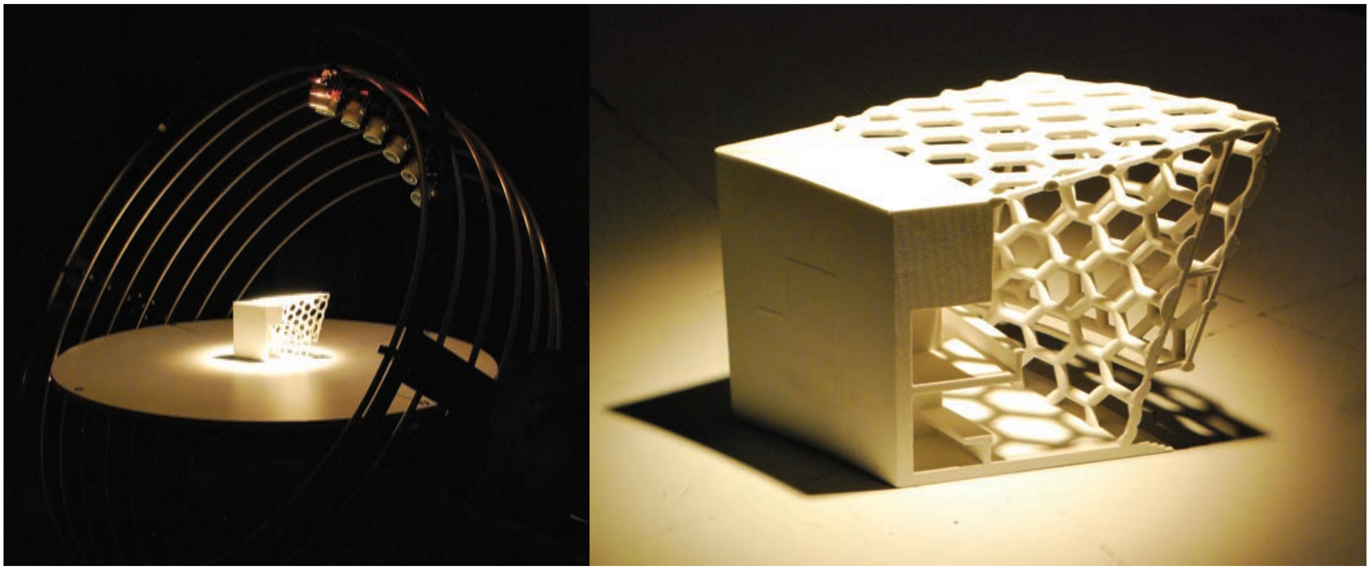

Figure 3.3

Heliodon in Use Testing a Model

By placing a model building on the heliodon's flat surface and making adjustments to the light/surface angle, the investigator can see how the building would look in the three dimensional solar beam at various dates and times of day. In this case, the model is being tested for solar penetration on the summer solstice at 30° N latitude.

Photograph by Dason Whitsett; model by Various Architects

point at the origin in the center of the sky dome. It can be used very effectively to test shading and direct or reflect sun penetration. It is most effective with smaller models because its accuracy diminishes at points on the model further away from the origin.

Figure 3.4 shows the alignment of the solar path band for various latitudes. On the equator ($L = 0°$), at solar noon on the equinox, the sun is directly overhead at the zenith, which is the point at the top of the sky dome directly over the origin on the ground. The sun's path moves exactly east to west, following a perfect arc overhead. As one moves to higher latitudes, the equinox path progressively drops toward the horizon in the direction of the equator, until it is parallel to the horizon at the poles (±90°).

As the equinox path tilts to adjust for latitude, so does the entire solar path band. The result is that the circles representing dates on either side of the equinox are either raised toward the zenith, or pushed down toward the ***nadir***, the point on bottom of the sky sphere opposite the zenith. In the northern hemisphere, those dates on the June solstice side of the equinox are lifted toward the zenith, which leads to higher sun angles at mid-day for these months compared to the others and more hours of daylight as more of those circles are lifted above the horizon. The dates on the December solstice side of the equinoxes have just the opposite situation. They are pushed down toward the horizon, resulting in lower noon sun angles and fewer hours of daylight as the ground plane clips off more of the arc. In the southern hemisphere, the same relationships hold, but on opposite sides of the year: in June, the smallest portion of the solar path arc is exposed above the horizon and in December, the largest segment is exposed.

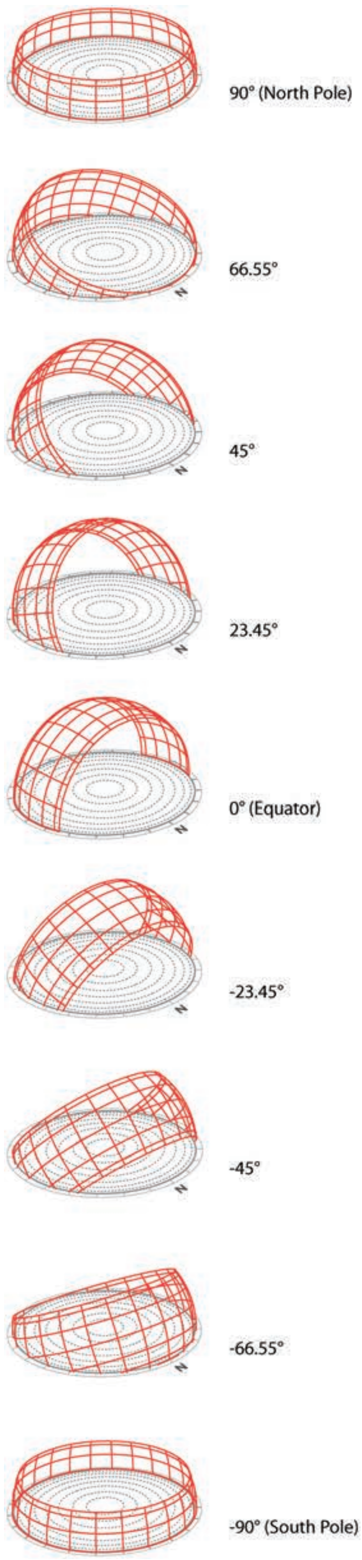

Figure 3.4
Solar Path Band for Various Latitudes
Greg Arcangeli

The result of this progression is that the solar path band is parallel to the horizon at the poles, with the equinox representing a single long sunrise on one equinox and sunset on the other. All dates on the summer side of the equinox are completely above the horizon, while dates on the winter side are completely below. The sun, as it rises, begins a three-month spiral upward toward the summer solstice at an altitude of 23.45°, then spirals back down toward the autumnal equinox, slowly setting for six months of darkness. Again, we model this spiraling as a set of parallel circles inscribed on the surface of the sky dome.

Once one develops a sound mental model of the solar path band and how it pivots on the sky dome, it is easy to mentally position it relative to any latitude. With nothing but this understanding, one can estimate with surprising accuracy the general path of the sun throughout the year as well as the position of the sun at any time. The following section will discuss how to calculate sun position precisely.

Describing Sun Position

Spherical Coordinates

The sun's position at any moment in time is most often described using spherical coordinates. ***Spherical coordinates*** are one method of locating any point in three-dimensional space by specifying its angular coordinates and a radius relative to an origin point. The ***origin*** in this context will always be at the center of the sky dome, wherever it is located. Because the sky dome may be imagined to be any size that is useful, the radius for solar spherical coordinates will always be a dimensionless "1" to simplify calculations and need not be specified. Regardless of the size of the sky dome, the sun's position will always be modeled as if it falls somewhere on the surface of that dome.

Therefore, only the two angular coordinates azimuth and altitude will serve to describe the location of the sun or any other point on the sky dome. It is useful to visualize a vector, or line, connecting the sun's position with the origin representing the direct rays of the sun. This line is known as the ***solar ray*** or ***solar vector***. As depicted in Figure 3.5, ***azimuth*** (α) describes the angular distance of the origin on the ground plane from a reference line to the point of interest. Azimuth conventions for various disciplines, reference sources, and computer programs vary substantially, so the user should always verify the system used in each context. In this book, 0° azimuth is due south, and positive rotation is clockwise (to the west). If there is no indication that it refers to something else, azimuth will refer to the true ***solar azimuth*** (α *sol*), the angle from due south to the solar ray projected straight down onto the ground plane.

Solar noon occurs throughout the year when the sun ***transits***, or crosses, the meridian passing through the origin of the sky dome. Azimuth at solar noon is always either 0° (due south) or 90° (due north), depending on the date and observer's latitude. Outside of the tropics, the sun is always due south at solar noon in the northern hemisphere and due north at solar noon in the southern hemisphere.

Altitude (β) is the angular elevation of the origin between the ground plane and the point of interest. Unless noted otherwise, altitude will refer to true ***solar altitude*** (β*sol*), the angle from the solar ray straight down to the ground plane, as shown in Figure 3.5. An alternative to the altitude angle, useful in

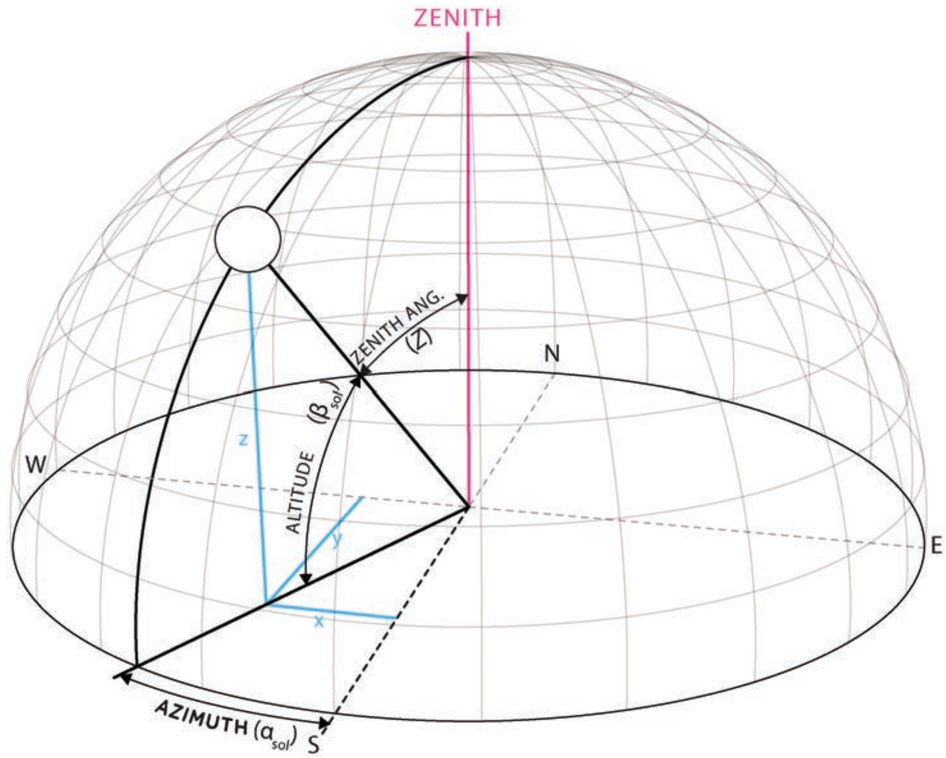

Figure 3.5

Spherical Coordinates of Sun Position

Greg Arcangeli

some contexts, is the zenith angle. The ***zenith angle*** (Z) is the complement of an altitude angle, measuring the angle of the origin down from vertical to a point or vector.

The sun's position at any moment in time may be determined quickly and with reasonable accuracy using graphic methods, but if a high degree of precision is desirable, calculations are necessary. Formulas for the spherical coordinates, solar azimuth (α_{sol}) and altitude (β_{sol}), are presented in Equations 3.1 through 3.3b. The parameters necessary are apparent solar declination (δ), hour angle (H), apparent solar time (AST), and latitude (L). For solar azimuth, a logical test is necessary to determine the proper sign. Equation 3.3b simply returns the negative of the afternoon azimuth for morning azimuths, reflecting the symmetry between morning and afternoon. Some sources, such as ASHRAE Fundamentals,[2] use a variation on this test involving both a cosine and sine function, accomplishing the same result.

Equation 3.1 Zenith and Altitude Angle Relationship

$$\beta = 90° - Z$$

Equation 3.2 Solar Altitude

$$\sin\beta_{sol} = \cos L \cos\delta \cos H + \sin L \sin\delta$$

Equation 3.3a Solar Azimuth If AST ≥ 12:00

$$\alpha_{sol} = \cos^{-1}\left(\frac{\cos H \cos\delta \sin L - \sin\delta \cos L}{\cos\beta}\right)$$

Equation 3.3b Solar Azimuth If AST < 12:00

$$\alpha_{sol} = -\cos^{-1}\left(\frac{\cos H \cos\delta \sin L - \sin\delta \cos L}{\cos\beta}\right)$$

EXAMPLE 3.1 CALCULATING SPHERICAL COORDINATES FROM SOLAR TIME

What are the spherical coordinates of the sun's position in Austin, Texas, at 14:14 solar time on July 11 (Figure 3.6)?

Austin $L = 30.29°$ $n = 192$ 14:14 = 14.24 h

Solution

1) Calculate the orbital angle for the current date using Equation 2.1. From Example 2.9, $\Gamma = 109.48°$.
2) Calculate the current hour angle using Equation 2.2.

$$H = 15°(AST - 12.00) = 15°(14.24 - 12.00) = 33.50°$$

3) Calculate the declination using Equation 2.9. In this case, we know $\delta = 22.11°$ from Example 2.9.
4) Calculate the solar altitude using Equation 3.2.

$$\sin\beta_{sol} = \cos L \cos\delta \cos H + \sin L \sin\delta$$
$$\sin\beta_{sol} = \cos(30.29°)\cos(22.11°)\cos(33.5°) + \sin(30.29°)\sin(22.11°)$$
$$\beta_{sol} = 58.97°$$

5) Calculate the solar azimuth using Equation 3.3a or b. In this example, the current solar time is after solar noon, so use Equation 3.3a, which will place the azimuth to the west of south.

$$\alpha_{sol} = \cos^{-1}\left(\frac{\cos H \cos\delta \sin L - \sin\delta \cos L}{\cos\beta}\right)$$
$$\alpha_{sol} = \cos^{-1}\left(\frac{\cos 33.50° \cos 22.11° \sin 30.29° - \sin 22.11° \cos 30.29°}{\cos 58.97°}\right)$$
$$\alpha_{sol} = 82.79°$$

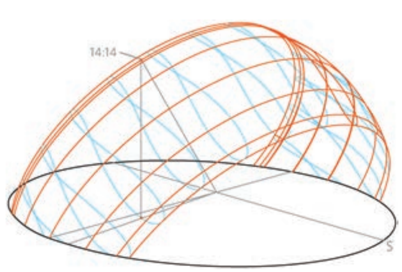

Figure 3.6
Sun Position in Example 3.1
Greg Arcangeli

If starting from local standard or daylight savings time, refer to Chapter 2 for the methods to convert to solar time.

EXAMPLE 3.2 CALCULATING SPHERICAL COORDINATES FROM LOCAL TIME IN THE SOUTHERN HEMISPHERE

What are the spherical coordinates for the sun's position at 10:41 in Sydney, Australia, on the May design day?

Sydney $L = -33.87°$ $LON = 151.20$ UTC $= +10$

Solution

1) To find the orbital angle, refer to Table 2.2 or calculate it with Equation 2.1. Using design days in increments of 30° yields an orbital angle of $\Gamma = 60°$ for the May design day. If we use May 21, $\Gamma = 59.18°$. This example will use the true 30° of the orbit design day.

2) Determine apparent solar time from local time. Australia is not under daylight saving time on this date, so local time = local standard time (*LST*) = 10:41 = 10.68h.

Using Equations 2.3 and 2.4, calculate the local standard meridian and the longitude time adjustment.

$$LSM = 15°(TZ) = 15°(10) = 150°$$

$$LA = \frac{LON - LSM}{15°} = \frac{151.20° - 90.00°}{15°} = 0.08\,\text{h} = 5\,\text{min}$$

3) Use Equation 3.7 to find solar time.

From Table 2.2, *ET* for the May design day = 3.69 min

$$AST = LST + \frac{ET}{60\,\text{min/h}} + LA = 10.68\,\text{h} + \frac{3.69\,\text{min}}{60\,\text{min/h}} + 0.08\,\text{h} = 10.82\,\text{h} = 10:49$$

4) Calculate the current hour angle using Equation 2.2.

$$H = 15°(AST - 12.00) = 15°(10.82 - 12.00) = -17.70°$$

5) Calculate the solar declination using Equation 2.9.

$$\delta = 23.45° \sin\Gamma = 23.45° \sin 60.00° = 20.31°$$

6) Calculate solar altitude using Equation 3.2.

$$\sin\beta_{sol} = \cos L \cos\delta \cos H + \sin L \sin\delta$$

$$\sin\beta_{sol} = \cos(-33.87°)\cos(20.31°)\cos(-17.70°) + \sin(-33.87°)\sin(20.31°)$$

$$\beta_{sol} = 33.26°$$

7) Calculate the solar azimuth using Equation 2.3b, as the time is before solar noon, which will place the azimuth to the east of south.

$$\alpha_{sol} = -\cos^{-1}\left(\frac{\cos H \cos\delta \sin L - \sin\delta \cos L}{\cos\beta}\right)$$

$$\alpha_{sol} = -\cos^{-1}\left(\frac{\cos -17.70° \cos 20.31° \sin -33.87° - \sin 20.31° \cos -33.87°}{\cos 33.26°}\right)$$

$$\alpha_{sol} = -160.07°$$

Based on these coordinates, the sun is positioned low in the sky in the northeast quadrant, which makes sense for a location in the southern hemisphere outside of the tropics on a late fall morning (Figure 3.7).

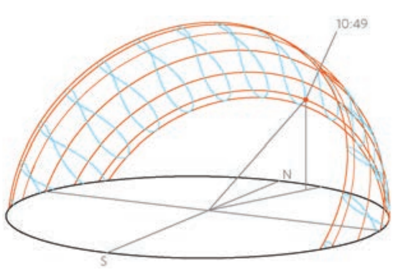

Figure 3.7
Sun Position in Example 3.2
Greg Arcangeli

Often, one is interested in not just one, but an entire array of solar position values to establish the path of the sun during the course of a day, season, or year. These calculations for one particular time are straightforward, but tedious to calculate for all of the necessary coordinates diagrams or tables require. These characteristics make the use of spreadsheets to calculate solar coordinates ideal. See Example 2.1 for tips on building such a spreadsheet.

Sunrise and Sunset

As noted previously, ***sunrise*** and ***sunset*** occur when the solar altitude is 0° and the zenith angle is 90°. Actually, the sun is large enough that it appears to us on Earth as a disk rather than a mere point. The calculations presented locate the center of the solar disk, so by the time the center of the sun has crested the horizon, the edge of the disk has been visible for a short time already. Between this effect and atmospheric refraction of light, true sunrise occurs slightly earlier and sunset slightly later than predicted by these equations. For design purposes, however, these effects are not important and will be ignored here.

The time at which sunset occurs is determined by solving the solar altitude equation for the hour angle at which solar altitude is 0°. This results in Equation 3.4 by Duffie and Beckman.[3] To convert the hour angle of sunset to solar time, solve Equation 2.2 for *AST*. Sunrise is the symmetrical time in the morning. Find the sunrise time by subtracting the time interval between solar noon and sunset from solar noon or by multiplying the sunset hour angle by (–) 1 and then solving for the solar time with which this angle corresponds.

Equation 3.4 Hour Angle at Sunset

$$\cos H_{ss} = -\tan L \tan\delta$$

EXAMPLE 3.3 DETERMINING THE TIMES OF SUNRISE AND SUNSET

What time do sunrise and sunset occur in Austin, Texas, on July 11?

Austin $L = 30.29°$ From Example 2.9, $\delta = 22.11$

Solution

1) Using Equation 3.4, find the hour angle at sunset.

$$\cos H_{ss} = -\tan L \tan\delta$$
$$\cos H_{ss} = -\tan(30.29°)\tan(22.11°)$$
$$H_{ss} = 103.73°$$

2) The hour angle at sunrise is the negative of hour angle at sunset. Determine the solar time of sunrise and sunset by rearranging Equation 2.2, solving for *AST*.

$$AST = \frac{H}{15°} + 12.0$$
$$AST = \frac{103.73°}{15°} + 12.0$$
$$AST = 18.91 = 18{:}55$$

Sunset occurs 6.91 hours after noon at 18:55; therefore, sunrise is 6.91 hours before noon, or at 5:05. The number of daylight hours is 2 x 6.91 = 13.82.

The previous section described how to visualize the position of the solar path band relative to any point on Earth with a single simple mental calculation, requiring only the latitude as input. The position of the sun at solar noon on any date follows from this model, and in particular we know that the solar position at noon on the June solstice will always be an additional 23.45° toward the north horizon while the noon position of the sun on the December solstice will be 23.45° toward the south horizon compared to the equinox position. The azimuth at sunrise and sunset are more difficult to visualize. The sun will always rise and set due east and west on the equinoxes, but how much of those date circles are cut off by the horizon on other dates? This question is straightforward to answer by calculating the hour angle at sunset, then calculating solar azimuth for that hour angle, but this process requires several steps of calculations. A quick solution for determining solar azimuth at sunrise and sunset in one step with no more information than the latitude and zenith angle at solar noon (Z_{12}) is presented in Equation 3.5.

Equation 3.5 Solar Azimuth at Sunset

$$\alpha_{ss} = 90° + \sin^{-1}(\cos Z_{12} \tan L - \sin Z_{12})$$

EXAMPLE 3.4 DETERMINE SOLAR AZIMUTH AT SUNRISE AND SUNSET USING EQUATION 3.5

What is the solar azimuth at sunrise and sunset on the solstices in Austin, Texas?

Austin $L = 30.29°$

Solution

From Example 2.10, at solar noon on the June solstice, $Z_{12} = 6.84°$, and at the December solstice, $Z_{12} = 53.74°$.

Using Equation 3.5 for the June solstice:

$$\alpha_{ss} = 90° + \sin^{-1}\left(\cos Z_{12} \tan L - \sin Z_{12}\right)$$
$$\alpha_{ss} = 90° + \sin^{-1}\left(\cos(6.84°)\tan(30.29°) - \sin(6.84°)\right)$$
$$\alpha_{ss} = 117.44°$$

Solar azimuth at sunset is 117.44° and sunrise is at −117.44°, 27.44° north of the east-west line.

For the December solstice:

$$\alpha_{ss} = 90° + \sin^{-1}\left(\cos(53.74°)\tan(30.29°) - \sin(53.74°)\right)$$
$$\alpha_{ss} = 62.56°$$

Solar azimuth at sunset is 62.56° and sunrise is at −62.56°, which is also 27.44° from the east-west line, but this time to the south. The angular offset of the sunset azimuth from east-west will always be an equal increment to the north and south at the two solstices.

A slightly obscure but occasionally useful task is to calculate the solar declination at which the sun will be on the horizon at a particular solar time using Equation 3.6. This phenomenon occurs at those hours where the hour lines of the solar path band intersect the horizon. This is especially useful when calculating coordinates for drawing sun-path diagrams. Once the declination is known, the date may be determined by solving Equation 2.9 for the ordinal date (n).

Equation 3.6 Declination at Hour Rise (for Sun-Path Diagrams)

$$\tan\delta = -\frac{\cos H}{\tan L}$$

Cartesian Coordinates

While spherical coordinates are used most frequently, specifying sun position via ***Cartesian coordinates*** is helpful for some applications. Also known as rectangular or x,y,z coordinates, this system makes it more difficult to visualize sun position but has advantages in some contexts such as determining relative insolation and plotting spherical sun-path diagrams. Three separate dimensionless coordinates are necessary to specify the position of a point on the sky dome, as shown in Figure 3.8. In order to correspond with the azimuth convention, we use a coordinate system where the positive x-direction is toward the west, the positive y-direction toward the south, and the positive z-direction vertically in the zenith. Corresponding to the west, south, and zenith directions, respectively, symbols σ_W, σ_S, σ_Z, also known as ***direction cosines*** or ***sigma values***, represent the Cartesian coordinates of a point on the sky dome. Use Equations 3.7–3.9 to convert spherical coordinates to Cartesian coordinates.

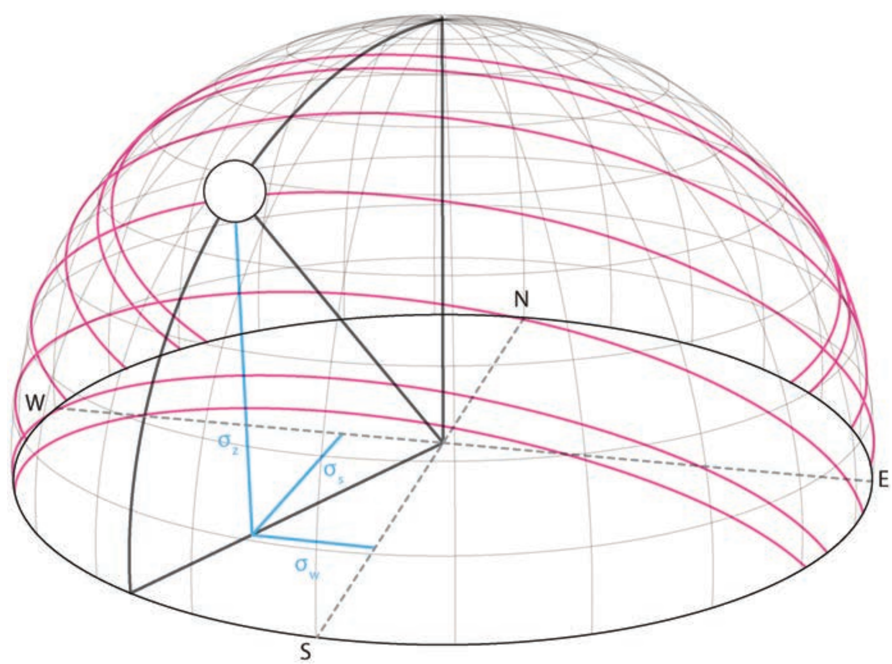

Figure 3.8

Cartesian Coordinates of Sun Position

Greg Arcangeli

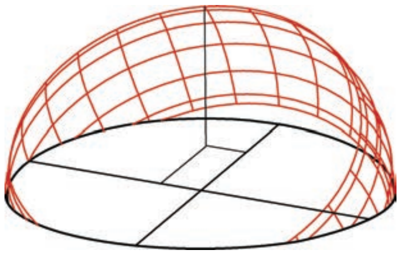

Figure 3.9
Sun Position in Example 3.5
Dason Whitsett

EXAMPLE 3.5 CALCULATING CARTESIAN COORDINATES OF SUN POSITION

What are the Cartesian coordinates of the sun's position at $L = 60°$ N at 11:00 *AST* on the June design day? The spherical solar coordinates at this time and location are $\alpha_{sol} = -22.67°$ and $\beta_{sol} = 51.97°$ (Figure 3.9).

Using Equations 3.7–3.9, calculate the direction cosines.

$$\sigma_w = \sin\alpha_{sol} \cos\beta_{sol}$$
$$\sigma_w = \sin(-22.97°)\cos(51.97°)$$
$$\sigma_w = -0.24$$
$$\sigma_s = \cos\alpha_{sol} \cos\beta_{sol}$$
$$\sigma_s = \cos(-22.97°)\cos(51.97°)$$
$$\sigma_s = 0.57$$
$$\sigma_z = \sin\beta_{sol}$$
$$\sigma_z = \sin(51.97°)$$
$$\sigma_z = 0.79$$

Try to visualize where this point falls on the sky dome using both the spherical and Cartesian coordinates.

Equation 3.7 West Direction Cosine

$$\sigma_w = \sin\sigma_{sol} \cos\beta_{sol}$$

Equation 3.8 South Direction Cosine

$$\sigma_s = \cos\alpha_{sol} \cos\beta_{sol}$$

Equation 3.9 Zenith Direction Cosine

$$\sigma_z = \sin\beta_{sol}$$

These three coordinates indicate the distance from the origin along each of the three cardinal axes of the sky dome, which has a dimensionless radius of 1. Positive σ values indicate distance along their respective axes while negative σ values indicate position opposite those cardinal directions. For example, if $\sigma_w = -0.50$, the point would be located half of the radius of the sky dome to the east of the origin.

The solar table is a useful means of displaying coordinate and other solar values over the course of a day or longer. Table 3.1 shows an example daily solar table and Appendix C provides annual solar tables for representative latitudes.

It is essential to remember that these three values are the coordinates of a point located *on the sky dome*. As a check to verify that the coordinates locate a point on the surface of the dome, we can apply Pythagoras's theorem in the form of Equation 3.10. If the right side of the equation does not equal 1, then there is a problem somewhere in the coordinate calculations. If it does, this does not guarantee the accuracy of the calculations, but there would have to be a mistake in two or more of the coordinates that coincide to represent another point somewhere on

Table 3.1 Solar Coordinates, June Solstice at 30.3° N Latitude

	Cartesian Coordinates			*Spherical Coordinates*	
AST	σ_w	σ_s	σ_z	β_{sol}	α_{sol}
5:01	–0.887	–0.461	0.000	0.00	–117.45
6:00	–0.917	–0.344	0.201	11.58	–110.53
7:00	–0.886	–0.224	0.406	23.94	–104.17
8:00	–0.794	–0.112	0.597	36.64	–98.04
9:00	–0.649	–0.016	0.761	49.54	–91.44
10:00	–0.459	0.057	0.887	62.47	–82.88
11:00	–0.237	0.103	0.966	74.99	–66.45
12:00	0.000	0.119	0.993	83.15	0.00
13:00	0.237	0.103	0.966	74.99	66.45
14:00	0.459	0.057	0.887	62.47	82.88
15:00	0.649	–0.016	0.761	49.54	91.44
16:00	0.794	–0.112	0.597	36.64	98.04
17:00	0.886	–0.224	0.406	23.94	104.17
18:00	0.917	–0.344	0.201	11.58	110.53
18:58	0.887	–0.461	0.000	0.00	117.45

the surface of the sky dome. The quantity on the left side of the equation reflects the dimensionless radius of "1" of the sky dome.

Equation 3.10 Pythagorean Check of Cartesian Coordinates

$$1^2 = \sqrt{\sigma_w^2 + \sigma_s^2 + \sigma_z^2}$$

EXAMPLE 3.6 CHECKING CARTESIAN COORDINATES WITH PYTHAGOREAN FORMULA

Use Equation 3.10, the Pythagorean theorem, to check the coordinates calculated in Example 3.5.

$$\sigma_w = -0.24 \ \sigma_s = 0.57 \ \sigma_z = 0.79$$

$$1^2 = \sqrt{\sigma_w^2 + \sigma_s^2 + \sigma_z^2}$$

$$1^2 = \sqrt{-0.24^2 + 0.57^2 + 0.79^2}$$

$$1 = 1$$

The coordinates check out, indicating that they correspond to a point located on the surface of the sky dome.

REPRESENTING SUN POSITION (SUN-PATH DIAGRAMS)

The geometry of the sun's apparent motion relative to an observer on Earth discussed in the preceding section takes the form of arcs inscribed on the surface of the sky dome. This is the true three-dimensional geometry that we are concerned with.

We often find it useful, however, to represent that geometry in two dimensions so that it is easier to work with and communicate about.

A convenient means of translating the solar position data described by the solar path band into a more readily usable form is to project or plot this geometry onto some plane, often a horizontal plane. Drawings of this type are known as ***sun-path diagrams*** and are essential tools for designers. Figure 3.10 shows two example projections.

A sun-path diagram condenses an entire year's worth of solar position information into one simple chart. Combined with a scale to indicate azimuth and altitude, the diagram quickly provides a visual representation of the sun's path throughout the year as well as reasonably accurate data on sun position at any given time. Compared to reliance on calculations or tables, sun-path diagrams excel at conveying a complete and readily visualized picture of the sun's relationship to a location to aid in design thinking. Sun-path diagrams can be drawn showing any dates and times desired, but usually have curves showing the sun's path for each design day and intersecting curves plotting the sun's position at each hour during the year.

While sun-path diagrams usually show solar time, it is possible to draw them to represent standard time, resulting in an analemma figure for each hour, as shown in Figure 3.10. If full alignment with clock time is necessary, an additional offset for daylight saving time may be included as well. For most applications, however, using

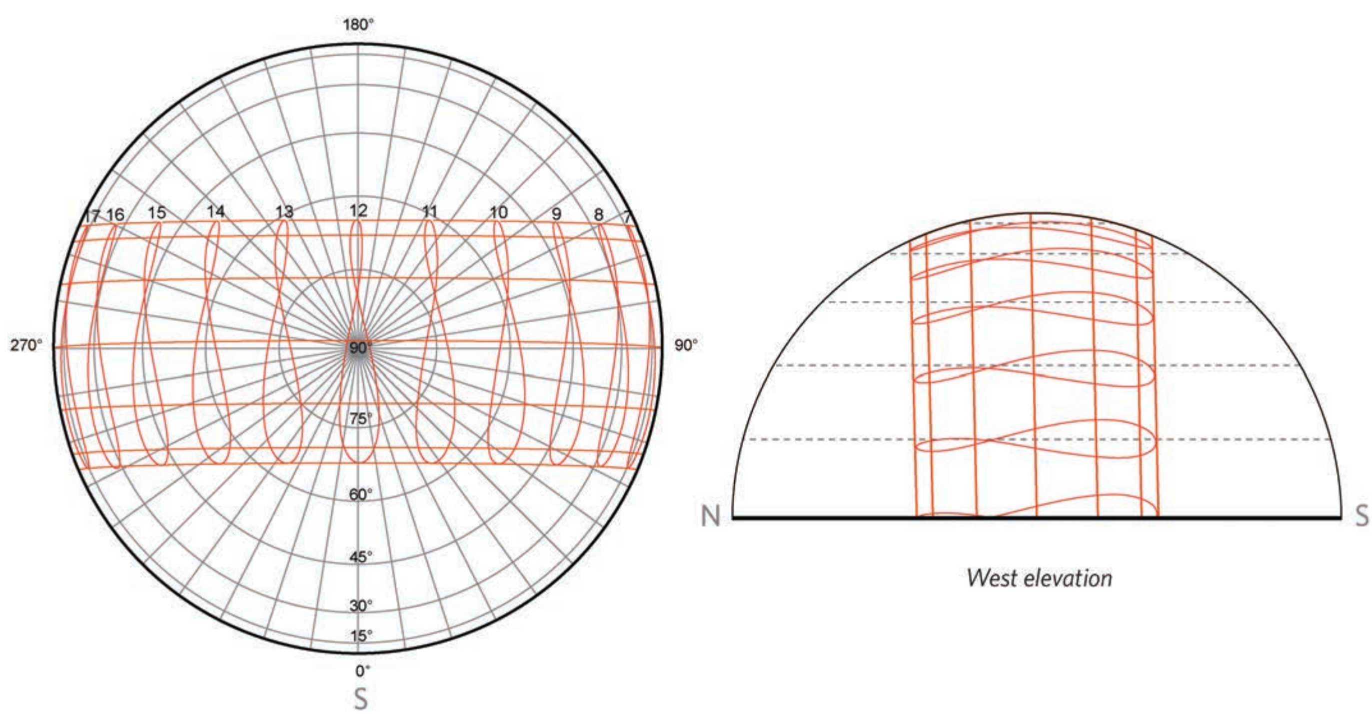

Figure 3.10

Example Sun-Path Projections

Spherical (orthographic) projections for Nairobi, Kenya at 1.3° S, 36.8° E. The circular diagram is a plan view and the semi-circular is a west elevation of the sky dome. The distinctive analemma shape of the hour lines reflects local standard time.

Greg Arcangeli

standard or local time adds unnecessary visual noise to the diagram and makes its use more difficult without providing significant benefits.

The sun-path diagram is not limited to representing sun position. Any object in space around the origin point can also be projected onto the sky dome and represented on the sun-path diagram, allowing one to assess when the point will be in sun or shade. In Chapters 7 and 8, additional techniques for using sun-path diagrams will be discussed.

The same issues that come into play in drawing cartographic projections arise with any attempt to represent the sun's path across the sky dome two-dimensionally. Numerous map projection techniques have been developed in an attempt to better represent the Earth's surface in two dimensions, all of which have advantages and disadvantages. Sometimes, the Earth is represented as if we are looking at the spherical globe from space, as in Figure 3.5. This is a geometrically correct view, but it makes it difficult to interpret geographic information except near the center of the map because one is looking progressively more obliquely at the Earth's surface moving toward the edge of the map until the view is tangent to the sphere of the Earth at the edge of the drawing. This approach is similar to the horizontal projections discussed next.

In other cases, the Earth's spherical surface is flattened into a neat rectangle. The Mercator map is probably both the best known and most harshly criticized of this style projection. It is very useful to navigators in particular because all straight lines represent a course of constant azimuth on a Mercator projection.[4] The problem with the Mercator map is that it greatly exaggerates relative area as latitude increases. At the extreme, the projection extends a single point in space (either pole) to a length equal to the Earth's full circumference. Mercator's map is a cylindrical projection similar to the vertical projections discussed in the following section.

The term ***projection*** refers to a drawing technique for creating various views of 3D objects. All true projections can be constructed graphically. The term ***diagram*** is used for other representations of the solar path, such as equidistant diagrams, which are not based on a constructed geometric relationship. Figure 3.11, after Szokolay[5], shows the construction techniques of some of the most common projection and diagram styles. Parallel-line projections, such as spherical projections, are the most straightforward to construct graphically; radial projections tend to take more work to draw manually.

Because graphical construction can be tedious, methods for calculating x-y coordinates to plot sun position based on known azimuth and altitude angles are provided for each method as well. To use this approach, one would start with a table of values of spherical solar position coordinates for each design day, convert these to x-y coordinates, plot the resulting series of points for each day on the diagram, and connect the points with a line. The shorter the time interval between coordinate points, the more precise the diagram will be. Hour lines can then be added by connecting the points for each hour from date line to date line. Increased resolution for hour lines may be gained by calculating sets of coordinates for each hour, keeping the hour fixed and using the date as the independent variable. The calculations involved are repetitive, but are done easily with a spreadsheet.

Horizontal Diagrams

Horizontal sun-path diagrams, such as the large circular diagram shown in Figure 3.10, are the most common type. They position the viewer at the center point of a circular

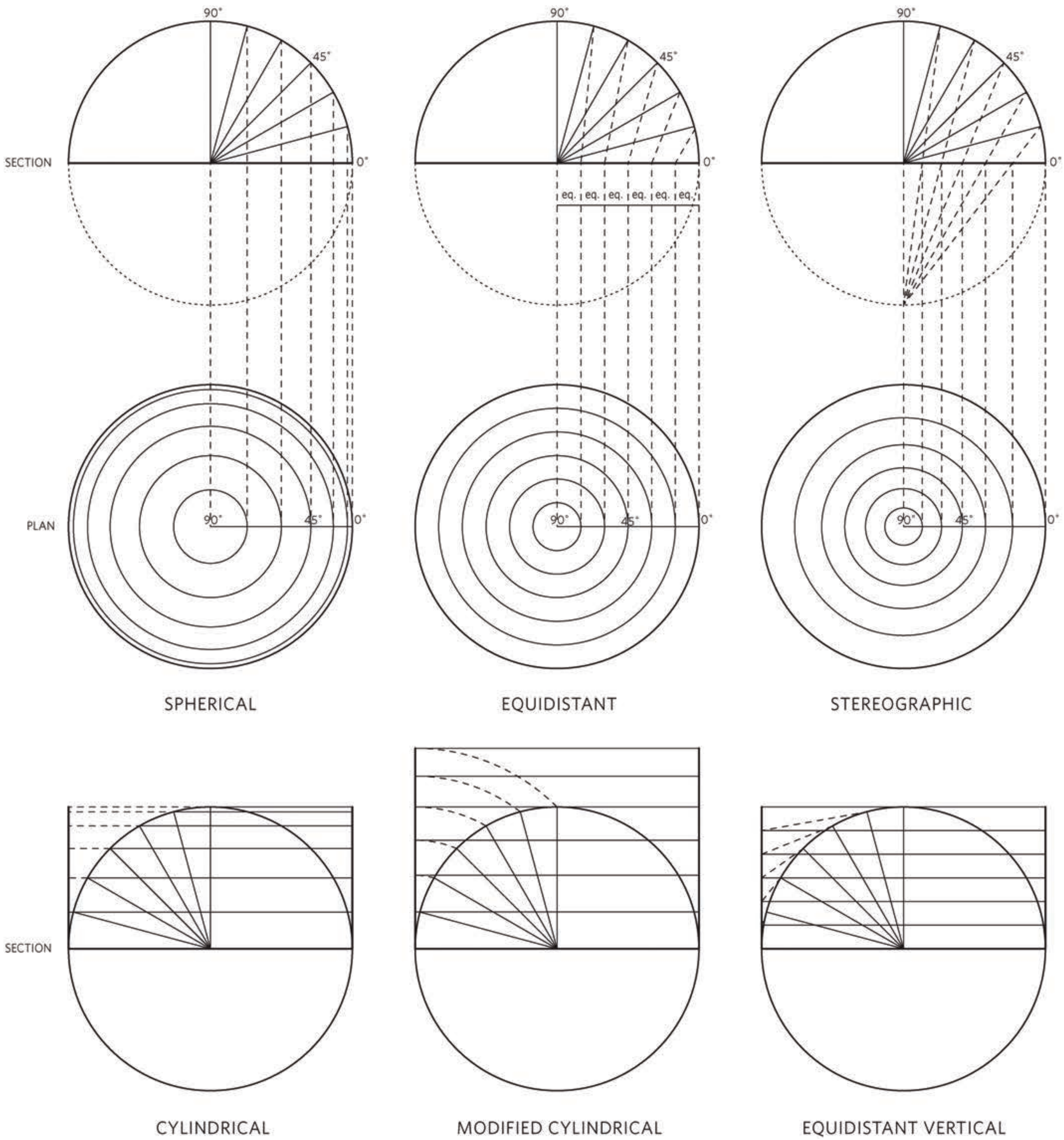

Figure 3.11

Construction of Various Projections

Greg Arcangeli

diagram surrounded by a projection of the sky dome onto the ground plane. The center of the diagram is known as the ***reference point*** or origin. It is crucial to note that the observer is always located at this reference point, and if the observer moves, the reference point moves along with him. This is important because all angles are taken relative to this reference point.

Azimuth is read on a scale around the perimeter of the diagram. The convention used in this book is that south is 0° of azimuth with positive rotation to the west. Altitude is read on a scale of concentric circles from the horizon at the perimeter of the diagram to the zenith at the center.

A series of curves running generally east-west trace the sun path for each date shown, usually the design days, but curves can be plotted for any date desired. These are crossed by roughly perpendicular curves representing time of day running more or less perpendicular to the date lines. Sunrise occurs at the point at which a date line intersects the eastern horizon at the edge of the diagram, and sunset at the symmetrical solar time in the afternoon.

To determine the solar azimuth and altitude at a particular date and time, first find the azimuth by extending a line from the reference point to the scale on the perimeter of the diagram. Then, read the altitude on the scale of concentric circles emanating from the reference point. Interpolation is usually necessary to determine altitude. Three styles of horizontal projection will be discussed in this section.

Spherical Projections

Spherical projections (Figure 3.12), also known as orthographic projections, are simply orthographic views of the sky dome. It is most common to see horizontal spherical projections where the observer is looking from above toward the reference point along the z-axis, but elevation views are frequently used as well.

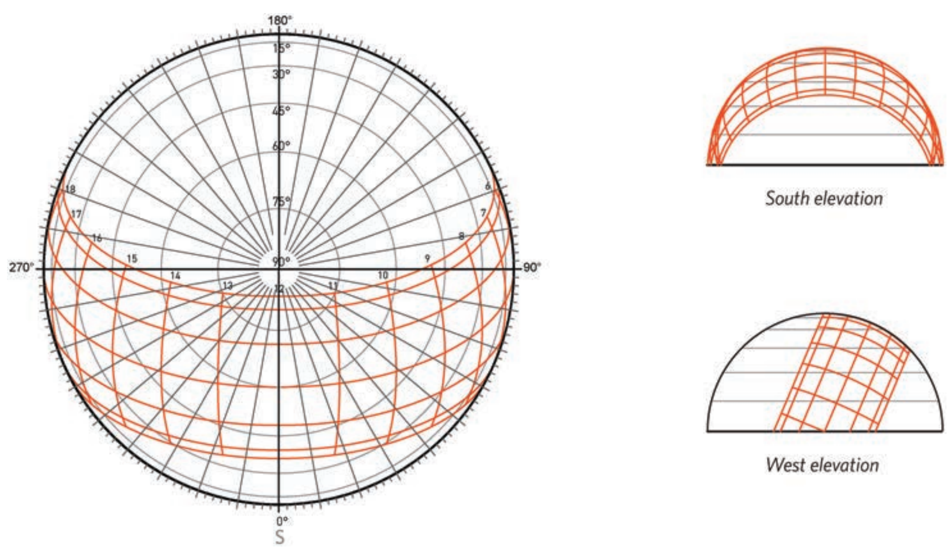

Figure 3.12

30° North Spherical Sun Path

The sky dome and spherical projections on the ground plane from the west and south for Austin, Texas.

Greg Arcangeli

For general purposes, the most useful spherical sun-path projection is the plan view. From this point of view, each of the circles representing the sun's path around the sky dome (sphere) appears as a partial ellipse being cut off by the ground plane at sunrise and sunset. The crossing curves indicating hours on the solar path band appear as ellipsoidal segments connecting each of the date curves, with the exception of solar noon, which is viewed entirely on edge, thus appearing as a straight line along the north-south axis.

Because spherical projections are true orthographic views of the sky dome, they are excellent tools to help the user visualize the geometry and position of the solar path band for a given location. The key to creating a good mental picture based on these diagrams is to remember that the drawing is a view of a sphere and to visualize the information three-dimensionally. Showing azimuth and altitude scale lines, which give the view a characteristic globe or beach-ball-like appearance, can greatly aid in this visualization.

Because of their geometric accuracy, spherical projections suffer from the same disadvantage orthographic views of the globe do in map-making. As one looks at the sky dome, resolution is high toward the center of the diagram, but it becomes progressively more difficult to read the drawing toward the edges. In plan view, altitude angles become highly compressed toward the horizon until it is impossible to read the diagram with any degree of accuracy. This problem may be mitigated by using an east or west elevation projection in addition to the ground plane projection, but the need for two diagrams reduces the convenience of using the projections.

The result of the bias toward the center of the diagram is that, while the sky directly overhead is shown quite clearly, areas near the horizon are represented poorly. This becomes problematic when reading low-altitude solar positions, or using the diagram with shading masks because low-angled obstructions are not clearly represented.

When using these diagrams to assess solar exposure of a point in space, it is necessary to draw the surrounding objects around that point projected onto the sun-path diagram as well. In design situations, surrounding points are often closer to the horizon than the zenith, reducing the utility of this style of projection.

Spherical projections are the easiest projection type to draw. It is relatively straightforward to take spherical views from any arbitrary azimuth and altitude angle. One convenient means of doing so is to build a 3D computer model of the sky dome and create views of it from different angles. When taking views of such a model, be sure to set the view to parallel-line or orthographic rather than perspective. Spherical projections are also readily drawn using 2D projection techniques. Figure 3.13 demonstrates how to draw the sun path for the December solstice in Austin, Texas ($L = 30°$ N), and locate 14:00 solar time. Start by drawing the equinox sun path in elevation on the sky sphere and adjusting it to the correct position based on the latitude of the location. From there, the paths for other dates can be drawn using either the method shown or by calculating the zenith angle at noon on the desired dates using Equation 3.10 or one of its variants. Remember that the zenith angle is relative to the reference point, but the sun-path circles will all be parallel to the equinox sun path.

Then, project an elevation of the sphere normal to the solar path band to determine where hours fall along the date lines. A day is 24 hours long, which translates to 15° of axial rotation per hour. Draw the hours on this elevation. Because the sun path for each date is a circle around the sky sphere, looking at the path from any angle other than normal or parallel, it will appear as an ellipse. To draw the solar path for the chosen date on the plan-view diagram, project the

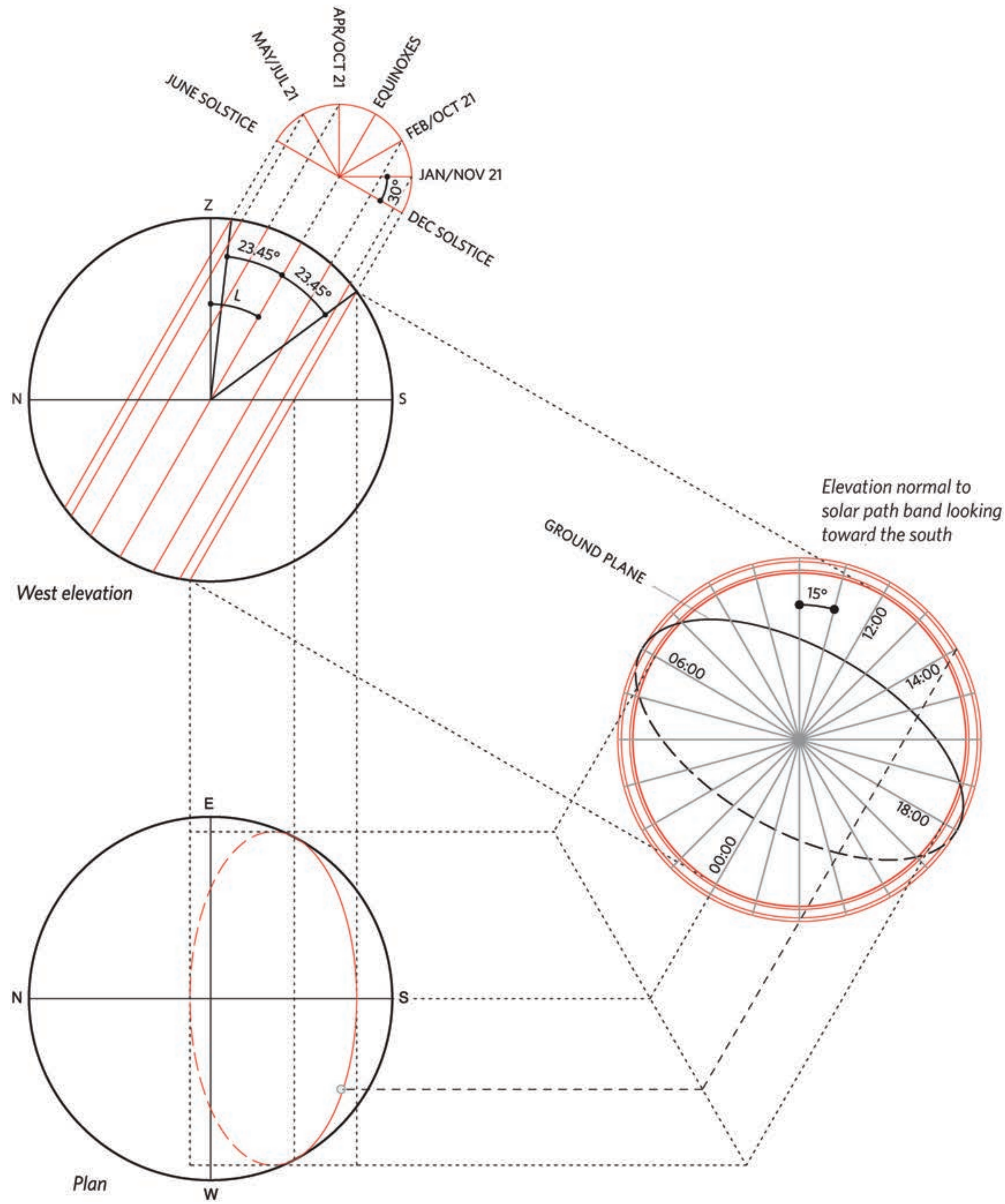

Figure 3.13

Construction of a Spherical Sun-Path Projection

Construction method for the December solstice sun path and locating the sun position at 14:00 for latitude 30° N.

Greg Arcangeli

position of solar noon and midnight from the west elevation to the plan. These lines are the width of the minor axis of the ellipse. Project the diameter of the date circle from the elevation of the solar path band onto the plan view. This will indicate the length of the major axis of the ellipse. Draw the ellipse representing the path of the sun around the sky sphere on the December solstice within these extents.

Sunrise and sunset occur where the solar path crosses the ground plane. This will be the point at which the ellipse is tangent to the circle of the ground plane, but is easier to locate by projecting from the west elevation. Remove the portion of the ellipse where the sun is below the horizon.

To locate the solar position at a particular time, project the intersection of the hour line and the date circle from the elevation of the solar path band to the plan view. The intersection of this projection line and the date ellipse is the position of the sun at that time. A completed spherical sun-path diagram, such as the one shown in Figure 3.12, will also have an azimuth and altitude scale allowing the user to determine solar coordinates for any point in time or a Cartesian grid, as shown in Figure 3.14.

To plot spherical projections using mathematically derived coordinates, calculate a table of Cartesian coordinates for sun position using Equations 3.7–3.9. Plot these coordinates directly onto the ground plane and connect the date and hour lines as outlined in the introduction to this section.

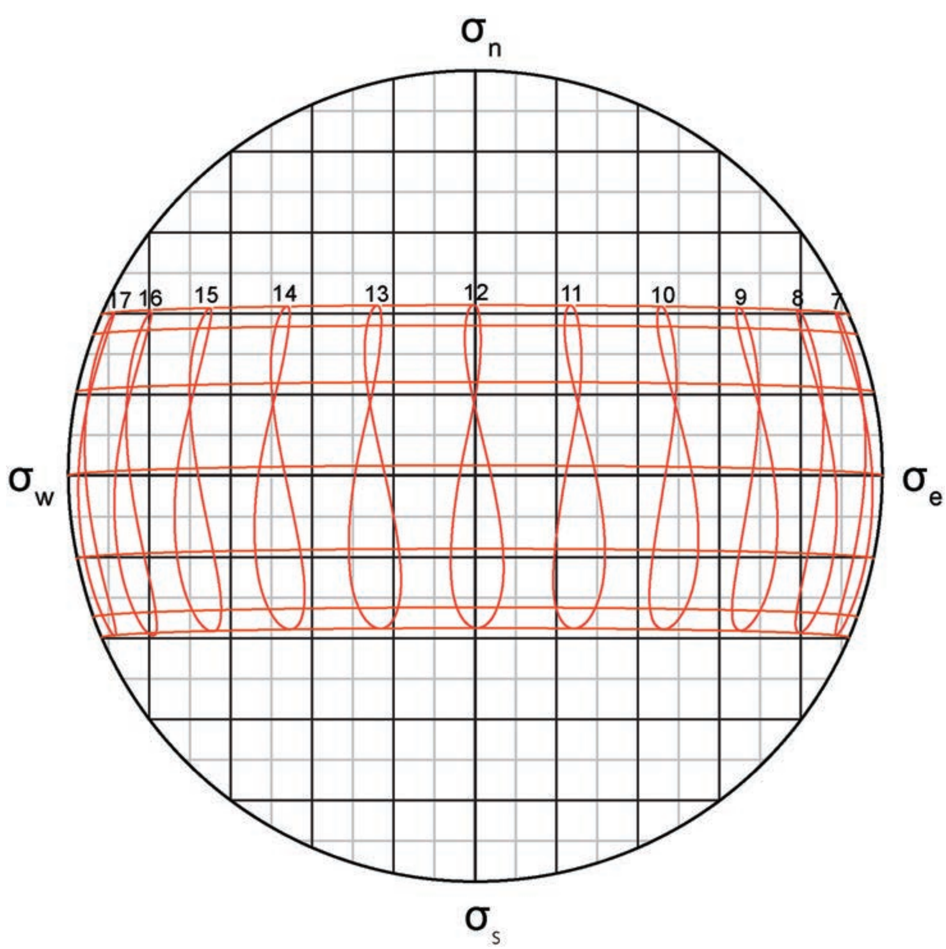

Figure 3.14

Spherical Sun-Path Projection with Cartesian Grid, Nairobi, Kenya

Either polar or Cartesian coordinates may be used for the coordinate grid.

Greg Arcangeli

Other Horizontal Diagrams

Because spherical projections suffer from the major shortcoming of poor usability at low solar altitudes, two other projection styles are used more often in practice. Although they lack the didactic power of true three-dimensional geometry represented by the spherical projection, these other diagrams provide a more useable representation of solar position at lower altitudes, making them much more practical for analytic use.

Equidistant Diagrams

In the United States, the ***equidistant diagram*** is the most common representation of the sun's path in two dimensions. The ease of use of this type of diagram, in combination with its use in the Sun Angle Calculator copyrighted originally by the Libby Owens Ford Glass Company beginning in the 1950s and now by Pilkington Glass Company, has made the equidistant diagram the de-facto standard. Figure 3.15 shows an example. Equidistant sun-path diagrams improve on the difficulties in reading and working with low altitudes in spherical projections

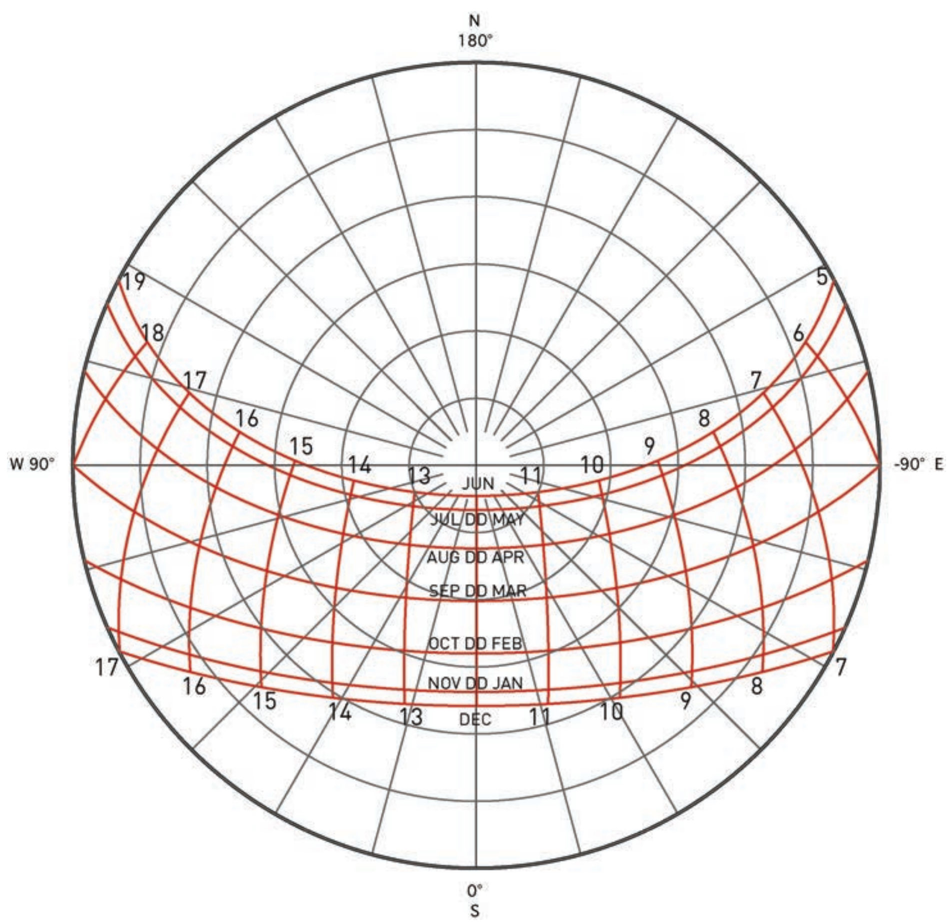

Figure 3.15

Equidistant Sun-Path Diagram for Austin, Texas 30.3°N

Greg Arcangeli

by spacing altitude in equal linear increments from the horizon to the zenith. In other words, the ratio of the radii of circles representing 0° and 45° altitude in an equidistant diagram is 2:1, compared to 1.4:1 in a spherical projection. As a result, equidistant diagrams provide good resolution at either high or low altitude angles.

This convenience does come at some cost, however. All projection techniques besides spherical distort the geometry in an attempt to better represent it from a particular point of view. As a result of this distortion, the diagram is no longer a literal model of three-dimensional geometry and there are no corresponding views of the sun path from other points of view. This makes it more difficult to use the diagram as a tool to visualize the solar path band as it relates to the three-dimensional reality of a building site. Because of these trade-offs, it is a good idea to use spherical projections for conceptual purposes, while relying on equidistant or other projection styles for analysis tasks.

Use Equations 3.11 and 3.12 to determine x and y coordinates for plotting equidistant diagrams from known spherical coordinates. Positive x values are toward the west and positive y toward the south.

Equation 3.11 X-Coordinate for Equidistant Diagram

$$x_{eq} = \sin\alpha_{sol}\left(\frac{90° - \beta_{sol}}{90°}\right)$$

Equation 3.12 Y-Coordinate for Equidistant Diagram

$$y_{eq} = \cos\alpha_{sol}\left(\frac{90° - \beta_{sol}}{90°}\right)$$

EXAMPLE 3.7 COORDINATES FOR EQUIDISTANT DIAGRAM

What are the coordinates on an equidistant diagram of the sun's position in Austin, Texas, at 14:14 solar time on July 11? Spherical coordinates of solar position at this time were calculated in Example 3.1: $\alpha_{sol} = 82.79°$ and $\beta_{sol} = 58.97°$.

Use Equations 3.11 and 3.12 to map the coordinates to the equidistant diagram.

$$x_{eq} = \sin\alpha_{sol}\left(\frac{90° - \beta_{sol}}{90°}\right)$$

$$x_{eq} = \sin(82.79°)\left(\frac{90° - 58.97°}{90°}\right)$$

$$x_{eq} = 0.34$$

$$y_{eq} = \cos\alpha_{sol}\left(\frac{90° - \beta_{sol}}{90°}\right)$$

$$y_{eq} = \cos(82.79°)\left(\frac{90° - 58.97°}{90°}\right)$$

$$y_{eq} = 0.04$$

Equidistant diagrams are not true projections because they are based on a geometrically arbitrary linear distribution of altitude rather than a true constructed projection onto a plane. In practice, however, this has no impact on the user of equidistant projections. Because of their wide acceptance, and other advantages, this book will use equidistant diagrams for most purposes in later chapters.

Stereographic Projections

Stereographic projections also address the low-altitude readability issue by using a radial projection technique, as depicted in Figure 3.16. The position of a point on the sky sphere is projected to the ***nadir***, the pole of the sky sphere opposite the zenith. The intersection of this projection line and the ground plane locates that point on the stereographic projection. These projections are the most common style in use outside of the United States.

Stereographic projections have the advantage of increasing the relative spacing between low altitude lines compared to those closer to the zenith. The ratio of the radii of circles representing 0° and 45° altitude in a stereographic diagram is 2.4:1. This characteristic makes the stereographic technique useful in solar site assessment because it provides a high resolution near the ground where many obstructions are

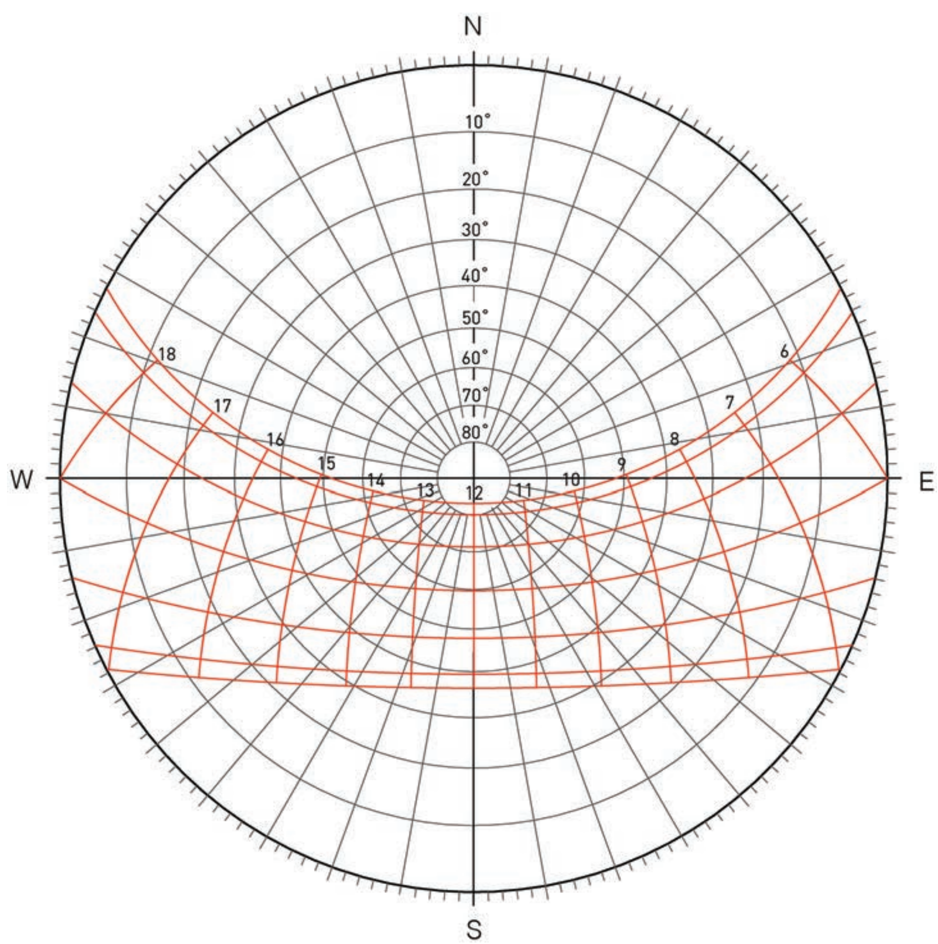

Figure 3.16

Stereographic Projection for Austin, Texas

Greg Arcangeli

located. The sacrifice for greater low-angle resolution is a de-emphasis of the zenith area, which, if unrecognized, could have an adverse impact from a daylighting point of view because under overcast skies, the zenith area has the highest luminance and is most important to maintain exposure to.

Szokolay[6] provides good instructions for graphically constructing stereographic projections in two dimensions using arcs without the necessity to cut a section for every azimuth. Use Equations 3.13 and 3.14 to plot coordinates for stereographic projections mathematically.

Equation 3.13 X-Coordinate for Stereographic Projection

$$x_{st} = \sin\alpha_{sol}\left(\frac{\sin(90° - \beta_{sol})}{\sin\beta_{sol} + 1}\right)$$

Equation 3.14 Y-Coordinate for Stereographic Projection

$$y_{st} = \cos\alpha_{sol}\left(\frac{\sin(90° - \beta_{sol})}{\sin\beta_{sol} + 1}\right)$$

EXAMPLE 3.8 COORDINATES FOR STEREOGRAPHIC DIAGRAM

What are the coordinates on a stereographic diagram of the sun's position from Example 3.7?

Use Equations 3.13 and 3.14 to calculate the coordinates.

$$x_{st} = \sin\alpha_{sol}\left(\frac{\sin(90° - \beta_{sol})}{\sin\beta_{sol} + 1}\right)$$

$$x_{st} = \sin(82.79°)\left(\frac{\sin(90° - 58.97°)}{\sin(58.97°) + 1}\right)$$

$$x_{st} = 0.27$$

$$y_{st} = \cos\alpha_{sol}\left(\frac{\sin(90° - \beta_{sol})}{\sin\beta_{sol} + 1}\right)$$

$$y_{st} = \cos(82.79°)\left(\frac{\sin(90° - 58.97°)}{\sin(58.97°) + 1}\right)$$

$$y_{st} = 0.03$$

Vertical Diagrams

The sun's path can also be represented on a Cartesian grid with the x-axis representing azimuth and the y-axis altitude. There are a variety of ways in which the solar path can be projected or plotted on a vertical diagram, but all are either literally or conceptually based on the idea that the sun's position on the sky dome is projected onto a cylinder surrounding that dome similar to the manner in which a Mercator map projection is drawn. The cylinder is then sliced lengthwise and unfurled to reveal a flat diagram.

Vertical projections are the easiest for the layperson to understand, but exhibit the same problem from which the Mercator map projection suffers. In mapping the spherical geometry onto a rectangular plane, points along the full 360° panorama of the horizon are separated proportionally to their true angular distance, while one single point, the zenith, is stretched to the entire length of the horizon at the top edge of the diagram. This tends to visually exaggerate the importance of objects in this region when shading masks are drawn on these diagrams and distort the sun path into shapes that do not visually relate to the spherical geometry the diagram represents.

There is more confusion around the terminology and variations on the construction of vertical sun-path diagrams than with the horizontal projections. Various authors use the same terms to apply to slightly different methods of constructing these diagrams. For the most part, these variations are not important as long as the user is consistent with conventions. Also note that vertical sun-path diagrams are sometimes referred to as orthographic because the grid they are plotted on is rectangular. The term orthographic projection properly applies to spherical projections, however, because they are a parallel-projection line representation of the actual geometry of the sun's path on the sky dome.

Cylindrical Projection

Cylindrical projections are a common type of vertical sun-path diagram. The most basic form of cylindrical projection projects altitude horizontally onto the surrounding cylinder, as shown in Figure. 3.17. This projection results in a diagram with a very large x- to y-axis aspect ratio of 2ϖ:1. This provides good resolution at lower solar altitudes, but higher altitudes are compressed significantly. To mathematically translate solar coordinates to cylindrical projection, use Equations 3.15 and 3.16.

Equation 3.15 X-Coordinate for Cylindrical Projection

$$x_{cy} = \left(\frac{\alpha_{sol}}{360°}\right)2\pi$$

Equation 3.16 Y-Coordinate for Cylindrical Projection

$$y_{cy} = \sin\beta_{sol}$$

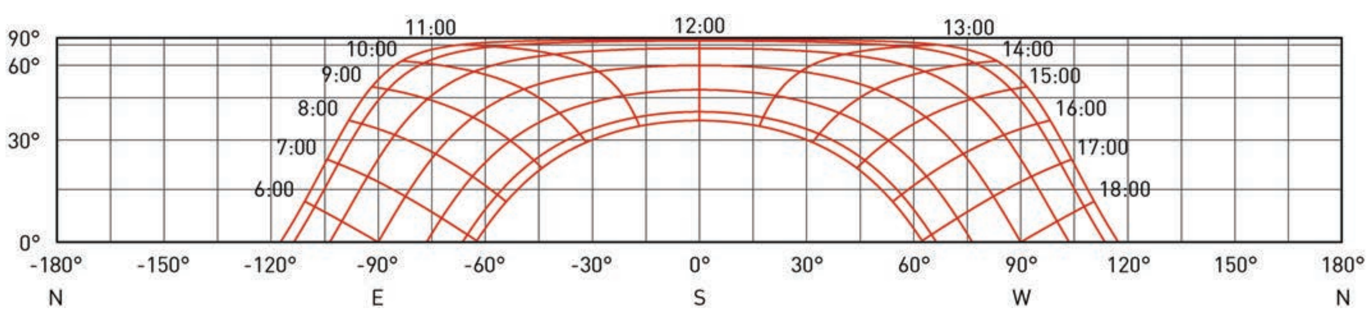

Figure 3.17

Cylindrical Projection of the Sun Path for Austin, Texas

Greg Arcangeli/Dason Whitsett

EXAMPLE 3.9 COORDINATES FOR CYLINDRICAL PROJECTION

What are the coordinates on a cylindrical projection of the sun's position from Example 3.7?

Use Equations 3.15 and 3.16 to calculate the coordinates.

$$x_{cy} = \left(\frac{\alpha_{sol}}{360°}\right)2\pi$$

$$x_{cy} = \left(\frac{82.79°}{360°}\right)2\pi$$

$$x_{cy} = 1.44$$

$$y_{cy} = \sin\beta_{sol}$$

$$y_{cy} = \sin(58.97°)$$

$$y_{cy} = 0.87$$

Modified Cylindrical Projection

Mazria[7] popularized these diagrams for solar site analysis. The modified cylindrical projection, shown in Figure 3.18, is similar to the standard cylindrical projection, but provides better high-solar altitude resolution by creating more space between altitude line parallels.

The geometric projection of a modified cylindrical sun-path diagram entails swinging an arc with its center at the horizon edge of the sky dome from an altitude point on the dome up to a vertical line intersecting that horizon edge. The vertical line represents a section through a cylinder surrounding the sky dome. If this arc is swept around the perimeter of the sky dome to draw a line of constant altitude on the cylinder, the surface resulting from the sweep of that arc will be a section of a torus. Once all the necessary points have been projected onto the inner surface of the cylinder, it is then unfurled into a flat diagram like the other vertical projections.

Equation 3.17 gives the formula for calculating the *y*-coordinate of a modified cylindrical projection. The *x*-coordinate is the same as for a standard cylindrical projection from Equation 3.15.

Equation 3.17 Y-Coordinate for Modified Cylindrical Projection

$$y_{mc} = \sqrt{(1-\cos\beta_{sol})^2 + (\sin\beta_{sol})^2}$$

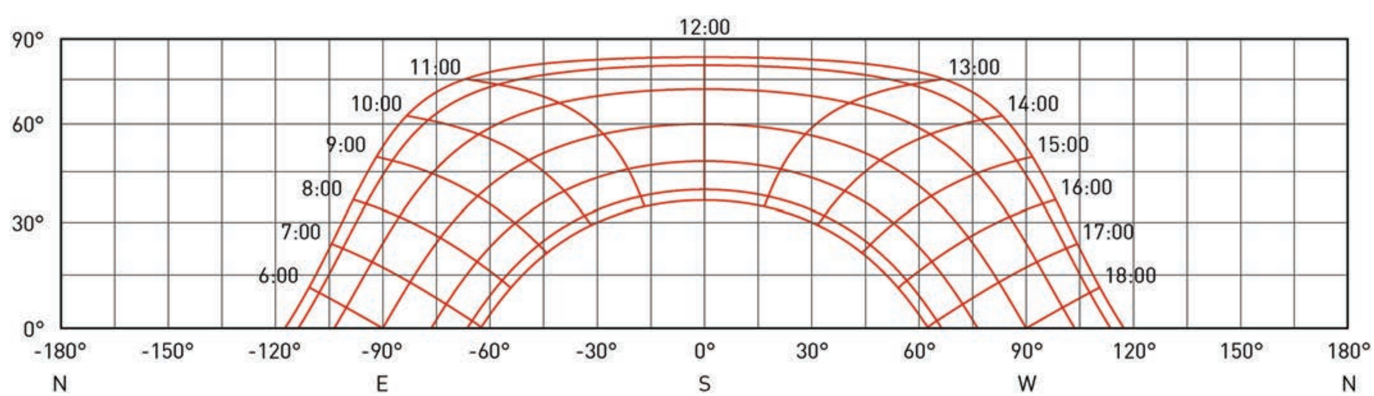

Figure 3.18

Modified Cylindrical Projection of the Sun Path for Austin, Texas

Greg Arcangeli/Dason Whitsett

EXAMPLE 3.10 COORDINATES FOR MODIFIED CYLINDRICAL PROJECTION

What are the coordinates on a modified cylindrical projection of the sun's position from Example 3.7?

$x_{cy} = 1.44$ as calculated in Example 3.9
Use Equation 3.17 to calculate the y-coordinate.

$$y_{mc} = \sqrt{(1 - \cos\beta_{sol})^2 + (\sin\beta_{sol})^2}$$

$$y_{mc} = \sqrt{(1 - \cos(58.97°))^2 + (\sin 58.97°)^2}$$

$$y_{mc} = 0.98$$

The ratio of the length of the x- to y-axes of a true 360° degree modified cylindrical projection is 4.4:1. Often, these diagrams are drawn only as wide as necessary to show all positions of the sun above the horizon. A particular shortcoming of the modified cylindrical projection is that it gives greater visual weight to the zenith than the horizon.

In the diagram, the zenith (90° altitude) is represented by the entire topmost line of the diagram even though in actuality it is just one point in space. The zenith line is the same length as the horizon line (0° altitude), which depicts a full 360° panorama.

Vertical Equidistant

The simplest form of vertical sun-path diagram, the equidistant vertical style shown in Figure 3.19, treats azimuth and altitude directly as *x* and *y*-coordinates, respectively. This is the style, for example, generated by the Climate Consultant software tool.[8] Both values are plotted on a linear scale throughout their range. The scale of altitude is often larger than that for azimuth, creating a diagram with a lower x-y aspect ratio that is easier to use. Although they are frequently referred to as cylindrical projections, many published vertical sun-path diagrams are actually vertical equidistant diagrams.

Other Projections

In addition to those just described, several other styles of projections are used sometimes in particular contexts. The Waldram diagram is a type of vertical projection, but with a non-linear vertical scale. It is used primarily for right-to-light analysis. Unlike the

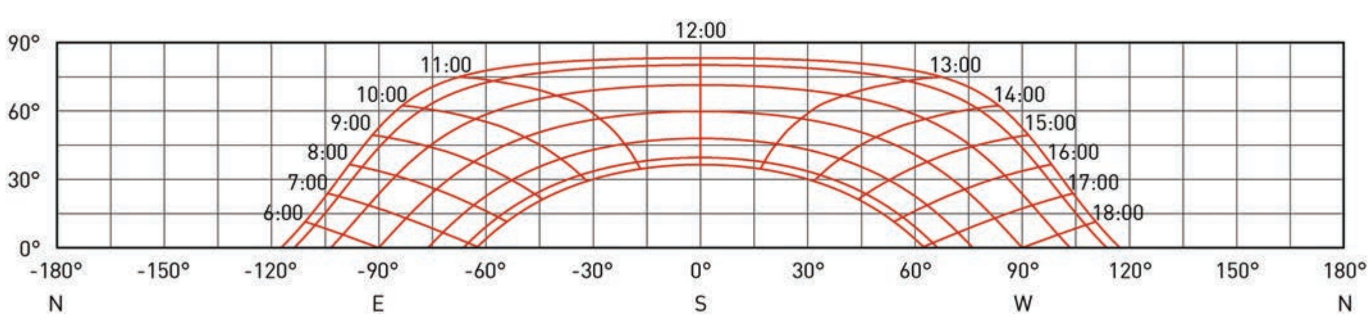

Figure 3.19

Vertical Equidistant Projection of the Sun Path for Austin, Texas

Greg Arcangeli/Dason Whitsett

other vertical diagrams discussed previously, it is crucial that the Waldram diagram be constructed according to a specific specialized method so that it may be used with its associated overlays.

Gnomonic projections have a unique style that plots shadow lengths rather than provides a representation of the sky dome. Sundials are gnomonic projections. These projections are particularly useful for model analysis because one may create a scale sundial, attach it to a model, then orient the model until the sundial shows the time of interest. That way, shadows and sun penetration may be quickly studied on the model.

Developing a clear, intuitive understanding of the sun's movement relative to any place on Earth is the first and most fundamental task for the designer to master in order to begin to design with nature's cycles. This chapter presented techniques that allow the designer to visualize the sun's path across the sky dome throughout the year as well as graphically estimate or precisely calculate the sun's position at any time. This knowledge is a prerequisite for making good decisions in the design process relative to comfort, energy use, and user experience, and it must be readily recalled and visualized by the designer in the flow of design thinking if it is to be effective.

The most essential component for a dependable mental model of the sun's movement is a thorough understanding of the solar path band. The section of this chapter on the solar path band describes the few basic pieces of information needed to mentally construct the solar path band for any location on Earth. With only this information, one may instantly visualize the sun's relationship to that place throughout the year and roughly estimate the implications of decisions about orientation, window placement, shading, daylighting, and so on.

Subsequent chapters will extend the investigation to how the sun interacts with buildings in terms of light and heat, evaluating these impacts in both quantitative and qualitative terms. In doing so, detailed analysis techniques will be presented to evaluate design decisions based on the general knowledge of solar geometry presented here.

NOTES

1 Steven Szokolay, "Solar Control," in *Time-Saver Standards for Architectural Design Data*, ed. Donald Watson, Michael J. Crosbie, and John Hancock Callender, 7th ed. (New York: McGraw-Hill, 1997), 35–62.
2 ASHRAE, *2009 ASHRAE Handbook: Fundamentals*, SI ed. (Atlanta, GA: American Society of Heating, Refrigerating and Air-Conditioning Engineers, Inc., 2009).
3 John A. Duffie and William A. Beckman, *Solar Engineering of Thermal Processes*, 3rd ed. (Hoboken, NJ: Wiley, 2006).
4 Peter H. Dana, "Map Projections," *Map Projections*, 1999, www.colorado.edu/geography/gcraft/notes/mapproj/mapproj_f.html.
5 Szokolay, "Solar Control."
6 Steven Szokolay, *Introduction to Architectural Science: The Basis of Sustainable Design*, 2nd ed., (Burlington: Elsevier, 2008).
7 Edward Mazria, *The Passive Solar Energy Book: A Complete Guide to Passive Solar Home, Greenhouse, and Building Design* (Emmaus, PA: Rodale Press, 1979).
8 *Climate Consultant*, version 6.0 (University of California Los Angeles; The Regents of the University of California, 2015).

4 CLIMATE AND SOLAR RADIATION

He who dwells in man and who dwells in the sun is one and the same.

—Taittiriya Upanishad

A SOLAR-POWERED EXISTENCE

Our connection to the sun registers in many ways, including the nourishment and development of our bodies as well as the assembly and configuration of our cultures and constructs (Figure 4.1). Sunlight is the basis of our being, and although we are often removed from direct sunlight, or even left without direct views of daylight, we are still innately linked to the sun. Buildings have gone so

Figure 4.1

Brooklyn, NY: Crowd Scene at Coney Island during Heat Wave

Photograph by Weegee, 1938; Bettmann/CORBIS far in the past century to remove us from the uncomfortable things about nature (extreme heat/cold, high winds) that we often forget about the great aspects of nature (cross-ventilation, fresh air, daylight, and dappled sunlight). Not many generations ago, humans spent the majority of their time outdoors, and also constructed shelters that more directly tracked the outdoor environment. Although many changes have occurred in our cities and environments, our historical and genetic makeup influence our evolving perceptions of comfort.[1] Similarly, our thresholds for comfort vary due to many factors, some of which seem contradictory, but the factor of choice plays a role in the tolerance of light and temperature levels. Furthermore, adaptive behavior plays an important role in humankind's ability to survive and thrive, although this relationship has recently changed as technology and fossil fuel energy have been used to adapt the environment to the liking of humans.[2]

CIVILIZATIONS ORGANIZED BY SUNLIGHT FOR SURVIVAL

The historical relationship between architecture and light is arguably as shaped by vernacular design as it is by Greek and Roman influence, both of which considered daylight in nuanced ways to determine city layouts. The former has typically occurred in a more circumstantial manner while the latter has usually been developed by design, or a master plan. Non-pedigree building, just as orthodox design, is more often picturesque in the way that nature is, in that it is design for a particular function, without regard to aesthetics, which is precisely what makes it interesting and harmonious. There is much to learn from architecture before it became a professional discipline. Indigenous cultures showed a great capacity to design and construct structures to carefully fit into their natural surroundings. Instead of trying to "conquer" nature, as modern man has often done, they embrace the climate and the challenge of topography to create spaces that intelligently and efficiently manage various environmental factors—particularly sunlight.

Traditional and vernacular Middle Eastern settlements are especially interesting in this regard. In an aerial view, the traditional market in Marrakesh, Morocco, appears to be a complex, ordered arrangement, bearing resemblance to a top-down man-made system (Figure 4.2). Instead, each building was constructed based on its own immediate circumstances, rather than a set masterplan, and as such, there are no continuous axes to order the entire layout. In this case, surface was the critical variable that drove the plan pattern. As the sun is extremely hot in the local Saharan climate, each building depends on being shaded by its neighbor, or in many cases, simply attached to its neighbor to avoid direct solar exposure on all facades throughout the day. Thus, each residence has a nearly square inner courtyard that allows sunlight but limits direct exposure. In order for the system to work, a critical density is required to ensure not only that each residence has the proper proportion of solar protection and penetration, but also that streets have a particular width to control the amount of light reaching them. Furthermore, makeshift canopies of lattice or wood constructions are often spanned from building to building to further modulate the light that reaches the street level.

The intricate neighborhood organization in Marrakesh provides an infrastructure in which the residents can live within tolerable comfort levels in an extremely hot climate. However, the physical structure of each individual residence and the overall cluster is only part of the strategy to enable thermal comfort within the climate.

Figure 4.2

Aerial View of Houses and Streets of Central Marrakesh

The medina of Marrakesh, Morocco, with its relaxed geometry, driven by surface optimization to regulate sunlight. The archetype of the Islamic town is based on quadrangular houses organized around interior courts. The density provides no traffic arteries, and the cool narrow alleys often lead to dead ends.

Darrin Jenkins/Alamy Stock Photo

Diurnal patterns of the inhabitants, based on the solar path, are ultimately what make the system function. In each residence, the various spaces or rooms are kept fairly unspecific programmatically, such that multiple daily functions can occur in each room throughout the day. Thus, the occupants can move around the house during the day to either follow or avoid the sun, depending on the season (Figure 4.3). The entire system exists as a complex infrastructure that developed organically, without any notion of a masterplan, and directly due to the need to physically sustain a population in a harsh solar climate.

Beginning in Roman times, many cities have been laid out on a north-south axis (cardo) and an east-west axis (decumanus). It can be speculated that this alignment is related to solar orientation and the fact that structures oriented in this way are more predictably illuminated by the east-to-west solar path than structures that are randomly oriented. In Roman cities and encampments, the cardo was the primary north-south oriented street. Cardo is derived from the same root as "cardinal" and is the hinge or axis of the city. The main cardo was called the cardo maximus. The cardo, a fundamental component in the planning of cities, was generally an economic strip, including buildings and spaces for commerce and public flow. Most Roman cities also had an east-west street that served as a secondary main street (decumanus maximus). The decumanus was originally based on separating groups within military camps, and was related to the proximity and exposure to enemies. As a result of geographical constraints, in some cities, the decumanus was the main street and the cardo was secondary.

The Forum is normally located close to the intersection of the cardo maximus and the decumanus maximus. This concept became deeply engrained in European city and town planning and eventually colonial America. It can be readily understood that

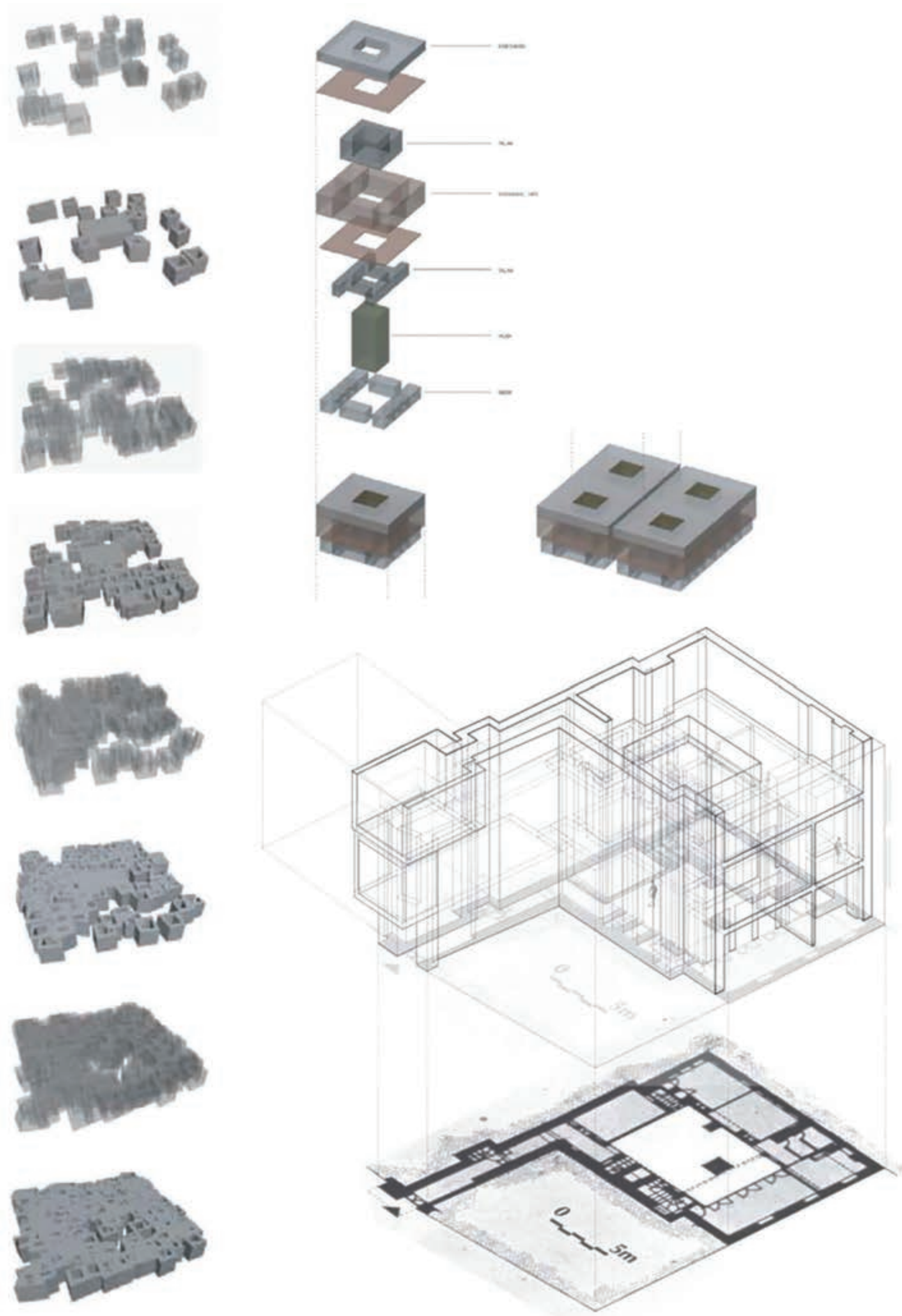

Figure 4.3

Analysis of the Typical Islamic House

An analysis of the typical Islamic house and its relationship to an overall system, such that density and optimization of surface is necessary for the entire network to function. Each individual house is inhabited in a diurnal fashion, where the occupant migrates around the structure during the day to evade direct sunlight.

Matt Fajkus

Romans laid out streets in this pattern, which has continued to modern day. On the island of Manhattan, for example, the avenues, which run north-south, are larger than the streets, which run east-west. This not only reinforces the cardo/decumanus hierarchy but also allows winter sunlight to penetrate more deeply into the mass of the city, while harsh west summer sun is limited by the narrower east-west streets

Figure 4.4
Barcelona (Barcino)
Matt Fajkus

(similar to Barcelona's streets, as shown in Figures 4.4, 4.5, and 4.6). Daylight and solar orientation are factors used to organize city layouts for intuitive wayfinding, and the nuanced manifestation of this creates a unique atmosphere and ambience. The character of a city is less defined by its specific individual buildings than the collection of buildings, and how they operate in density and establish a legible fabric to regulate light and shadow.[3]

René Descartes, referenced in the first chapter of this book, was influenced by Kepler's theories, which explained the world through the mathematical principles of planetary motion, and proposed a new concept of space. He determined that the nature of the entire universe must be explicable in pure mathematical terms. The signature feature of this theory is the Cartesian system, or Cartesian grid, which is

Figure 4.5
Barcelona (Barcino)
Matt Fajkus

the proclamation that space is a plenum, or a predominantly two-dimensional flat continuous space filled with matter or air.[4]

The Cartesian grid later dominated proper architectural discourse and in many ways became the default system by which the architect starts the design process. This also manifests itself in modular construction materials including dimensional lumber, flat panels, and masonry units, all of which are orthogonally based. The Cartesian grid has direct implications to the solar impact of urban planning, in addition to the fact that it better accommodates most types of transportation. This organization system allows for strategies to be scaled up and down, and perhaps most importantly, it allows portions to be segmented and broken down into smaller components that can be more readily understood at the human scale.

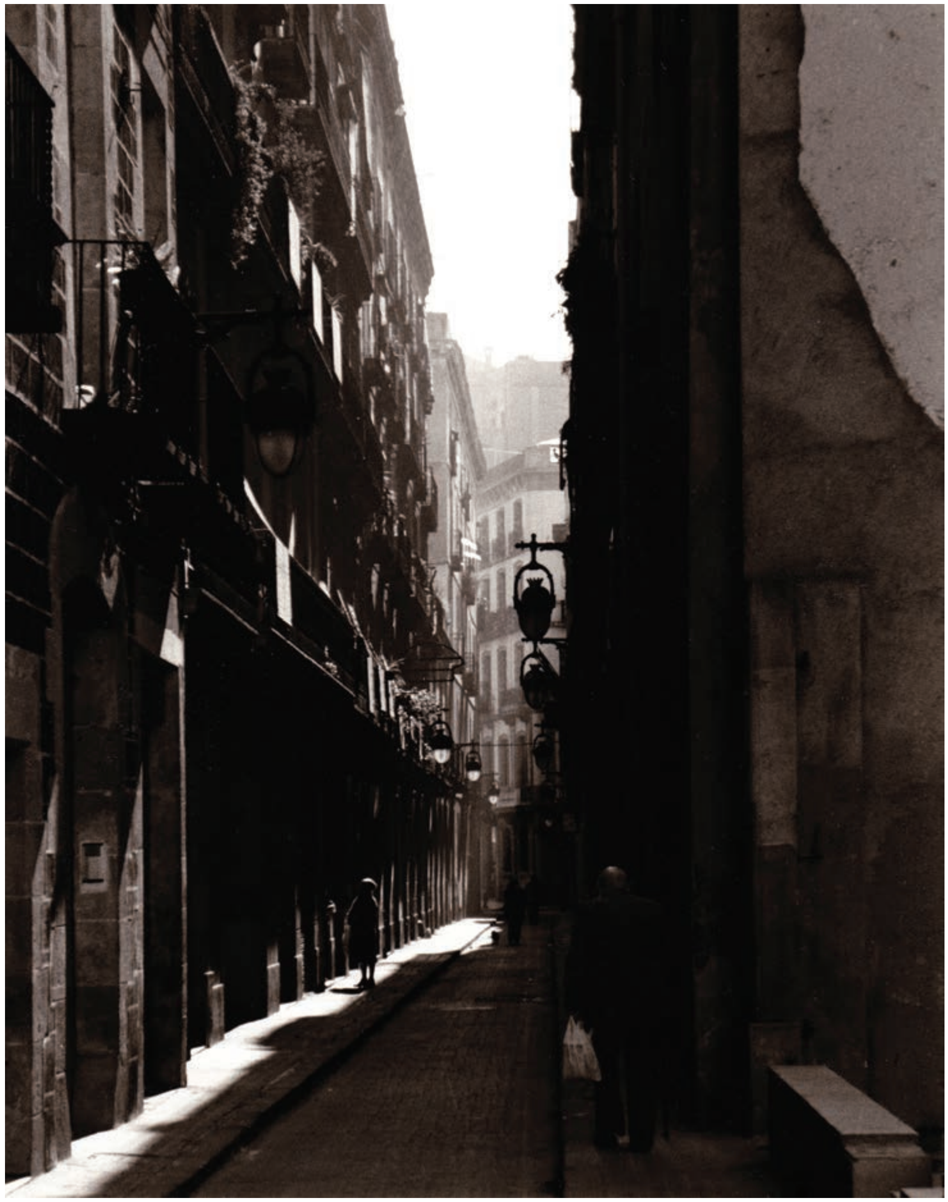

Figure 4.6
Barcelona (Barcino)
Matt Fajkus

PROPERTIES OF SOLAR RADIATION

For inhabitants of Earth, the sun is almost incomprehensibly large and powerful. While as stars go, it is not particularly notable, its diameter is 109 times that of Earth and each hour it emits 2.5 *billion* times the amount of energy consumed on Earth each year. The sun is powered by a fusion of hydrogen atoms into helium in its core. In its 4.5 billion-year life, the sun has used up approximately half of its total hydrogen stores. Photons emanate from the core of the sun, getting absorbed and re-emitted numerous times on their way to the surface. It takes one photon between 10,000 and 170,000 years to reach the surface of the sun,[5] but only eight minutes to travel to Earth.

The sun provides energy and heat that drives the weather process and is, ultimately, the source of all energy consumed by humans, whether present or ancient, except for nuclear sources. Solar radiation falls on the ***electromagnetic spectrum***

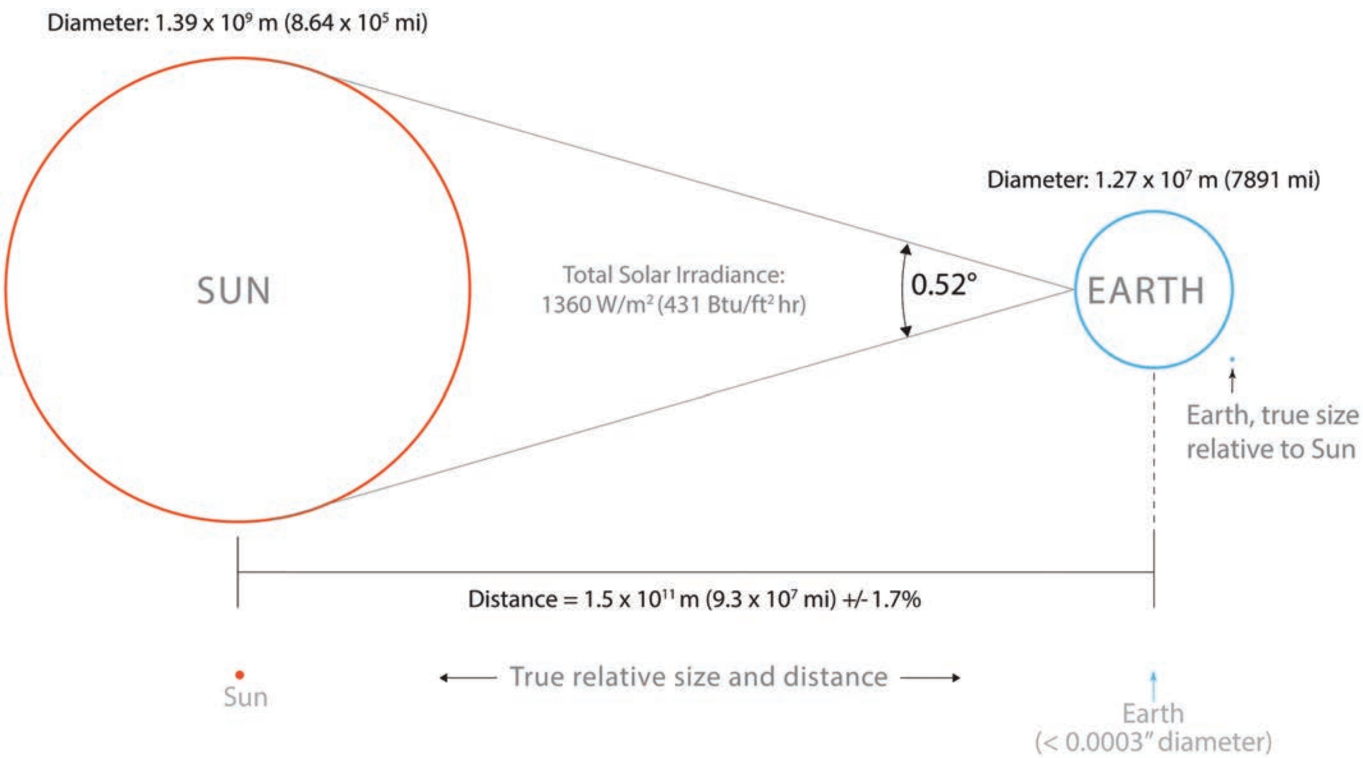

Figure 4.7

Relationship of the Sun and Earth

Due to the enormous distance between the sun and Earth, radiation from all portions of the sun facing the Earth arrive near parallel. For design purposes, we assume that the rays are in fact parallel at any position on Earth. The approximate half-degree solid angle encompassing the sun's diameter is not significant enough to affect design decisions.

Diagram after Duffie and Beckman, 2006; Greg Arcangeli

and is not to be confused with nuclear radiation. While electromagnetic radiation has characteristics of both particles and waves, nuclear radiation is composed of elementary particles emitted from the nuclei of atoms. Figure 4.7 shows some of the basic properties of the relationship between Sun and Earth.

The power of the various wavelengths in the solar spectrum varies dramatically. Figure 4.8 shows the power of different wavelengths outside and within the atmosphere. The red line represents the radiation of an ideal blackbody radiator at 5777 K. The sun is not a perfect blackbody, but the distribution of spectral power shows that it does approximate one. Note that the visible portion of the solar spectrum corresponds with the most powerful region. Humans evolved under solar radiation and our eyes developed to respond to the most abundant wavelengths of light. In fact, the visible section is centered on yellow-green at approximately 555 nanometers, the wavelength to which the eye is most sensitive.

Solar irradiance (*G*) measures the instantaneous power of incident solar radiation across the entire solar spectrum. It may be measured either in space perpendicular to the solar vector or on a surface in a particular orientation. Irradiance is the radiant flux, or rate of energy transfer per unit of time. Units of irradiance are usually W/m^2 (Btu/ft^2 h).

Solar irradiation (*I* for hourly, *D* for daily total) is the irradiance received on a surface over a given time period. Commonly referred to as ***insolation*** in the context of solar design, the terms irradiation and insolation are used interchangeably in this text. Units of irradiation are usually J/m^2 or Wh/m^2 (Btu/ft^2).

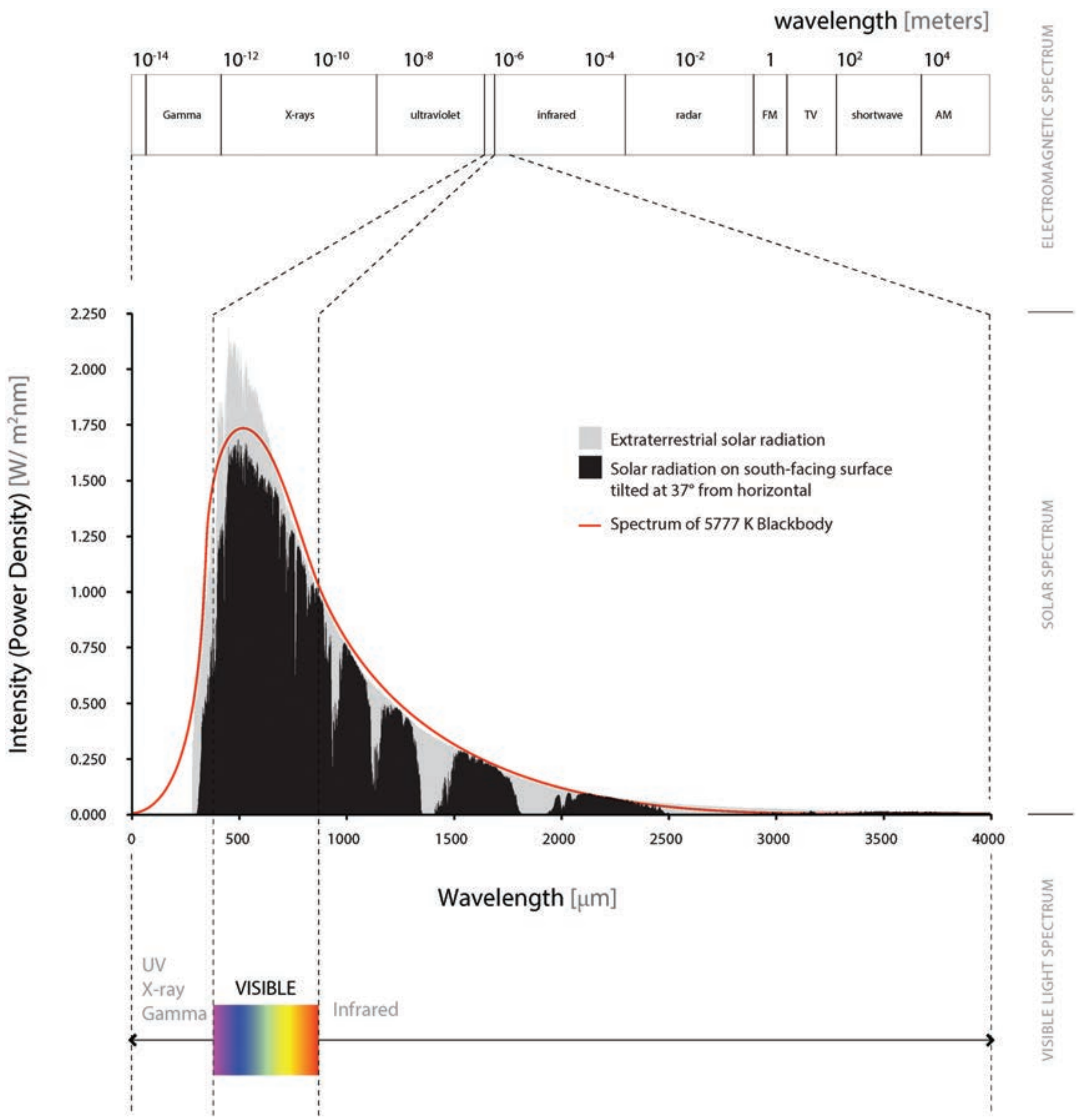

Figure 4.8
The Solar Radiation Spectrum
Greg Arcangeli

Extraterrestrial Solar Radiation

While the sun's radiation is emitted at a roughly constant rate, as a result of Earth's elliptical orbit, the power of radiation incident on the outer atmosphere varies over the course of the year. ***Total solar irradiance*** (*TSI*) is the radiant flux of the sun, or power of solar irradiance per unit area.[6] Formerly known as the ***solar constant***, *TSI* fluctuates approximately 0.1% over the 11-year solar sunspot cycle. Various studies have arrived at differing values for the *TSI*, but 1,360 W/m^2 (431 Btu/ft^2 h) is the value currently used by NASA.[7] The density of radiation arriving at the outer atmosphere varies with the Earth's position in its elliptical orbit as well. Calculate the actual ***extraterrestrial radiant flux*** (G_o) for any day of the year with a level of accuracy adequate for design using Equation 4.1.[8] For a more precise formula, see Iqbal.[9]

Equation 4.1 Extraterrestrial Radiant Flux

$$G_o = TSI\left[1 + 0.033\cos\left(\frac{360°n}{365}\right)\right]$$

EXAMPLE 4.1 CALCULATING EXTRATERRESTRIAL RADIANT FLUX

What is the extraterrestrial radiant flux on August 16?

$n = 136 \qquad TSI = 1{,}360\ \mathrm{W/m^2}$

Use Equation 4.1 to calculate.

$$G_o = TSI\left[1 + 0.033\cos\left(\frac{360°n}{365}\right)\right]$$

$$G_o = 1{,}360\,\frac{\mathrm{Wh}}{\mathrm{m}^2}\left[1 + 0.033\cos\left(\frac{360°*228}{365}\right)\right]$$

$$G_o = 1328\,\frac{\mathrm{Wh}}{\mathrm{m}^2}$$

The extraterrestrial radiant flux is uniform for the entire Earth on any given day, but the power of solar radiation arriving at the Earth's surface near the poles will be much lower than that striking the ground at solar noon near the equator because the same radiant flux is distributed over a significantly larger area due to the Earth's curvature. See Figure 4.9.

Because irradiance measures power, or a rate value at a particular instant, it tends to be easier to visualize than irradiation. *Insolation* is the cumulative effect of these

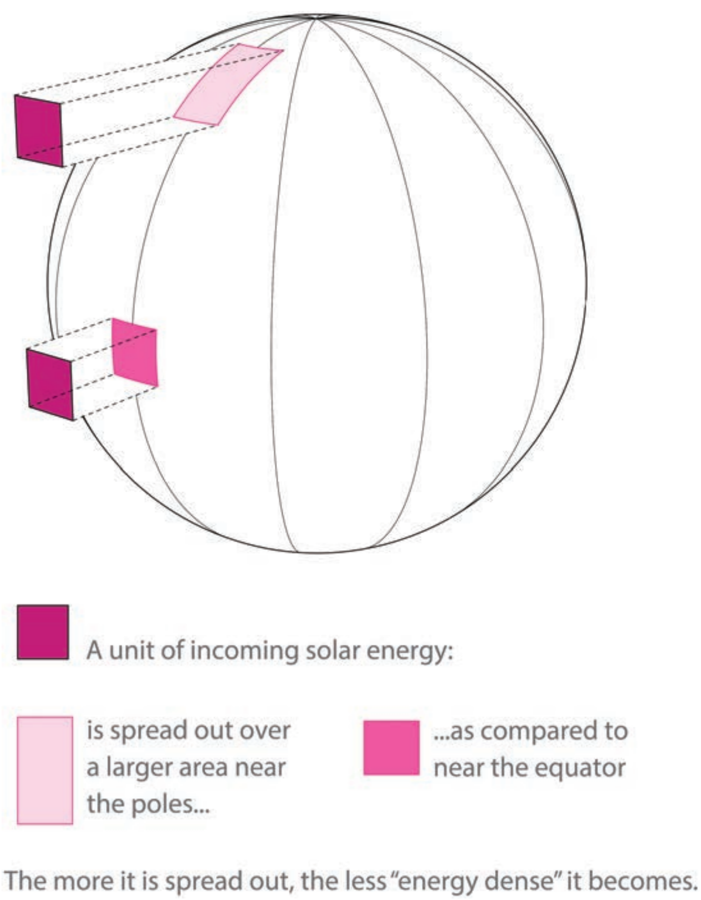

Figure 4.9

Solar Radiation Density on the Earth's Surface

Greg Arcangeli

instantaneous values integrated over time. As the power usually varies, the area under the curve of a power graph reflects total energy expended. In design practice, one usually works from hourly irradiance values that are taken to represent the average over that hour, and the totals for each hour are summed to approximate the total energy over the day, month, or year.

The three basic components of solar radiation (beam, sky diffuse, and reflected) transform into a wide array of parameters depending on how they are measured, classified, and aggregated. The intrinsic distance between observer experience and quantity of energy arriving from the sun over time makes this an abstract concept that takes some work to grasp intuitively.

Power vs. Energy—the Time Factor

The differences between instantaneous irradiance (*G*) values and energy values for irradiation (*I* for hourly, *D* for daily) were discussed previously. Any of the three radiation components can be, and frequently are, measured in all three of these forms. It is frequently necessary to convert between them. In many cases, the same formulas apply when doing calculations based on these different values. One must be careful, however, to avoid applying a variable that aggregates radiation values over time to an equation that depends on a particular sun position, or vice versa.

When looking at tables of hourly data, irradiance (*G*) and hourly irradiation (*I*) are usually interchangeable. For example, Table 4.1 (which gives hourly irradiance values

Table 4.1 Solar Radiation Data for Austin, Texas, May 9, 1980

Time	*Gb* (W/m^2)	*Gd* (W/m^2)
0:01–1:00	0	0
1:01–2:00	0	0
2:01–3:00	0	0
3:01–4:00	0	0
4:01–5:00	0	0
5:01–6:00	1	6
6:01–7:00	202	53
7:01–8:00	505	102
8:01–9:00	658	143
9:01–10:00	743	174
10:01–11:00	795	194
11:01–12:00	816	205
12:01–13:00	823	209
13:01–14:00	814	204
14:01–15:00	789	192
15:01–16:00	734	171
16:01–17:00	637	142
17:01–18:00	470	99
18:01–19:00	153	50
19:01–20:00	0	1
20:01–21:00	0	0
21:01–22:00	0	0
22:01–23:00	0	0
23:01–24:00	0	0
		1,945 Wh/m^2

from a weather file for Austin, Texas, used for energy simulation[10]) shows sky diffuse irradiance (G_d) from 10:01–11:00 as 194 W/m^2. This irradiance value is meant to represent an average for the preceding hour. Using Equation 4.1, the irradiation over that hour would be 194 W/m^2 x 1 hour = 194 Wh/m^2.

Likewise, when irradiation is given in hourly tables, dividing by one hour gives the average irradiation over that hour. If maximum or minimum irradiance values are indicated, this translation is not valid. If sub-hourly values are given, or if doing sub-hourly calculations based on hourly data, appropriate adjustments are required.

This text will primarily work in terms of hourly irradiation (I) and daily total irradiation (D) when looking at surfaces because those values are more commonly available and represent metrics most useful in energy analysis. When designing buildings, we are more concerned about typical conditions than moment-to-moment fluctuations. If working with sub-hourly calculations, this is not the case.

Daily total irradiation (D) is generally calculated as the sum of the irradiation over each timestep during the day. Looking at Table 4.1 once more, the daily total sky diffuse irradiation (D_d) is the sum of the hourly horizontal sky diffuse values—1,945 Wh/m^2. This value may be read as energy in Wh/m^2, although the hourly values are power (W/m^2) for the reason described previously. Direct beam values are not summed because these are measured normal to the ray of the sun, so a total would only make sense for a surface tracking the sun.

Terrestrial Solar Radiation

When extraterrestrial radiation strikes the atmosphere, one of several things happens—it is either reflected, transmitted directly, scattered, or absorbed by the atmosphere, as shown in Figure 4.10. The radiation that does make it to the surface of the Earth impacts building surfaces in three primary forms: direct beam, sky diffuse, and ground reflected radiation. These components of solar radiation will be discussed in the following section.

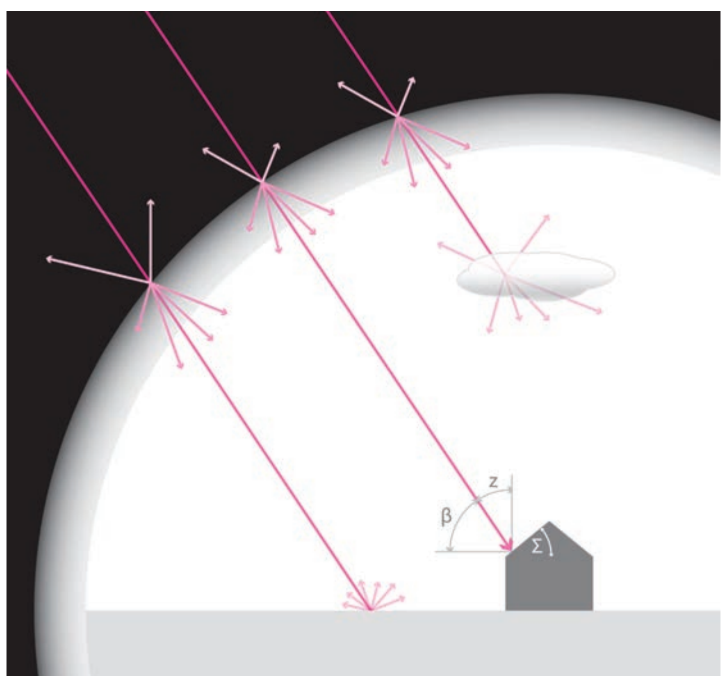

Figure 4.10

Interaction of Solar Radiation and the Atmosphere

Greg Arcangeli

Each of these three forms can be measured in terms of instantaneous power or energy over a period of time. Instantaneous power values are useful to understand the impact of the continually moving solar ray on a surface at any moment in time, while energy values provide insight into the net impact of the sun on a surface over time. Common timeframes to consider range from one day to a month, a season, or a year. Each of these provides important information in different contexts.

Figure 4.11 shows proportionately how the components of radiation are distributed in the atmosphere and how they contribute to the Earth's heat balance.

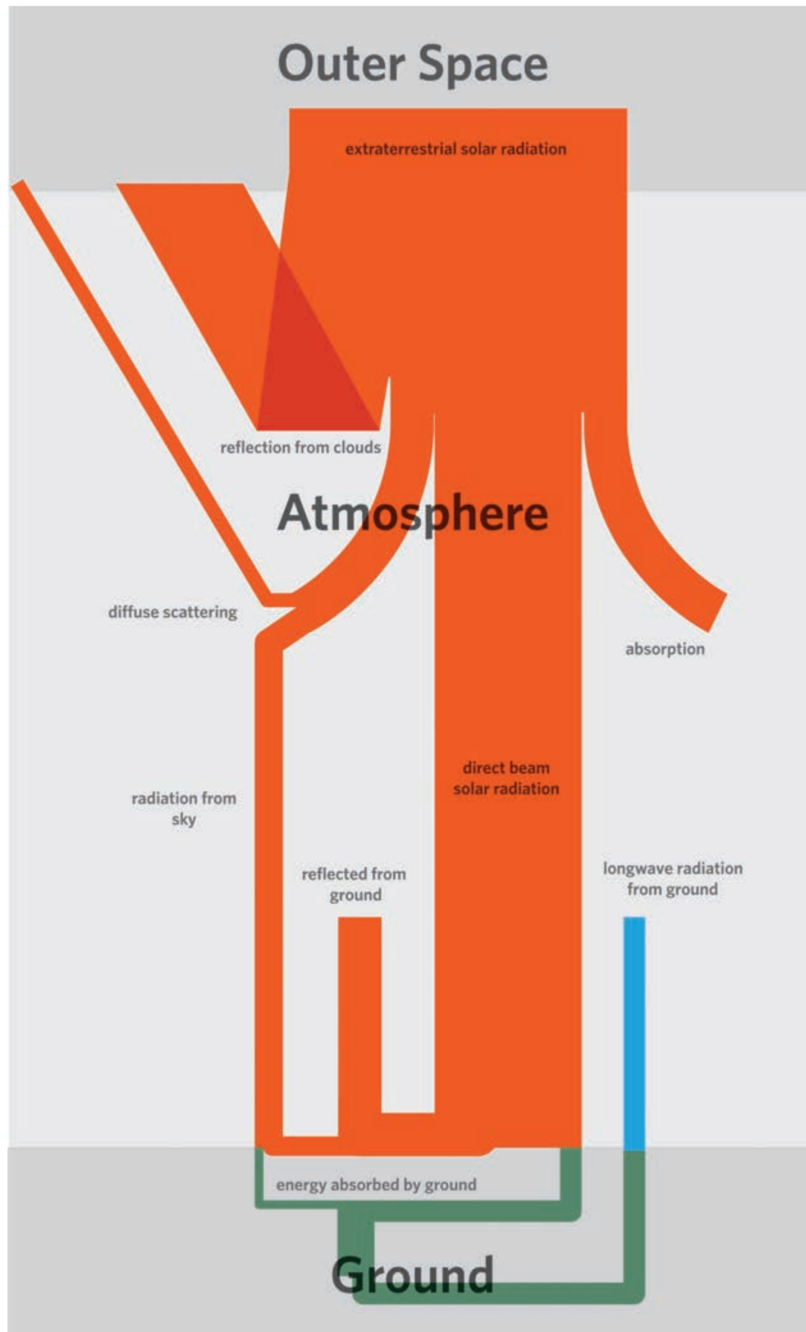

Figure 4.11
Solar Radiation Flows
Greg Arcangeli

SOLAR RADIATION COMPONENTS

Calculating the quantity of radiation falling on a surface is a relatively straightforward process once one has the relevant surface and climatic data. Often, the primary challenge lies not in determining the radiation received on a surface, but in determining the appropriate solar radiation values to use for a given location. Understanding the components of solar radiation that affect building surfaces is necessary in order to identify appropriate data types.

Beam Radiation

The component of solar radiation that first comes to mind for most is ***direct beam irradiance*** (G_b), also known as *beam, direct, and direct normal irradiance*. The corresponding symbol for ***hourly direct beam insolation*** is I_b and for ***daily total direct beam insolation***, it is D_{tb}. This is the portion of solar radiation arriving from the sun, passing through the atmosphere unobstructed, and directly striking a surface—in other words, the direct rays of the sun. When you turn your face to the sun on a cold winter day and soak up its pleasing heat, you are relishing direct beam irradiance.

The direct beam component of irradiance is measured as a rate of heat flux or power per unit area on a surface normal to the solar ray in W/m^2. The value of direct beam irradiance is always reduced from the full extraterrestrial value (G_o), as some of the radiation is reflected, scattered, and absorbed by the atmosphere. Because the sun is in constant motion relative to an observer on Earth, the imaginary plane normal to the sun's ray upon which beam radiation is measured is constantly rotating as well.

To develop a sense of what irradiance values mean in the real world, the high end of direct beam irradiance that most of us are likely to experience is around 1,000 W/m^2 (the highest beam irradiance value in NREL's TMY3 dataset for Phoenix, Arizona, is 1,034 W/m^2).[11] The solar flux at which photovoltaic cell power ratings are set also happens to be 1,000 W/m^2. On the average August day in Austin, Texas (known for its hot summers), direct beam irradiance reaches a maximum 567 W/m^2.[12] On the average December day in London, direct beam irradiance only reaches 137 W/m^2.[13] Near sunset, typical values are in the range of 10–20 W/m^2, and of course go to zero after sunset.

Diffuse Sky Radiation

A substantial amount of solar radiation is scattered in the atmosphere, arriving on surfaces as non-directional diffuse radiation. Under clear skies, ***sky diffuse irradiance*** (G_d) is mainly the result of ***Rayleigh scattering***, the diffusion of light by particles smaller than the wavelength of the radiation. The sky appears blue because this scattering is more pronounced at the shorter wavelengths of the visible spectrum. Conversely, the sun appears yellowish because the radiation in the longer wavelengths of its spectrum have not been scattered as much. Overcast skies have the effect of producing a more uniform diffusion of light and can fully convert the direct component to diffuse. The corresponding symbol for ***hourly sky diffuse insolation*** is I_d and for ***daily total sky diffuse insolation***, it is D_d.

Reflected Radiation

Radiation also arrives at surfaces having been reflected by other surfaces. The importance of this component ranges from nominal to significant depending on the circumstances. ***Ground reflected diffuse irradiance*** ($G\gamma$) results from both direct beam and diffuse sky radiation that has struck the ground and been reflected. Ground surfaces tend to be highly diffuse, meaning that they scatter light non-directionally, with the exception of water, which can be highly specular at low sun angles. The corresponding symbol for ***hourly ground reflected diffuse insolation*** is I_g and for ***daily total ground reflected diffuse insolation***, it is D_g.

Ground reflected radiation is usually the most important source of reflected radiation. Urban contexts are the most common exception to this, where other buildings, especially those with mirrored glass or geometries that focus radiation on a certain area, can have an enormous impact. In such cases, the reflected radiation may either be specular or diffuse and must be taken into account by analyzing the specific additional components.

Global Radiation

Global radiation (G, I, or D) is the sum of all components of solar radiation incident on a horizontal surface. Often, climate data report this value. Global horizontal values include only the beam and sky diffuse components incident on the horizontal. Because a horizontal surface faces the zenith, there is no ground reflected component to this value. If one also knows the corresponding sky diffuse horizontal value, subtraction will yield the beam radiation on a horizontal plane.

Perception of Solar Radiation Components

Under clear or mostly clear skies, the direct beam component dominates the various components of solar irradiance. This is apparent from the experience almost everyone has had on a hot summer day. Imagine first standing with your back to a west-facing wall on a summer afternoon exposed to the blistering sun, then moving to stand in the shade on the other side of the wall, blocking the direct sun. Being shaded from the direct rays of the sun provides immediate relief even though the ambient temperature and exposure to diffuse radiation from the sky and ground have not changed. The radiant temperature, however, has dropped considerably due to the obstruction of the sun's direct radiation. Sky diffuse radiation is the most desirable source for daylight, although many people have also had the experience of getting sunburned even on overcast days by diffuse radiation.

The potential power of ground reflected radiation is apparent to anyone who has spent time around snow in the sun. The high reflectivity of fresh snow means that nearly as much reflected radiation is coming from the ground as global radiation from above (see Table 5.1). This results in not only bright, potentially sunburn-inducing conditions, but also a relatively high radiant temperature despite the low temperature of the snow. The moment the sun passes behind a cloud, however, the radiant temperature drops dramatically and immediately changes one's perception of comfort without any change in air temperature.

SOLAR RADIATION DATA

Extraterrestrial solar radiation incident on the Earth's atmosphere may be calculated using Equation 4.1, but the fraction of that radiation making it to the surface of the Earth varies based on local weather conditions. It is possible to estimate the values for terrestrial radiation components through calculations, but these calculations are not very reliable, and obtaining the necessary input parameters is difficult. It is preferable to have actual measured data for a given location if it is available.

Data Collection

Because of the ways solar radiation measurement instruments work, as well as varying conventions, one will often find the three basic components of solar radiation (beam, sky diffuse, and ground reflected) aggregated in several different ways. Two instrument types are used for taking solar radiation measurements. Pyroheliometers measure beam radiation and must be aimed directly at the sun, posing a challenge to their use in a weather station. Pyranometers have a fixed hemispherical dome over a sensor and measure beam and diffuse radiation. They are simpler to use and are more common than pyroheliometers for solar radiation data collection.[14]

Because a pyranometer measures both beam and diffuse radiation and is generally mounted horizontally, the basic value recorded is global horizontal irradiance (G). To determine beam radiation values, a second pyranometer with a shield to block the beam portion of radiation is used to measure the horizontal diffuse irradiance (G_{dh}). Beam irradiance on the horizontal (G_{bh}) is derived by subtracting the diffuse value from global. Once beam on the horizontal is known, direct beam normal may be calculated with the knowledge of solar altitude.

Because the pyranometer has only one sensor, it cannot differentiate the direction of received diffuse radiation, so the availability of measured data on the brightness of different portions of the sky dome is limited. The instrument also cannot detect ground reflected radiation because it is horizontal, but this can be calculated based on the other known values. Individual sources of radiation data then parse the collected data in various ways, ranging from aggregating longer time periods to breaking out the components differently.

Solar Radiation Data Types

In order to quantify the impact of solar radiation on a surface, one needs data on the amount of radiation available. Determining the best source of solar radiation data to use for analysis is not as simple as it might seem. Reliable empirical data averaged or otherwise selected over the long-term to provide a good picture of typical solar radiation values for a particular location is best for use in design. Specific weather data from a particular day or year is only useful when attempting to reproduce particular performance conditions, such as when calibrating a simulation model to actual performance data. For design purposes, it is important to use data that are representative of expected trends.

Data for a Changing Climate

How climate data should be selected in the context of accelerating climate change is an area of ongoing exploration and several methods have been proposed for producing data reflecting predicted trends.[15] This will be an area of expanding interest as the effects of climate change become increasingly apparent. Organizations that create weather data files will likely begin to produce climate-change scenario data files for general use in the future.

At present, however, the available solar data are primarily based on historical trends. Data for a huge number of sites worldwide are readily available today, and most of these datasets include solar radiation values.

To estimate how solar radiation impacts building surfaces, two values are needed for each hour: direct beam normal and sky diffuse irradiance or irradiation (G_b and G_d, or I_b and I_d). Several sources for radiation data, as well as procedures for extracting these values from the available data, will be discussed in the following section.

Historical Weather Data

Historical weather data come direct from weather stations for particular time periods with little or no processing. Its main use to architects and engineers is for calibrated energy simulation of existing buildings in the attempt to align modeled performance with actual utility bills and other measured operational data. This type of data is readily available, but of limited use in design because it reflects day-to-day weather that may not be representative of typical conditions.

Weather Data Files

Weather data files are designed to provide the climatic input for energy simulation. It should be noted that weather data files are compiled using a protocol that attempts to reproduce a typical year of weather for a specific location, including normal day-to-day variability. This is accomplished by compiling 12 individual 1-month periods of actual measured data statistically most representative of each month during the total period of the dataset. So, weather data files are frequently composed of 12 actual months from different years.

Unfortunately, solar radiation values are among the least reliable data contained in weather files because few weather stations have equipment for collecting this data, and of those that do, calibration and data collection problems are common.[16] For those stations that do not have radiation monitoring equipment, radiation data are estimated through calculations that attempt to account for weather conditions.

One of the most comprehensive sources for this type of climatic data is the EnergyPlus Weather Data for Simulation available for free through the United States Department of Energy.[17] Data for thousands of locations worldwide can be viewed by importing the files into a spreadsheet program or with other specialized viewer applications. In addition, typical values of important climatic variables, including average hourly solar radiation for each month, may be downloaded along with the weather data files.

For U.S. locations, another excellent source of weather data is the National Solar Radiation Database Typical Meteorological Year 3 (TMY3) files.[18] Files are provided in .csv format and the hourly average direct beam normal irradiance (G_b) values are in column H, labeled DNI (W/m^2). Hourly average diffuse irradiance on the horizontal (G_d) is in column K, labeled DHI (W/m^2). As noted previously, these values may be read as irradiation for each hour in W/m^2 as well.

The data in weather files are generally recorded in local standard time, so the appropriate conversion to apparent solar time for determining solar position is necessary. If local (clock) time is desired, one must convert for daylight saving time as well.

Within energy simulation programs that model building performance hour-by-hour for the entire year, simulating the day-to-day variability in weather conditions is desirable in order to model how the building will respond to realistic weather conditions. For hand or spreadsheet calculations in design, however, day-by-day calculations are impractical and we are generally more interested in average values for a month or season rather than the conditions on one particular day. Therefore, weather data files are not well-suited for design calculations without additional processing.

One excellent tool for processing and analyzing weather data files to evaluate climatic conditions is Climate Consultant.[19] This free computer program analyzes and creates plots of typical weather data according to a set of input parameters provided by the user.

Statistical Summary Data

For design calculations, we are interested in typical conditions, so it is usually most desirable to have radiation values that represent averages. Typical extreme conditions can also be valuable. Statistical summary data may be broken out into hourly values, but often are aggregated into monthly average daily total values that should be broken out into hourly values for the purpose of calculations.

Statistical summary data files may also be downloaded with EnergyPlus weather files. These files provide one of the best sources of solar radiation data for design because of their ease of use and plethora of locations. Table 4.2 shows the typical radiation data for Austin, Texas, from the EnergyPlus weather statistics file. Direct Average is the average daily total of direct beam irradiance that a surface tracking the sun's position would receive each month. Direct Maximum is the highest direct beam value for the month and the day of the month on which that maximum occurs. Diffuse Average is the daily total diffuse radiation a horizontal surface would receive each day of that month (D_d), and Global Average is the average total irradiation a horizontal surface would receive on a typical day of the month (D). The total of Direct Average and Diffuse Average exceeds Global Horizontal Average because direct is measured normal to the sun's rays while diffuse and global are taken on a horizontal surface. Note that the maximum direct beam total for each month ranges from 1.6–2.5 times the average for this location. In areas with very clear skies, this multiple tends to be smaller.

The data in Table 4.2 include hourly direct beam normal values (I_b) that are ready to use for surface insolation calculations. In cases where beam insolation on the horizontal (I_{bh}) is given, rearrange Equation 5.13 to solve for I_b. For the average hourly values of direct normal radiation, the units for the time bins shown are Wh/m^2, a unit of energy. This table may also be read as representing the average power of solar radiation in W/m^2 during each hour of the day. Note, however, that any given hour of direct sun can have significantly varying irradiance levels with the passing of clouds. Figure 4.12 is a plot of the values from this table for four representative months. Here, it is interesting to note that direct normal irradiance levels during the course of a day are similar in November, January, and April, with only the month of July showing a significant increase in power, which also coincides with the longest days of the months shown.

Table 4.2 Average Solar Radiation Values for Austin, Texas, from EnergyPlus Weather Statistics File

Austin, Texas, USA

WMO Station 722544	L = *30.3° N*, LON = *97.8° W*	*UTC -6.0 Hours*

Monthly Statistics for Solar Radiation: Direct Normal, Diffuse, Global Horizontal [Wh/m²]

	Jan	*Feb*	*Mar*	*Apr*	*May*	*Jun*	*Jul*	*Aug*	*Sep*	*Oct*	*Nov*	*Dec*
Direct Average	3,622	3,840	4,907	4,533	4,464	5,523	6,093	5,900	4,783	5,012	3,982	3,609
Direct Maximum	8,826	9,442	10,196	10,227	8,565	9,939	10,250	9,294	9,385	8,046	8,275	8,374
Day of Month	24	23	20	6	24	7	22	27	26	14	11	8
Diffuse Average	1,320	1,565	1,847	2,232	2,608	2,534	2,311	2,191	2,012	1,483	1,363	1,182
Global Horizontal Average	3,016	3,627	4,850	5,403	5,914	6,666	6,760	6,353	5,228	4,300	3,341	2,790
Maximum Direct Normal Solar of 10,250 Wh/m² on Jul 22												

Average Hourly Statistics for Direct Normal Solar Radiation [Wh/m²]

	Jan	*Feb*	*Mar*	*Apr*	*May*	*Jun*	*Jul*	*Aug*	*Sep*	*Oct*	*Nov*	*Dec*
0:01–1:00	0	0	0	0	0	0	0	0	0	0	0	0
1:01–2:00	0	0	0	0	0	0	0	0	0	0	0	0
2:01–3:00	0	0	0	0	0	0	0	0	0	0	0	0
3:01–4:00	0	0	0	0	0	0	0	0	0	0	0	0
4:01–5:00	0	0	0	0	0	0	0	0	0	0	0	0
5:01–6:00	0	0	0	0	2	10	6		0	0	0	0
6:01–7:00	0	0	11	45	64	124	158	121	37	9	3	0
7:01–8:00	45	89	207	200	195	212	276	372	187	208	142	70
8:01–9:00	233	266	344	304	295	366	421	438	313	356	288	248
9:01–10:00	364	331	393	370	387	462	526	540	436	451	388	369
10:01–11:00	405	412	442	457	424	529	592	595	477	453	424	409
11:01–12:00	439	425	469	486	444	581	589	610	553	495	482	432
12:01–13:00	478	480	551	482	483	596	601	576	536	564	501	455
13:01–14:00	448	468	522	520	477	541	606	560	550	626	501	459
14:01–15:00	421	418	542	520	400	537	539	567	497	612	485	444
15:01–16:00	397	419	549	418	432	481	562	494	492	583	411	391
16:01–17:00	283	326	473	345	424	440	495	508	410	466	299	275
17:01–18:00	108	191	344	279	302	400	432	362	254	188	56	57
18:01–19:00	0	14	59	105	130	223	260	151	43	0	0	0
19:01–20:00	0	0	0	0	4	22	28	4	0	0	0	0
20:01–21:00	0	0	0	0	0	0	0	0	0	0	0	0
21:01–22:00	0	0	0	0	0	0	0	0	0	0	0	0
22:01–23:00	0	0	0	0	0	0	0	0	0	0	0	0
23:01–24:00	0	0	0	0	0	0	0	0	0	0	0	0
Max Hour	13	13	13	14	13	13	14	12	12	14	13	14
Min Hour	1	1	1	1	1	1	1	1	1	1	1	1

Values extracted from Austin-Camp Mabry 722544 (TMY3) stat file.[20]

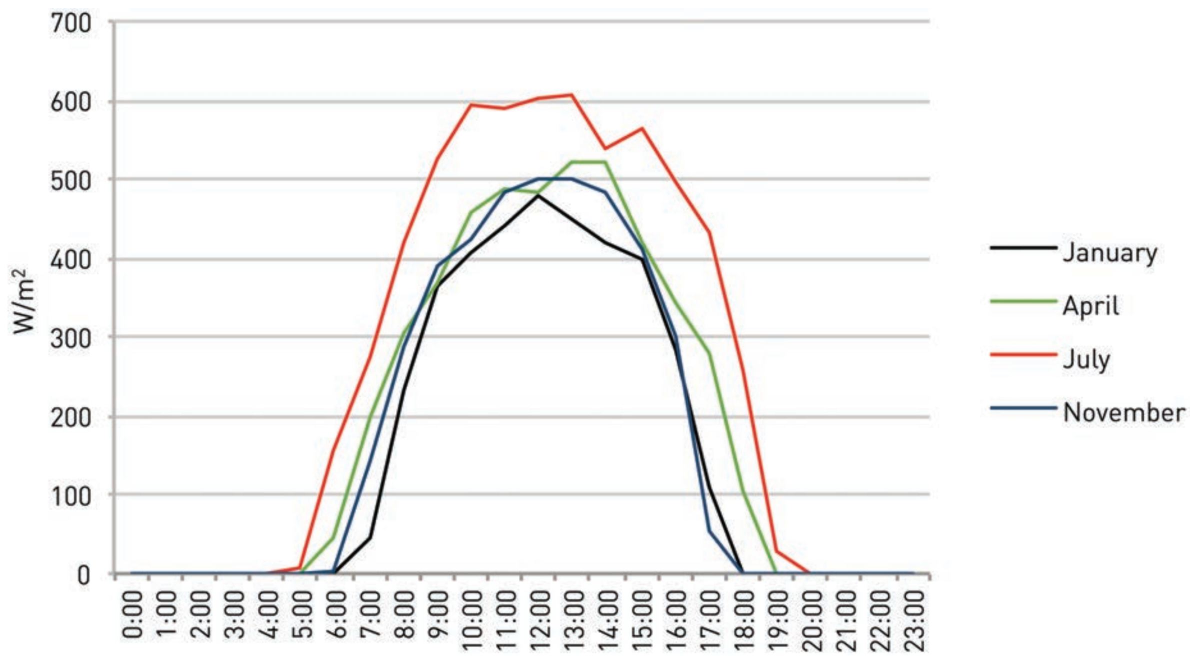

Figure 4.12

Hourly Average Direct Normal Irradiance for Austin, Texas, in Selected Months

Dason Whitsett

For diffuse, daily total (D_d) values are shown in Table 4.2. These must be converted to hourly diffuse (I_d) values for surface insolation calculations. Doing so first requires calculating the *hourly fraction of sky diffuse insolation* (r_d) from the equations by Liu and Jordan[21] as cited by Duffie and Beckman.[22] This is the estimated ratio of sky diffuse radiation for a given hour to the daily total. Equation 4.2 calculates this ratio such that the average daily total diffuse radiation incident on the horizontal for a given location is distributed in a typical proportion over the hours between sunrise and sunset. Use the hour angle (H) for the hour in question. This equation does not capture the actual variability that might occur in a day due to changing cloud cover, but it does allow one to use statistical daily total data for diffuse radiation. Once the hourly diffuse fraction is obtained, multiply by the daily total diffuse on the horizontal value to obtain the hourly diffuse insolation, as shown in Equation 4.3.

Equation 4.2 Hourly Fraction of Sky Diffuse Insolation

$$r_d = \frac{\pi}{24}\left(\frac{\cos H - \cos H_{ss}}{\sin H_{ss} - \frac{\pi H_{ss}}{180}\cos H_{ss}}\right)$$

Equation 4.3 Estimated Hourly Sky Diffuse Insolation from Daily Value

$$I_d = D_d\, r_d$$

EXAMPLE 4.2 CONVERTING DAILY TOTAL DIFFUSE RADIATION TO ESTIMATED HOURLY VALUE

Based on the summary radiation data in Table 4.2, what is the estimated hourly diffuse insolation in the $LST = 16{:}01 = 17{:}00$ hour for the typical August day in Austin, Texas?

The daily total diffuse insolation value (D_d) from the table is 2,191 Wh/m^2. To arrive at the most representative value for the hour, the calculations will be performed for $LST = 16{:}30$ using August 16 as the average day of the month. Using methods developed in Chapter 3, we find the following:

16:30 $LST = 15{:}54$ AST, $H = 58.59°$, and $H_{ss} = 98.04°$

1) Use Equation 4.2 to calculate r_d.

$$r_d = \frac{\pi}{24} \cdot \frac{\cos H - \cos H_{ss}}{\sin H_{ss} - \frac{\pi H_{ss}}{180} \cos H_{ss}}$$

$$r_d = \frac{\pi}{24} \cdot \frac{\cos(58.59°) - \cos(98.04°)}{\sin(98.04°) - \frac{\pi(98.04°)}{180} \cos(98.04°)}$$

$$r_d = 0.07$$

So, 7% of the day's total horizontal diffuse insolation is estimated to arrive in the 16:00 hour.

2) Use Equation 4.3 to find I_d.

$$I_d = D_d\, r_d = \left(2{,}191 \frac{Wh}{m^2}\right)(0.07) = 153 \frac{Wh}{m^2}$$

Figure 4.13 shows graphs of the daily total radiation month-by-month from the data in Table 4.2. In this example location, direct normal radiation levels are lowest in December and January as one would expect, and peak in July. The dip in direct normal radiation in the more overcast months of April and May coincides with the peak in diffuse radiation as a result of scattering by clouds. Although the totals for

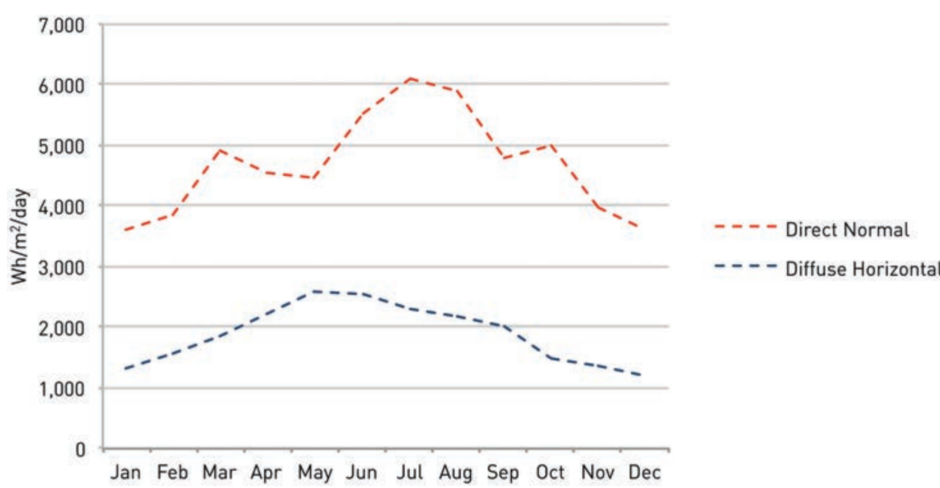

Figure 4.13

Average Daily Total Irradiation for Austin, Texas.

Dason Whitsett

TIP

The weather data statistics (.stat) file that is available along with EnergyPlus weather files comes as part of the compressed .zip file for any location. This file is in text format and may be read with any common text reader application. To make use of this data, however, it is much more useful to access it from a spreadsheet. To use it in most spreadsheet applications, import it as a tab delimited text file. Often, the application will detect this automatically. Finishing the import process will create a long table of data in the new worksheet. Scroll down to locate the solar radiation data. Once the data are in the spreadsheet, you can use the lookup functions to find the appropriate values for a given date within the data.

winter are significantly lower than summer, the global average value of 2,790 Wh/m^2 in December is plenty to justify the utilization of passive or active solar strategies. The July global value of 6,760 Wh/m^2 indicates that shading is a primary concern in summer.

Global Daily Total Statistical Data

For quick estimates of the solar impact on surfaces of various tilts and orientations, a good source for United States locations is the National Renewable Energy Laboratory's Solar Radiation Data Manual (SRDM).[23] This is a compendium providing average directional daily radiation values along with other climatic and design data for 239 locations. Of these, 56 are primary stations that measure solar radiation directly, while the remainder are secondary stations with solar radiation values modeled based on meteorological data collected at the station location.

As shown in Table 4.3, the SRDM gives values for daily total global (D_h) and diffuse (D_d) incident on surfaces facing in each of the cardinal directions as well as horizontal for each month of the year. To determine the direct beam component, subtract the diffuse from the global value. This type of chart is extremely useful for quickly estimating the impact of building and window orientation on solar heat gain. Clear Day Global is the value expected for global insolation on a day with completely clear skies. The difference between the global and clear day global values gives a good sense of how overcast a place tends to be in that month. For Austin, Texas, clear day global values are generally somewhat higher than the average global values, indicating a moderate level of average cloud cover. Note that in January, however, global values are higher for north-facing and horizontal surfaces. At that time of year, cloud cover brings more diffuse radiation to those surfaces that experience no direct gain or high angles of incidence under clear skies.

The manual also provides general climatic information and estimates of the heat gain through windows facing each of these directions with and without a basic shading overhang.

If only daily totals for global horizontal and diffuse radiation are available, then both will need to be converted. Use Equations 4.2 and 4.3 for diffuse. For global values, start by calculating the ***hourly fraction of global insolation*** (r_t) developed by Collares-Pereira and Rabl.[25] This is the ratio of hourly to daily total global radiation on the horizontal. Equation 4.4 makes use of the hourly diffuse ratio calculated by Equation 4.2 from the previous section. Estimate the hourly value for global horizontal radiation (I) by multiplying the hourly fraction by the daily total for global (D) per Equation 4.5.

Equation 4.4 Hourly Fraction of Global Insolation

$$r_t = (a + b^*\cos H) r_d$$

where

Equation 4.4a Hourly Global Ratio Coefficient A

$$a = 0.409 + 0.5016\sin(H_{ss} - 60°)$$

Equation 4.4b Hourly Global Ratio Coefficient B

$$b = 0.6609 - 0.4767\sin(H_{ss} - 60°)$$

Table 4.3 Daily Total Insolation for Austin, Texas

Average Insolation (Wh/m²) Uncertainty = 9%

Surface Direction	*Component*	*Jan*	*Feb*	*Mar*	*Apr*	*May*	*Jun*	*Jul*	*Aug*	*Sep*	*Oct*	*Nov*	*Dec*	*Annual*
Horizontal	Global	2,965	3,786	4,732	5,426	5,899	6,593	6,782	6,341	5,237	4,353	3,312	2,776	4,858
	Std.Dev.	243	306	366	508	470	410	432	350	372	344	325	215	101
	Minimum	2,524	3,091	3,912	4,669	4,574	5,710	5,584	5,489	4,448	3,502	2,524	2,429	4,732
	Maximum	3,502	4,416	5,489	6,625	6,656	7,287	7,508	7,035	6,088	4,890	3,943	3,407	5,079
	Diffuse	1,293	1,546	1,987	2,334	2,618	2,555	2,366	2,208	2,019	1,577	1,325	1,199	1,924
	Clear Day Global	1,320	5,142	6,404	7,508	8,076	8,265	8,107	7,571	6,625	5,426	4,322	3,817	6,278
North	Global	852	1,009	1,262	1,451	1,767	2,019	1,924	1,577	1,293	1,073	883	789	1,325
	Diffuse	852	1,009	1,262	1,420	1,577	1,640	1,609	1,451	1,293	1,073	883	789	1,230
	Clear Day Global	757	915	1,136	1,388	1,861	2,240	2,050	1,546	1,167	978	789	726	1,293
East	Global	1,798	2,177	2,555	2,744	2,839	3,186	3,470	3,375	2,871	2,461	1,956	1,703	2,587
	Diffuse	1,009	1,199	1,483	1,703	1,830	1,924	1,924	1,830	1,609	1,325	1,073	946	1,483
	Clear Day Global	2,776	3,312	3,849	4,227	4,385	4,385	4,322	4,227	3,880	3,375	2,839	2,587	3,691
South	Global	3,786	3,817	3,407	2,681	2,082	1,861	2,019	2,587	3,281	3,975	3,975	3,786	3,091
	Diffuse	1,325	1,451	1,640	1,672	1,640	1,609	1,609	1,672	1,703	1,577	1,388	1,262	1,546
	Clear Day Global	6,467	6,088	5,047	3,439	2,334	1,924	2,082	2,934	4,290	5,584	6,246	6,435	4,385
West	Global	1,924	2,397	2,902	3,155	3,344	3,691	3,659	3,470	3,060	2,744	2,145	1,830	2,871
	Diffuse	1,041	1,230	1,546	1,767	1,924	1,987	1,956	1,861	1,640	1,356	1,104	946	1,514
	Clear Day Global	2,776	3,312	3,849	4,227	4,385	4,385	4,322	4,227	3,880	3,375	2,839	2,587	3,691

The values in this table come from the NREL SRDM[24] and have been converted to SI units.

Equation 4.4 Hourly Fraction of Global Insolation

$r_t = (a + b^{*}\cos H)r_d$

where:

Equation 4.4a) $a = 0.409 + 0.5016\sin(H_{ss} - 60°)$
Equation 4.4b) $b = 0.6609 - 0.4767\sin(H_{ss} - 60°)$
Equation 4.5 Estimated Hourly Global Horizontal Insolation from Daily Total

$I = D\, r_t$

Rearranging and combining the terms from other equations yields the expression for hourly direct beam (I_b) in terms of I and I_d shown in Equation 4.6.

Equation 4.6 Hourly Beam Insolation from Global Horizontal and Sky Diffuse

$$I_b = \frac{I - I_d}{\sin\beta_{sol}}$$

EXAMPLE 4.3 CONVERTING DAILY TOTAL GLOBAL INSOLATION TO ESTIMATED HOURLY BEAM VALUE

What is the estimated amount of daily total global irradiation expected in the 16:01–17:00 hour in Austin, Texas?

To arrive at the most representative value for the hour, the calculations will be performed for LST = 16:30 using August 16 as the average day of the month. Using methods developed in Chapter 3, we found the following in Example 4.2:

16:30 LST = 15:54 AST, $H = 58.59°$, $H_{ss} = 98.04°$, $r_d = 0.07$, and $I_d = 153\ \text{Wh/m}^2$

From Table 4.2, the average global horizontal daily total insolation (D) is 6,353 Wh/m^2.

1) Use Equations 4.4 and 4.4a–b to find r_t.

$a = 0.409 + 0.5016\sin(H_{ss} - 60°)$

$a = 0.409 + 0.5016\sin(98.04° - 60.00°)$

$a = 0.72$

$b = 0.6609 - 0.4767\sin(H_{ss} - 60°)$

$b = 0.6609 - 0.4767\sin(98.04° - 60.00°)$

$b = 0.37$

$r_t = (a + b\cos H)r_d$

$r_t = (0.72 + 0.37\cos(58.59°))0.07$

$r_t = r_t = 0.06$

2) Use Equation 4.5 to find the estimated hourly global insolation.

$$I = D\, r_t = 6{,}353\,\frac{\text{Wh}}{\text{m}^2} * 0.06 = 381\,\frac{\text{Wh}}{\text{m}^2}$$

3) Use Equation 4.6 to calculate the direct beam normal insolation from global and diffuse.

$$I_b = \frac{I - I_d}{\sin\beta_{sol}}$$

$$I_b = \frac{381\frac{\text{Wh}}{\text{m}^2} - 153\frac{\text{Wh}}{\text{m}^2}}{\sin(33.71°)}$$

$$I_b = 411\frac{\text{Wh}}{\text{m}^2}$$

Hypothetical Clear-Sky Radiation

Sometimes, one may be left without available empirical data for a location due to a remote site or because many weather stations do not routinely monitor solar radiation. In other cases, the data are unreliable. At times, the worst-case scenario for solar heat gain is desired, such as is used in some methods of cooling load calculations, although this can potentially lead to significant over-sizing of HVAC systems.[26] When empirical data are unavailable or deemed unreliable, or needs dictate a type of data different than what is available, one must choose a method for calculating appropriate solar radiation values.

Calculated clear-sky solar radiation data provide an estimate for a given latitude of the level of solar radiation under completely clear-sky conditions. Figure 4.14 shows the frequency with which completely clear skies occur globally. The average frequency of occurrence of totally clear skies worldwide (over land) is only 17.4%,[27] so clear-sky values are obviously of limited utility for understanding climatic trends, although some areas in the Middle East experience around 70% completely clear conditions.

Clouds are influential because they cover an average of 56% of the sky during daytime hours globally.[28] Figure 4.15 shows the global distribution of cloud cover.

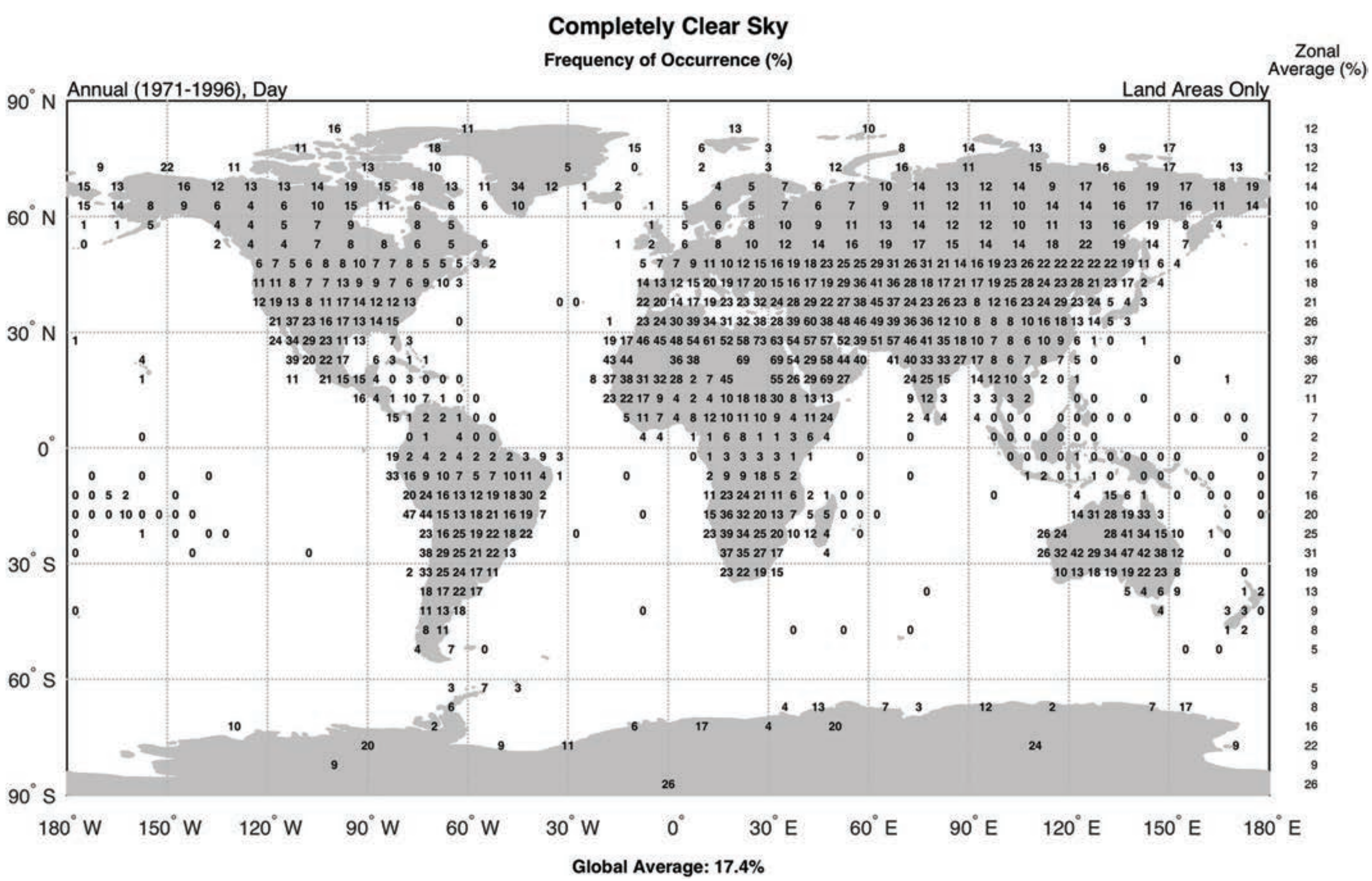

Figure 4.14

Global Frequency of Occurrence of Completely Clear Skies.

Ryan Eastman, Stephen G. Warren, and Carole J. Hahn. *Climatic Atlas of Clouds Over Land and Ocean.*

Values represent the percentage of daytime hours when no cloud cover is present for each geodesic grid cell shown.[29]

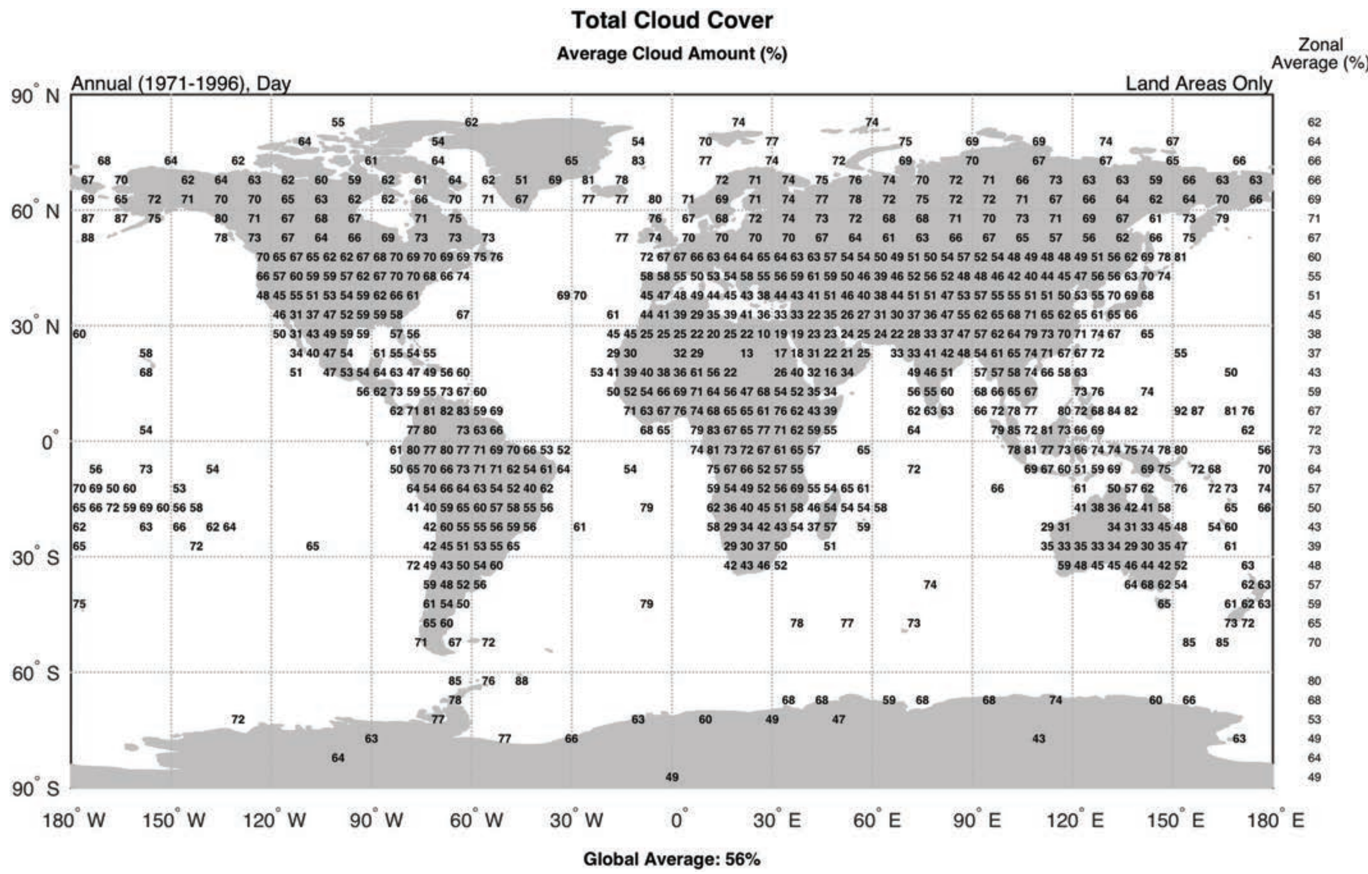

Figure 4.15

Global Average Amount of Cloud Cover.

Ryan Eastman, Stephen G. Warren, and Carole J. Hahn. *Climatic Atlas of Clouds Over Land and Ocean.* Values represent the annual average percentage of cloud cover during daytime hours for each geodesic grid cell shown.[30]

The importance of cloud cover necessitates the use of climate data specific to one's location for design purposes. Clear-sky conditions are not the norm in most locations, however, so for more realistic modeling of typical conditions, other methods are preferable.

Numerous methods have been proposed for calculating solar irradiance values in clear-sky and other conditions. See Muneer[31] for a summary of many of these approaches. These models range from relatively simple to highly complex, but ultimately are no better than the climatic assumptions fed into them. For design purposes, such calculations are not generally useful because measured data are preferable. For weather stations that lack solar radiation monitoring, often these methods have been used to estimate appropriate values.

Clear-sky values, if used improperly, will grossly overestimate the amount of available radiation. For example, the clear-sky beam insolation value for 30° N latitude is 914 Wh/m^2 in the 12:00–13:00 hour on the typical August day. In Kuwait City, the data show just 749 Wh/m^2 is typical, Austin normally receives 576 Wh/m^2, and Shanghai just 219 Wh/m^2 (24% of the clear-sky value). In other words, proceed with extreme caution when using clear-sky radiation values.

Perhaps the most valuable use of clear-sky radiation values, however, is for didactic purposes. It is very useful for the designer to develop an understanding of how a location's solar geometry affects its solar potential. Studying graphs

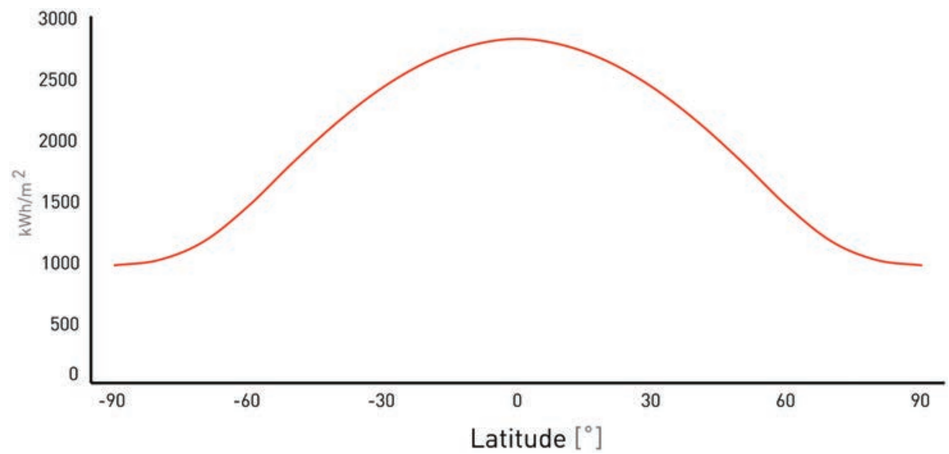

Figure 4.16

Clear-Sky Annual Total Global Horizontal Insolation by Latitude.

Dason Whitsett

of clear-sky radiation values during the course of the year for various latitudes (Figure 4.16) and the way that radiation is distributed over surfaces of varying orientations (covered in Chapter 5) provides the designer with insight into fundamental principles governing passive design. Once the essential trends for a given latitude are understood, it is relatively easy to synthesize this knowledge with information on local climatic trends to understand how the sun will affect a form in a particular climate.

Of the numerous models for calculating clear-sky radiation values that have been developed, the model presented here is one of the simplest. It is based on the method used in the 2005 ASHRAE Handbook of Fundamentals.[32]

Refer to Table 4.4 for the coefficients needed in Equations 4.7 and 4.8.

Equation 4.7 Clear Day Hourly Direct Beam Insolation

$$G_b = \frac{A}{\exp\left(\dfrac{B}{\sin\beta_{sol}}\right)}$$

Table 4.4 Irradiance Data for Clear-Sky Calculations

	G_o *(W/m²)*	ET *(min)*	A *(W/m²)*	B	C
Jan	1,402	−11.2	1,190	0.141	0.103
Feb	1,389	−13.9	1,177	0.142	0.104
Mar	1,368	−7.5	1,153	0.149	0.109
Apr	1,345	1.1	1,121	0.164	0.12
May	1,326	3.3	1,098	0.177	0.13
Jun	1,316	−1.4	1,076	0.185	0.137
Jul	1,318	−6.2	1,078	0.186	0.138
Aug	1,331	−2.4	1,101	0.182	0.134
Sep	1,352	7.5	1,130	0.165	0.121
Oct	1,375	15.4	1,162	0.152	0.111
Nov	1,394	13.8	1,181	0.144	0.106
Dec	1,404	1.6	1,193	0.141	0.103

After ASHRAE[33] with values updated to reflect current estimate of *TSI*.

Equation 4.8 Clear Day Hourly Sky Diffuse Insolation

$$G_d = G_b, C$$

EXAMPLE 4.4 CALCULATING CLEAR-SKY IRRADIATION VALUES

What are the clear-sky direct beam normal and sky diffuse insolation values for the August design day in the 16:01–17:00 hour in Austin, Texas?

Calculations will be based on 16:30 *LST* to give the average sun position for the hour. Using the equations from Chapter 2 and 3, we find: 16:30 *LST* = 15:55 *AST*, β_{sol} = 32.65°

1) Use Equations 4.7 and 4.8 to calculate.
From Table 4.4: $A = 1{,}101\ \mathrm{W/m^2}$, $B = 0.182$, $C = 0.134$

$$G_b = \frac{A}{\exp\left(\frac{B}{\sin\beta_{sol}}\right)}$$

$$G_b = \frac{1{,}101\frac{\mathrm{W}}{\mathrm{m}^2}}{\exp\left(\frac{0.182}{\sin(32.65^\circ)}\right)}$$

$$G_b = 786\frac{\mathrm{W}}{\mathrm{m}^2}$$

$$G_d = G_b, C$$

$$G_d = 786\frac{\mathrm{W}}{\mathrm{m}^2} * 0.134$$

$$G_d = 105\frac{\mathrm{W}}{\mathrm{m}^2}$$

2) These will be treated as average irradiance values for the hour, so multiply by one hour to convert to insolation.

$$I_b = G_b * 1h = 786\frac{\mathrm{Wh}}{\mathrm{m}^2}$$

$$I_d = G_d * 1h = 105.32\frac{\mathrm{Wh}}{\mathrm{m}^2}$$

Solar tables provide a quick reference for solar coordinates on design days for a given latitude. To save space, Table 4.5 only lists hours from sunrise to noon. Afternoon values are symmetrical across the north-south axis; it also shows the Cartesian coordinates of sun position and clear-sky direct beam (I_b), horizontal diffuse (I_d), and global horizontal ($_I$) irradiation values. Daily totals for the horizontal values are shown at the bottom of each design day section. These totals are for the entire day, not just up to noon. It is *crucial* not to use these clear-sky values for general design purposes. Most locations will typically experience dramatically lower direct beam values than the clear-sky values shown in the table. Appendix C contains solar tables for various other latitudes.

The value in studying clear-sky annual trends is that they expose the maximum solar potential of a place based on the geometry that governs the relationship of the sun to a site's latitude without the confounding variable of weather to complicate understanding. Armed with an understanding of these fundamental relationships, the designer can easily assess how local climatic trends affect the actual solar potential of a specific place. Clear-sky radiation trends will be discussed in Chapter 5.

Table 4.5 Solar Table for 30° North Latitude

$L = 30°$	Approx. Clear-Sky Irradiation (Wh/m^2)								
	AST	$\alpha_{sol}(°)$	$\beta_{sol}(°)$	σ_s	σ_w	σ_z	I_b	I_d	I
Dec	6:58	–62.64	0.00	0.46	–0.89	0.00			
	7:00	–62.40	0.38	0.46	–0.89	0.01	0	0	0
	8:00	–54.15	11.44	0.57	–0.79	0.20	591	61	178
	9:00	–44.12	21.27	0.67	–0.65	0.36	816	84	380
	10:00	–31.73	29.28	0.74	–0.46	0.49	902	93	534
	11:00	–16.77	34.64	0.79	–0.24	0.57	940	97	631
	12:00	0.00	36.55	0.80	0.00	0.60	950	98	664
								767	4,111 *D* ($Wh/m^2/day$)
Jan/Nov	6:49	–66.37	0.00	0.40	–0.92	0.00			
	7:00	–65.0	32.10	0.42	–0.91	0.04	25	3	3
	8:00	–56.63	13.45	0.54	–0.81	0.23	648	68	218
	9:00	–46.37	23.63	0.63	–0.66	0.40	838	88	423
	10:00	–33.57	31.99	0.71	–0.47	0.53	914	96	580
	11:00	–17.86	37.66	0.75	–0.24	0.61	947	99	678
	12:00	0.00	39.69	0.77	0.00	0.64	957	100	711
								805	4,517 *D* ($Wh/m^2/day$)
Feb/Oct	6:27	–76.43	0.00	0.23	–0.97	0.00			
	7:00	–72.25	6.77	0.30	–0.95	0.12	338	36	76
	8:00	–63.61	18.81	0.42	–0.85	0.32	746	80	321
	9:00	–52.98	29.87	0.52	–0.69	0.50	876	94	530
	10:00	–39.21	39.25	0.60	–0.49	0.63	933	100	690
	11:00	–21.33	45.84	0.65	–0.25	0.72	959	103	791
	12:00	0.00	48.28	0.67	0.00	0.75	966	104	825
								932	5,641 *D* ($Wh/m^2/day$)
Mar/Sep	6:00	–90.00	0.00	0.00	–1.00	0.00			
	7:00	–82.37	12.95	0.13	–0.97	0.22	571	66	194
	8:00	–73.90	25.66	0.25	–0.87	0.43	800	92	439
	9:00	–63.43	37.76	0.35	–0.71	0.61	890	102	647
	10:00	–49.11	48.59	0.43	–0.50	0.75	933	107	807
	11:00	–28.19	56.77	0.48	–0.26	0.84	953	110	907
	12:00	0.00	60.00	0.50	0.00	0.87	959	110	941
								1,064	6,928 *D* ($Wh/m^2/day$)
Apr/Aug	5:32	–103.57	0.00	–0.23	–0.97	0.00			
	6:00	–100.19	5.83	–0.18	–0.98	0.10	204	26	47
	7:00	–92.98	18.73	–0.05	–0.95	0.32	653	83	292
	8:00	–85.36	31.71	0.07	–0.85	0.53	805	102	525
	9:00	–76.19	44.52	0.17	–0.69	0.70	874	111	724
	10:00	–63.14	56.72	0.25	–0.49	0.84	909	115	876
	11:00	–40.48	67.02	0.30	–0.25	0.92	927	118	971
	12:00	0.00	71.73	0.31	0.00	0.95	932	118	1,004
								1,229	7,873 *D* ($Wh/m^2/day$)
May/Jul	5:10	–113.63	0.00	–0.40	–0.92	0.00			
	6:00	–107.77	9.99	–0.30	–0.94	0.17	386	52	119
	7:00	–101.19	22.57	–0.18	–0.91	0.38	685	92	355
	8:00	–94.65	35.42	–0.07	–0.81	0.58	804	108	574
	9:00	–87.32	48.40	0.03	–0.66	0.75	863	116	761
	10:00	–77.32	61.27	0.11	–0.47	0.88	894	120	904
	11:00	–57.88	73.35	0.15	–0.24	0.96	910	122	993
	12:00	0.00	80.31	0.17	0.00	0.99	915	123	1,024
								1,340	8,434 *D* ($Wh/m^2/day$)
Jun	5:01	–117.36	0.00	–0.46	–0.89	0.00			
	6:00	–110.59	11.48	–0.34	–0.92	0.20	431	59	145
	7:00	–104.30	23.87	–0.23	–0.89	0.40	691	95	374
	8:00	–98.26	36.60	–0.12	–0.79	0.60	801	110	587
	9:00	–91.79	49.53	–0.02	–0.65	0.76	856	117	769
	10:00	–83.46	62.50	0.05	–0.46	0.89	886	121	908
	11:00	–67.48	75.11	0.10	–0.24	0.97	902	124	995
	12:00	0.00	83.45	0.11	0.00	0.99	906	124	1,025
								1,376	8,580 *D* ($Wh/m^2/day$)
									2,419 $kWh/m^2/year$

These tables contain solar coordinates in solar time and *clear-sky* insolation values for the latitude shown. To keep the tables compact, values are only included up to noon. Afternoon values are symmetrical around the north-south axis. Irradiation/Insolation values are calculated using a slight variation on the clear-sky method presented in this chapter. See Appendix C for more detail on this modification.

USING SOLAR RADIATION DATA TO ESTIMATE SURFACE INSOLATION

Chapter 5 will cover methods for calculating the insolation incident on surfaces of any orientation. Frequently, the biggest challenge in performing these calculations is to obtain available solar radiation values in a form necessary for calculating how much of the beam, sky diffuse, and reflected components available at that time is striking the surface. For irradiance or hourly insolation calculations, only two climatic values are necessary for each timestep to be calculated: direct beam insolation (I_b) and sky diffuse insolation (I_d). Four common scenarios corresponding with the example solar radiation data sources discussed previously are listed with references to the equations to convert them to the necessary beam and diffuse values.

SCENARIO 1: USING HOURLY BEAM AND DIFFUSE INSOLATION (I_B AND I_D) OR IRRADIANCE (G_B AND G_D) VALUES.

This is the most straightforward because no conversion is necessary; simply plug the values straight into the formulas in Chapter 5. It is unusual, however, to find typical or average solar data in this format, so this scenario has limited application to design calculations.

SCENARIO 2: USING HOURLY BEAM AND DAILY TOTAL DIFFUSE (I_B AND D_D) VALUES

This scenario corresponds to the values provided in EnergyPlus weather statistics files. No conversion is necessary for the beam value. Use Equations 4.2 and 4.3 to convert the diffuse to an approximate hourly value.

SCENARIO 3: USING DAILY TOTAL GLOBAL AND DIFFUSE INSOLATION (D AND D_D) VALUES

These values are provided in the NREL SRDM tables. Use Equations 4.2 and 4.3 to approximate the hourly diffuse component. Use Equations 4.4–4.6 to estimate the hourly beam component.

SCENARIO 4: CALCULATING HYPOTHETICAL CLEAR-SKY INSOLATION VALUES

If the need dictates using clear-sky radiation values, use Equations 4.7 and 4.8 to calculate the two necessary components. Remember, however, that clear-sky values are substantially higher than what nearly all locations on Earth experience virtually all the time.

NOTES

1 Nick Baker, "We Really Are Outdoor Animals," in *Conference Proceedings: Moving Thermal Comfort Standards into the 21st Century* (Moving Thermal Comfort Standards into the 21st Century, Oxford: Oxford Brookes University, 2001).

2 Marialena Nikolopoulou and Spyros Lykoudis, "Thermal Comfort in Outdoor Urban Spaces: The Human Parameter," *Solar Energy* 70, no. 3 (2001).

3 Mireia Vergés, Julie Meyers, and Inma Alavedra, *Light in Architecture* (Antwerp: Tectum Publishers, 2007).

4 Edmund T. Whittaker, *From Euclid to Eddington, a Study of Conceptions of the External World* (Cambridge, England: University Press, 1949).

5 "#50 Ancient Sunlight," *NASA—Sun-Earth Day—Technology Through Time*, accessed February 28, 2016, http://sunearthday.nasa.gov/2007/locations/ttt_sunlight.php.

6 "Solar Radiation," *NASA Climate and Radiation Science Research Portal*, accessed February 28, 2016, http://atmospheres.gsfc.nasa.gov/climate/index.php?section=136.

7 Ibid.

8 John A. Duffie and William A. Beckman, *Solar Engineering of Thermal Processes*, 3rd ed. (Hoboken, NJ: Wiley, 2006), 9.

9 Muhammad Iqbal, *An Introduction to Solar Radiation* (Toronto: Academic Press, 1983), 3.

10 "Weather Data Download: Austin-Camp Mabry 722544 (TMY3)," *EnergyPlus-Weather Data by Location*, accessed February 28, 2016, https://energyplus.net/weather-location/north_and_central_america_wmo_region_4/USA/TX/USA_TX_Austin-Camp.Mabry.722544_TMY3.

11 "Weather Data Download: Phoenix-Sky Harbor Intl AP 722780 (TMY3)," *EnergyPlus-Weather Data by Location*, accessed February 28, 2016, https://energyplus.net/weather-location/north_and_central_america_wmo_region_4/USA/AZ/USA_AZ_Phoenix-Sky.Harbor.Intl.AP.722780_TMY3.

12 "Weather Data Download: Austin-Camp Mabry 722544 (TMY3)."

13 "Weather Data Download: London Gatwick 037760 (IWEC)," *EnergyPlus-Weather Data by Location*, accessed February 28, 2016, https://energyplus.net/weather-location/europe_wmo_region_6/GBR//GBR_London.Gatwick.037760_IWEC.

14 Duffie and Beckman, *Solar Engineering of Thermal Processes*.

15 Drury B. Crawley, "Creating Weather Files for Climate Change and Urbanization Impacts Analysis," in *Proceedings: Building Simulation 2007* (Beijing, China: IBPSA, 2007); Amélie Robert and Michaël Kummert, "Designing Net-Zero Energy Buildings for the Future Climate, Not for the Past," *Building and Environment, Implications of a Changing Climate for Buildings* 55 (September 2012): 150–158, doi:10.1016/j.buildenv.2011.12.014; Lisa Guan, "Preparation of Future Weather Data to Study the Impact of Climate Change on Buildings," *Building and Environment* 44, no. 4 (April 2009): 793–800, doi:10.1016/j.buildenv.2008.05.021.

16 Duffie and Beckman, *Solar Engineering of Thermal Processes*, 55–56.

17 "EnergyPlus Energy Simulation Software: Weather Data," *U.S. Department of Energy—Energy Efficiency & Renewable Energy*, 2011, https://energyplus.net/weather/simulation.

18 "NSRDB: 1991–2005 Update: TMY3," *National Renewable Energy Laboratory*, accessed March 4, 2016, http://rredc.nrel.gov/solar/old_data/nsrdb/1991-2005/tmy3/.

19 *Climate Consultant*, version 6.0 (University of California Los Angeles; The Regents of the University of California, 2015).

20 "Weather Data Download: Austin-Camp Mabry 722544 (TMY3)."

21 Benjamin Y. H. Liu and Richard C. Jordan, "The Long-Term Average Performance of Flat-Plate Solar-Energy Collectors: With Design Data for the U.S., Its Outlying Possessions and Canada," *Solar Energy* 7, no. 2 (April 1963): 53–74, doi:10.1016/0038-092X(63)90006-9.

22 Duffie and Beckman, *Solar Engineering of Thermal Processes*, 81.

23 William Marion and Stephen Wilcox, *Solar Radiation Data Manual for Buildings* (National Renewable Energy Laboratory, September 1995), http://rredc.nrel.gov/solar/pubs/bluebook/.

24 Ibid., 206.

25 Manuel Collares-Pereira and Ari Rabl, "The Average Distribution of Solar Radiation-Correlations between Diffuse and Hemispherical and between Daily and Hourly Insolation Values," *Solar Energy* 22, no. 2 (1979): 150, doi:10.1016/0038-092X(79)90100-2.

26 Tariq Muneer, *Solar Radiation and Daylight Models*, 2nd ed. (Oxford: Elsevier Butterworth Heinemann, 2004), xxxvi.

27 Iqbal, *An Introduction to Solar Radiation*.

28 Stephen G. Warren and Carole Hahn, *Climatic Atlas of Clouds Over Land and Ocean*, 2010, www.atmos.washington.edu/CloudMap/index.html.

29 "Completely Clear Sky-Day," *Climatic Atlas of Clouds Over Land and Ocean*, accessed February 29, 2016, www.atmos.washington.edu/CloudMap/.

30 "Average Cloud Amount-Day," *Climatic Atlas of Clouds Over Land and Ocean*, accessed February 29, 2016, www.atmos.washington.edu/CloudMap/.

31 Muneer, *Solar Radiation and Daylight Models*.

32 ASHRAE, *2005 ASHRAE Handbook: Fundamentals*, SI ed. (Atlanta, GA: American Society of Heating, Refrigerating and Air-Conditioning Engineers, Inc., 2005), 31.16.

33 Ibid.

5 THE SUN AND FORM

INTRODUCTION

> We step inside a dark cave. With no light in the cave, we cannot form any conception of it. Were you to describe the cave by running your hands over every inch of it, ceiling, floor and walls, it would take several lifetimes to gain any sense of how the cave looks. But the moment you strike a light you see the cave as a room, instantly perceiving it as a space. Space is a much more complex concept than form, and only much later in life do we learn to relate to it.
>
> —*Henning Larsen*

Architecture is defined by form and our perception thereof, and no element more comprehensively influences our perception of architecture than light. It renders architecture's physical aspects, allowing for intangible and illusive perceptions. In some respects, the continuum of architectural styles throughout regions and time can be understood in relation to solar response within microclimate cycles as well as seasonal and daily cycles.

In a design context, what we ultimately care about is not solar position or radiation levels per se, but how our built environment responds to the sun's light and heat. To understand this relationship, we need to describe not just the position of the sun, but also the position of points, lines, and surfaces in relationship to the sun. This chapter will begin with a discussion of how to model the geometry of surfaces relative to the sky dome, then cover how to combine that information with solar radiation data to evaluate radiation gains on a surface, and finally conclude with an exploration of how building form can be tuned to climate to optimize solar radiation exposure.

SURFACE GEOMETRY

To understand how a surface is affected by solar radiation, one must first describe its position relative to the sun. Surface orientation can be described with either spherical or Cartesian vector coordinates in the same way that solar position is identified. A surface is defined by the position of its ***surface normal vector*** on the sky dome. This is an imaginary line perpendicular to a surface extending outward from its center. Such a vector is modeled as if it begins at the origin and extends to a particular point on the surface of the sky dome.

Using spherical coordinates, the ***surface azimuth*** (α_{sf}), like the solar azimuth, defines the bearing of the surface normal vector on the ground plane relative to south. The ***surface altitude*** (β_{sf}) is the angular elevation of that vector up from the ground plane. Because the surface normal vector is an imaginary line perpendicular to the surface, its altitude is not obvious, but one can determine it easily enough. The information usually on hand for a surface is its tilt up from horizontal, therefore ***surface tilt*** (Σ) will be used for all surface position coordinates in this text, and equations have been modified accordingly. See Figure 5.1 for a graphic representation of these parameters.

Alternatively, Cartesian coordinates may also be used to describe a surface normal vector. These coordinates (n_w, n_s, n_z) are found using equations identical to those translating spherical coordinates for solar position, but adapted for use with surface tilt rather than altitude of the surface normal. These coordinates are represented by the symbol n, indicating they are the surface normal components rather than solar components. Subscripts indicate the axis of each coordinate. Use Equations 5.1–5.4 to determine the Cartesian surface normal vector components and check them using the Pythagorean theorem.

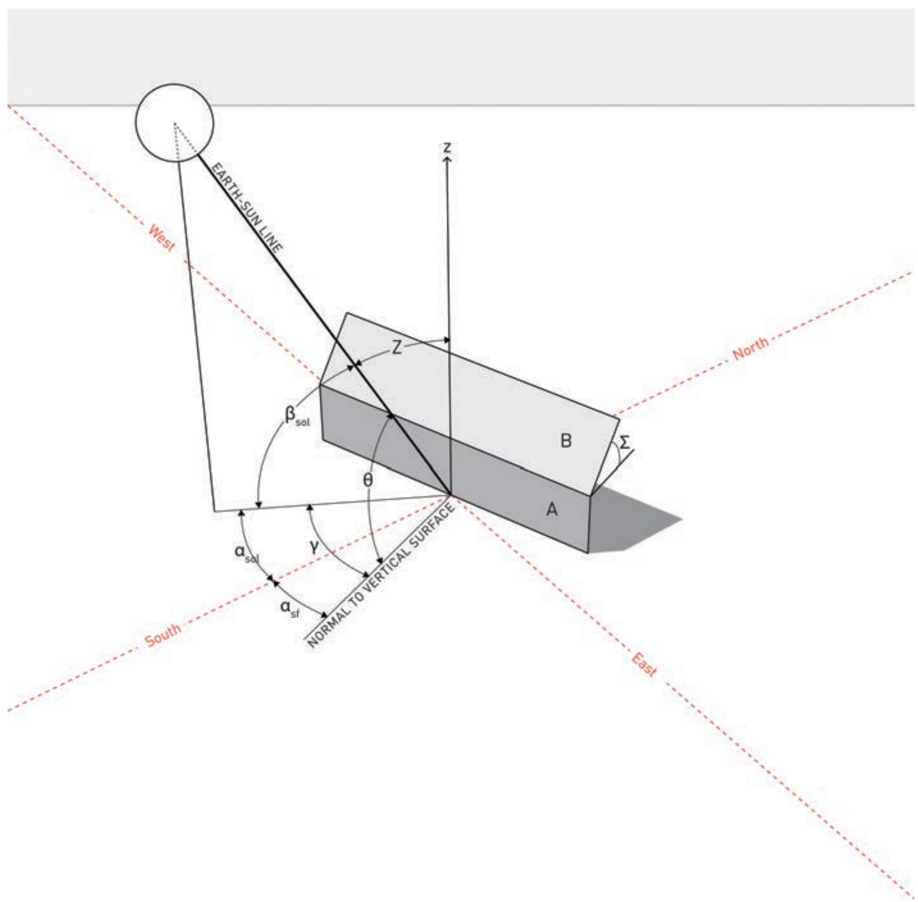

Figure 5.1

Solar Angles Relative to a Surface.

Most of the angles are shown for surface A, a vertical surface with an azimuth to the east of south. The solar azimuth (αsol) and altitude (βsol) are shown along with the surface-solar azimuth (γ) and angle of incidence (θ). Surface B is tilted and its tilt angle (Σ) is shown behind it.

Greg Arcangeli

Equation 5.1 South Normal Vector Component

$$n_s = \cos\alpha_{sf}\cos(90° - \Sigma)$$

Equation 5.2 West Normal Vector Component

$$n_w = \sin\alpha_{sf}\cos(90° - \Sigma)$$

Equation 5.3 Zenith Normal Vector Component

$$n_z = \sin(90° - \Sigma)$$

Equation 5.4 Pythagorean Theorem Check for Normal Vector Components

$$1^2 = \sqrt{n_s^2 + n_w^2 + n_z^2}$$

EXAMPLE 5.1 CALCULATING CARTESIAN SURFACE NORMAL VECTOR COMPONENTS

What is the angle of incidence of the solar ray on a surface with an azimuth of 70° and a tilt of 30° in Austin, Texas ($L = 30.29°$ $LON = -97.74°$), at 16:30 *LST* on August 16?

Given: $\alpha_{sf} = 70.00°$ $\Sigma_{sf} = 30.00°$ $n = 228$

Use Equations 5.1–5.3 to calculate the surface normal vector components.

$$n_s = \cos\alpha_{sf}\cos(90° - \Sigma) = \cos(70.00°)\cos(90° - 30.00°) = 0.17$$
$$n_s = \cos\alpha_{sf}\cos(90° - \Sigma) = \cos(70.00°)\cos(90° - 30.00°) = 0.17$$
$$n_z = \sin(90° - 30.00°) = 0.87$$

Use Equation 5.4 to check that these coordinates place the surface normal vector on the surface of the sky dome:

$$1^2 = \sqrt{n_s^2 + n_w^2 + n_z^2} = \sqrt{0.17^2 + 0.47^2 + 0.87^2} = 1.00$$

Unlike solar coordinates, which are constantly changing as the Earth orbits the sun and rotates on its axis, coordinates for stationary surfaces remain constant.

Solar Coordinates Relative to Surfaces

Any time the solar azimuth is not perpendicular to a given surface (almost all times), it is helpful to translate the solar coordinates from the cardinal directions to the frame of reference of the surface. Doing so makes it much easier to visualize and work with the geometry. Casting shadows and the design of shading devices becomes much easier because angles are defined relative to the surface in question and are drawn easily in standard orthographic projection drawings. This process is necessary to determine the solar exposure of a surface for evaluating insolation.

Surface-Solar Transformation Using Spherical Coordinates

The ***surface-solar azimuth*** (γ) is simply the azimuth of the sun's position relative to the normal vector of a surface, as shown in Figure 5.1. The horizontal shading angle is a special case of the surface-solar azimuth that is useful in shading design and will be covered in Chapter 8. Use Equation 5.5 to calculate the surface-solar azimuth.

Equation 5.5 Surface-Solar Azimuth

$$\gamma = \alpha_{sol} - \alpha_{sf}$$

Once the surface-solar azimuth is known, one can determine the ***angle of incidence*** (θ), which is the absolute angle between the solar ray and the surface's normal vector. Because the angle of incidence is relative to the normal vector, when $\theta = 0°$, the sun is perpendicular to the surface. When $\theta = 90°$, the sun is in plane with the surface. The angle of incidence is important because it determines how much relative insolation a surface receives and because the light transmission of glass is highly dependent on the angle of incidence. Calculate the angle of incidence using Equation 5.6.

Equation 5.6 Angle of Incidence

$$\cos\theta = \cos\beta_{sol} \cos\gamma \sin\Sigma + \sin\beta_{sol} \cos\Sigma$$

EXAMPLE 5.2 CALCULATING ANGLE OF INCIDENCE

What is the angle of incidence of the solar ray on a surface with an azimuth of 70° and a tilt of 30° in Austin, Texas ($L = 30.29°$ $LON = -97.74°$), at 16:30 *LST* on August 16?

Given: $\alpha_{sf} = 70.00°$ $\Sigma_{sf} = 30.00°$ $n = 228$

1) Using the methods described in Chapter 3, calculate the coordinates of the sun's position at the given time: 16:30 $LST = $ 15:54 *AST*, $\alpha_{sol} = 86.23°$, and $\beta_{sol} = 33.71°$.
2) Using Equation 5.5, calculate the surface-solar azimuth:

$$\gamma = \alpha_{sol} - \alpha_{sf}$$
$$\gamma = 86.23° - 70.00°$$
$$\gamma = 16.23°$$

Using Equation 5.6, calculate the angle of incidence:

$$\cos\theta = \cos\beta_{sol} \cos\gamma \sin\Sigma + \sin\beta_{sol} \cos\Sigma$$
$$\cos\theta = \cos(33.71°) \cos(16.23°) \sin(30.00°) + \sin(33.71°) \cos(30.00°)$$
$$\theta = 28.36°$$

Additional solar coordinate transformations for profile angle and elevation angle are covered in Chapter 6.

Onset/Offset

Onset and ***offset*** are the times at which the direct rays of the sun move onto and off of a surface, also known as the ***surface sunrise*** (H'_{sr}) and ***sunset*** (H'_{ss}). If the surface has a view of true sunrise or sunset, onset and offset will occur at those times. If not, onset and offset will occur at times when the angle of incidence (θ) is 90°. Surfaces facing the poles may have two periods per day when the sun sees the surface as it rises and sets toward the poles, but is toward the equator at solar noon.

Equation 5.7 Offset Hour Angle for Tilted Surface Facing Equator in Northern Hemisphere

$$H'_{ss} = \min\begin{bmatrix} \cos^{-1}(-\tan L \tan\delta) \\ \cos^{-1}(-\tan(L-\Sigma)\tan\delta) \end{bmatrix}$$

Use Equation 5.7 from Duffie and Beckman[1] to find the offset hour angle on a south-facing tilted surface in the northern hemisphere. It tests whether the surface is exposed to the true sunset and simulates shifting the latitude of the receiving surface to a position on Earth where, at the same tilt relative to the ecliptic plane, the surface would be horizontal relative to the surface of the Earth. In the southern hemisphere for a north-facing surface, substitute (L+Σ) for (L−Σ) in the second set of terms. For surface sunrise, take the negative of the surface sunset hour angle.

EXAMPLE 5.3 OFFSET ON A TILTED SURFACE FACING THE EQUATOR

What is the offset time in solar time on the December solstice for a surface with an azimuth of 180.00° and a tilt of 60.00° located at −45.00° latitude?

$L = -45.00°\ \Sigma = 60.00°\ \delta = -23.45°$

1) Use Equation 5.7, substituting (L+Σ) for (L−Σ) because the surface is in the southern hemisphere.

$$H'_{ss} = \min\begin{bmatrix} \cos^{-1}(-\tan L \tan\delta) \\ \cos^{-1}(-\tan(L+\Sigma)\tan\delta) \end{bmatrix}$$

$$H'_{ss} = \min\begin{bmatrix} \cos^{-1}(-\tan(-45.00°)\tan(-23.45°)) \\ \cos^{-1}(-\tan((-45.00°)+(60.00°))\tan(-23.45°)) \end{bmatrix}$$

$$H'_{ss} = \min\begin{bmatrix} 115.71° \\ 83.33° \end{bmatrix}$$

$$H'_{ss} = 83.33°$$

2) Rearrange Equation 2.2 to solve for apparent solar time at surface sunset.

$$AST = \frac{83.33°}{15.00°} - 12.00\,\text{h}$$

$$AST = 17.56 = 17{:}34$$

For surfaces of an arbitrary orientation, the equations become slightly more complex. Sunrise and sunset are no longer symmetrical, and two sunrises per day may occur on surfaces facing the poles. Equations 5.8a–g[2] give the sunrise and sunset time for surfaces of any tilt or orientation.

Equations 5.8a–g Offset Hour Angle on Surfaces of Arbitrary Tilt and Azimuth

Equation 5.8a Absolute Value of Hour Angle of Onset for Surface of Arbitrary Tilt and Orientation

$$|H'_{sr}| = \min\left[H_{ss}, \cos^{-1}\frac{AB + C\sqrt{A^2 - B^2 + C^2}}{A^2 + C^2}\right]$$

Equation 5.8b Onset Hour Angle for Surface of Arbitrary Tilt and Orientation

$$H'_{sr} = \begin{Bmatrix} -\left|H'_{sr}\right| & if\left(A>0\, and\, B>0\right) or \left(A \geq B\right) \\ +\left|H'_{sr}\right| & otherwise \end{Bmatrix}$$

Equation 5.8c Absolute Value of Hour Angle of Offset for Surface of Arbitrary Tilt and Orientation

$$\left|H'_{ss}\right| = \min\left[H_{ss}, \cos^{-1}\frac{AB - C\sqrt{A^2 - B^2 + C^2}}{A^2 + C^2}\right]$$

Equation 5.8d Offset Hour Angle for Surface of Arbitrary Tilt and Orientation

$$H'_{ss} = \begin{Bmatrix} +\left|H'_{ss}\right| & if\left(A>0\, and\, B>0\right) or \left(A \geq B\right) \\ -\left|H'_{ss}\right| & otherwise \end{Bmatrix}$$

where:

Equation 5.8e) $A = \cos\Sigma + \tan L \cos\gamma \sin\Sigma$

Equation 5.8f) $B = \cos H_{ss} \cos\Sigma + \tan\delta \sin\Sigma \cos\gamma$

Equation 5.8g) $C = \dfrac{\sin\Sigma \sin\gamma}{\cos L}$

Using these equations, one may determine exactly how many hours the sun will see a surface each day.

SOLAR RADIATION ON SURFACES

In evaluating the amount of solar radiation incident on a surface, at least three components must always be considered: direct beam, sky diffuse, and ground reflected. Chapter 4 dealt with sources of available solar radiation data and approaches to extracting values necessary for surface insolation calculations from various data types. The basic input values one needs for evaluating surface radiation exposure are direct beam normal and sky diffuse values for either instantaneous power values of irradiance (G_b and G_d,) or energy values for insolation/irradiation (I_b and I_d).

Calculations in this section will be based for insolation because it is generally more relevant to designers. The same processes may be used for irradiance calculations by substituting irradiance values (G) wherever insolation values (I) are used. Remember, however, that power values cannot be summed without multiplying by the timestep to convert them to energy.

Irradiance and insolation only describe the amount of radiation incident on a surface. Just as with the atmosphere, the radiation that arrives at a surface will be reflected, absorbed, and transmitted according to the physical properties of the surface. How solar radiation interacts with windows is covered in Chapter 9. The interaction of solar radiation and the opaque building envelope is beyond the scope of this book, but covered by many other sources.

Beam Radiation

As noted in Chapter 4, beam radiation is solar radiation from the direct ray of the sun and is also known as direct, direct beam, and direct beam normal.

Relative Beam Radiation (R_b)

Although a surface may be in full view of the sun, unless the surface is normal to the sun's position, the radiant flux on the surface will be lower than the full beam normal value because the same density of radiation spreads out over a larger area as it strikes the surface at an angle. Figure 4.9 demonstrates this principle on a global scale, but it also applies at the scale of an individual surface.

The fraction of the total direct normal beam radiation incident on a surface at any given time is known as the ***relative beam radiation*** (R_b). This ratio is based on a geometric relationship with the angle of incidence, as shown in Equation 5.9. The product of this equation is the ratio of the direct beam radiation incident on the surface compared to the total radiation the surface would receive if oriented normal to the sun's position at that time. Another way to state this is that R_b is the ratio of the projected area of the surface from the sun's point of view to the true area of that surface. When working with hourly irradiance or insolation values, calculate the relative beam radiation using solar coordinates on the half hour to represent the average angle of incidence over that timespan.

Equation 5.9 Relative Beam Radiation

$$R_b = \cos\theta$$

EXAMPLE 5.4 RELATIVE BEAM RADIATION

What is the relative beam radiation on the surface from Example 5.2?

From Example 5.2, $\theta = 28.36°$.

Use Equation 5.9 to calculate relative beam radiation:

$$R_b = \cos\theta$$
$$R_b = \cos(28.36°)$$
$$R_b = 0.88$$

Therefore, the surface is currently receiving 88% of the radiation it would receive if oriented normal to the sun. This also indicates the projected area of the surface onto the direction of the solar ray is 88% of its actual size.

If working in Cartesian coordinates, the relative beam radiation is found as the dot product of the solar and surface coordinates as demonstrated in Equation 5.10. In evaluating beam insolation, the Cartesian solar coordinates become particularly useful because the individual components are equal to the relative beam radiation for a surface facing in any of the cardinal directions or toward the zenith.

Equation 5.10 Relative Beam Radiation—Cartesian

$$R_b = \sigma_s n_s + \sigma_w n_w + \sigma_z n_z$$

EXAMPLE 5.5 RELATIVE BEAM RADIATION USING CARTESIAN COORDINATES

Using the Cartesian coordinate system, determine the relative beam radiation for the same surface and time used in Example 5.1.

Given: $\alpha_{sf} = 70.00°$ $\Sigma_{sf} = 30.00°$ $n = 228$ 16:30 *LST* $L = 30.29°$ $LON = -97.74°$

1) Using the methods described in Chapter 3, calculate the Cartesian coordinates of the sun's position at the given time: $\sigma_s = 0.05$, $\sigma_w = 0.83$, $\sigma_z = 0.56$.

2) Use Equation 5.10 to calculate the relative beam radiation on the surface at this time.

$R_b = \sigma_s n_s + \sigma_w n_w + \sigma_z n_z$
$R_b = (0.05)(0.17) + (0.83)(0.47) + (0.56)(0.87)$
$R_b = 0.89$

Notice there is a difference of 0.01 between the rounded values for R_b calculated with the Cartesian coordinates in this example and the value calculated for spherical coordinates in Example 5.4. This is the result of rounding at each step in the examples. The values would be identical if we carried the calculations for each of the components to more digits and rounded at the end. The difference only amounts to slightly over 1% and is not significant enough to cause concern. For greater precision, use a spreadsheet to calculate the values.

Any surface facing in one of the cardinal directions or the zenith direction will have a normal vector component of 1.00 for the direction the surface faces and components of 0.00 for the other directions, canceling the contribution of the solar beam from other directions and leaving only the contribution of the direction it faces. The Cartesian coordinates are also referred to as direction cosines because they indicate the cosine of the angle of incidence of the sun's rays on a surface facing along the axis to which the coordinate refers. Note that Equation 5.9 shows that the cosine of the angle of incidence is the relative beam radiation on the surface. In other words, each coordinate describes the ratio of the projected area of the surface onto the rays of the sun compared to the true area.

Therefore, when looking at a solar table including Cartesian coordinates, one can very quickly develop a sense of the relative solar exposure of surfaces facing the cardinal directions as well as horizontal surfaces over the course of a day or year by examining the Cartesian coordinates for sun position. For example, Figure 5.2 shows the sun position from the west elevation of the sky dome for a time at which the solar altitude is 30.00° and azimuth is 0.00°. This results in direction cosine values of $\sigma_s = 0.87$, $\sigma_w = 0.00$, and $\sigma_z = 0.50$. The bottom portion of the diagram shows how these values result in relative insolation.

Surface Direct Beam Radiation (G_{tb}, I_{tb}, D_{tb})

Hourly direct beam insolation (irradiation) on a surface (I_{tb}) measures the actual beam solar radiation incident on a surface, which is a function of the angle at which the sun strikes the surface. As indicated in Equation 5.11, for hourly insolation, multiply the relative beam radiation (R_b) by the direct beam (I_b) value to obtain the surface hourly beam insolation. Methods for determining appropriate available solar radiation values are discussed in Chapter 4.

Equation 5.11 Hourly Beam Insolation on a Surface

$I_{tb} = I_b, R_b$

EXAMPLE 5.6 HOURLY BEAM INSOLATION ON A SURFACE

What is the hourly beam insolation on the surface used in Examples 5.1 and 5.4 at the same date and time?

From Table 4.2, the available beam normal insolation (I_b) in Austin for the hour from 14:01 to 15:00 is 508 Wh/m^2. From Example 5.4, $R_b = 0.88$.

$$I_{tb} = I_b R_b = \left(508 \frac{\text{Wh}}{\text{m}^2}\right)(0.88) = 447 \frac{\text{Wh}}{\text{m}^2}$$

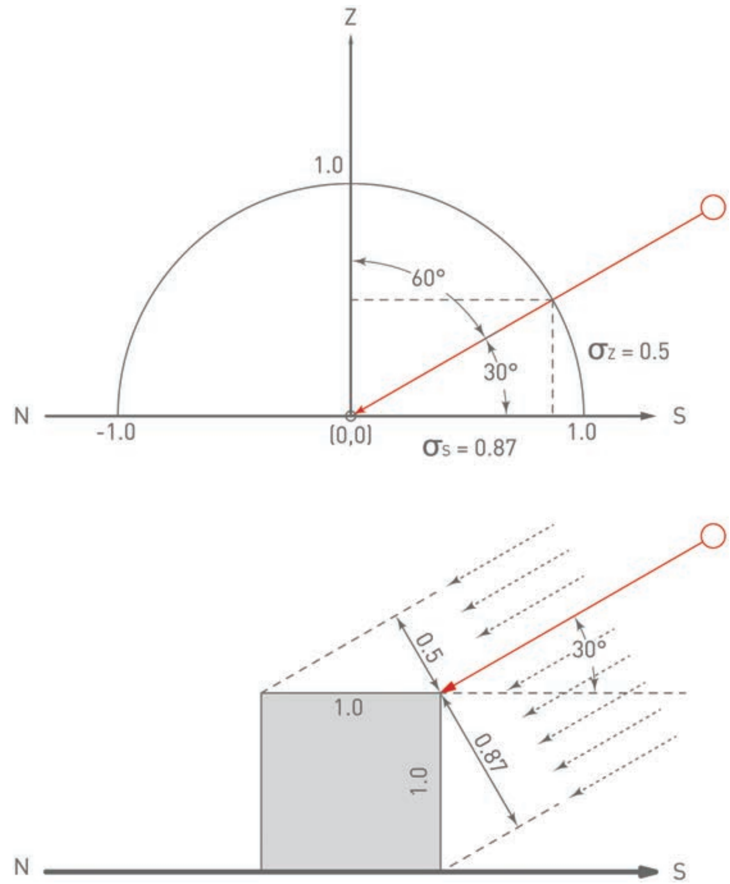

Figure 5.2

Relative Insolation.

Relative insolation on surfaces corresponds to the projected area of the surface from the point of view of the solar ray. For surfaces facing in the cardinal directions or horizontal, this is the same as the Cartesian coordinates for sun position at any time.

Francois Levy

To find the ***daily total direct beam insolation*** (D_{tb}) for a surface, calculate I_b for each hour of the day (or shorter timestep if data are available) and sum the values.

Beam Radiation on a Horizontal Plane (G_{bh}, I_{bh}, D_{bh})

A special case of the relative beam radiation, which is used in calculating ground reflected radiation and sometimes reported separately in solar radiation data, is ***hourly horizontal beam insolation*** (I_{bh}). Convert between beam normal and horizontal beam irradiation values using Equations 5.12 and 5.13.

The ***relative beam radiation on the horizontal*** (R_{bh}) is the ratio of direct beam radiation falling on a horizontal surface to the amount that would fall on a plane normal to the sun's ray at a given time. The angle of incidence on a horizontal surface is always equal to the zenith angle. Equation 5.12 eliminates the need to calculate the angle of incidence separately by using the sine of solar altitude, which is equal to the cosine of the zenith angle.

Equation 5.12 Relative Beam Radiation on the Horizontal

$$R_{bh} = \sin\beta_{sol}$$

Use Equation 5.13 (I_{bh}) to solve for the beam insolation on the horizontal, or rearrange it to obtain I_b when I_{bh} is known.

Equation 5.13 Hourly Beam Insolation on the Horizontal

$$I_{bh} = I_b, R_{bh}$$

EXAMPLE 5.7 HOURLY BEAM INSOLATION ON THE HORIZONTAL

What is the hourly beam insolation on the horizontal for the location and time used in Examples 5.2 and 5.4?

From the previous examples: $I_b = 508$ Wh/m² and $\beta_{sol} = 33.71°$.

1) Using Equation 5.12, calculate R_{bh}.

$$R_{bh} = \sin\beta_{sol} = \sin(33.71°) = 0.55$$

2) Using Equation 5.13, calculate I_{bh}.

$$I_{bh} = I_b\, R_{bh} = \left(508\,\frac{Wh}{m^2}\right)(0.55) = 279\,\frac{Wh}{m^2}$$

Sky Diffuse Radiation

The second component that must always be factored into insolation calculations is the portion of solar radiation that makes its way to the Earth's surface after being diffused and scattered by the atmosphere. The power of diffuse radiation may not be as apparent as direct beam, but for example, in Austin, Texas, at noon in August, the diffuse radiation on a vertical south-facing surface is roughly equal to the direct beam.

Diffuse Sky Radiation Calculations (G_d, I_d, D_d)

If one were to measure the diffuse radiation arriving from different portions of the sky, the values would vary significantly. The actual distribution depends primarily on sun position and cloud cover. Recording, modeling, and working with the enormous amount of data that would represent the distribution of diffuse radiation over the sky dome is impractical, so sky diffuse irradiance is usually recorded as a single value for the entire sky dome on a horizontal plane. We will discuss two models for working with this data to account for its distribution to non-horizontal surfaces.

Sky Diffuse Model 1—Isotropic Sky

Because of the complexity of modeling the actual distribution of diffuse irradiance from the sky, particularly under partly cloudy conditions, frequently the assumption for the purpose of radiation calculations is that sky diffuse radiation is distributed uniformly across the sky dome. This idealized model developed by Liu and Jordan[3] is known as the ***isotropic sky*** model and is highly convenient for calculation purposes.

The amount of diffuse sky irradiance modeled for a surface when using the isotropic model is dependent upon its view of the sky. A surface facing the zenith has a sky view of 1.0, while a vertical surface without obstructions between it and the horizon has a view factor of 0.5. Use Equation 5.14 to determine the ***sky view factor*** (V_s) for surfaces of any arbitrary tilt.

Equation 5.14 Sky View Factor

$$V_s = \frac{1 + \cos\Sigma}{2}$$

The ***sky diffuse insolation on a surface*** (I_{td}) describes the diffuse sky insolation incident on the surface under examination. Find this value by multiplying the sky view factor by the diffuse sky hourly insolation on the horizontal (I_d) as indicated by Equation 5.15.

Equation 5.15 Hourly Sky Diffuse Insolation on a Surface—Isotropic

$$I_{td} = I_d, V_s$$

EXAMPLE 5.8 HOURLY SKY DIFFUSE INSOLATION USING THE ISOTROPIC SKY MODEL

Calculate the sky diffuse irradiance on the surface from Example 5.2 at the same date and time using the *isotropic* sky model.

In Example 4.2, we found at this time I_d = 153 Wh/m^2, and Σ_{sf} = 30.00°.

1) Calculate the sky view factor using Equation 5.14.

$$V_s = \frac{1+\cos\Sigma}{2} = \frac{1+\cos(30.00°)}{2} = 0.93$$

2) Calculate the hourly sky diffuse insolation on the surface using Equation 5.15.

$$I_{td} = I_d V_s = \left(153\frac{Wh}{m^2}\right)(0.93) = 142\frac{Wh}{m^2}$$

Although desirable in its simplicity, the isotropic sky model may in some cases exaggerate the amount of diffuse radiation incident on vertical surfaces.[4]

Sky Diffuse Model 2—Anisotropic

Numerous models have been developed to attempt to better estimate the distribution of diffuse irradiance across the sky dome. Termed anisotropic models because they model diffuse radiation non-uniformly across the sky dome, these models range from straightforward to fairly complex and tend to focus on the effects of the increased intensity of diffuse irradiance around the solar disc and near the horizon under clear-sky conditions. For summaries and comparisons of many of these models, see Iqbal[5] and Duffie and Beckman.[6]

The simple anisotropic model presented here is the one employed by ASHRAE Fundamentals,[7] based on work by Stephenson[8] and Threlkeld.[9] It is recommended only for use in clear or nearly clear-sky conditions. If conditions are overcast or partly cloudy, use actual weather data or the isotropic model if weather data are not available.

The first step in using the anisotropic model is to calculate the ***anisotropic sky factor*** (Y) using Equation 5.16. This value is always calculated based on the angle of incidence of the sun's rays on a vertical surface with the same azimuth of the surface being investigated ($\theta_{\Sigma 90}$), regardless of the actual tilt of the surface.

Equation 5.16 Anisotropic Sky Factor

$$Y = \max\{0.45,\ 0.55 + 0.437\cos\theta_{\Sigma 90} + 0.313\cos^2\theta_{\Sigma 90}\}$$

To find the surface sky diffuse insolation using the anisotropic model, use Equations 5.17a–b.

Equations 5.17a–b Hourly Sky Diffuse Insolation on a Surface—Anisotropic

Equation 5.17a) if $\Sigma \geq 90°$: $I_{td} = I_d Y \sin\Sigma$

Equation 5.17b) if $\Sigma < 90°$: $I_{td} = I_d\left(Y\sin\Sigma + \cos\Sigma\right)$

EXAMPLE 5.9 HOURLY SKY DIFFUSE INSOLATION USING THE ANISOTROPIC SKY MODEL

Calculate the sky diffuse irradiance on the surface from Example 5.2 at the same date and time using the *anisotropic* sky model.

Given: $\alpha_{sf} = 70.00°$ $\Sigma_{sf} = 30.00°$ $n = 228$

Using methods from Chapter 3, we found: $\alpha_{sol} = 86.23°$ and $\beta_{sol} = 33.71°$. In Example 4.2, we found at this time $I_d = 153$ Wh/m², and $\Sigma_{sf} = 30.00°$. In Example 5.2, we calculated that $\gamma = 16.23°$.

1) Calculate the angle of incidence on a vertical surface of the same bearing using Equation 5.6.

$\Sigma_{sf-90} = 90.00°$

$$\cos\theta_{\Sigma 90} = \cos\beta_{sol}\cos\gamma\sin\Sigma_{90} + \sin\beta_{sol}\cos\Sigma_{90}$$

$$\cos\theta_{\Sigma 90} = \cos(33.71°)\cos(16.23°)\sin(90.00°) + \sin(33.71°)\cos(90.00°)$$

$$\theta_{\Sigma 90} = 36.99°$$

2) Calculate the anisotropic sky factor using Equation 5.16.

$$Y = \max\left\{0.45, 0.55 + 0.437\cos\theta_{\Sigma 90} + 0.313\cos^2\theta_{\Sigma 90}\right\}$$

$$Y = \max\left\{0.45, 0.55 + 0.437\cos(36.99°) + 0.313\cos^2(36.99°)\right\}$$

$$Y = 1.10$$

3) Calculate the anisotropic hourly sky diffuse insolation on the surface using Equation 5.17 a or b as appropriate. In this case, because tilt is ≤ 90°, use 5.17b.

$$I_{td} = I_d\left(Y\sin\Sigma + \cos\Sigma\right)$$

$$I_{td} = 153\frac{\text{Wh}}{\text{m}^2}\left(1.10 * \sin(30.00°) + \cos(30.00°)\right)$$

$$I_{td} = 217\frac{\text{Wh}}{\text{m}^2}$$

Reflected Radiation

Reflected solar radiation may come from a variety of sources, but the only one that is virtually always present is the ground. In most cases, reflection from other surfaces is minimal, but it can be extremely important. This section will focus on ground reflected radiation (I_{tg}) but adjustments should be made if other sources are present. Ground reflected radiation is assumed to be diffuse.

Ground Reflected Radiation Calculations (G_{tg}, I_{tg}, D_{tg})

The amount of radiation reflected by the ground depends on the physical properties of the ground around the receiving surface to be modeled. Reflectance properties may also change due to factors such as seasonal variation of plant foliage, material weathering, snow cover, or wetness. Sometimes, ***albedo*** is used to refer to reflection only in the visible range of wavelengths, whereas ***ground reflectance*** (ρ_g) covers the entire solar spectrum, but in many cases, the two terms are used interchangeably as they will be here. Twenty percent is a common assumption for the magnitude of ground reflectance in the absence of specific information because that value represents a rough average of the albedo of typical surfaces found around buildings, such as grass and other vegetation, crushed rock, weathered concrete,

Table 5.1 Solar Reflectivity of Various Surfaces

Material	ρ
New concrete*	0.31
Weathered concrete**	0.22
Grass**	0.20
Crushed rock**	0.20
Asphalt**	0.09
Fresh snow**	0.75–0.90
Old snow**	0.40–0.70
Building surfaces—dark**	0.27
Building surfaces—light**	0.60
White cool roof membrane—new***	0.83
White cool roof membrane—3 years old***	0.70

* from Threlkeld (1962)
** from Muneer (2004)
*** based on author's analysis of typical new and three-year aged reflectance of rated products from CRRC (2016)

and bare soil. In the case of a building located adjacent to highly reflective surfaces, such as white sand, ice, or especially snow, it is essential to adjust for the proper reflectance value because ground reflectance can become a large contributor to insolation in these situations. It is also important to consider that ground reflected radiation, while diffuse, is coming from below rather than above, so it will tend to strike ceilings and the underside of overhangs first. For building surfaces adjacent to ground surfaces of very low albedo such as asphalt, the differences are not as extreme, but should still be accounted for. In these cases, the solar heat absorbed and re-radiated by very low albedo surfaces is a more pressing concern. Table 5.1—adapted from the Cool Roof Ratings Council,[10] Muneer,[11] and Thevenard and Haddad[12]—lists the solar reflectivity values for common surfaces found on and around buildings.

The fraction of reflected radiation incident on a surface is also dependent on that surface's ground view (V_g) from the model by Liu and Jordan.[13] Equation 5.18 is used to calculate the appropriate ground view for surfaces of any tilt. For a vertical surface, the ground view is 0.5, implying an unobstructed view to the horizon. While a true view of the horizon is unusual in practice, closer ground surfaces are much more important, and the error introduced with this assumption is usually minimal if obstructions are distant. In cases where ground reflectance is very high and potential overheating becomes a concern, this assumption is conservative. In tight urban environments, adjustments may need to be made to account for less view of the ground, but more view of other building surfaces.

Equation 5.18 Ground View Factor

$$V_g = \frac{1 - \cos\Sigma}{2}$$

In order to determine how much radiation is reflected from the ground, one must first know how much is incident upon it. If an hourly value for ***global horizontal insolation*** (I) is not available in the solar radiation data, calculate it by adding the beam insolation on the horizontal (I_{bh}) from Equation 5.13 to sky diffuse (I_d), as shown in Equation 5.19.

Equation 5.19 Global Horizontal Insolation

$$I = I_{bh} + I_d$$

To find the ***ground reflected insolation*** (I_{tg}) on the surface, use Equation 5.20, multiplying the ground view (V_g) and global horizontal insolation (I) values by the surface reflectance.

Equation 5.20 Ground Reflected Insolation on a Surface

$$I_{tg} = I\rho_g V_g$$

EXAMPLE 5.10 GROUND REFLECTED INSOLATION ON A SURFACE

Calculate the ground reflected insolation on the surface from Example 5.2. Assume ground reflectance of 20%.

From Example 4.2, I_d = 153 Wh/m², and from Example 5.7, I_{bh} = 279 Wh/m², and $\Sigma = 30.00°$.

1) Using Equation 5.18, calculate the ground view factor.

$$V_g = \frac{1-\cos\Sigma}{2} = \frac{1-\cos(30.00°)}{2} = 0.07$$

2) Using Equation 5.19, determine the total radiation incident on the horizontal.

$$I = I_{bh} + I_d = 279\frac{Wh}{m^2} + 153\frac{Wh}{m^2} = 432\frac{Wh}{m^2}$$

3) Using Equation 5.20, calculate the ground reflected insolation on the surface.

$$I_{tg} = I\rho_g V_g = \left(432\frac{Wh}{m^2}\right)(0.20)(0.07) = 6\frac{Wh}{m^2}$$

In most cases, reflected radiation is diffuse in nature, but in some extreme cases, it can be specular and must be dealt with as such. This type of problem arises most often with mirrored glass curtain walls that reflect light into adjacent spaces. In one extreme example, the concave façade of a hotel in Las Vegas was found to focus reflected solar radiation on the pool deck below with an intensity that could cause severe sunburns.[14] More commonly, reflective glass walls cause glare that negatively impacts drivers, pedestrians, and occupants of other buildings and can also result in excessive heat gain in adjacent buildings.

Surface Global Radiation (G_T, I_T, D_T)

Surface global radiation is the total of all solar radiation components incident on a surface of arbitrary orientation. This is distinct from global radiation, which is the sum of components incident on a horizontal surface. Equation 5.21 shows the formulation for determining hourly surface global insolation. Any additional reflected components in a given situation would be added to this total. Duffie and Beckman present a method for dealing with additional diffuse reflected components.[15] For irradiance or daily total insolation, substitute the appropriate symbols and values into the same equation.

Equation 5.21 Surface Global Insolation

$$I_T = I_{tb} + I_{td} + I_{tg}$$

EXAMPLE 5.11 SURFACE GLOBAL INSOLATION

Calculate the global insolation on the surface from Examples 5.1, 5.4, 5.6, 5.8, and 5.10 using both the isotropic and anisotropic sky models.

From Example 5.6, $I_{tb} = 447\ \mathrm{Wh/m^2}$.
From Example 5.8, $I_{td\text{-}isotropic} = 142\ \mathrm{Wh/m^2}$.
From Example 5.9, $I_{td\text{-}anisotropic} = 217\ \mathrm{Wh/m^2}$.
From Example 5.10, $I_{tg} = 6\ \mathrm{Wh/m^2}$.

1) Use Equation 5.21 to calculate I_T.

Isotropic

$$I_T = I_{tb} + I_{td} + I_{tg} = 447\frac{Wh}{m^2} + 142\frac{Wh}{m^2} + 6\frac{Wh}{m^2} = 595\frac{Wh}{m^2}$$

Anisotropic

$$I_T = I_{tb} + I_{td} + I_{tg} = 447\frac{Wh}{m^2} + 217\frac{Wh}{m^2} + 6\frac{Wh}{m^2} = 670\frac{Wh}{m^2}$$

In this case, the anisotropic value is quite a bit higher than the isotropic because the surface is facing toward the area of the sky dome where the sun is. Vertical surfaces facing away from the sun modeled with the anisotropic model will have slightly lower values for diffuse insolation compared to the isotropic model.

Equation 5.22 combines the equations for the beam, sky diffuse, and ground reflected components of hourly surface global insolation into one formula for surface global insolation using the isotropic sky model.

Equation 5.22 Surface Global Insolation—All Components (Isotropic Model)

$$I_T = I_b \cos\theta + I_d\left(\frac{1+\cos\Sigma}{2}\right) + \left(I_b \sin\beta_{sol} + I_d\right)\rho_g\left(\frac{1-\cos\Sigma}{2}\right)$$

Daily Total Radiation

Daily total insolation values indicate the total solar energy, either global or by component, incident on a surface over the course of one day. Often used to provide a simple metric to summarize solar insolation levels, daily totals have the advantage of providing insight into the net impact over time of the sun on a surface or volume. Looking solely at individual hourly insolation values allows one to gauge the momentary intensity of solar radiation on a surface, but provides no indication of what happens at other times during the day.

Daily total beam, sky diffuse, reflected, and surface global insolation values (D_{tb}, D_{td}, D_{tg}, and D_T, respectively) are readily found by calculating the various insolation components for each hour (minimum) and summing them over the course of a day (Equation 5.23). If daily total data are given for available radiation components, see Chapter 4 for methods of breaking it up into approximate hourly values.

Equation 5.23 Daily Total Insolation

$$D = \sum_{24:00}^{0:00} I_T$$

EXAMPLE 5.12 DAILY TOTAL INSOLATION

What is the daily total diffuse and surface global insolation totals using the anisotropic sky model for the surface described in Example 4.2?

1) Use the techniques covered in this chapter to calculate hourly insolation values in tabular form.
2) Sum the diffuse and surface global values for the day to obtain daily totals. See Table 5.2.

Table 5.2 Daily Total Insolation on Surface (Wh/m²) from Example 5.2

Date	*Calc Time*	α_{sol} (°)	β_{sol} (°)	I_{tb}	I_{tg}	I_{td}	I_T
08/16	5:27	−105.63	0.00				
	5:54	−102.36	5.55	0	1	29	30
	6:54	−95.18	18.34	0	3	95	98
	7:54	−87.73	31.28	24	5	157	186
	8:54	−78.97	44.14	160	8	211	378
	9:54	−66.76	56.52	310	10	253	573
	10:54	−45.54	67.36	437	11	284	732
	11:54	−4.74	73.11	499	11	308	818
	12:54	39.63	69.01	539	10	317	867
	13:54	63.72	58.73	566	10	308	883
	14:54	77.03	46.52	479	8	275	761
	15:54	86.23	33.71	447	6	218	671
	16:54	93.82	20.77	266	3	142	411
	17:54	100.99	7.94	82	1	55	138
	18:32	105.63	0.00				
						$D_{td} = 2{,}654$	$D_T = 6{,}548$

Methods also exist for estimating daily total insolation on a surface direct from daily total radiation values; however, these approaches are not as well developed as the hourly approach[16] and involve several cumbersome steps. For single-step methods of working with daily total radiation data for tilted surfaces facing the equator and for any arbitrary orientation, see Hay[17] and Klein and Theilacker.[18]

INSOLATION AND BUILDING FORM

Available radiation for a given location is determined partially by the solar geometry of its latitude, and partially by local conditions of clouds and particulates in the air. As discussed at length in Chapter 4, clear-sky solar radiation values have serious shortcomings for making sound design decisions. Even in the clearest of climates, clear-sky beam values are considerably higher than typical conditions. For studying the relationship of building form and solar geometry as it relates to insolation, clear-sky values are very helpful. Where the details of local weather conditions muddy the picture, studying trends of insolation based on clear-sky calculations provides a clear view of the general principles of the relationship of building form and solar radiation. Armed with that knowledge of the principles, one can investigate a specific climate to evaluate to what extent the local conditions modify those general principles.

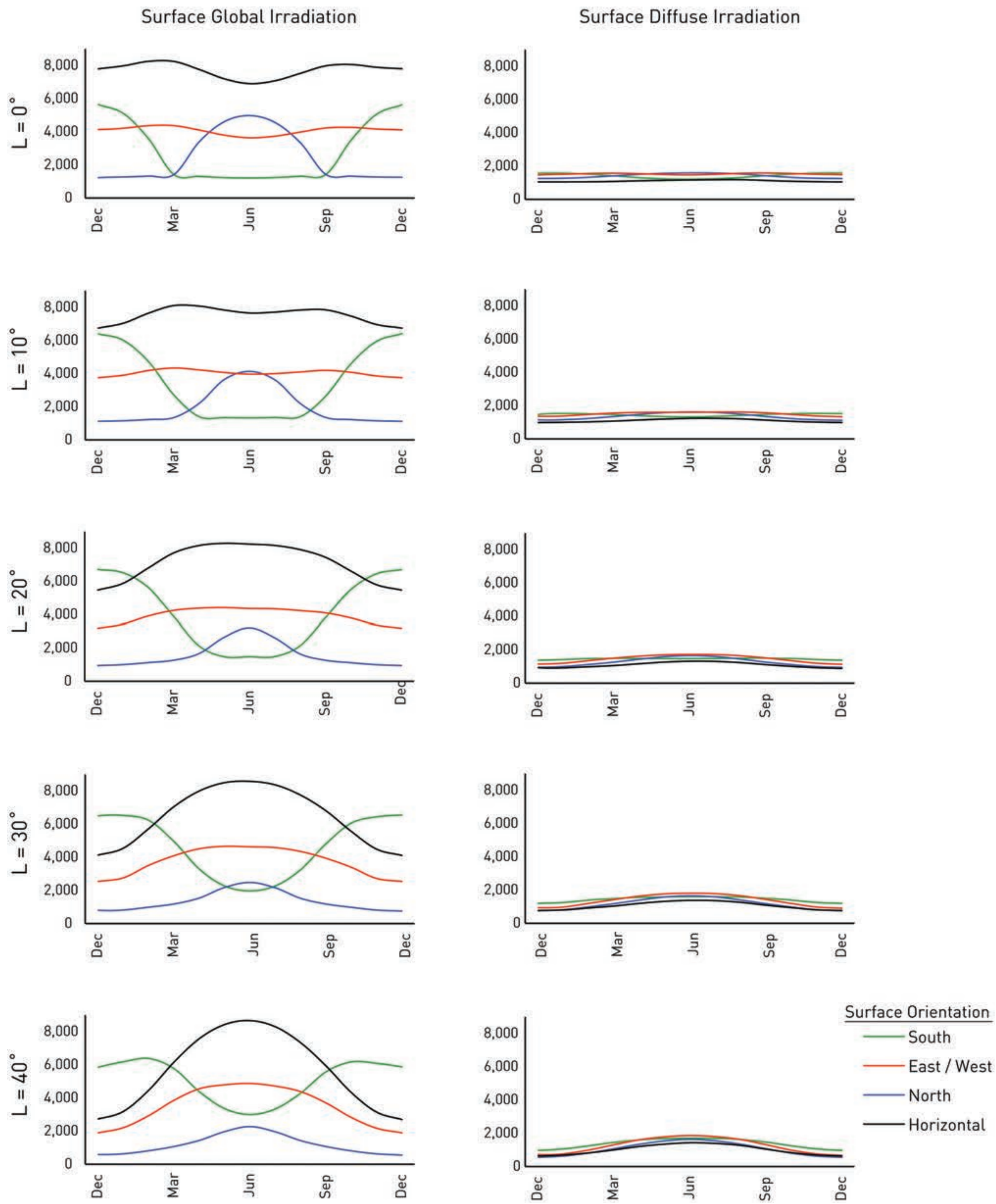

(a)

Figure 5.3a–b

Calculated Clear-Sky Insolation for Surfaces of Five Standard Orientations at Various Latitudes. The curves represent the daily total clear-sky insolation in Wh/m^2 for surfaces at the four cardinal orientations plus horizontal.

Dason Whitsett

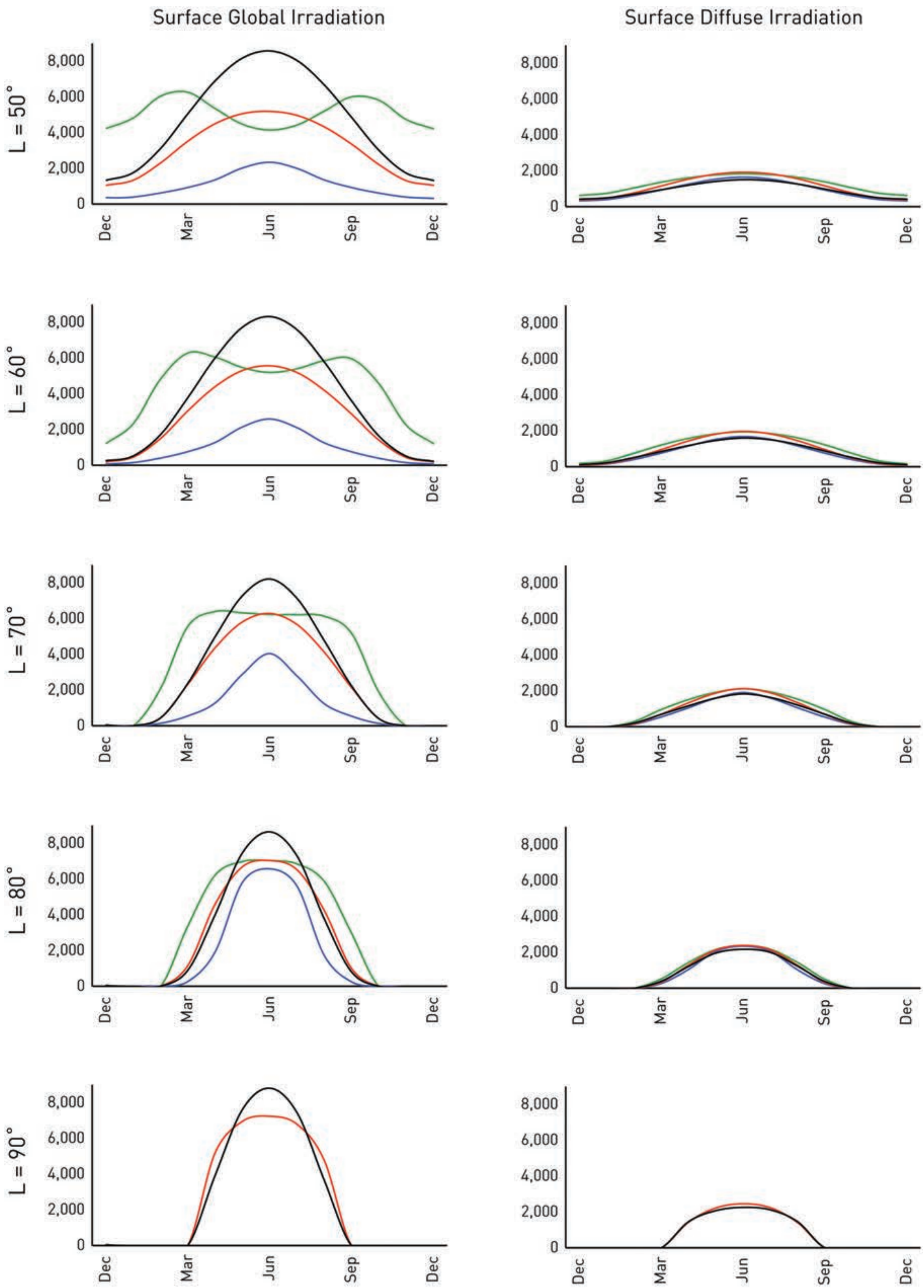

(b)

Figure 5.3a–b
(Continued)

Global Clear-Sky Insolation Trends

The graphs in Figures 5.3a and b show clear-day insolation on vertical surfaces facing each of the cardinal directions and a horizontal surface in Wh/m^2. Latitudes from the equator to the North Pole are shown. In the southern hemisphere, one must reverse north and south surfaces. Clear-sky radiation levels were calculated using the method presented in Chapter 4. Diffuse values were obtained with the anisotropic sky model and include both the sky component and ground reflected radiation incident on the surfaces. Ground reflectivity of 20% is assumed.

Studying the daily total insolation by surface graphs, several trends emerge:

1. At all latitudes in summer, a horizontal surface receives more insolation than any vertical surface.
2. Above approximately 15°, a south-facing surface will receive more radiation per unit area than any other vertical or horizontal surface in winter when the sun is above the horizon.
3. Up to approximately 45°, a south-facing surface will receive substantially more insolation on the cool side of the year than in summer.
4. Above approximately 20°, east- and west-facing surfaces receive more insolation in summer than winter. As you move further toward the pole, the proportion of summer to winter radiation on east and west surfaces increases.
5. Up to approximately 33°, a north-facing surface will receive more insolation than a south-facing surface at the summer solstice.

Local Insolation Patterns

To effectively design using knowledge of the sun, one must combine knowledge of the general principles revealed by study of clear-sky insolation patterns with knowledge of local climate. Figure 5.4 shows a graph of daily total surface global insolation levels on surfaces facing the cardinal directions and the horizontal for Austin, Texas.

The value of this type of graph almost cannot be overstated. It boils down nearly everything one needs to know about passive design into one neat package. Every designer should have a version of this chart for her location committed to memory. Combined with just a little more knowledge, it tells us where shading is important, which surfaces will receive solar gain when it is cool, and which ones will be most exposed when it is hot. It suggests daylighting strategies, and what properties the building envelope should have for different surfaces. In short, it shows one how to choreograph the relationship of building and climate for effective passive performance.

To tease out some of those characteristics, start by examining which surface receives the most solar radiation in December and which receives the least in June. Many people are shocked to see that these are the characteristics of a south-facing surface at this latitude and climate. In fact, the south-facing surface receives even less radiation in June than a north-facing one does. This is the result of extremely high angles of incidence and a short period of exposure to the south and the sun rising and setting to the north at this time.

East and west surfaces see a significant peak in summer, but are not close to receiving the highest total levels of radiation. This is because they are each only exposed for half of the day. Nevertheless, east and especially west surfaces are

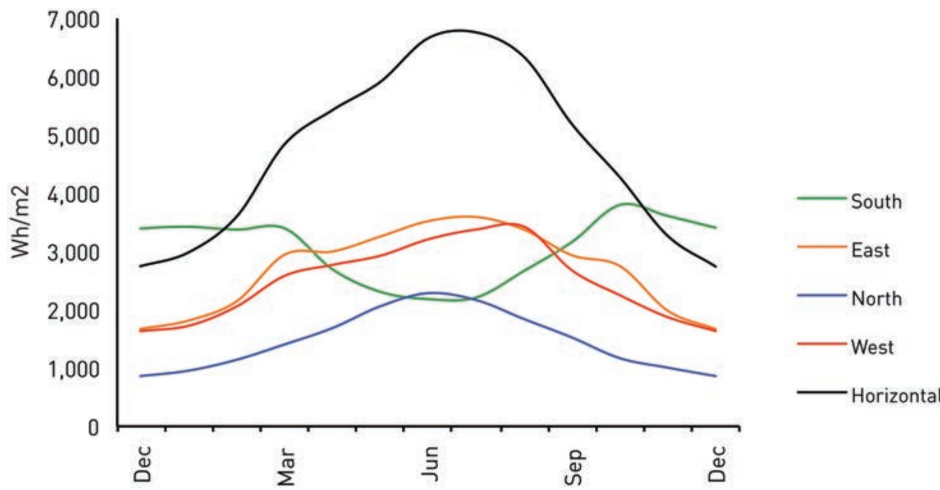

Figure 5.4

Daily Total Global Insolation on Five Surfaces in Austin, Texas, throughout the Year.

Graph shows average insolation month-by-month for vertical surfaces facing in the cardinal directions and a horizontal surface.

Dason Whitsett

crucial to pay attention to because of very low angles of incidence in morning and afternoon. West is particularly a problem because the low-angle sun that is very difficult to shade occurs at the hottest time of the day.

The horizontal surface shows a huge peak in summer as the result of intense low angle of incidence sun for most of the day. During winter, when the sun is low, solar impact on the roof is not nearly as significant, as demonstrated in Figure 5.2. So, it is clear that in a place with very hot summers, such as Austin, highly reflective roofs are a big advantage. Cool roofs reject much of the summer heat, yet do not result in much of a cool weather penalty because they receive so little relative insolation in winter.

Solar gain through opaque walls does not tend to be one of the biggest sources of heat gain in modern buildings, but solar gain through windows does. Figure 5.4 makes strong suggestions about where to place fenestration. The east and west walls and the roof all see their peak exposure levels in summer and are very difficult to shade due to low angles of incidence; hence, they are problematic orientations for windows. The north surface sees relatively moderate insolation levels all year round, and even when it does receive direct-beam radiation in summer, that radiation is at a high angle of incidence, so little of the direct beam component will be transmitted by the window. This concept will be discussed in more detail in Chapter 9. Because it is primarily exposed to relatively consistent levels of diffuse radiation, the north is the optimal location for daylighting fenestration.

The south wall has unique properties because it sees its maximum exposure level at the December solstice. As the result, it is the only direction to place windows for effective passive solar gain, and it also can provide good daylighting as long as appropriate controls are put in place. Because of solar geometry, the south is also the easiest orientation to shade.

Many of the characteristics described regarding Figure 5.4 would also apply in other climates at similar latitudes. As one moves further to the north or south, however, things change significantly, as shown by Figures 5.3a and b.

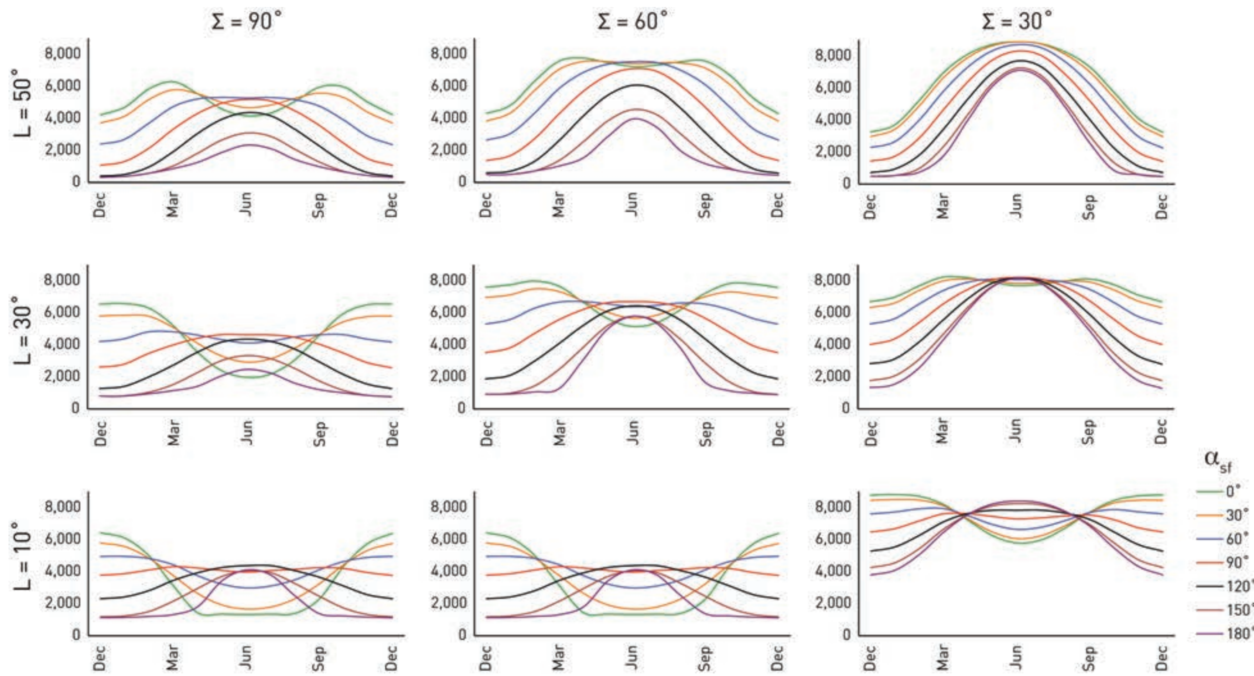

Figure 5.5

Clear-Sky Insolation for Surfaces at Various Latitudes and Tilt Angles.

The curves represent the daily total clear-sky insolation in Wh/m^2 for vertical surfaces at the azimuths shown in the legend. Latitude is shown on the left and surface tilt angle across the top.

Dason Whitsett

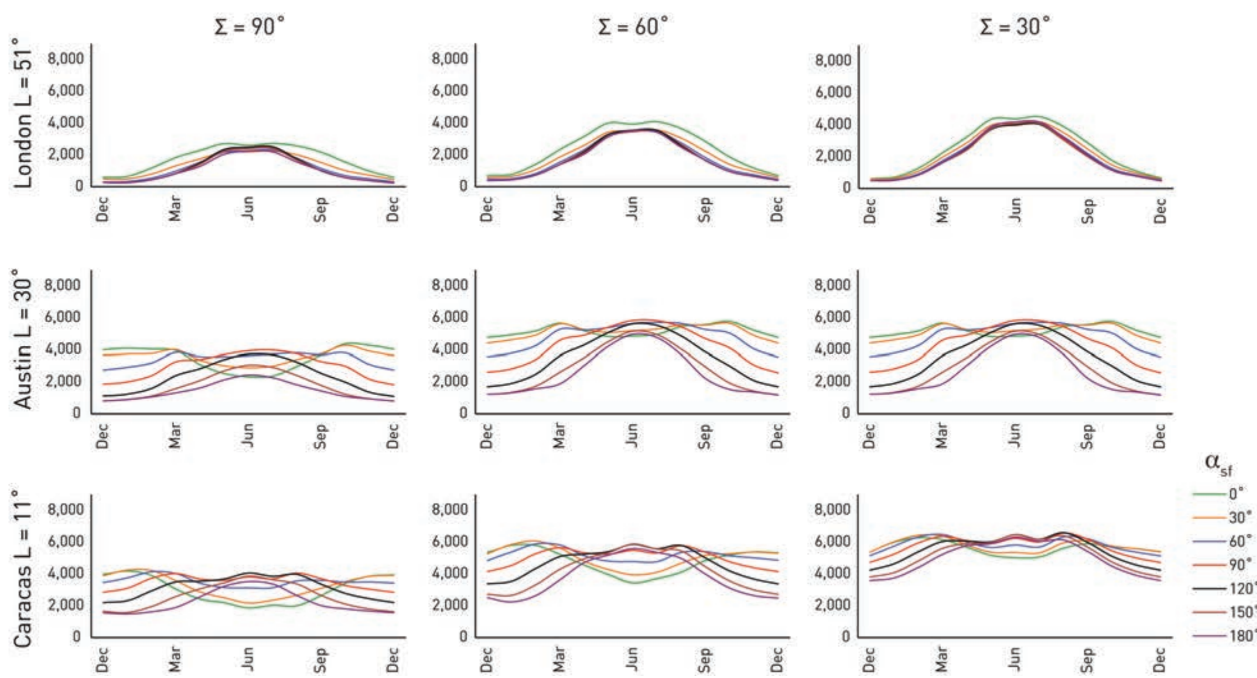

Figure 5.6

Typical Insolation for Surfaces at Three Locations and Various Tilt Angles.

The curves represent the average daily total insolation in Wh/m^2 for surfaces at the azimuths shown in the legend in three representative cities. Location and latitude is shown on the left and surface tilt angle across the top. Note the substantial reduction in insolation compared to clear-sky levels in all three locations due to cloud cover.

Dason Whitsett

Comparing Clear-Sky and Typical Radiation Values

Figures 5.5 and 5.6 show a comparison of clear-day insolation with actual climatic norms for three cities. Surfaces are vertical and are at various azimuths, as shown in the legend. It is clear that in all of these cases, the typical irradiation levels are much lower than the clear-sky values. In a highly overcast climate such as London, surface orientation plays a minimal role in determining typical insolation levels, for which the surface values bear only marginal resemblance to the trend shown by the clear-sky calculations. In Austin and Caracas, however, the trends are similar between the clear-sky calculations and typical conditions, but with a reduced magnitude in the typical conditions.

Insolation and Building Form

Building orientation is commonly cited as one of the most important performance-influencing decisions the designer should think about early in the design process. But to what extent does orientation affect energy use and comfort in buildings? Figure 5.7 compares total building insolation values for forms of various aspect ratios and numbers of stories at a variety of plan orientations. Each building form has the same floor area and values are in Wh/m^2 of gross floor area. Data are grouped into seasonal series so that heating/cooling/transition seasonal comparisons may be made. The calculations use anisotropic *clear-sky* values at 30° N latitude, which allows one to clearly examine the relationship between form and solar geometry. As such, the values are higher than would be expected in any particular location, but seasonal trends would generally be expected to remain similar.

Several very interesting observations may be made about the data in Figure 5.7:

1. In June-July-August, the volume that receives the most insolation (5:1, 1 story, +/– 90°) gets 77% more than the form that receives the least (3:1, 3 story, 0°).
2. In December-January-February, the form that receives the most insolation (5:1, 5 story, 0°) gets 61% more than the scheme that receives the least (1:1, 3 story, +/–45°).
3. The most compact form (1:1, 3 story) receives uniformly low levels of insolation year-round regardless of orientation.
4. The cubic volume (1:1, 3 story) in summer and winter sees a maximum of 5% variation in insolation depending on orientation. On an annual basis, the variation is less than 1%.
5. The 3:1 and 5:1, 5 story, 0° forms receive the most insolation in winter and least in summer.
6. The large surface-to-volume ratio of the single story schemes results in high total insolation on those during summer when the roof is exposed to a great deal of radiation.

The amount of solar radiation a building receives does not automatically dictate its energy use; however, if that energy arrives when the building could use a boost and is minimized when it is already hot, that is obviously advantageous. How solar radiation affects a building depends on solar heat gain through glass and solar absorptance and heat gain through the envelope, which is dependent on the physical properties of the materials with which it is built. Chapter 9 will cover solar heat gain through glazing.

Solar heat gain through the opaque fabric of a building is usually a primary driver of energy use in today's well-insulated buildings, which often have highly reflective

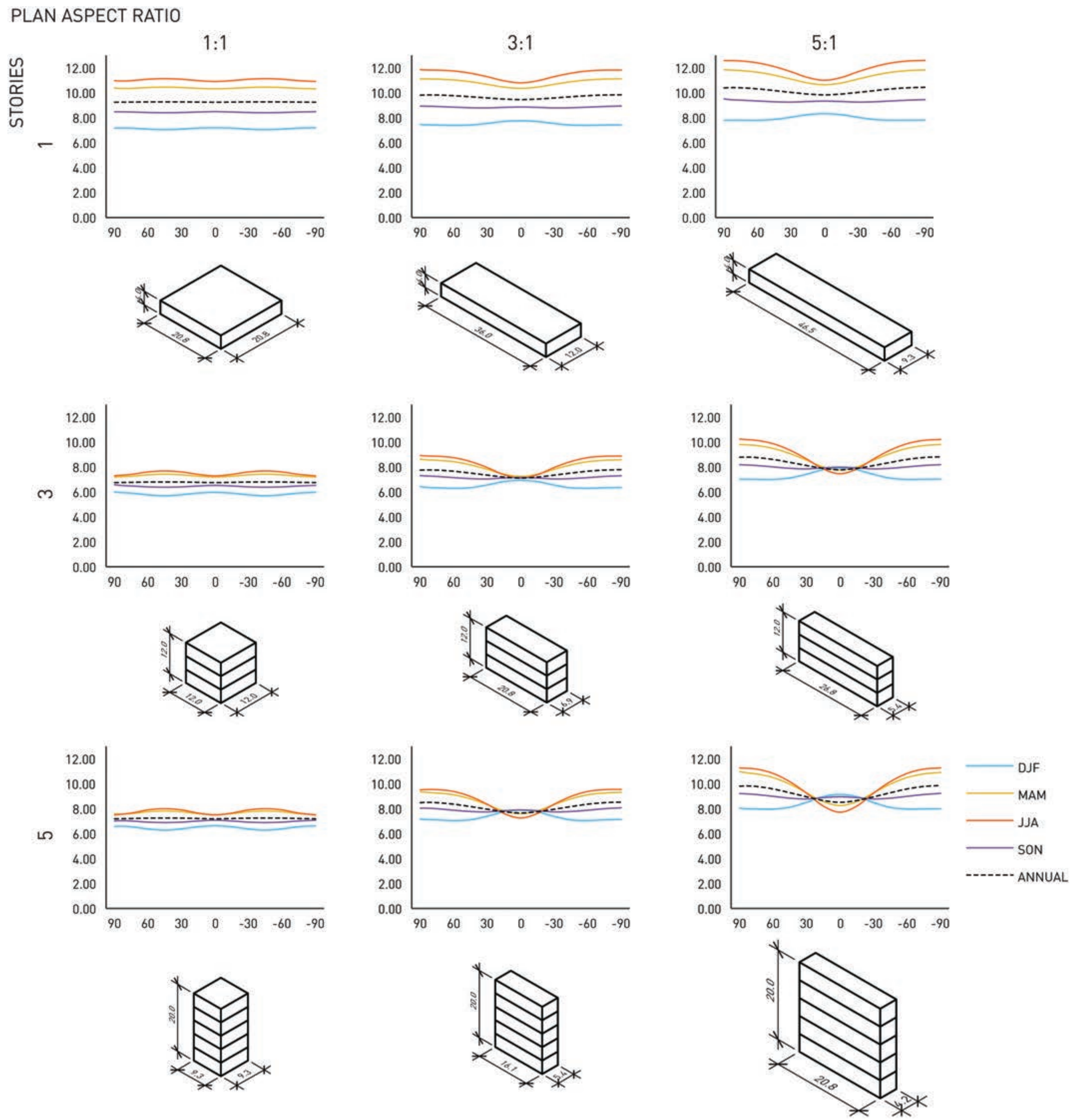

Figure 5.7

Insulation on a Building by Orientation, Plan Aspect Ratio, and Height.

Values are based on clear-sky conditions. The values on the vertical scale are in kWh/m²/day.

Dason Whitsett

roofs. One of the primary lessons relative to building form and insolation is that the availability of surfaces to fenestration is the most important factor relative to building orientation. That is, a building with large north- and south-facing surfaces and narrow east and west ones will tend to have the majority of its glazing on the north and south. These are generally the most desirable directions for windows because the north provides excellent even light for natural lighting and solar geometry/climate patterns are aligned to the south with heating and cooling seasons coinciding with most and least insolation, respectively.

East-, west-, and zenith-facing surfaces, on the other hand, receive the most radiation when one does not want it and the least when we do. To compound the problem, it is very difficult to effectively shade east- and west-facing windows, with the result that solar gain through those windows is often a major driver of cooling loads or discomfort in skin-load dominated buildings. Chapter 8 will delve into the challenges of shading east- and west-facing windows. Therefore, the concern for orientation is, in part, about total building insolation, but more importantly is a question of where windows will be placed.

CONCLUSION

Understanding irradiance and insolation gives the designer tools to adapt the form of the building to the climate. Incident radiation, however, should not be confused with solar gain. The amount of solar heat transferred through a surface into a building or solar collector results from the interplay of a number of factors, which are discussed in Chapter 9, but will always be less than the total irradiance received upon the surface.

NOTES

1 John A. Duffie and William A. Beckman, *Solar Engineering of Thermal Processes*, 3rd ed. (Hoboken, NJ: Wiley, 2006), 104.
2 Ibid., 111.
3 Benjamin Y. H. Liu and Richard C. Jordan, "The Long-Term Average Performance of Flat-Plate Solar-Energy Collectors: With Design Data for the U.S., Its Outlying Possessions and Canada," *Solar Energy* 7, no. 2 (April 1963): 57, doi:10.1016/0038-092X(63)90006-9.
4 Tariq Muneer, *Solar Radiation and Daylight Models*, 2nd ed. (Oxford: Elsevier Butterworth Heinemann, 2004), xxxvi.
5 Muhammad Iqbal, *An Introduction to Solar Radiation* (Toronto: Academic Press, 1983).
6 Duffie and Beckman, *Solar Engineering of Thermal Processes*.
7 ASHRAE, *2009 ASHRAE Handbook: Fundamentals*, SI ed. (Atlanta, GA: American Society of Heating, Refrigerating and Air-Conditioning Engineers, Inc., 2009), 14.10.
8 Donald G. Stephenson, "Equations for Solar Heat Gain through Windows," *Solar Energy* 9, no. 2 (April 1965): 81–86, doi:10.1016/0038-092X(65)90207-0.
9 James L. Threlkeld, "Solar Irradiation of Surfaces on Clear Days," *ASHRAE Transactions* 69, no. 24 (1963).
10 CRRC, "Find Rated Products: Cool Roof Rating Council," accessed February 26, 2016, http://coolroofs.org/products/results/search&channel=products&orderby=cf_product_manufacturer+cf_product_brand+cf_product_model+asc&keywords=thermoplastic&cf_product_slope=Low.
11 Muneer, *Solar Radiation and Daylight Models*.
12 Didier Thevenard and Kamel Haddad, "Ground Reflectivity in the Context of Building Energy Simulation," *Energy and Buildings* 38, no. 8 (August 2006): 972–80, doi:16/j.enbuild.2005.11.007.
13 Liu and Jordan, "The Long-Term Average Performance of Flat-Plate Solar-Energy Collectors," 57.

14 Tony Illia, "Viñoly's Vdara Hotel Accused of Scorching Sunbathers | News | Architectural Record," *Architectural Record*, accessed October 15, 2010, http://archrecord.construction.com/news/daily/archives/2010/10/101015Vdara.asp.
15 John A. Duffie and William A. Beckman, *Solar Engineering of Thermal Processes*, 4th ed. (Hoboken: Wiley, 2013), 97–100.
16 Ibid., 103.
17 John E. Hay, "Calculation of Monthly Mean Solar Radiation for Horizontal and Inclined Surfaces," *Solar Energy* 23, no. 4 (1979): 301–307, doi:10.1016/0038-092X(79)90123-3.
18 Sanford A. Klein and Jay C. Theilacker, "An Algorithm for Calculating Monthly-Average Radiation on Inclined Surfaces," *Journal of Solar Energy Engineering* 103, no. 1 (February 1, 1981): 31, doi:10.1115/1.3266201.

6 RECEIVED SHADOWS

The duality of sunlight and shadows, as referenced in the first chapter of this book, is an ancient binary opposition. Tree canopies modulate sunlight, scattering it about the ground beneath. Although there is an inherent geometric rigor about these projections, due to the irregularity of the tree canopy form, it appears to the human eye to be random, making it more compelling. This is further enhanced by the fluttering movement. The same occurs with the movement of clouds overhead, which provides a dynamic setting and an ephemeral sense of natural light.[1] Shadows have a role in folklore; it was once considered a terrible curse to lose one's shadow, and anyone with a headless shadow was predicted to die within a year.[2] Although an eclipse of the sun, where the moon passes between the sun and Earth, is a rare occurrence, it is often referred to and highly anticipated. This is partially related to the fact that it is an anomaly within the typical daily solar pattern, and even a partial eclipse creates a highly unique shadow.

In one of the most well-known writings in ancient western civilization, *The Republic*, Plato described a cave in which the only things to see were shadows, and dismissed this knowledge gathered by the inhabitants of the cave as inferior. The scene, represented in an engraving entitled "The Miracle in the Cave" by Pieter Saenredam in 1604, is set in a subterranean passage beneath the ground (Figure 6.1). In a dimly lit room, the occupants are supposedly part of an experiment. They are unaware of the state of the outside world, as they have been kept in the cave since they were young. Their only focal point is a shadow performance, upon which they fixate. They are unaware of their unusual circumstances, as it is all they know. They are witnessing projections of shadows from statues, which they cannot see, and this becomes their understanding of reality. They have no way of knowing that this two-dimensional performance is not reality, and that they are witnessing a twice-removed representation of reality. Likewise, even though we have more information from which to deduct "reality," we are still also part of an illusion. Plato maintains that no one has a comprehensive understanding of what truly exists, but shadows are one way we begin to make sense of three dimensions and the world around us.

It could also be argued that Plato attempts to diminish the value of the shadow as only having a limited ability to represent the object from which it is projected. The fact is that shadows do help us more thoroughly understand our surroundings and to establish constructs at various scales. Shadows are both a tool and deeply meaningful entities that help describe formal characteristics of any object and also remind us of the passage of time.

A clear architectural design strategy at the scale of volumetric massing typically includes careful consideration between a building and its light and shade. Greek

Figure 6.1
"The Miracle in The Cave," Peter Saenredam, Engraving, 1604

temples are composed of rhythmic patterns of solid and void from the column spacing and solid walls, setting up a dynamic interplay of light and shadow. The careful proportional design of the Parthenon can be argued to be as much about light and shadow on an object to be seen in the round as it is about occupiable space. Light and shadow intensify the relationship between the facade and the viewer, and their ever-changing nature heightens the relationship between the architectural object and the observer.

Louis Kahn brought natural light to the forefront in the discourse of Modern architecture. Not only his work but also his writings clearly define light as the essence of all nature, which is ultimately what architecture should aspire to approximate. In Kahn's interpretation, light is the source of all things: "All material in nature, the mountains, the great rivers and we ourselves are extinguished light, and this decayed mass that we call material casts a shadow, and the shadow belongs to the light." He thought it was important that architectural space allowed for abundant light, partially to allow the occupant to track time and the changes in the day. "Natural light has the moods of the time of the day, the seasons of the year, [which] year for year and day for day are different from the day preceding."[3] His view that structure enables or even "gives" light lends to the fact that Kahn's buildings possess a great physical monumentality, to the extent that design for function may be considered secondary to the overall presence of the structure as a form and the spaces as ambient environments. The monumentality of his buildings was also reinforced by their materiality of concrete and masonry in monolithic configurations as primary components, creating unity in the buildings and a restrained canvas to receive light. Kahn was certainly an advocate of daylight in all spaces, declaring, "[A] room without natural light is not a proper room."[4]

In Kahn's work, the construct of the wall plays a role; relief, texture, color, size, and the rhythm of the openings decide how light is transformed or to what extent the proposed building requires light modulation. It is the openings in his heavy walls that make for the depth and richness of the shadows in the work. His work can often be seen as stereotomic, as a series of large openings carved out of an otherwise solid volumetric mass, which acts as an instrument to modulate light for the functional spaces in the interior (see Figure 6.2). In many of his buildings, deep skylight monitors, deep openings, and deep overhangs minimize direct solar gain and manage daylight in the spaces, aiding in the diffusion of light before it reaches interior surfaces.

The seemingly intuitive work done by Kahn was in fact the result of a rigorous investigation and observation regarding the balance of sunlight, architectural structure, and experiential space. He took a critical distance from each of his projects with the intent to continually learn and improve his craft. Through qualitative and quantitative investigations and diagram sets on the relationship between form and daylight distribution, the aim of this book is to help the reader build a knowledge base upon which a light-driven design "intuition" can be developed as a practical tool.

Figure 6.2

Phillips Exeter Library Reading Desks, Louis I. Kahn Architect.

Greg Arcangeli

In the following generation of architects, the work and writing of Tadao Ando stands out as particularly steeped in its response to and generation of light and shadow. Referring to his Koshino House design, Tadao Ando states, "Light gives objects existence as objects and connects space and form. A beam of light isolated within architectural space lingers on the surfaces of objects and evokes shadows from the background." There is a sort of give and take relationship between light and objects. Appearances of objects are altered with changes of season and passage of time; conversely, light is not given form until it is accepted by physical objects. An individual object is articulated and given shape at the boundary between light and dark.[5]

Ando once visited a medieval monastery built of rough stone masonry and devoid of ornament. However, the interaction of light and dark within the building conferred a feeling of great power. Ando felt a similarity between this and the mood conveyed in a Japanese tea ceremony room. Japan's distinctive culture has been created by importing and assimilating elements from other countries. Ando feels that there is a tendency today to submerge that distinctive culture, resulting in much of what was particularly Japanese vanishing. In his opinion, one important thing being lost is a sense of the depth and richness of darkness.[6] When everything is uniformly illuminated, we forget the subtle patterns created by light and shade.

Ando states:

> Although they are essentially very different from the normal regularity of daily life, geometric principles both give order to architectural form and serve as a mediator in making architecture a material representation of an intangible theory of life. Introducing the processes of nature and human movement brings dynamism to architecture that has acquired self-control and tranquility as a result of the imposition of geometric order.[7]

As a person walks through such an ordered space, the eye encounters various overlapping scenes that merge into a whole. The parts have an enriching effect on each individual scene within the whole.

Ando speaks of a "dialogue with materials." For example, he uses concrete to produce, or receive, light along its homogeneous surfaces. When light is drawn into the smooth surfaces and sharp edges, a cool, tranquil space is created. Ando's aim is to eliminate all nonessentials and to limit materials, interweaving into his spaces the totality of the human being.[8] He says that "to achieve this effect, it is necessary to return to the point where the interplay of light and dark reveals forms, and in this way to bring richness back into architectural space."[9]

Architecture takes its form by the means of light and shadow. Light defines contours and shadows capture depth. The work of Tadao Ando makes exceptional use of sunlight, and therefore shadow, as it changes throughout the day, in contrast to the static quality of artificial light. One can argue that contemporary architecture lacks the power that can be derived from the intentional manipulation of shadows. In that respect, Ando's architecture is both a spectacle to behold as well as a humble backdrop for light and the life that exists within it. Light and shadow take the center stage, and the buildings have a certain confident stoic presence, seeming ready to endure and withstand. Like the work of Kahn, volumetric mass as well as mass created by sheer thickness of walls plays a role in the perception of volume, light, and form. Furthermore, the large solid planar masses are in direct contrast with the openings. This polarization leaves no middle ground, but rather just either extreme, with no translucency or screening devices. Ando has stated, "To create space in architecture is nothing more than to concentrate and refine light," acknowledging that light and shadow are necessarily complementary counterparts.[10] In a broader sense, architecture is meant to use tangible materials to create the setting for the intangible patterns of the human experience. Part of creating meaningful architecture is the intentional embrace of light and shadow, with a fundamental understanding of shadow-casting, as a key element in the generation of transcendent space.

SHADOW GEOMETRY

In the 3rd century BCE, the Greek natural philosopher Eratosthenes learned that, in Swenet, Egypt, no shadows are cast at solar noon on the June solstice. He knew, however, that 800 km north at his home in Alexandria, a pole did cast a shadow. He measured the angle of that shadow and concluded that the two cities were separated by an angular distance equal to 7.2°. It just so happened that the pharaohs employed surveyors to keep accurate records of distances between cities. Using this information, he made a remarkably accurate estimate of the circumference of the Earth. While there is debate about which version of the "stadia" length measurement he was using, at the worst, his estimate was within approximately 15% and, at best, within approximately 1%. Either way, it was a remarkable feat for a philosopher to achieve using primitive methods and without leaving Egypt.

We will let the reader match wits with Eratosthenes. Alexandria is slightly west of Swenet. The actual distance between the two cities is approximately 845 km. The distance along a meridian between the latitudes of the two cities, however, is almost exactly 800 km. Try to reproduce his logic and circumference estimate and check your answer against Table 2.3. With his keen observation of shadows, Eratosthenes proved the Earth was spherical and deduced its size, although it would be well over a millennium before much of the world accepted this insight.

Figure 6.3

The Magic of the Shadow

Recently, while taking my girls to school, one of them exclaimed, 'Look at my shadow!' I looked up and here was this magical moment in a banal place we've walked by countless times without thinking anything about it. It was cold, and the sun was just cresting above the building on the opposite side of the street. We felt the warmth of the sun on our backs and heard the rustling of the leaves in the breeze. Her legs looked impossibly long, but her body was its real dimension. The low morning sun brought out the warm honey-color of a normally dull cedar fence. The low sun lit up the little escarpment of the crack in the concrete like neon. Then there was the peculiar situation where the tree appeared to be casting a shadow onto itself, which was actually the shadow of a telephone pole behind us.

—*Dason Whitsett*

Dason Whitsett

Some previous generations of architects were taught to draw shadows where a 45° line from the roof intersects the ground; today, most students and designers have 3D CAD do the work of casting shadows for them. For a designer without an understanding of actual shadow geometry, however, these tools provide little useful insight. Learning to visualize and predict shadows is essential to effective design, whether harnessing the power of the sun for heating, intentionally creating shadows for comfort, or avoiding glare.

Shadows occur where an object blocks the direct rays of the sun or another light source from striking another surface. Generally, we have to see the boundary of the obscured area with the contrast of direct sun on an adjacent area to perceive it as a shadow and not simply shade. These are closely related concepts in that shade only occurs within a shadow.

To be precise, a *shadow* is the projected shape of an object onto another along the ray of a light source. Every child has observed the distortions that occur in her shadow on the ground (Figure 6.3). When the sun is high, the shadow is short, but it grows very long as the sun moves closer to the horizon. When walking next to a wall, her shadow miraculously folds up the wall. As the topography of the surfaces that the shadow lands on becomes more varied, the shadow becomes more complex.

Predicting the shape of a shadow is conceptually simple. Imagine the solar vector as a giant pencil at a fixed angle tracing along the edges of the shadow-casting object—in this case, the child. The tip of the pencil is extended until it contacts a surface. The area that falls within the boundary is in shadow, while the area outside the boundary receives direct light. Geometrically predicting the resulting shape is almost as straightforward when working with simple solids casting shadows onto horizontal surfaces, but complexity increases quickly when the forms and the receiving surfaces are more intricate.

One might assume that the ready availability of 3D drawing tools today would make the study of 2D orthographic projections of shadows obsolete. To the contrary, the difficulty of mental visualization of multiple intersecting planes and vectors in three dimensions makes the 2D orthographic projection the best tool to understand shadow principles.

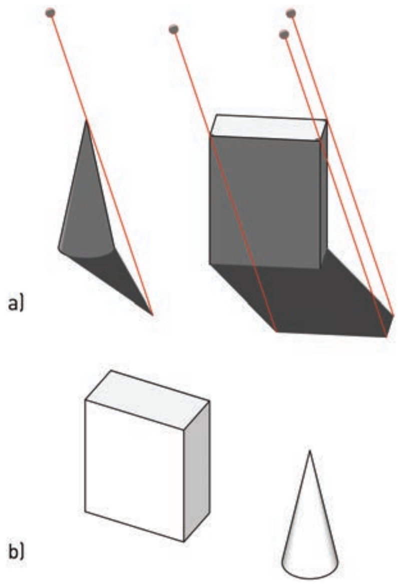

Figure 6.4

Shadows and Solar Views

Drawing *a* shows the shadows cast by these simple solids with the sun in a particular position. Because the sun is so far away that all the rays are effectively parallel, the solar vector is projected past each shadow-casting point until it strikes a surface—in this case, the ground plane. Drawing *b* shows solar views of the same objects at the same date and time.

Dason Whitsett

SOLAR VIEWS

Solar views are parallel-line projections taken from the point of view of the sun, as shown in Figure 6.4. These are closely related to shadows in that the parallel-line projection of an object one sees from this vantage point is the same as the projection of a shadow onto whatever surfaces it strikes. In other words, in a solar view, the area obscured by the object itself is in shade and the outline of the object matches the shadow perimeter. The construction of solar views is beyond the scope of this book, but some 3D programs allow the user to easily create these. Solar views for site evaluation will be covered in Chapter 7.

CONSTRUCTING SHADOWS

To construct shadow geometry, only the solar coordinates at a particular date and time are necessary. Start by projecting lines at the solar azimuth angle in plan view past potential shadow-casting edges, as shown in Figure 6.5. Next, draw an elevation of the object looking perpendicular to the azimuth angle. On that elevation, project lines at the solar altitude angle from potential shadow-casting points until they strike another object or the ground plane. Then, project these intersection points back to the plan view, find the intersection with the azimuth-line projections, and draw the perimeter of the shadow. If unsure about whether a point or edge will form part of the shadow outline, just project it to verify.

While straightforward, this method requires drawing a separate elevation for the current azimuth angle, which is tedious, especially if drawing shadows for multiple different times of day. Usually, it is more desirable to adapt the solar coordinates to the frame of reference of the drawing rather than doing a specific drawing for the solar position. This is accomplished through some simple algebraic manipulation.

PROFILE AND ELEVATION ANGLES

In Chapter 5, two angles that represent a transformation of solar coordinates to the frame of reference of the surface were discussed. The surface-solar azimuth is the azimuth of the sun relative to the bearing of the surface. The angle of incidence is the true angle between the surface normal vector and the solar vector.

To describe solar altitude relative to the surface, we use the profile and elevation angles. These exceedingly important angles, shown in Figure 6.6, measure the apparent solar altitude perpendicular and parallel to a plane. The ***profile angle*** (Ω_{pf}) is the altitude of the sun as viewed looking at a surface in section or "profile." From this point of view, the solar vector is projected onto a vertical plane perpendicular to the surface, and the profile angle is the apparent angle between the solar vector and the ground plane.

The ***elevation angle*** (Ω_{el}) is a variation on the profile angle concept, viewing the surface in elevation with the solar vector projected onto the vertical surface. When $\Omega_{el} > 0$, the solar vector is to the left side of the surface, and when $\Omega_{el} < 0$, it is to the right.

The profile angle and elevation angles are the same concept from different frames of reference. For example, in Figure 6.6, the profile angle of the gray wall is the same as the elevation angle of the magenta wall. When viewing an elevation drawing of a wall, the profile angle determines the length that shadows project down the wall while the elevation angle defines the angle at which shadows rake across its surface. Profile and elevation angles will always be greater than the true solar altitude angle due to the foreshortening that results from viewing the angle from a position other than normal to the azimuth. If the view is parallel to the azimuth, the profile or elevation angle is 90° because the altitude vector appears vertical.

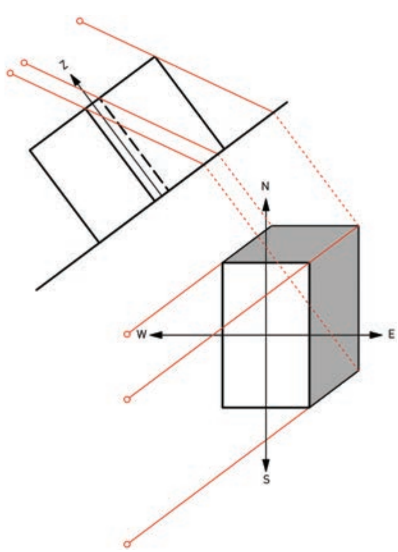

Figure 6.5

Shadow Geometry

Dason Whitsett

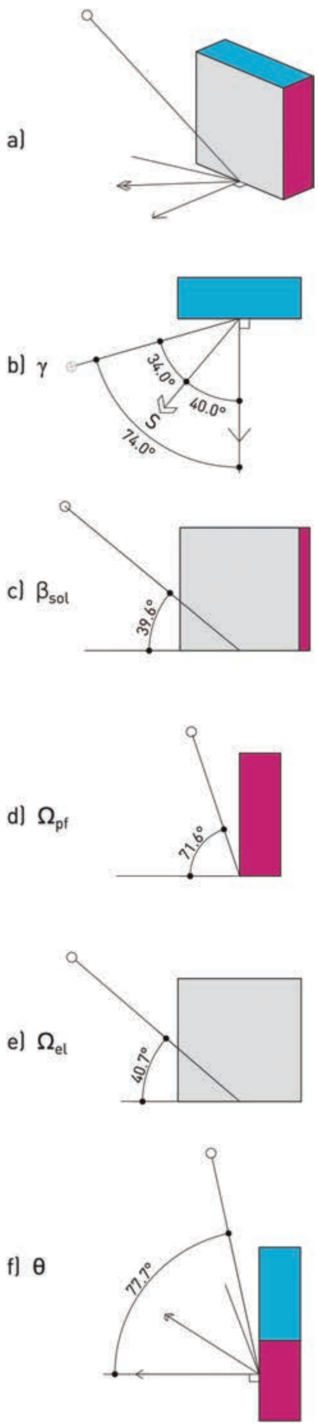

Figure 6.6

Transformation of Solar Coordinates

Views of a surface relative to the sun in Austin, Texas, on the February design day at 13:45. Solar position is: αsol = 34.0° and βsol = 39.6°. The surface in question is the grey surface with a surface azimuth of –40° and tilt of 90° (vertical). View *a* shows the surface and solar ray in 3D. View *b* shows the solar, surface, and surface-solar azimuth in plan view. Views *c–f* show the true solar altitude, profile angle, elevation angle, and angle of incidence relative to the grey surface.

Dason Whitsett

Figure 6.7 shows isopleth curves on the sky dome for these various angles. Each red line represents points on the sky dome that have a constant profile, elevation, or incidence angle relative to the normal vector of the vertical dashed surface. Note that profile and elevation angle curves become ellipses when shown in plan view while the angle of incidence forms straight lines. These plan views are spherical (true) projections of the sky dome. When the same curves are translated to the equidistant projection used most commonly, their shape changes, making it more difficult to interpret their geometric meaning.

Profile, elevation, and incidence angles are essential in shading device design, shadow-casting, and projection drawing. While profile and elevation angles are most frequently used to describe the position of the sun relative to a surface, these two angles can just as easily be used to describe the relationship between any plane and vector. These angles may also be calculated directly using Equations 6.1 and 6.2, or found using diagrams or protractor-type tools.

Equation 6.1 Profile Angle

$$\tan\Omega_{pf} = \frac{\tan\beta_{sol}}{\cos\gamma}$$

Equation 6.2 Elevation Angle

$$\tan\Omega_{el} = \frac{\tan\beta_{sol}}{\sin\gamma}$$

EXAMPLE 6.1 PROFILE AND ELEVATION ANGLES

Find the surface-solar azimuth, profile, and elevation angles for the plan-south and plan-west surfaces in Figure 6.8 on the October design day at 14:00 in Austin, Texas.

Plan-south surface: $\alpha_{sf\text{-}south}$= 15.00°, $\Sigma_{sf\text{-}south}$= 90.00°.
Plan-west surface: $\alpha_{sf\text{-}west}$= 105.00°, $\Sigma_{sf\text{-}south}$= 90.00°.

Using methods from Chapter 3: α_{sol}= 39.06° and β_{sol}= 39.02°.

1) For the plan-south surface:

Use Equation 5.5 to find the surface-solar azimuth:

$$\gamma_{south} = \alpha_{sol} - \alpha_{sf-south} = 39.06° - 15.00° = 24.06°$$

Use Equation 6.1 to find the profile angle:

$$\tan\Omega_{pf-south} = \frac{\tan\beta_{sol}}{\cos\gamma} = \frac{\tan(39.02°)}{\cos(24.06°)} = 41.59°$$

Use Equation 6.2 to find the elevation angle:

$$\tan\Omega_{el-south} = \frac{\tan(39.02°)}{\sin(24.06°)} = 63.29°$$

2) For the plan-west surface:

$$\gamma_{west} = \alpha_{sol} - \alpha_{sf-south} = 39.06° - 105.00° = -65.94°$$

$$\tan\Omega_{pf-east} = \frac{\tan\beta_{sol}}{\cos\gamma} = \frac{\tan(39.02°)}{\cos(-65.94°)} = 63.29°$$

$$\tan\Omega_{el-south} = \frac{\tan(39.02°)}{\sin(-65.94°)} = -41.59°$$

Note that the elevation angle of the plan-south surface is the same as the profile angle of the plan-west surface. The profile angle of the plan-south surface is the same as the negative of the elevation angle of the plan-east surface. The surfaces are rotated 90° from one another, so it is natural that the angles match. The utility of separating the two concepts is that when working relative to one surface, one does not have to switch back and forth between frames of reference. For shadow-casting, it is only necessary to calculate the solar profile and elevation angles for a plane aligned with one axis.

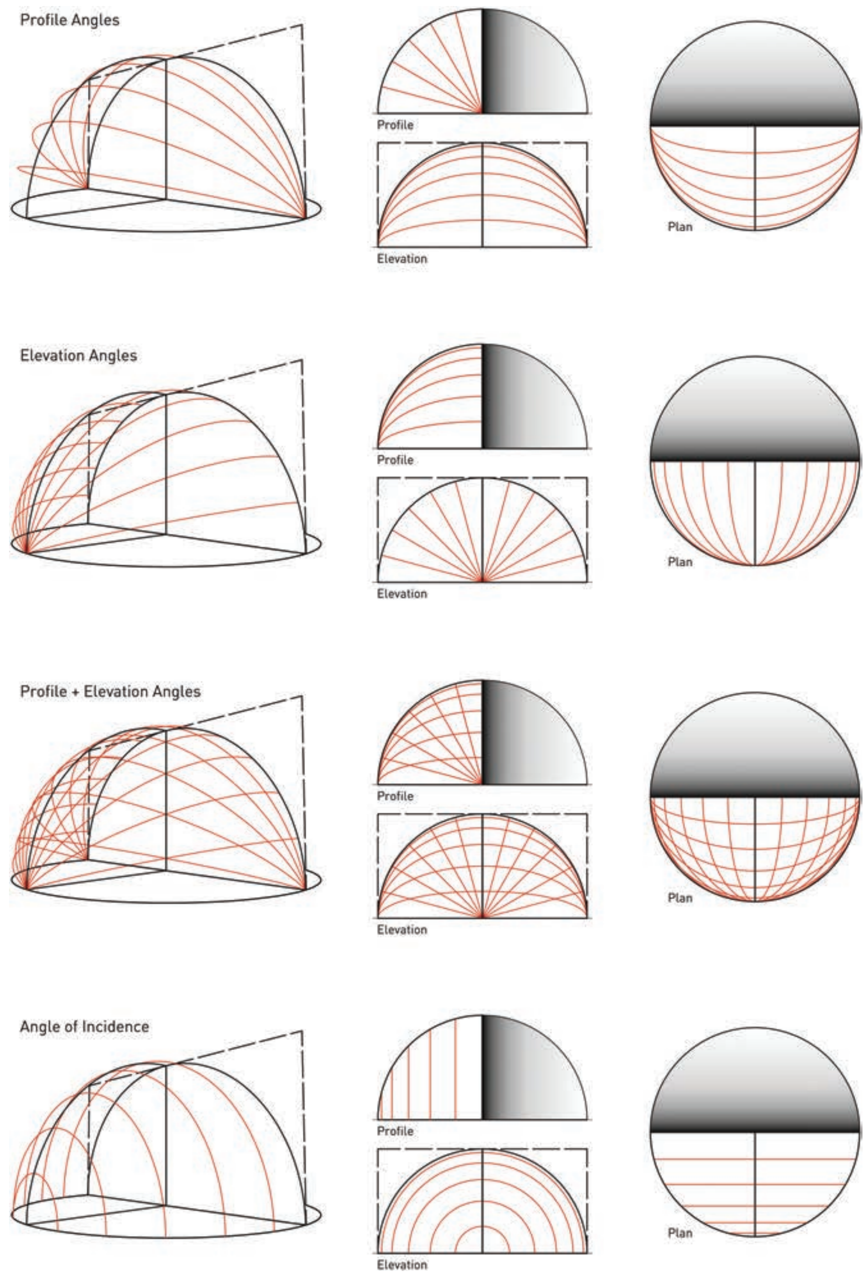

Figure 6.7

Surface Coordinate Transformations on the Sky Dome

The diagram shows lines of constant profile angle relative to a vertical surface aligned with the x-x axis. A point of the sky dome that falls anywhere on one of these lines will have the same profile angle relative to that surface. Note that the sky dome is a projection of the surroundings from one particular point (not a 3D view), so the dashed vertical surface is shown for reference only.

Dason Whitsett

COMPLEX SHADOW-CASTING

As the volumes casting shadows become more complex, and the surfaces onto which shadows fall more contoured, visualizing the shape of shadows is much more difficult. Figure 6.8 is an example of a slightly more involved shadow construction. For this figure, the surface-solar azimuth, profile, and elevation angles were calculated in Example 6.1. The process for casting shadows in this case is conceptually the same

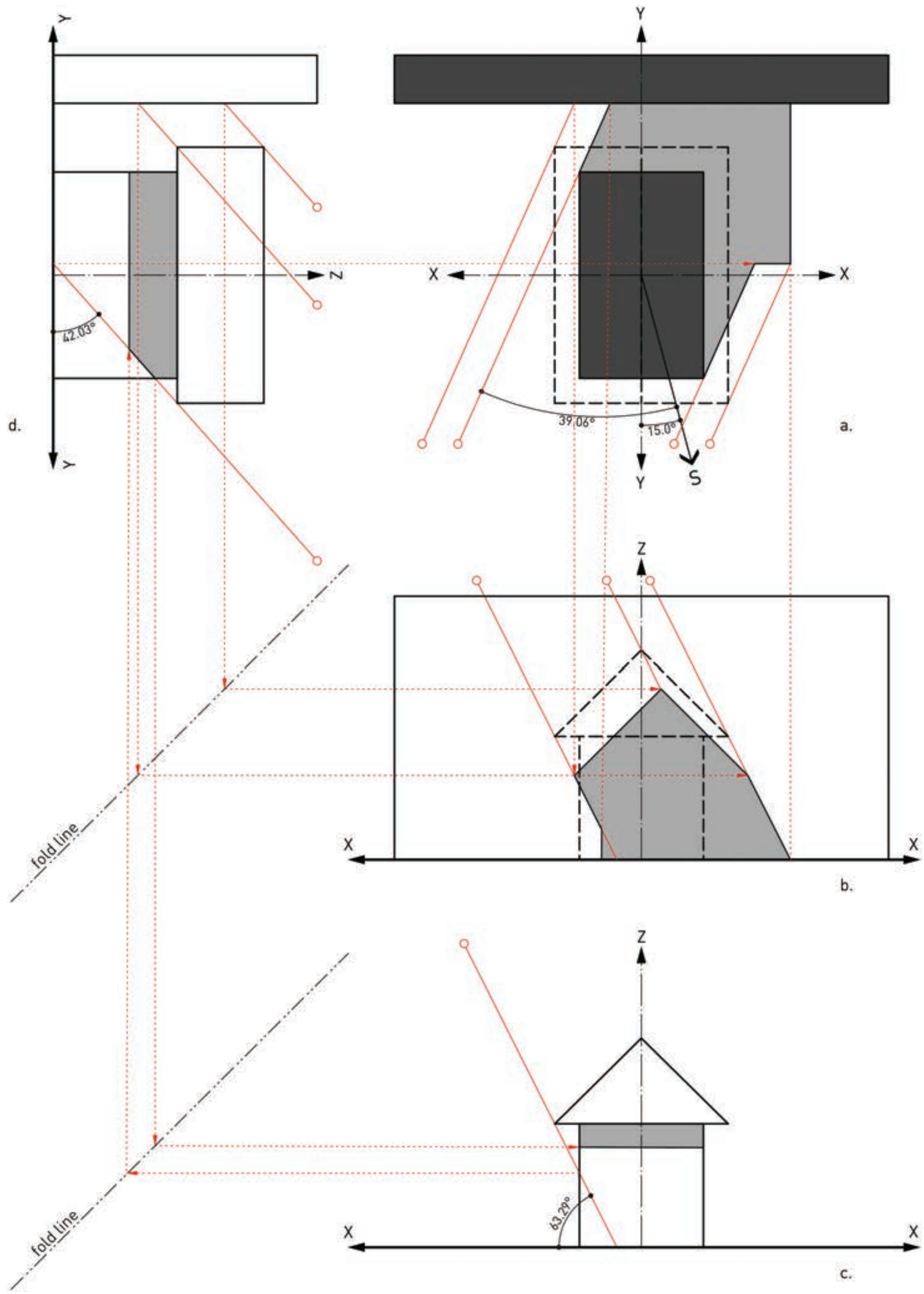

Figure 6.8
Complex Shadow Example
Dason Whitsett

as that used in Figure 6.5 except that we will substitute these angles for the solar coordinates, allowing us to use only the typical orthographic views.

First, project lines in plan view at the angle of the surface-solar azimuth past potential shadow-casting points. The east elevation view shows the south wall in profile. Therefore, use $\Omega_{el\text{-}east}$ or $\Omega_{pf\text{-}south}$ to project the solar vector past potential shadow points until striking another surface. Do the same in the south elevation view using $\Omega_{pf\text{-}east}$ or $\Omega_{el\text{-}south}$. Usually, it is only necessary to project angles in two views, but the third is convenient to have for certain points and provides a good check, as the projection from any view should connect with any other. Project the contact points back to the other views and find the vertices of the shadow perimeter.

Where shadow vectors contact a vertical surface rather than the ground plane, the same principles apply. Simply find the intersecting point in one view and project it to another to identify the shadow location. It can be helpful to project all the possible shadow-casting points rather than guessing which ones form the shadow perimeter to ensure the proper shadow is drawn.

CALCULATING SHADOW COORDINATES

It is also possible to calculate the coordinates of shadow points directly rather than constructing them graphically. Equations 6.3 and 6.4 provide x-y coordinates for a shadow point on a horizontal plane. These equations use the profile angles of sun position relative to a vertical plane aligned with the surface axes to project the location of a point along the solar vector onto a horizontal plane where *h* is the height of the shadow-casting object.

Equation 6.3 Location of Shadow on Horizontal Plane (X)

$$x = \frac{h}{\tan\Omega_{pf-xx}}$$

Equation 6.4 Location of Shadow on Horizontal Plane (Y)

$$y = \frac{h}{\tan\Omega_{pf-yy}}$$

For shadows on a plane of arbitrary tilt, use Equations 6.5–6.8 to translate the shadow of a point onto another surface.

Equation 6.5 Transposition of Sunposition to Arbitrary Surface-Sigma X Component

$$\sigma_x = -\sin(\alpha_{sf})\ \sigma_s + \cos(\alpha_{sf})\ \sigma_w$$

Equation 6.6 Transposition of Sunposition to Arbitrary Surface-Sigma Y Component

$$\sigma_y = \cos(\Sigma)\ \cos(\alpha_{sf})\ \sigma_s + \cos(\Sigma)\ \sin(\alpha_{sf})\ \sigma_w - \sin(\Sigma)\ \sigma_z$$

Equation 6.7 Shadow Point Coordinate-X Component

$$x = -h\frac{\delta_x}{R_b}$$

Equation 6.8 Shadow Point Coordinate-Y Component

$$y = -h\frac{\delta_y}{R_b}$$

Mastering the control of shadows (and their inverse, patches of direct sun) is essential to the designer for building energy and comfort performance, daylighting, and for crafting the experience of architecture. Subsequent chapters will delve into methods to employ knowledge of shadows in analysis and design.

NOTES

1 Marcel Minnaert, *Light and Color in the Outdoors* (New York, NY: Springer, 1993).
2 Ibid.
3 Louis I. Kahn and Nell E. Johnson, *Light Is the Theme: Louis I. Kahn and the Kimbell Art Museum: Comments on Architecture* (Fort Worth, TX: Kimbell Art Foundation, 1975), 11, 18.
4 William H. Jordy et al., *Louis Kahn: Silence and Light*, 2014, www.kanopystreaming.com/node/69924.
5 Arden Reed, "Light, Shadow and Form: The Koshino House by Tadao Ando," *Via* 11, no. Architecture and Shadow: Special Issue (1990): 52–61.
6 Ibid.
7 Ibid.
8 Ibid.
9 Ibid.
10 Ibid.

7 THE SOLAR MICROCLIMATE

Microclimatic effects are often very important factors in the comfort and energy performance of a building. The best-known microclimatic phenomenon is the urban heat island effect, where developed areas, especially those with large portions of exposed paving and heat-absorbing building surfaces, absorb and store solar radiation during the day. Then, at night, these surfaces slowly lose their heat to the surrounding air and raise the temperature of cities compared to surrounding less-developed areas. There are numerous complex physical interactions in play and occasionally inversions of this effect occur, but in general, the phenomenon has only increased along with development since the 1980s when it was first brought to general attention by Oke.[1] Arnfield points out, though, that there may be an even bigger difference between the climate on the north and south sides of a building than there is between different land use zones.[2] That is, building-site level microclimates can be even more important than regional ones.

The term ***microclimate*** refers to climatic conditions in a localized area that differ from the prevailing climate of the area. A microclimate can be impacted by topography, vegetation, bodies of water, or man-made structures. The actual physical processes that alter localized conditions include the influence of insolation, wind flow patterns, evaporation, evapotranspiration, convection, advection, and thermal radiation, all of which in turn are affected by surface properties such as roughness and albedo. Here, we will focus on assessing shading/exposure to solar radiation as a means for the designer to evaluate the solar microclimate. For a consideration of the impact of topography on solar radiation gain, see Brown and DeKay.[3]

Imagine the difference between standing exposed on a barren concrete parking lot on a sweltering hot clear day compared to relaxing under the lush canopy of a grove of trees on that same day. Under the trees, a number of influences are likely at play, the most important of which is the obstruction of direct solar radiation by casting a shadow on the area below. The individual standing on the parking lot, on the other hand, receives not only the direct beam irradiation from above, but also a tremendous amount of radiation reflected off the light-colored concrete below. Anyone who has spent time on snow or white sand on a clear day can attest to the intensity of radiation off of reflective surfaces. By the same token, absorptive ground surfaces such as asphalt are just as, if not more, important to the microclimate of a site. Asphalt absorbs a large fraction of the solar radiation striking it, stores it in the mass of the asphalt and ground, and then re-radiates that energy as heat as the surroundings cool off.

All of these factors ultimately depend on the quantity of solar radiation striking surfaces on the site. In order to analyze how a site will perform relative to these criteria, one must be able to predict where shadows are cast and for what portion of the day throughout the year a particular point on the site will be in shade. Thus, shadows are the mechanism by which the solar climate of a site is directly modified and the designer must understand how shadows fall on the site to make effective design decisions.

ORTHOGRAPHIC METHODS FOR SOLAR SITE ANALYSIS

The impact of the incident insolation on the microclimate depends on other factors such as albedo, emissivity, and thermal mass. Shadows on a site may be created by any obstruction, including vegetation, topography, signage, and buildings either on or off the site. Therefore, including the surrounding context is extremely important when evaluating a building site (see, for example, Figure 7.1).

A solar site analysis pinpoints where on the building site shadows will be cast and at what time. There are several methods for evaluating this, each with advantages and disadvantages. The most obvious of these methods is the shadow study.

Shadow Studies

Shadow studies have the advantage of being intuitive and of showing shading conditions over a large area simultaneously. They are also easy to generate using almost any 3D CAD software. The weakness of this approach is that shadows only represent conditions at one moment in time, while the objective of a site analysis is to glean general information for making design decisions. This challenge may be partially overcome by overlaying shadows at multiple times to show the progression through a day or year; however, these can become very difficult to read with any level of accuracy quickly.

Figure 7.2 shows a composite shadow study of the shading conditions on the building site in Figure 7.1. For each design day indicated, shadows are shown from 7:30 to 16:30. It shows, for example, that all parts of the open plaza area between the buildings receive at least some shade on the December solstice. A casual reading of the diagram might suggest that the entire central plaza is in heavy shade almost all day on that date, but it is not! Figure 7.3 shows the shadows each hour on the December solstice, demonstrating that there is a significant amount of direct solar exposure in the middle of the day in the plaza area.

It is also important to remember that the shadows in this kind of study are only indicative of what is happening on the surface onto which they are cast—in this case, the ground plane. If one were interested in building a multi-story building in the open plaza space, this diagram provides little useful information about the exposure of anything above the ground-floor level. Figure 7.4 shows the shadows at 9:00, when most of the plaza is in shade, on a proposed cylindrical form. Even with the low altitude of the sun at that time, the shadow only strikes the lower part of the proposed object. As the sun gets higher toward mid-day, it will be more exposed.

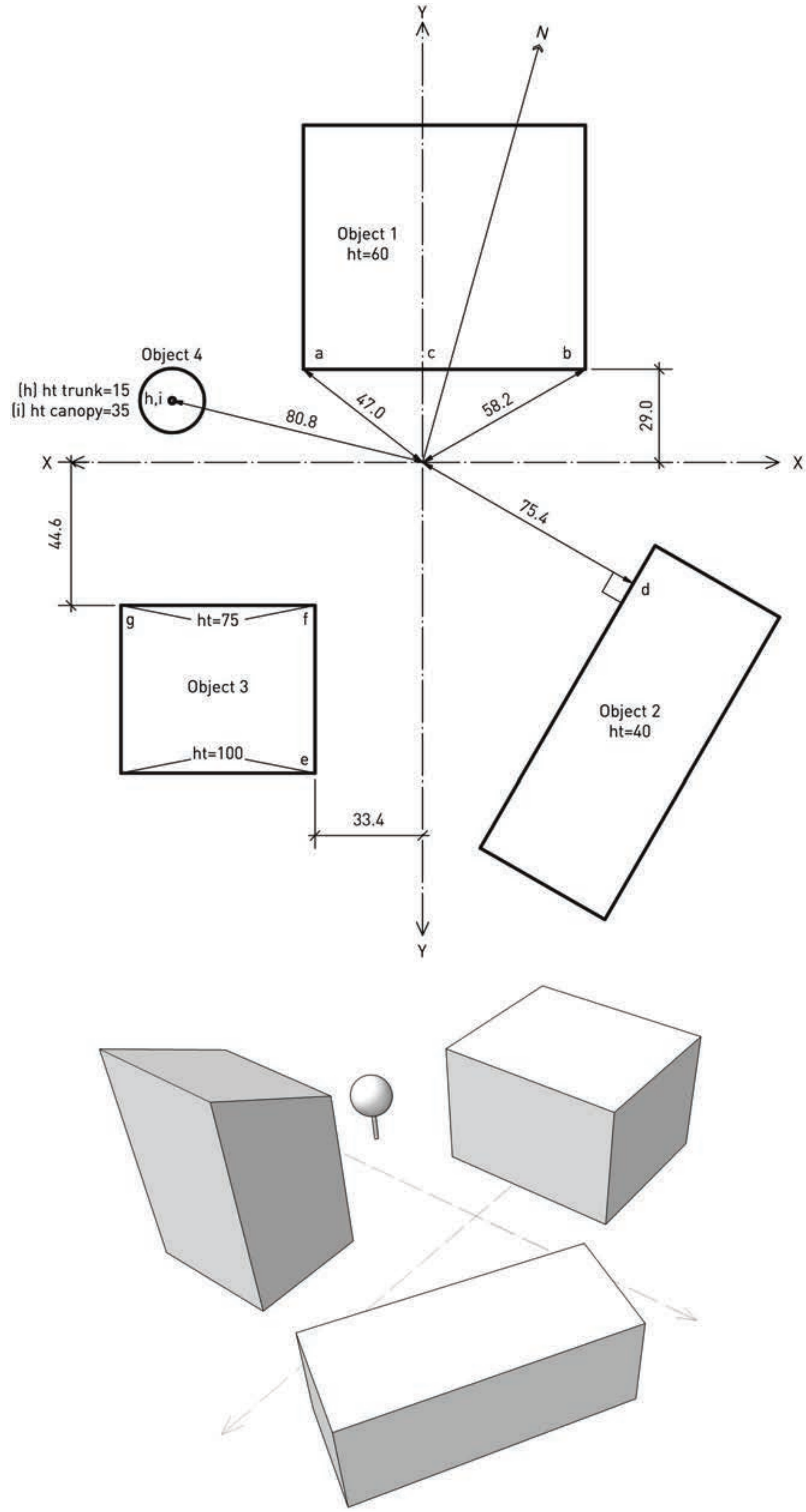

Figure 7.1

Example Site Plan for Studies in Chapter 7

Example site plan of building site in Austin, Texas ($L = 30.3°$), for solar analyses in Chapter 7.

Dason Whitsett

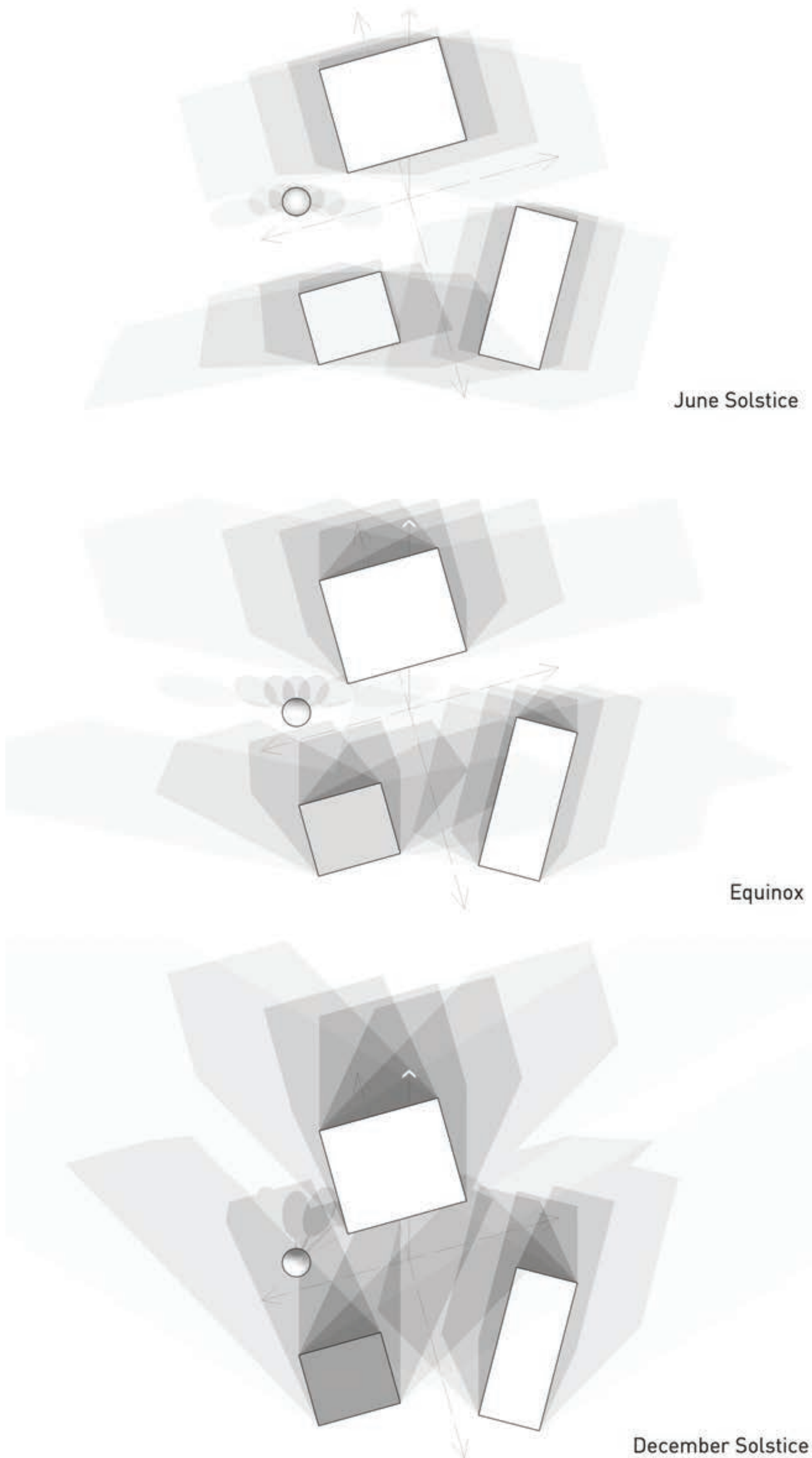

Figure 7.2

Composite Shadow Study

Composite shadow analysis for building site shown in Figure 7.1.

Dason Whitsett

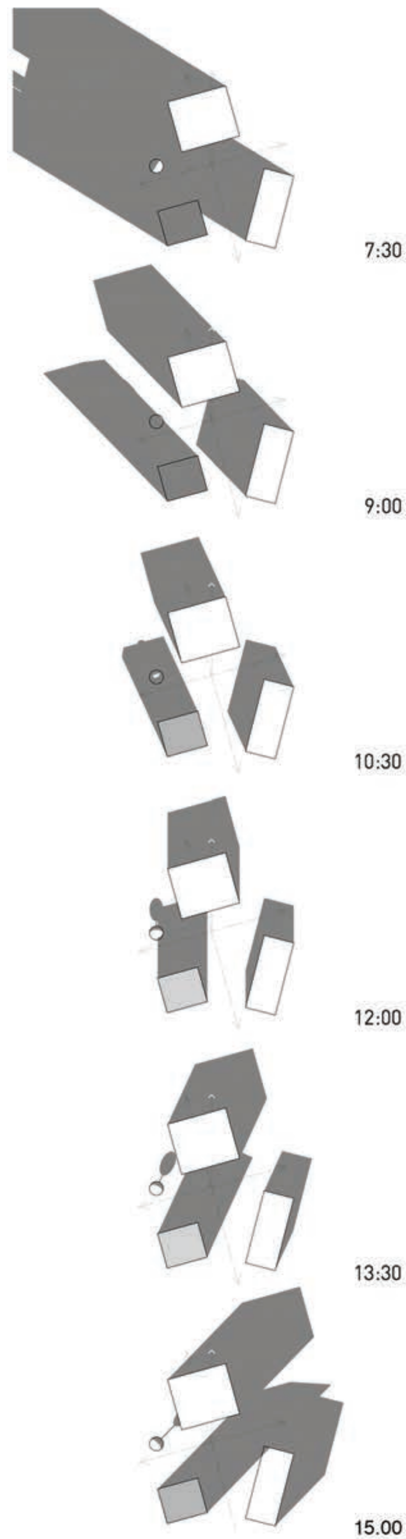

Figure 7.3

December Solstice Shadows on Example Site

Dason Whitsett

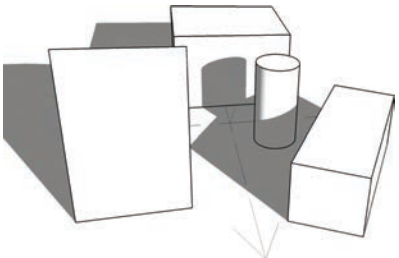

Figure 7.4

Shadow Height on Proposed Object

Dason Whitsett

Solar Views

Solar views, discussed briefly in Chapter 6, are another useful solar site analysis tool. A solar view is an orthographic drawing from the point of view of the sun. As such, the surfaces shown in the drawing are in direct sun, while concealed areas are in shade. Solar views of the same site are shown in Figure 7.5. Solar views have the advantage of showing exposed areas very clearly, but are not easily combined to condense a day's worth of views into one composite image. Some software will generate solar views or animations automatically. Even if the software does not have the capability built in, it is relatively easy in most programs to place a camera looking toward the model along the solar azimuth and altitude vector to generate a solar view using a parallel line projection.

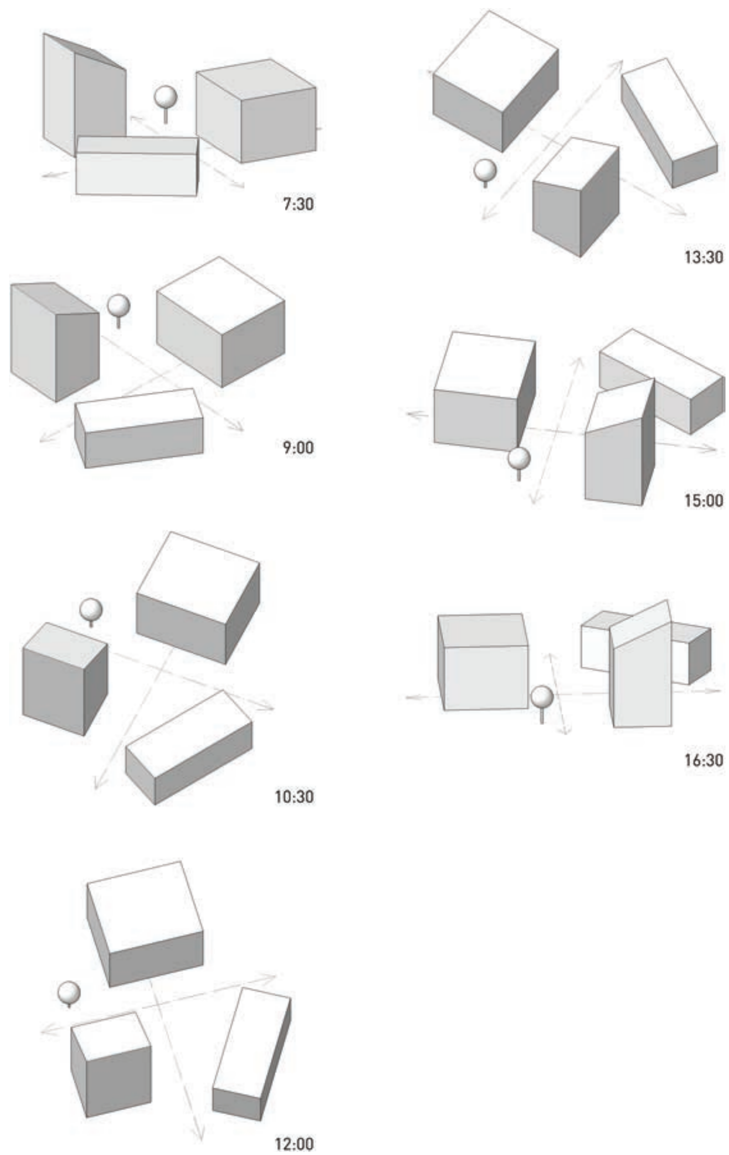

Figure 7.5

Site Solar Views

Solar views of the site in Figure 7.1 on the equinox.

Dason Whitsett

SKY DOME PROJECTIONS

Previous sections of this book have primarily used the sky dome as a means to represent the path of the sun. This, however, is not the most important use of this valuable tool. Just as the sun's path can be projected onto the sky dome, any geometry around a point in space may also be projected onto the dome. Doing so allows one to examine the relationship of the solar vector and everything surrounding the reference point. The reference point will be in shade at dates and times when the path of the sun crosses an object in the projection. If nothing obscures a portion of the sun path, the reference point will be in direct sun if it is not overcast. Day-to-day weather, then, ultimately determines whether the point will receive direct sun. It is possible, although unusual, to combine these diagrams with typical climatic information plotted onto the sun path to factor in the influence of clouds and make the diagram specific to a particular location.

Such diagrams are known as ***sky dome projections*** or ***overshadowing diagrams***. It is helpful to note that the geometry of objects around the reference point is fixed and does not relate to a particular location. The projection of a particular scene would not change no matter where on Earth one moved all of its elements as long as they have the same relationship to one another. Once a solar path band is applied to the sky dome, the relationship to latitude is fixed, although the scene could still be moved any place with the same latitude.

These projections are generally challenging for the uninitiated to interpret because of the distortion that results. Even those familiar with sun-path diagrams sometimes have trouble reading the projection of objects onto the dome at first. The appearance of a sky dome projection is similar to a fisheye lens photograph or the reflection from a domed mirror. Everything in the hemisphere around the reference point is present but distorted.

Compared to shadow studies, the advantage of sky dome projections is that they show the relationship between a point and the whole sky throughout the entire year in one diagram. Their disadvantage is that the projection only relates to one specific point in space, so it is more difficult to establish the general conditions on the site as a whole.

Several tools exist for generating sky dome projections of existing conditions. The most intuitive of these is a commercially available device known as the Solar Pathfinder, shown in use with the resulting projection in Figure 7.6. It is a simple instrument that consists of a transparent plastic dome over an equidistant sun-path projection with a compass needle mounted on the base. One aligns the device with true north in the reference location, then observes the reflection of the surroundings on the plastic dome. The dome is shaped to distort the reflection of the surroundings to match the equidistant sun-path projection used. The shape of the reflection of surrounding objects is traced onto the sun-path diagram or a photograph is taken from above showing both the reflection of the surroundings and the sun path below.

The result is a sky dome projection of everything around the reference point overlaid on a sun-path diagram. One can instantly see when at the reference point if the sun will be occluded by obstructions or not. To determine how much time in a day the reference point is exposed, count the hours on the sun-path diagram. The diagram also includes values for the estimated percentage of daily total global radiation (*D*) incident each hour. To estimate the fraction of *D* that the point receives per day, sum the percentage values shown for each hour that the point is exposed. Current weather conditions at the time the view is taken are not relevant to the projection, and in fact, the device is easier to use when it is overcast or the sun is blocked by objects so that the bright reflection of the sun itself is not an issue.

Because the view in a sky dome projection changes as the reference point moves, it is imperative to document the exact locations and elevations where views are taken with this tool. Multiple views will almost always be required to obtain all the necessary information on a site. Often, it is necessary to use a ladder or other means

Figure 7.6

Solar Pathfinder in Use

The frames show the instrument in use, a top-view with sky dome reflection, and the sun-path diagram produced. In this case, the colonnade shades the reference point from approximately 10:00 *AST* through the afternoon on the summer solstice. On the winter solstice, there are only on average three hours of unimpeded sun and two more in late afternoon of partial sun coming through the trees. The tall building to the south shades the point for approximately 1:20 on the winter solstice and its shading impact ends by the Feb/Oct design days. Late morning to late afternoon is exposed through the transition months.

Dason Whitsett

to reach a higher elevation to record a view at the level of a window or some other key element of a proposed design.

The Solar Pathfinder instrument is commonly employed by photovoltaic designers to evaluate the potential for solar arrays. It is also a valuable tool for designers. Passive House Institute U.S. requires a site assessment using this instrument for projects pursuing Passive House certification. It is very handy because one can carry it around to quickly investigate approximate overshadowing at numerous different points on a site, including window overhangs, before deciding where to take more precise readings.

The Solar Pathfinder may also be used to determine the height and shape of objects such as trees and buildings so that they can then be accurately modeled in 3D or energy simulation software. To do so, measure the altitude and azimuths of key points in the surroundings from the projection, then locate these in space relative to the reference point. Having a plan location for the base of an object allows one to determine its height using Equation 7.1. For trees, one can get a very good estimate of the tree profile, with two perpendicular views. While it is an excellent site analysis tool, the Solar Pathfinder is not very useful for testing design proposals because it needs surroundings to reflect.

Also available are digital instruments and smartphone apps to superimpose a sun path onto photographs using either fisheye or standard lenses. These have various levels of reliability and the user should critically evaluate the output. If used properly, these can provide an excellent way of evaluating specific overshadowing conditions. Understanding the general principles outlined in this chapter will allow the designer to evaluate and interpret the output from such tools.

The Solar Pathfinder has great didactic value in providing a tangible demonstration of how sky dome projections work. One can readily see how everything from the ground to the zenith surrounding the instrument is reflected in the dome and superimposed on the sun path.

Figure 7.7 shows the geometrical construction of a sky dome projection. The shape of the projection of the orthogonal surface in the foreground is determined by

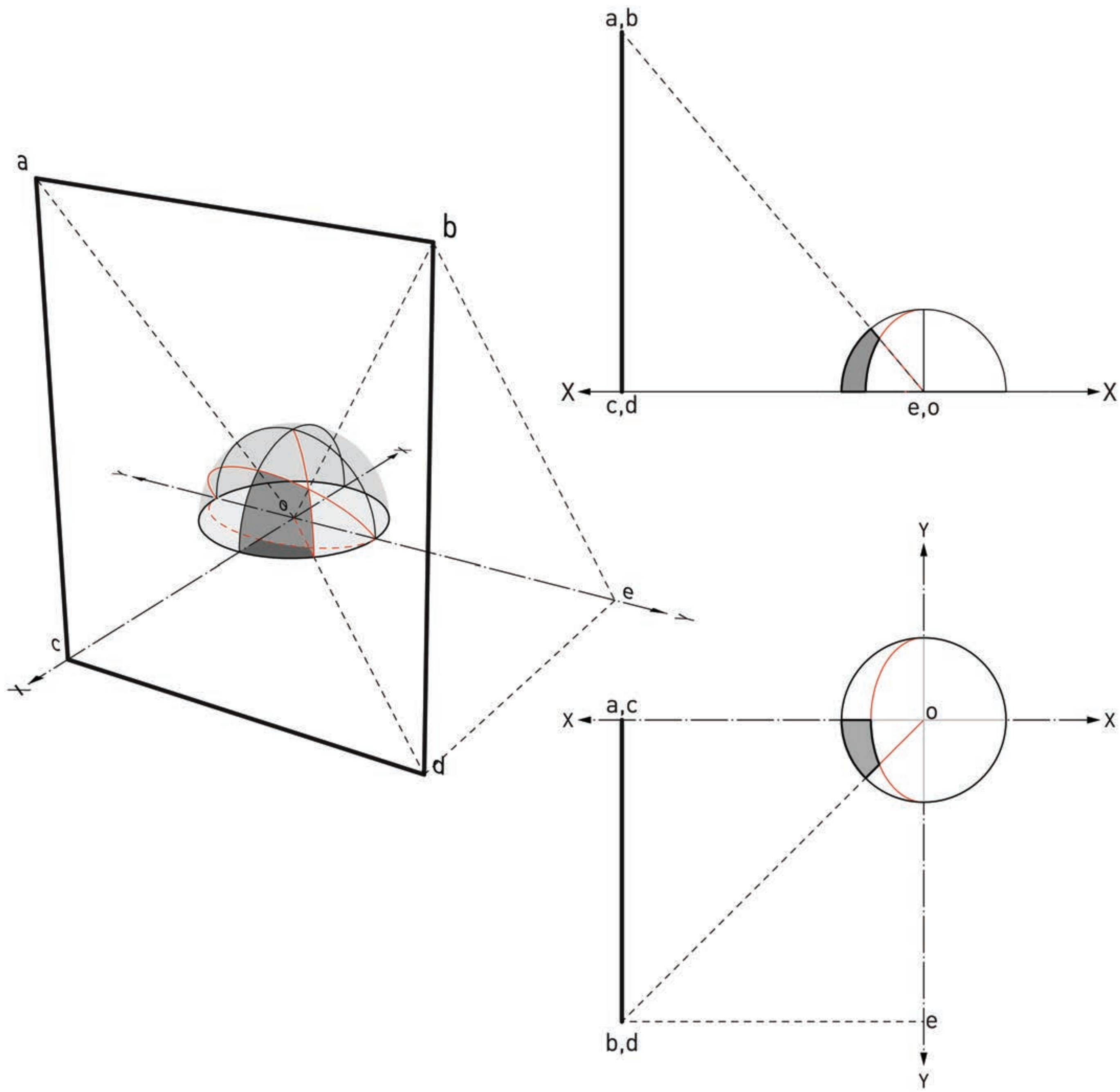

Figure 7.7

Sky Dome Projection Construction

The shaded area on the sky dome is the projection of the transparent rectangle in the foreground onto the hemispherical dome. Because this is a projection from one point, notice that all projection lines emanate from the reference point.

To locate the projection of a point in space on the sky dome, first draw a line from the origin to that point. The projected point is where that line intersects the sky dome.

Because of this, the size of the dome or absolute dimensions of the objects are irrelevant. The plan and elevation views of this projection are also shown.

Dason Whitsett

the points where lines connecting the edges of the surface and the reference point intersect the surface of the sky dome. From this point of view, it is easy to see why changing the reference point changes the projection.

While any view of the sky dome may be used, the plan view is the most common and broadly useful. All points are described by their azimuth and altitude relative to the reference point. The entire projection could be created by plotting enough points along each edge to generate the projection geometry. Several important principles, however, allow a greatly simplified method of construction of most of the geometry and assist in the interpretation of these diagrams.

Principles of Sky Dome Projection Geometry:

1. Vertical edges occur as segments of great arcs on the sky dome between the ground plane and the zenith point. In plan view, these appear as radiating straight lines and as segments of ellipses in elevation. These lines will be aligned with the azimuth of the vertical edge relative to the origin. See segments *a-c* and *b-d* in Figure 7.7, for example.
2. Horizontal edges form segments of great arcs on the sky dome inclined at the profile angle of the edge relative to the reference point. In the elevation view where the surface is shown in profile, note that in Figure 7.7, angles *a-o-c*, *b-o-d* (the true altitude of point *b*), and *b-e-d* are all the same, i.e. the profile angles of points *a* and *b* are the same relative to the reference axis. In plan view, horizontal edges appear as segments of ellipses following the appropriate profile angle lines, as depicted in Figure 6.7 If using equidistant or stereographic projections, the curve of the profile angle lines will not be elliptical, but will follow the projected shape specific to that diagram style.
3. Edges that are neither horizontal nor vertical will have their own unique geometry in the projection.
4. Points on the ground plane appear at the perimeter of the plan view and a point directly overhead is at the center.
5. Any object that crosses the zenith point overhangs the reference point; if the zenith point is not covered, nothing is directly overhead.

In practice, 3D drafting is not an efficient means to produce a sky dome projection. Some computer programs can automatically generate such drawings, but these are not widely available at present. To construct sky dome projections manually, 2D methods are most convenient and useful for analysis.

Solar Protractors

A solar protractor is a device that combines a representation of the sun path with overlays that allow one to determine not only solar coordinates, but also transformed coordinates for vertical surfaces such as surface-solar azimuth, profile and elevation angle, and angle of incidence. Some of these devices have included typical illuminance distribution on the sky dome or radiation values. The Pilkington Sun Angle Calculator (PSAC), shown in Figure 7.8, is the best-known example of this type of solar protractor. These simple hand instruments capture an astonishing volume of information in a very simple geometric device.

In this type of solar protractor, the base is a sun-path diagram that serves as the background. The most important part of the tool, however, is the overlay, which is bisected by a line representing a vertical surface. The overlay has scale lines for

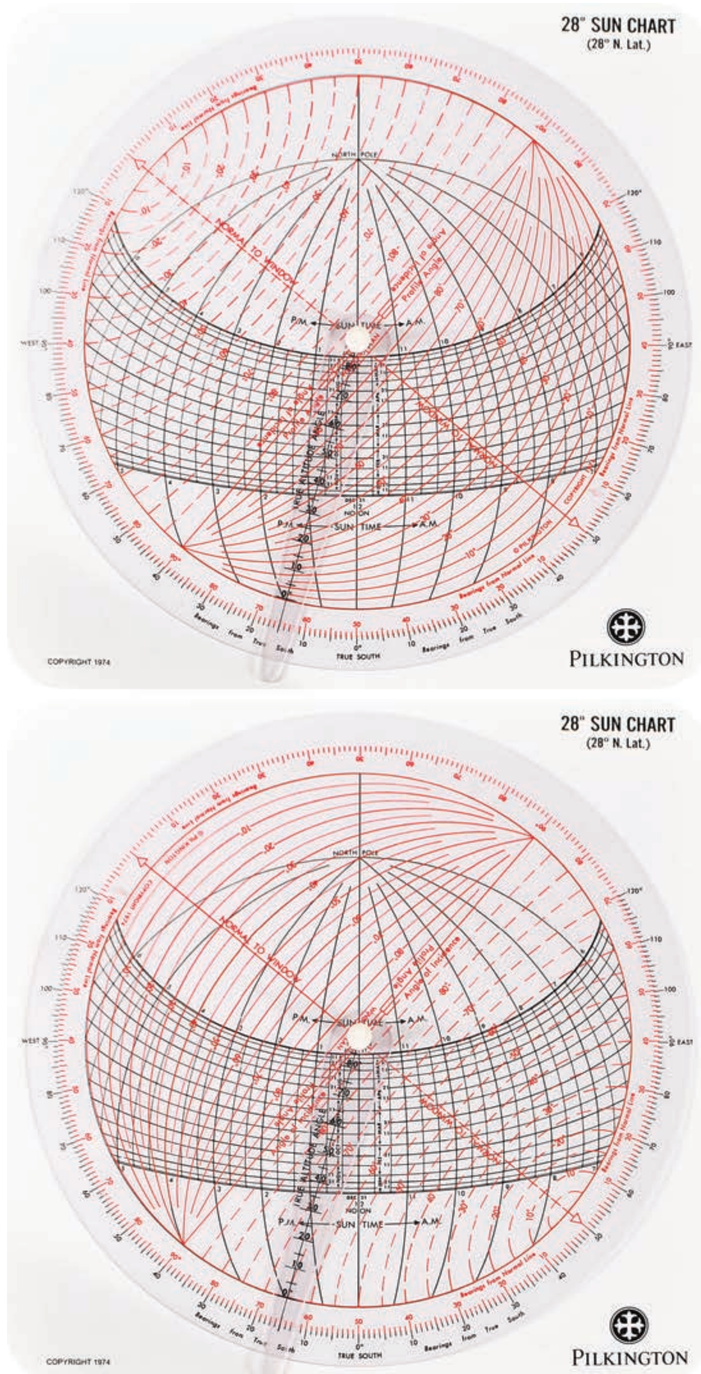

Figure 7.8

Pilkington Sun Angle Calculator

Solar protractor for a vertical surface at 28° N latitude. The overlay is adjusted by aligning "normal to window" with the surface azimuth (αsf) on the black azimuth scale, in this case, –50°. The top image shows the profile angle overlay and the lower, the angle of incidence overlay. On January 21 at 12:45, the solar azimuth (αsol) is 15°, read off of the black azimuth scale by aligning the stylus with the current sun position. The surface-solar azimuth (γ) is 65°, read off of the red azimuth scale. Solar altitude (βsol) is 41°, read off of the rotating stylus. The profile angle (Ωpf) is 64°, read off of the red overlay in the upper image. The angle of incidence (θ) is 72°, read off of the red overlay with the dashed lines in the lower image.

Dason Whitsett

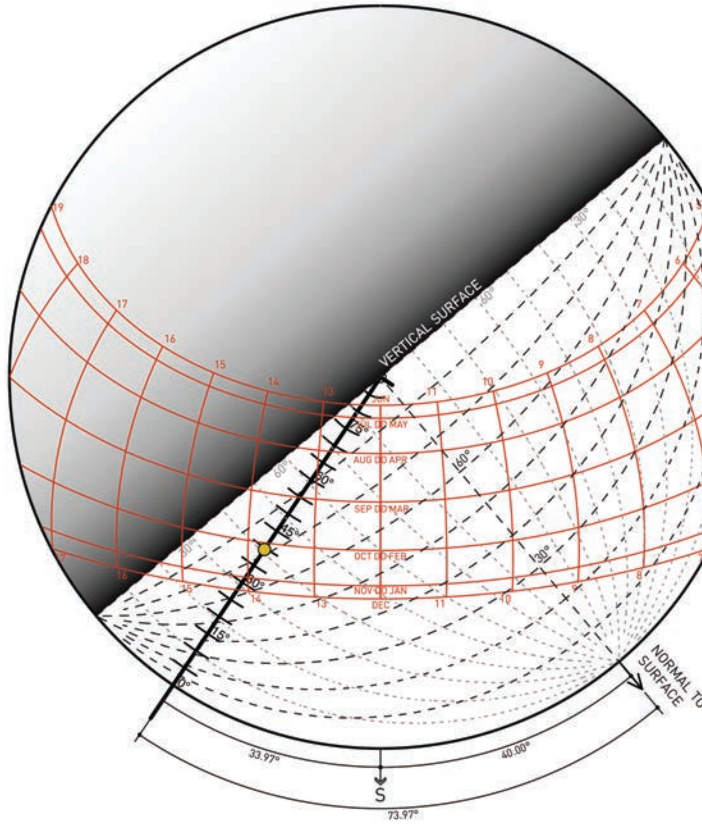

Figure 7.9

Equidistant Solar Protractor *L* = 30°—Profile and Elevation Angles

To use a solar protractor, first align the "normal to surface" line with the bearing of the surface. In this case, the surface azimuth is (–) 40°.Read azimuth and surface-solar azimuth off the perimeter scale. Profile and elevation angles may be read from the dashed overlay.

Dason Whitsett

profile and elevation angles and the angle of incidence. On top of that is a stylus with a scale for true altitude.

To use a solar protractor, first align the "normal to surface" line with the azimuth, or bearing, of the surface using the scale on the underlay with the sun path, as shown in Figure 7.9. Locate the date and time on the sun-path underlay diagram, equidistant in this case, and align the stylus with that point. Read the true solar azimuth off the underlay and surface-solar azimuth off the azimuth scale on the overlay. The true altitude may also be read on the scale on the stylus.

With the overlay aligned properly, one can immediately see at what times throughout the year the vertical surface represented will be exposed to direct sun and when it will be in shade. Areas of the sun path in front of the surface line represent times at which the sun can "see" the surface, and times at which the sun path is behind the line indicate that the surface is in shade. One can count the daylight hours during which the surface is in direct sun to determine how much exposure time the surface receives on a given date. The times at which the sun path crosses the surface line represent sunrises and sunsets for the surface.

The crossing curved black dashed lines in Figure 7.9 are lines of constant profile and elevation angle relative to the surface. Refer to Figures 6.6 and 6.7 to interpret these. To determine the profile angle of the sun relative to a surface at a particular time, find that point on the sun-path diagram, then interpolate within the profile

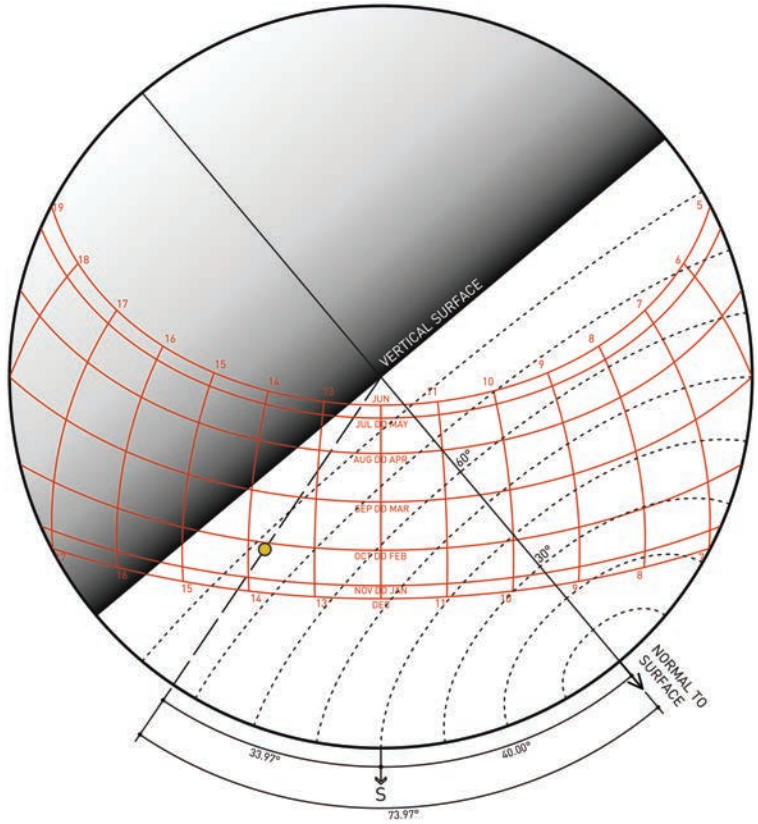

Figure 7.10

Equidistant Solar Protractor *L* = 30°—Angle of Incidence

Read angle of incidence off the dashed underlay. Solar protractor for a surface with an azimuth of (–) 40°.

Dason Whitsett

angle lines on the overlay. To find the elevation angle, use the same process with the elevation angle lines. If your overlay does not have elevation angle lines marked on the same overlay as profile angles, simply rotate the overlay 90° toward the sun from the surface normal to find the profile of an adjacent surface at 90°. This is the same as the elevation angle of the original surface.

Reading the angle of incidence (θ) off the appropriate overlay works the same as the profile angle. As shown in Figure 7.10, align "normal to surface" with the proper surface azimuth and interpolate to read the current angle of incidence. The angle of incidence is 0° when the sun is on the horizon normal to the surface, and 90° when the solar azimuth is parallel to the surface.

Solar protractors are valuable tools for drawing sky dome projections, described in the following section, and for designing shading devices, as covered in Chapter 8.

Constructing Plan-View Sky Dome Projections

To draw a plan-view sky dome projection, one first needs to establish the azimuth of significant points relative to the reference axes. Figure 7.1 shows a plan and axonometric view of an example site with certain dimensions given, including heights of the objects. One could determine the missing dimensions easily, but for the sake of this example, we will use various concepts already developed to draw the projection without the need for the missing dimensions. Figure 7.11 shows the construction of the projections of the various objects in the example site plan.

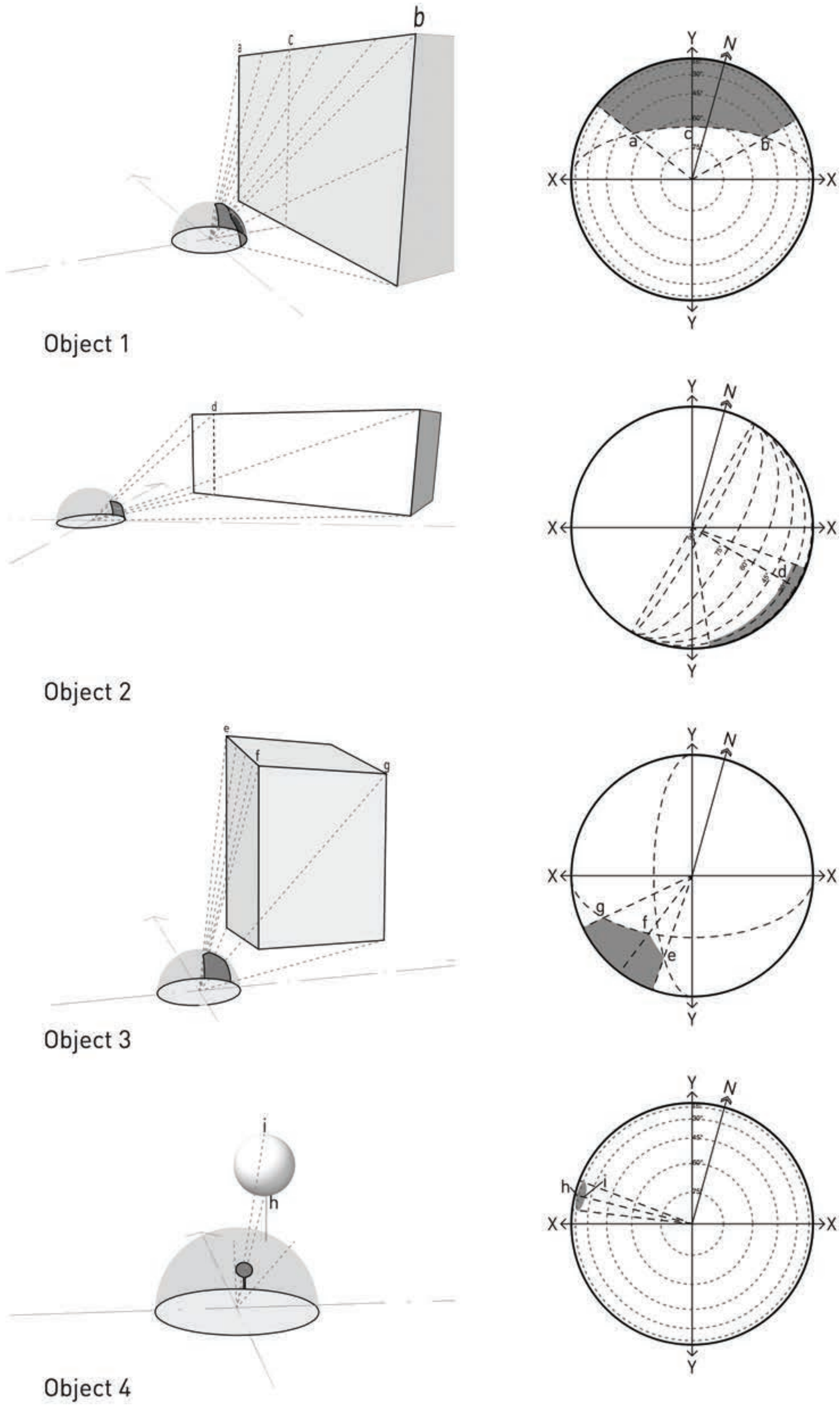

Figure 7.11

Sky Dome Projection Example Construction

Dason Whitsett

Table 7.1 Altitude and Profile Angles for Example Sky Dome Projection

Point	*ht*	*d*	*Angle (°)*	*Alt or Profile?*	*Note for profile angles*
a	60.0	47.0	51.9	β	
b	60.0	58.2	45.9	β	
c	60.0	29.0	64.2	Ω	with respect to x-x axis
d	40.0	75.4	27.9	Ω	with respect to object axis
e	100.0	33.4	71.5	Ω	with respect to y-y axis
f	75.0	33.4	66.0	Ω	with respect to y-y axis
f, g	75.0	44.6	59.3	Ω	with respect to x-x axis
h	35.0	80.8	23.4	β	
i	15.0	80.0	10.6	β	

The projection is drawn as spherical to demonstrate the true geometry from different points of view, but the same method applies to any plan-view projection type. First, determine the azimuth of each vertical edge relative to the reference point. One time-saving trick is to trace these azimuth lines from the plan view of the site, but remember that a hemispherical sky dome projection and site plan of a building site do not share the same frame of reference, so do not trace the buildings themselves onto the projection. The view of those buildings from the perspective of the sky dome projection is in fact what the projection will depict.

Once the azimuths are found, one must determine the altitude of the points to locate. For point *a* on Object 1, the altitude is found using the basic trigonometric relationship of Equation 7.1. In this case, $\beta_{pt} = 51.9°$. Table 7.1 shows the altitude and profile angles for all key points in the drawing. To locate point *a* on the plan-view diagram, use an altitude scale to mark its height on the line of its azimuth. Do the same for point *b*. For point *c*, note that it is both the true altitude of the top edge of Object 1 as well as the profile angle of that point with respect to the x-x axis. Points *a* and *b*, therefore, also have the same profile angle. Refer back to Figure 7.7 to demonstrate this principle.

In order to draw the top edge of Object 1, we could locate numerous points manually and connect the dots. However, given that we know all points along the top edge fall on the same profile angle with regard to the x-x axis, it is much easier to use a solar protractor or other tool to draw a line of constant profile for that horizontal edge. Just align "normal to surface" where it is perpendicular to the surface of Object 1, which in this case is along the y-y axis, and draw in the correct curve. If using a protractor overlay for this task, interpolation between profile angle lines will usually be necessary.

Equation 7.1 Altitude or Profile Angle of a Point

$$\tan \beta_{p_t} = \frac{h_t}{d}$$

To draw Object 2, only one distance dimension is given to point *d*. Using the same principle from point *c*, this is clearly a profile angle as well, but at an orientation off the established axes. The relationship to the axes is not important, however. Align "normal to surface" perpendicular to the surface that point *d* is on. Table 7.1 indicates that Ω_{pf} of point *d* is 27.9°, so interpolate to locate that profile angle and draw it in, cutting off the two vertical edges in the process.

From the reference point, one can actually see two sides of Object 3, and possibly even some of the roof. In this case, the top surface of the object is not level. Point *e* is clearly a profile angle because the dimension given is perpendicular to the surface rather than along its azimuth. Align the profile angle overlay normal to the surface and use the overlay to mark the point terminating the vertical edge below it.

Points *f* and *g* have the same profile angle relative to the x-x axis. Use the profile angle overlay again by aligning "normal to surface" normal to the north surface of the object. Note that even though the center line of the overlay bypasses the object itself, the profile angles are correct. This is not uncommon. Draw the edge between points *f* and *g* at the profile angle of 59.3°.

Use the value for the profile angle of point *f* taken from the opposite direction as a check on the height found with the profile angle from the adjacent surface. The two intersect at the same point. That still leaves the sloping top edge of Object 3 to draw in. Plot the azimuth and altitude of multiple points along the edge and connect them to fill in the shape of edge *e–f*. Further investigation reveals that the roof is not in view from the reference point, so the projection of Object 3 is complete.

Lastly, Object 4 presents some challenges. It is a tree modeled as a sphere on a stick. The top and bottom of the canopy, points *h* and *i*, may be located using the methods described previously. Mark the respective azimuths of the sides of the canopy. For surfaces with a wide-view factor to the reference point (close or very large), it is important to make the projected profile precise because a small difference can have a substantial effect. In this case, however, its small size and relative distance from the reference point indicate the tree will be a very minor contributor to overshadowing. So, the canopy shape is estimated with an ellipse bounded by the top, bottom, and width points of the canopy. If it were an important element, it would be necessary to plot individual points to create the shape of the projection.

With the completed diagram shown in Figure 7.12, one can now see the entire projection of the context of the reference point onto the sky dome. Shaded areas block

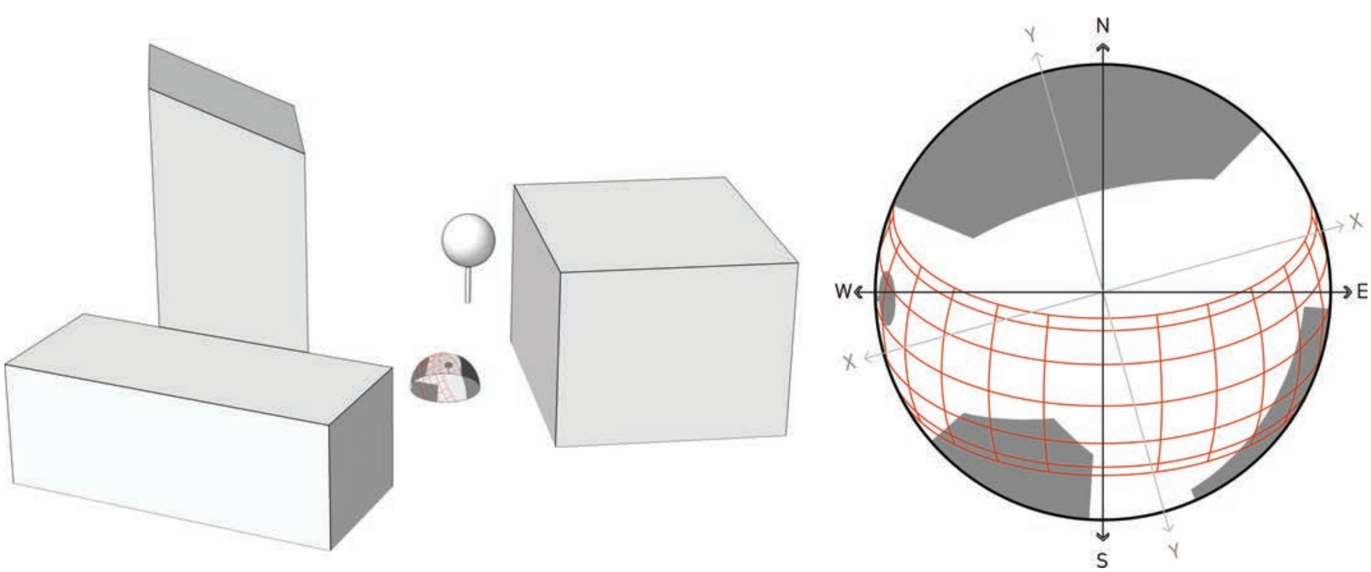

Figure 7.12

Completed Sky Dome Projection of a Site

Dason Whitsett

the view of that portion of the sky dome. Where the sky is not covered, the reference point sees the sky. Assuming that these objects are fixed in place, the projection will not change regardless of location or date.

Upon superimposing the solar path band onto the projection at its proper orientation, it is easy to see what portions of the sky are blocked and when the reference point is exposed to direct sun if the sun is out. In this case, the reference point is exposed for the entire day on the June solstice, except for a few minutes at sunset. On the equinoxes, the sun comes over Object 2 at approximately 8:10 *AST*, and is visible all day. At 17:00, it skims the canopy of the tree. On the December solstice, Objects 2 and 3 present some significant shading. The reference point is exposed from approximately 9:15 to 12:15, in shade from 12:15 to 15:20, then exposed again until sunset.

It is also important to note how much of the sky, especially north sky, is obstructed. Daylighting potential is dependent on unobstructed views of the sky because that controls the amount of diffuse insolation received. In the northern hemisphere, north sky is the most desirable because the light is most even, and direct sun is not a problem except at high latitudes. In this case, much of the sky to the north is obstructed by Object 1, so a north-facing window placed at this location will not have optimal daylight access.

This projection was taken at the ground plane. If one is interested in exposure at another elevation or plan location, another projection must be drawn. Taking several projections at different locations can provide a good evaluation of the solar microclimatic conditions on a site. These drawings involve several steps, but can be generated quickly once the principles are understood. In most cases, a high level of precision is not important because design decisions usually do not involve levels of exposure down to the minute. It is possible to sketch these very quickly using a solar protractor and its overlays as a guide to create diagrams with plenty of accuracy for most design situations.

Solar Microclimate Analysis Using Sky Dome Projections

The sky dome projection is an excellent tool to evaluate the solar exposure on a building site or localized areas on a site. The projection in Figure 7.13 is of an open pergola shading cover with various walls and buildings around it. The diagram, created using Ecotect Analysis software,[4] shows when a spot below the canopy will be in sun and shade throughout the year. The reference point is in shade through mid-day for most of the year with direct sun in early morning and late afternoon. For approximately a month on either side of the December solstice, the point is exposed for most of the day. The vertical turn-down was added to expand the period of the year when shading is available, and the covered portion does not extend all the way to the north of the frame because it is unnecessary for shading.

Figure 7.14 shows an example solar microclimate analysis for a building site with a mature tree canopy. It was performed with the aid of a Solar Pathfinder instrument to show how the existing trees shade various surfaces of the proposed new building, in particular the large west-facing windows.

These diagrams were used to create a shading and landscape strategy minimizing glare and solar heat gain while providing good daylighting. All new windows were analyzed to ensure that solar gain is minimal. The sun-path diagram indicates the large bank of west-facing windows will receive substantial shading from the large tree but some overhang would be desirable to block early to mid-afternoon high-angle sun. The wide area of south-facing glazing at the connector space is in full shade from

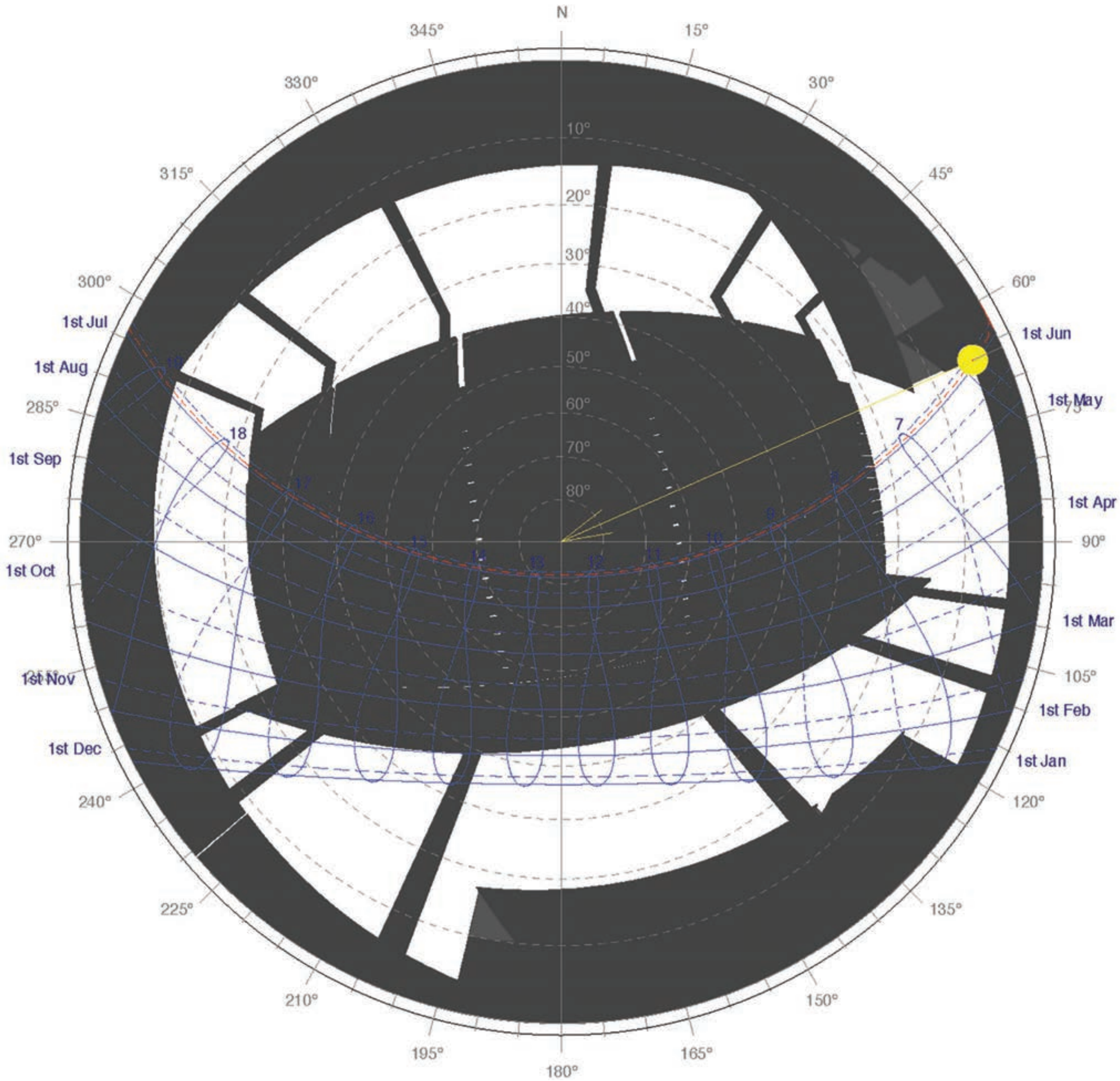

Figure 7.13
Sky Dome Projection of an Open Pergola
Pollen Architecture and Design

the tree canopy and adjacent structure almost all year except for a few evening hours in the winter.

These projections were also used to obtain dimensioned profiles of the trees on site for accurate modeling in the thermal simulation software. Some of the projection points are inside or outside the building footprint because design changes were made after the projections were taken, but between the range of projections available and the 3D model created with their aid, effective design-decision making was still possible using this set of views.

Solar microclimate analysis methods are like the uncertainty principle: one can either evaluate all shadows in a large area at a moment in time or see exposure

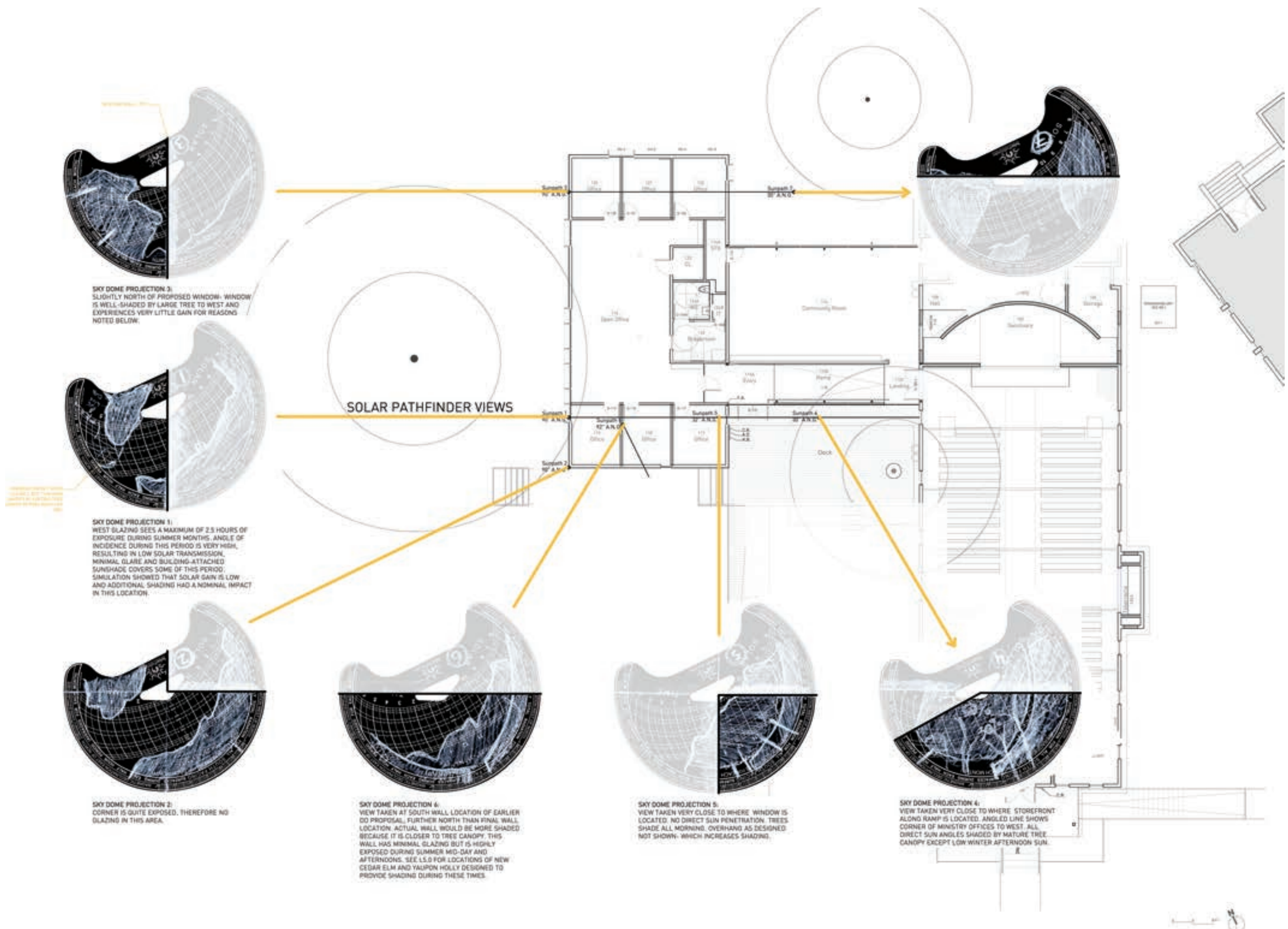

Figure 7.14

Site Analysis Using Sky Dome Projections

Pollen Architecture and Design

and shading for the entire year for one point using a single diagram. However, there is no way to show overshadowing conditions for an entire site for the entire year. Therefore, a combination of the two techniques is usually the best approach to understand the solar microclimate of a proposed site.

NOTES

1 Timothy R. Oke, *Review of Urban Climatology, 1973–1976* (Geneva: World Meteorological Organization, 1979).
2 A. John Arnfield, "Two Decades of Urban Climate Research: A Review of Turbulence, Exchanges of Energy and Water, and the Urban Heat Island," *International Journal of Climatology* 23, no. 1 (January 1, 2003): 2, doi:10.1002/joc.859.
3 G. Z. Brown and Mark DeKay, *Sun, Wind & Light: Architectural Design Strategies*, 2nd ed. (New York: Wiley, 2001), 86–88.
4 *Ecotect Analysis*, version 2010 (Autodesk, n.d.), http://usa.autodesk.com/adsk/servlet/index?id=12602821&siteID=123112.

8 CREATING SHADOWS

Shadows have been intentionally described in various ways throughout this book, due to their very ephemerality. The Merriam Webster dictionary defines shadow as "partial darkness or obscurity within a part of space from which rays from a source of light are cut off by an interposed opaque body."[1] This definition describes a cast shadow as different from an attached shadow, which refers to an unlit area of an object. Shadows could be defined as voids in the light. The silhouette of an object casts a shadow, or leaves a void in the light, creating a recognizable geometry or image. Shadows can also be understood as an interruption of the flow of light. In the 18th century, John Locke proposed an innovative theory that uniquely framed the way we perceive the three-dimensional world. He offered that experience is key to our understanding of form, in conjunction with our expectation of shadow behavior.[2] We therefore make associations between actual geometric shapes and their two-dimensional representations in an empirical and rational manner (see, for example, Figure 8.1).[3]

Norberg-Schulz claims that architecture is a means to frame the world in an immediate location, particularly if it directly responds to light and shadow. The term he used for this is "genius loci," or the spirit of a place, which was later embedded in the history of architecture. Light and shadow provide a way to situate architecture, defining "place" and "environment" as an important part of human existence. He extends this to argue that the very basis of human identity is dependent on a notion of "place." He maintains that a deep understanding through a long-term lens and rooted in a place is necessary for meaningful architecture and a meaningful life in general.[4] Bringing this to the current day, although contemporary definitions of sustainability in architecture widely vary, one common denominator is the notion of locale, or regional responses to optimize material resources and energy efficiency.

The character and atmosphere of any given space can greatly differ depending on the distribution of light across its volume and surfaces. Even through intentional and simulated daylight harvesting studies in the design process, buildings cannot, and arguably should not, fully control or homogenize the varying light conditions throughout the day. This change allows interior spaces to more directly track the exterior environment and keep our bodies in sync with circadian rhythms and natural flows. Similarly, the exterior form of a building should manage light and shadow in a manner to change and evolve throughout the day and during the changing seasons (see, for example, Figure 8.2).

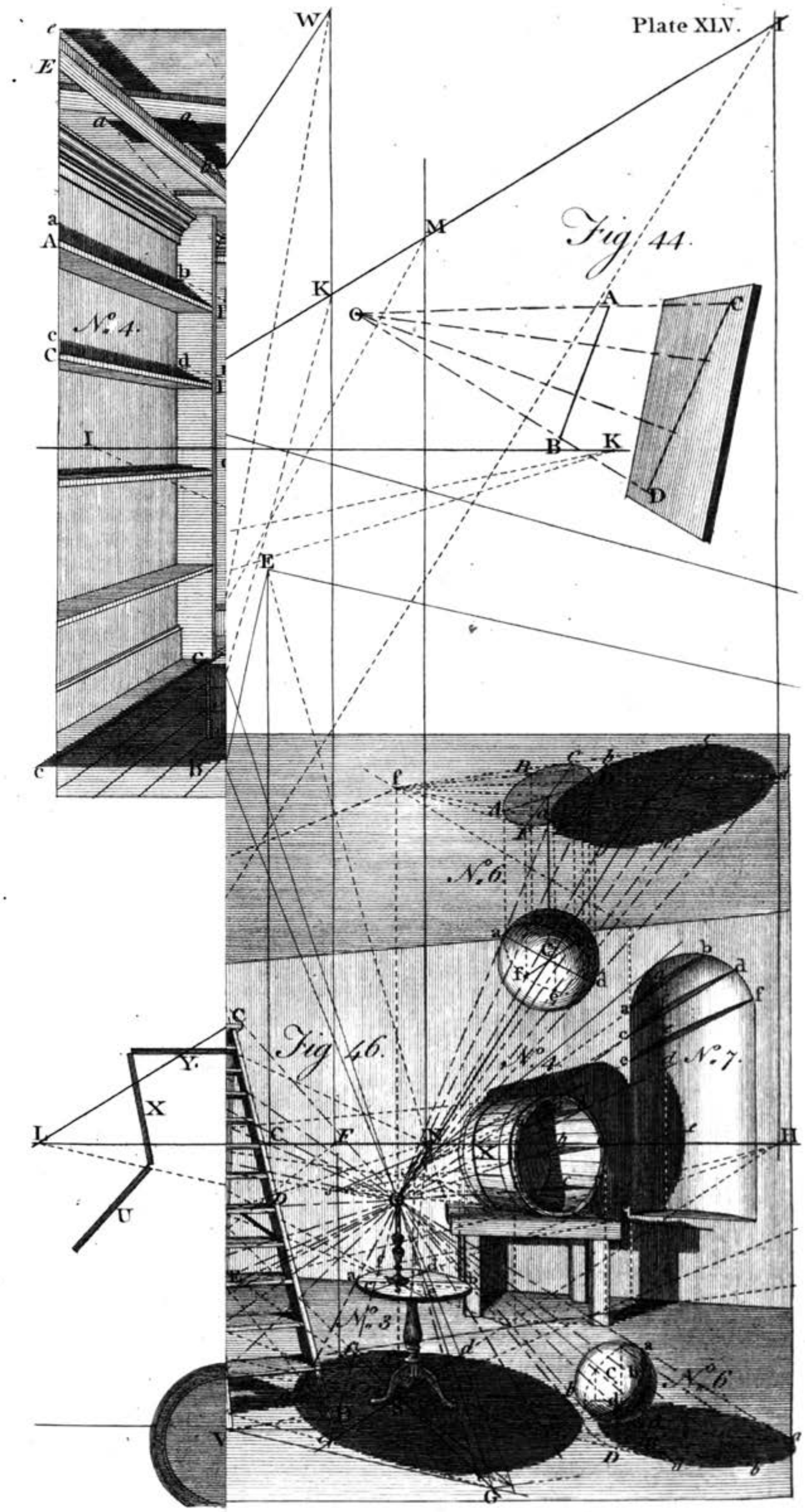

Figure 8.1

"Treatise on Perspective," Thomas Malton, London, 1788

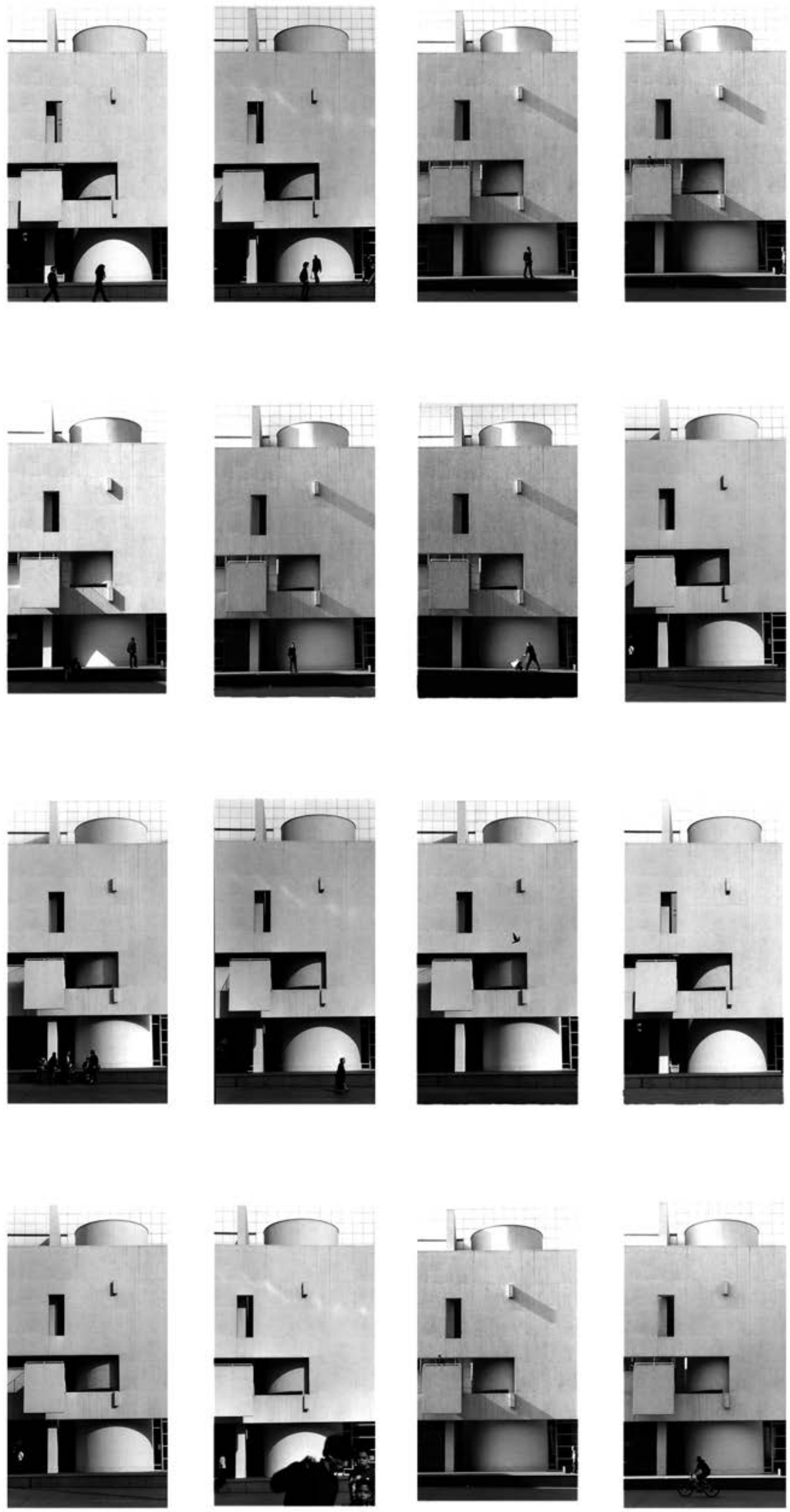

Figure 8.2

Diurnal Changing Shadows on the MOCA Barcelona

Diurnal changing shadows on the Museum of Contemporary Art in Barcelona, Spain.

Matt Fajkus

SHADOW GEOMETRY

In the United States, energy use for heating is nearly 5 times the energy used for cooling in commercial buildings[5] and 6.7 times the cooling energy use in the residential sector.[6] Globally, heating consumes more energy than transportation.[7] The sun provides an incredibly valuable resource as a free, renewable source of energy to offset some of this heating energy consumption.

At the same time, a large portion of the world at lower latitudes, where cooling is a more pressing concern, is experiencing rapid economic growth, which drives demand for air-conditioning. Even at the upper temperate latitudes, most modern buildings would benefit from shading in summer.

This chapter is concerned with methods to manage these considerations—designing for shade and solar exposure. Shading design is really shadow-casting in reverse. To effectively design shading devices, one must first have a clear understanding of the geometry of the sun's movement relative to the surface one wishes to shade. Most frequently, this surface is a vertical window in a wall, but it could just as easily be fenestration in a tilted plane or an outdoor table. Regardless of the surface, the principles remain the same.

Consider the architectural/programmatic function of the window. What other functions does it need to fulfill? Views and daylighting are two of the most important considerations in this regard. Small windows that are tightly bound by fins and overhangs often feel very constricted and may not provide a sense of expansive view for the occupant. Tight fins and, especially, overhangs also adversely affect daylighting by limiting access to diffuse sky light.

THE SOLAR VECTOR ENVELOPE

The *solar vector envelope* is the imaginary surface modeled by the sweep of the solar ray throughout the course of a day. This envelope, shown in Figure 8.3, is conical on any day except the equinoxes, when it is flat. The vector envelope forms a surface connecting the path of the sun on the sky dome for that day to the origin of the sky dome. From the point of view of an observer looking across the origin toward the equator, the conical surface is concave in summer and convex in winter. In other words, to an observer in the northern hemisphere in the winter, the vector envelope folds downward away from the observer, reaching its high point at solar noon. Sunrise and sunset will be located to the south of east and west. The closer one moves toward the North Pole, the further south sunrise and sunset will occur and the lower the sun will be at solar noon.

On the equinox, the vector envelope forms a planar surface rising and setting due east and west and inclined at a zenith angle equal to the latitude. On the summer

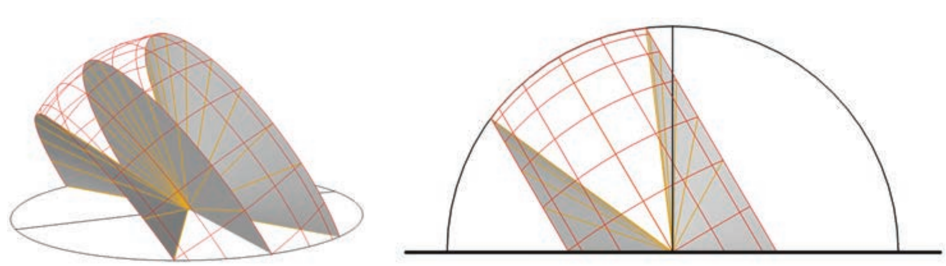

Figure 8.3
The Solar Vector Envelope
Dason Whitsett

solstice, the envelope will wrap back around the observer with the sun rising and setting to the north of east and west. The higher the latitude, the further north the sun will rise. Outside the tropics, the sun will be toward the equator at solar noon, and will spend a good portion of the day north of east and west.

Because solar geometry is symmetrical on the north-south axis, it is helpful to use this as our frame of reference, regardless of the orientation of the surface we are trying to shade. For an equator-facing surface in either hemisphere, on the winter solstice, the *highest* solar profile angle will occur at solar noon. On the same surface, the profile angle remains constant on the day of the equinox. Outside the tropics, on the summer solstice, the *lowest* solar profile angle relative to an equator-facing surface will occur at solar noon and the surface will only see the sun for part of the day. Within the tropics, an equator-facing vertical surface will not see the sun at all on the summer solstice.

To visualize the fluctuation in the vector envelope during the course of the year, imagine the cone folding back and forth like the stroke of a butterfly's wings. This dynamic geometry is the basis of passive design, as it allows one to tune the fixed form of a building to the dynamic movement of the sun. By orienting surfaces with care, we can choose how much solar radiation they will receive and at what angle at different times of the year. We can create form such that it deliberately casts shadows on a particular point at some times, but not others. Glazing can be placed so that it maximizes daylight and desirable heat gain and avoids unwanted heat gain. Using these principles, the designer can craft a building that *dances with the sun.*

For equator-facing surfaces outside of the tropics, a simple overhang that cuts off the lowest profile angle on a given day will guarantee full shading for all dates closer to the summer solstice, provided the overhang is long enough. This is the result of the concave vector envelope.

The same principle works in reverse when considering passive solar gain. Because the solar vector envelope folds toward the equator on the winter side of the equinoxes, if one designs building-attached shading to ensure that the window is fully exposed on a given day, it will be exposed at all times on the winter solstice side of that date.

If the climate or internal loads of the building determine that shading on the winter side of the equinoxes is necessary, the benefits of this geometry are lost and shading with fixed devices becomes more challenging.

SHADING/EXPOSURE CRITERIA

Before one can design appropriate shading or consider exposure measures, a clear objective is important. Establishing shading and exposure criteria should include analysis of characteristics of the building, climate, and physical properties of glazing to be shaded.

Balance Point

The ***balance point*** of a building is the outdoor temperature below which heating is necessary to offset heat loss through the envelope and maintain comfortable indoor conditions. Occupied buildings always have internal sources of heat, such as people, lighting, computers, and equipment, so some amount of heat loss is always necessary to maintain comfort. In the absence of solar gain, when the outdoor temperature drops below the balance point, additional heating will be necessary. Therefore, the balance point can range from just below the low end of the comfort zone to below freezing in extreme cases of high internal loads. See Utzinger and Wasley[8] for a detailed description of the balance point and how to calculate it.

Smaller residential buildings are usually skin-load dominated, meaning heating and cooling loads are mainly driven by heat loss and gain through the envelope, and have higher balance point temperatures. High-performance buildings, such as those built to the Passive House standard, will have lower balance point temperatures than other skin-load dominated buildings.

Larger commercial buildings are more commonly internally load dominated because of their surface-to-volume ratio and density of internal heat sources with the result that heat loss or gain from the outside plays a less important role. These buildings will have lower balance point temperatures, in extreme cases even below freezing.

The balance point is independent of climate and depends on the thermal characteristics of the building envelope, occupancy, and internal loads. When outdoor temperatures drop below the balance point, the necessary heating may be provided by solar gain, mechanical heating, or a combination thereof. This is where climate comes in.

Climate

For all buildings, if average daily outdoor air temperature is within the comfort zone or above, any solar gain, whether diffuse or beam, is a liability from a cooling load point of view. Because of the high luminous efficacy of sunlight, the value of light from a well-designed daylighting system will outperform electric lighting, but admitting more solar radiation than necessary for lighting will quickly increase cooling loads. Designers should provide as much shading from direct beam radiation as possible when outside conditions are at or above the balance point.

Internally load dominated buildings will be affected less by solar gain in terms of its impact on cooling loads. However, even if solar loads are a small fraction of the total load, uncontrolled sun coming in through windows in the occupant's field of view creates glare and discomfort for users. This often results in users closing window blinds that then stay closed even after the sun has moved, eventually leading to an increase in electric lighting use that would otherwise have been offset by daylight if the blinds were open.

When average outside conditions are below the balance point of a given building, providing for exposure to solar radiation, especially direct beam radiation coming in through windows, is a valuable free source of heating. One must be careful with this heat source, however—the biggest challenges with passive solar heat are overheating during the day and excessive heat loss through glazing at night.

Figure 8.4 shows hourly outdoor temperatures plotted on a sun-path diagram generated by the Climate Consultant software.[9] This type of plot is a valuable tool in evaluating dates at which exposure or shading from solar radiation is desirable. The plots illustrate the approximate six-week offset between the cycles of solar geometry and maximum/minimum temperatures. In the case of Austin, regardless of the balance point of the building, shading is desirable at least up to the equinoxes. On the winter side of the cycle, some moderate solar gain is desirable for buildings with high balance points, but probably has limited value for internally load dominated ones.

Solar radiation levels should also be considered. In a climate that is heavily overcast in either the shading or exposure period, these criteria are less important. It is not always necessary to provide full exposure to allow for adequate solar gain in climates where the need for heating is minimal. If local conditions and building design make exposure unnecessary, solar controls may be created based on shading angles alone.

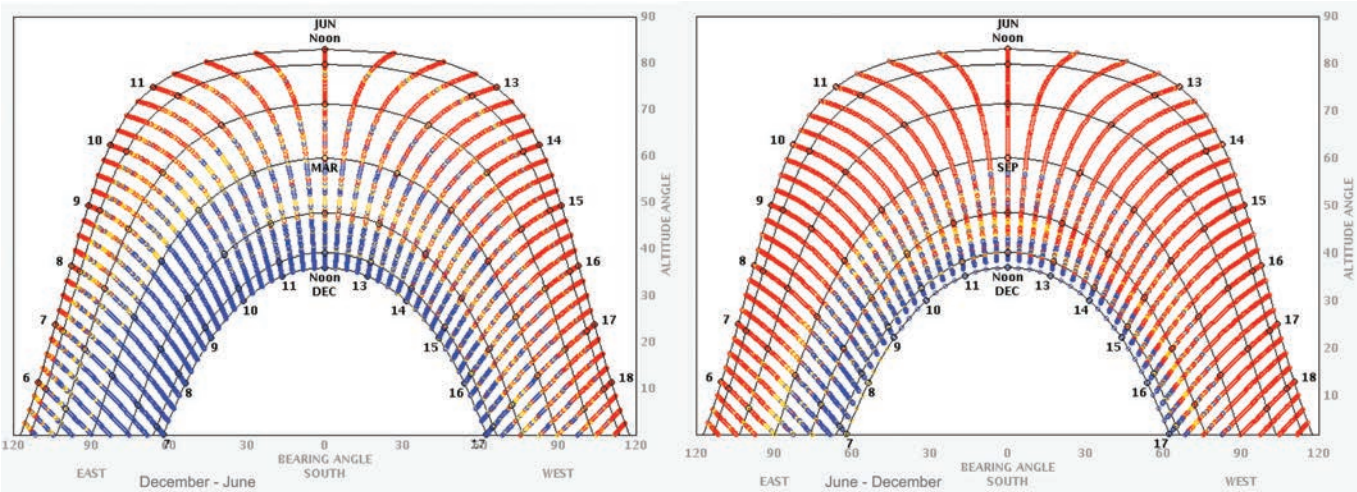

Figure 8.4

Climate Consultant Over/Underheated Periods for Austin, Texas

This diagram shows over and underheated periods for Austin, Texas, using the ASHRAE 55–2010 Adaptive Comfort Model superimposed on a vertical sun-path projection for Austin, Texas. Red dots indicate hours where the outside temperature is > 27°C, blue dots underheated times when the temperature is < 20° C, and yellow dots comfortable periods when the temperature is in between those two values.

Dason Whitsett

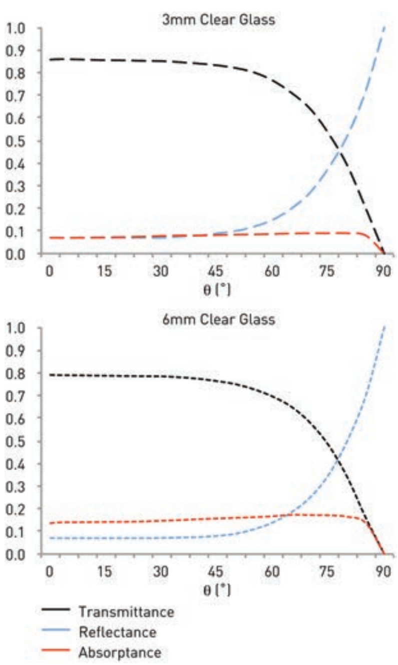

Figure 8.5

Dielectric Properties of Glass

Transmittance (T), reflectance (r), and absorptance (a) of clear float glass. These properties are averaged over the solar spectrum and vary across wavelengths.

Dason Whitsett

Angle of Incidence

When solar radiation strikes a glass surface, portions of that radiation are transmitted through the glass, absorbed by the glass, and reflected back to the exterior. Figure 8.5 shows the relative proportions of these reactions are determined both by the angle of incidence (θ) of the radiation on the glass and by the physical properties of the glass assembly. Standard clear 3mm glass is approximately 86% transparent at a normal angle of incidence, but transmission drops off steeply starting around 65°. At angles of incidence close to 90° (parallel to the surface), transmission is near zero, while reflectance increases proportionally. Absorptance stays roughly constant until θ approaches 90°, when it drops to zero.

As glass thickness increases, the same trends are apparent, although transmission values are reduced while absorptance increases, as shown in Figure 8.5 for 6mm thick clear glass. Modern glazing products with multiple layers, gas fills, and low-E coatings also show similar trends, but with further reduced transmission values.

As the angle of incidence increases, the net insolation is reduced, as demonstrated in Figure 4.9 and for glass, the level of reflected radiation increases to the point where reflectivity approaches 100% near a 90° angle of incidence. Most modern windows in use in cooling climates today have a low solar heat gain coefficient, further reducing transmitted solar radiation. The interaction of these three phenomena means that the designer may ignore times of sufficiently high angle of incidence in shading design because very little radiation is likely to be transmitted into the building. Therefore, evaluating the angle of incidence relative to shading and exposure criteria can uncover times at which shading is unnecessary even if suggested by outside temperatures and help reduce the size of solar controls.

Looking at the solar protractor for a south-facing surface at 30° N latitude shown in Figure 8.6, it is apparent that the sun only sees the surface for less than six hours on the summer solstice, that the lowest solar profile angle is 83.5°, and the angle of incidence is also 83.5° at its lowest. Therefore, shading of windows

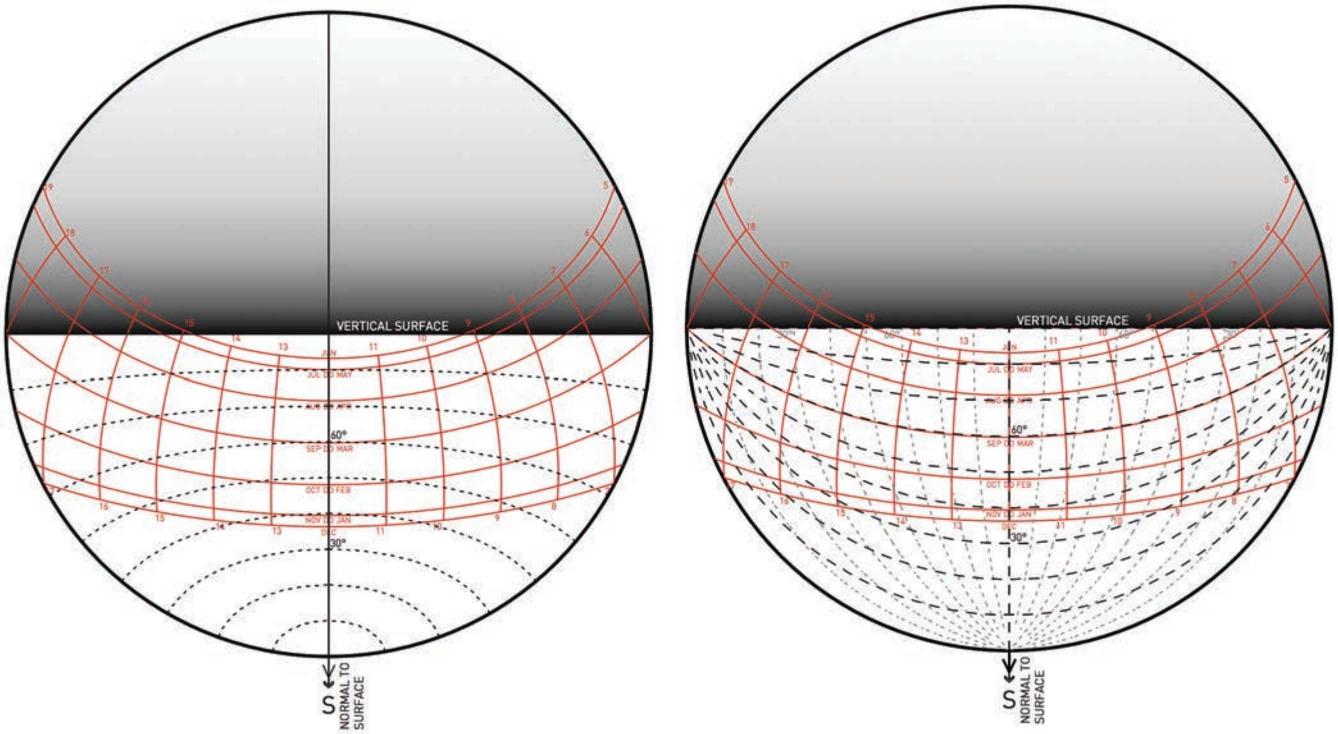

Figure 8.6

Solar Protractor for South-Facing Surface at 30° N Latitude—Angle of Incidence and Profile/Elevation Angles

Dason Whitsett

on that surface will have very limited impact on that date. By September, however, $\theta = 60°$ at solar noon and the sun spends six hours below 70° angle of incidence. Shading at this time is very important.

Setting the Criteria

Using knowledge of the solar vector envelope, building balance point, climatic knowledge, and glass properties, the designer can establish effective shading and exposure criteria. In the temperate latitudes, to remain practical, the shading date should be on the summer side of the equinoxes and the exposure date should be on the winter side of the cycle. Otherwise, as the solar vector surface folds past the equinox and into winter, it becomes very difficult or impossible to maintain full shading on a surface with a fixed device. The closer the shading and exposure dates are to one another, the larger the necessary geometry will be to satisfy the criteria.

DESIGN FOR SOLAR EXPOSURE: THE WINTER FUNNEL

If a window is to be fully exposed on a certain date, all portions of the window need to have an unobstructed view of the sun on that day. The geometric expression of these criteria is a funnel-like shape around the window that must be kept open. To create this funnel geometry is conceptually simple. To do so, one would take the conical shape of the solar vector envelope for the day when full exposure is desired and sweep it around the edges of that window. Figure 8.7 illustrates this concept. The outer boundary defined by this sweep forms a new envelope around the window, which we call the *winter funnel*.

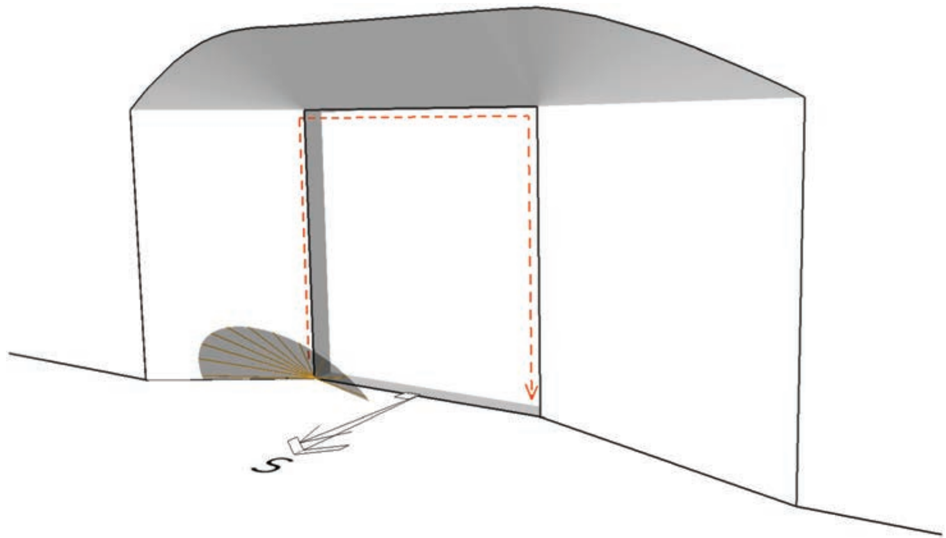

Figure 8.7
Winter Funnel for Solar Exposure
Dason Whitsett

DESIGN FOR SHADING: SHADING DEVICE GEOMETRY

Minimum Solar Shade Geometry

Once the winter funnel is established, geometry to provide the necessary summer shading can be generated. Arumí established a method for finding absolute minimum shading geometry to fit an established set of shading criteria.[10] To create the minimum geometry, one takes the vector envelope for the summer shading day and sweeps it down the sides and across the bottom edge of the window, creating another shell at the outer boundary formed by this sweep. The winter funnel is then clipped where it intersects with this summer shading shell. The remaining portion of the winter funnel represents the optimum geometry to satisfy the defined shading criteria.

Figure 8.8 shows a variety of examples of the geometry for different azimuths resulting from this method. The criteria used in the examples are to provide full shading on the summer solstice and full exposure on the winter solstice. For a due-south-facing surface, the optimal shade is small. But even with these most minimal of shading and exposure criteria, the shade geometry grows quickly as the window azimuth rotates to the west, expanding to the point of being impractical in most situations. For more restrictive shading goals, the shade becomes very large even at 20–30° of azimuth as it seeks the south direction to maintain the defined exposure.

While the sail-like shape of this geometry renders it unlikely to be used in a literal way very often, the concept is helpful in the creation of other shading geometry.

Shading Masks

A ***shading mask*** is a tool for expressing shading and exposure criteria and generating shading geometry. Shadings masks look like sky dome projections of a particular geometry, but they are not. A shading mask is best read as a composite of sky dome projections from the different corners of a window (and the mid-points if drawn). The mask indicates the areas of the sky dome that must either be blocked or exposed

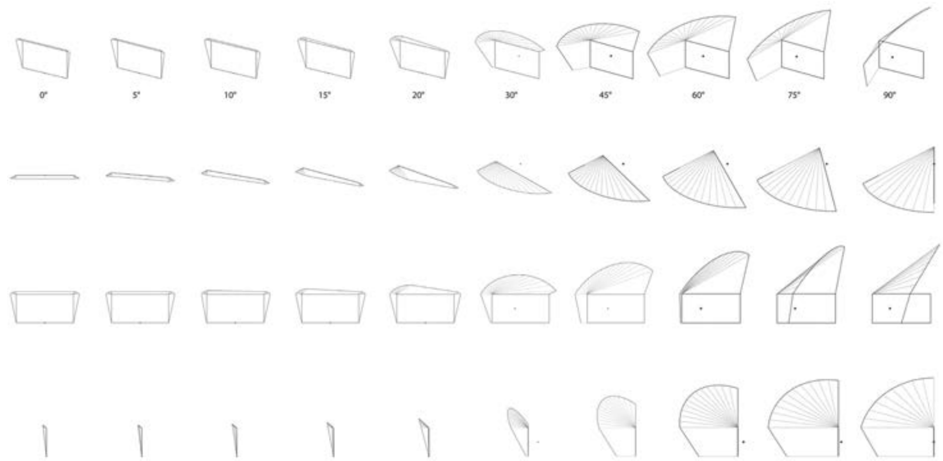

Figure 8.8

Minimum Solar Shading Geometry

Solar shading for various azimuths at 30° N latitude providing full shading on the summer solstice and full exposure on the winter solstice.

Dason Whitsett

from all points of view on the window, depending on the date, to meet the established shading and exposure criteria. See Figure 8.9 for example shading masks for combinations of vertical and horizontal elements and Figure 8.10 for masks for other typical geometries.

In the figures, magenta represents the area of the sky dome that is obstructed by the example geometry, which is drawn as if the horizontal and vertical elements are infinitely long. In practice, it is very important to consider the practical size of such elements. The mask may be read as a projection from the two opposite lower corners of the window and split at the black dashed line. The pink area is a projection from the mid-point indicated.

The shading mask itself is orientation independent, being a representative only of geometry relative to a surface. Shading masks may be overlaid on different sun-path diagrams or oriented in different directions to test the performance of a certain geometry under different conditions, as shown in the figures.

For the classic analysis of an extensive "vocabulary" of shading device geometries using shading masks, see Olgyay.[11]

Shading and Exposure Angles

The critical shading angles for design of solar controls may be measured off of the shading mask overlay on a sun-path diagram. Using a solar protractor for this purpose is helpful. The discussion of these angles assumes a window in the northern hemisphere. For windows in the southern hemisphere, reverse the references to left and right.

The most commonly recognized shading angle is the ***vertical shading angle*** (*VSA*). The *VSA* is the lowest profile angle of the solar ray relative to a building surface during a shading period. To meet the shading criteria, this angle must be obstructed by a shading device, as shown in Figure 8.9. The *VSA* always springs from the sill of the window.

The ***elevation shading angle*** (*ESA*) is the elevation angle of the solar ray on the building surface at the beginning or end of the shading period. The *ESA* determines how far down the wall a horizontal shading device must extend to fully shade the

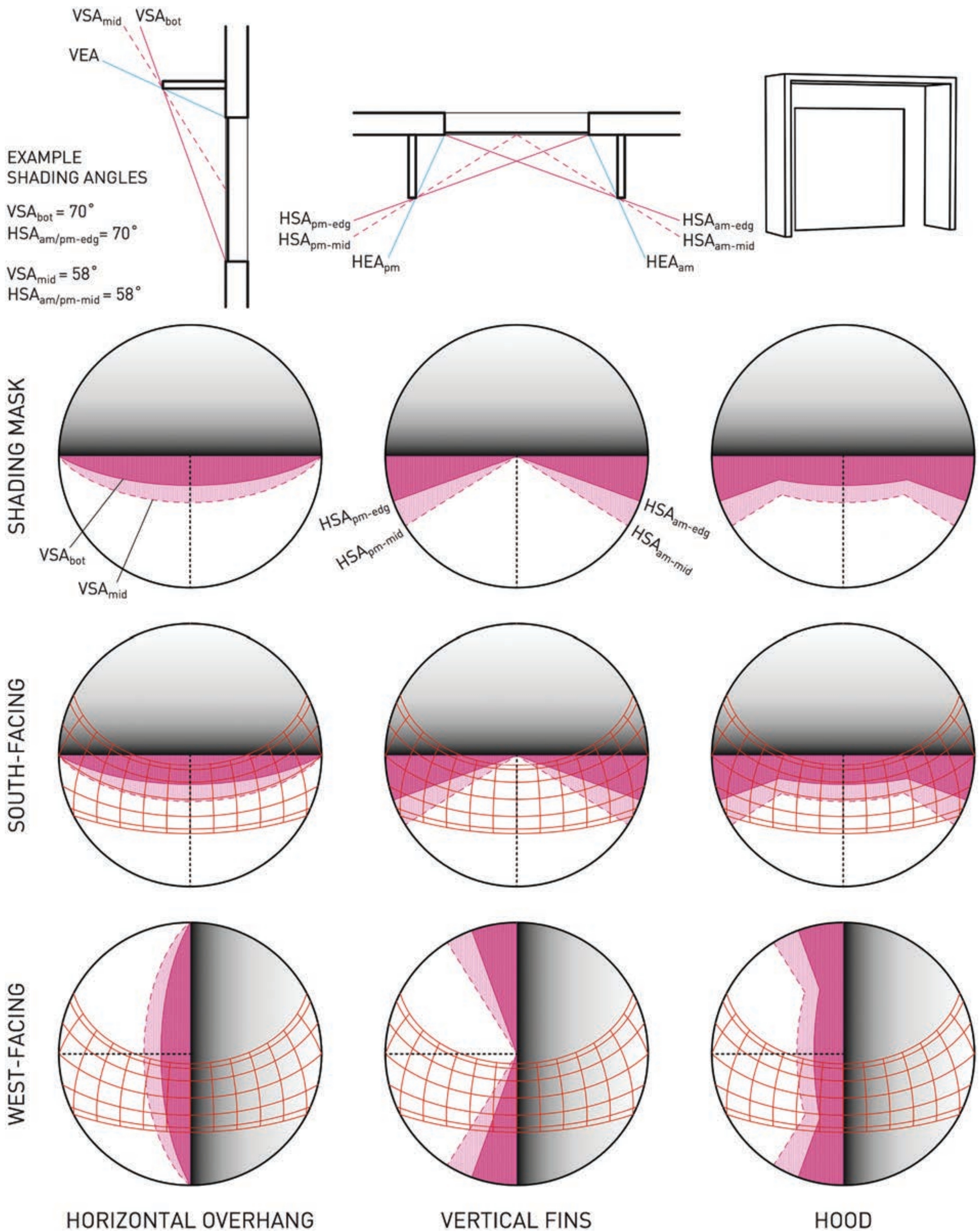

Figure 8.9

Shading Masks for Common Shading Geometries

Shading masks for various common geometries alone, and overlaid on a sun-path diagram for 30° N latitude in south and west orientations. The mask may be overlaid on any sun-path diagram to test performance at a given latitude and rotated to any orientation. The horizontal and vertical elements are drawn as if they are infinitely long and should be adjusted in practice for actual length. After Olgyay (1957).

Dason Whitsett

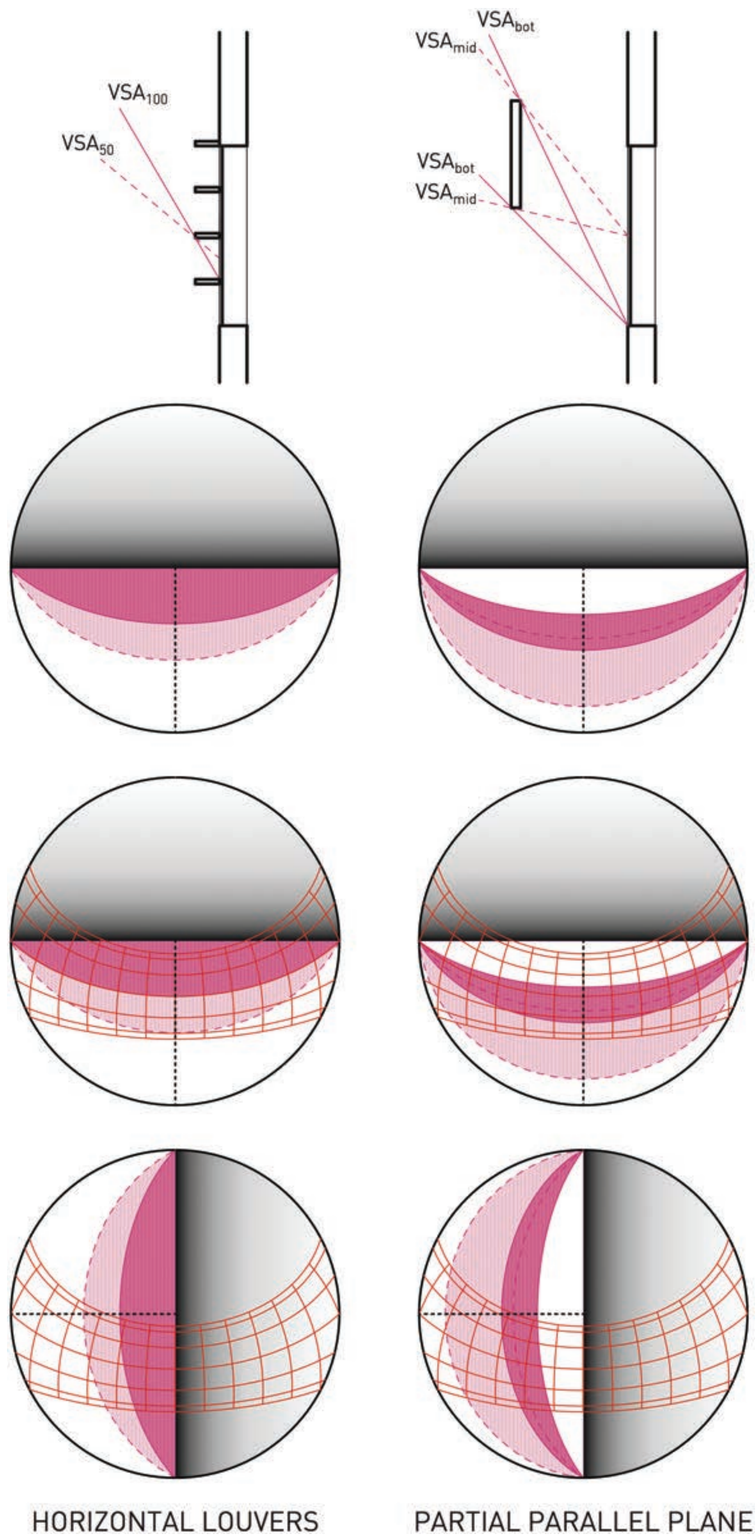

Figure 8.10

Shading Masks for Other Example Geometries

Dason Whitsett

window within a defined period. To avoid excessive length of required shading, often, the time period during which shading is required is reduced to the period when the angle of incidence is low enough to be a concern. The ESA_{am} springs from the lower right corner of the window in elevation and the ESA_{pm} from the lower left.

The ***horizontal shading angle*** (*HSA*) is the surface-solar azimuth at the beginning or end of a shading period or the angle to a fixed shading surface. The *HSA* springs from the opposite edge of the window; for example, the HSA_{am} for a fin on the right side of a window springs from the opposite (left) edge of that window.

The ***vertical exposure angle*** (*VEA*) is the highest solar profile angle of the sun relative to a surface during the exposure period. In order to maintain the desired window exposure, a shading device must not encroach beyond the *VEA*. The *VEA* springs off the top edge of the window.

The ***horizontal exposure angle*** (*HEA*) is the surface-solar azimuth at the beginning or end of an exposure period. In order to maintain the desired window exposure, a shading device must not encroach beyond the *HEA*. The HEA_{am} springs off the right jamb of the window to be exposed and HEA_{pm} off the left jamb.

Shading Geometries

Horizontal Overhangs

Horizontal overhangs are the most versatile fixed shading geometry and include elements such as eaves, awnings, horizontal shading devices, and so on. The outermost edge of a horizontal overhang follows a constant profile angle line in the shading mask and comes from overhead at the zenith. Overhangs are most effective at blocking sun with a high profile angle. As the profile angle drops, horizontal overhangs must get deeper to provide shading, reaching a practical limit at some point. Figure 8.9 shows that these characteristics are optimal for equator-facing surfaces, but less so for east or west surfaces. Nevertheless, a west overhang can easily add several hours of shade on a surface.

When working with horizontal overhangs, it is essential to check their length to avoid end-around exposure from the elevation angle, as illustrated in Figure 8.11. Often, it is necessary to extend a horizontal overhang a significant distance down the wall or to combine it with other geometry to prevent this.

Utzinger and Klein[12] found that under the following conditions, the end effect of solar exposure past a horizontal overhang became negligible, where *width* refers to the width of the window and *extension* to the length of extension of the overhang beyond each side of the window.

$width \geq 25$ and $extension \geq 0$
$width \geq 4$ and $extension \geq 2$
$width \geq 1$ and $extension \geq 3$

In other words, as the window gets wider, the effect of the extension is reduced to the point where, for very wide windows, it may be ignored. For narrow windows, the extension may need to be multiples of the width of the window itself to prevent all effects from end-around exposure.

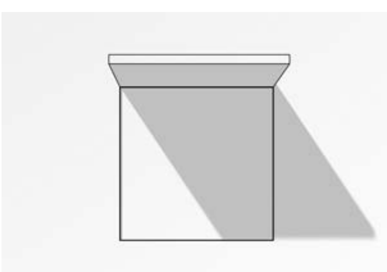

Figure 8.11

Importance of Elevation Angle in Shading Design

South-facing window at 30° N latitude with shading device designed to provide full shading at noon on the equinox. By 14:00 on the equinox, 1/3 of the window is exposed to radiation bypassing the overhang from the side. Exposure will increase during the afternoon and the same problem will occur in the morning.

Dason Whitsett

Vertical Fins

Vertical fins are most effective at blocking sun positions with a high surface-solar azimuth and low elevation angle. There is a persistent rule of thumb in architecture that vertical fins are the best remedy for east- and west-facing windows, but Figure 8.9 shows their weakness in this application unless they are extremely deep or angled in front of the window. Vertical fins are much more effective for a southwest- or north-northwest-facing surface where, at overheated times, the sun will be at a high surface-solar azimuth.

As latitude increases, however, vertical fins become more versatile because the solar path band is tilted closer to perpendicular relative to the vertical element. This results in less time that the sun spends in the surface-solar azimuth window left exposed by the fins.

Hoods

Hoods are shading geometries that combine horizontal overhangs and vertical fins, as shown in Figure 8.9. Egg crate or bris soleil structures would fall into this category as well. This strategy is useful in particular for limiting the length along the wall of horizontal overhangs or for dealing with southeast- and southwest-facing windows.

Detached Shades

By far the most difficult challenge in shading design is dealing with sun positions with a low surface-solar azimuth and low profile angle, the combination of which translates to a low angle of incidence. In other words, if the sun is shining nearly straight onto a surface, it is very difficult to block without putting something entirely in front of the surface, which is usually antithetical to the purpose of the window.

Detached floating planar surfaces parallel to the window surface are one way to deal with this, as shown in Figure 8.10. If the panel extended as low as the sill of the window, direct sun would be blocked all the way to the horizon, but building users would also look out the window at the back of the shading surface.

Louvers

Louvers are a technique to effectively break up a shading control into a more manageable dimension while maintaining the performance of a much larger shading element. For example, it is fairly easy to create a louvered element with a *VSA* of 45°, while a shading angle that low would generally be prohibitively large for a single horizontal building-attached shading element. Louvers result in shading performance very similar to overhangs or fins at the same shading angle.

Other Geometries

Shadows are created by anything that comes between the solar ray and a surface. Shading controls can take on any geometry and work equally as well under the same principles described here. Looking at a sky dome projection, for example, it is not possible to discern whether the projection of a surface following a constant profile angle line is a horizontal plane or a sloping surface with a change in depth and height that results in a constant profile angle. The minimum shading geometry discussed previously is an example of this.

Operable Elements

Operable shading controls have the enormous advantage that they can be adjusted based on both typical seasonal variation as well as day-to-day weather to optimize their performance to the conditions. The disadvantages of such systems, however, are cost and reliability of the mechanical elements along with the risk that they will not be operated in practice and could negatively impact comfort and performance.

Moveable shades can be anything from operable louvers to exterior blinds, curtains, or operable sections of building-attached elements. These are not to be confused, however, with interior window treatments. Shading on the inside of a window can have some impact, but once radiation has been transmitted through glass, the vast majority of it remains inside. So, to be effective, shading must be on the outside of glass.

Other Shading Elements

Forms to create shade need not be attached to the building. For example, trees are incredibly effective shaders, particularly excelling at shading east- and west-facing windows that would otherwise be subject to challenging low angles of incidence during peak periods.

Trees have the added advantage that looking out a window into a tree is generally considered desirable, while looking into a built element is rarely ideal. In addition to trees, other detached elements such as other portions of the building, pergolas, fences, landscape elements, etc. should not be overlooked as potential shadow-casting elements.

EQUATOR-FACING SOLAR CONTROLS

Shading controls for windows facing the equator are the easiest to design because of the symmetry of the sun's geometry on the north-south axis. They also result in the smallest forms for maximum shading effect.

EXAMPLE 8.1 EQUATOR-FACING SOLAR CONTROLS

Establish shading and exposure criteria and design a solar control for a 1m^2 window facing south in Austin, Texas. Assume there is an adjacent building that makes shading unnecessary before 10:30 am.

Solution

Step 1: Shading and Exposure Criteria

Exposure Criteria

Austin, Texas, has mild winters and few heating degree days compared to much of the country, but some minimal solar gain in winter is still desirable for skin-load dominated buildings. It is important, however, not to provide for excessive gain, which can easily lead to overheating. For the sake of this example, we will assume there is a limited south-facing glazed area and that substantial exposure is desirable on the few small windows that do exist. Actual passive solar gain needs should be evaluated based on the project specifics. Here, full exposure will be maintained on the December solstice.

Limiting the full exposure period to hours with useful levels of radiation for passive solar gain helps by narrowing the winter funnel, which in turn will minimize the size of the summer controls necessary. Because of the moderate heating needs, the hours of 9:00–15:00 *AST* when beam radiation is at its highest will be chosen as the period to maintain full exposure.

Shading Criteria

Figure 8.4 shows that Austin has a cooling load-dominated climate, and that shading all the way up to the equinox is desirable in any application. March mornings are often on the cool side, but by afternoon, it is generally too warm, and in September, mornings and afternoons are overheated. Additional shading even beyond the equinox would be desirable in most cases, but the shape of the solar vector envelope makes this difficult to accomplish with building-attached shades. So, the equinox would be the minimum preferred shading date.

Looking at a solar protractor, one can see that at 16:00 *AST* on the equinoxes, the angle of incidence is approximately 75° and increases quickly thereafter. Per Figure 8.5, that means that transmittance of clear glass is down to around 40% of incident radiation, and actual glazing used in this climate in practice is likely to have a much lower transmittance. Therefore, we will choose 16:00 as the time at which the period of full shading will end on the equinox.

Step 2: Draw Shading and Exposure Mask

See Figure 8.12. Note that the occluded area extends from the shading date line to the wall on a constant elevation angle line that correlates with a form projecting

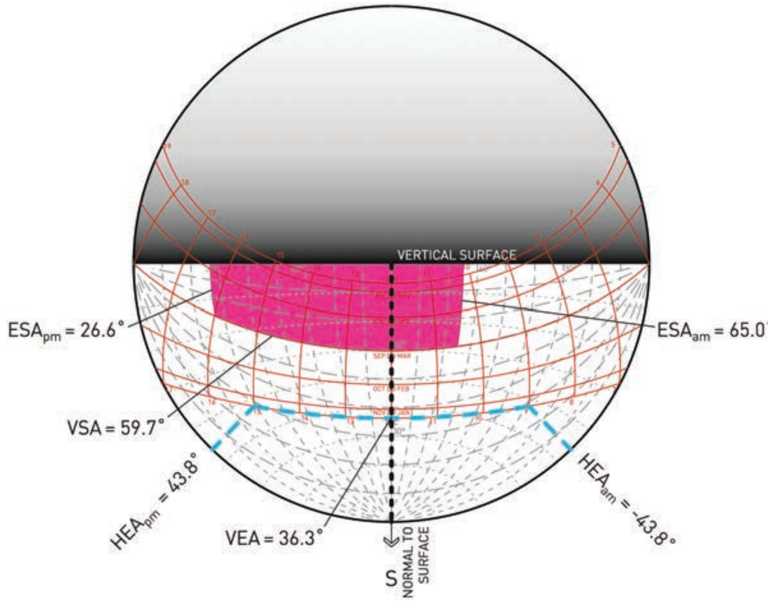

Figure 8.12

Shading Mask for Specific Shading Criteria (Not Infinite)

Shading mask showing the shading/exposure criteria for Example 8.1. The period of full shading is shown in magenta and the period for full exposure is outlined by the dashed blue line. A shading mask is not a literal sky dome projection, but rather a set of guidelines for the generation of shading/exposure geometry. See Figure 8.14 for an illustration of the relationship.

Dason Whitsett

perpendicular to the wall. Based on the criteria, the minimum geometry could follow the 10:30 and 16:00 lines back to the wall, but in practice is not likely to reflect that geometry.

Step 3: Determine Shading Angles

HEA_{am} is the surface-solar azimuth at the time in the morning when the full exposure period is to start; in this case, −43.8°.

HEA_{pm} is the surface-solar azimuth at the time in the morning when the full exposure period is to end; in this case, 43.8°.

The *VEA* is the lowest profile angle of the sun within this time frame, 36.3°.

The ESA_{am} is the elevation shading angle at the beginning of the shading period. At 10:30, this is 65.0°.

The ESA_{pm} is the elevation shading angle at the end of the shading period. At 16:00, this is 26.6°.

The *VSA* is the lowest profile angle of the sun within this time frame, which on the equinox for a south-facing surface is constant at the complement of the latitude, 59.7°.

There is nothing setting a particular *HSA* yet, so that angle will be ignored for now.

Step 4: Design Shading Control

Figure 8.13 shows one possible solution to meeting these criteria. This is not the absolute minimum geometry, and there are an infinite number of solutions that also meet the criteria. This solution does, however, illustrate a way to minimize the geometry with fairly simple forms.

Draw the shading angles onto the plan, section, and elevation views of the window. Remember that the horizontal angles are surface-solar azimuths so the angle is relative to the normal vector of the wall, not the wall itself. The exposure

EXAMPLE 8.1 CONTINUED

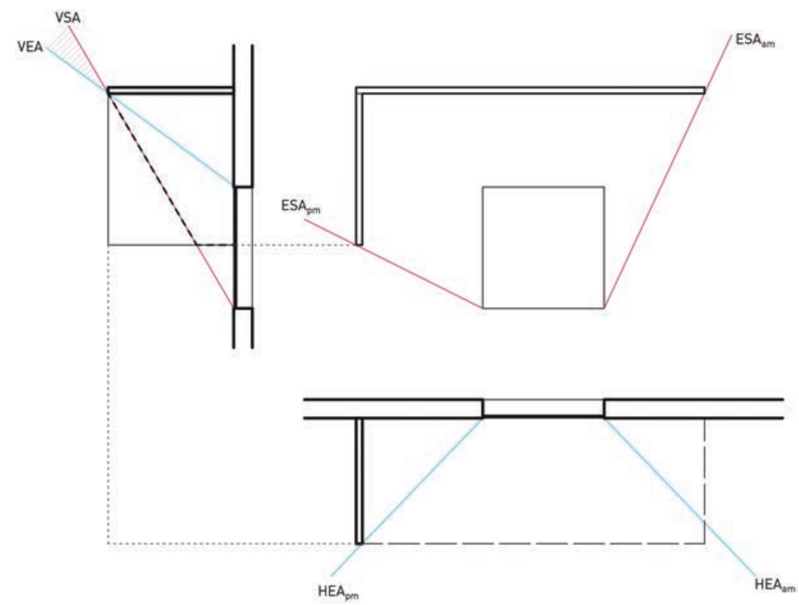

Figure 8.13
Design of Equator-Facing Solar Controls
Dason Whitsett

angles should project off the edge of the window on the side of the sun and the shading angles off the opposite edges.

In the section view, the point where the *VSA* and *VEA* intersect is the minimum depth of overhang that must exist to meet the criteria. Geometry that projects into the hatched area above this intersection will also meet the criteria, extending the shading period and reducing window exposure. Because the shading date is the equinox and the solar vector envelope will begin folding down toward the equator after this date, further extension will not provide full shading throughout the day.

Project the depth of the horizontal overhang into the plan and elevation views. In the elevation to the right of the window, the overhang may be cut off by the ESA_{am}. On the left side of the window, the overhang could be extended horizontally to intersect the ESA_{pm}, but this would result in an unreasonably large form unless the overhang was an eave or some other similar building element that serves additional functions.

To determine where the overhang could fold down into a fin, find the intersection of its depth with the HEA_{pm} in the plan view. Turn the overhang down at that depth. In the elevation again, there is no need for the fin to extend lower than the ESA_{pm}.

Step 5: Check Solution

It is important to check the solution to ensure it is performing as expected. Figure 8.14 shows sky dome projections from the four corners of the window overlaid with the outline of the shading mask. The solution does, indeed, perform as intended. The area in the lower two projections between the shaded area and the exposure period is where a deeper overhang that still meets the criteria as discussed previously would encroach.

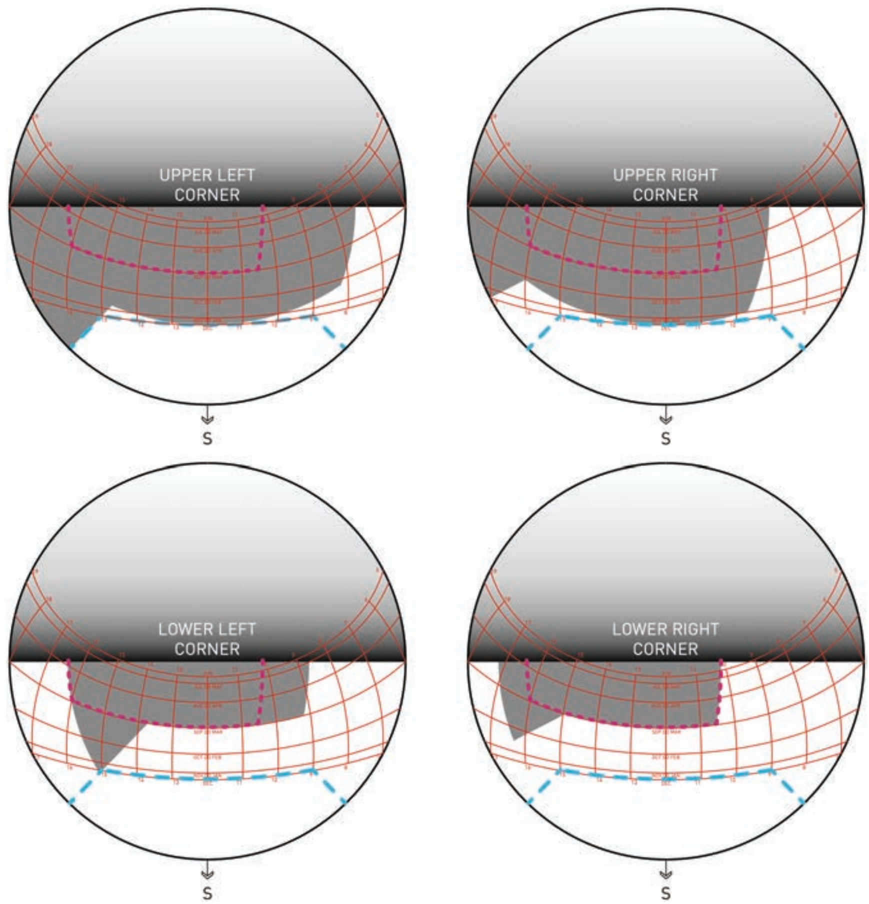

Figure 8.14

Sky-Dome Projection of Shading Device Design (at Four Corners)

Sky dome projections from the four corners of the window from Example 8.1. The shading/exposure criteria from the shading mask in Figure 8.12 are superimposed on the projections showing that the solution meets the criteria reflected in the shading mask.

Dason Whitsett

Notice the difference between the projected view of the shading device and the shading mask but also note how the shading mask defines most of the edges. The exception is the triangular area at the bottom of the fin that serves no shading purpose. The dashed line matching the *VSA* in the section view shows the portion of the fin that could be removed to further optimize the shading control without adversely impacting the shading criteria.

Note that although some steps were taken to minimize the size of the shading device in Example 8.1, it is still large in proportion to the window. We do not have control over the path of the sun, so the geometric relationships are fixed. However, there are a number of other measures to consider in order to reduce its size. First, one could evaluate other types of shading solutions in lieu of or in addition to a fixed shading element. For example trees, louvers, or operable elements might be an option. Second, look at whether the shading criteria can be altered. A sensitivity study on solar gain is an excellent method for doing this. While the balance point and climatic information might indicate that certain dates for full shading and full

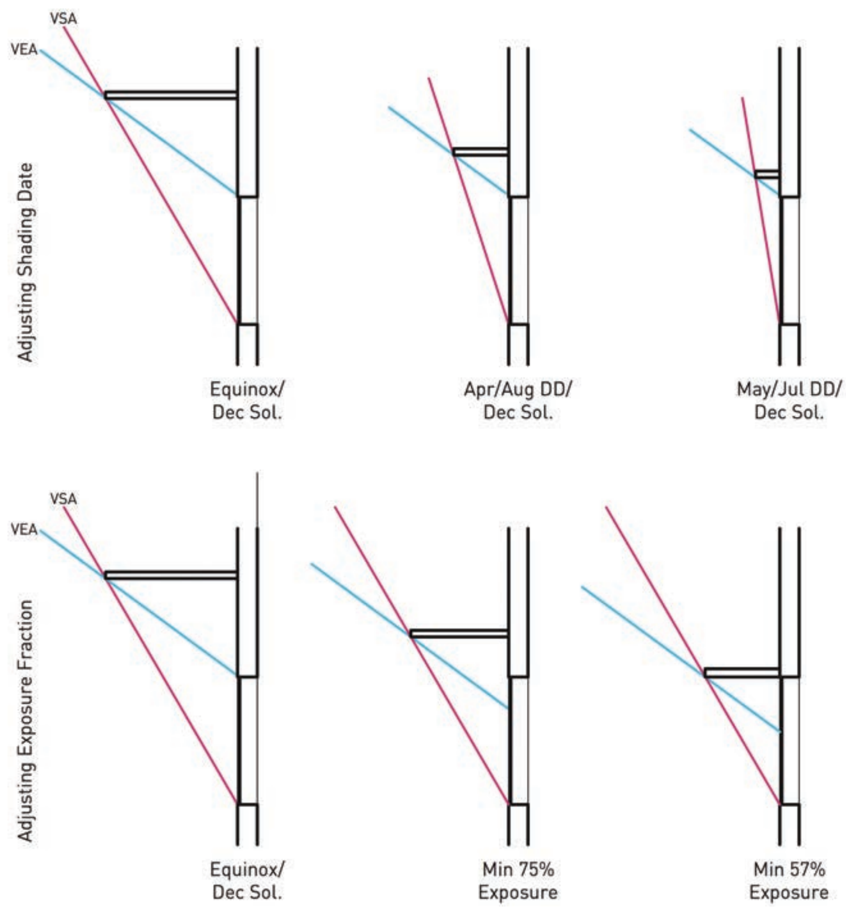

Figure 8.15

Overhang Proportions for South-Facing Surface

Dason Whitsett

exposure are desirable, it is worth evaluating what the impact of scaling back the criteria is. Remember that backing off of full shading or full exposure does not mean there is no shading or exposure. In cooling climates, if compromise is necessary, generally preserving shading in overheated periods is higher priority than maintaining exposure at underheated times.

Figure 8.15 shows the impact of adjusting either the full shading date or exposure fraction of an equator-facing window at 30.3° N. The examples start with the criteria used in Example 8.1. Note in particular the large difference between the equinox and the August shading dates due to the rapid change in solar declination over that period. Selecting a shading date between design days could be a good compromise solution in this case. Many, if not most, buildings in climates at around 30° latitude would not need or want full exposure even in winter, so the scenarios where the exposure fraction is reduced are useful to consider. As the shading device comes closer to the top of the window, however, it is important to be aware of the reduction in daylight and obstruction of views from the interior that will result.

SHADING FOR WINDOWS OF ANY ORIENTATION

As the window azimuth rotates away from the south, maintaining constant shading criteria will cause the controls to increase in size quite rapidly, as illustrated in Figure 8.8.

EXAMPLE 8.2

Design a shading control for a 1m² window with an azimuth of 15° at 30.3° N latitude to fully shade the window between 11:00 and 17:00 on the April and August design days and fully expose it from 8:00 to 16:00 *AST* on the December solstice.

This example is intended to show the types of conflicts and trade-offs that must be considered in actual practical applications and how much difference even a small rotation off of south makes in shading device requirements.

Solution

Step 1: Shading and Exposure Criteria

Fully expose window from 8:00 to 16:00 *AST* on the December solstice.

Fully shade the window between 11:00 and 17:00 on the April and August design days.

Step 2: Draw Shading and Exposure Mask

See Figure 8.16.

Step 3: Determine Shading Angles

$HEA_{am} = -69.1°$
$HEA_{pm} = 39.2°$

VEA is the highest profile angle within that period, which is 39.0° at approximately 10:30.

$ESA_{am} = 71.0°$
$ESA_{pm} = 19.0°$
$VSA = 59.1°$

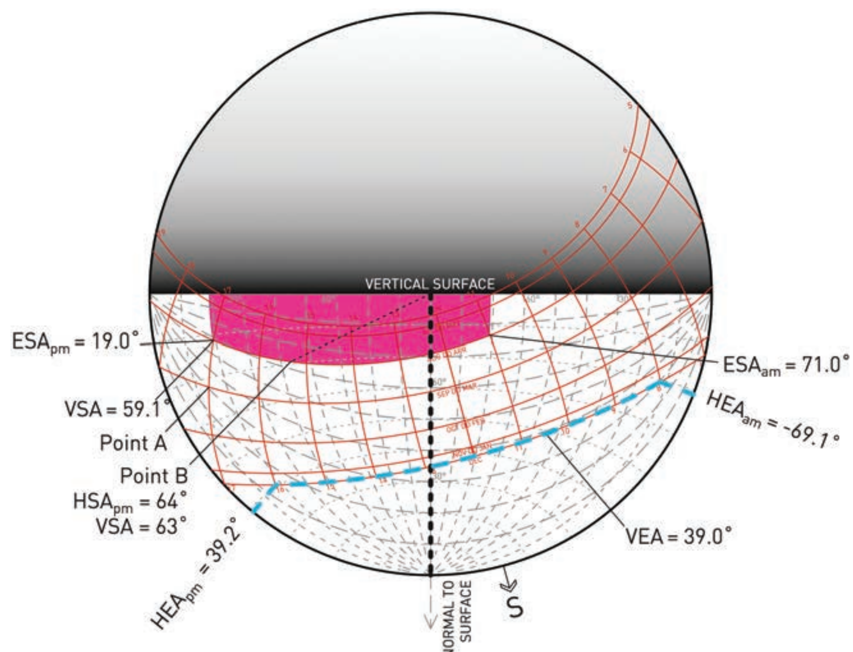

Figure 8.16
Shading Mask for Example 8.2
Dason Whitsett

EXAMPLE 8.2 CONTINUED

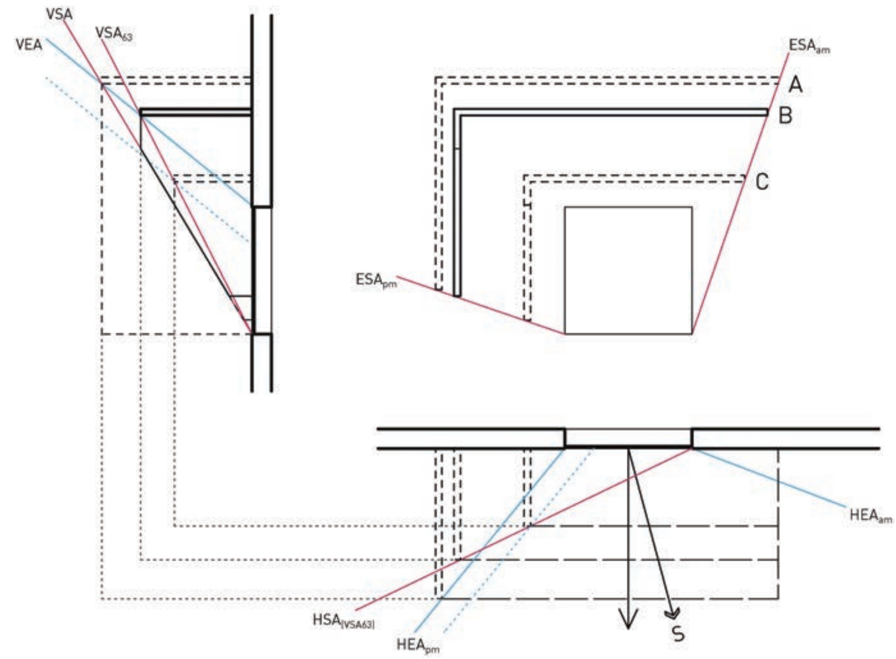

Figure 8.17

Solar Control Design for Surface of Arbitrary Orientation—Example 8.2

Dason Whitsett

Note that if the same shading date from Example 8.1 was used, point *a* shows that the *VSA* would be 31°, an impossible solution for a horizontal overhang because the *VSA* and *ESA* would never intersect.

Step 4: Design Shading Control

Version A in Figure 8.17 shows the design of a shading control based on these criteria following the same method used in Example 8.1. This results in an enormous shading form. Likely this is too big to be feasible, so other means to optimize the form should be explored.

Exploration on the shading mask shows that dropping a fin with an HSA_{pm} of 64° would yield a *VSA* at that time of 63°. This combination allows the control to shrink and the fin to be brought in while still keeping the winter funnel clear, as shown in version B.

Version C shows the effect of reducing the requirement for exposure to 75% of the height and width of the window and using the same shading angles in version B. Clearly, reducing or eliminating exposure criteria has a major impact on shading device size. At lower latitudes, this is an important option to explore.

Step 5: Check Solution

Figure 8.18 shows the shadows cast by version B at key times on the shading and exposure dates, indicating that the shading device performs as intended.

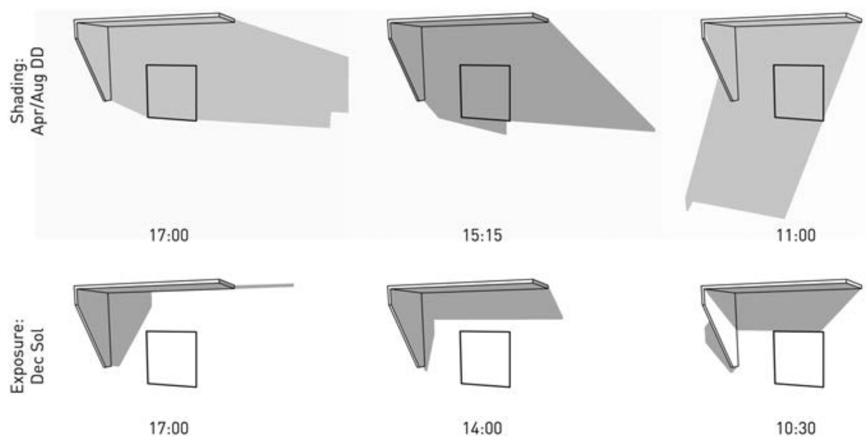

Figure 8.18

Shadow Study Confirming Expected Performance of Shading Device

Dason Whitsett

There is no absolute set of rules for shading device design and there are nearly always tradeoffs to be made with other considerations. However, the following set of guidelines outline a process that is useful in many situations. Refer to the section titled *Shading and Exposure Angles* in this chapter for definitions of the various acronyms that follow.

Method for the Design of Fixed Shading Devices

1. Establish exposure and shading criteria as discussed previously.
2. Draw the shading/exposure mask for the window.
3. Determine the shading and exposure angles for the window and draw onto the window views. Shading angles will spring from the opposite edge of the window while exposure angles spring from the side nearest the sun.
   a. The *VEA* and *HEA* represent a crude version of the winter funnel.
   b. The *VSA*, *ESA*, and *HSA* are used to clip the winter funnel or otherwise create geometry beyond it.
   c. If there are no exposure criteria, use the shading angles alone to define the minimum depth of shading controls.
4. Design the shading controls based on these angles. If the solution is unworkable:
   a. look for opportunities to reduce its size by introducing other elements such as fins, louvers, or dropped elements.
   b. look for ways to improve the orientation of the fenestration or modify its physical properties.
   c. evaluate the impact of relaxing the shading or exposure criteria on building performance.
5. Check the design using sky-dome projections, by casting shadows, or by drawing solar views.

OTHER TOOLS FOR SHADING DESIGN

Another useful approach to shading design is the production of tables of key angles and solar exposure, as shown in Table 8.1. Here, times at which insolation is

Table 8.1 Surface Insolation and Solar Gain Analysis

Unshaded Surface Insolation and Solar Gain Analysis

Location: Austin, TX L= 30.3° LON=-97.7° Time Zone: UTC -6 Calculation Time Standard: AST Solar Radiation Data Source: EPW Stat File Diffuse Sky Model: Isotropic

sf1 South — αsf (°) 0.00, Σ (°) 90.00, A_{sf} (m²) 1.00, A_{win} (m²) 1.00, ρ 0.20, SHGC 0.25

Date	Time	α_{sol} (°)	β_{sol} (°)	γ (°)	Ωpf (°)	Ωel (°)	θ (°)	I_{tb} (Wh)	I_T (Wh)	Q_b (Wh)	Q_T (Wh)
Jun 15	5:01	-117	0	-	-	-	-	-	-	-	-
	5:30	-114	6	-	-	-	-	-	17	-	3
	6:30	-107	18	-	-	-	-	-	57	-	10
	7:30	-101	30	-	-	-	-	-	99	-	16
	8:30	-95	43	-	-	-	-	-	145	-	21
	9:30	-87	56	-87	**88**	-56	89	**12**	196	**0**	26
	10:30	-76	69	-76	**85**	-69	85	**46**	259	**2**	31
	11:30	-46	80	-46	**83**	-83	83	**68**	299	**4**	35
	12:30	46	80	46	**83**	83	83	**70**	302	**4**	35
	13:30	76	69	76	**85**	69	85	**47**	261	**2**	31
	14:30	87	56	87	**88**	56	89	**14**	204	**0**	26
	15:30	95	43	-	-	-	-	-	153	-	21
	16:30	101	30	-	-	-	-	-	111	-	16
	17:30	107	18	-	-	-	-	-	65	-	10
	18:30	114	6	-	-	-	-	-	19	-	3
	18:58	117	0	-	-	-	-	-	-	-	-
								257	2187	**11**	284
Jul 16	5:07	-115	0	-	-	-	-	-	-	-	-
	5:30	-112	5	-	-	-	-	-	13	-	2
	6:30	-105	17	-	-	-	-	-	52	-	8
	7:30	-99	29	-	-	-	-	-	94	-	14
	8:30	-92	42	-	-	-	-	-	138	-	20
	9:30	-84	55	-84	**86**	-55	87	**31**	208	**1**	25
	10:30	-71	68	-71	**83**	-69	83	**71**	277	**4**	31
	11:30	-39	79	-39	**81**	-83	81	**89**	307	**6**	35
	12:30	39	79	39	**81**	83	81	**91**	310	**6**	35
	13:30	71	68	71	**83**	69	83	**73**	280	**4**	31
	14:30	84	55	84	**86**	55	87	**31**	210	**1**	25
	15:30	92	42	-	-	-	-	-	148	-	20
	16:30	99	29	-	-	-	-	-	104	-	14
	17:30	105	17	-	-	-	-	-	60	-	8
	18:30	112	5	-	-	-	-	-	15	-	2
	18:52	115	0	-	-	-	-	-	-	-	-
								386	2213	**21**	270
Aug 16	5:27	-106	0	-	-	-	-	-	-	-	-
	6:30	-98	13	-	-	-	-	-	41	-	7
	7:30	-91	26	-	-	-	-	-	89	-	13
	8:30	-83	39	-83	**81**	-39	84	**43**	175	**2**	21
	9:30	-72	52	-72	**76**	-53	79	**102**	275	**8**	32
	10:30	-56	63	-56	**74**	-67	75	**150**	352	**16**	43
	11:30	-24	72	-24	**73**	-82	73	**174**	390	**21**	49
	12:30	24	72	24	**73**	82	73	**164**	378	**20**	48
	13:30	56	63	56	**74**	67	75	**141**	340	**15**	42
	14:30	72	52	72	**76**	53	79	**107**	282	**9**	32
	15:30	83	39	83	**81**	39	84	**48**	184	**2**	21
	16:30	91	26	-	-	-	-	-	95	-	13
	17:30	98	13	-	-	-	-	-	46	-	7
	18:32	106	0	-	-	-	-	-	-	-	-
								930	2651	**93**	327

sf2 West — αsf (°) 90.00, Σ (°) 90.00, A_{sf} (m²) 1.00, A_{win} (m²) 1.00, ρ 0.20, SHGC 0.25

Date	Time	γ (°)	Ωpf (°)	Ωel (°)	θ (°)	I_{tb} (Wh)	I_T (Wh)	Q_b (Wh)	Q_T (Wh)
Jun 15	5:01	-	-	-	-	-	-	-	-
	5:30	-	-	-	-	-	17	-	3
	6:30	-	-	-	-	-	57	-	10
	7:30	-	-	-	-	-	99	-	16
	8:30	-	-	-	-	-	145	-	21
	9:30	-	-	-	-	-	184	-	26
	10:30	-	-	-	-	-	213	-	29
	11:30	-	-	-	-	-	231	-	31
	12:30	-44	**83**	-83	83	**71**	304	**4**	35
	13:30	-14	**69**	-85	69	**190**	404	**27**	57
	14:30	-3	**56**	-88	56	**300**	490	**60**	87
	15:30	5	**43**	85	43	**350**	503	**80**	101
	16:30	11	**31**	72	32	**373**	484	**88**	104
	17:30	17	**18**	47	24	**364**	430	**87**	97
	18:30	24	**6**	13	24	**203**	222	**49**	52
	18:58	27	**0**	0	27	**0**	-	**0**	-
						1853	3783	**395**	668
Jul 16	5:07	-	-	-	-	-	-	-	-
	5:30	-	-	-	-	-	13	-	2
	6:30	-	-	-	-	-	52	-	8
	7:30	-	-	-	-	-	94	-	14
	8:30	-	-	-	-	-	138	-	20
	9:30	-	-	-	-	-	177	-	24
	10:30	-	-	-	-	-	206	-	27
	11:30	-	-	-	-	-	218	-	29
	12:30	-51	**83**	-81	83	**73**	292	**4**	33
	13:30	-19	**69**	-83	69	**216**	423	**31**	58
	14:30	-6	**55**	-86	55	**306**	484	**62**	86
	15:30	2	**42**	88	42	**415**	563	**95**	114
	16:30	9	**30**	75	31	**426**	530	**101**	115
	17:30	15	**17**	49	23	**399**	458	**96**	105
	18:30	22	**5**	12	23	**240**	255	**58**	60
	18:52	25	**0**	0	25	**0**	-	**0**	-
						2075	3902	**447**	696
Aug 16	5:27	-	-	-	-	-	-	-	-
	6:30	-	-	-	-	-	41	-	7
	7:30	-	-	-	-	-	89	-	13
	8:30	-	-	-	-	-	132	-	19
	9:30	-	-	-	-	-	173	-	23
	10:30	-	-	-	-	-	202	-	27
	11:30	-	-	-	-	-	216	-	28
	12:30	-66	**82**	-73	83	**73**	286	**4**	32
	13:30	-34	**67**	-74	68	**208**	407	**31**	58
	14:30	-18	**53**	-76	54	**336**	511	**70**	93
	15:30	-7	**39**	-81	40	**381**	517	**88**	107
	16:30	1	**26**	88	26	**456**	552	**109**	122
	17:30	8	**13**	59	15	**349**	395	**85**	92
	18:32	16	**0**	0	16	**0**	-	**0**	-
						1949	3670	**423**	658

sf3 North — αsf (°) 180.00, Σ (°) 90.00, A_{sf} (m²) 1.00, A_{win} (m²) 1.00, ρ 0.20, SHGC 0.25

Date	Time	γ (°)	Ωpf (°)	Ωel (°)	θ (°)	I_{tb} (Wh)	I_T (Wh)	Q_b (Wh)	Q_T (Wh)
Jun 15	5:01	-297	**0**	0	63	**0**	-	**0**	-
	5:30	-294	**13**	6	66	**4**	21	**1**	4
	6:30	-287	**47**	18	74	**35**	92	**4**	14
	7:30	-281	**72**	31	81	**35**	134	**2**	18
	8:30	-275	**85**	43	87	**22**	167	**1**	22
	9:30	-	-	-	-	-	184	-	26
	10:30	-	-	-	-	-	213	-	29
	11:30	-	-	-	-	-	231	-	31
	12:30	-	-	-	-	-	232	-	31
	13:30	-	-	-	-	-	214	-	29
	14:30	-	-	-	-	-	190	-	26
	15:30	-85	**85**	-43	87	**29**	182	**1**	22
	16:30	-79	**72**	-31	81	**72**	183	**5**	21
	17:30	-73	**47**	-18	74	**112**	178	**13**	23
	18:30	-66	**13**	-6	66	**90**	109	**14**	17
	18:58	-63	**0**	0	63	**0**	-	**0**	-
						399	2329	**41**	314
Jul 16	5:07	-295	**0**	0	65	**0**	-	**0**	-
	5:30	-292	**12**	5	68	**2**	15	**0**	3
	6:30	-285	**49**	17	75	**40**	92	**4**	13
	7:30	-279	**75**	30	82	**37**	131	**2**	17
	8:30	-272	**88**	42	88	**12**	150	**0**	20
	9:30	-	-	-	-	-	177	-	24
	10:30	-	-	-	-	-	206	-	27
	11:30	-	-	-	-	-	218	-	29
	12:30	-	-	-	-	-	219	-	29
	13:30	-	-	-	-	-	207	-	27
	14:30	-	-	-	-	-	178	-	24
	15:30	-88	**88**	-42	88	**16**	163	**0**	20
	16:30	-81	**75**	-30	82	**67**	171	**4**	18
	17:30	-75	**49**	-17	75	**109**	169	**12**	20
	18:30	-68	**12**	-5	68	**98**	113	**15**	17
	18:52	-65	**0**	0	65	**0**	-	**0**	-
						381	2208	**38**	286
Aug 16	5:27	-286	**0**	0	74	**0**	-	**0**	-
	6:30	-278	**59**	13	82	**17**	57	**1**	8
	7:30	-271	**88**	26	89	**5**	94	**0**	13
	8:30	-	-	-	-	-	132	-	19
	9:30	-	-	-	-	-	173	-	23
	10:30	-	-	-	-	-	202	-	27
	11:30	-	-	-	-	-	216	-	28
	12:30	-	-	-	-	-	213	-	28
	13:30	-	-	-	-	-	199	-	27
	14:30	-	-	-	-	-	175	-	23
	15:30	-	-	-	-	-	136	-	19
	16:30	-89	**88**	-26	89	**7**	102	**0**	13
	17:30	-82	**59**	-13	82	**50**	96	**3**	10
	18:32	-74	**0**	0	74	**0**	-	**0**	-
						118	1838	**9**	243

sf4 East — αsf (°) 270.00, Σ (°) 90.00, A_{sf} (m²) 1.00, A_{win} (m²) 1.00, ρ 0.20, SHGC 0.25

Date	Time	γ (°)	Ωpf (°)	Ωel (°)	θ (°)	I_{tb} (Wh)	I_T (Wh)	Q_b (Wh)	Q_T (Wh)
Jun 15	5:01	-387	**0**	0	27	**0**	-	**0**	-
	5:30	-384	**6**	-13	24	**9**	26	**2**	5
	6:30	-377	**18**	-47	24	**113**	170	**27**	37
	7:30	-371	**31**	-72	32	**180**	279	**43**	58
	8:30	-365	**43**	-85	43	**267**	412	**61**	82
	9:30	-357	**56**	88	56	**258**	442	**52**	78
	10:30	-346	**69**	85	69	**186**	399	**27**	56
	11:30	-316	**83**	83	83	**70**	300	**4**	35
	12:30	-	-	-	-	-	232	-	31
	13:30	-	-	-	-	-	214	-	29
	14:30	-	-	-	-	-	190	-	26
	15:30	-	-	-	-	-	153	-	21
	16:30	-	-	-	-	-	111	-	16
	17:30	-	-	-	-	-	65	-	10
	18:30	-	-	-	-	-	19	-	3
	18:58	-	-	-	-	-	-	-	-
						1082	3013	**215**	488
Jul 16	5:07	-385	**0**	0	25	**0**	-	**0**	-
	5:30	-382	**5**	-12	23	**6**	18	**1**	4
	6:30	-375	**17**	-49	23	**146**	197	**35**	44
	7:30	-369	**30**	-75	31	**237**	331	**56**	71
	8:30	-362	**42**	-88	42	**311**	449	**71**	91
	9:30	-354	**55**	86	55	**298**	475	**60**	84
	10:30	-341	**69**	83	69	**211**	417	**31**	58
	11:30	-309	**83**	81	83	**72**	289	**4**	32
	12:30	-	-	-	-	-	219	-	29
	13:30	-	-	-	-	-	207	-	27
	14:30	-	-	-	-	-	178	-	24
	15:30	-	-	-	-	-	148	-	20
	16:30	-	-	-	-	-	104	-	14
	17:30	-	-	-	-	-	60	-	8
	18:30	-	-	-	-	-	15	-	2
	18:52	-	-	-	-	-	-	-	-
						1281	3108	**259**	508
Aug 16	5:27	-376	**0**	0	16	**0**	-	**0**	-
	6:30	-368	**13**	-59	15	**117**	157	**29**	35
	7:30	-361	**26**	-88	26	**334**	424	**80**	93
	8:30	-353	**39**	81	40	**338**	470	**78**	97
	9:30	-342	**53**	76	54	**320**	493	**66**	90
	10:30	-326	**67**	74	68	**221**	423	**33**	60
	11:30	-294	**82**	73	83	**77**	294	**4**	33
	12:30	-	-	-	-	-	213	-	28
	13:30	-	-	-	-	-	199	-	27
	14:30	-	-	-	-	-	175	-	23
	15:30	-	-	-	-	-	136	-	19
	16:30	-	-	-	-	-	95	-	13
	17:30	-	-	-	-	-	46	-	7
	18:32	-	-	-	-	-	-	-	-
						1407	3128	**291**	525

sf5 Roof — αsf (°) 0.00, Σ (°) 0.00, A_{sf} (m²) 1.00, A_{win} (m²) 1.00, ρ 0.20, SHGC 0.25

Date	Time	γ (°)	Ωpf (°)	Ωel (°)	θ (°)	I_{tb} (Wh)	I_T (Wh)	Q_b (Wh)	Q_T (Wh)
Jun 15	5:01	-117	**0**	0	90	**0**	-	**0**	-
	5:30	-114	**-13**	-6	84	**1**	29	**0**	6
	6:30	-107	**-47**	-18	72	**38**	126	**5**	24
	7:30	-101	**-72**	-31	60	**107**	254	**20**	52
	8:30	-95	**-85**	-43	47	**250**	450	**55**	98
	9:30	-87	**88**	-56	34	**383**	626	**90**	142
	10:30	-76	**85**	-69	21	**493**	766	**119**	178
	11:30	-46	**83**	-83	10	**573**	862	**142**	204
	12:30	46	**83**	83	10	**588**	876	**145**	207
	13:30	76	**85**	69	21	**504**	778	**122**	181
	14:30	87	**88**	56	34	**445**	688	**105**	157
	15:30	95	**-85**	43	47	**328**	528	**73**	116
	16:30	101	**-72**	31	60	**221**	369	**42**	73
	17:30	107	**-47**	18	72	**121**	210	**15**	34
	18:30	114	**-13**	6	84	**21**	50	**1**	7
	18:58	117	**0**	0	90	**0**	-	**0**	-
						4073	6612	**934**	1480
Jul 16	5:07	-115	**0**	0	90	**0**	-	**0**	-
	5:30	-112	**-12**	-5	85	**0**	22	**0**	5
	6:30	-105	**-49**	-17	73	**46**	124	**6**	22
	7:30	-99	**-75**	-30	61	**136**	269	**25**	54
	8:30	-92	**-88**	-42	48	**283**	466	**63**	102
	9:30	-84	**86**	-55	35	**432**	655	**101**	149
	10:30	-71	**83**	-69	22	**549**	800	**132**	186
	11:30	-39	**81**	-83	11	**578**	844	**142**	200
	12:30	39	**81**	83	11	**590**	856	**145**	203
	13:30	71	**83**	69	22	**562**	813	**135**	190
	14:30	84	**86**	55	35	**443**	666	**104**	152
	15:30	92	**-88**	42	48	**378**	561	**84**	123
	16:30	99	**-75**	30	61	**243**	377	**45**	74
	17:30	105	**-49**	17	73	**125**	203	**15**	32
	18:30	112	**-12**	5	85	**20**	42	**1**	5
	18:52	115	**0**	0	90	**0**	-	**0**	-
						4384	6699	**999**	1496
Aug 16	5:27	-106	**0**	0	90	**0**	-	**0**	-
	6:30	-98	**-59**	-13	77	**27**	91	**3**	16
	7:30	-91	**-88**	-26	64	**163**	285	**28**	54
	8:30	-83	**81**	-39	51	**275**	450	**59**	97
	9:30	-72	**76**	-53	38	**423**	641	**98**	145
	10:30	-56	**74**	-67	27	**531**	780	**127**	180
	11:30	-24	**73**	-82	18	**579**	843	**141**	198
	12:30	24	**73**	82	18	**547**	811	**133**	190
	13:30	56	**74**	67	27	**500**	748	**120**	173
	14:30	72	**76**	53	38	**444**	662	**103**	150
	15:30	83	**81**	39	51	**311**	485	**66**	104
	16:30	91	**-88**	26	64	**223**	345	**38**	64
	17:30	98	**-59**	13	77	**82**	145	**8**	22
	18:32	106	**0**	0	90	**0**	-	**0**	-
						4108	6291	**924**	1393

Sep	15	5:54	-93	0	-	-	-	-	-	-	-	-
		6:30	-88	8	-88	**76**	-8	88	**1**	25	**0**	4
		7:30	-80	20	-80	**65**	-21	81	**30**	98	**2**	13
		8:30	-71	33	-71	**63**	-34	74	**86**	199	**10**	27
		9:30	-59	45	-59	**62**	-49	68	**160**	315	**24**	46
		10:30	-41	55	-41	**62**	-65	64	**206**	390	**35**	61
		11:30	-16	61	-16	**62**	-82	62	**258**	461	**46**	74
		12:30	16	61	16	**62**	82	62	**250**	452	**45**	72
		13:30	41	55	41	**62**	65	64	**238**	427	**40**	66
		14:30	59	45	59	**62**	49	68	**182**	342	**27**	49
		15:30	71	33	71	**63**	34	74	**135**	258	**16**	33
		16:30	80	20	80	**65**	21	81	**65**	142	**5**	16
		17:30	88	8	88	**76**	8	88	**8**	35	**0**	4
		18:05	93	0	-	-	-	-	-	-	-	-
									1619	3142	**249**	466
Oct	16	6:23	-78	0	-78	**0**	0	78	**0**	-	**0**	-
		6:30	-78	1	-78	**6**	-1	78	**2**	6	**0**	1
		7:30	-70	14	-70	**35**	-15	70	**71**	114	**10**	17
		8:30	-60	25	-60	**44**	-29	63	**161**	246	**28**	41
		9:30	-48	36	-48	**47**	-44	57	**245**	367	**49**	66
		10:30	-32	44	-32	**49**	-62	53	**276**	421	**58**	78
		11:30	-11	49	-11	**50**	-80	50	**318**	478	**69**	91
		12:30	11	49	11	**50**	80	50	**362**	527	**78**	100
		13:30	32	44	32	**49**	62	53	**381**	538	**80**	101
		14:30	48	36	48	**47**	44	57	**333**	464	**66**	83
		15:30	60	25	60	**44**	29	63	**263**	358	**46**	59
		16:30	70	14	70	**35**	15	70	**158**	208	**22**	29
		17:30	78	1	78	**6**	1	78	**40**	45	**4**	4
		17:36	78	0	78	**0**	0	78	**0**	-	**0**	-
									2610	3772	**510**	669
Nov	15	6:46	-68	0	-68	**0**	0	68	**0**	-	**0**	-
		7:30	-62	8	-62	**17**	-10	62	**66**	96	**12**	17
		8:30	-53	19	-53	**30**	-24	55	**165**	237	**34**	45
		9:30	-41	29	-41	**36**	-40	49	**257**	365	**56**	72
		10:30	-27	36	-27	**39**	-58	44	**307**	442	**70**	89
		11:30	-9	40	-9	**40**	-79	41	**364**	516	**84**	105
		12:30	9	40	9	**40**	79	41	**379**	531	**87**	109
		13:30	27	36	27	**39**	58	44	**362**	502	**82**	102
		14:30	41	29	41	**36**	40	49	**321**	434	**70**	86
		15:30	53	19	53	**30**	24	55	**236**	311	**48**	59
		16:30	62	8	62	**17**	10	62	**139**	171	**25**	30
		17:13	68	0	68	**0**	0	68	**0**	-	**0**	-
									2596	3604	**568**	714
Dec	16	6:58	-63	0	-63	**0**	0	63	**0**	-	**0**	-
		7:30	-58	6	-58	**11**	-7	59	**36**	56	**7**	10
		8:30	-49	16	-49	**24**	-21	51	**155**	214	**33**	42
		9:30	-38	25	-38	**31**	-37	45	**262**	357	**59**	73
		10:30	-25	32	-25	**35**	-57	40	**315**	435	**73**	90
		11:30	-9	36	-9	**36**	-78	37	**346**	480	**81**	100
		12:30	9	36	9	**36**	78	37	**365**	499	**85**	104
		13:30	25	32	25	**35**	57	40	**354**	476	**82**	99
		14:30	38	25	38	**31**	37	45	**315**	413	**71**	85
		15:30	49	16	49	**24**	21	51	**244**	307	**52**	61
		16:30	58	6	58	**11**	7	59	**143**	165	**28**	31
		17:01	63	0	63	**0**	0	63	**0**	-	**0**	-
									2535	3402	**570**	698

Sep	15	5:54	-	-	-	-	-	-	-	-
		6:30	-	-	-	-	-	24	-	4
		7:30	-	-	-	-	-	68	-	11
		8:30	-	-	-	-	-	113	-	17
		9:30	-	-	-	-	-	155	-	22
		10:30	-	-	-	-	-	183	-	26
		11:30	-	-	-	-	-	203	-	28
		12:30	-74	**82**	-62	83	**70**	272	**4**	32
		13:30	-49	**65**	-62	68	**210**	400	**32**	58
		14:30	-31	**49**	-62	53	**302**	462	**64**	86
		15:30	-19	**34**	-63	38	**390**	513	**91**	108
		16:30	-10	**21**	-65	23	**379**	455	**91**	102
		17:30	-2	**8**	-76	8	**252**	278	**62**	67
		18:05	3	**0**	0	3	**0**	-	**0**	-
							1603	3126	**344**	561
Oct	16	6:23	-	-	-	-	-	-	-	-
		6:30	-	-	-	-	-	4	-	1
		7:30	-	-	-	-	-	44	-	7
		8:30	-	-	-	-	-	85	-	13
		9:30	-	-	-	-	-	122	-	17
		10:30	-	-	-	-	-	145	-	20
		11:30	-	-	-	-	-	160	-	22
		12:30	-79	**80**	-50	83	**73**	238	**4**	26
		13:30	-58	**62**	-49	68	**236**	393	**36**	56
		14:30	-42	**44**	-47	53	**367**	498	**77**	94
		15:30	-30	**29**	-44	39	**456**	550	**106**	118
		16:30	-20	**15**	-35	25	**424**	474	**102**	109
		17:30	-12	**1**	-6	12	**184**	188	**45**	46
		17:36	-12	**0**	0	12	**0**	-	**0**	-
							1739	2901	**369**	528
Nov	15	6:46	-	-	-	-	-	-	-	-
		7:30	-	-	-	-	-	30	-	5
		8:30	-	-	-	-	-	71	-	11
		9:30	-	-	-	-	-	109	-	16
		10:30	-	-	-	-	-	135	-	20
		11:30	-	-	-	-	-	151	-	22
		12:30	-81	**79**	-40	83	**62**	214	**3**	25
		13:30	-63	**58**	-39	69	**181**	321	**27**	46
		14:30	-49	**40**	-36	55	**279**	392	**57**	73
		15:30	-37	**24**	-30	41	**308**	384	**71**	82
		16:30	-28	**10**	-17	29	**261**	293	**62**	67
		17:13	-22	**0**	0	22	**0**	-	**0**	-
							1091	2099	**220**	366
Dec	16	6:58	-	-	-	-	-	-	-	-
		7:30	-	-	-	-	-	20	-	3
		8:30	-	-	-	-	-	59	-	9
		9:30	-	-	-	-	-	95	-	14
		10:30	-	-	-	-	-	120	-	18
		11:30	-	-	-	-	-	133	-	19
		12:30	-81	**78**	-36	83	**55**	189	**3**	22
		13:30	-65	**57**	-35	69	**161**	284	**23**	41
		14:30	-52	**37**	-31	56	**248**	346	**50**	64
		15:30	-41	**21**	-24	43	**285**	348	**65**	74
		16:30	-32	**7**	-11	32	**233**	255	**55**	59
		17:01	-27	**0**	0	27	**0**	-	**0**	-
							982	1849	**196**	323

Sep	15	5:54	-273	**0**	0	87	**0**	-	**0**	-
		6:30	-	-	-	-	-	24	-	4
		7:30	-	-	-	-	-	68	-	11
		8:30	-	-	-	-	-	113	-	17
		9:30	-	-	-	-	-	155	-	22
		10:30	-	-	-	-	-	183	-	26
		11:30	-	-	-	-	-	203	-	28
		12:30	-	-	-	-	-	202	-	28
		13:30	-	-	-	-	-	189	-	26
		14:30	-	-	-	-	-	159	-	22
		15:30	-	-	-	-	-	123	-	17
		16:30	-	-	-	-	-	76	-	11
		17:30	-	-	-	-	-	27	-	4
		18:05	-87	**0**	0	87	**0**	-	**0**	-
							0	1524	**0**	217
Oct	16	6:23	-	-	-	-	-	-	-	-
		6:30	-	-	-	-	-	4	-	1
		7:30	-	-	-	-	-	44	-	7
		8:30	-	-	-	-	-	85	-	13
		9:30	-	-	-	-	-	122	-	17
		10:30	-	-	-	-	-	145	-	20
		11:30	-	-	-	-	-	160	-	22
		12:30	-	-	-	-	-	165	-	22
		13:30	-	-	-	-	-	157	-	20
		14:30	-	-	-	-	-	131	-	17
		15:30	-	-	-	-	-	95	-	13
		16:30	-	-	-	-	-	50	-	7
		17:30	-	-	-	-	-	4	-	1
		17:36	-	-	-	-	-	-	-	-
							0	1162	**0**	159
Nov	15	6:46	-	-	-	-	-	-	-	-
		7:30	-	-	-	-	-	30	-	5
		8:30	-	-	-	-	-	71	-	11
		9:30	-	-	-	-	-	109	-	16
		10:30	-	-	-	-	-	135	-	20
		11:30	-	-	-	-	-	151	-	22
		12:30	-	-	-	-	-	152	-	22
		13:30	-	-	-	-	-	139	-	20
		14:30	-	-	-	-	-	113	-	16
		15:30	-	-	-	-	-	76	-	11
		16:30	-	-	-	-	-	32	-	5
		17:13	-	-	-	-	-	-	-	-
							0	1008	**0**	147
Dec	16	6:58	-	-	-	-	-	-	-	-
		7:30	-	-	-	-	-	20	-	3
		8:30	-	-	-	-	-	59	-	9
		9:30	-	-	-	-	-	95	-	14
		10:30	-	-	-	-	-	120	-	18
		11:30	-	-	-	-	-	133	-	19
		12:30	-	-	-	-	-	135	-	19
		13:30	-	-	-	-	-	123	-	18
		14:30	-	-	-	-	-	98	-	14
		15:30	-	-	-	-	-	63	-	9
		16:30	-	-	-	-	-	22	-	3
		17:01	-	-	-	-	-	-	-	-
							0	867	**0**	128

Sep	15	5:54	-363	**0**	0	3	**0**	-	**0**	-
		6:30	-358	**8**	76	8	**37**	61	**9**	13
		7:30	-350	**21**	65	23	**173**	241	**42**	53
		8:30	-341	**34**	63	38	**248**	362	**58**	75
		9:30	-329	**49**	62	53	**265**	420	**56**	78
		10:30	-311	**65**	62	68	**182**	366	**28**	54
		11:30	-286	**82**	62	83	**72**	275	**4**	32
		12:30	-	-	-	-	-	202	-	28
		13:30	-	-	-	-	-	189	-	26
		14:30	-	-	-	-	-	159	-	22
		15:30	-	-	-	-	-	123	-	17
		16:30	-	-	-	-	-	76	-	11
		17:30	-	-	-	-	-	27	-	4
		18:05	-	-	-	-	-	-	-	-
							977	2501	**197**	413
Oct	16	6:23	-348	**0**	0	12	**0**	-	**0**	-
		6:30	-348	**1**	6	12	**9**	13	**2**	3
		7:30	-340	**15**	35	25	**189**	233	**45**	52
		8:30	-330	**29**	44	39	**278**	363	**65**	77
		9:30	-318	**44**	47	53	**270**	392	**57**	74
		10:30	-302	**62**	49	68	**171**	316	**26**	46
		11:30	-281	**80**	50	83	**64**	224	**4**	26
		12:30	-	-	-	-	-	165	-	22
		13:30	-	-	-	-	-	157	-	20
		14:30	-	-	-	-	-	131	-	17
		15:30	-	-	-	-	-	95	-	13
		16:30	-	-	-	-	-	50	-	7
		17:30	-	-	-	-	-	4	-	1
		17:36	-	-	-	-	-	-	-	-
							981	2143	**198**	357
Nov	15	6:46	-338	**0**	0	22	**0**	-	**0**	-
		7:30	-332	**10**	17	29	**124**	153	**29**	34
		8:30	-323	**24**	30	41	**216**	287	**49**	61
		9:30	-311	**40**	36	55	**223**	332	**46**	62
		10:30	-297	**58**	39	69	**153**	288	**23**	42
		11:30	-279	**79**	40	83	**59**	211	**3**	25
		12:30	-	-	-	-	-	152	-	22
		13:30	-	-	-	-	-	139	-	20
		14:30	-	-	-	-	-	113	-	16
		15:30	-	-	-	-	-	76	-	11
		16:30	-	-	-	-	-	32	-	5
		17:13	-	-	-	-	-	-	-	-
							776	1784	**150**	297
Dec	16	6:58	-333	**0**	0	27	**0**	-	**0**	-
		7:30	-328	**7**	11	32	**59**	79	**14**	17
		8:30	-319	**21**	24	43	**181**	240	**41**	50
		9:30	-308	**37**	31	56	**206**	301	**41**	56
		10:30	-295	**57**	35	69	**144**	264	**21**	38
		11:30	-279	**78**	36	83	**52**	185	**3**	22
		12:30	-	-	-	-	-	135	-	19
		13:30	-	-	-	-	-	123	-	18
		14:30	-	-	-	-	-	98	-	14
		15:30	-	-	-	-	-	63	-	9
		16:30	-	-	-	-	-	22	-	3
		17:01	-	-	-	-	-	-	-	-
							642	1508	**120**	247

Sep	15	5:54	-93	**0**	0	90	**0**	-	**0**	-
		6:30	-88	**76**	-8	82	**5**	44	**0**	9
		7:30	-80	**65**	-21	70	**65**	168	**9**	31
		8:30	-71	**63**	-34	57	**170**	331	**34**	68
		9:30	-59	**62**	-49	45	**307**	514	**69**	114
		10:30	-41	**62**	-65	35	**390**	630	**91**	143
		11:30	-16	**62**	-82	29	**484**	742	**115**	171
		12:30	16	**62**	82	29	**469**	727	**112**	167
		13:30	41	**62**	65	35	**449**	690	**105**	157
		14:30	59	**62**	49	45	**350**	557	**79**	123
		15:30	71	**63**	34	57	**268**	429	**53**	88
		16:30	80	**65**	21	70	**143**	246	**20**	43
		17:30	88	**76**	8	82	**34**	73	**2**	10
		18:05	93	**0**	0	90	**0**	-	**0**	-
							3134	5151	**690**	1123
Oct	16	6:23	-78	**0**	0	90	**0**	-	**0**	-
		6:30	-78	**6**	-1	89	**0**	7	**0**	1
		7:30	-70	**35**	-15	76	**50**	114	**5**	19
		8:30	-60	**44**	-29	65	**153**	270	**26**	51
		9:30	-48	**47**	-44	54	**265**	424	**55**	89
		10:30	-32	**49**	-62	46	**316**	505	**71**	111
		11:30	-11	**50**	-80	41	**374**	579	**86**	130
		12:30	11	**50**	80	41	**426**	631	**98**	142
		13:30	32	**49**	62	46	**437**	626	**98**	139
		14:30	48	**47**	44	54	**359**	518	**74**	109
		15:30	60	**44**	29	65	**251**	367	**42**	67
		16:30	70	**35**	15	76	**111**	175	**11**	25
		17:30	78	**6**	1	89	**4**	11	**0**	1
		17:36	78	**0**	0	90	**0**	-	**0**	-
							2747	4226	**566**	884
Nov	15	6:46	-68	**0**	0	90	**0**	-	**0**	-
		7:30	-62	**17**	-10	82	**21**	67	**1**	11
		8:30	-53	**30**	-24	71	**95**	198	**13**	35
		9:30	-41	**36**	-40	61	**187**	337	**34**	66
		10:30	-27	**39**	-58	54	**249**	433	**52**	91
		11:30	-9	**40**	-79	50	**310**	510	**67**	110
		12:30	9	**40**	79	50	**322**	523	**70**	113
		13:30	27	**39**	58	54	**295**	478	**61**	100
		14:30	41	**36**	40	61	**234**	384	**43**	75
		15:30	53	**30**	24	71	**136**	239	**19**	41
		16:30	62	**17**	10	82	**44**	90	**3**	13
		17:13	68	**0**	0	90	**0**	-	**0**	-
							1893	3258	**362**	656
Dec	16	6:58	-63	**0**	0	90	**0**	-	**0**	-
		7:30	-58	**11**	-7	84	**7**	39	**0**	7
		8:30	-49	**24**	-21	74	**70**	157	**8**	27
		9:30	-38	**31**	-37	65	**158**	290	**27**	55
		10:30	-25	**35**	-57	58	**218**	381	**42**	78
		11:30	-9	**36**	-78	54	**253**	433	**52**	91
		12:30	9	**36**	78	54	**266**	446	**55**	94
		13:30	25	**35**	57	58	**244**	408	**48**	83
		14:30	38	**31**	37	65	**190**	322	**32**	60
		15:30	49	**24**	21	74	**110**	197	**13**	32
		16:30	58	**11**	7	84	**28**	60	**1**	8
		17:01	63	**0**	0	90	**0**	-	**0**	-
							1546	2733	**279**	534

Highlighting Settings

10	Full highlight solar altitude above (°)
5	Ignore solar altitude below (°)
65	Full highlight angle of incidence below (°)
85	Ignore angle of incidence above (°)

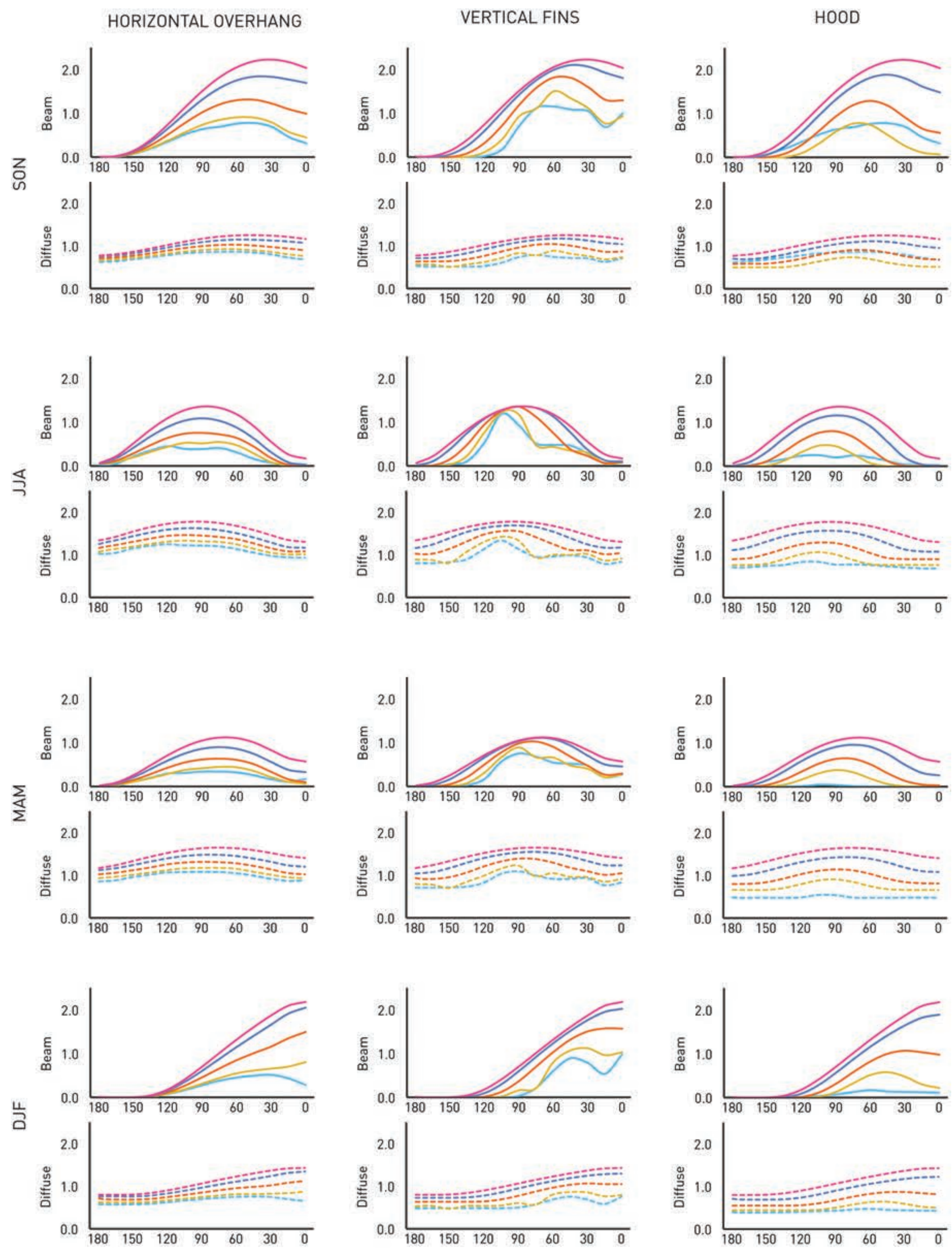

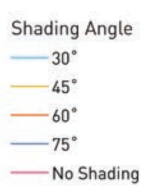

Figure 8.19

Effect of Shading Angle on Insolation Received by Fenestration at Various Orientations

These graphs show the average daily total insolation received on a 1m^2 window with different shading configurations in Kuwait City, Kuwait, at 29° N latitude. The shading surfaces are offset from the window by 0.2m. Each line represents a different shading angle (*VSA* or *HSA*), as indicated in the legend. Results are grouped by season. The horizontal overhang and vertical fins are modeled as if they are effectively infinitely long to prevent end-around exposure.

The vertical scale in the graphs is in kWh and the horizontal scale in degrees of azimuth. The graphs with the solid lines are for direct beam and the dotted lines for diffuse radiation.

Dason Whitsett

significant and the angle of incidence low for multiple surfaces are highlighted, along with important angles for shading design.

Three-dimensional CAD programs are valuable tools for shading design, but suffer from a lack of obvious methods to generate a solution to meet a rational set of criteria. Armed with a thorough understanding of solar geometry and shading design principles, however, the ability to design in 3D and cast shadows automatically can greatly speed the process. Be sure to set the latitude and north offset of the model properly and adjust for the difference between *LST* and *AST*.

IMPACT OF SHADING ON INSOLATION OF WINDOWS

Figure 8.19 shows the impact of three common shading strategies on windows of varying orientation. Kuwait City, Kuwait, at 29° N latitude was chosen for the location of this study due to its clear climate and location near the world's most populous parallel. Although insolation values differ based on cloudiness, the trends are similar for other locations at a similar latitude unless there are significant asymmetries in cloud cover during the day. The shading angle is modified in each scenario to compare the effect of shading device size. The lowest shading angle, 30°, would necessarily result in a very large shading device except on small windows. Observations on the results follow.

- Direct beam insolation is negligible on due-south-facing surfaces regardless of shading strategy in summer, but increases quickly as the surface is rotated westward.
- For south-facing surfaces in the fall, insolation is very high without shading, but drops by over 50% with a horizontal overhang at a *VSA* of 60° (roughly equal to the zenith angle at solar noon on the equinox). Vertical fins provide less shading, but a hood at the same depth provides an approximate 75% reduction in solar exposure.
- In winter, all of the shading strategies have a significant impact on insolation. The intent of this study was to evaluate shading performance, so exposure criteria were ignored. Using the techniques described previously, it would be possible to achieve the same shading performance for most of the shading angles while maintaining full exposure in winter, but the shading geometry would increase in size significantly.
- Southwest-facing surfaces benefit similarly from overhangs and fins in summer and fall, but a hood substantially out-performs either one alone.
- West-facing surfaces receive very little benefit from fins in summer while an overhang or hood can provide significant reductions in insolation. In fall, the differences are much less pronounced.
- Vertical fins are useless for surfaces with a west-northwest azimuth—essentially looking straight at the sunset—while a deep horizontal overhang can provide a large benefit.
- Diffuse insolation, the source of effective daylight, should be considered when evaluating a shading strategy because increasing the depth of a shading control decreases the sky view from that surface. Very deep shading controls can reduce diffuse insolation by well over 50%.

SHADING STRATEGIES BY LATITUDE

Latitude has a major impact on the effectiveness of shading strategies due to differences in tilt of the solar path band relative to building surfaces, as shown in Figure 3.4. See Figures 5.3a and b to reference clear-sky radiation levels on surfaces at the cardinal orientations at various latitudes.

Lower Tropics

Near the equator, north- and south-facing surfaces will be exposed to direct sun for significant periods on respective solstices. At the equator, the angle of incidence stays constant on north- and south-facing surfaces all day. For these surfaces, hood shading geometries are ideal.

East- and west-facing surfaces will experience long periods of exposure with low surface-solar azimuth throughout the year. These surfaces are difficult to shade without obstructing views and daylight. If fenestration cannot be relocated to another surface, detached shades, louvers, or other elements such as trees will be most effective.

Upper Tropics

Equator-facing surfaces will have similar characteristics as at the equator, but lower profile angles and more change in the angle of incidence during the day than at the equator. Horizontal overhangs or hoods can provide shading well beyond the equinox if sufficiently deep.

East- and west-facing surfaces experience conditions similar to those in the lower tropics.

Pole-facing surfaces at one of the tropics will receive direct sun all day on the summer solstice, but at a higher angle of incidence than at the equator. The surface-solar azimuth is high at times when the angle of incidence is low enough to be of concern. Vertical fins can be effective on these surfaces.

Lower Temperate Latitudes

Equator-facing surfaces receive the highest solar gain in winter and lowest in summer. Geometry is ideally suited for horizontal overhangs or hoods that choreograph shading and exposure periods.

Pole-facing surfaces do not generally receive enough direct radiation at a low enough angle of incidence to warrant shading. Minor azimuth rotations can make a significant difference, however.

East- and west-facing surfaces are nearly as difficult to shade as in the tropics.

Upper Temperate Latitudes

Equator-facing surfaces experience peak insolation in spring and fall with less irradiation in winter and summer. The tilt of the solar path band toward the horizon results in low angles of incidence and lower profile angles, creating challenging shading conditions, especially in spring and fall. The need for shading of skin-load dominated buildings varies greatly with climate in this latitude range and the shading period is generally shorter. The net effect may result in shading controls similar in size to those at lower latitudes, but allowing exposure earlier in the year due to the low profile angle.

East- and west-facing surfaces see a very high peak of insolation in summer. With the solar path band tilted toward the horizon, the surface-solar azimuth will be high enough at times that vertical fins can be effective, with hoods improving on that performance. Horizontal overhangs alone are limited in their effectiveness unless very deep. Operable louvers are a versatile option to compensate for the high shading angles otherwise necessary.

Pole-facing surfaces will receive enough insolation in summer to warrant solar controls if the shading criteria call for it. Vertical fins are a good solution in this location, as the surface-solar azimuth will be high most of the time.

OTHER CONSIDERATIONS FOR SHADING DEVICE DESIGN

The design of shading touches on many other architectural issues, some of the most important of which are discussed briefly here.

Reduction of Air Flow: Most of the time, the purpose of a shading device is to minimize heat gain and promote comfort in hot weather. If it traps a layer of warm air next to the building, this will tend to increase heat gains and slow heat loss on the nighttime side of the cycle.

Thermal Bridging: As an exterior element of the building structure, shading devices are usually connected to the structure and protrude out of the envelope. As such, thermal bridging is an important heat-loss pathway to consider and minimize.

Thermal Mass: Shading devices should be low-mass whenever possible. Massive materials such as concrete will absorb solar heat during the day and slowly release it at night, raising the surrounding air temperature.

Reflectance: Reflectance should be controlled. In the case of light shelves, reflectance is desirable so that maximum natural light makes it into the space. In other cases, it is preferable that shading devices not reflect excessive amounts of radiation.

Detailing: Along with the protrusion through the envelope of the shading control structure comes the challenge of avoiding water penetration past the drainage plane. Shading elements may also unintentionally provide habitat for birds and other creatures.

Daylight: The fundamental purpose of windows is to provide views and light. Daylight is a very important consideration in shading design. Diffuse daylight levels are driven by the sky view factor, which is reduced when a shading control is put above a window and reduced severely when that overhang is immediately above the window. This is an important and often overlooked consideration.

Views: If the shading controls are within the field of view of the occupants from inside, this has a substantial impact on their experience of a view. If screens or detached planar elements are used, the impact on view will be significant.

Perception from Inside: Shading should not give the feeling of encroaching in the occupant's field of vision or creating a cage-like sensibility.

NOTES

1 Philip Babcock Gove, *Webster's Third New International Dictionary of the English Language Unabridged* (Springfield, MA: Merriam-Webster, 2002).
2 Michael Baxandall, *Shadows and Enlightenment* (New Haven: Yale University Press, 1995).
3 Ibid.
4 Christian Norberg-Schulz, *Genius Loci: Towards a Phenomenology of Architecture* (New York: Rizzoli, 1980).
5 "2003 CBECS Detailed Tables," *U.S. Energy Information Administration*, September 2008, www.eia.gov/consumption/commercial/data/archive/cbecs/cbecs2003/detailed_tables_2003/detailed_tables_2003.html#buildingchar03.
6 "Residential Energy Consumption Survey Data (RECS)-2009 RECS Survey Data," *U.S. Energy Information Administration*, accessed November 10, 2015, www.eia.gov/consumption/residential/data/2009/index.cfm?view=consumption#end-use.
7 Anselm Eisentraut and Adam Brown, *Heating without Global Warming: Market Developments and Policy Considerations for Renewable Heat* (Paris, France: International Energy Agency, 2014).
8 Michael Utzinger and James H. Wasley, "Building Balance Point," in *Vital Signs Curriculum Materials Project* (Johnson Controls Institute for Environmental Quality in Architecture, School of Architecture and Urban Planning, University of Wisconsin, Milwaukee, August 1997).

9 *Climate Consultant*, version 6.0 (University of California Los Angeles; The Regents of the University of California, 2015).
10 Francisco Arumí-Noé, "Algorithm for the Geometric Construction of an Optimum Shading Device," *Automation in Construction* 5 (1996): 211–217.
11 Aladar Olgyay, *Solar Control & Shading Devices* (Princeton: Princeton University Press, 1957), 88–92.
12 D. Michael Utzinger and Sanford A. Klein, "A Method of Estimating Monthly Average Solar Radiation on Shaded Receivers," *Solar Energy* 23, no. 5 (1979): 375, doi:10.1016/0038-092X(79)90145-2.

9 FENESTRATION AND THE SUN

Historically, fenestration was simply a means of creating a thermal barrier within punched openings of a building's load-bearing enclosure. The building envelope has become increasingly detached from the building structure and floor plates, such that fenestration can be conceived of as an autonomous building system, which, among other things, manages solar gain. With vastly more freedom for facade and fenestration design, criteria for facade design are important to establish. Facade glazing can thus be considered both a concept and a tectonic assembly, as it influences both the performance and experience of a building. Fenestration plays a very significant role fundamental to the experience and function of buildings. Windows literally and figuratively connect the building occupant to their external environment.

Lisa Heschong, in her canonical book titled *Thermal Delight in Architecture*, establishes that the thermal qualities of a building significantly affect the individual's experience of the space. Thermal qualities are of course often directly related to management of light as a form of energy.[1] They not only influence what an individual does there but also how the individual feels about the space, and ultimately the success of the space as a designed element. She argues that the thermal function holds as much importance as the programmatic function. Due to the connection of light to heat and thermal factors, this is extended to an emphasis on the rigorous use of light quality as a design element. The quality of light, in its different varieties from direct to diffuse and beyond, must be coupled with thermal considerations in the design process. Heschong aptly points out that thermal systems are typically standardized in contemporary buildings, effectively removing that variable from the design equation.[2] When mechanical systems function independently and are detached from the overall design concept, an opportunity is missed.

Heschong points out the relatively small range of temperature within which all life on Earth exists, as well as its sensitivity to subtle changes in temperature. Animals have specific strategies to deal with these changes, as did indigenous cultures, which not only did not have climate control but also did not use formal standards or abstract ideals such as Classical proportioning systems. According to Heschong:

> The Anasazi Indians of the southwestern United States were remarkably clever in choosing the sites for their cliff dwellings. They invariably chose locations shaded in the summer by an overhanging ledge of the cliff, but exposed to full sun all winter long. With their backs to the cliff, the dwellings were protected from the winter winds and took advantage of the thermal mass of the earth to moderate the temperature flux.[3]

This may be contrasted with self-referential tendencies or prescriptions to abstract ideals seen in contemporary architecture. Artificial climate control by way of heating and cooling systems has enabled the possibility for buildings to ignore their immediate microclimate and override its conditions. This can be achieved through the use of energy, which also has its limitations and costs. Heschong is not suggesting a revival of Regionalism, but rather that its merits be understood. Perhaps the most prudent approach is a blend of regionalist strategies while incorporating technological advancements, such as solar panels to harvest energy from the sun or glazing technology with calibrated insulation and emissivity control.

Fenestration design should acknowledge the need for a variety of thermal and lighting conditions within the same building or space with a program that allows for building occupants to move throughout the day and find their own comfort. By consciously noticing this range, end users can more readily appreciate the space and develop awareness of their own senses and how each of these senses provides a different amount of collective information about our surrounding environment. Heschong's revered text can be read as a call for integration in a design, or at least a design agenda that considers systems beyond pragmatic and quantifiable values. Rather than simply containing mechanical systems, building structures can be designed as instruments to manage light and thermal energy, and this starts with fenestration, or the building envelope. Regarding terminology, a building envelope can be considered its own collective system, rather than independent facades and a roof.

Building envelopes, in fundamental terms, are composed of a combination of opaque, transparent, and translucent materials. Each of these material properties directly affects light transmission. Transparency is by definition the property of allowing the direct passage of light and view through a surface, and it has played a dominant role in contemporary architecture. The most common transparent material used in buildings is glass, or glazing. Glazing properties have radically changed over the years, both in terms of strength and energy efficiency, but the primary function is the same. The compositional balance of solids and voids is an integral part of formal architectural design, where void is often considered "transparent" by default in the view of the architect. However, transparency is not quite as simple and reductive as its definition because it is dependent on which side of the transparent surface has the higher illuminance level, in addition to other characteristics, including reflections, condensation, or residual layers of dirt and other particulates.[4] Mies van der Rohe saw glass as the closest approximation to nothingness—he wanted it to disappear completely. This can be contrasted with the approach of glass artists such as James Carpenter or even any application of double or triple-glazed windows, which necessarily generate more reflections, exposing their make-up. In the work of Mies and other Modern architects, glass is often used not only to allow exterior views, but to blur the line between inside and outside, while also providing for more direct flows of natural light into interior architectural spaces. This concept was taken to its logical extreme in his Farnsworth House design, which was not functionally successful in the view of the client, with its relentless openness.[5] Hand in hand with this was the advent of structural steel, which spearheaded the five tenets of Modern architecture and enabled the premise of glass and steel frames, rather than load-bearing walls with punched openings. Steel and glass systems are the predominant type of fenestration for commercial buildings.

Translucency is the property of allowing light to flow through a material while limiting vision. This is done by diffusing or scattering light, which obscures the view. Translucent materials also smooth out the variation between light and dark, generally softening the experience of light. As such, translucent materials are inherently more enigmatic than their transparent or opaque counterparts. In contemporary architecture, glass is the primary material used for translucency, although synthetic materials such as plastics have been on the rise in the early 21st century. Synthetic plastics include polycarbonate panels, which are composed as extruded cells of thick plastic surfaces.[6] Translucency in glass is produced through various treatments, including etching, coating, or lamination methods. The quality of opaqueness can be achieved through a wide range of materials. For the sake of studying fenestration in this chapter, opaque or solid materials are considered the default or controlled variable, whereas openings are the element under consideration, particularly in the illuminance diagrams.

Glass on buildings can take on different characteristics throughout the day, and the property of reflection has a large impact on the presence of a building. Reflection can either help a building blend into its surroundings or stand out within its context, or even cause glare in the external environment. Refraction, which is a slight deviation of rays of light, can also occur in uneven panes of glass. This effect is also seen when light passes from air into water: A stick in the water appears to be broken where it enters the water due to refraction. It does not represent the image of a broken ray of light because the line of sight is also skewed.[7]

Beyond the binary characteristics of solid and void, light filtration is a strategy to further manage amounts of light in a space, manage extremes, and maintain human comfort. Building envelopes have increasingly included screens and shading devices to manage sunlight.[8] In the book *Light in Architecture*, the authors state:

> Facades have been designed as responsive and selective filters since antiquity, including overhangs and balconies, venetian blinds, porticos, thickened walls incorporating curtains. Contemporary facades are now responsive in more sophisticated ways, sometimes in an overly complicated manner and to their peril. While the double shell of radial trusses in the Berlin Free Library by Foster + Partners passively manages light and thermal exchange, the failed active facade system of the Institute du Monde Arabe by Jean Nouvel was derived from cultural patterned geometries.[9]

Light filtration of many types can also be found in nature. Crepuscular rays are a profound natural phenomenon where beams of sunlight are filtered and isolated as projections through the sky. The atmospheric aesthetics are a result of the dramatic modulation of light, rather than the extreme of full daylight or complete darkness. In that way, building envelopes, or fenestration design, is responsible for modulating sunlight to harvest and manage daylight for interior spaces.

During daylight hours, exterior illuminance varies between approximately 1,000 and 100,000 lux, ranging from overcast conditions to direct sunlight. Relative to any form of electric light, daylight is the most balanced light, spanning the chromatic spectrum. The characteristics of natural light change over the course of the day, within the daily and yearly cycles of the sun. This constant change of natural illuminance throughout the day links us to the patterns and flows of the universe. The qualities of natural light vary greatly and are related to atmospheric conditions of the sky, including humidity, cloud cover, and particulates in the air, including pollutants.

"Daylight factor" is the proportion of light inside a space relative to the light level outside the space or structure. It is the direct result of aperture percentages and placement, and it can be calculated as a quantitative value. This ratio provides some sense of the amount of light transmitted into a space; the desirable amount varies depending upon functional program and climate, yet it is typically between 1% and 10%. The illuminance diagrams of Figures 9.1a–o visually illustrate this

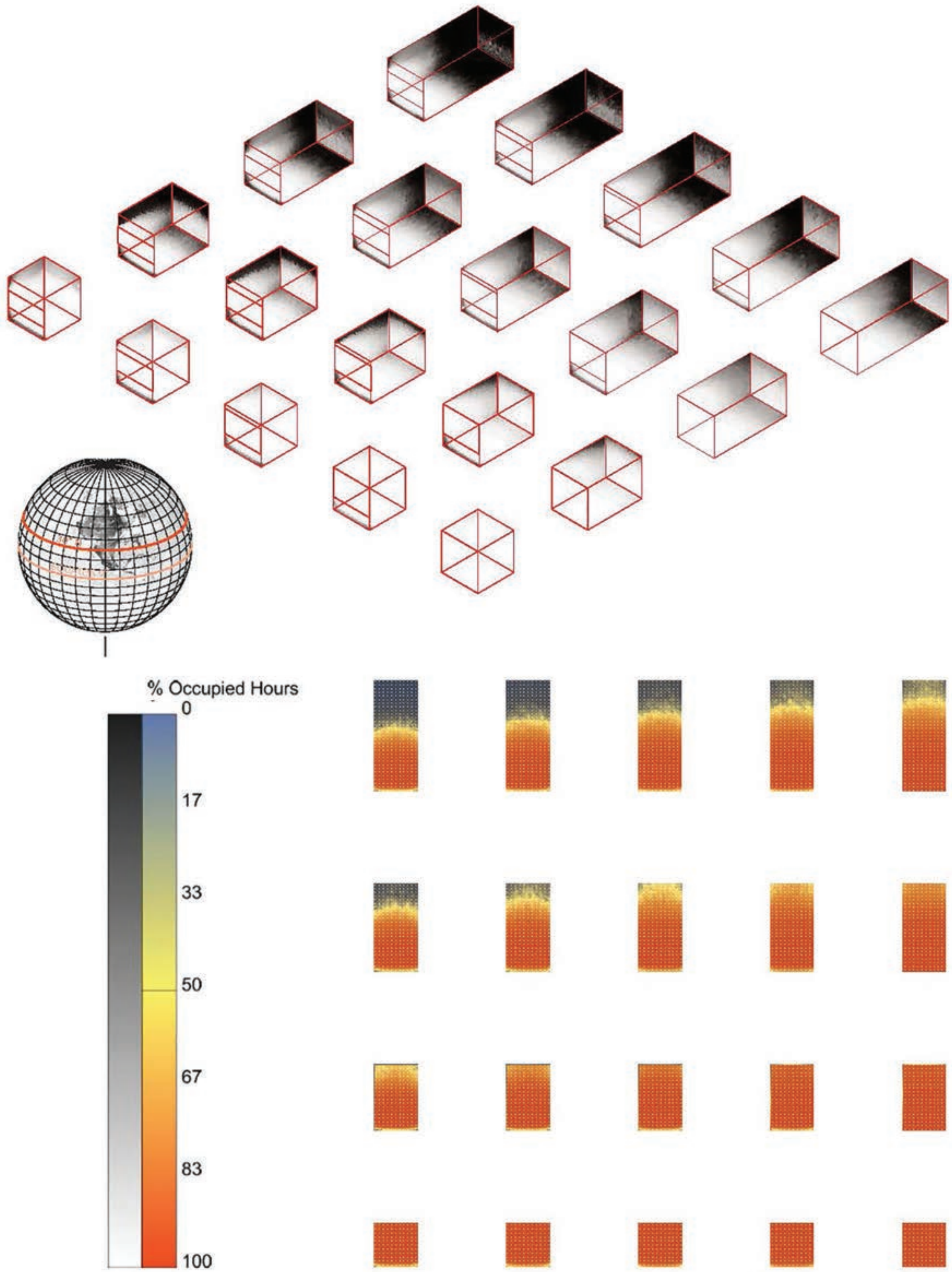

Figure 9.1a–o

Illuminance Diagrams

Visual depictions of the difference in illuminance as variables change, including latitude, solar orientation, and aperture size.

Nic Allinder and Jesefa Templo

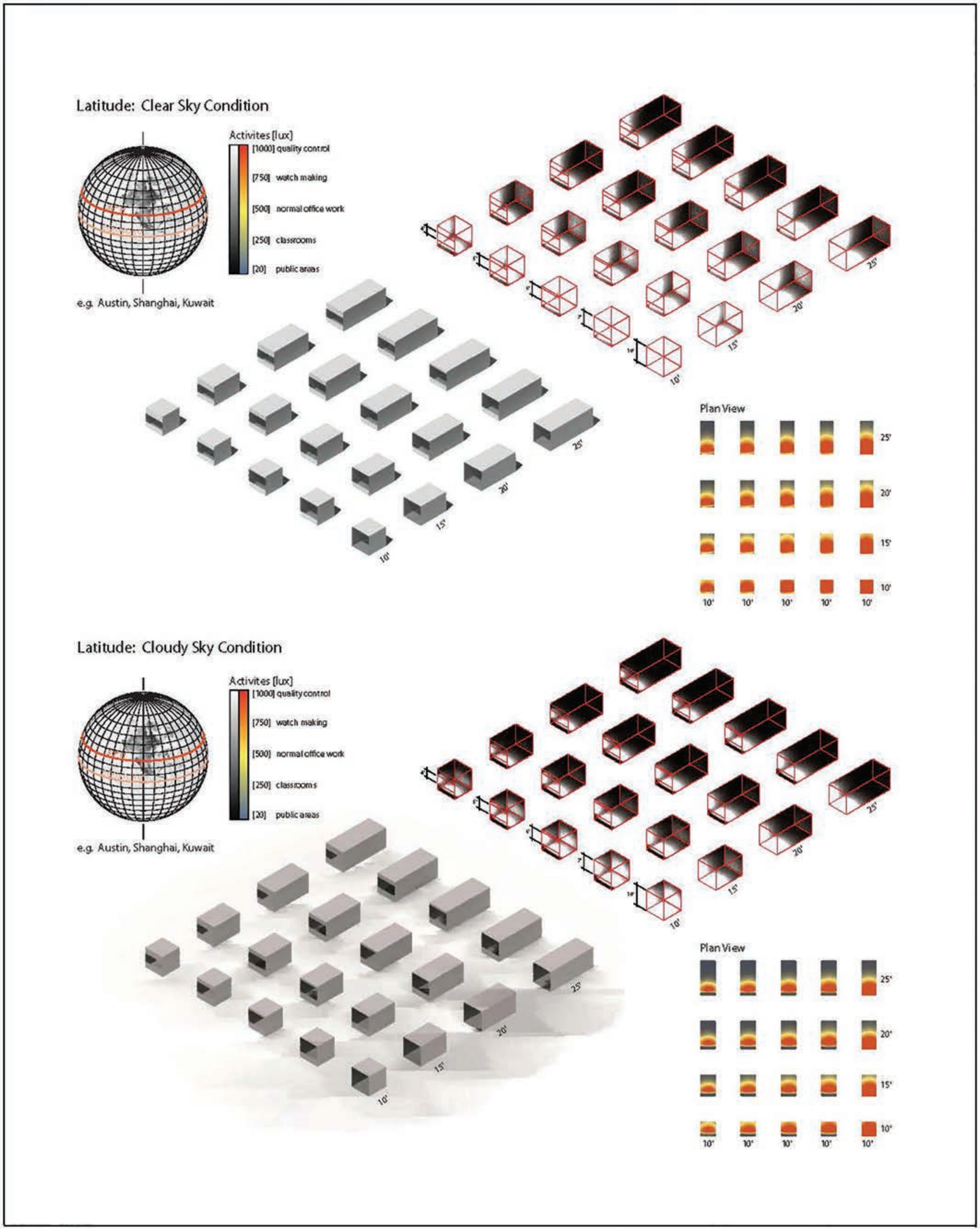
Latitude: Clear Sky Condition
Activites [lux]
[1000] quality control
[750] watch making
[500] normal office work
[250] classrooms
[20] public areas
e.g. Austin, Shanghai, Kuwait
Plan View
25'
20'
15'
10'
Latitude: Cloudy Sky Condition
Activites [lux]
[1000] quality control
[750] watch making
[500] normal office work
[250] classrooms
[20] public areas
e.g. Austin, Shanghai, Kuwait
Plan View

Figure 9.1b

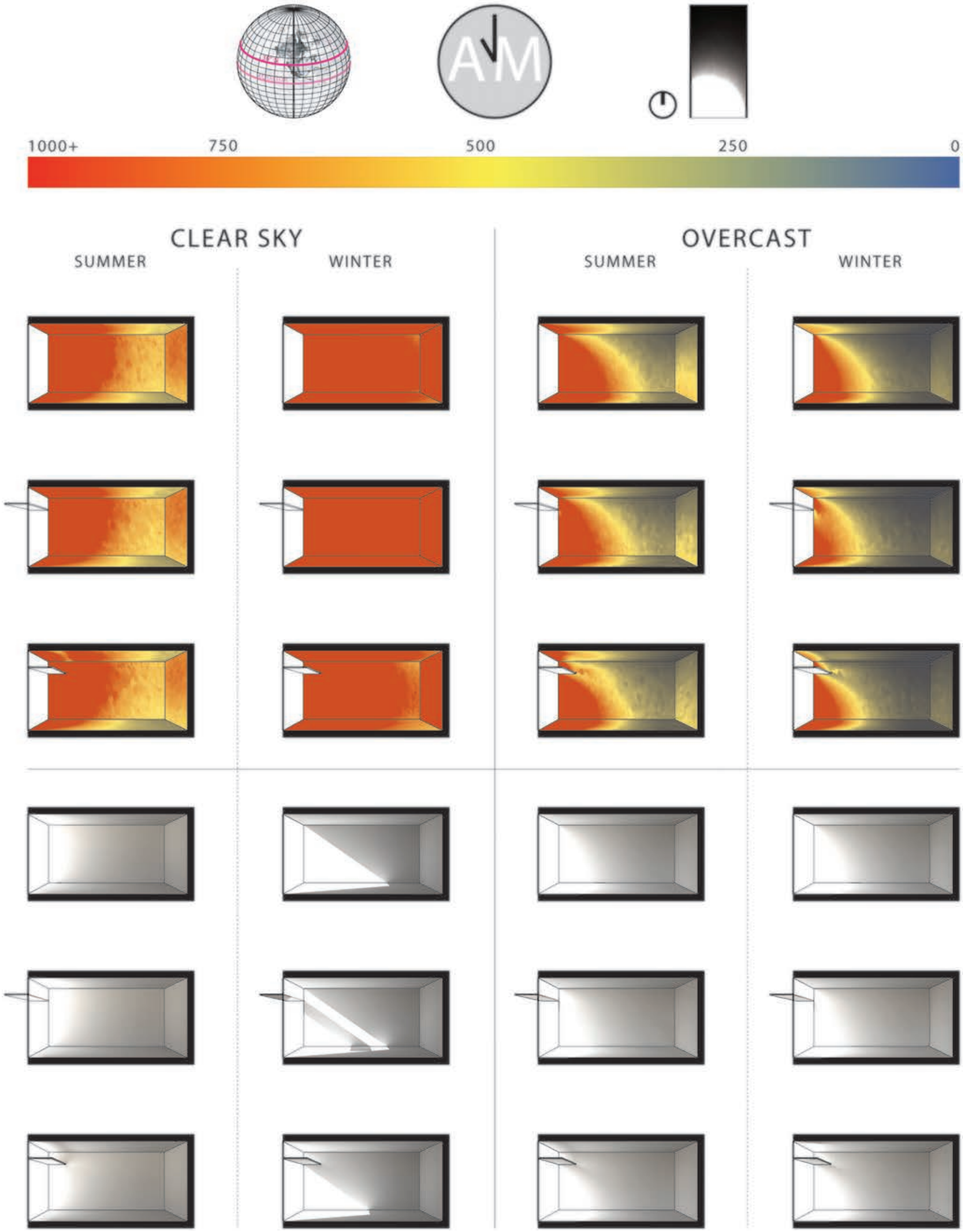
AM
1000+
750
500
250
0
CLEAR SKY
SUMMER
WINTER
OVERCAST
SUMMER
WINTER

Figure 9.1c

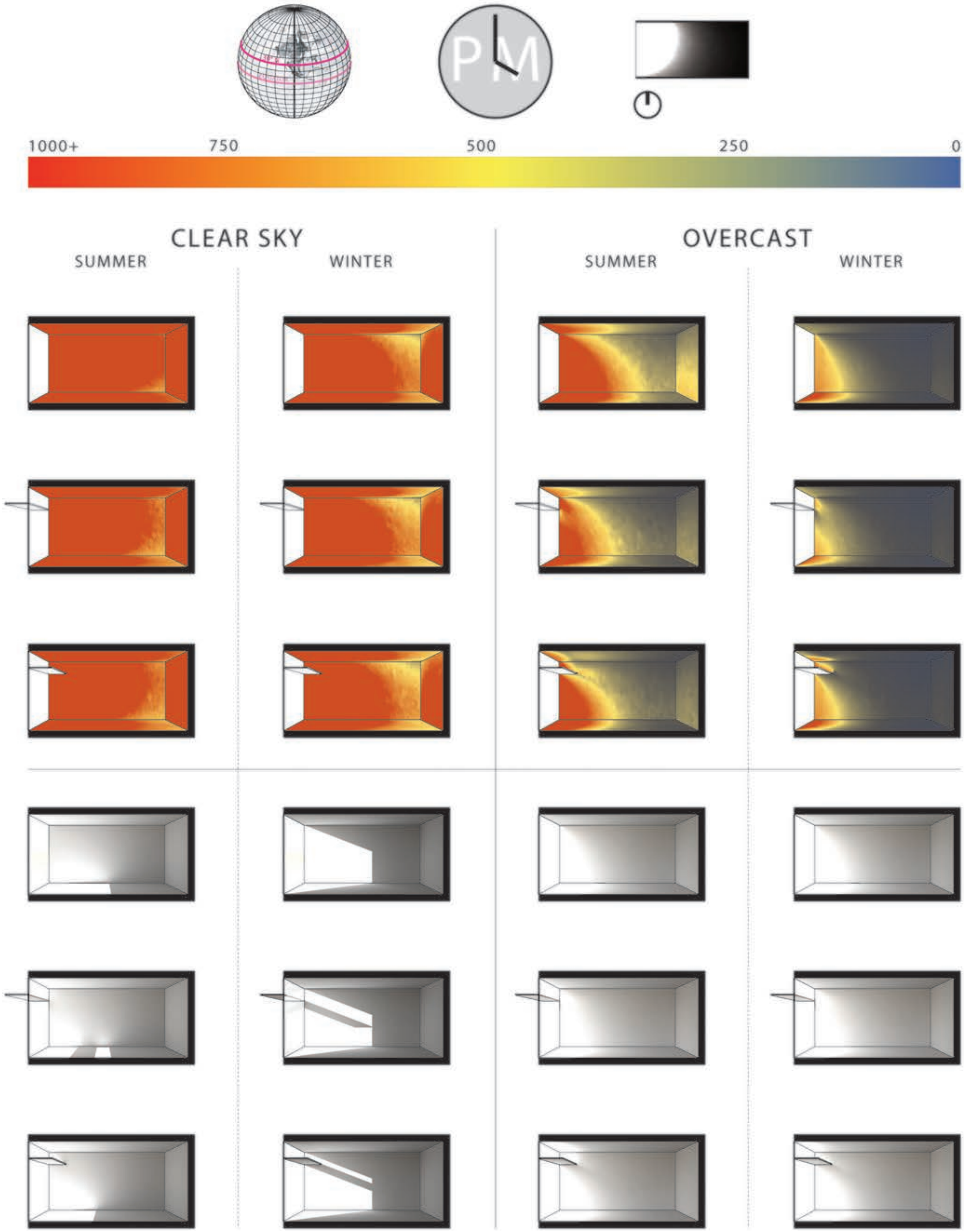
PM
1000+
750
500
250
0
CLEAR SKY
SUMMER
WINTER
OVERCAST
SUMMER
WINTER

Figure 9.1d

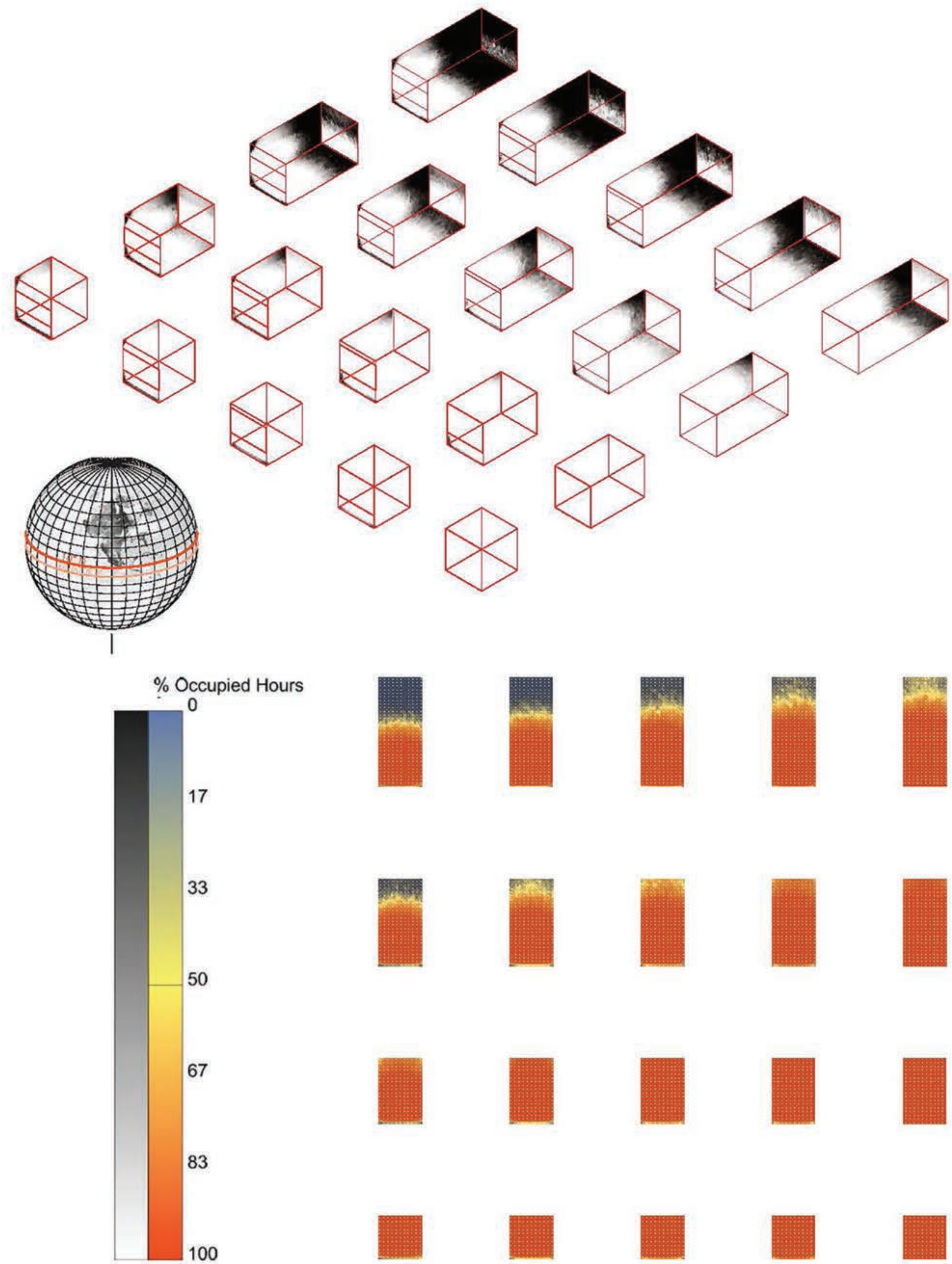

Figure 9.1e

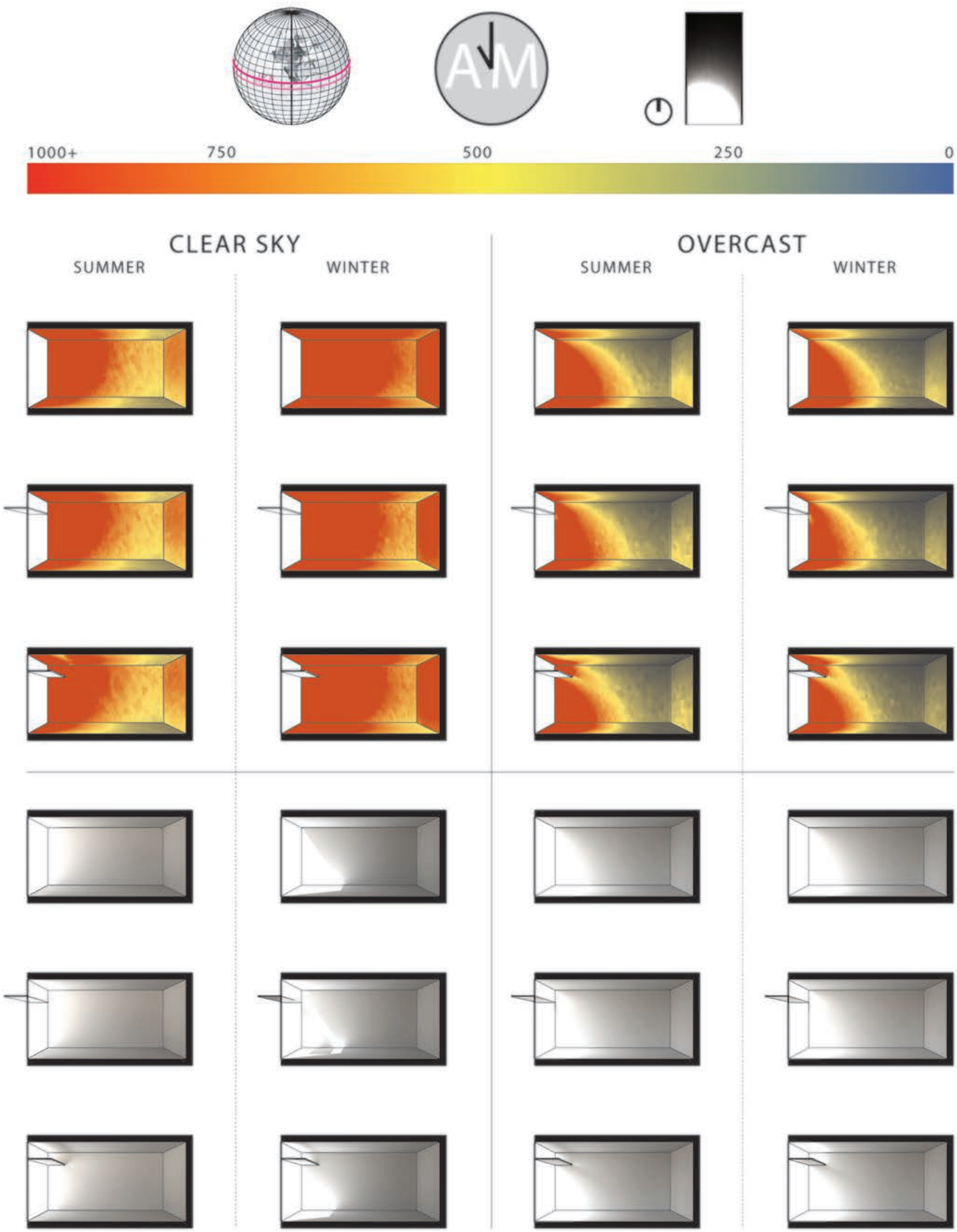
AM
1000+
750
500
250
0
CLEAR SKY
SUMMER
WINTER
OVERCAST
SUMMER
WINTER

Figure 9.1f

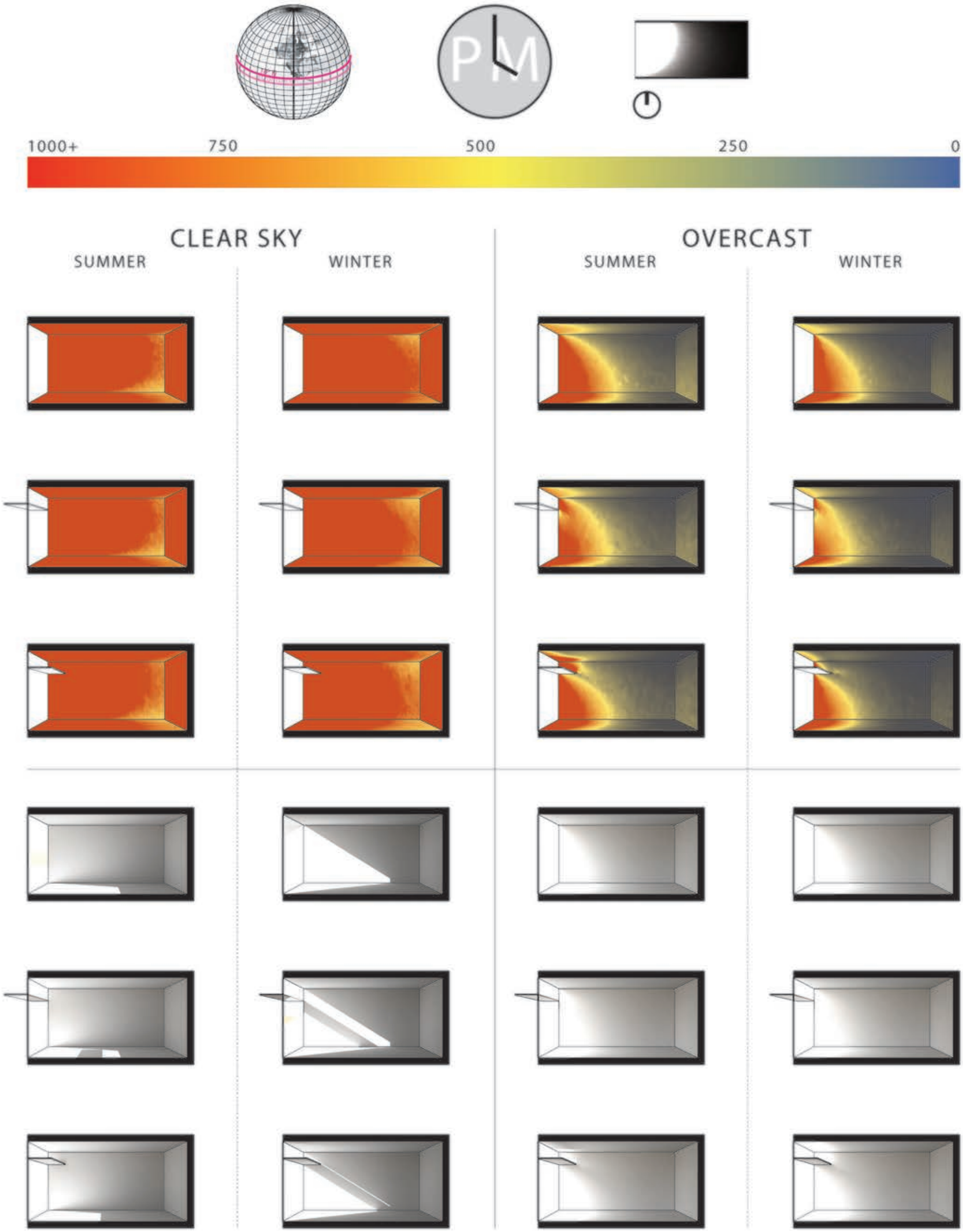

PM
1000+
750
500
250
0
CLEAR SKY
SUMMER
WINTER
OVERCAST
SUMMER
WINTER

Figure 9.1g

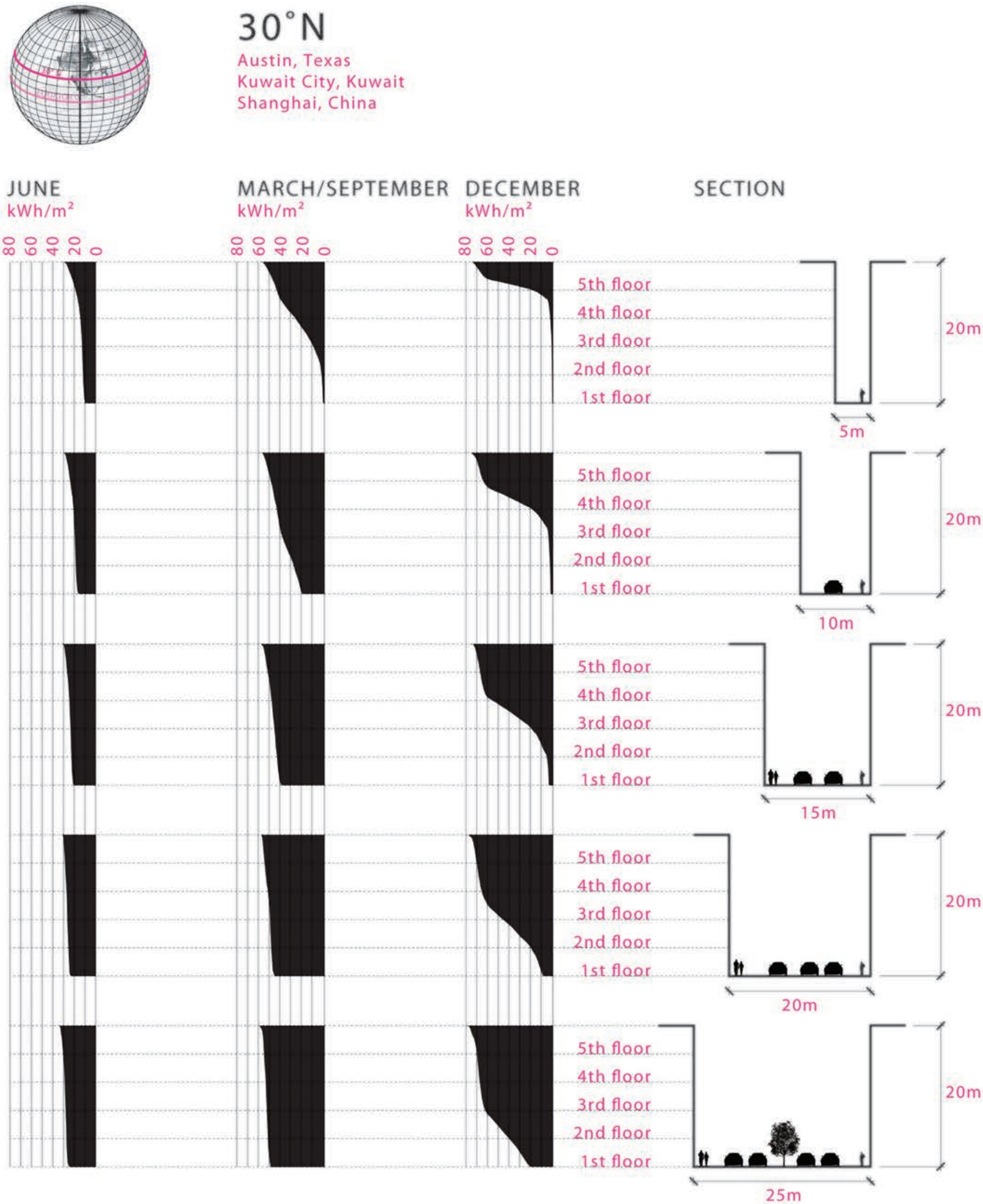
30°N
Austin, Texas
Kuwait City, Kuwait
Shanghai, China
JUNE
kWh/m²
MARCH/SEPTEMBER
kWh/m²
DECEMBER
kWh/m²
SECTION
80 60 40 20 0
5th floor
4th floor
3rd floor
2nd floor
1st floor
20m
5m
10m
15m
20m
25m

Figure 9.1h

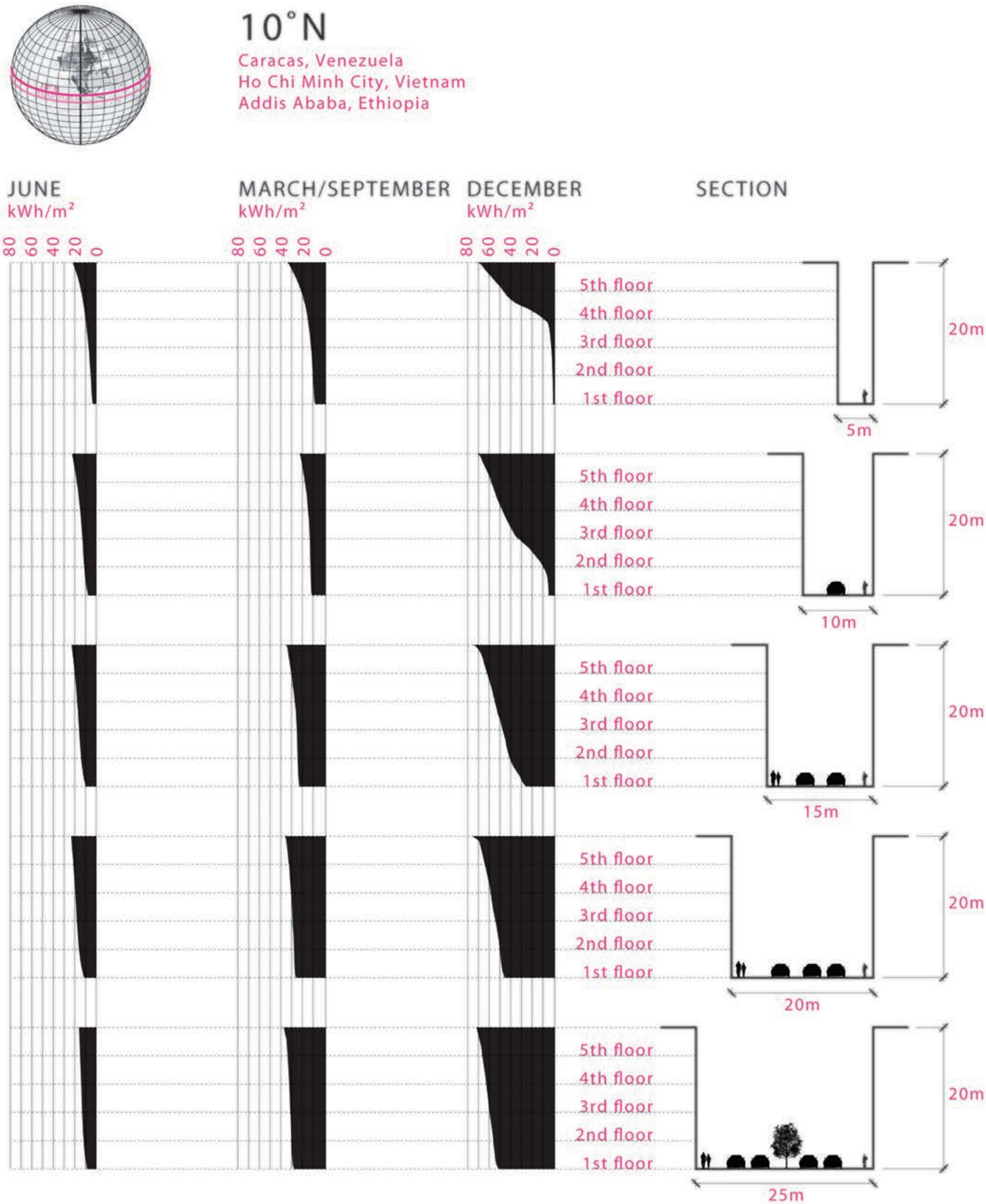
10°N
Caracas, Venezuela
Ho Chi Minh City, Vietnam
Addis Ababa, Ethiopia
JUNE
kWh/m²
MARCH/SEPTEMBER
kWh/m²
DECEMBER
kWh/m²
SECTION
80 60 40 20 0
5th floor
4th floor
3rd floor
2nd floor
1st floor
20m
5m
10m
15m
20m
25m

Figure 9.1i

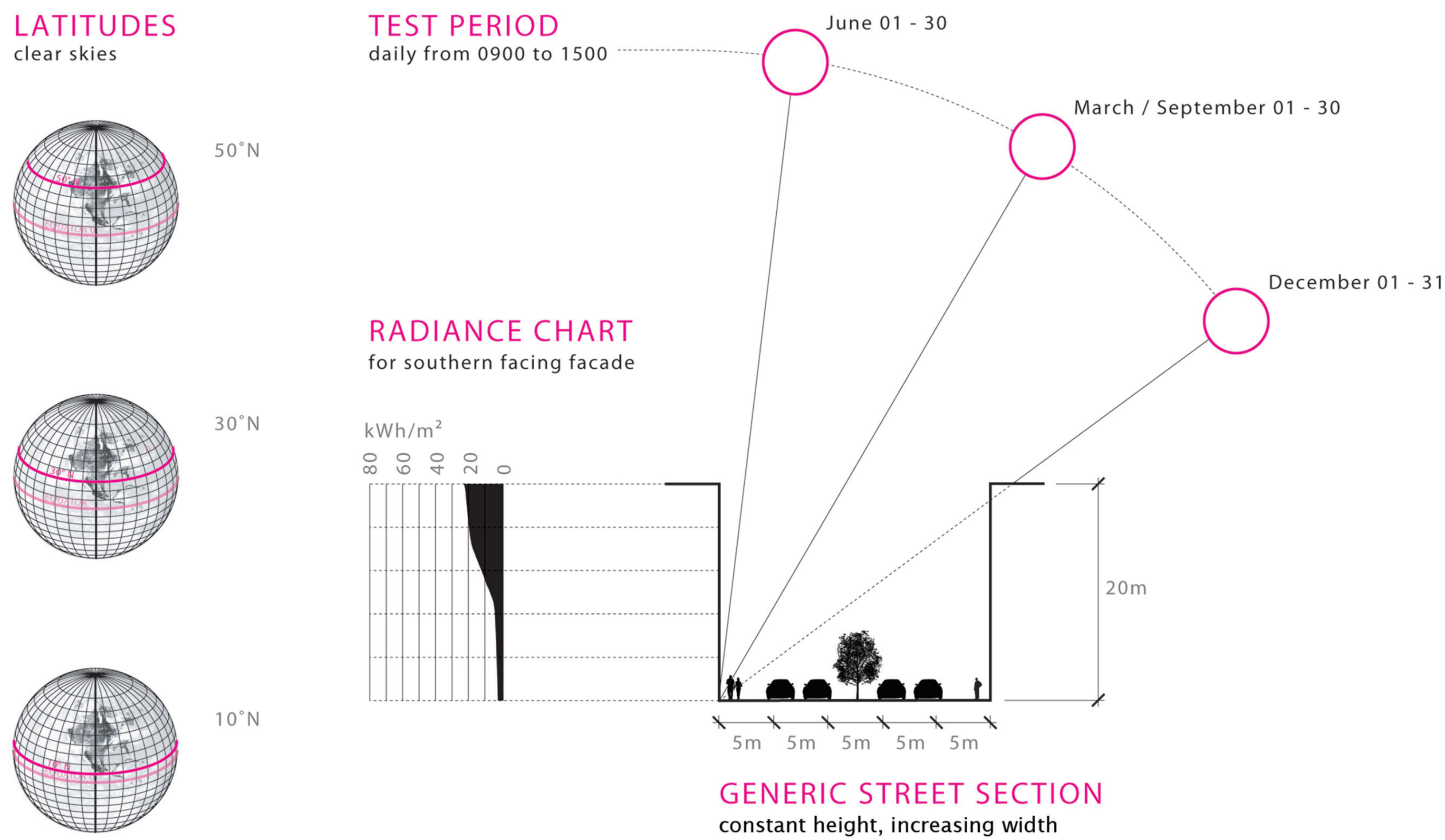

LATITUDES
clear skies
50°N
30°N
10°N
TEST PERIOD
daily from 0900 to 1500
June 01 - 30
March / September 01 - 30
December 01 - 31
RADIANCE CHART
for southern facing facade
kWh/m²
80
60
40
20
0
20m
5m
5m
5m
5m
5m
GENERIC STREET SECTION
constant height, increasing width

Figure 9.1j

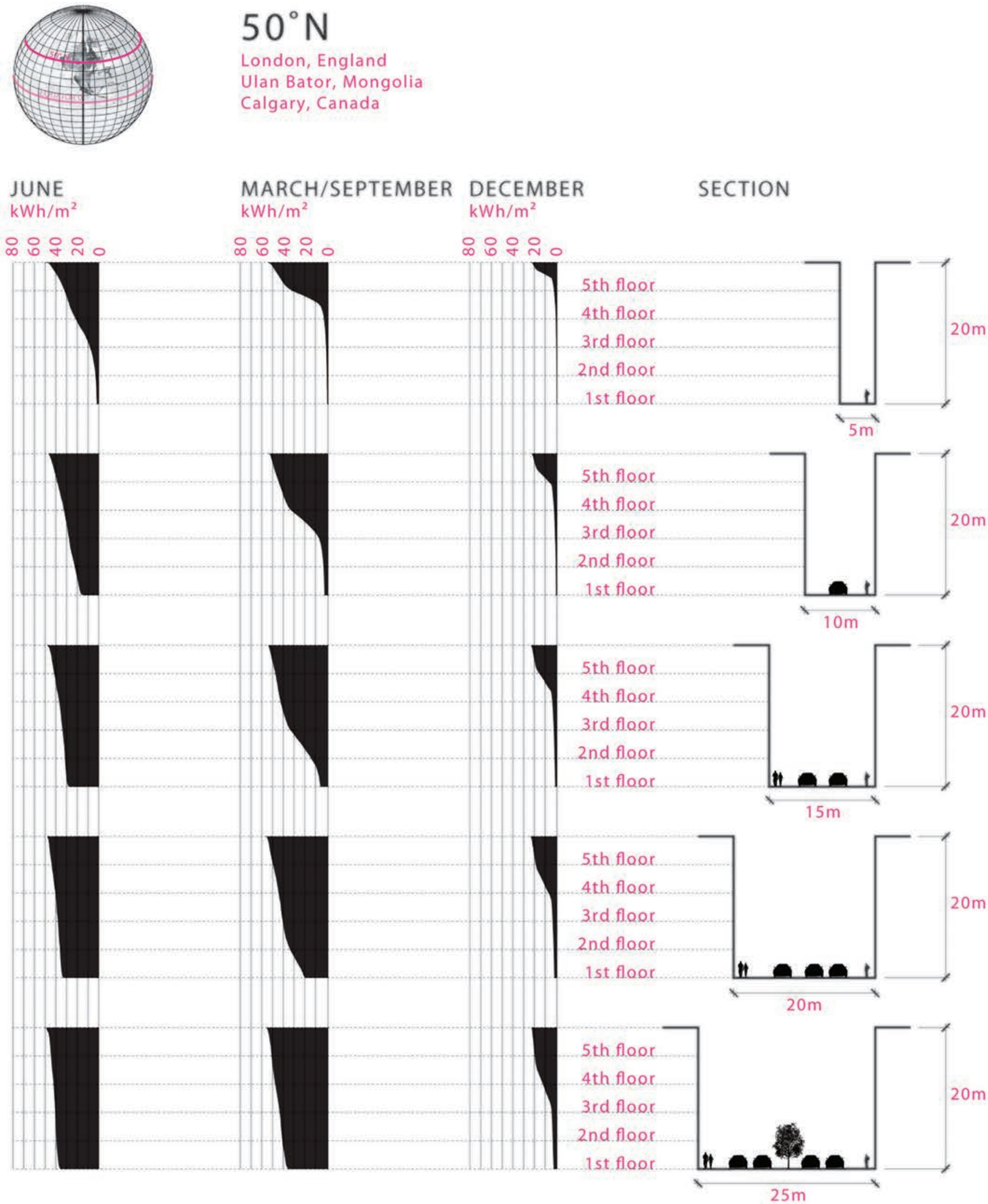
50°N
London, England
Ulan Bator, Mongolia
Calgary, Canada
JUNE
kWh/m²
MARCH/SEPTEMBER
kWh/m²
DECEMBER
kWh/m²
SECTION
80 60 40 20 0
5th floor
4th floor
3rd floor
2nd floor
1st floor
20m
5m
10m
15m
20m
25m

Figure 9.1k

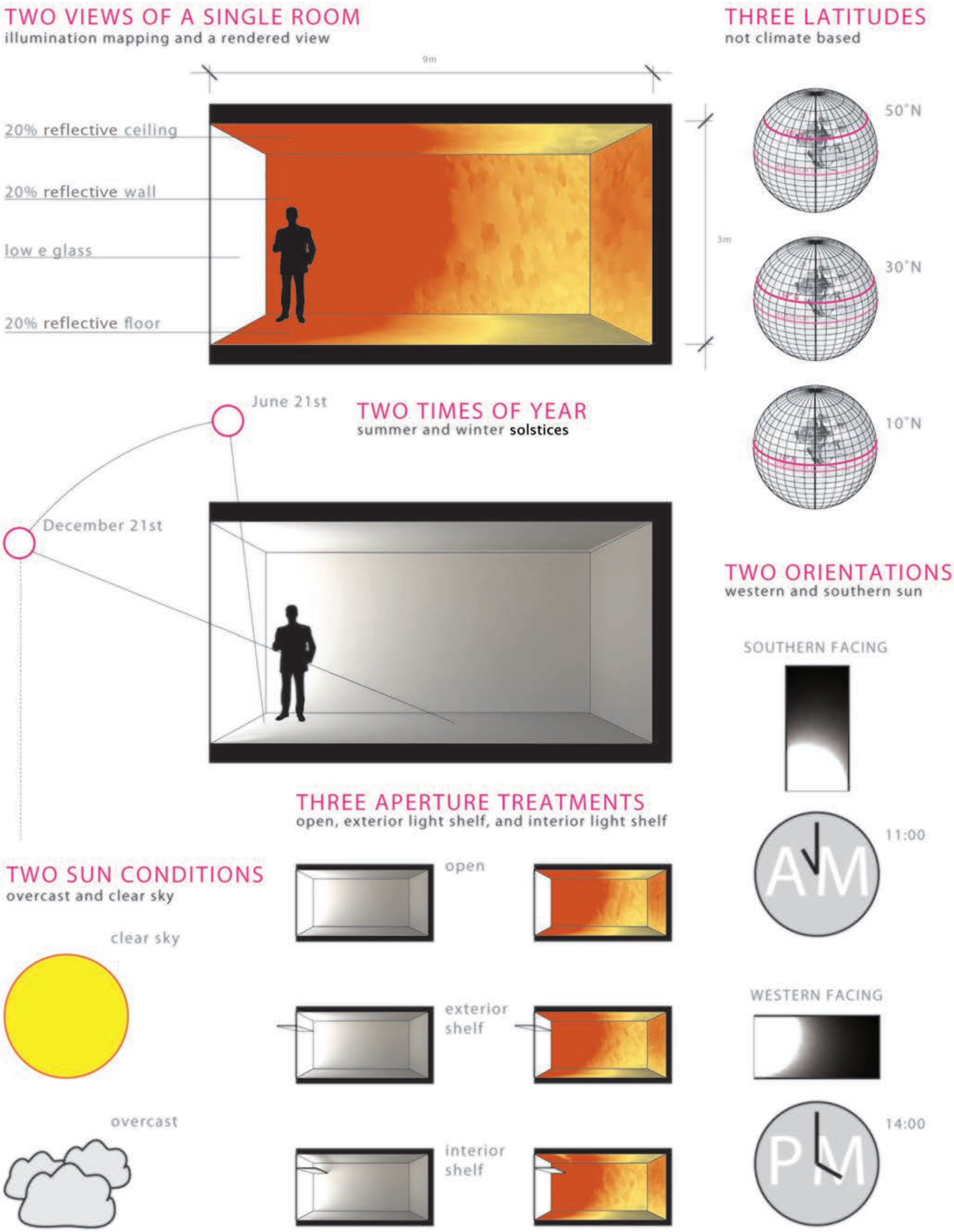
TWO VIEWS OF A SINGLE ROOM
illumination mapping and a rendered view
9m
3m
20% reflective ceiling
20% reflective wall
low e glass
20% reflective floor
THREE LATITUDES
not climate based
50°N
30°N
10°N
June 21st
TWO TIMES OF YEAR
summer and winter solstices
December 21st
TWO ORIENTATIONS
western and southern sun
SOUTHERN FACING
11:00
AM
THREE APERTURE TREATMENTS
open, exterior light shelf, and interior light shelf
TWO SUN CONDITIONS
overcast and clear sky
open
clear sky
exterior
shelf
WESTERN FACING
overcast
interior
shelf
14:00
PM

Figure 9.1l

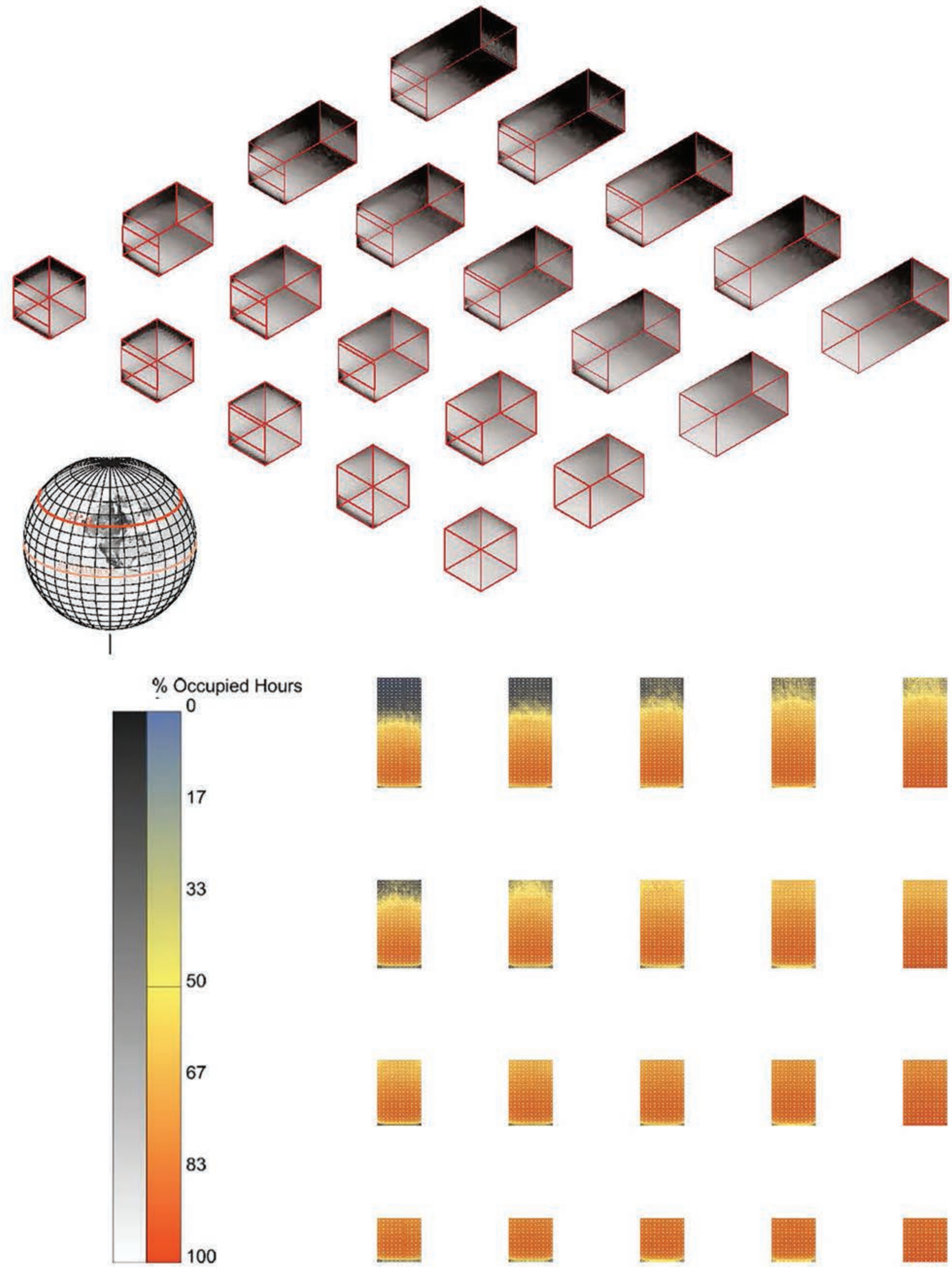

Figure 9.1m

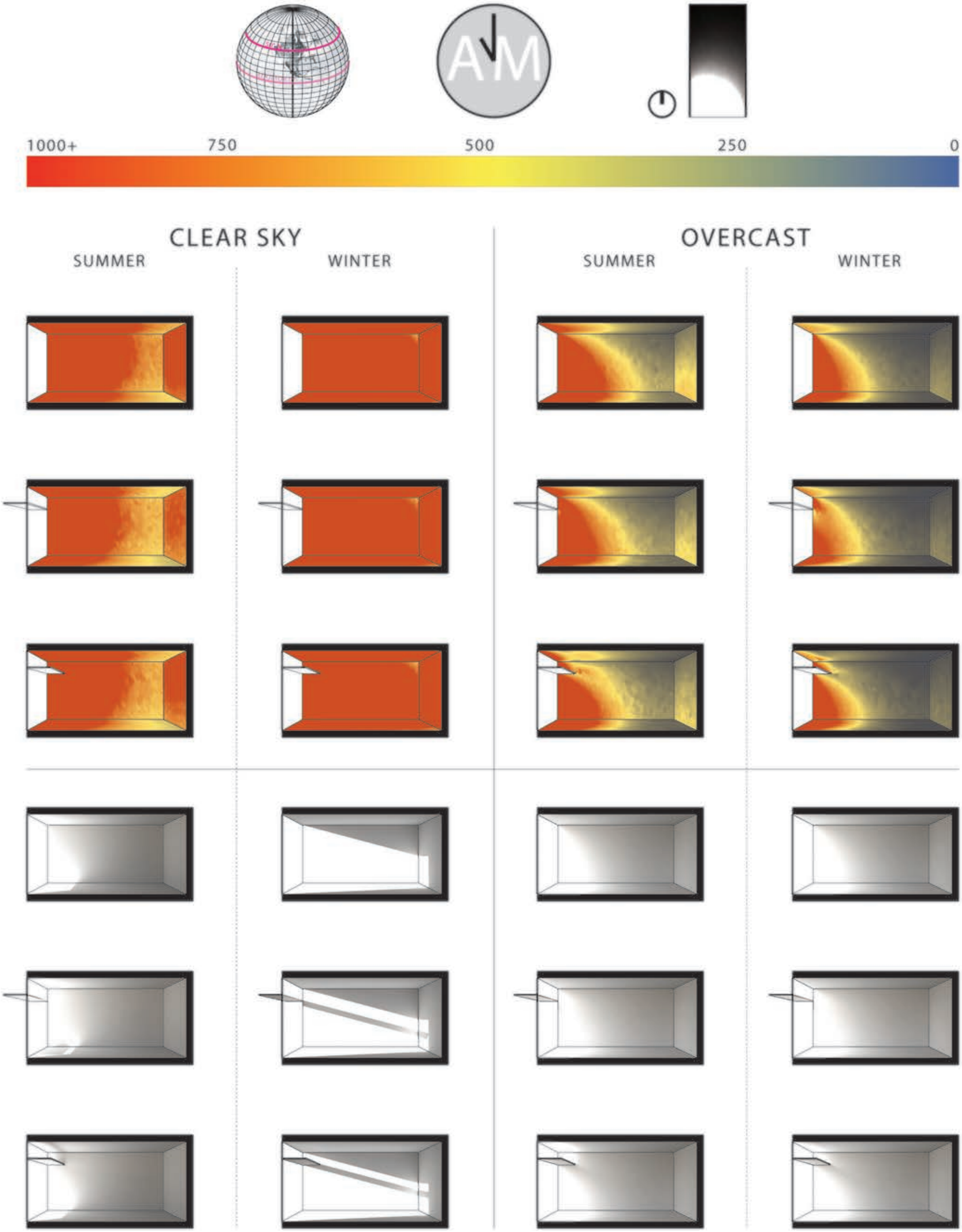
AM
1000+
750
500
250
0
CLEAR SKY
SUMMER
WINTER
OVERCAST
SUMMER
WINTER

Figure 9.1n

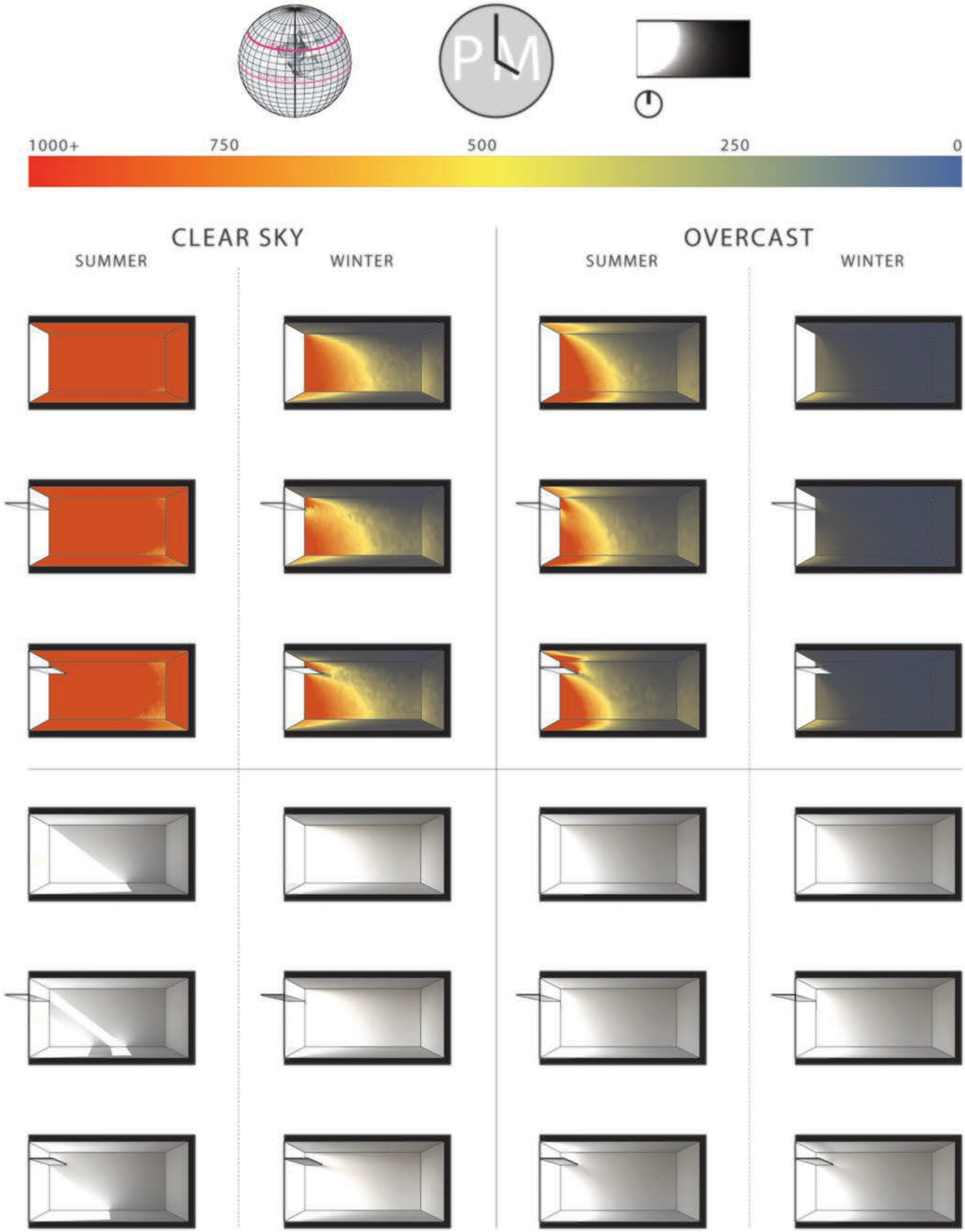
PM
1000+
750
500
250
0
CLEAR SKY
SUMMER
WINTER
OVERCAST
SUMMER
WINTER

Figure 9.1o

principle, and are intended to provide an intuitive resource for designers as a supplement to charts and graphs. The diagrams visually depict the difference in illuminance as variables change, including latitude, solar orientation, and aperture size. Convention establishes that the effective horizontal reach of daylight into a space is 2.5 times the height of an aperture in the facade, although the illuminance diagrams show that it is largely dependent on latitude and solar orientation factors. "Daylight autonomy" is indirectly related, as it is the percentage of time that a certain level of illuminance is reached throughout the year, and therefore the amount of time that no electric light is needed in a space. Based on a desired amount of lux in a space, this may also be loosely inferred from the illuminance diagrams.

While previous chapters presented detailed methods for assessing how much solar radiation falls on surfaces and how to control it, in this chapter, we will start to examine how that radiation affects occupants inside the building. This text will focus on the solar radiation transmitted through windows. Heat conducted through the envelope plays an important role in building energy and comfort performance as well, but is beyond the scope of this book. With the exception of dark-colored roofs or poorly insulated walls, the contribution to total heat gain of solar heat falling on opaque portions of the building envelope is usually insignificant compared to solar radiation transmitted through glazing. In order to determine how much of the incident insolation enters the building through a piece of fenestration, it first is necessary to examine some of the properties of glass.

GLAZING FUNDAMENTALS

Transparent materials play a unique role in the heat flows of a building. All building assemblies are subject to the three primary pathways of heat transfer—conduction, convection, and radiation. ***Conduction*** is the molecule-to-molecule transfer of heat energy. ***Convection*** is the transfer of heat by the circulation of a fluid—generally air in the case of buildings. ***Radiation*** is the transfer of heat or energy by electromagnetic waves. Radiation relevant to buildings takes either the form of short-wave solar radiation or long-wave thermal radiation.

In the opaque portions of the building (roofs, walls, floors), convection and radiation usually stop and start at the assembly surface with heat transfer through a well-built wall or floor assembly itself, primarily taking the form of conduction. Windows, on the other hand, provide a pathway for solar radiation (and convection if the window is open) to transfer heat around the thermal barrier of the insulated skin and directly into the envelope. Think of this as a thermal "short circuit." In an electrical system, a short circuit is never a benefit, but in the case of glazing, it can be either positive or negative, depending on the circumstances. It is the designer's task to understand and control this phenomenon, putting it to work to benefit occupant comfort, perception, and building energy use.

Fenestration products sold in the United States are rated by the National Fenestration Rating Council (NFRC) for energy performance based on five parameters: U-factor (*U*), solar heat gain coefficient (*SHGC*), visible transmittance (*VT*), air leakage (*AL*), and condensation resistance (*CR*). Of these parameters, the one most closely tied to solar gain is the solar heat gain coefficient. Visible transmittance is a key factor in daylighting and will be discussed later.

The ***solar heat gain coefficient*** (*SHGC*) is the fraction of incident solar radiation transmitted through glazing. *SHGC* includes both direct transmission and the inward-flowing portion of absorbed radiation. *SHGC* is found using Equation 9.1[10] where T is the transmittance of the glazing at normal incidence, a_{glass} is the solar absorptance of the glazing, and N is the inward-flowing fraction of absorbed radiation.

Equation 9.1 Solar Heat Gain Coefficient

$$SHGC = T + a_{glass}\, N$$

The solar heat gain coefficient is given at a normal angle of incidence. Most of the time, however, radiation is not striking the window at normal or even near-normal angles of incidence. We know from the graph of the dielectric properties of glass (Figure 8.5) that the transmittance of radiation through glass drops off significantly at higher angles of incidence. Therefore, a method is needed to adjust the *SHGC* based on the angle of incidence at a particular time.

The methods for doing so with high accuracy are complex and unsuitable for design calculations, but it is possible to estimate these values with reasonable accuracy using Equation 9.2. This is the same formula that EnergyPlus uses to calculate appropriate *SHGC* values when the simple window model is used.[11] This equation gives an estimate of the transmittance value, T_θ, of the fenestration at any arbitrary angle of incidence (θ).

Equation 9.2 Glass Transmittance at Arbitrary Angle of Incidence

$$T_\theta = SHGC \cos\theta \, [1 + (0.768 + 0.817\, SHGC^4)\sin^3 \theta]$$

The equation is an approximation but it closely matches the profile we would expect, including the rapid fall-off in transmittance starting at an angle of incidence of approximately 65°. This equation has plenty of accuracy for design purposes, as shown in Figure 9.2.

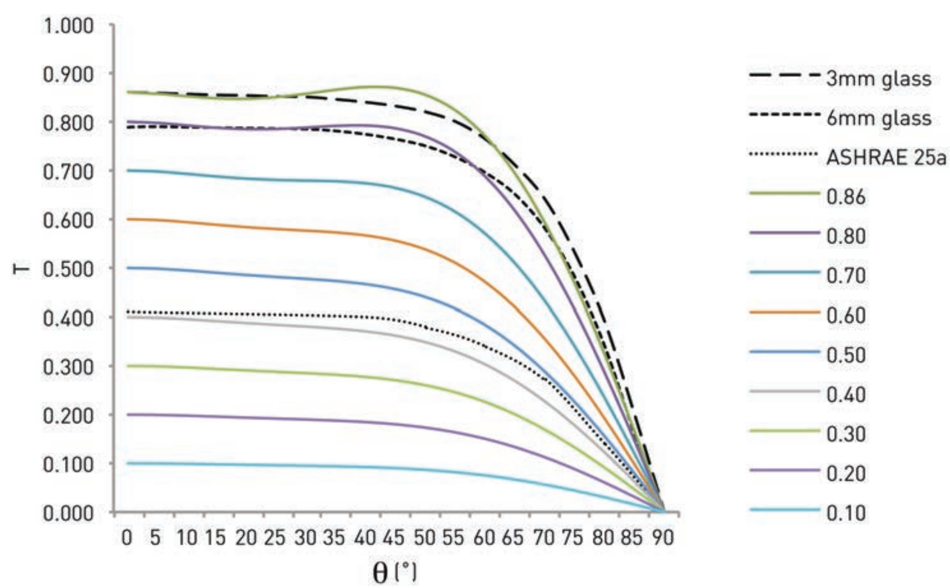

Figure 9.2

Transmittance Value by Angle of Incidence

Radiation transmission for clear and low-E glass by angle of incidence for various *SHGC* values. These curves are derived from Equation 9.1. The dashed lines show the actual transmission characteristics of 3mm and 6mm clear glass as well as assembly 25a from the ASHRAE Handbook of Fundamentals, which is comprised of two layers of 1/8″ clear glass with a low-E coating with an emissivity of 0.005 on surface 2 for comparison.

Dason Whitsett

Transmission of diffuse radiation either from the sky or ground through glazing presents a slightly different problem. Diffuse radiation comes from all directions off of the sky dome as well as being reflected from the ground and other surfaces, so we also need to determine the radiation transmittance value averaged over the hemisphere, which the surface sees. Methods for making this determination precisely are, again, complex. For clear and low-E glazing, however, a simple rule of thumb will provide a good approximation. Using 86% of the *SHGC* at normal incidence provides a reasonable estimate of the hemispherical diffuse transmittance value, as indicated by Equation 9.3. This rule of thumb was derived by comparing the hemispherical diffuse transmittance values to the *SHGC at the normal angle of incidence* for the representative glazing assemblies listed in ASHRAE Fundamentals 2009.[12]

Equation 9.3 Estimate of Hemispherical Diffuse Transmittance

$$T_d = 0.86\ SHGC$$

SOLAR GAIN THROUGH UNSHADED WINDOWS

Once the *SHGC* at a particular angle of incidence is known, calculating solar gain for each hour through the window is a simple matter. For direct beam radiation (Q_b), multiply the hourly direct beam insolation incident on the window (I_{tb}) by the area of the window (A) and the transmittance value for the current angle of incidence (T_θ), as shown in Equation 9.4. As with any insolation calculations, the solar coordinates at the midpoint of each hour should be used to correspond with the insolation data that are generally available as average hourly values.

Equation 9.4 Hourly Direct Beam Solar Gain through Window

$$Q_b = I_{tb} A T_\theta$$

Equation 9.5 Hourly Diffuse Solar Gain through Window

$$Q_d = I_{td} A T_d$$

For solar gain from diffuse radiation (Q_d), multiply the total ground and sky diffuse irradiation incident on the window by the hemispherical diffuse transmittance value, as shown in Equation 9.5.

CAVITY ABSORPTANCE

Some of the radiation coming in through windows will be reflected back out through those same windows. Sometimes, the assumption is made in passive heating situations that interior surfaces need to be dark to ensure that valuable heat is not lost through the windows. This seems to pose a conflict with the desire for effective daylighting, for which more reflective surfaces are desirable. In reality, these two desires are usually not in significant conflict. Most spaces retain the vast majority of solar radiation that enters, so even though light bounces longer off reflective surfaces, increasing daylight levels, nearly all of the light will eventually be absorbed as heat by the building or removed by an air conditioner.

Albedo (a) is the term used to describe the ratio of radiation reflected from a surface or volume. Most building interior volumes have a very low albedo. This means that, of the solar radiation transmitted through glass into the building, most is absorbed inside and only a small portion is reflected back out. Windows usually look dark from the outside during the day because our eyes see light, and if there is relatively little light reflected off objects beyond the window, travelling through the glass, and received by the observer's eyes, the window will appear dark from the outside due to the high level of contrast with the luminance of other outdoor objects in the observer's field of view. Even on a cloudy day, outdoor illumination levels are frequently two orders of magnitude higher than indoors and the eye tends to adapt to the ambient condition, making the relatively weak luminance of the window appear comparatively dark. Common exceptions to the dark window phenomenon are nighttime, spaces with views to other windows, and spaces with unusually high reflectance or illumination inside. When the luminance of the window is similar to or higher than surrounding surfaces, such as at night with lights on indoors, our eyes can clearly perceive what lies beyond the glazing and windows will appear bright. Similarly, when an observer has a significant view of a window beyond the glazing, light coming in the far window can travel straight through to the viewer's eye.

The albedo or reflectance of a space is a function of its interior surface area, reflectivity of interior surfaces, glazing area, and glazing properties. ***Absorptance*** is the inverse of albedo, describing the ratio of radiation absorbed by a surface or volume. This is, thermally speaking, what ultimately impacts a building as it relates to the sun.

The method presented here for determining the cavity absorptance of a volume was adapted from Duffie and Beckman.[13] Equation 9.6 gives the ratio of the radiation absorbed in the space to the total radiation transmitted into the space through glazing, including the portion that is reflected back out through the windows. The ***effective cavity absorptance*** (a_{cav}) is a dimensionless ratio. In this equation, a_i represents the mean absorptance of diffuse radiation for the surfaces on the inside of the cavity. This should be determined as a weighted average by summing the absorptance of each surface multiplied by its area less glazing and dividing the total by the total interior surface area less windows. T_d is the hemispherical diffuse transmittance of the glazing (also weighted by area if multiple different glazing types are present). A_{win} is the total window area and A_i is the total inside surface area less windows.

Equation 9.6 Effective Cavity Absorptance

$$a_{cav} = \frac{a_i}{a_i + (1 - a_i) T_d \frac{A_{win}}{A_i}}$$

EXAMPLE 9.1

Determine the effective cavity absorptance for a volume 10m long, 5m deep, and 3.5m high. Assume a mean internal surface absorptance (a_i) of 0.30 and 3mm single glazing ($SHGC = 0.86$). One of the 10m long sides is glazed for 50% of its surface area.

Solution

$A_{win} = 10.0m \times 3.5m \times 0.50 = 17.5m^2$

$A_i = 2(10.0m \times 3.5m + 5.0m \times 3.5m + 10.0m \times 5.0m) - 17.5m^2 = 187.5m^2$

Use the actual average hemispherical diffuse radiation transmission value, if available, or the rule of thumb presented in Equation 9.3 to find T_d.

$$T_d = 0.86SHGC = 0.86\text{Í}0.86 = 0.74$$

$$a_{cav} = \frac{a_i}{a_i + (1 - a_i)T_d \dfrac{A_{win}}{A_i}} = \frac{0.30}{0.30 + (1 - 0.30)0.74\dfrac{17.7m^2}{187.5m^2}} = 0.86$$

Even the room in Example 9.1, with half of its long side glazed with the highest transmittance glazing available and a very high internal reflectance level, still absorbs 86% of the radiation that enters. Most new buildings today use multi-pane glazing, often with spectrally selective coatings that reduce *SHGC* dramatically, and lead to even higher cavity absorptance values, although absolute gain may be less. Figure 9.3 shows the effective cavity absorptance for a range of conditions for the same volume. Albedo increases substantially in narrow spaces such as corridors and shop-front windows, but even with the atypical condition of single-glazing equal to the surface area of the wall and a depth of only two meters, the volume only reflects back out approximately 40% of the radiation that enters.

In most cases, the vast majority of radiation entering the space will be absorbed within it, and the light-colored internal surfaces beneficial for daylighting do not significantly affect the amount of solar radiation captured.

Once the effective cavity absorptance is known, multiply the total radiation transmitted through the glazing by this value to obtain the net solar gain for the space, as shown in Equation 9.7.

Equation 9.7 Net Solar Gain

$$Q_{sol} = (Q_b + Q_d)a_{cav}$$

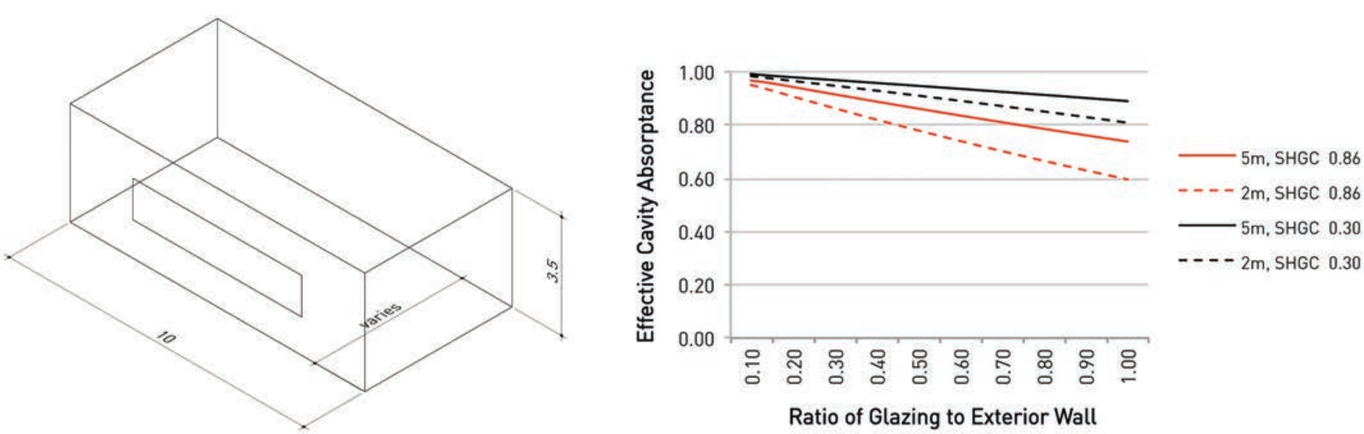

Figure 9.3

Example Cavity Absorptance

The chart shows the effective cavity absorptance for the volume depicted. The volume is 10m long and 3.5m high with a mean internal absorptance of 30%. Two depths are considered. The 5m depth represents a typical room depth while the 2m depth represents a corridor, which results in higher albedo for the space. Glazing is modeled as both 3mm clear glass (*SHGC* 0.86) and a typical low-E dual glazing (*SHGC* 0.30). The ratio of the window to wall area is shown along the horizontal axis.

Dason Whitsett

SOLAR GAIN THROUGH SHADED OR PARTIALLY SHADED WINDOWS

In cases where solar controls or other shadow-casting elements are present, it is essential to incorporate the impact of shading choices on the solar gain of a building or space.

Direct Beam Gain through Partially Shaded Windows

To solve for direct beam solar gain through a partially shaded window, determine the exposed area of the window for each hour. This is conceptually extremely simple, and for idealized shading geometries, easy to implement in practice. If an overhang or fin is infinitely long, using the profile or elevation angle to determine the unshaded fraction of the window is straightforward. For hoods, these two methods may be combined to calculate the unshaded fraction. In situations where the shadow geometry is not as simple, such as the condition shown in Figure 8.11, complex algorithms such as those proposed by Sutherland and Hodgman,[14] Maillot,[15] or Weiler and Atherton[16] are necessary to find the unshaded fraction. Generally, for the designer, a graphic solution is the easier route. By casting shadows and measuring the exposed area, one can readily determine how much of the window is exposed to beam radiation at a particular time. Use Equation 9.4 to calculate direct beam gains, adjusting the exposed area of the window at each timestep in the calculations.

Given that the most important factor in considering solar gain is monthly performance rather than hour-by-hour conditions, using the graphic method for each hour of the day would be impractical. For methods to calculate daily total solar gain for horizontal overhangs without end effects, see Jones,[17] and for shorter overhangs, see Utzinger and Klein.[18] In practice, simulation tools are a far more efficient approach for analyzing solar gain in partially shaded conditions except in the most idealized situations noted previously. For early design decision-making, one can use a shoebox model approach to study solar gain in isolation without the burden of whole-building complexity.

Diffuse Solar Gain through Partially Shaded Windows

Because a shading device cuts off some of the view of the sky from a window, it also affects diffuse insolation on the window. Jones[19] and Utzinger and Klein[20] present methods for calculating the impact of horizontal shading on the diffuse insolation received on a surface. The latter paper summarizes the results of these calculations nicely in a table of values for various shading extensions, offset heights, window widths, and overhang depths, as shown in Table 9.1. The values assume a window height of 1.0, and they are proportional, so units do not make a difference. The values provided are adjusted sky view factors ($V_{s\text{-}shd}$) for vertical surfaces using the isotropic sky model. This value may be substituted into Equation 5.15 to determine diffuse insolation on the partially shaded window. For comparison, an unshaded vertical surface has a sky view factor of 0.5 using Equation 5.14.

The table shows that deep overhangs with no offset above the window, especially on wide windows, result in major reductions in diffuse insolation. Increasing the offset of the overhang above the window, however, significantly reduces this impact. Overhang extension width is important for narrow windows, but becomes insignificant on wider ones.

Table 9.1 Adjusted Sky View Factors for Windows Shaded by Horizontal Overhangs ($V_{s\text{-}shd}$)

Extension Past Window Edge	*Offset Above Window*	*Window Width*	*Overhang Projection Depth*								
			0.10	*0.20*	*0.30*	*0.40*	*0.50*	*0.75*	*1.00*	*1.50*	*2.00*
0.00	0.00	1	0.46	0.42	0.40	0.37	0.35	0.32	0.30	0.28	0.27
		4	0.46	0.41	0.38	0.35	0.32	0.27	0.23	0.19	0.16
		25	0.45	0.41	0.37	0.35	0.31	0.25	0.21	0.15	0.12
	0.25	1	0.49	0.48	0.46	0.45	0.43	0.40	0.38	0.35	0.34
		4	0.49	0.48	0.45	0.43	0.40	0.35	0.31	0.26	0.23
		25	0.49	0.47	0.45	0.42	0.39	0.34	0.29	0.22	0.18
	0.50	1	0.50	0.49	0.49	0.48	0.47	0.44	0.42	0.40	0.38
		4	0.50	0.49	0.48	0.46	0.45	0.41	0.37	0.31	0.28
		25	0.50	0.49	0.47	0.46	0.44	0.39	0.35	0.27	0.23
	1.00	1	0.50	0.50	0.50	0.49	0.49	0.48	0.47	0.45	0.43
		4	0.50	0.50	0.49	0.49	0.48	0.46	0.43	0.39	0.35
		25	0.50	0.50	0.49	0.48	0.47	0.44	0.41	0.35	0.30
0.30	0.00	1	0.46	0.41	0.38	0.35	0.33	0.28	0.25	0.22	0.20
		4	0.46	0.41	0.37	0.34	0.31	0.26	0.22	0.17	0.15
		25	0.45	0.41	0.37	0.34	0.31	0.25	0.21	0.15	0.12
	0.25	1	0.49	0.48	0.46	0.43	0.41	0.37	0.34	0.30	0.28
		4	0.49	0.47	0.45	0.42	0.40	0.34	0.30	0.27	0.21
		25	0.49	0.47	0.45	0.42	0.39	0.33	0.29	0.22	0.18
	0.50	1	0.50	0.49	0.48	0.47	0.45	0.42	0.39	0.35	0.33
		4	0.50	0.49	0.47	0.46	0.44	0.39	0.34	0.27	0.26
		25	0.50	0.49	0.47	0.46	0.44	0.39	0.34	0.27	0.22
	1.00	1	0.50	0.50	0.49	0.49	0.48	0.47	0.45	0.42	0.40
		4	0.50	0.50	0.49	0.48	0.48	0.45	0.43	0.38	0.34
		25	0.50	0.50	0.49	0.48	0.47	0.44	0.41	0.35	0.30

From Utzinger and Klein (1979) as cited in Duffie and Beckman (2013)

NOTES

1 Lisa Heschong, *Thermal Delight in Architecture* (Cambridge, MA: MIT Press, 1979).
2 Ibid.
3 Ibid.
4 Mireia Vergés, Julie Meyers, and Inma Alavedra, *Light in Architecture* (Antwerp: Tectum Publishers, 2007), 18–19.
5 Ibid.
6 Ibid., 42–43.
7 Marcel Minnaert, *Light and Color in the Outdoors* (New York, NY: Springer, 1993).
8 Vergés, Meyers, and Alavedra, *Light in Architecture*, 42–43.
9 Ibid., 304–305.
10 ASHRAE, *2009 ASHRAE Handbook: Fundamentals*, SI ed. (Atlanta, GA: American Society of Heating, Refrigerating and Air-Conditioning Engineers, Inc., 2009), 17.
11 *Energy Plus Engineering Reference* (The Board of Trustees of the University of Illinois and the Regents of the University of California through the Ernest Orlando Lawrence Berkeley National Laboratory, Berkeley, CA, May 24, 2012).
12 ASHRAE, *2009 ASHRAE Handbook*.
13 John A. Duffie and William A. Beckman, *Solar Engineering of Thermal Processes*, 4th ed. (Hoboken: Wiley, 2013), 229.

14 Ivan Sutherland and Gary W. Hodgman, "Reentrant Polygon Clipping," *Communication of Association for Computing Machinery (CACM)* 17 (1974): 32–42.
15 Patrick-Gilles Maillot, "A New, Fast Method for 2D Polygon Clipping: Analysis and Software Implementation," *ACM Transactions on Graphics* 11, no. 3 (July 1992): 276–290, doi:10.1145/130881.130894.
16 Kevin Weiler and Peter Atherton, "Hidden Surface Removal Using Polygon Area Sorting," *Computer Graphics* 11, no. 2 (1977): 214–222.
17 Robert E. Jones, "Effects of Overhang Shading of Windows Having Arbitrary Azimuth," *Solar Energy* 24, no. 3 (January 1, 1980): 305–312, doi:10.1016/0038-092X(80)90488-0.
18 D. Michael Utzinger and Sanford A. Klein, "A Method of Estimating Monthly Average Solar Radiation on Shaded Receivers," *Solar Energy* 23, no. 5 (1979): 369–378, doi:10.1016/0038-092X(79)90145-2.
19 Jones, "Effects of Overhang Shading of Windows Having Arbitrary Azimuth."
20 Utzinger and Klein, "A Method of Estimating Monthly Average Solar Radiation on Shaded Receivers."

10 LIGHT AND EFFECT

In addition to understanding the scientific fundamentals of solar design, sound architectural design also considers phenomenological factors of light as an equally significant counterpart. Architecture is best when it is not only based on quantitative measurements, but also upon perception of space and color, as well as health and wellbeing. By optimizing daylight in a given space, the occupant directly and indirectly benefits from these factors and is ultimately connected to the natural environment in meaningful ways. Building standards have been created to respond to these factors, beginning around the time that electric light became required in buildings, as they were designed as internalized spaces. This was especially the case for department stores and other artifacts of commercial spaces during an economic rise. Floor plates in office buildings could then be extended and expanded due to electric light, which was then used during daylight hours.[1]

As buildings scaled up in size and electric light consumption increased, more attention was given to energy efficiency. As Mohamed Boubekri points out in his book *Daylighting, Architecture, and Health*, the emphasis for daylighting has primarily been from the perspective of energy savings.[2] Furthermore, despite technological advances in terms of electrical lighting, it continues to be one of the major energy consumers in large buildings, and even though daylighting has the potential to significantly reduce energy usage, it is not commonplace in the design of most current buildings.[3] There are many factors at play, and there is no silver bullet for enacting a way to standardize design procedures in this respect. Regulation can be difficult to quantify due to microclimatic variations and the inconsistency of daylight throughout the year. Boubekri maintains that due to these difficulties, legislation related to daylighting varies across the world and can generally be categorized into three types. The first is regarding the amount of access to sunlight a building must have, and is usually referred to as "solar zoning legislation." The second type is with regard to window requirements, in terms of their number and size. These regulations are usually contained in building codes. The third type has to do with the quantity of light in the rooms of the building.[4]

Daylit spaces have been shown to increase user comfort while also helping to stabilize circadian rhythms, increasing sleep duration and quality, and conversely increasing work productivity. In addition to revenue increases for the workplace and reduced energy costs, daylight is more broadly important for human health. Daylight is important for improved metabolism and mood levels, all of which can have a compounding effect on wellbeing. These elements rarely enter the architectural discourse at the academic and professional levels, as design critiques are typically based more exclusively on proof of concept, programmatic functionalism, and formal aesthetics. However, it has been long established that vitamin D is critical to overall health, even if it is not routinely acknowledged in architectural and engineering design processes. Boubekri notes that the sun provides us with vitamin D, through the process of photosynthesis on our skin, and that although we can get vitamin D from other sources, these amounts are small when compared to the amount we get through photosynthesis. Vitamin D deficiency is related to a number of health concerns, including depression, cancer, diabetes, high blood pressure, multiple sclerosis, and rheumatoid arthritis.[5] Beyond these conditions and hormonal issues related to a lack of sunlight, it is also problematic to not have access to windows, which can lead to stress, especially in the workplace, where employees might have limited access to windows for a number of hours at a time. Studies have shown a correlation between stress caused by lack of windows and job burnout.[6]

Although the history of solar zoning regulations is rooted in managing overshadowing and blockage of view in dense urban scenarios, it remains of prime significance due to the health concerns highlighted previously, in addition to energy conservation. This is not to mention phenomenological aspects that ultimately allow us to connect buildings to life and tangible experience. Merleau-Ponty's description of phenomenology suggests that it is much more complex than the immediacy of sensation of touch. Rather, it is based upon a history of knowledge and preconceptions, all of which influence our senses.[7] He also blurs the distinction between subject and object, which further emphasizes the potential for designers to create impactful space beyond the pure function and pragmatics.

At its essence, Modern architecture was not only based on the ethos of "form follows function," but also about boiling down physical components such that buildings could be deferential to nature—including light, air, and views. The notion of the "machine in the garden" suggested a deliberate crafting of an object that would have an inverse relationship with its natural surroundings, although not attempting to blend in. There were also negative connotations with the "International Style," as it implied that there was a "one size fits all" solution to architectural form, regardless of climate or cultural context. The linear "ribbon window" apertures were applied similarly in very different climates, giving the perception that the buildings were in fact not as responsive to their local environment as was hoped. Successful Modern architecture does fulfill this hope, and the framework for the movement allows for calibration to respond to diverse circumstances and for tailored daylighting and rich phenomenological experiences.

Directly and indirectly related to light and architecture is the element of color, an attribute that is typically not integrally addressed in the design processes of architecture and engineering. We have established that light levels and quantities affect our sensorial perceptions, and color also has a significant impact on emotional reactions, concentration, and efficiency, as well as health. Colors are known to trigger specific feelings, tying back to anthropological associations and cultural symbolism.[8] While the latter varies due to the unique values and contexts of a given culture, the former can be considered quite universal, causing subconscious reactions to stimuli across the color spectrum. Warm and cool colors are generally grouped together to represent general sets of emotions within a range of excitement or calming, respectively. Black and white have deep symbolic associations in many cultures, where white typically represents innocence and black is connected to mourning and sadness. Similarly, pairings of colors conjure up different types of emotions, as do tones and saturation levels.[9]

Perception of color is dependent on an array of criteria, and is partially related to the way that we attempt to define color with terminology. As in other realms, terminology and definition of labels, while convenient for classification, can be limiting and miss the subtlety of the actual phenomenon—in this case, the infinite spectrum of possible colors. Josef Albers argued for relativity of color, and his artworks were deliberate studies on the comparative analysis of colors.[10] His use of color paper instead of paint had to do with his interest in accuracy and consistency in the experiments. He was even interested in the purity of the color paper surface, as opposed to the texture from the applied paint brush. By eliminating the variables of inconsistent texture, Albers was able to truly study the interplay of light and color.[11] In doing so, his work gets to the essence of portraying colors that support or contrast one another, providing a different reading of a color than if it were viewed independently. As such, context is paramount in the understanding of color and its attributes, as is the case with most aspects of design. With color, there are also illusory effects that allow the context to linger or bleed into a subsequent image separated by time. This is the case with an after image or simultaneous contrast, where viewing a color physically changes the components of the retina, and this psycho-physiological phenomenon proves that "color deception," as referred to by Albers, can and does exist in at least some capacities.

In black and white photography, a conventionally ideal image has both pure white tones and pure black tones, as well as countless tones of gray between either end of the spectrum. Albers explains light intensity as lightness and color intensity as brightness, and argues the former is based on physical facts while the latter is dependent upon perceptual reactions "which permit either a factual measure or an interpretation of illusions."[12] This is precisely the type of cognizant interrelationship that architects might aspire to when designing space based on measurable criteria, yet intended to evoke subjective and personal reactions to provide meaning and experience beyond the prosaic.

Color and light are innately interconnected at all scales and across artificial and natural phenomena. Through an established grouping of sensations, it is commonly agreed upon that the sky is "blue."[13] The very fact that this is conventional thought speaks to the complexity of color optics. Infinitely varying blue skies seemingly stretch across our planet, changing daily and throughout the seasons. Although the sun is not blue, its scattered light creates the perception of the color blue in our eyes. In actuality, the sky is more violet, but our eyes are not as sensitive to the violet end of the color spectrum. The molecules within the air itself scatter the light. We see sunlight as a yellow color, as a result of the blue and violet rays that have been scattered, which becomes increasingly orange and red before sunset—a function of refraction and Rayleigh's law of small scattering particles.[14] The color of the blue sky changes in proportion to the amount of dust and water droplets present in the air. The darkest blue is experienced during the temporary cleaning up of the weather between two showers of rain, related to high pressure. Conversely, the sky becomes pale or almost white when covered with cirrus clouds, or due to dust-filled air or the summer months.[15]

In the Fine Arts, particularly painting, color and light are used as tools to evoke phenomenological sensation and set moods. The source for this ultimately goes back to inspiration from the natural environment, and the varying light and color in the atmosphere. Artist Brice Marden directly acknowledges as much:

> When I talk about the grayish white that runs up through 'White Light,' I have to talk about what it is for me to be in that grayish-white place. As I was coming uptown to the Museum this afternoon, there was the most beautiful light. New York has a great silvery light and today the city was filled with that light. The air was cleansed and the atmosphere was brilliant. As I was standing on a street corner thinking . . . I looked up and I saw one bank of clouds slightly in front going in another direction. And I look at those clouds and I feel those two large movements with real empathy, and that's just what happens in 'White Light.' Different movements work against each other and with each

> other, and this grayish white starts moving through the painting in one way [versus another].[16]

Marden is referring to Jackson Pollock's painting *White Light* and its range of gray tones as a gradient between black and white, as a tonal composition. Rather than any content or subject, Marden believes that the piece of art is defined by its interplay of light and the emotion it evokes. It can be argued that in its most pure form, architectural space can be defined by its unique qualities of light and color, rather than the overall form or the content of the space.

Marden elaborates to suggest that light is the prime subject in his art, and he views everything in terms of light. When speaking of the work of Cezanne, Marden states, "Color is a way of arriving at light. The illusion of light is one of the things that the painter works with. Without light, there is no visible image."[17] Marden is known to spend up to three days mixing a single hue of a given color because its relative light is critical to get right in consideration of where it sits in the layering of strokes and colors. To Marden, the single color itself somehow is not of significance, but rather the "weights and leanings" of the light. Cezanne, like many of the Impressionists, emphasized light over color, allowing certain colors to come to the forefront in order to create the illusion of light radiating from the canvas plane. Marden's work can be seen as an evolution in the use of light, and his "Cold Mountain" series can be seen *as* light—open with polyvalence. In the broadest and perhaps flimsiest of metaphorical generalizations, it is almost as if Marden's earlier paintings depict interior/indoor light (the viewer is outside looking into shadow), and the later paintings, exterior/outdoor light (the viewer is inside looking out to the sun).

Light brilliantly animates our surroundings in its wide ranges of tones and color, inspiring artists, photographers, and architects. The elusive allure of light can capture imaginations and create powerful atmospheres in its shifting light throughout the day, especially just before sunrise and just after sunset. There is implied depth from layers of atmospheric variation, including mist and haze, which help to reinforce foreground, middle ground, and background in the built world and with natural formations. The very fact that some weather conditions limit the possibility of a long prospect view makes a clear view much more powerful when it can be seen, such that it is not taken for granted.

Light is necessarily associated with the arts, and when paired with shadows is used to create definition and clarity in representation. Similarly, light and shadow allow us to comprehend everything around them, including depth and dimensionality. It was a breakthrough during the Renaissance for artists to accurately represent depth in general—through perspective and a realistic use of light and shadow. These characteristics are precisely what were challenged by art movements to follow. Cubism, for example, deliberately created ambiguity between two and three dimensions, and used light and dark in ways that were inconsistent with realism. This type of abstractionism is based on an understanding of the classical convention of painting, and intentionally bending the rules for effect.

Edward Hopper, a prominent 20th-century realist painter, used light for symbolic reference in his paintings. Consistency of representation of the lighting effects of everyday nuances led to his distinction as an important American artist of his era, by the very fact that he epitomized his time. In his work, Hopper utilized light, primarily daylight, to define sharp edges and contrast, while also establishing definite ambience. In addition to the deliberate use of light, Hopper also focused on repetitive themes. Gail Levins astutely observes these themes and offers interpretations of each. When painting architecture, rather than focusing on buildings as objects or spectacles, he treats it more abstractly, featuring walls, surfaces, openings (windows), and interior corners to allow the space to be understood. Typologically, Hopper often featured the theater, as he saw it as a metaphor for life, and in his paintings, he was able to direct and stage his own scenes, props, and characters.[18] Time is also a common theme in the body of work, with the mood connected to the specific time.[19] In this sense, his work responds to the ever-changing characteristics of sunlight and daylight, as well as the lack thereof, as his few night scenes portrayed a different, more somber tone. By capturing these moments, represented as nonspecific in terms of regionality and with abstracted architectural styles, the work is more transcendent, universal, and timeless. As Levins observes, Hopper uses light to paint in a way that expresses the psychological pulse of his time, while also relating to all times.[20]

Innovation in the Fine Arts also transforms our understanding of the placemaking capacity of light and at least indirectly influences architectural trajectory, particularly in the work of James Turrell, who aims to frame light and the sky in a specific fashion to require the viewer to see and understand light in a very particular way. Lighting is important for all art, although it is typically to illuminate and spotlight a piece of art, whereas the work of Turrell is *about* the light, and the piece is more of an environment in which the visitor directly visits, rather than an object or surface (i.e., painting) to observe in an otherwise diffusely and neutrally lit room. Therefore, the work of Turrell requires the attention of the viewer and transcends to a more mystical character because the materiality and construct of the work itself is not readily apparent. One might argue that successful architecture has the same level of mystery. Architecture can aspire to the same level of mysticism, while also achieving programmatic and functional agendas. In the words of Louis Kahn, "A great building must begin with the immeasurable, must go through measurable means when it is being designed, and in the end must be unmeasured."[21]

Architectural presentation drawings and renderings often aim for realism to allow the client or audience to better understand the design through an illustration that more accurately depicts how an overall form or space might look and feel, as opposed to orthographic and technical drawings used for the trade. For this very reason, some architectural renderings or illustrations choose to abstract certain aspects of view. The risk of literal representation in architectural renderings presented during the design process is that the client or viewer may focus on insignificant details that have yet to be resolved. Abstraction in architectural representation can be beneficial, particularly when that representation can tap into phenomenological realms of light and atmospherics. By boiling down the simulated experience of a space to its atmospheric light effects, both the designer and the viewer may then better discuss the essence and ultimate result of a given design. This is not to discount functional efficiency, which is either a prerequisite or must be developed hand-in-hand with the effects of light. Likewise, atmospheric renderings can delude, and should be based on a fundamental understanding, if not proper testing, of illuminance. This refers to the illuminance diagram matrices in Chapter 9 of this book. However, due to the numerous elements involved in creating the actual experience of light in a space—including light, surfaces, reflections, and colors—it can be difficult to simulate with complete accuracy. Therefore, there are limits to virtual representation in architecture, although it is often a worthwhile pursuit, rather than solely focusing on programmatic function, at the neglect of experience.

Taken to the other logical extreme, the Fine Arts have the potential to create an exclusively experiential space, with no function in the sense of a conventional architectural program. This principle is demonstrated with light as the primary ingredient by Olafur Eliasson's *Weather Project*, a 2003 installation at the Tate Modern in London. Consisting of a mechanical sun created by yellow mono-frequency lamps, mirrors, and artificial fog streamed into the space, the hazy sun captivated its audiences. It was displayed in the Turbine Hall of the museum, the largest single gallery space in the world at approximately 500 feet in length, and its presence filled the entire space in a way that made it impossible to ignore. Visitors acclimated to the melancholic London winters were able to experience a simulation of the sun and they indeed soaked it in. Eliasson believes that weather is a societal construct as much as it is a scientific phenomenon, and that it affects many elements of life from political to sensorial realms. With the artificial sun placed at the far end of the gallery space, the installation allowed for a long procession sequence to the device itself before the revelation of the sun's tectonic assembly. Intensifying the experience, suspended from the ceiling was an aluminum frame, clad with reflective mirrored foil, extending the perceptual height of the space and further blurring any concrete sense of the surroundings.

The *Weather Project* was Eliasson's most popular installation—one in which visitors lingered to fully experience it—which is highly atypical in a gallery. At most, visitors will observe a piece of art for a moment and read the placard description, but not stop and sit or lie to simply "be" with it. This careful use of light as an attractor and socially unifying element can be a lesson to architects and engineers, as it proves that the character of a space is much more than the proportion and tectonics of the structure. The installation harkens back to the primordial instinctual tendencies of sun worship by our ancestors, relating to its mysticism. At some point, the dimensional attributes of a space can be trumped by other sensorial effects. A single focal point can attract attention in the space at a particular spot while also consuming the majority of the space in its effect. Sanford Kwinter points out that Eliasson claims that his work intends for us to "see ourselves seeing" by being in tune with the way the world affects us and also how we manipulate it once we understand it within our senses. Kwinter states, "The 'world neither pre-exists us nor do we exist separately and passively within it. We are not 'in' the world but in fact *are* part of the world itself."[22]

Conversely, the Moonlight Towers in Austin, Texas, were given their name due to their inspiration from moonlight. Constructed in the late 19th century at more than 150 feet in height, the towers acted as beacons that transformed their surrounding environment at night, providing district lighting. However, unlike Eliasson's *Weather Project*, they were completely utilitarian in purpose, intended to increase safety following a string of murders in the city. Originally, illumination was created by carbon arc lamps atop the towers, and could provide light over a radius of one quarter mile. The lamps were replaced by newer types throughout the years, but with the same effect. Long after street lamps popped up in the city and other forms of illumination made the towers less functional, they were later recognized to have historical value, and those remaining were reconstructed by the city.

Figure 10.1
Olafur Eliasson's *Weather Project*.
Weather Project by Olafur Eliasson at Tate Modern, 2003
©Mike Kemp/In Pictures/Corbis

Architects possess control of light in many means, including the crafting of an overall form. Le Corbusier (Jeanneret) stated, "The elements of architecture are light and shade, walls and space."[23] In practical terms, the calibration of light is determined by quantitative factors, including aperture ratios and locations. The effects, however, are decidedly qualitative and sensorial. Steven Holl eloquently states:

> The experience of space, light, and material as well as the socially condensing forces of architecture are the fruit of a developed idea. When the intellectual realm, the realm of ideas, is in balance with the experiential realm, the realm of phenomena, form is animated with meaning. In this balance, architecture has both intellectual and physical intensity, with the potential to touch the mind, eye, and soul.[24]

Fundamentally, there are limits to understanding phenomenology in a cerebral sense. Steven Holl describes phenomenology as a sort of hidden dimension that can only be understood by direct and haptic experience.[25] Light and shadow communicate with the occupant of a space, and the phenomenon of light reflecting off a brightly colored surface onto a white surface can subtly project color onto a neutrally colored surface, which creates a unique spatial perception. In his view, for architecture to genuinely address perception, pragmatism must be suspended to allow for exploration.[26] Furthermore, Holl makes a direct case for subjectivity in architecture, in conjunction with objectivity, and parses out a difference between visual appearance and core substance. This is a bold and refreshing stance, as architects often err strictly on the side of rationalization to explain their work, including creating endless series of diagrams to explain operations and design moves. The intent of this book is to address the objective, or scientific, aspects of light and design, while also addressing and including subjective and poetic elements.

Light, as an ever-present element throughout all aspects of life, is critical to understand and carefully incorporate in the architectural design and engineering processes. For architecture to have meaning for its occupants, it must respond to their cultural, social, and environmental concerns. Light, as a predecessor for all existence, is directly related to energy, health, function, and perceptual experiences. Architectural science and architectural theory are typically not integrated or even generally understood by a single entity in the architectural design process. Poetic and aesthetic aspects are conventionally the responsibility of the architect while the pragmatic and scientific components are relegated to the engineer and/or other consultants. In addition to acting as a handbook and reference guide for solar design principles, this book is a call for a discourse addressing both realms, for the sake of designing more efficient and effective structures. There has been a recent proliferation of design standards and building standards, all of which have the noble intent to improve the performance of buildings and the wellbeing of its occupants. However, said standards should exist as more than boxes to check to prove compliance. Instead, the standards are inherently more valuable and successful if the larger intent of the standards is understood and embraced by designers as they relate to quantitative measures and qualitative results. As the term "sustainability" becomes more ubiquitous, it becomes diluted and requires a thorough understanding beyond collecting points in a standards system. In this vein, it is critical to keep sight on the less tangible, phenomenological impacts of light. When applied properly in architecture, light enriches health and the soul through artistic and aesthetic means, as well as overall efficiency and effectiveness such that structures may respond to the immediacy of their place as well as larger universal principles that unite all of humankind.

NOTES

1 Chris van Uffelen, *Light in Architecture* (Salenstein, Switzerland: Braun, 2012).
2 Mohamed Boubekri, *Daylighting, Architecture and Health: Building Design Strategies* (Amsterdam; Boston; London: Architectural, 2008), http://site.ebrary.com/id/10251259.
3 Ibid.
4 Ibid.
5 Ibid.
6 Ibid.
7 Maurice Merleau-Ponty, *Phenomenology of Perception* (London and New York: Routledge, 1962).
8 Mireia Vergés, Julie Meyers, and Inma Alavedra, *Light in Architecture* (Antwerp: Tectum Publishers, 2007), 154–155.
9 Ibid.
10 Josef Albers, Fred Licht, and Nicholas F. Weber, *Josef Albers Glass, Color, and Light* (New York, NY: Guggenheim Museum, 1994).
11 Ibid.
12 Ibid.

13 Edmund T. Whittaker, *From Euclid to Eddington, a Study of Conceptions of the External World* (Cambridge, England: University Press, 1949), 2.
14 Marcel G. J. Minnaert, *The Nature of Light & Colour in the Open Air* (New York: Dover Publications, 1954).
15 Ibid.
16 Brenda Richardson, *Brice Marden: Cold Mountain* (Houston, TX: Houston Fine Art Press, 1992).
17 Ibid.
18 Edward Hopper and Gail Levin, *Edward Hopper: The Art and the Artist* (New York: Norton; Whitney Museum of American Art, 1980).
19 Ibid.
20 Ibid.
21 Louis Kahn, “The Value and Aim in Sketching,” *T Square Club Journal* 1, no. 6 (May 1930).
22 Sanford Kwinter, “The Reenchantment of the Interior: Olafur Eliasson’s Weather Project,” *Harvard Design Magazine*, Fall/Winter 2008/2009.
23 Charles-Édouard Jeanneret, *Vers une Architecture* (Paris: Crès, 1923).
24 Steven Holl and Architektur Zentrum Wien, *Steven Holl: Idea and Phenomena* (Baden, Switzerland: Lars Müller, 2002).
25 Ibid.
26 Ibid.

APPENDICES

APPENDIX A: MATHEMATICAL SYMBOLS

Term	*Symbol*
area	A
effective absorptance of a room cavity	a_{cav}
mean absorptance of room cavity surfaces	a_i
projected area	A
solar time, apparent solar time	AST
area of window	A_{win}
calendar date orbital angle	B
insolation, daily total (without subscript refers to global)	D
daylight saving time	DST
elevation shading angle	ESA
equation of time	ET
solar irradiance (without subscript refers to available global)	G
hour angle	H
hour angle at (subscript)	H'
horizontal exposure angle	HEA
horizontal shading angle	HSA
insolation, hourly (without subscript refers to available global)	I
inch-pound system	IP
latitude	L
longitude time adjustment	LA
longitude	LON
local standard meridian	LSM
local standard time	LST
ordinal date	n
surface normal vector components	n_s, n_w, n_z
heat flux	Q
relative beam radiation	R_b
relative beam radiation on the horizontal	R_{bh}
relative diffuse radiation	R_d
solar heat gain coefficient	$SHGC$
system international	SI
transmittance of glass at normal incidence	T
total solar irradiance	TSI
time zone	TZ
transmittance	T_θ
U factor (U value)	U

Term	*Symbol*
Coordinated Universal Time	*UTC*
vertical exposure angle	*VEA*
ground view factor	V_g
sky view factor	V_s
vertical shading angle	*VSA*
visible transmittance	*VT*
zenith angle	Z
azimuth	α
surface azimuth, bearing	α_{sf}
solar azimuth	α_{sol}
altitude	β
solar altitude	β_{sol}
surface-solar azimuth	$\mathit{\Gamma}$
orbital angle	$\mathit{\Gamma}$
declination	$\mathit{\Delta}$
angle of incidence	$\mathit{\Theta}$
ground reflected radiation	P
tilt angle	$\mathit{\Sigma}$
normal direction cosine, sigma normal	σ_n
direction cosines	σ_s, σ_w, σ_z
elevation angle	$\mathit{\Omega}_{el}$
profile angle	$\mathit{\Omega}_{pf}$

SUBSCRIPT SYMBOLS

Term	*Symbol*
at solar noon	*12*
at 90°	*90*
morning	*am*
available direct beam	*b*
direct beam on a horizontal surface	*bh*
cavity	*cav*
available sky diffuse	*d*
east	*e*
elevation	*el*
elevation shading angle	*ESA*
exposure	*exp*
ground reflected	*g*
horizontal	*h*
horizontal exposure angle	*HEA*
horizontal shading angle	*HSA*
internal	*i*
normal	*n*
extraterrestrial	*on*
projected	*p*
profile	*pf*
afternoon	*pm*

(*Continued*)

Term	*Symbol*
relative to a point	*pt*
south, sky	*s*
surface	*sf*
shaded	*shd*
sun, solar	*sol*
sunrise	*sr*
sunset	*ss*
total on surface	*T*
total direct beam on surface	*tb*
total sky diffuse global on surface	*td*
total ground reflected on surface	*tg*
vertical exposure angle	*VEA*
vertical shading angle	*VSA*
west	*w*
window	*win*
"plan" east-west	*x*
relative to the x-x axis	*xx*
"plan" north-south	*y*
relative to the y-y axis	*yy*
zenith direction	*z*
at a given angle of incidence	θ
as if surface had a tilt of 90°	$\Sigma 90$

APPENDIX B: EQUATIONS LIST

List Equation Number	*Description*	*Actual Equation*
Equation 2.1	Orbital Angle	$\Gamma = 360°\left(\frac{n+284}{365}\right)$
Equation 2.2	Hour Angle	$H = 15°(AST - 12.00\ \text{h})$
Equation 2.3	Local Standard Meridian	$LSM = 15°(TZ)$
Equation 2.4	Longitude Time Adjustment	$LA = \frac{LON - LSM}{15°}$
Equation 2.5a	Calendar Date Orbital Angle	$B = 360°\left(\frac{n-1}{365}\right)$
Equation 2.5b	Calendar Date Orbital Angle from Solar Orbital Angle	$B = \Gamma - 281.096$
Equation 2.6	Equation of Time	$ET = 2.2918\,[0.0075 + 0.1868\cos(B) - 3.2077\sin(B) - 1.4615\cos(2B) - 4.089\sin(2B)]$
Equation 2.7	Apparent Solar Time Conversion from LST	$AST = LST + \frac{ET}{60\ \text{min}} + LA$
Equation 2.8	Convert DST to LST	LST=DST-1
Equation 2.9	Solar Declination	$\delta = 23.45°\ \Gamma$
Equation 2.10	Zenith Angle at Solar Noon	$Z_{12} = L - \delta$
Equation 2.11	Zenith Angle at Solar Noon on Equinox	Z_{12}=L
Equation 3.1	Zenith And Altitude Angle Relationship	$\beta = 90^{\circ} - Z$
Equation 3.2	Solar Altitude	$\sin\beta_{sol} = \cos L \cos\delta \cos H + \sin L \sin\delta$
Equation 3.3a	Solar Azimuth if AST ≥ 12:00	$\alpha_{sol} = \cos^{-1}\left(\frac{\cos H \cos\delta \sin L - \sin\delta \cos L}{\cos\beta}\right)$
Equation 3.3b	Solar Azimuth if AST < 12:00	$\alpha_{sol} = -\cos^{-1}\left(\frac{\cos H \cos\delta \sin L - \sin\delta \cos L}{\cos\beta}\right)$
Equation 3.4	Hour Angle at Sunset	$\cos H_{ss} = -\tan L \tan\delta$

(*Continued*)

List Equation Number	*Description*	*Actual Equation*
Equation 3.5	Solar Azimuth at Sunset	$\alpha_{ss} = 90° + \sin^{-1}(\cos Z_{12} \tan L - \sin Z_{12})$
Equation 3.6	Declination at Hour Rise (for Sun-Path Diagrams)	$\tan\delta = -\frac{\cos H}{\tan L}$
Equation 3.7	West Direction Cosine	$\sigma_w = \sin\alpha_{sol} \cos\beta_{sol}$
Equation 3.8	South Direction Cosine	$\sigma_s = \cos\alpha_{sol} \cos\beta_{sol}$
Equation 3.9	Zenith Direction Cosine	$\sigma_z = \sin\beta_{sol}$
Equation 3.10	Pythagorean Check of Cartesian Coordinates	$1^2 = \sqrt{\sigma_w^2 + \sigma_s^2 + \sigma_z^2}$
Equation 3.11	X-Coordinate for Equidistant Diagram	$x_{eq} = \sin\alpha_{sol}\left(\frac{90° - \beta_{sol}}{90°}\right)$
Equation 3.12	Y-Coordinate for Equidistant Diagram	$y_{eq} = \cos\alpha_{sol}\left(\frac{90° - \beta_{sol}}{90°}\right)$
Equation 3.13	X-Coordinate for Stereographic Projection	$x_{st} = \sin\alpha_{sol}\left(\frac{\sin(90° - \beta_{sol})}{\sin\beta_{sol} + 1}\right)$
Equation 3.14	Y-Coordinate for Stereographic Projection	$y_{st} = \cos\alpha_{sol}\left(\frac{\sin(90° - \beta_{sol})}{\sin\beta_{sol} + 1}\right)$
Equation 3.15	X-Coordinate for Cylindrical Projection	$x_{cy} = \left(\frac{\alpha_{sol}}{360°}\right)2\pi$
Equation 3.16	Y-Coordinate for Cylindrical Projection	$y_{cy} = \sin\beta_{sol}$
Equation 3.17	Y-Coordinate for Modified Cylindrical Projection	$y_{mc} = \sqrt{(1 - \cos\beta_{sol})^2 + (\sin\beta_{sol})^2}$
Equation 4.1	Extraterrestrial Radiant Flux	$G_o = TSI\left[1 + 0.033\cos\left(\frac{360° n}{365}\right)\right]$
Equation 4.2	Hourly Fraction of Sky Diffuse Insolation	$r_d = \frac{\pi}{24}\left(\frac{\cos H - \cos H_{ss}}{\sin H_{ss} - \frac{\pi H_{ss}}{180}\cos H_{ss}}\right)$
Equation 4.3	Estimated Hourly Sky Diffuse Insolation from Daily Value	$I_d = D_d\, r_d$
Equation 4.4	Hourly Fraction of Global Insolation	$r_t = (a + b\cos H)\, r_d$
Equation 4.4a	Hourly Global Ratio Coefficient A	$a = 0.409 + 0.5016\sin(H_{ss} - 60°)$
Equation 4.4b	Hourly Global Ratio Coefficient B	$b = 0.6609 - 0.4767\sin(H_{ss} - 60°)$
Equation 4.5	Estimated Hourly Global Horizontal Insolation from Daily Total	$I = D\ r_t$
Equation 4.6	Hourly Beam Insolation from Global Horizontal and Sky Diffuse	$I_b = \frac{I - I_d}{\sin\beta_{sol}}$
Equation 4.7	Clear Day Direct Beam Irradiance	$G_b = \frac{A}{\exp\left(\frac{B}{\sin\beta_{sol}}\right)}$

List Equation Number	*Description*	*Actual Equation*
Equation 4.8	Clear Day Hourly Sky Diffuse Irradiance	$G_d = G_b \ C$
Equation 5.1	South Normal Vector Component	$n_s = \cos\alpha_{sf}\cos(90° - \Sigma)$
Equation 5.2	West Normal Vector Component	$n_w = \sin\alpha_{sf}\cos(90° - \Sigma)$
Equation 5.3	Zenith Normal Vector Component	$n_z = \sin(90° - \Sigma)$
Equation 5.4	Pythagorean Check for Surface Normal Vector Components (Cartesian) (4)	$1^2 = \sqrt{n_s^2 + n_w^2 + n_z^2}$
Equation 5.5	Surface-Solar Azimuth	$\gamma = \alpha_{sol} - \alpha_{sf}$
Equation 5.6	Angle of Incidence	$\cos\theta = \cos\beta_{sol}\cos\gamma\sin\Sigma + \sin\beta_{sol}\cos\Sigma$
Equation 5.7	Offset Hour Angle for Surface Facing Equator in Northern Hemisphere	$H'_{ss} = \min\begin{bmatrix}\cos^{-1}(-\tan L\tan\delta)\\ \cos^{-1}(-\tan(L-\Sigma)\tan\delta)\end{bmatrix}$
Equation 5.8a	Absolute Value of Hour Angle of Onset for Surface of Arbitrary Tilt and Orientation	$\lvert H'_{sr}\rvert = \min\left[H_{ss}, \cos^{-1}\frac{AB + C\sqrt{A^2 - B^2 + C^2}}{A^2 + C^2}\right]$
Equation 5.8b	Onset Hour Angle for Surface of Arbitrary Tilt and Orientation	$H'_{sr} = \begin{Bmatrix}-\lvert H'_{sr}\rvert & if\,(A>0\ and\ B>0)\,or\,(A\geq B)\\ +\lvert H'_{sr}\rvert & otherwise\end{Bmatrix}$
Equation 5.8c	Absolute Value of Hour Angle of Offset for Surface of Arbitrary Tilt and Orientation	$\lvert H'_{ss}\rvert = \min\left[H_{ss}, \cos^{-1}\frac{AB - C\sqrt{A^2 - B^2 + C^2}}{A^2 + C^2}\right]$
Equation 5.8d	Offset Hour Angle for Surface of Arbitrary Tilt and Orientation	$H'_{ss} = \begin{Bmatrix}+\lvert H'_{ss}\rvert & if\,(A>0\ and\ B>0)\,or\,(A\geq B)\\ -\lvert H'_{ss}\rvert & otherwise\end{Bmatrix}$
Equation 5.8e	Surface Onset/Offset Coefficient A	$A = \cos\Sigma + \tan L\cos\gamma\sin\Sigma$
Equation 5.8f	Surface Onset/Offset Coefficient B	$B = \cos H_{ss}\cos\Sigma + \tan\delta\sin\Sigma\cos\gamma$
Equation 5.8g	Surface Onset/Offset Coefficient C	$C = \frac{\sin\Sigma\sin\gamma}{\cos L}$
Equation 5.9	Relative Beam Radiation	$R_b = \cos\theta$
Equation 5.10	Relative Beam Radiation, Cartesian	$R_b = \sigma_s n_s + \sigma_w n_w + \sigma_z n_z$
Equation 5.11	Hourly Beam Insolation on a Surface	$I_{tb} = I_b R_b$
Equation 5.12	Relative Beam Radiation on the Horizontal	$R_{bh} = \sin\beta_{sol}$
Equation 5.13	Hourly Beam Insolation on the Horizontal	$I_{bh} = I_b R_{bh}$
Equation 5.14	Isotropic Sky View Factor	$V_s = \frac{1 + \cos\Sigma}{2}$
Equation 5.15	Hourly Sky Diffuse Insolation on a Surface, Isotropic	$I_{tb} = I_d V_s$
Equation 5.16	Anisotropic Sky Factor	$Y = \max\{0.45, 0.55 + 0.437\cos\theta_{\Sigma 90} + 0.313\cos^2\theta_{\Sigma 90}\}$
Equation 5.17a	Hourly Sky Diffuse Insolation on a Surface, Anisotropic	$I_{td} = I_d \ Y\sin\Sigma$
Equation 5.17b	Surface Sky Diffuse Insolation, Anisotropic	$I_{td} = I_d(Y\sin\Sigma + \cos\Sigma)$

(*Continued*)

List Equation Number	*Description*	*Actual Equation*
Equation 5.18	View Factor, Ground	$V_g = \frac{1-\cos\Sigma}{2}$
Equation 5.19	Global Horizontal Insolation	$I = I_{bh} + I_d$
Equation 5.20	Ground Reflected Insolation on a Surface	$I_{tg} = I\,\rho_g V_g$
Equation 5.21	Surface Global Insolation	$I_T = I_{tb} + I_{td} + I_{tg}$
Equation 5.22	Surface Global Insolation, All Components (Isotropic Model)	$I_T = I_b \cos\theta + I_d\left(\frac{1+\cos\Sigma}{2}\right) + \left(I_b \sin\beta_{sol} + I_d\right)\rho_g\left(\frac{1-\cos\Sigma}{2}\right)$
Equation 5.23	Daily Total Insolation	$D = \sum_{24:00}^{0:00} I_T$
Equation 6.1	Profile Angle (Solar)	$\tan\Omega_{pf} = \frac{\tan\beta_{sol}}{\cos\gamma}$
Equation 6.2	Elevation Angle	$\tan\Omega_{el} = \frac{\tan\beta_{sol}}{\sin\gamma}$
Equation 6.3	Location of Shadow on Horizontal Plane (X)	$x = \frac{h}{\tan\Omega_{pf-xx}}$
Equation 6.4	Location of Shadow on Horizontal Plane (Y)	$y = \frac{h}{\tan\Omega_{pf-yy}}$
Equation 6.5	Transposition of Sun Position to Arbitrary Surface, Sigma X Component	$\sigma_x = -\sin(\alpha_{sf})\sigma_s + \cos(\alpha_{sf})\sigma_w$
Equation 6.6	Transposition of Sun Position to Arbitrary Surface, Sigma Y Component	$\sigma_y = \cos(\Sigma)\cos(\alpha_{sf})\sigma_s + \cos(\Sigma)\sin(\alpha_{sf})\sigma_w - \sin(\Sigma)\sigma_z$
Equation 6.7	Shadow Point Coordinate, X Component	$x = -h\,\frac{\delta_x}{R_b}$
Equation 6.8	Shadow Point Coordinate, Y Component	$y = -h\,\frac{\delta_y}{R_b}$
Equation 7.1	Altitude of a Point	$tan\beta_{p_t} = \frac{ht}{d}$
Equation 9.1	Solar Heat Gain Coefficient	$SHGC = T + a_{glass} \cdot N$
Equation 9.2	Transmission of Direct Beam Radiation through Glass	$T_\theta = SHGC\ cos\theta\ \left[1+\left(0.768+0.817SHGC^4\right)\sin^3\theta\right]$
Equation 9.3	Estimate of Hemispherical Diffuse Transmittance	$T_d = 0.86\,SHGC$
Equation 9.4	Hourly Direct Beam Heat Gain through Window	$Q_b = I_{tb}AT_\theta$
Equation 9.5	Hourly Diffuse Heat Gain through Window	$Q_d = I_{td}AT_d$
Equation 9.6	Effective Absorptivity of Room	$a_{cav} = \frac{a_i}{a_i + (1-a_i)T_d\frac{A_{win}}{A_i}}$
Equation 9.7	Solar Gain through Windows	$Q_{sol} = (Q_b + Q_d)a_{cav}$

APPENDIX C: SOLAR TABLES

SOLAR POSITION COORDINATES

The following solar tables give solar data at the indicated latitude in apparent solar time for the design days. The first value for each month is the time of sunrise, followed by solar data for each hour up to solar noon. Because solar geometry is symmetrical around solar noon, the second half of the day is omitted. Solar azimuth in the afternoon is simply the negative of the position at the symmetrical hour in the morning and, likewise, the west direction cosine for the afternoon is the negative of the morning value. For example, if at 10:00 $\alpha_{sol} = -31.16°$ and $\sigma_w = -0.46$, then at 14:00 $\alpha_{sol} = 31.16°$ and $\sigma_w = 0.46$.

A single Cartesian coordinate in the table may reach 1.00, particularly for the south direction, while also having a value slightly greater than zero for other directions. This is especially apparent at high latitudes when the sun is close to the horizon and is due to rounding the values to two digits for the tables. When any one coordinate reaches unity (the radius of the sky dome), this indicates the sun is positioned on the surface of the sky dome along that axis. When this is the case, the other coordinate values must be zero, as is evident from the Pythagorean theorem check (Equation 3.10) for Cartesian coordinates.

Insolation

Irradiation/Insolation values are calculated using a slight variation on the clear-sky method presented in Chapter 4. These values are useful to illustrate the effect of latitude on irradiation. They are meant only to provide a rough estimate of extreme-case scenarios; in most cases, actual irradiation levels will be substantially less on average due to atmospheric attenuation.

In order to keep the tables compact, several approximations were made in the irradiation calculations. The three coefficients used for each month in the clear-sky model are not quite symmetrical across the solstices due to the eccentricity of the Earth's orbit, although solar position relative to a point on Earth is. For the values in the tables, these coefficients were averaged for symmetrical design days, such as those for May and July. Because clear-sky radiation values are not indicative of typical conditions for any given location anyway, the small amount of error this approach introduces is not of consequence for most applications. For design purposes, one should always consult typical weather data. See Chapter 4 for a discussion of various solar radiation data sources.

$L = 0°$	Approx. Clear-Sky Irradiation (Wh/m^2)									
	AST	α_{sol}(°)	β_{sol} (°)	σ_s	σ_w	σ_z	I_b	I_d	I	
Dec	6:00	–66.55	0.00	0.40	–0.92	0.00				
	7:00	–65.82	13.74	0.40	–0.89	0.24	665	68	226	
	8:00	–63.39	27.30	0.40	–0.79	0.46	885	91	497	
	9:00	–58.47	40.44	0.40	–0.65	0.65	969	100	728	
	10:00	–49.06	52.61	0.40	–0.46	0.79	1,008	104	905	
	11:00	–30.82	62.39	0.40	–0.24	0.89	1,027	106	1,016	
	12:00	0.00	66.55	0.40	0.00	0.92	1,032	106	1,054	
								1,044	7,799	D (Wh/m^2/day)
Jan/Nov	6:00	–69.69	0.00	0.35	–0.94	0.00				
	7:00	–69.04	14.05	0.35	–0.91	0.24	665	69	231	
	8:00	–66.86	27.96	0.35	–0.81	0.47	883	92	506	
	9:00	–62.37	41.54	0.35	–0.66	0.66	965	101	741	
	10:00	–53.49	54.31	0.35	–0.47	0.81	1,004	105	920	
	11:00	–34.97	64.94	0.35	–0.24	0.91	1,022	107	1,033	
	12:00	0.00	69.69	0.35	0.00	0.94	1,027	107	1,071	
								1,056	7,931	D (Wh/m^2/day)
Feb/Oct	6:00	–78.28	0.00	0.20	–0.98	0.00				
	7:00	–77.87	14.68	0.20	–0.95	0.25	659	71	238	
	8:00	–76.52	29.31	0.20	–0.85	0.49	871	94	520	
	9:00	–73.64	43.82	0.20	–0.69	0.69	951	102	761	
	10:00	–67.46	57.99	0.20	–0.49	0.85	989	106	945	
	11:00	–51.27	71.04	0.20	–0.25	0.95	1,007	108	1,061	
	12:00	0.00	78.28	0.20	0.00	0.98	1,012	109	1,100	
								1,072	8,150	D (Wh/m^2/day)
Mar/Sep	6:00	–90.00	0.00	0.00	–1.00	0.00				
	7:00	–90.00	15.00	0.00	–0.97	0.26	627	72	234	
	8:00	–90.00	30.00	0.00	–0.87	0.50	840	97	517	
	9:00	–90.00	45.00	0.00	–0.71	0.71	921	106	757	
	10:00	–90.00	60.00	0.00	–0.50	0.87	959	110	941	
	11:00	–90.00	75.00	0.00	–0.26	0.97	977	112	1,057	
	12:00	0.00	90.00	0.00	0.00	1.00	983	113	1,096	
								1,108	8,108	D (Wh/m^2/day)
Apr/Aug	6:00	–101.73	0.00	–0.20	–0.98	0.00				
	6:00	–101.73	0.00	–0.20	–0.98	0.00	0	0	0	
	7:00	–102.13	14.68	–0.20	–0.95	0.25	565	72	215	
	8:00	–103.48	29.31	–0.20	–0.85	0.49	786	100	484	
	9:00	–106.36	43.82	–0.20	–0.69	0.69	871	111	714	
	10:00	–112.54	57.99	–0.20	–0.49	0.85	912	116	889	
	11:00	–128.73	71.04	–0.20	–0.25	0.95	932	118	999	
	12:00	180.00	78.28	–0.20	0.00	0.98	937	119	1,037	
								1,152	7,640	D (Wh/m^2/day)
May/Jul	6:00	–110.31	0.00	–0.35	–0.94	0.00				
	7:00	–110.96	14.05	–0.35	–0.91	0.24	521	70	196	
	8:00	–113.14	27.96	–0.35	–0.81	0.47	747	100	450	
	9:00	–117.63	41.54	–0.35	–0.66	0.66	836	112	667	
	10:00	–126.51	54.31	–0.35	–0.47	0.81	879	118	832	
	11:00	–145.03	64.94	–0.35	–0.24	0.91	900	121	936	
	12:00	180.00	69.69	–0.35	0.00	0.94	906	121	971	
								1,162	7,132	D (Wh/m^2/day)
Jun	6:00	–113.45	0.00	–0.40	–0.92	0.00				
	7:00	–114.18	13.74	–0.40	–0.89	0.24	501	69	188	
	8:00	–116.61	27.30	–0.40	–0.79	0.46	730	100	435	
	9:00	–121.53	40.44	–0.40	–0.65	0.65	821	112	645	
	10:00	–130.94	52.61	–0.40	–0.46	0.79	865	119	806	
	11:00	–149.18	62.39	–0.40	–0.24	0.89	886	121	907	
	12:00	180.00	66.55	–0.40	0.00	0.92	893	122	941	
								1,164	6,901	D (Wh/m^2/day)
									2,816	kWh/m^2/year

L = 2°	*Approx. Clear-Sky Irradiation (Wh/m²)*								
	AST	α_{sol}*(°)*	β_{sol} *(°)*	σ_s	σ_w	σ_z	I_b	I_d	I
Dec	6:03	–00.53	0.00	0.40	–0.92	0.00			
	7:00	–05.38	12.91	0.41	–0.89	0.22	641	66	209
	8:00	–02.49	26.39	0.41	–0.79	0.44	877	90	480
	9:00	–57.00	39.38	0.42	–0.65	0.63	964	99	711
	10:00	–47.10	51.27	0.43	–0.46	0.78	1,005	104	887
	11:00	–28.98	60.66	0.43	–0.24	0.87	1,024	105	998
	12:00	0.00	64.55	0.43	0.00	0.90	1,030	106	1,036
								1,035	7,608 *D* (Wh/m²/day)
Jan/Nov	0:02	–09.08	0.00	0.35	–0.94	0.00			
	7:00	–08.58	13.32	0.36	–0.91	0.23	644	67	216
	8:00	–05.91	27.16	0.36	–0.81	0.46	875	91	491
	9:00	–00.84	40.59	0.37	–0.66	0.65	961	100	726
	10:00	–51.34	53.09	0.38	–0.47	0.80	1,001	105	905
	11:00	–32.07	63.28	0.38	–0.24	0.89	1,020	107	1,017
	12:00	0.00	67.69	0.38	0.00	0.93	1,025	107	1,056
								1,048	7,765 *D* (Wh/m²/day)
Feb/Oct	0:01	–78.27	0.00	0.20	–0.98	0.00			
	7:00	–77.37	14.25	0.21	–0.95	0.25	648	70	229
	8:00	–75.44	28.83	0.22	–0.85	0.48	867	93	511
	9:00	–71.83	43.22	0.23	–0.69	0.68	949	102	752
	10:00	–04.58	57.18	0.23	–0.49	0.84	988	106	936
	11:00	–47.03	69.74	0.24	–0.25	0.94	1,006	108	1,052
	12:00	0.00	76.28	0.24	0.00	0.97	1,011	109	1,091
								1,067	8,052 *D* (Wh/m²/day)
Mar/Sep	0:00	–90.00	0.00	0.00	–1.00	0.00			
	7:00	–89.40	14.99	0.01	–0.97	0.26	627	72	234
	8:00	–88.85	29.98	0.02	–0.87	0.50	840	97	516
	9:00	–88.00	44.97	0.02	–0.71	0.71	921	106	757
	10:00	–80.54	59.94	0.03	–0.50	0.87	959	110	941
	11:00	–82.58	74.87	0.03	–0.26	0.97	977	112	1,056
	12:00	0.00	88.00	0.03	0.00	1.00	983	113	1,095
								1,108	8,102 *D* (Wh/m²/day)
Apr/Aug	5:58	–101.73	0.00	–0.20	–0.98	0.00			
	0:00	–101.72	0.41	–0.20	–0.98	0.01	0	0	0
	7:00	–101.61	15.09	–0.19	–0.95	0.26	576	73	223
	8:00	–102.37	29.76	–0.19	–0.85	0.50	789	100	492
	9:00	–104.49	44.35	–0.18	–0.69	0.70	873	111	721
	10:00	–109.51	58.71	–0.17	–0.49	0.85	914	116	897
	11:00	–123.87	72.23	–0.17	–0.25	0.95	933	118	1,007
	12:00	180.00	80.28	–0.17	0.00	0.99	938	119	1,044
								1,157	7,723 *D* (Wh/m²/day)
May/Jul	5:57	–110.32	0.00	–0.35	–0.94	0.00			
	0:00	–110.30	0.69	–0.35	–0.94	0.01	0	0	0
	7:00	–110.48	14.76	–0.34	–0.91	0.25	539	72	210
	8:00	–112.14	28.73	–0.33	–0.81	0.48	754	101	463
	9:00	–116.02	42.44	–0.32	–0.66	0.67	840	113	680
	10:00	–124.19	55.47	–0.32	–0.47	0.82	882	118	845
	11:00	–142.40	66.56	–0.32	–0.24	0.92	902	121	949
	12:00	180.00	71.69	–0.31	0.00	0.95	908	122	984
								1,172	7,276 *D* (Wh/m²/day)
Jun	5:50	–113.47	0.00	–0.40	–0.92	0.00			
	0:00	–113.44	0.80	–0.40	–0.92	0.01	0	0	0
	7:00	–113.72	14.55	–0.39	–0.89	0.25	523	72	203
	8:00	–115.66	28.18	–0.38	–0.79	0.47	738	101	450
	9:00	–120.04	41.47	–0.38	–0.65	0.66	826	113	660
	10:00	–128.89	53.89	–0.37	–0.46	0.81	869	119	821
	11:00	–147.08	64.09	–0.37	–0.24	0.90	889	122	921
	12:00	180.00	68.55	–0.37	0.00	0.93	895	123	956
								1,176	7,065 *D* (Wh/m²/day)
									2,813 kWh/m²/year

L = 4°	Approx. Clear-Sky Irradiation (Wh/m²)								
	AST	α_{sol}(°)	β_{sol} (°)	σ_s	σ_w	σ_z	I_b	I_d	I
Dec	6:06	–66.49	0.00	0.40	–0.92	0.00			
	7:00	–64.98	12.07	0.41	–0.89	0.21	613	63	191
	8:00	–61.63	25.46	0.43	–0.79	0.43	867	89	462
	9:00	–55.72	38.27	0.44	–0.65	0.62	959	99	693
	10:00	–45.40	49.89	0.45	–0.46	0.76	1,001	103	869
	11:00	–27.36	58.90	0.46	–0.24	0.86	1,021	105	980
	12:00	0.00	62.55	0.46	0.00	0.89	1,027	106	1,017
								1,025	7,407 *D* (Wh/m²/day)
Jan/Nov	6:05	–69.64	0.00	0.35	–0.94	0.00			
	7:00	–68.15	12.59	0.36	–0.91	0.22	622	65	201
	8:00	–64.99	26.33	0.38	–0.81	0.44	867	91	475
	9:00	–59.38	39.59	0.39	–0.66	0.64	956	100	709
	10:00	–49.33	51.81	0.40	–0.47	0.79	998	104	888
	11:00	–30.66	61.58	0.41	–0.24	0.88	1,017	106	1,001
	12:00	0.00	65.69	0.41	0.00	0.91	1,023	107	1,039
								1,039	7,588 *D* (Wh/m²/day)
Feb/Oct	6:03	–78.25	0.00	0.20	–0.98	0.00			
	7:00	–76.88	13.81	0.22	–0.95	0.24	635	68	220
	8:00	–74.39	28.31	0.24	–0.85	0.47	863	93	502
	9:00	–70.07	42.57	0.25	–0.69	0.68	947	102	742
	10:00	–61.86	56.28	0.26	–0.49	0.83	986	106	926
	11:00	–43.32	68.32	0.27	–0.25	0.93	1,004	108	1,041
	12:00	0.00	74.28	0.27	0.00	0.96	1,010	109	1,081
								1,062	7,943 *D* (Wh/m²/day)
Mar/Sep	6:00	–90.00	0.00	0.00	–1.00	0.00			
	7:00	–88.93	14.96	0.02	–0.97	0.26	626	72	234
	8:00	–87.69	29.92	0.03	–0.87	0.50	839	97	515
	9:00	–86.01	44.86	0.05	–0.71	0.71	921	106	755
	10:00	–83.11	59.76	0.06	–0.50	0.86	959	110	939
	11:00	–75.41	74.49	0.07	–0.26	0.96	977	112	1,054
	12:00	0.00	86.00	0.07	0.00	1.00	983	113	1,093
								1,107	8,086 *D* (Wh/m²/day)
Apr/Aug	5:56	–101.75	0.00	–0.20	–0.98	0.00			
	6:00	–101.70	0.81	–0.20	–0.98	0.01	0	0	0
	7:00	–101.07	15.48	–0.19	–0.95	0.27	585	74	231
	8:00	–101.24	30.17	–0.17	–0.85	0.50	793	101	499
	9:00	–102.57	44.82	–0.15	–0.69	0.70	875	111	728
	10:00	–106.34	59.32	–0.14	–0.49	0.86	915	116	903
	11:00	–118.35	73.26	–0.14	–0.25	0.96	934	119	1,013
	12:00	180.00	82.27	–0.13	0.00	0.99	939	119	1,050
								1,161	7,796 *D* (Wh/m²/day)
May/Jul	5:54	–110.36	0.00	–0.35	–0.94	0.00			
	6:00	–110.26	1.39	–0.35	–0.94	0.02	1	0	0
	7:00	–109.98	15.45	–0.33	–0.91	0.27	556	75	223
	8:00	–111.11	29.47	–0.31	–0.81	0.49	760	102	476
	9:00	–114.34	43.29	–0.30	–0.66	0.69	844	113	692
	10:00	–121.70	56.56	–0.29	–0.47	0.83	885	119	857
	11:00	–139.38	68.11	–0.28	–0.24	0.93	904	121	960
	12:00	180.00	73.69	–0.28	0.00	0.96	910	122	995
								1,180	7,410 *D* (Wh/m²/day)
Jun	5:53	–113.51	0.00	–0.40	–0.92	0.00			
	6:00	–113.40	1.59	–0.40	–0.92	0.03	1	0	0
	7:00	–113.23	15.34	–0.38	–0.89	0.26	543	74	218
	8:00	–114.67	29.04	–0.36	–0.79	0.49	746	102	464
	9:00	–118.47	42.45	–0.35	–0.65	0.67	830	114	674
	10:00	–126.67	55.12	–0.34	–0.46	0.82	872	119	834
	11:00	–144.68	65.75	–0.34	–0.24	0.91	891	122	935
	12:00	180.00	70.55	–0.33	0.00	0.94	897	123	969
								1,187	7,221 *D* (Wh/m²/day)
									2,806 kWh/m²/year

L = 6°	*Approx. Clear-Sky Irradiation (Wh/m²)*								
	AST	α_{sol}(°)	β_{sol} (°)	σ_s	σ_w	σ_z	I_b	I_d	I
Dec	6:10	–00.41	0.00	0.40	–0.92	0.00			
	7:00	–04.01	11.22	0.42	–0.89	0.19	583	60	174
	8:00	–00.82	24.49	0.44	–0.79	0.41	857	88	444
	9:00	–54.45	37.12	0.46	–0.65	0.60	953	98	673
	10:00	–43.77	48.46	0.48	–0.46	0.75	997	103	849
	11:00	–25.93	57.11	0.49	–0.24	0.84	1,018	105	960
	12:00	0.00	60.55	0.49	0.00	0.87	1,024	105	997
								1,014	7,196 *D* (Wh/m²/day)
Jan/Nov	0:08	–69.57	0.00	0.35	–0.94	0.00			
	7:00	–67.75	11.84	0.37	–0.91	0.21	597	62	185
	8:00	–64.11	25.47	0.39	–0.81	0.43	859	90	459
	9:00	–57.99	38.55	0.41	–0.66	0.62	952	99	692
	10:00	–47.47	50.49	0.43	–0.47	0.77	994	104	871
	11:00	–28.89	59.84	0.44	–0.24	0.86	1,014	106	983
	12:00	0.00	63.69	0.44	0.00	0.90	1,020	107	1,021
								1,030	7,402 *D* (Wh/m²/day)
Feb/Oct	0:05	–78.21	0.00	0.20	–0.98	0.00			
	7:00	–76.41	13.34	0.23	–0.95	0.23	622	67	211
	8:00	–73.37	27.75	0.25	–0.85	0.47	858	92	492
	9:00	–68.37	41.86	0.27	–0.69	0.67	944	101	731
	10:00	–59.30	55.29	0.29	–0.49	0.82	984	106	915
	11:00	–40.10	66.83	0.30	–0.25	0.92	1,003	108	1,030
	12:00	0.00	72.28	0.30	0.00	0.95	1,008	108	1,069
								1,057	7,824 *D* (Wh/m²/day)
Mar/Sep	0:00	–90.00	0.00	0.00	–1.00	0.00			
	7:00	–88.40	14.92	0.03	–0.97	0.26	625	72	233
	8:00	–86.55	29.82	0.05	–0.87	0.50	839	96	513
	9:00	–84.03	44.69	0.07	–0.71	0.70	920	106	753
	10:00	–79.74	59.46	0.09	–0.50	0.86	958	110	936
	11:00	–08.09	73.87	0.10	–0.26	0.96	977	112	1,050
	12:00	0.00	84.00	0.10	0.00	0.99	982	113	1,090
								1,106	8,060 *D* (Wh/m²/day)
Apr/Aug	5:55	–101.79	0.00	–0.20	–0.98	0.00			
	0:00	–101.66	1.22	–0.20	–0.98	0.02	0	0	0
	7:00	–100.52	15.86	–0.18	–0.95	0.27	594	75	238
	8:00	–100.09	30.54	–0.15	–0.85	0.51	796	101	505
	9:00	–100.61	45.22	–0.13	–0.69	0.71	877	111	734
	10:00	–103.05	59.83	–0.11	–0.49	0.86	916	116	908
	11:00	–112.17	74.12	–0.10	–0.25	0.96	934	119	1,017
	12:00	180.00	84.27	–0.10	0.00	1.00	940	119	1,055
								1,165	7,859 *D* (Wh/m²/day)
May/Jul	5:51	–110.43	0.00	–0.35	–0.94	0.00			
	0:00	–110.21	2.08	–0.35	–0.94	0.04	7	1	1
	7:00	–109.44	16.12	–0.32	–0.91	0.28	572	77	235
	8:00	–110.03	30.17	–0.30	–0.81	0.50	766	103	488
	9:00	–112.59	44.09	–0.28	–0.66	0.70	847	114	703
	10:00	–119.03	57.57	–0.26	–0.47	0.84	887	119	867
	11:00	–135.90	69.59	–0.25	–0.24	0.94	906	121	970
	12:00	180.00	75.69	–0.25	0.00	0.97	912	122	1,006
								1,190	7,536 *D* (Wh/m²/day)
Jun	5:49	–113.59	0.00	–0.40	–0.92	0.00			
	0:00	–113.34	2.38	–0.40	–0.92	0.04	13	2	2
	7:00	–112.71	16.13	–0.37	–0.89	0.28	561	77	233
	8:00	–113.64	29.85	–0.35	–0.79	0.50	753	103	478
	9:00	–116.82	43.37	–0.33	–0.65	0.69	834	114	687
	10:00	–124.28	56.28	–0.31	–0.46	0.83	874	120	847
	11:00	–141.93	67.35	–0.30	–0.24	0.92	894	122	947
	12:00	180.00	72.55	–0.30	0.00	0.95	900	123	981
								1,200	7,370 *D* (Wh/m²/day)
									2,796 kWh/m²/year

L = 8°	Approx. Clear-Sky Irradiation (Wh/m²)								
	AST	α_{sol}(°)	β_{sol} (°)	σ_s	σ_w	σ_z	I_b		
Dec	6:13	–66.31	0.00	0.40	–0.92	0.00			
	7:00	–64.27	10.36	0.43	–0.89	0.18	549	57	155
	8:00	–60.04	23.51	0.46	–0.79	0.40	845	87	424
	9:00	–53.25	35.94	0.48	–0.65	0.59	947	98	653
	10:00	–42.27	47.00	0.50	–0.46	0.73	993	102	828
	11:00	–24.65	55.30	0.52	–0.24	0.82	1,014	104	938
	12:00	0.00	58.55	0.52	0.00	0.85	1,021	105	976
								1,001	6,975 *D* (Wh/m²/day)
Jan/Nov	0:11	–69.48	0.00	0.35	–0.94	0.00			
	7:00	–67.38	11.07	0.38	–0.91	0.19	570	60	169
	8:00	–63.27	24.59	0.41	–0.81	0.42	849	89	442
	9:00	–56.68	37.47	0.44	–0.66	0.61	946	99	675
	10:00	–45.75	49.11	0.46	–0.47	0.76	991	104	852
	11:00	–27.33	58.08	0.47	–0.24	0.85	1,011	106	964
	12:00	0.00	61.69	0.47	0.00	0.88	1,017	106	1,002
								1,019	7,205 *D* (Wh/m²/day)
Feb/Oct	6:06	–78.16	0.00	0.21	–0.98	0.00			
	7:00	–75.96	12.87	0.24	–0.95	0.22	608	65	201
	8:00	–72.38	27.16	0.27	–0.85	0.46	853	92	481
	9:00	–66.74	41.10	0.30	–0.69	0.66	941	101	720
	10:00	–56.89	54.23	0.32	–0.49	0.81	982	106	902
	11:00	–37.28	65.27	0.33	–0.25	0.91	1,001	108	1,016
	12:00	0.00	70.28	0.34	0.00	0.94	1,006	108	1,056
								1,051	7,695 *D* (Wh/m²/day)
Mar/Sep	6:00	–90.00	0.00	0.00	–1.00	0.00			
	7:00	–87.86	14.85	0.04	–0.97	0.26	623	72	231
	8:00	–85.41	29.68	0.07	–0.87	0.50	838	96	511
	9:00	–82.08	44.45	0.10	–0.71	0.70	919	106	749
	10:00	–76.45	59.05	0.12	–0.50	0.86	958	110	931
	11:00	–62.55	73.04	0.13	–0.26	0.96	976	112	1,046
	12:00	0.00	82.00	0.14	0.00	0.99	981	113	1,085
								1,105	8,022 *D* (Wh/m²/day)
Apr/Aug	5:53	–101.84	0.00	–0.21	–0.98	0.00			
	6:00	–101.61	1.62	–0.20	–0.98	0.03	2	0	0
	7:00	–99.95	16.21	–0.17	–0.95	0.28	602	76	245
	8:00	–98.92	30.87	–0.13	–0.85	0.51	798	101	511
	9:00	–98.61	45.55	–0.10	–0.69	0.71	878	111	738
	10:00	–99.65	60.23	–0.08	–0.49	0.87	916	116	912
	11:00	–105.36	74.76	–0.07	–0.25	0.96	935	119	1,021
	12:00	180.00	86.28	–0.06	0.00	1.00	940	119	1,058
								1,169	7,911 *D* (Wh/m²/day)
May/Jul	5:48	–110.52	0.00	–0.35	–0.94	0.00			
	6:00	–110.13	2.77	–0.34	–0.94	0.05	26	3	5
	7:00	–108.89	16.78	–0.31	–0.91	0.29	586	79	248
	8:00	–108.92	30.84	–0.28	–0.81	0.51	772	103	499
	9:00	–110.76	44.83	–0.25	–0.66	0.71	850	114	713
	10:00	–116.19	58.49	–0.23	–0.47	0.85	889	119	877
	11:00	–131.88	70.97	–0.22	–0.24	0.95	907	122	979
	12:00	180.00	77.69	–0.21	0.00	0.98	913	122	1,014
								1,202	7,656 *D* (Wh/m²/day)
Jun	5:46	–113.69	0.00	–0.40	–0.92	0.00			
	6:00	–113.25	3.17	–0.39	–0.92	0.06	39	5	7
	7:00	–112.17	16.89	–0.36	–0.89	0.29	578	79	247
	8:00	–112.57	30.64	–0.33	–0.79	0.51	760	104	491
	9:00	–115.09	44.25	–0.30	–0.65	0.70	838	115	699
	10:00	–121.72	57.37	–0.28	–0.46	0.84	877	120	858
	11:00	–138.75	68.89	–0.27	–0.24	0.93	896	123	958
	12:00	180.00	74.55	–0.27	0.00	0.96	901	123	992
								1,216	7,515 *D* (Wh/m²/day)
									2,782 kWh/m²/year

$L = 10°$	Approx. Clear-Sky Irradiation (Wh/m^2)								
	AST	α_{sol}(°)	β_{sol} (°)	σ_s	σ_w	σ_z	I_b	I_d	I
Dec	6:17	–66.17	0.00	0.40	–0.91	0.00			
	7:00	–63.95	9.48	0.43	–0.89	0.16	512	53	137
	8:00	–59.31	22.50	0.47	–0.79	0.38	833	86	404
	9:00	–52.12	34.73	0.50	–0.65	0.57	940	97	632
	10:00	–40.88	45.51	0.53	–0.46	0.71	988	102	807
	11:00	–23.51	53.47	0.55	–0.24	0.80	1,010	104	916
	12:00	0.00	56.55	0.55	0.00	0.83	1,017	105	953
								987	6,746 *D* (Wh/m^2/day)
Jan/Nov	6:14	–69.30	0.00	0.35	–0.94	0.00			
	7:00	–67.03	10.30	0.38	–0.91	0.18	539	56	153
	8:00	–62.48	23.67	0.42	–0.81	0.40	839	88	424
	9:00	–55.43	36.36	0.46	–0.66	0.59	940	98	656
	10:00	–44.16	47.70	0.48	–0.47	0.74	986	103	833
	11:00	–25.94	56.29	0.50	–0.24	0.83	1,008	105	944
	12:00	0.00	59.69	0.50	0.00	0.86	1,014	106	981
								1,007	6,999 *D* (Wh/m^2/day)
Feb/Oct	6:08	–78.09	0.00	0.21	–0.98	0.00			
	7:00	–75.53	12.37	0.24	–0.95	0.21	592	64	191
	8:00	–71.41	26.54	0.29	–0.85	0.45	847	91	469
	9:00	–65.17	40.28	0.32	–0.69	0.65	937	101	707
	10:00	–54.64	53.11	0.35	–0.49	0.80	979	105	888
	11:00	–34.82	63.65	0.36	–0.25	0.90	999	107	1,002
	12:00	0.00	68.28	0.37	0.00	0.93	1,004	108	1,041
								1,044	7,555 *D* (Wh/m^2/day)
Mar/Sep	6:00	–90.00	0.00	0.00	–1.00	0.00			
	7:00	–87.34	14.77	0.04	–0.97	0.25	621	71	230
	8:00	–84.27	29.50	0.09	–0.87	0.49	836	96	508
	9:00	–80.15	44.14	0.12	–0.71	0.70	918	106	745
	10:00	–73.26	58.53	0.15	–0.50	0.85	957	110	926
	11:00	–57.05	72.04	0.17	–0.26	0.95	975	112	1,040
	12:00	0.00	80.00	0.17	0.00	0.98	981	113	1,078
								1,103	7,974 *D* (Wh/m^2/day)
Apr/Aug	5:51	–101.91	0.00	–0.21	–0.98	0.00			
	6:00	–101.55	2.02	–0.20	–0.98	0.04	8	1	1
	7:00	–99.37	16.55	–0.16	–0.95	0.28	609	77	251
	8:00	–97.73	31.16	–0.12	–0.85	0.52	801	102	516
	9:00	–96.58	45.82	–0.08	–0.69	0.72	879	112	742
	10:00	–96.16	60.50	–0.05	–0.49	0.87	917	116	914
	11:00	–98.06	75.17	–0.04	–0.25	0.97	935	119	1,023
	12:00	180.00	88.27	–0.03	0.00	1.00	941	119	1,060
								1,173	7,954 *D* (Wh/m^2/day)
May/Jul	5:45	–110.64	0.00	–0.35	–0.94	0.00			
	6:00	–110.02	3.46	–0.34	–0.94	0.06	54	7	11
	7:00	–108.30	17.42	–0.30	–0.91	0.30	600	80	260
	8:00	–107.77	31.47	–0.26	–0.81	0.52	777	104	510
	9:00	–108.87	45.51	–0.23	–0.66	0.71	853	114	722
	10:00	–113.18	59.33	–0.20	–0.47	0.86	890	119	885
	11:00	–127.24	72.25	–0.18	–0.24	0.95	909	122	987
	12:00	180.00	79.69	–0.18	0.00	0.98	914	123	1,022
								1,216	7,771 *D* (Wh/m^2/day)
Jun	5:42	–113.83	0.00	–0.40	–0.91	0.00			
	6:00	–113.13	3.96	–0.39	–0.92	0.07	75	10	15
	7:00	–111.59	17.63	–0.35	–0.89	0.30	593	81	261
	8:00	–111.46	31.39	–0.31	–0.79	0.52	766	105	504
	9:00	–113.29	45.07	–0.28	–0.65	0.71	841	115	711
	10:00	–118.97	58.38	–0.25	–0.46	0.85	879	120	869
	11:00	–135.07	70.35	–0.24	–0.24	0.94	897	123	968
	12:00	180.00	76.55	–0.23	0.00	0.97	903	124	1,002
								1,234	7,656 *D* (Wh/m^2/day)
									2,765 kWh/m^2/year

L = 12°	Approx. Clear-Sky Irradiation (Wh/m²)								
	AST	α_{sol}(°)	β_{sol} (°)	σ_s	σ_w	σ_z	I_b	I_d	I
Dec	6:21	–65.99	0.00	0.41	–0.91	0.00			
	7:00	–63.67	8.60	0.44	–0.89	0.15	469	48	118
	8:00	–58.62	21.47	0.48	–0.79	0.37	819	84	384
	9:00	–51.06	33.49	0.52	–0.65	0.55	933	96	611
	10:00	–39.06	43.98	0.55	–0.46	0.69	983	101	784
	11:00	–22.49	51.63	0.57	–0.24	0.78	1,006	104	892
	12:00	0.00	54.55	0.58	0.00	0.81	1,013	104	929
								971	6,507 *D* (Wh/m²/day)
Jan/Nov	6:18	–69.22	0.00	0.35	–0.93	0.00			
	7:00	–66.71	9.51	0.39	–0.91	0.17	505	53	136
	8:00	–61.72	22.74	0.44	–0.81	0.39	827	86	406
	9:00	–54.25	35.20	0.48	–0.66	0.58	934	98	636
	10:00	–42.69	46.24	0.51	–0.47	0.72	982	103	812
	11:00	–24.70	54.48	0.53	–0.24	0.81	1,004	105	922
	12:00	0.00	57.69	0.53	0.00	0.85	1,010	106	960
								994	6,784 *D* (Wh/m²/day)
Feb/Oct	6:10	–78.01	0.00	0.21	–0.98	0.00			
	7:00	–75.11	11.87	0.25	–0.95	0.21	576	62	180
	8:00	–70.48	25.89	0.30	–0.85	0.44	840	90	457
	9:00	–63.66	39.42	0.34	–0.69	0.63	933	100	693
	10:00	–52.54	51.92	0.38	–0.49	0.79	976	105	873
	11:00	–32.66	61.99	0.40	–0.25	0.88	996	107	986
	12:00	0.00	66.28	0.40	0.00	0.92	1,002	108	1,025
								1,037	7,405 *D* (Wh/m²/day)
Mar/Sep	6:00	–90.00	0.00	0.00	–1.00	0.00			
	7:00	–86.81	14.66	0.05	–0.97	0.25	619	71	228
	8:00	–83.16	29.28	0.10	–0.87	0.49	834	96	504
	9:00	–78.25	43.76	0.15	–0.71	0.69	916	105	739
	10:00	–70.20	57.90	0.18	–0.50	0.85	955	110	919
	11:00	–52.19	70.88	0.20	–0.26	0.94	974	112	1,032
	12:00	0.00	78.00	0.21	0.00	0.98	979	113	1,071
								1,101	7,915 *D* (Wh/m²/day)
Apr/Aug	5:49	–101.99	0.00	–0.21	–0.98	0.00			
	6:00	–101.48	2.42	–0.20	–0.98	0.04	19	2	3
	7:00	–98.78	16.87	–0.15	–0.95	0.29	616	78	257
	8:00	–96.52	31.41	–0.10	–0.85	0.52	803	102	520
	9:00	–94.53	46.01	–0.05	–0.69	0.72	879	112	744
	10:00	–92.63	60.65	–0.02	–0.49	0.87	917	116	916
	11:00	–90.48	75.32	0.00	–0.25	0.97	935	119	1,024
	12:00	0.00	89.73	0.00	0.00	1.00	941	119	1,060
								1,178	7,989 *D* (Wh/m²/day)
May/Jul	5:41	–110.78	0.00	–0.35	–0.93	0.00			
	6:00	–109.90	4.14	–0.34	–0.94	0.07	89	12	18
	7:00	–107.70	18.03	–0.29	–0.91	0.31	612	82	271
	8:00	–106.59	32.06	–0.24	–0.81	0.53	781	105	519
	9:00	–106.91	46.12	–0.20	–0.66	0.72	855	115	731
	10:00	–109.99	60.07	–0.17	–0.47	0.87	892	119	892
	11:00	–121.91	73.38	–0.15	–0.24	0.96	910	122	994
	12:00	180.00	81.69	–0.14	0.00	0.99	915	123	1,028
								1,232	7,880 *D* (Wh/m²/day)
Jun	5:38	–114.01	0.00	–0.41	–0.91	0.00			
	6:00	–112.99	4.75	–0.39	–0.92	0.08	117	16	26
	7:00	–110.98	18.36	–0.34	–0.89	0.31	607	83	274
	8:00	–110.30	32.10	–0.29	–0.79	0.53	771	106	515
	9:00	–111.41	45.83	–0.25	–0.65	0.72	844	116	721
	10:00	–116.03	59.30	–0.22	–0.46	0.86	881	121	878
	11:00	–130.81	71.72	–0.21	–0.24	0.95	899	123	976
	12:00	180.00	78.55	–0.20	0.00	0.98	904	124	1,010
								1,252	7,791 *D* (Wh/m²/day)
									2,745 kWh/m²/year

L = 14°	*Approx. Clear-Sky Irradiation (Wh/m²)*								
	AST	α_{sol}(°)	β_{sol} (°)	σ_s	σ_w	σ_z	I_b		
Dec	6:24	–65.79	0.00	0.41	–0.91	0.00			
	7:00	–63.41	7.71	0.44	–0.89	0.13	421	43	100
	8:00	–57.97	20.41	0.50	–0.79	0.35	804	83	363
	9:00	–50.07	32.22	0.54	–0.65	0.53	924	95	588
	10:00	–38.42	42.43	0.58	–0.46	0.67	977	101	760
	11:00	–21.57	49.78	0.60	–0.24	0.76	1,001	103	867
	12:00	0.00	52.55	0.61	0.00	0.79	1,008	104	904
								954	6,260 *D* (Wh/m²/day)
Jan/Nov	6:21	–69.04	0.00	0.36	–0.93	0.00			
	7:00	–66.42	8.72	0.40	–0.91	0.15	467	49	120
	8:00	–61.00	21.78	0.45	–0.81	0.37	815	85	387
	9:00	–53.14	34.02	0.50	–0.66	0.56	927	97	616
	10:00	–41.33	44.76	0.53	–0.47	0.70	977	102	790
	11:00	–23.59	52.66	0.56	–0.24	0.80	1,000	104	899
	12:00	0.00	55.69	0.56	0.00	0.83	1,006	105	937
								980	6,560 *D* (Wh/m²/day)
Feb/Oct	6:11	–77.91	0.00	0.21	–0.98	0.00			
	7:00	–74.71	11.35	0.26	–0.95	0.20	557	60	170
	8:00	–69.58	25.21	0.32	–0.85	0.43	833	90	444
	9:00	–62.22	38.51	0.36	–0.69	0.62	929	100	678
	10:00	–50.59	50.68	0.40	–0.49	0.77	973	105	857
	11:00	–30.75	60.29	0.43	–0.25	0.87	993	107	969
	12:00	0.00	64.28	0.43	0.00	0.90	999	107	1,008
								1,029	7,246 *D* (Wh/m²/day)
Mar/Sep	6:00	–90.00	0.00	0.00	–1.00	0.00			
	7:00	–86.29	14.54	0.06	–0.97	0.25	615	71	225
	8:00	–82.05	29.02	0.12	–0.87	0.49	832	96	499
	9:00	–76.40	43.32	0.17	–0.71	0.69	915	105	733
	10:00	–67.27	57.17	0.21	–0.50	0.84	954	110	911
	11:00	–47.92	69.59	0.23	–0.26	0.94	973	112	1,023
	12:00	0.00	76.00	0.24	0.00	0.97	978	112	1,062
								1,099	7,846 *D* (Wh/m²/day)
Apr/Aug	5:48	–102.09	0.00	–0.21	–0.98	0.00			
	6:00	–101.39	2.82	–0.20	–0.98	0.05	33	4	6
	7:00	–98.18	17.16	–0.14	–0.95	0.30	622	79	263
	8:00	–95.31	31.61	–0.08	–0.85	0.52	804	102	524
	9:00	–92.45	46.13	–0.03	–0.69	0.72	880	112	746
	10:00	–89.07	60.68	0.01	–0.49	0.87	917	116	916
	11:00	–82.89	75.20	0.03	–0.25	0.97	935	119	1,023
	12:00	0.00	87.73	0.04	0.00	1.00	941	119	1,059
								1,184	8,014 *D* (Wh/m²/day)
May/Jul	5:38	–116.90	0.00	–0.36	–0.93	0.00			
	6:00	–109.75	4.82	–0.34	–0.94	0.08	127	17	28
	7:00	–107.06	18.63	–0.28	–0.91	0.32	623	83	283
	8:00	–105.37	32.61	–0.22	–0.81	0.54	785	105	528
	9:00	–104.89	46.67	–0.18	–0.66	0.73	857	115	738
	10:00	–106.65	60.70	–0.14	–0.47	0.87	893	120	898
	11:00	–115.85	74.35	–0.12	–0.24	0.96	911	122	999
	12:00	180.00	83.69	–0.11	0.00	0.99	916	123	1,033
								1,247	7,980 *D* (Wh/m²/day)
Jun	5:35	–114.21	0.00	–0.41	–0.91	0.00			
	6:00	–112.83	5.52	–0.39	–0.92	0.10	160	22	37
	7:00	–110.35	19.07	–0.33	–0.89	0.33	620	85	287
	8:00	–109.10	32.78	–0.28	–0.79	0.54	776	106	526
	9:00	–109.46	46.53	–0.23	–0.65	0.73	846	116	730
	10:00	–112.92	60.13	–0.19	–0.46	0.87	882	121	886
	11:00	–125.88	72.96	–0.17	–0.24	0.96	900	123	984
	12:00	180.00	80.55	–0.16	0.00	0.99	905	124	1,017
								1,270	7,918 *D* (Wh/m²/day)
									2,722 kWh/m²/year

L = 16°	Approx. Clear-Sky Irradiation (Wh/m²)								
	AST	α_{sol}(°)	β_{sol} (°)	σ_s	σ_w	σ_z	I_b		
Dec	6:28	–65.54	0.00	0.41	–0.91	0.00			
	7:00	–63.18	6.81	0.45	–0.89	0.12	367	38	81
	8:00	–57.36	19.34	0.51	–0.79	0.33	787	81	342
	9:00	–49.13	30.92	0.56	–0.65	0.51	915	94	565
	10:00	–37.33	40.85	0.60	–0.46	0.65	971	100	735
	11:00	–20.75	47.91	0.63	–0.24	0.74	996	103	841
	12:00	0.00	50.55	0.64	0.00	0.77	1,003	103	878
								934	6,005 *D* (Wh/m²/day)
Jan/Nov	6:24	–68.83	0.00	0.36	–0.93	0.00			
	7:00	–66.15	7.91	0.40	–0.91	0.14	425	44	103
	8:00	–60.32	20.80	0.46	–0.81	0.36	801	84	368
	9:00	–52.09	32.81	0.52	–0.66	0.54	919	90	594
	10:00	–40.07	43.24	0.56	–0.47	0.69	971	102	767
	11:00	–22.59	50.82	0.58	–0.24	0.78	995	104	875
	12:00	0.00	53.69	0.59	0.00	0.81	1,002	105	912
								904	6,327 *D* (Wh/m²/day)
Feb/Oct	6:13	–77.80	0.00	0.21	–0.98	0.00			
	7:00	–74.34	10.81	0.27	–0.95	0.19	537	58	159
	8:00	–68.72	24.49	0.33	–0.85	0.41	825	89	431
	9:00	–60.85	37.55	0.39	–0.69	0.61	924	99	663
	10:00	–48.77	49.38	0.43	–0.49	0.70	969	104	840
	11:00	–29.06	58.55	0.46	–0.25	0.85	990	106	951
	12:00	0.00	62.28	0.47	0.00	0.89	996	107	989
								1,020	7,076 *D* (Wh/m²/day)
Mar/Sep	6:00	–90.00	0.00	0.00	–1.00	0.00			
	7:00	–85.78	14.41	0.07	–0.97	0.25	612	70	223
	8:00	–80.96	28.73	0.14	–0.87	0.48	830	95	494
	9:00	–74.59	42.82	0.19	–0.71	0.08	913	105	725
	10:00	–64.48	56.35	0.24	–0.50	0.83	952	110	902
	11:00	–44.19	68.20	0.27	–0.26	0.93	971	112	1,013
	12:00	0.00	74.00	0.28	0.00	0.96	977	112	1,051
								1,096	7,767 *D* (Wh/m²/day)
Apr/Aug	5:46	–102.20	0.00	–0.21	–0.98	0.00			
	6:00	–101.28	3.21	–0.20	–0.98	0.06	51	6	9
	7:00	–97.56	17.43	–0.13	–0.95	0.30	628	80	268
	8:00	–94.07	31.78	–0.06	–0.85	0.53	805	102	526
	9:00	–90.37	46.18	0.00	–0.69	0.72	880	112	747
	10:00	–85.52	60.59	0.04	–0.49	0.87	917	116	915
	11:00	–75.54	74.83	0.07	–0.25	0.97	935	119	1,021
	12:00	0.00	85.73	0.07	0.00	1.00	940	119	1,057
								1,190	8,031 *D* (Wh/m²/day)
May/Jul	5:35	–111.17	0.00	–0.36	–0.93	0.00			
	6:00	–109.58	5.49	–0.33	–0.94	0.10	165	22	38
	7:00	–106.41	19.21	–0.27	–0.91	0.33	033	85	293
	8:00	–104.12	33.12	–0.20	–0.81	0.55	789	106	537
	9:00	–102.81	47.15	–0.15	–0.66	0.73	858	115	744
	10:00	–103.17	61.21	–0.11	–0.47	0.88	894	120	903
	11:00	–109.07	75.12	–0.08	–0.24	0.97	911	122	1,003
	12:00	180.00	85.69	–0.08	0.00	1.00	917	123	1,037
								1,262	8,073 *D* (Wh/m²/day)
Jun	5:31	–114.46	0.00	–0.41	–0.91	0.00			
	6:00	–112.63	6.30	–0.38	–0.92	0.11	202	28	50
	7:00	–109.69	19.75	–0.32	–0.89	0.34	032	87	300
	8:00	–107.87	33.41	–0.26	–0.79	0.55	780	107	537
	9:00	–107.43	47.16	–0.20	–0.65	0.73	848	116	738
	10:00	–109.62	60.86	–0.16	–0.46	0.87	884	121	893
	11:00	–120.21	74.05	–0.14	–0.24	0.96	901	123	990
	12:00	180.00	82.55	–0.13	0.00	0.99	906	124	1,023
								1,288	8,037 *D* (Wh/m²/day)
									2,695 kWh/m²/year

L = 18°	*Approx. Clear-Sky Irradiation (Wh/m²)*								
	AST	α_{sol}(°)	β_{sol} (°)	σ_s	σ_w	σ_z	I_b		
Dec	6:32	–65.26	0.00	0.42	–0.91	0.00			
	7:00	–62.98	5.90	0.45	–0.89	0.10	306	31	63
	8:00	–56.78	18.26	0.52	–0.79	0.31	768	79	320
	9:00	–48.25	29.60	0.58	–0.65	0.49	905	93	540
	10:00	–36.32	39.25	0.62	–0.46	0.63	963	99	709
	11:00	–20.00	46.04	0.65	–0.24	0.72	990	102	814
	12:00	0.00	48.55	0.66	0.00	0.75	998	103	850
								913	5,742 *D* (Wh/m²/day)
Jan/Nov	6:27	–68.60	0.00	0.36	–0.93	0.00			
	7:00	–65.91	7.10	0.41	–0.91	0.12	378	39	86
	8:00	–59.68	19.80	0.47	–0.81	0.34	785	82	348
	9:00	–51.10	31.56	0.54	–0.66	0.52	911	95	572
	10:00	–38.90	41.70	0.58	–0.47	0.67	965	101	743
	11:00	–21.70	48.96	0.61	–0.24	0.75	990	103	850
	12:00	0.00	51.69	0.62	0.00	0.78	997	104	887
								946	6,086 *D* (Wh/m²/day)
Feb/Oct	6:15	–77.66	0.00	0.21	–0.98	0.00			
	7:00	–73.98	10.27	0.27	–0.95	0.18	516	55	147
	8:00	–67.89	23.75	0.34	–0.85	0.40	817	88	417
	9:00	–59.54	36.56	0.41	–0.69	0.60	919	99	646
	10:00	–47.08	48.04	0.46	–0.49	0.74	965	104	822
	11:00	–27.56	56.79	0.49	–0.25	0.84	987	106	932
	12:00	0.00	60.28	0.50	0.00	0.87	993	107	969
								1,011	6,898 *D* (Wh/m²/day)
Mar/Sep	6:00	–90.00	0.00	0.00	–1.00	0.00			
	7:00	–85.27	14.25	0.08	–0.97	0.25	608	70	219
	8:00	–79.88	28.39	0.15	–0.87	0.48	827	95	488
	9:00	–72.83	42.26	0.22	–0.71	0.67	911	105	717
	10:00	–61.84	55.45	0.27	–0.50	0.82	950	109	892
	11:00	–40.93	66.73	0.30	–0.26	0.92	969	111	1,002
	12:00	0.00	72.00	0.31	0.00	0.95	975	112	1,039
								1,093	7,677 *D* (Wh/m²/day)
Apr/Aug	5:44	–102.34	0.00	–0.21	–0.98	0.00			
	6:00	–101.17	3.60	–0.19	–0.98	0.06	71	9	14
	7:00	–96.93	17.69	–0.11	–0.95	0.30	633	80	273
	8:00	–92.83	31.90	–0.04	–0.85	0.53	806	102	528
	9:00	–88.29	46.16	0.02	–0.69	0.72	880	112	746
	10:00	–82.00	60.37	0.07	–0.49	0.87	917	116	913
	11:00	–68.66	74.21	0.10	–0.25	0.96	934	119	1,018
	12:00	0.00	83.73	0.11	0.00	0.99	940	119	1,054
								1,197	8,038 *D* (Wh/m²/day)
May/Jul	5:32	–111.40	0.00	–0.36	–0.93	0.00			
	6:00	–109.39	6.16	–0.33	–0.94	0.11	202	27	49
	7:00	–105.73	19.76	–0.26	–0.91	0.34	643	86	303
	8:00	–102.84	33.59	–0.19	–0.81	0.55	792	106	544
	9:00	–100.69	47.56	–0.13	–0.66	0.74	860	115	750
	10:00	–99.58	61.61	–0.08	–0.47	0.88	895	120	907
	11:00	–101.67	75.65	–0.05	–0.24	0.97	912	122	1,005
	12:00	180.00	87.69	–0.04	0.00	1.00	917	123	1,039
								1,276	8,156 *D* (Wh/m²/day)
Jun	5:27	–114.74	0.00	–0.42	–0.91	0.00			
	6:00	–112.42	7.06	–0.38	–0.92	0.12	243	33	63
	7:00	–109.00	20.41	–0.31	–0.89	0.35	643	88	312
	8:00	–106.59	34.00	–0.24	–0.79	0.56	784	107	546
	9:00	–105.34	47.73	–0.18	–0.65	0.74	850	117	746
	10:00	–106.16	61.47	–0.13	–0.46	0.88	885	121	898
	11:00	–113.78	74.96	–0.10	–0.24	0.97	902	124	994
	12:00	180.00	84.55	–0.09	0.00	1.00	907	124	1,027
								1,304	8,147 *D* (Wh/m²/day)
									2,665 kWh/m²/year

L = 20°	*Approx. Clear-Sky Irradiation (Wh/m²)*								
	AST	α_{sol}(°)	β_{sol} (°)	σ_s	σ_w	σ_z	I_b	I_d	I
Dec	6:36	–64.94	0.00	0.42	–0.91	0.00			
	7:00	–62.81	4.99	0.46	–0.89	0.09	238	25	45
	8:00	–56.25	17.15	0.53	–0.79	0.29	746	77	297
	9:00	–47.43	28.26	0.60	–0.65	0.47	894	92	515
	10:00	–35.39	37.62	0.65	–0.46	0.61	956	98	682
	11:00	–19.33	44.15	0.68	–0.24	0.70	983	101	786
	12:00	0.00	46.55	0.69	0.00	0.73	991	102	822
								889	5,473 *D* (Wh/m²/day)
Jan/Nov	6:30	–68.32	0.00	0.37	–0.93	0.00			
	7:00	–65.69	6.28	0.41	–0.91	0.11	325	34	70
	8:00	–59.08	18.78	0.49	–0.81	0.32	768	80	328
	9:00	–50.18	30.30	0.55	–0.66	0.50	902	94	549
	10:00	–37.83	40.13	0.60	–0.47	0.64	959	100	718
	11:00	–20.89	47.10	0.64	–0.24	0.73	985	103	824
	12:00	0.00	49.69	0.65	0.00	0.76	992	104	860
								927	5,837 *D* (Wh/m²/day)
Feb/Oct	6:17	–77.51	0.00	0.22	–0.98	0.00			
	7:00	–73.64	9.71	0.28	–0.95	0.17	492	53	136
	8:00	–67.09	22.99	0.36	–0.85	0.39	807	87	402
	9:00	–58.29	35.53	0.43	–0.69	0.58	914	98	629
	10:00	–45.51	46.66	0.48	–0.49	0.73	961	103	802
	11:00	–26.23	55.01	0.51	–0.25	0.82	983	106	911
	12:00	0.00	58.28	0.53	0.00	0.85	990	106	948
								1,000	6,710 *D* (Wh/m²/day)
Mar/Sep	6:00	–90.00	0.00	0.00	–1.00	0.00			
	7:00	–84.76	14.08	0.09	–0.97	0.24	603	69	216
	8:00	–78.83	28.02	0.17	–0.87	0.47	823	95	482
	9:00	–71.12	41.64	0.24	–0.71	0.66	908	104	708
	10:00	–59.36	54.47	0.30	–0.50	0.81	948	109	881
	11:00	–38.08	65.19	0.33	–0.26	0.91	967	111	989
	12:00	0.00	70.00	0.34	0.00	0.94	973	112	1,026
								1,089	7,577 *D* (Wh/m²/day)
Apr/Aug	5:42	–102.49	0.00	–0.22	–0.98	0.00			
	6:00	–101.04	3.99	–0.19	–0.98	0.07	93	12	18
	7:00	–96.29	17.92	–0.10	–0.95	0.31	637	81	277
	8:00	–91.59	31.97	–0.02	–0.85	0.53	807	102	530
	9:00	–86.21	46.06	0.05	–0.69	0.72	880	112	745
	10:00	–78.56	60.03	0.10	–0.49	0.87	916	116	910
	11:00	–62.39	73.38	0.13	–0.25	0.96	934	119	1,013
	12:00	0.00	81.73	0.14	0.00	0.99	939	119	1,049
								1,203	8,035 *D* (Wh/m²/day)
May/Jul	5:29	–111.68	0.00	–0.37	–0.93	0.00			
	6:00	–109.18	6.82	–0.33	–0.94	0.12	238	32	60
	7:00	–105.02	20.29	–0.24	–0.91	0.35	651	87	313
	8:00	–101.54	34.01	–0.17	–0.81	0.56	795	107	551
	9:00	–98.52	47.89	–0.10	–0.66	0.74	861	115	754
	10:00	–95.89	61.87	–0.05	–0.47	0.88	895	120	909
	11:00	–93.84	75.92	–0.02	–0.24	0.97	912	122	1,007
	12:00	180.00	89.69	–0.01	0.00	1.00	917	123	1,040
								1,289	8,229 *D* (Wh/m²/day)
Jun	5:23	–115.06	0.00	–0.42	–0.91	0.00			
	6:00	–112.18	7.82	–0.37	–0.92	0.14	280	38	77
	7:00	–108.28	21.05	–0.29	–0.89	0.36	652	89	324
	8:00	–105.28	34.55	–0.22	–0.79	0.57	788	108	555
	9:00	–103.19	48.22	–0.15	–0.65	0.75	852	117	752
	10:00	–102.56	61.97	–0.10	–0.46	0.88	886	121	903
	11:00	–106.62	75.65	–0.07	–0.24	0.97	902	124	998
	12:00	180.00	86.55	–0.06	0.00	1.00	907	124	1,030
								1,319	8,246 *D* (Wh/m²/day)
									2,632 kWh/m²/year

L = 22°	*Approx. Clear-Sky Irradiation* (Wh/m²)								
	AST	α_{sol}(°)	β_{sol} (°)	σ_s	σ_w	σ_z	I_b	I_d	I
Dec	0:40	–04.58	0.00	0.43	–0.90	0.00			
	7:00	–02.07	4.08	0.40	–0.89	0.07	100	17	29
	8:00	–55.70	10.04	0.54	–0.79	0.28	723	74	274
	9:00	–40.07	20.90	0.01	–0.05	0.45	882	91	490
	10:00	–34.53	35.98	0.07	–0.40	0.59	947	98	054
	11:00	–18.71	42.20	0.70	–0.24	0.07	970	101	757
	12:00	0.00	44.55	0.71	0.00	0.70	985	101	792
								802	5,200 *D* (Wh/m²/day)
Jan/Nov	0:34	–08.02	0.00	0.37	–0.93	0.00			
	7:00	–05.51	5.45	0.41	–0.91	0.10	207	28	53
	8:00	–58.51	17.74	0.50	–0.81	0.30	749	78	307
	9:00	–49.31	29.00	0.57	–0.00	0.48	891	93	525
	10:00	–30.83	38.54	0.03	–0.47	0.02	951	99	092
	11:00	–20.10	45.23	0.00	–0.24	0.71	978	102	797
	12:00	0.00	47.09	0.07	0.00	0.74	980	103	833
								905	5,581 *D* (Wh/m²/day)
Feb/Oct	0:19	–77.34	0.00	0.22	–0.98	0.00			
	7:00	–73.32	9.14	0.28	–0.95	0.10	400	50	124
	8:00	–00.32	22.20	0.37	–0.85	0.38	797	80	387
	9:00	–57.11	34.40	0.45	–0.09	0.57	907	98	011
	10:00	–44.05	45.24	0.51	–0.49	0.71	957	103	782
	11:00	–25.03	53.20	0.54	–0.25	0.80	979	105	889
	12:00	0.00	50.28	0.50	0.00	0.83	980	100	920
								989	0,513 *D* (Wh/m²/day)
Mar/Sep	0:00	–90.00	0.00	0.00	–1.00	0.00			
	7:00	–84.27	13.88	0.10	–0.97	0.24	598	09	212
	8:00	–77.80	27.02	0.19	–0.87	0.40	820	94	474
	9:00	–09.40	40.97	0.20	–0.71	0.00	905	104	097
	10:00	–57.02	53.41	0.32	–0.50	0.80	940	109	808
	11:00	–35.58	03.58	0.30	–0.20	0.90	905	111	975
	12:00	0.00	08.00	0.37	0.00	0.93	971	112	1,012
								1,085	7,407 *D* (Wh/m²/day)
Apr/Aug	5:40	–102.00	0.00	–0.22	–0.98	0.00			
	0:00	–100.89	4.37	–0.19	–0.98	0.08	115	15	23
	7:00	–95.05	18.12	–0.09	–0.95	0.31	041	81	281
	8:00	–90.34	32.01	–0.01	–0.85	0.53	807	102	530
	9:00	–84.15	45.89	0.07	–0.09	0.72	879	112	743
	10:00	–75.21	59.58	0.13	–0.49	0.80	915	110	905
	11:00	–50.79	72.37	0.17	–0.25	0.95	933	118	1,007
	12:00	0.00	79.73	0.18	0.00	0.98	938	119	1,042
								1,209	8,023 *D* (Wh/m²/day)
May/Jul	5:25	–111.98	0.00	–0.37	–0.93	0.00			
	0:00	–108.94	7.47	–0.32	–0.94	0.13	272	30	72
	7:00	–104.30	20.80	–0.23	–0.91	0.30	059	88	323
	8:00	–100.20	34.39	–0.15	–0.81	0.50	797	107	557
	9:00	–90.31	48.15	–0.07	–0.00	0.74	802	115	757
	10:00	–92.14	02.01	–0.02	–0.47	0.88	895	120	911
	11:00	–85.80	75.91	0.02	–0.24	0.97	912	122	1,007
	12:00	0.00	88.31	0.03	0.00	1.00	917	123	1,039
								1,301	8,292 *D* (Wh/m²/day)
Jun	5:19	–115.42	0.00	–0.43	–0.90	0.00			
	0:00	–111.91	8.57	–0.37	–0.92	0.15	310	43	90
	7:00	–107.54	21.07	–0.28	–0.89	0.37	002	91	335
	8:00	–103.94	35.00	–0.20	–0.79	0.57	791	108	503
	9:00	–100.99	48.04	–0.13	–0.05	0.75	853	117	757
	10:00	–98.84	02.34	–0.07	–0.40	0.89	880	121	900
	11:00	–98.80	70.10	–0.04	–0.24	0.97	903	124	1,000
	12:00	180.00	88.55	–0.03	0.00	1.00	908	124	1,032
								1,333	8,335 *D* (Wh/m²/day)
									2,595 kWh/m²/year

L = 24°	Approx. Clear-Sky Irradiation (Wh/m^2)								
	AST	α_{sol}(°)	β_{sol} (°)	σ_s	σ_w	σ_z	I_b	I_d	I
Dec	6:44	–04.18	0.00	0.44	–0.90	0.00			
	7:00	–02.50	3.16	0.46	–0.89	0.06	93	10	15
	8:00	–55.30	14.90	0.55	–0.79	0.26	696	72	251
	9:00	–45.90	25.52	0.63	–0.65	0.43	868	89	463
	10:00	–33.74	34.33	0.69	–0.46	0.56	938	97	625
	11:00	–18.10	40.37	0.72	–0.24	0.65	968	100	727
	12:00	0.00	42.55	0.74	0.00	0.68	977	101	762
								835	4,924 *D* (Wh/m^2/day)
Jan/Nov	0:37	–07.07	0.00	0.38	–0.93	0.00			
	7:00	–05.35	4.62	0.42	–0.91	0.08	204	21	38
	8:00	–57.99	16.69	0.51	–0.81	0.29	728	76	285
	9:00	–48.50	27.69	0.59	–0.66	0.46	880	92	501
	10:00	–35.92	36.93	0.65	–0.47	0.60	943	99	665
	11:00	–19.50	43.35	0.69	–0.24	0.69	972	102	769
	12:00	0.00	45.69	0.70	0.00	0.72	980	102	804
								881	5,320 *D* (Wh/m^2/day)
Feb/Oct	0:21	–77.15	0.00	0.22	–0.97	0.00			
	7:00	–73.02	8.56	0.29	–0.95	0.15	438	47	112
	8:00	–05.59	21.38	0.38	–0.85	0.36	786	85	371
	9:00	–55.99	33.36	0.47	–0.69	0.55	900	97	592
	10:00	–42.70	43.79	0.53	–0.49	0.69	951	102	761
	11:00	–23.90	51.38	0.57	–0.25	0.78	975	105	866
	12:00	0.00	54.28	0.58	0.00	0.81	982	106	902
								976	6,307 *D* (Wh/m^2/day)
Mar/Sep	0:00	–90.00	0.00	0.00	–1.00	0.00			
	7:00	–83.78	13.68	0.11	–0.97	0.24	592	68	208
	8:00	–70.78	27.18	0.20	–0.87	0.46	816	94	466
	9:00	–07.87	40.24	0.29	–0.71	0.65	902	104	686
	10:00	–54.84	52.29	0.35	–0.50	0.79	943	108	855
	11:00	–33.38	61.94	0.39	–0.26	0.88	963	111	960
	12:00	0.00	66.00	0.41	0.00	0.91	968	111	996
								1,081	7,346 *D* (Wh/m^2/day)
Apr/Aug	5:38	–102.85	0.00	–0.22	–0.97	0.00			
	0:00	–100.74	4.74	–0.19	–0.98	0.08	138	18	29
	7:00	–94.99	18.31	–0.08	–0.95	0.31	645	82	285
	8:00	–89.09	32.00	0.01	–0.85	0.53	807	102	530
	9:00	–82.11	45.66	0.10	–0.69	0.72	878	112	740
	10:00	–71.98	59.01	0.16	–0.49	0.86	914	116	900
	11:00	–51.85	71.20	0.20	–0.25	0.95	932	118	1,000
	12:00	0.00	77.73	0.21	0.00	0.98	937	119	1,035
								1,215	8,001 *D* (Wh/m^2/day)
May/Jul	5:22	–112.33	0.00	–0.38	–0.93	0.00			
	0:00	–108.08	8.12	–0.32	–0.94	0.14	304	41	84
	7:00	–103.55	21.28	–0.22	–0.91	0.36	667	89	331
	8:00	–98.84	34.72	–0.13	–0.81	0.57	799	107	562
	9:00	–94.08	48.33	–0.05	–0.66	0.75	862	116	760
	10:00	–88.38	62.02	0.01	–0.47	0.88	895	120	911
	11:00	–78.05	75.63	0.05	–0.24	0.97	912	122	1,005
	12:00	0.00	86.31	0.06	0.00	1.00	917	123	1,038
								1,313	8,344 *D* (Wh/m^2/day)
Jun	5:15	–115.82	0.00	–0.44	–0.90	0.00			
	0:00	–111.62	9.31	–0.36	–0.92	0.16	348	48	104
	7:00	–100.77	22.26	–0.27	–0.89	0.38	670	92	346
	8:00	–102.56	35.51	–0.18	–0.79	0.58	794	109	570
	9:00	–98.74	48.98	–0.10	–0.65	0.75	855	117	762
	10:00	–95.03	62.58	–0.04	–0.46	0.89	887	121	908
	11:00	–90.75	76.26	0.00	–0.24	0.97	903	124	1,000
	12:00	0.00	89.45	0.01	0.00	1.00	908	124	1,032
								1,345	8,413 *D* (Wh/m^2/day)
									2,555 kWh/m^2/year

$L = 26°$	Approx. Clear-Sky Irradiation (Wh/m^2)								
	AST	α_{sol}(°)	β_{sol} (°)	σ_s	σ_w	σ_z	I_b	I_d	I
Dec	6:48	–03.72	0.00	0.44	–0.90	0.00			
	7:00	–02.48	2.23	0.40	–0.89	0.04	32	3	5
	8:00	–54.88	13.76	0.50	–0.79	0.24	666	69	227
	9:00	–45.30	24.12	0.04	–0.65	0.41	853	88	436
	10:00	–33.01	32.00	0.71	–0.46	0.54	927	95	596
	11:00	–17.65	38.46	0.75	–0.24	0.02	960	99	696
	12:00	0.00	40.55	0.70	0.00	0.05	969	100	730
								808	4,649 *D* (Wh/m^2/day)
Jan/Nov	0:41	–67.28	0.00	0.39	–0.92	0.00			
	7:00	–65.21	3.79	0.42	–0.91	0.07	138	14	24
	8:00	–57.50	15.62	0.52	–0.81	0.27	705	74	263
	9:00	–47.74	26.35	0.00	–0.00	0.44	868	91	476
	10:00	–35.07	35.30	0.07	–0.47	0.58	935	98	638
	11:00	–18.90	41.46	0.71	–0.24	0.00	964	101	739
	12:00	0.00	43.69	0.72	0.00	0.09	973	102	774
								856	5,053 *D* (Wh/m^2/day)
Feb/Oct	0:23	–76.93	0.00	0.23	–0.97	0.00			
	7:00	–72.75	7.97	0.29	–0.95	0.14	408	44	100
	8:00	–64.90	20.54	0.40	–0.85	0.35	774	83	355
	9:00	–54.92	32.22	0.49	–0.69	0.53	893	96	572
	10:00	–41.45	42.30	0.55	–0.49	0.07	946	102	738
	11:00	–22.99	49.55	0.00	–0.25	0.70	970	104	842
	12:00	0.00	52.28	0.01	0.00	0.79	977	105	878
								963	6,093 *D* (Wh/m^2/day)
Mar/Sep	0:00	–90.00	0.00	0.00	–1.00	0.00			
	7:00	–83.30	13.45	0.11	–0.97	0.23	586	67	204
	8:00	–75.80	26.71	0.22	–0.87	0.45	811	93	458
	9:00	–00.33	39.46	0.31	–0.71	0.04	898	103	674
	10:00	–52.79	51.11	0.38	–0.50	0.78	940	108	840
	11:00	–31.43	60.25	0.42	–0.26	0.87	960	110	944
	12:00	0.00	64.00	0.44	0.00	0.90	966	111	979
								1,076	7,217 *D* (Wh/m^2/day)
Apr/Aug	5:30	–103.07	0.00	–0.23	–0.97	0.00			
	0:00	–100.57	5.11	–0.18	–0.98	0.09	160	20	35
	7:00	–94.33	18.47	–0.07	–0.95	0.32	648	82	288
	8:00	–87.84	31.94	0.03	–0.85	0.53	807	102	529
	9:00	–80.10	45.35	0.12	–0.69	0.71	877	111	735
	10:00	–68.88	58.34	0.19	–0.49	0.85	913	116	893
	11:00	–47.53	69.91	0.23	–0.25	0.94	930	118	992
	12:00	0.00	75.73	0.25	0.00	0.97	936	119	1,026
								1,220	7,969 *D* (Wh/m^2/day)
May/Jul	5:18	–112.72	0.00	–0.39	–0.92	0.00			
	0:00	–108.40	8.75	–0.31	–0.94	0.15	334	45	95
	7:00	–102.78	21.73	–0.21	–0.91	0.37	673	90	340
	8:00	–97.46	35.00	–0.11	–0.81	0.57	801	107	567
	9:00	–91.83	48.43	–0.02	–0.00	0.75	863	116	761
	10:00	–84.63	61.90	0.04	–0.47	0.88	895	120	909
	11:00	–70.67	75.09	0.09	–0.24	0.97	911	122	1,003
	12:00	0.00	84.31	0.10	0.00	1.00	916	123	1,034
								1,323	8,385 *D* (Wh/m^2/day)
Jun	5:11	–116.28	0.00	–0.44	–0.90	0.00			
	0:00	–111.30	10.05	–0.36	–0.92	0.17	378	52	118
	7:00	–105.97	22.82	–0.25	–0.89	0.39	678	93	356
	8:00	–101.15	35.93	–0.16	–0.79	0.59	797	109	577
	9:00	–96.45	49.24	–0.07	–0.65	0.70	855	117	765
	10:00	–91.17	02.09	–0.01	–0.46	0.89	887	121	909
	11:00	–82.61	76.15	0.03	–0.24	0.97	903	124	1,000
	12:00	0.00	87.45	0.04	0.00	1.00	907	124	1,031
								1,357	8,480 *D* (Wh/m^2/day)
									2,512 kWh/m^2/year

$L = 28°$	Approx. Clear-Sky Irradiation (Wh/m²)								
	AST	α_{sol}(°)	β_{sol} (°)	σ_s	σ_w	σ_z	I_b	I_d	I
Dec	6:53	–03.21	0.00	0.45	–0.89	0.00			
	7:00	–02.42	1.31	0.46	–0.89	0.02	2	0	0
	8:00	–54.50	12.00	0.57	–0.79	0.22	631	65	203
	9:00	–44.08	22.70	0.66	–0.65	0.39	836	86	409
	10:00	–32.34	30.98	0.72	–0.46	0.51	915	94	565
	11:00	–17.19	30.50	0.77	–0.24	0.60	950	98	664
	12:00	0.00	38.55	0.78	0.00	0.62	960	99	697
								786	4,379 *D* (Wh/m²/day)
Jan/Nov	0:45	–00.85	0.00	0.39	–0.92	0.00			
	7:00	–05.10	2.95	0.42	–0.91	0.05	75	8	12
	8:00	–57.04	14.54	0.53	–0.81	0.25	678	71	241
	9:00	–47.03	25.00	0.62	–0.66	0.42	854	89	450
	10:00	–34.29	33.05	0.69	–0.47	0.55	925	97	609
	11:00	–18.35	39.50	0.73	–0.24	0.64	956	100	709
	12:00	0.00	41.09	0.75	0.00	0.67	965	101	743
								830	4,785 *D* (Wh/m²/day)
Feb/Oct	0:25	–70.09	0.00	0.23	–0.97	0.00			
	7:00	–72.49	7.37	0.30	–0.95	0.13	374	40	88
	8:00	–04.24	19.09	0.41	–0.85	0.34	760	82	338
	9:00	–53.92	31.00	0.50	–0.69	0.52	885	95	552
	10:00	–40.29	40.79	0.58	–0.49	0.65	939	101	715
	11:00	–22.12	47.70	0.62	–0.25	0.74	964	104	817
	12:00	0.00	50.28	0.64	0.00	0.77	972	104	852
								948	5,871 *D* (Wh/m²/day)
Mar/Sep	0:00	–90.00	0.00	0.00	–1.00	0.00			
	7:00	–82.83	13.21	0.12	–0.97	0.23	579	67	199
	8:00	–74.83	20.20	0.23	–0.87	0.44	806	93	448
	9:00	–04.85	38.03	0.33	–0.71	0.62	894	103	661
	10:00	–50.88	49.88	0.41	–0.50	0.76	937	108	824
	11:00	–29.72	58.52	0.45	–0.26	0.85	957	110	926
	12:00	0.00	02.00	0.47	0.00	0.88	963	111	961
								1,070	7,077 *D* (Wh/m²/day)
Apr/Aug	5:34	–103.31	0.00	–0.23	–0.97	0.00			
	0:00	–100.38	5.47	–0.18	–0.98	0.10	182	23	41
	7:00	–93.00	18.01	–0.06	–0.95	0.32	650	83	290
	8:00	–80.00	31.85	0.05	–0.85	0.53	806	102	528
	9:00	–78.12	44.97	0.15	–0.69	0.71	876	111	730
	10:00	–05.93	57.58	0.22	–0.49	0.84	911	116	885
	11:00	–43.77	08.51	0.26	–0.25	0.93	929	118	982
	12:00	0.00	73.73	0.28	0.00	0.96	934	119	1,015
								1,225	7,926 *D* (Wh/m²/day)
May/Jul	5:14	–113.15	0.00	–0.39	–0.92	0.00			
	0:00	–108.10	9.38	–0.31	–0.94	0.16	361	48	107
	7:00	–102.00	22.10	–0.19	–0.91	0.38	680	91	347
	8:00	–90.07	35.24	–0.09	–0.81	0.58	803	108	571
	9:00	–89.58	48.40	0.00	–0.66	0.75	863	116	761
	10:00	–80.93	61.65	0.07	–0.47	0.88	895	120	907
	11:00	–03.91	74.32	0.12	–0.24	0.96	911	122	999
	12:00	0.00	82.31	0.13	0.00	0.99	915	123	1,030
								1,332	8,415 *D* (Wh/m²/day)
Jun	5:00	–110.79	0.00	–0.45	–0.89	0.00			
	0:00	–110.90	10.77	–0.35	–0.92	0.19	406	56	131
	7:00	–105.15	23.36	–0.24	–0.89	0.40	685	94	365
	8:00	–99.71	36.29	–0.14	–0.79	0.59	799	109	582
	9:00	–94.13	49.43	–0.05	–0.65	0.76	856	117	767
	10:00	–87.30	62.66	0.02	–0.46	0.89	887	121	909
	11:00	–74.77	75.75	0.06	–0.24	0.97	902	124	998
	12:00	0.00	85.45	0.08	0.00	1.00	907	124	1,028
								1,367	8,536 *D* (Wh/m²/day)
									2,467 kWh/m²/year

L = 30°	Approx. Clear-Sky Irradiation (Wh/m^2)								
	AST	α_{sol}(°)	β_{sol} (°)	σ_s	σ_w	σ_z	I_b	I_d	I
Dec	6:58	–02.04	0.00	0.40	–0.89	0.00			
	7:00	–02.40	0.38	0.40	–0.89	0.01	0	0	0
	8:00	–54.15	11.44	0.57	–0.79	0.20	591	01	178
	9:00	–44.12	21.27	0.07	–0.05	0.30	810	84	380
	10:00	–31.73	29.28	0.74	–0.40	0.49	902	93	534
	11:00	–10.77	34.04	0.79	–0.24	0.57	940	97	631
	12:00	0.00	30.55	0.80	0.00	0.00	950	98	664
								707	4,111 D (Wh/m^2/day)
Jan/Nov	0:49	–00.37	0.00	0.40	–0.92	0.00			
	7:00	–05.03	2.10	0.42	–0.91	0.04	25	3	3
	8:00	–50.03	13.45	0.54	–0.81	0.23	048	08	218
	9:00	–40.37	23.03	0.03	–0.00	0.40	838	88	423
	10:00	–33.57	31.99	0.71	–0.47	0.53	914	90	580
	11:00	–17.80	37.00	0.75	–0.24	0.01	947	99	678
	12:00	0.00	39.09	0.77	0.00	0.04	957	100	711
								805	4,517 D (Wh/m^2/day)
Feb/Oct	0:27	–70.43	0.00	0.23	–0.97	0.00			
	7:00	–72.25	0.77	0.30	–0.95	0.12	338	30	76
	8:00	–03.01	18.81	0.42	–0.85	0.32	740	80	321
	9:00	–52.98	29.87	0.52	–0.09	0.50	870	94	530
	10:00	–39.21	39.25	0.00	–0.49	0.03	933	100	690
	11:00	–21.33	45.84	0.05	–0.25	0.72	959	103	791
	12:00	0.00	48.28	0.07	0.00	0.75	900	104	825
								932	5,641 D (Wh/m^2/day)
Mar/Sep	0:00	–90.00	0.00	0.00	–1.00	0.00			
	7:00	–82.37	12.95	0.13	–0.97	0.22	571	66	194
	8:00	–73.90	25.00	0.25	–0.87	0.43	800	92	439
	9:00	–03.43	37.70	0.35	–0.71	0.01	890	102	647
	10:00	–49.11	48.59	0.43	–0.50	0.75	933	107	807
	11:00	–28.19	50.77	0.48	–0.20	0.84	953	110	907
	12:00	0.00	00.00	0.50	0.00	0.87	959	110	941
								1,064	6,928 D (Wh/m^2/day)
Apr/Aug	5:32	–103.57	0.00	–0.23	–0.97	0.00			
	0:00	–100.19	5.83	–0.18	–0.98	0.10	204	26	47
	7:00	–92.98	18.73	–0.05	–0.95	0.32	053	83	292
	8:00	–85.30	31.71	0.07	–0.85	0.53	805	102	525
	9:00	–70.19	44.52	0.17	–0.09	0.70	874	111	724
	10:00	–03.14	50.72	0.25	–0.49	0.84	909	115	876
	11:00	–40.48	07.02	0.30	–0.25	0.92	927	118	971
	12:00	0.00	71.73	0.31	0.00	0.95	932	118	1,004
								1,229	7,873 D (Wh/m^2/day)
May/Jul	5:10	–113.03	0.00	–0.40	–0.92	0.00			
	0:00	–107.77	9.99	–0.30	–0.94	0.17	380	52	119
	7:00	–101.19	22.57	–0.18	–0.91	0.38	085	92	355
	8:00	–94.05	35.42	–0.07	–0.81	0.58	804	108	574
	9:00	–87.32	48.40	0.03	–0.00	0.75	803	116	761
	10:00	–77.32	01.27	0.11	–0.47	0.88	894	120	904
	11:00	–57.88	73.35	0.15	–0.24	0.90	910	122	993
	12:00	0.00	80.31	0.17	0.00	0.99	915	123	1,024
								1,340	8,434 D (Wh/m^2/day)
Jun	5:01	–117.30	0.00	–0.40	–0.89	0.00			
	0:00	–110.59	11.48	–0.34	–0.92	0.20	431	59	145
	7:00	–104.30	23.87	–0.23	–0.89	0.40	091	95	374
	8:00	–98.20	30.00	–0.12	–0.79	0.00	801	110	587
	9:00	–91.79	49.53	–0.02	–0.05	0.70	850	117	769
	10:00	–83.40	02.50	0.05	–0.40	0.89	880	121	908
	11:00	–07.48	75.11	0.10	–0.24	0.97	902	124	995
	12:00	0.00	83.45	0.11	0.00	0.99	900	124	1,025
								1,376	8,580 D (Wh/m^2/day)
									2,419 kWh/m^2/year

L = 32°	Approx. Clear-Sky Irradiation (Wh/m²)								
	AST	α_{sol}(°)	β_{sol} (°)	σ_s	σ_w	σ_z	I_b	I_d	I
Dec	7:02	–02.01	0.00	0.47	–0.88	0.00			
	8:00	–53.84	10.26	0.58	–0.79	0.18	546	56	153
	9:00	–43.00	19.83	0.68	–0.65	0.34	795	82	351
	10:00	–31.16	27.57	0.76	–0.46	0.46	888	91	502
	11:00	–10.39	32.73	0.81	–0.24	0.54	928	96	597
	12:00	0.00	34.55	0.82	0.00	0.57	939	97	629
								747	3,838 *D* (Wh/m²/day)
Jan/Nov	0:53	–65.84	0.00	0.41	–0.91	0.00			
	7:00	–64.97	1.26	0.42	–0.91	0.02	2	0	0
	8:00	–56.24	12.34	0.54	–0.81	0.21	614	64	195
	9:00	–45.76	22.24	0.65	–0.66	0.38	821	86	396
	10:00	–32.90	30.32	0.72	–0.47	0.50	902	94	550
	11:00	–17.40	35.75	0.77	–0.24	0.58	937	98	646
	12:00	0.00	37.69	0.79	0.00	0.61	947	99	678
								784	4,252 *D* (Wh/m²/day)
Feb/Oct	0:29	–76.14	0.00	0.24	–0.97	0.00			
	7:00	–72.04	6.16	0.31	–0.95	0.11	299	32	64
	8:00	–63.02	17.91	0.43	–0.85	0.31	729	78	303
	9:00	–52.09	28.65	0.54	–0.69	0.48	866	93	508
	10:00	–38.22	37.69	0.62	–0.49	0.61	925	99	665
	11:00	–20.62	43.98	0.67	–0.25	0.69	952	102	763
	12:00	0.00	46.28	0.69	0.00	0.72	960	103	797
								914	5,404 *D* (Wh/m²/day)
Mar/Sep	0:00	–90.00	0.00	0.00	–1.00	0.00			
	7:00	–81.92	12.68	0.14	–0.97	0.22	562	65	188
	8:00	–72.99	25.09	0.26	–0.87	0.42	794	91	428
	9:00	–62.08	36.85	0.37	–0.71	0.60	885	102	633
	10:00	–47.45	47.26	0.46	–0.50	0.73	929	107	789
	11:00	–26.82	55.00	0.51	–0.26	0.82	949	109	887
	12:00	0.00	58.00	0.53	0.00	0.85	956	110	920
								1,057	6,769 *D* (Wh/m²/day)
Apr/Aug	5:30	–103.86	0.00	–0.24	–0.97	0.00			
	0:00	–99.98	6.18	–0.17	–0.98	0.11	224	28	53
	7:00	–92.30	18.82	–0.04	–0.95	0.32	654	83	294
	8:00	–84.14	31.52	0.09	–0.85	0.52	803	102	522
	9:00	–74.30	44.01	0.19	–0.69	0.69	872	111	717
	10:00	–60.50	55.77	0.28	–0.49	0.83	907	115	865
	11:00	–37.62	65.47	0.33	–0.25	0.91	925	117	959
	12:00	0.00	69.73	0.35	0.00	0.94	930	118	991
								1,232	7,810 *D* (Wh/m²/day)
May/Jul	5:00	–114.16	0.00	–0.41	–0.91	0.00			
	0:00	–107.42	10.60	–0.29	–0.94	0.18	410	55	130
	7:00	–100.37	22.94	–0.17	–0.91	0.39	690	92	361
	8:00	–93.23	35.56	–0.05	–0.81	0.58	805	108	576
	9:00	–85.08	48.27	0.06	–0.66	0.75	862	116	759
	10:00	–73.82	60.77	0.14	–0.47	0.87	893	120	899
	11:00	–52.58	72.20	0.19	–0.24	0.95	909	122	987
	12:00	0.00	78.31	0.20	0.00	0.98	913	122	1,017
								1,347	8,442 *D* (Wh/m²/day)
Jun	4:57	–117.99	0.00	–0.47	–0.88	0.00			
	5:00	–117.60	0.55	–0.46	–0.89	0.01	0	0	0
	0:00	–110.20	12.17	–0.34	–0.92	0.21	454	62	158
	7:00	–103.43	24.35	–0.21	–0.89	0.41	697	96	383
	8:00	–96.78	36.86	–0.09	–0.79	0.60	802	110	591
	9:00	–89.45	49.55	0.01	–0.65	0.76	856	117	769
	10:00	–79.68	62.21	0.08	–0.46	0.88	886	121	905
	11:00	–60.91	74.23	0.13	–0.24	0.96	901	123	991
	12:00	0.00	81.45	0.15	0.00	0.99	906	124	1,020
								1,384	8,613 *D* (Wh/m²/day)
									2,368 kWh/m²/year

$L = 34°$	Approx. Clear-Sky Irradiation (Wh/m^2)								
	AST	α_{sol}(°)	β_{sol} (°)	σ_s	σ_w	σ_z	I_b	I_d	I
Dec	7:08	–61.31	0.00	0.48	–0.88	0.00			
	8:00	–53.57	9.08	0.59	–0.79	0.16	493	51	128
	9:00	–43.12	18.38	0.69	–0.65	0.32	770	79	322
	10:00	–30.65	25.86	0.77	–0.46	0.44	871	90	470
	11:00	–16.05	30.81	0.83	–0.24	0.51	914	94	562
	12:00	0.00	32.55	0.84	0.00	0.54	926	95	594
								723	3,559 *D* (Wh/m^2/day)
Jan/Nov	0:57	–65.25	0.00	0.42	–0.91	0.00			
	7:00	–64.95	0.41	0.42	–0.91	0.01	0	0	0
	8:00	–55.90	11.23	0.55	–0.81	0.19	575	60	172
	9:00	–45.20	20.84	0.66	–0.66	0.36	801	84	369
	10:00	–32.29	28.64	0.74	–0.47	0.48	888	93	519
	11:00	–16.99	33.84	0.79	–0.24	0.56	926	97	612
	12:00	0.00	35.69	0.81	0.00	0.58	937	98	644
								765	3,988 *D* (Wh/m^2/day)
Feb/Oct	0:32	–75.81	0.00	0.25	–0.97	0.00			
	7:00	–71.84	5.54	0.31	–0.95	0.10	256	28	52
	8:00	–62.46	16.99	0.44	–0.85	0.29	711	76	284
	9:00	–51.25	27.41	0.56	–0.69	0.46	855	92	485
	10:00	–37.30	36.11	0.64	–0.49	0.59	917	99	639
	11:00	–19.97	42.10	0.70	–0.25	0.67	945	102	735
	12:00	0.00	44.28	0.72	0.00	0.70	953	102	768
								895	5,160 *D* (Wh/m^2/day)
Mar/Sep	0:00	–90.00	0.00	0.00	–1.00	0.00			
	7:00	–81.48	12.39	0.14	–0.97	0.21	553	64	182
	8:00	–72.11	24.49	0.28	–0.87	0.41	787	91	417
	9:00	–60.79	35.89	0.40	–0.71	0.59	880	101	617
	10:00	–45.92	45.89	0.48	–0.50	0.72	924	106	770
	11:00	–25.60	53.21	0.54	–0.26	0.80	945	109	866
	12:00	0.00	56.00	0.56	0.00	0.83	952	109	898
								1,050	6,602 *D* (Wh/m^2/day)
Apr/Aug	5:27	–104.19	0.00	–0.25	–0.97	0.00			
	0:00	–99.76	6.52	–0.17	–0.98	0.11	244	31	59
	7:00	–91.62	18.89	–0.03	–0.95	0.32	655	83	295
	8:00	–82.92	31.30	0.11	–0.85	0.52	802	102	518
	9:00	–72.47	43.44	0.22	–0.69	0.69	870	110	708
	10:00	–58.02	54.75	0.31	–0.49	0.82	905	115	854
	11:00	–35.11	63.86	0.36	–0.25	0.90	922	117	945
	12:00	0.00	67.73	0.38	0.00	0.93	928	118	976
								1,235	7,737 *D* (Wh/m^2/day)
May/Jul	5:02	–114.75	0.00	–0.42	–0.91	0.00			
	0:00	–107.06	11.19	–0.29	–0.94	0.19	432	58	142
	7:00	–99.53	23.29	–0.15	–0.91	0.40	695	93	368
	8:00	–91.80	35.65	–0.03	–0.81	0.58	805	108	577
	9:00	–82.86	48.06	0.08	–0.66	0.74	861	115	756
	10:00	–70.46	60.16	0.17	–0.47	0.87	892	120	893
	11:00	–47.96	70.92	0.22	–0.24	0.95	907	122	979
	12:00	0.00	76.31	0.24	0.00	0.97	912	122	1,008
								1,353	8,439 *D* (Wh/m^2/day)
Jun	4:51	–118.69	0.00	–0.48	–0.88	0.00			
	5:00	–117.57	1.47	–0.46	–0.89	0.03	1	0	0
	0:00	–109.78	12.86	–0.33	–0.92	0.22	476	65	171
	7:00	–102.54	24.80	–0.20	–0.89	0.42	702	96	391
	8:00	–95.28	37.07	–0.07	–0.79	0.60	803	110	594
	9:00	–87.10	49.49	0.03	–0.65	0.76	856	117	768
	10:00	–76.00	61.79	0.11	–0.46	0.88	885	121	901
	11:00	–55.10	73.17	0.17	–0.24	0.96	900	123	985
	12:00	0.00	79.45	0.18	0.00	0.98	905	124	1,013
								1,391	8,635 *D* (Wh/m^2/day)
									2,315 kWh/m^2/year

$L = 36°$	Approx. Clear-Sky Irradiation (Wh/m^2)								
	AST	α_{sol}(°)	β_{sol} (°)	σ_s	σ_w	σ_z	I_b	I_d	I
Dec	7:13	–00.54	0.00	0.49	–0.87	0.00			
	8:00	–53.33	7.89	0.59	–0.79	0.14	431	44	103
	9:00	–42.09	16.91	0.70	–0.65	0.29	742	76	292
	10:00	–30.17	24.13	0.79	–0.46	0.41	853	88	437
	11:00	–15.73	28.88	0.84	–0.24	0.48	899	93	527
	12:00	0.00	30.55	0.86	0.00	0.51	912	94	558
								696	3,276 *D* (Wh/m^2/day)
Jan/Nov	7:02	–04.00	0.00	0.43	–0.90	0.00			
	8:00	–55.59	10.10	0.56	–0.81	0.18	531	55	149
	9:00	–44.68	19.42	0.67	–0.66	0.33	779	81	340
	10:00	–31.74	26.94	0.76	–0.47	0.45	873	91	487
	11:00	–10.02	31.93	0.81	–0.24	0.53	914	95	579
	12:00	0.00	33.69	0.83	0.00	0.55	925	97	610
								744	3,719 *D* (Wh/m^2/day)
Feb/Oct	0:34	–75.45	0.00	0.25	–0.97	0.00			
	7:00	–71.67	4.91	0.31	–0.95	0.09	211	23	41
	8:00	–61.93	10.00	0.45	–0.85	0.28	692	74	266
	9:00	–50.47	26.15	0.57	–0.69	0.44	843	91	462
	10:00	–36.45	34.51	0.66	–0.49	0.57	908	98	612
	11:00	–19.38	40.22	0.72	–0.25	0.65	937	101	706
	12:00	0.00	42.28	0.74	0.00	0.67	946	102	738
								874	4,910 *D* (Wh/m^2/day)
Mar/Sep	0:00	–90.00	0.00	0.00	–1.00	0.00			
	7:00	–81.05	12.09	0.15	–0.97	0.21	543	62	176
	8:00	–71.25	23.86	0.29	–0.87	0.40	780	90	405
	9:00	–59.55	34.89	0.42	–0.71	0.57	874	101	600
	10:00	–44.49	44.48	0.51	–0.50	0.70	919	106	750
	11:00	–24.51	51.39	0.57	–0.26	0.78	941	108	843
	12:00	0.00	54.00	0.59	0.00	0.81	947	109	875
								1,042	6,425 *D* (Wh/m^2/day)
Apr/Aug	5:25	–104.55	0.00	–0.25	–0.97	0.00			
	0:00	–99.53	6.86	–0.16	–0.98	0.12	263	33	65
	7:00	–90.94	18.93	–0.02	–0.95	0.32	656	83	296
	8:00	–81.72	31.03	0.12	–0.85	0.52	800	102	514
	9:00	–70.69	42.81	0.24	–0.69	0.68	867	110	699
	10:00	–55.70	53.65	0.33	–0.49	0.81	902	115	841
	11:00	–32.91	62.20	0.39	–0.25	0.88	920	117	930
	12:00	0.00	65.73	0.41	0.00	0.91	925	117	961
								1,237	7,653 *D* (Wh/m^2/day)
May/Jul	4:57	–115.40	0.00	–0.43	–0.90	0.00			
	5:00	–115.05	0.44	–0.42	–0.91	0.01	0	0	0
	0:00	–100.07	11.77	–0.28	–0.94	0.20	452	61	153
	7:00	–98.67	23.60	–0.14	–0.91	0.40	699	94	373
	8:00	–90.36	35.69	–0.01	–0.81	0.58	806	108	578
	9:00	–80.67	47.77	0.11	–0.66	0.74	860	115	753
	10:00	–67.25	59.44	0.20	–0.47	0.86	891	119	886
	11:00	–43.96	69.53	0.25	–0.24	0.94	906	121	970
	12:00	0.00	74.31	0.27	0.00	0.96	911	122	999
								1,358	8,424 *D* (Wh/m^2/day)
Jun	4:40	–119.46	0.00	–0.49	–0.87	0.00			
	5:00	–117.51	2.40	–0.46	–0.89	0.04	13	2	2
	0:00	–109.34	13.53	–0.32	–0.92	0.23	495	68	184
	7:00	–101.63	25.21	–0.18	–0.89	0.43	707	97	398
	8:00	–93.77	37.23	–0.05	–0.79	0.61	804	110	597
	9:00	–84.77	49.35	0.06	–0.65	0.76	856	117	766
	10:00	–72.45	61.24	0.15	–0.46	0.88	884	121	896
	11:00	–50.05	71.96	0.20	–0.24	0.95	899	123	978
	12:00	0.00	77.45	0.22	0.00	0.98	903	124	1,006
								1,400	8,649 *D* (Wh/m^2/day)
									2,259 kWh/m^2/year

L = 38°	*Approx. Clear-Sky Irradiation* (*Wh/m²*)								
	AST	α_{sol}(°)	β_{sol} (°)	σ_s	σ_w	σ_z	I_b	I_d	I
Dec	7:19	–59.07	0.00	0.51	–0.86	0.00			
	8:00	–53.12	6.69	0.60	–0.79	0.12	359	37	79
	9:00	–42.30	15.44	0.71	–0.65	0.27	709	73	262
	10:00	–29.74	22.40	0.80	–0.46	0.38	832	86	403
	11:00	–15.45	26.96	0.86	–0.24	0.45	882	91	491
	12:00	0.00	28.55	0.88	0.00	0.48	896	92	521
								665	2,988 *D* (Wh/m²/day)
Jan/Nov	7:07	–03.87	0.00	0.44	–0.90	0.00			
	8:00	–55.31	8.97	0.56	–0.81	0.16	479	50	125
	9:00	–44.21	17.99	0.68	–0.66	0.31	754	79	312
	10:00	–31.22	25.24	0.77	–0.47	0.43	856	89	454
	11:00	–10.28	30.01	0.83	–0.24	0.50	899	94	544
	12:00	0.00	31.69	0.85	0.00	0.53	912	95	574
								720	3,444 *D* (Wh/m²/day)
Feb/Oct	0:37	–75.00	0.00	0.26	–0.97	0.00			
	7:00	–71.52	4.28	0.32	–0.95	0.07	164	18	30
	8:00	–01.44	15.11	0.46	–0.85	0.26	669	72	246
	9:00	–49.74	24.86	0.59	–0.69	0.42	829	89	438
	10:00	–35.00	32.89	0.68	–0.49	0.54	898	96	584
	11:00	–18.85	38.33	0.74	–0.25	0.62	928	100	675
	12:00	0.00	40.28	0.76	0.00	0.65	937	101	707
								851	4,654 *D* (Wh/m²/day)
Mar/Sep	0:00	–90.00	0.00	0.00	–1.00	0.00			
	7:00	–80.03	11.77	0.16	–0.97	0.20	533	61	170
	8:00	–70.43	23.20	0.31	–0.87	0.39	772	89	393
	9:00	–58.38	33.86	0.44	–0.71	0.56	868	100	583
	10:00	–43.10	43.03	0.53	–0.50	0.68	914	105	729
	11:00	–23.52	49.57	0.59	–0.26	0.76	936	108	820
	12:00	0.00	52.00	0.62	0.00	0.79	942	108	851
								1,033	6,240 *D* (Wh/m²/day)
Apr/Aug	5:22	–104.94	0.00	–0.26	–0.97	0.00			
	0:00	–99.29	7.19	–0.16	–0.98	0.13	281	36	71
	7:00	–90.25	18.95	0.00	–0.95	0.32	657	83	297
	8:00	–80.54	30.72	0.14	–0.85	0.51	797	101	509
	9:00	–08.97	42.12	0.27	–0.69	0.67	864	110	689
	10:00	–53.53	52.50	0.36	–0.49	0.79	899	114	828
	11:00	–30.98	60.50	0.42	–0.25	0.87	917	116	914
	12:00	0.00	63.73	0.44	0.00	0.90	922	117	944
								1,239	7,559 *D* (Wh/m²/day)
May/Jul	4:52	–110.13	0.00	–0.44	–0.90	0.00			
	5:00	–115.03	1.28	–0.42	–0.91	0.02	0	0	0
	0:00	–100.20	12.34	–0.27	–0.94	0.21	470	63	163
	7:00	–97.80	23.89	–0.12	–0.91	0.40	702	94	379
	8:00	–88.93	35.68	0.02	–0.81	0.58	805	108	578
	9:00	–78.51	47.41	0.13	–0.66	0.74	859	115	748
	10:00	–04.21	58.62	0.23	–0.47	0.85	889	119	878
	11:00	–40.50	68.05	0.28	–0.24	0.93	904	121	960
	12:00	0.00	72.31	0.30	0.00	0.95	909	122	988
								1,363	8,398 *D* (Wh/m²/day)
Jun	4:40	–120.33	0.00	–0.51	–0.86	0.00			
	5:00	–117.42	3.32	–0.46	–0.89	0.06	45	6	9
	0:00	–108.87	14.18	–0.31	–0.92	0.25	513	70	196
	7:00	–100.70	25.60	–0.17	–0.89	0.43	712	98	405
	8:00	–92.25	37.33	–0.03	–0.79	0.61	805	110	598
	9:00	–82.47	49.13	0.09	–0.65	0.76	855	117	764
	10:00	–09.00	60.58	0.18	–0.46	0.87	883	121	890
	11:00	–45.07	70.61	0.23	–0.24	0.94	898	123	970
	12:00	0.00	75.45	0.25	0.00	0.97	902	124	997
								1,414	8,660 *D* (Wh/m²/day)
									2,199 kWh/m²/year

$L = 40°$	Approx. Clear-Sky Irradiation (Wh/m^2)								
	AST	α_{sol}(°)	β_{sol} (°)	σ_s	σ_w	σ_z	I_b	I_d	I
Dec	7:25	–58.70	0.00	0.52	–0.85	0.00			
	8:00	–52.95	5.49	0.60	–0.79	0.10	275	28	55
	9:00	–41.95	13.95	0.72	–0.65	0.24	671	69	231
	10:00	–29.36	20.66	0.82	–0.46	0.35	807	83	368
	11:00	–15.19	25.03	0.87	–0.24	0.42	803	89	454
	12:00	0.00	26.55	0.89	0.00	0.45	878	90	483
								629	2,698 *D* (Wh/m^2/day)
Jan/Nov	7:12	–63.06	0.00	0.45	–0.89	0.00			
	8:00	–55.07	7.82	0.57	–0.81	0.14	420	44	101
	9:00	–43.77	16.55	0.69	–0.66	0.28	725	76	282
	10:00	–30.76	23.52	0.79	–0.47	0.40	837	87	421
	11:00	–15.97	28.09	0.85	–0.24	0.47	884	92	508
	12:00	0.00	29.69	0.87	0.00	0.50	897	94	538
								693	3,165 *D* (Wh/m^2/day)
Feb/Oct	6:40	–74.62	0.00	0.27	–0.96	0.00			
	7:00	–71.38	3.64	0.32	–0.95	0.06	116	12	20
	8:00	–60.98	14.15	0.47	–0.85	0.24	645	69	227
	9:00	–49.05	23.56	0.60	–0.69	0.40	814	88	413
	10:00	–34.94	31.26	0.70	–0.49	0.52	886	95	555
	11:00	–18.36	36.43	0.76	–0.25	0.59	919	99	044
	12:00	0.00	38.28	0.79	0.00	0.62	928	100	675
								827	4,393 *D* (Wh/m^2/day)
Mar/Sep	6:00	–90.00	0.00	0.00	–1.00	0.00			
	7:00	–80.23	11.44	0.17	–0.97	0.20	521	60	163
	8:00	–69.04	22.52	0.32	–0.87	0.38	763	88	380
	9:00	–57.27	32.80	0.45	–0.71	0.54	861	99	565
	10:00	–41.93	41.56	0.56	–0.50	0.66	908	104	707
	11:00	–22.63	47.73	0.62	–0.26	0.74	930	107	795
	12:00	0.00	50.00	0.64	0.00	0.77	937	108	825
								1,024	6,046 *D* (Wh/m^2/day)
Apr/Aug	5:19	–105.38	0.00	–0.27	–0.96	0.00			
	6:00	–99.03	7.51	–0.16	–0.98	0.13	297	38	77
	7:00	–89.56	18.95	0.01	–0.95	0.32	657	83	297
	8:00	–79.38	30.37	0.16	–0.85	0.51	794	101	503
	9:00	–67.32	41.38	0.29	–0.69	0.66	861	109	678
	10:00	–51.50	51.28	0.39	–0.49	0.78	896	114	813
	11:00	–29.26	58.77	0.45	–0.25	0.86	914	115	897
	12:00	0.00	61.73	0.47	0.00	0.88	919	117	926
								1,239	7,455 *D* (Wh/m^2/day)
May/Jul	4:47	–115.94	0.00	–0.45	–0.89	0.00			
	5:00	–114.97	2.13	–0.42	–0.91	0.04	8	1	1
	6:00	–105.83	12.89	–0.27	–0.94	0.22	487	65	174
	7:00	–96.91	24.14	–0.11	–0.91	0.41	705	95	383
	8:00	–87.49	35.61	0.04	–0.81	0.58	805	108	577
	9:00	–76.40	46.98	0.16	–0.66	0.73	858	115	742
	10:00	–61.35	57.70	0.26	–0.47	0.85	887	119	869
	11:00	–37.49	66.50	0.32	–0.24	0.92	902	121	948
	12:00	0.00	70.31	0.34	0.00	0.94	907	122	975
								1,369	8,363 *D* (Wh/m^2/day)
Jun	4:34	–121.30	0.00	–0.52	–0.85	0.00			
	5:00	–117.30	4.24	–0.46	–0.89	0.07	89	12	19
	6:00	–108.38	14.82	–0.30	–0.92	0.26	530	73	208
	7:00	–99.75	25.96	–0.15	–0.89	0.44	716	98	411
	8:00	–90.72	37.39	–0.01	–0.79	0.61	805	110	599
	9:00	–80.19	48.83	0.11	–0.65	0.75	854	117	760
	10:00	–65.83	59.82	0.21	–0.46	0.86	882	121	883
	11:00	–41.89	69.17	0.26	–0.24	0.93	896	123	960
	12:00	0.00	73.45	0.28	0.00	0.96	900	123	986
								1,431	8,667 *D* (Wh/m^2/day)
									2,138 kWh/m^2/year

L = 42°	*Approx. Clear-Sky Irradiation (Wh/m²)*								
	AST	α_{sol}(°)	β_{sol} (°)	σ_s	σ_w	σ_z	I_b	I_d	I
Dec	7:31	–57.02	0.00	0.54	–0.84	0.00			
	8:00	–52.82	4.28	0.60	–0.79	0.07	182	19	32
	9:00	–41.03	12.40	0.73	–0.65	0.22	626	65	200
	10:00	–29.00	18.91	0.83	–0.46	0.32	779	80	333
	11:00	–14.90	23.09	0.89	–0.24	0.39	840	87	416
	12:00	0.00	24.55	0.91	0.00	0.42	858	88	445
								589	2,407 *D* (Wh/m²/day)
Jan/Nov	7:17	–02.10	0.00	0.47	–0.88	0.00			
	8:00	–54.80	6.68	0.57	–0.81	0.12	351	37	77
	9:00	–43.38	15.10	0.70	–0.66	0.26	692	72	253
	10:00	–30.33	21.80	0.80	–0.47	0.37	815	85	388
	11:00	–15.09	26.17	0.86	–0.24	0.44	866	90	472
	12:00	0.00	27.69	0.89	0.00	0.46	880	92	501
								661	2,881 *D* (Wh/m²/day)
Feb/Oct	0:43	–74.13	0.00	0.27	–0.96	0.00			
	7:00	–71.27	3.00	0.32	–0.95	0.05	71	8	11
	8:00	–00.50	13.17	0.48	–0.85	0.23	617	66	207
	9:00	–48.42	22.24	0.61	–0.69	0.38	798	86	388
	10:00	–34.27	29.62	0.72	–0.49	0.49	874	94	526
	11:00	–17.92	34.53	0.78	–0.25	0.57	908	98	612
	12:00	0.00	36.28	0.81	0.00	0.59	918	99	642
								801	4,130 *D* (Wh/m²/day)
Mar/Sep	0:00	–90.00	0.00	0.00	–1.00	0.00			
	7:00	–79.84	11.09	0.17	–0.97	0.19	508	58	156
	8:00	–08.88	21.81	0.33	–0.87	0.37	754	87	367
	9:00	–50.21	31.70	0.47	–0.71	0.53	853	98	546
	10:00	–40.79	40.06	0.58	–0.50	0.64	901	104	684
	11:00	–21.82	45.88	0.65	–0.26	0.72	924	106	770
	12:00	0.00	48.00	0.67	0.00	0.74	931	107	799
								1,013	5,844 *D* (Wh/m²/day)
Apr/Aug	5:10	–105.87	0.00	–0.27	–0.96	0.00			
	0:00	–98.77	7.82	–0.15	–0.98	0.14	313	40	82
	7:00	–88.88	18.92	0.02	–0.95	0.32	656	83	296
	8:00	–78.24	29.99	0.18	–0.85	0.50	791	100	496
	9:00	–05.72	40.58	0.31	–0.69	0.65	857	109	667
	10:00	–49.02	50.01	0.42	–0.49	0.77	892	113	797
	11:00	–27.74	57.02	0.48	–0.25	0.84	910	116	879
	12:00	0.00	59.73	0.50	0.00	0.86	915	116	907
								1,239	7,341 *D* (Wh/m²/day)
May/Jul	4:42	–117.84	0.00	–0.47	–0.88	0.00			
	5:00	–114.89	2.97	–0.42	–0.91	0.05	33	4	6
	0:00	–105.38	13.43	–0.26	–0.94	0.23	503	67	184
	7:00	–90.02	24.37	–0.10	–0.91	0.41	708	95	387
	8:00	–80.07	35.50	0.06	–0.81	0.58	804	108	575
	9:00	–74.35	46.47	0.19	–0.66	0.73	856	115	735
	10:00	–58.00	56.70	0.29	–0.47	0.84	885	119	858
	11:00	–34.88	64.88	0.35	–0.24	0.91	900	121	935
	12:00	0.00	68.31	0.37	0.00	0.93	904	121	962
								1,378	8,324 *D* (Wh/m²/day)
Jun	4:28	–122.38	0.00	–0.54	–0.84	0.00			
	5:00	–117.10	5.15	–0.45	–0.89	0.09	139	19	32
	0:00	–107.87	15.44	–0.30	–0.92	0.27	545	75	220
	7:00	–98.78	26.28	–0.14	–0.89	0.44	719	99	417
	8:00	–89.19	37.38	0.01	–0.79	0.61	805	110	599
	9:00	–77.90	48.45	0.14	–0.65	0.75	853	117	755
	10:00	–02.79	58.95	0.24	–0.46	0.86	880	121	874
	11:00	–38.02	67.64	0.30	–0.24	0.92	894	122	949
	12:00	0.00	71.45	0.32	0.00	0.95	898	123	975
								1,448	8,667 *D* (Wh/m²/day)
									2,074 kWh/m²/year

L = 44°	*Approx. Clear-Sky Irradiation (Wh/m²)*								
	AST	α_{sol}(°)	β_{sol} (°)	σ_s	σ_w	σ_z	I_b	I_d	I
Dec	7:39	–56.41	0.00	0.55	–0.83	0.00			
	8:00	–52.72	3.07	0.60	–0.79	0.05	86	9	14
	9:00	–41.36	10.96	0.74	–0.65	0.19	574	59	168
	10:00	–28.69	17.16	0.84	–0.46	0.30	747	77	297
	11:00	–14.75	21.16	0.90	–0.24	0.36	815	84	378
	12:00	0.00	22.55	0.92	0.00	0.38	834	86	406
								543	2,119 *D* (Wh/m²/day)
Jan/Nov	7:23	–61.15	0.00	0.48	–0.88	0.00			
	8:00	–54.68	5.52	0.58	–0.81	0.10	272	28	55
	9:00	–43.03	13.65	0.71	–0.66	0.24	654	68	223
	10:00	–29.95	20.07	0.81	–0.47	0.34	790	83	353
	11:00	–15.44	24.24	0.88	–0.24	0.41	845	88	435
	12:00	0.00	25.69	0.90	0.00	0.43	861	90	463
								625	2,595 *D* (Wh/m²/day)
Feb/Oct	6:46	–73.59	0.00	0.28	–0.96	0.00			
	7:00	–71.19	2.36	0.32	–0.95	0.04	33	4	5
	8:00	–60.17	12.18	0.49	–0.85	0.21	586	63	187
	9:00	–47.83	20.91	0.63	–0.69	0.36	779	84	362
	10:00	–33.66	27.96	0.74	–0.49	0.47	860	92	496
	11:00	–17.51	32.63	0.80	–0.25	0.54	896	96	579
	12:00	0.00	34.28	0.83	0.00	0.56	906	97	608
								776	3,864 *D* (Wh/m²/day)
Mar/Sep	6:00	–90.00	0.00	0.00	–1.00	0.00			
	7:00	–79.46	10.73	0.18	–0.97	0.19	495	57	149
	8:00	–68.15	21.08	0.35	–0.87	0.36	743	85	353
	9:00	–55.21	30.57	0.49	–0.71	0.51	845	97	527
	10:00	–39.73	38.53	0.60	–0.50	0.62	894	103	660
	11:00	–21.09	44.01	0.67	–0.26	0.69	917	106	743
	12:00	0.00	46.00	0.69	0.00	0.72	925	106	771
								1,002	5,634 *D* (Wh/m²/day)
Apr/Aug	5:13	–106.41	0.00	–0.28	–0.96	0.00			
	6:00	–98.49	8.12	–0.15	–0.98	0.14	328	42	88
	7:00	–88.19	18.87	0.03	–0.95	0.32	655	83	295
	8:00	–77.12	29.56	0.19	–0.85	0.49	788	100	489
	9:00	–64.20	39.73	0.33	–0.69	0.64	853	108	654
	10:00	–47.87	48.69	0.44	–0.49	0.75	888	113	780
	11:00	–26.39	55.23	0.51	–0.25	0.82	906	115	859
	12:00	0.00	57.73	0.53	0.00	0.85	912	116	886
								1,238	7,217 *D* (Wh/m²/day)
May/Jul	4:36	–118.85	0.00	–0.48	–0.88	0.00			
	5:00	–114.78	3.81	–0.42	–0.91	0.07	72	10	14
	6:00	–104.91	13.95	–0.25	–0.94	0.24	518	69	194
	7:00	–95.11	24.56	–0.08	–0.91	0.42	711	95	391
	8:00	–84.65	35.34	0.08	–0.81	0.58	803	108	572
	9:00	–72.35	45.90	0.21	–0.66	0.72	854	114	728
	10:00	–56.15	55.62	0.31	–0.47	0.83	882	118	847
	11:00	–32.60	63.22	0.38	–0.24	0.89	897	120	921
	12:00	0.00	66.31	0.40	0.00	0.92	902	121	947
								1,390	8,281 *D* (Wh/m²/day)
Jun	4:20	–123.59	0.00	–0.55	–0.83	0.00			
	5:00	–116.98	6.06	–0.45	–0.89	0.11	190	26	46
	6:00	–107.33	16.05	–0.29	–0.92	0.28	559	77	231
	7:00	–97.80	26.57	–0.12	–0.89	0.45	722	99	422
	8:00	–87.67	37.33	0.03	–0.79	0.61	805	110	598
	9:00	–75.78	47.99	0.16	–0.65	0.74	851	117	749
	10:00	–59.92	57.99	0.27	–0.46	0.85	878	120	865
	11:00	–35.79	66.05	0.33	–0.24	0.91	892	122	937
	12:00	0.00	69.45	0.35	0.00	0.94	896	123	962
								1,465	8,659 *D* (Wh/m²/day)
									2,009 kWh/m²/year

L = 46°	*Approx. Clear-Sky Irradiation (Wh/m²)*								
	AST	α_{sol}(°)	β_{sol} (°)	σ_s	σ_w	σ_z	I_b		
Dec	7:46	–55.05	0.00	0.57	–0.82	0.00			
	8:00	–52.65	1.86	0.61	–0.79	0.03	15	2	2
	9:00	–41.12	9.46	0.74	–0.65	0.16	511	53	137
	10:00	–28.41	15.41	0.85	–0.46	0.27	708	73	261
	11:00	–14.56	19.23	0.91	–0.24	0.33	785	81	339
	12:00	0.00	20.55	0.94	0.00	0.35	806	83	366
								499	1,844 *D* (Wh/m²/day)
Jan/Nov	7:30	–60.02	0.00	0.50	–0.87	0.00			
	8:00	–54.54	4.36	0.58	–0.81	0.08	184	19	33
	9:00	–42.72	12.18	0.72	–0.66	0.21	609	64	192
	10:00	–29.60	18.33	0.83	–0.47	0.31	760	79	319
	11:00	–15.21	22.31	0.89	–0.24	0.38	822	86	398
	12:00	0.00	23.69	0.92	0.00	0.40	839	88	425
								584	2,308 *D* (Wh/m²/day)
Feb/Oct	6:49	–72.99	0.00	0.29	–0.96	0.00			
	7:00	–71.12	1.71	0.32	–0.95	0.03	9	1	1
	8:00	–59.81	11.18	0.49	–0.85	0.19	551	59	166
	9:00	–47.29	19.56	0.64	–0.69	0.33	758	82	335
	10:00	–33.10	26.29	0.75	–0.49	0.44	844	91	465
	11:00	–17.14	30.72	0.82	–0.25	0.51	882	95	546
	12:00	0.00	32.28	0.85	0.00	0.53	893	96	573
								751	3,599 *D* (Wh/m²/day)
Mar/Sep	6:00	–90.00	0.00	0.00	–1.00	0.00			
	7:00	–79.09	10.36	0.19	–0.97	0.18	480	55	142
	8:00	–67.45	20.32	0.36	–0.87	0.35	732	84	338
	9:00	–54.27	29.42	0.51	–0.71	0.49	835	96	506
	10:00	–38.75	36.98	0.62	–0.50	0.60	886	102	635
	11:00	–20.43	42.14	0.69	–0.26	0.67	910	105	715
	12:00	0.00	44.00	0.72	0.00	0.69	917	105	743
								989	5,416 *D* (Wh/m²/day)
Apr/Aug	5:10	–107.01	0.00	–0.29	–0.96	0.00			
	6:00	–98.20	8.41	–0.14	–0.98	0.15	343	43	94
	7:00	–87.51	18.80	0.04	–0.95	0.32	654	83	294
	8:00	–76.03	29.10	0.21	–0.85	0.49	784	100	481
	9:00	–62.73	38.84	0.36	–0.69	0.63	849	108	640
	10:00	–46.24	47.33	0.47	–0.49	0.74	884	112	762
	11:00	–25.17	53.43	0.54	–0.25	0.80	902	115	839
	12:00	0.00	55.73	0.56	0.00	0.83	907	115	865
								1,237	7,083 *D* (Wh/m²/day)
May/Jul	4:29	–119.98	0.00	–0.50	–0.87	0.00			
	5:00	–114.65	4.65	–0.42	–0.91	0.08	117	16	25
	6:00	–104.42	14.46	–0.24	–0.94	0.25	531	71	204
	7:00	–94.20	24.73	–0.07	–0.91	0.42	712	95	393
	8:00	–83.24	35.13	0.10	–0.81	0.58	802	107	569
	9:00	–70.42	45.26	0.24	–0.66	0.71	852	114	719
	10:00	–53.80	54.47	0.34	–0.47	0.81	880	118	834
	11:00	–30.59	61.51	0.41	–0.24	0.88	894	120	906
	12:00	0.00	64.31	0.43	0.00	0.90	899	120	931
								1,404	8,231 *D* (Wh/m²/day)
Jun	4:13	–124.95	0.00	–0.57	–0.82	0.00			
	5:00	–116.78	6.97	–0.45	–0.89	0.12	238	33	61
	6:00	–106.77	16.63	–0.28	–0.92	0.29	572	78	242
	7:00	–96.80	26.82	–0.11	–0.89	0.45	725	99	426
	8:00	–86.15	37.22	0.05	–0.79	0.60	804	110	597
	9:00	–73.66	47.47	0.19	–0.65	0.74	850	116	742
	10:00	–57.25	56.95	0.30	–0.46	0.84	876	120	854
	11:00	–33.33	64.40	0.36	–0.24	0.90	889	122	924
	12:00	0.00	67.45	0.38	0.00	0.92	894	122	948
								1,480	8,642 *D* (Wh/m²/day)
									1,942 kWh/m²/year

L = 48°	*Approx. Clear-Sky Irradiation (Wh/m²)*								
	AST	α_{sol}(°)	β_{sol} (°)	σ_s	σ_w	σ_z	I_b	I_d	I
Dec	7:55	–53.51	0.00	0.59	–0.80	0.00			
	8:00	–52.01	0.04	0.61	–0.79	0.01	0	0	0
	9:00	–40.92	7.95	0.75	–0.65	0.14	434	45	105
	10:00	–28.17	13.04	0.86	–0.46	0.24	662	68	224
	11:00	–14.40	17.29	0.92	–0.24	0.30	749	77	300
	12:00	0.00	18.55	0.95	0.00	0.32	773	80	326
								460	1,584 *D* (Wh/m²/day)
Jan/Nov	7:37	–58.70	0.00	0.52	–0.85	0.00			
	8:00	–54.44	3.20	0.58	–0.81	0.06	93	10	15
	9:00	–42.45	10.71	0.73	–0.66	0.19	555	58	161
	10:00	–29.29	10.59	0.84	–0.47	0.29	726	76	283
	11:00	–15.01	20.38	0.91	–0.24	0.35	794	83	360
	12:00	0.00	21.09	0.93	0.00	0.37	813	85	386
								538	2,024 *D* (Wh/m²/day)
Feb/Oct	0:53	–72.32	0.00	0.30	–0.95	0.00			
	7:00	–71.07	1.06	0.32	–0.95	0.02	0	0	0
	8:00	–59.48	10.17	0.50	–0.85	0.18	512	55	145
	9:00	–40.79	18.20	0.65	–0.69	0.31	735	79	308
	10:00	–32.58	24.61	0.77	–0.49	0.42	827	89	433
	11:00	–10.81	28.80	0.84	–0.25	0.48	867	93	511
	12:00	0.00	30.28	0.86	0.00	0.50	879	94	538
								727	3,333 *D* (Wh/m²/day)
Mar/Sep	0:00	–90.00	0.00	0.00	–1.00	0.00			
	7:00	–78.74	9.97	0.19	–0.97	0.17	465	53	134
	8:00	–00.78	19.55	0.37	–0.87	0.33	719	83	323
	9:00	–53.38	28.24	0.53	–0.71	0.47	825	95	485
	10:00	–37.84	35.41	0.64	–0.50	0.58	877	101	609
	11:00	–19.83	40.27	0.72	–0.26	0.65	902	104	687
	12:00	0.00	42.00	0.74	0.00	0.67	909	105	713
								976	5,190 *D* (Wh/m²/day)
Apr/Aug	5:00	–107.08	0.00	–0.30	–0.95	0.00			
	0:00	–97.91	8.69	–0.14	–0.98	0.15	356	45	99
	7:00	–80.83	18.70	0.05	–0.95	0.32	652	83	292
	8:00	–74.90	28.59	0.23	–0.85	0.48	779	99	472
	9:00	–01.33	37.90	0.38	–0.69	0.61	844	107	626
	10:00	–44.73	45.92	0.49	–0.49	0.72	879	112	743
	11:00	–24.09	51.62	0.57	–0.25	0.78	897	114	817
	12:00	0.00	53.73	0.59	0.00	0.81	902	115	842
								1,234	6,939 *D* (Wh/m²/day)
May/Jul	4:22	–121.24	0.00	–0.52	–0.85	0.00			
	5:00	–114.49	5.48	–0.41	–0.91	0.10	164	22	38
	0:00	–103.91	14.95	–0.23	–0.94	0.26	544	73	213
	7:00	–93.28	24.86	–0.05	–0.91	0.42	714	96	396
	8:00	–81.80	34.87	0.12	–0.81	0.57	800	107	565
	9:00	–08.55	44.56	0.26	–0.66	0.70	849	114	709
	10:00	–51.02	53.26	0.37	–0.47	0.80	877	117	820
	11:00	–28.83	59.78	0.44	–0.24	0.86	891	119	889
	12:00	0.00	62.31	0.46	0.00	0.89	896	120	913
								1,417	8,174 *D* (Wh/m²/day)
Jun	4:04	–120.49	0.00	–0.59	–0.80	0.00			
	5:00	–110.55	7.87	–0.44	–0.89	0.14	283	39	77
	0:00	–100.19	17.20	–0.27	–0.92	0.30	584	80	253
	7:00	–95.79	27.04	–0.09	–0.89	0.45	727	100	430
	8:00	–84.04	37.06	0.07	–0.79	0.60	803	110	594
	9:00	–71.00	46.87	0.22	–0.65	0.73	847	116	735
	10:00	–54.75	55.83	0.32	–0.46	0.83	873	120	842
	11:00	–31.19	62.71	0.39	–0.24	0.89	887	121	910
	12:00	0.00	65.45	0.42	0.00	0.91	891	122	933
								1,493	8,614 *D* (Wh/m²/day)
									1,874 kWh/m²/year

L = 50°	*Approx. Clear-Sky Irradiation* (Wh/m^2)								
	AST	α_{sol}(°)	β_{sol} (°)	σ_s	σ_w	σ_z	I_b	I_d	I
Dec	8:04	–51.75	0.00	0.02	–0.79	0.00			
	9:00	–40.75	0.44	0.75	–0.05	0.11	342	35	74
	10:00	–27.95	11.88	0.80	–0.40	0.21	007	03	187
	11:00	–14.25	15.35	0.93	–0.24	0.20	707	73	200
	12:00	0.00	10.55	0.90	0.00	0.28	734	70	285
								417	1,327 *D* (Wh/m^2/day)
Jan/Nov	7:44	–57.32	0.00	0.54	–0.84	0.00			
	8:00	–54.30	2.04	0.58	–0.81	0.04	22	2	3
	9:00	–42.21	9.23	0.73	–0.00	0.10	492	51	130
	10:00	–29.02	14.84	0.85	–0.47	0.20	080	72	247
	11:00	–14.83	18.45	0.92	–0.24	0.32	702	80	321
	12:00	0.00	19.09	0.94	0.00	0.34	784	82	340
								492	1,749 *D* (Wh/m^2/day)
Feb/Oct	0:57	–71.57	0.00	0.32	–0.95	0.00			
	7:00	–71.05	0.41	0.32	–0.95	0.01	0	0	0
	8:00	–59.19	9.15	0.51	–0.85	0.10	407	50	124
	9:00	–40.33	10.82	0.00	–0.09	0.29	708	70	281
	10:00	–32.11	22.92	0.78	–0.49	0.39	807	87	401
	11:00	–10.51	20.89	0.80	–0.25	0.45	850	91	470
	12:00	0.00	28.28	0.88	0.00	0.47	803	93	501
								701	3,005 *D* (Wh/m^2/day)
Mar/Sep	0:00	–90.00	0.00	0.00	–1.00	0.00			
	7:00	–78.40	9.58	0.20	–0.97	0.17	448	51	120
	8:00	–00.14	18.75	0.38	–0.87	0.32	700	81	308
	9:00	–52.55	27.03	0.54	–0.71	0.45	814	94	404
	10:00	–37.00	33.83	0.00	–0.50	0.50	807	100	583
	11:00	–19.28	38.38	0.74	–0.20	0.02	893	103	057
	12:00	0.00	40.00	0.77	0.00	0.04	901	104	083
								901	4,957 *D* (Wh/m^2/day)
Apr/Aug	5:02	–108.43	0.00	–0.32	–0.95	0.00			
	0:00	–97.00	8.90	–0.13	–0.98	0.10	308	47	104
	7:00	–80.10	18.58	0.00	–0.95	0.32	050	83	290
	8:00	–73.92	28.00	0.24	–0.85	0.47	774	98	403
	9:00	–00.00	30.92	0.40	–0.09	0.00	839	107	010
	10:00	–43.33	44.49	0.52	–0.49	0.70	874	111	723
	11:00	–23.11	49.78	0.59	–0.25	0.70	892	113	794
	12:00	0.00	51.73	0.02	0.00	0.79	897	114	818
								1,231	0,780 *D* (Wh/m^2/day)
May/Jul	4:15	–122.08	0.00	–0.54	–0.84	0.00			
	5:00	–114.30	0.31	–0.41	–0.91	0.11	211	28	51
	0:00	–103.38	15.42	–0.22	–0.94	0.27	550	74	222
	7:00	–92.35	24.95	–0.04	–0.91	0.42	715	90	398
	8:00	–80.49	34.50	0.14	–0.81	0.57	798	107	500
	9:00	–00.75	43.80	0.28	–0.00	0.09	840	113	099
	10:00	–49.00	51.99	0.40	–0.47	0.79	873	117	805
	11:00	–27.27	58.01	0.47	–0.24	0.85	888	119	872
	12:00	0.00	00.31	0.50	0.00	0.87	892	120	895
								1,429	8,108 *D* (Wh/m^2/day)
Jun	3:55	–128.25	0.00	–0.02	–0.79	0.00			
	4:00	–127.39	0.57	–0.01	–0.79	0.01	0	0	0
	5:00	–110.29	8.70	–0.44	–0.89	0.15	324	44	94
	0:00	–105.58	17.75	–0.20	–0.92	0.30	595	82	203
	7:00	–94.77	27.22	–0.07	–0.89	0.40	729	100	433
	8:00	–83.14	30.85	0.10	–0.79	0.00	802	110	591
	9:00	–09.01	40.21	0.24	–0.05	0.72	845	110	720
	10:00	–52.43	54.04	0.35	–0.40	0.82	870	119	829
	11:00	–29.30	00.98	0.42	–0.24	0.87	884	121	894
	12:00	0.00	03.45	0.45	0.00	0.89	888	122	910
								1,505	8,575 *D* (Wh/m^2/day)
									1,805 kWh/m^2/year

L = 52°	Approx. Clear-Sky Irradiation (Wh/m²)								
	AST	α_{sol}(°)	β_{sol} (°)	σ_s	σ_w	σ_z	I_b	I_d	I
Dec	8:14	–49.73	0.00	0.65	–0.76	0.00			
	9:00	–40.03	4.92	0.76	–0.65	0.09	233	24	44
	10:00	–27.77	10.11	0.87	–0.46	0.18	539	56	150
	11:00	–14.13	13.41	0.94	–0.24	0.23	656	68	220
	12:00	0.00	14.55	0.97	0.00	0.25	687	71	243
								365	1,071 *D* (Wh/m²/day)
Jan/Nov	7:53	–55.09	0.00	0.56	–0.83	0.00			
	8:00	–54.32	0.87	0.58	–0.81	0.02	0	0	0
	9:00	–42.01	7.75	0.74	–0.66	0.13	415	43	99
	10:00	–28.78	13.09	0.85	–0.47	0.23	638	67	211
	11:00	–14.07	16.51	0.93	–0.24	0.28	724	76	282
	12:00	0.00	17.69	0.95	0.00	0.30	748	78	306
								450	1,490 *D* (Wh/m²/day)
Feb/Oct	7:01	–70.73	0.00	0.33	–0.94	0.00			
	7:00	–71.05	–0.24	0.32	–0.95	0.00	0	0	0
	8:00	–58.93	8.12	0.51	–0.85	0.14	416	45	103
	9:00	–45.91	15.43	0.67	–0.69	0.27	677	73	253
	10:00	–31.08	21.22	0.79	–0.49	0.36	784	84	368
	11:00	–10.23	24.97	0.87	–0.25	0.42	831	89	440
	12:00	0.00	26.28	0.90	0.00	0.44	844	91	464
								673	2,793 *D* (Wh/m²/day)
Mar/Sep	0:00	–90.00	0.00	0.00	–1.00	0.00			
	7:00	–78.08	9.17	0.20	–0.97	0.16	429	49	118
	8:00	–05.54	17.93	0.39	–0.87	0.31	691	79	292
	9:00	–51.70	25.81	0.56	–0.71	0.44	802	92	441
	10:00	–30.23	32.22	0.68	–0.50	0.53	857	99	555
	11:00	–18.78	36.49	0.76	–0.26	0.59	883	102	627
	12:00	0.00	38.00	0.79	0.00	0.62	891	102	651
								945	4,717 *D* (Wh/m²/day)
Apr/Aug	4:58	–109.27	0.00	–0.33	–0.94	0.00			
	0:00	–97.28	9.21	–0.13	–0.98	0.16	380	48	109
	7:00	–85.49	18.43	0.07	–0.95	0.32	647	82	287
	8:00	–72.91	27.49	0.26	–0.85	0.46	769	98	453
	9:00	–58.73	35.90	0.42	–0.69	0.59	833	106	594
	10:00	–42.03	43.01	0.54	–0.49	0.68	868	110	702
	11:00	–22.23	47.94	0.62	–0.25	0.74	886	113	770
	12:00	0.00	49.73	0.65	0.00	0.76	892	113	793
								1,226	6,624 *D* (Wh/m²/day)
May/Jul	4:00	–124.31	0.00	–0.56	–0.83	0.00			
	5:00	–114.09	7.13	–0.40	–0.91	0.12	255	34	66
	0:00	–102.84	15.87	–0.21	–0.94	0.27	566	76	231
	7:00	–91.42	25.02	–0.02	–0.91	0.42	716	96	399
	8:00	–79.14	34.21	0.16	–0.81	0.56	796	107	554
	9:00	–05.02	42.98	0.31	–0.66	0.68	843	113	687
	10:00	–47.72	50.67	0.43	–0.47	0.77	870	117	789
	11:00	–25.89	56.22	0.50	–0.24	0.83	884	118	853
	12:00	0.00	58.31	0.53	0.00	0.85	888	119	875
								1,440	8,033 *D* (Wh/m²/day)
Jun	3:45	–130.27	0.00	–0.65	–0.76	0.00			
	4:00	–127.30	1.79	–0.61	–0.79	0.03	3	0	0
	5:00	–110.00	9.64	–0.43	–0.89	0.17	362	50	110
	0:00	–104.95	18.28	–0.25	–0.92	0.31	605	83	273
	7:00	–93.74	27.37	–0.06	–0.89	0.46	730	100	436
	8:00	–81.66	36.58	0.12	–0.79	0.60	801	110	587
	9:00	–67.69	45.48	0.27	–0.65	0.71	842	115	716
	10:00	–50.28	53.39	0.38	–0.46	0.80	867	119	815
	11:00	–27.65	59.22	0.45	–0.24	0.86	880	121	877
	12:00	0.00	61.45	0.48	0.00	0.88	885	121	898
								1,516	8,526 *D* (Wh/m²/day)
									1,734 kWh/m²/year

L = 54°	Approx. Clear-Sky Irradiation (Wh/m²)								
	AST	α_{sol}(°)	β_{sol} (°)	σ_s	σ_w	σ_z	I_b	I_d	I
Dec	8:20	–47.39	0.00	0.68	–0.74	0.00			
	9:00	–40.53	3.40	0.76	–0.65	0.06	112	12	18
	10:00	–27.02	8.34	0.88	–0.46	0.15	455	47	113
	11:00	–14.02	11.47	0.95	–0.24	0.20	593	61	179
	12:00	0.00	12.55	0.98	0.00	0.22	629	65	202
								304	822 *D* (Wh/m²/day)
Jan/Nov	8:02	–53.81	0.00	0.59	–0.81	0.00			
	8:00	–54.31	–0.30	0.58	–0.81	–0.01	0	0	0
	9:00	–41.85	6.26	0.74	–0.66	0.11	324	34	69
	10:00	–28.57	11.34	0.86	–0.47	0.20	579	61	174
	11:00	–14.53	14.58	0.94	–0.24	0.25	679	71	242
	12:00	0.00	15.69	0.96	0.00	0.27	706	74	265
								404	1,236 *D* (Wh/m²/day)
Feb/Oct	7:00	–09.77	0.00	0.35	–0.94	0.00			
	7:00	–71.00	–0.89	0.32	–0.95	–0.02	0	0	0
	8:00	–58.70	7.09	0.52	–0.85	0.12	357	38	82
	9:00	–45.53	14.04	0.68	–0.69	0.24	642	69	225
	10:00	–31.29	19.51	0.81	–0.49	0.33	758	81	335
	11:00	–15.99	23.05	0.88	–0.25	0.39	808	87	403
	12:00	0.00	24.28	0.91	0.00	0.41	823	88	427
								640	2,517 *D* (Wh/m²/day)
Mar/Sep	0:00	–90.00	0.00	0.00	–1.00	0.00			
	7:00	–77.77	8.75	0.21	–0.97	0.15	410	47	109
	8:00	–04.90	17.09	0.40	–0.87	0.29	674	78	276
	9:00	–51.03	24.56	0.57	–0.71	0.42	788	91	418
	10:00	–35.51	30.60	0.70	–0.50	0.51	845	97	527
	11:00	–18.33	34.59	0.78	–0.26	0.57	872	100	595
	12:00	0.00	36.00	0.81	0.00	0.59	880	101	619
								927	4,471 *D* (Wh/m²/day)
Apr/Aug	4:53	–110.23	0.00	–0.35	–0.94	0.00			
	0:00	–90.90	9.46	–0.12	–0.98	0.16	391	50	114
	7:00	–84.83	18.26	0.09	–0.95	0.31	644	82	284
	8:00	–71.93	26.88	0.28	–0.85	0.45	763	97	442
	9:00	–57.52	34.85	0.44	–0.69	0.57	826	105	577
	10:00	–40.83	41.52	0.57	–0.49	0.66	862	109	680
	11:00	–21.43	46.08	0.65	–0.25	0.72	880	112	745
	12:00	0.00	47.73	0.67	0.00	0.74	885	112	767
								1,221	6,452 *D* (Wh/m²/day)
May/Jul	3:57	–120.19	0.00	–0.59	–0.81	0.00			
	5:00	–113.84	7.94	–0.40	–0.91	0.14	295	40	80
	0:00	–102.27	16.31	–0.20	–0.94	0.28	576	77	239
	7:00	–90.48	25.05	–0.01	–0.91	0.42	716	96	399
	8:00	–77.82	33.81	0.18	–0.81	0.56	793	106	548
	9:00	–03.37	42.11	0.33	–0.66	0.67	839	112	675
	10:00	–45.98	49.30	0.45	–0.47	0.76	865	116	772
	11:00	–24.05	54.41	0.53	–0.24	0.81	880	118	833
	12:00	0.00	56.31	0.55	0.00	0.83	884	118	854
								1,449	7,947 *D* (Wh/m²/day)
Jun	3:33	–132.01	0.00	–0.68	–0.74	0.00			
	4:00	–127.29	3.00	–0.61	–0.79	0.05	32	4	6
	5:00	–115.08	10.51	–0.43	–0.89	0.18	396	54	126
	0:00	–104.30	18.78	–0.23	–0.92	0.32	615	84	282
	7:00	–92.70	27.48	–0.04	–0.89	0.46	731	100	438
	8:00	–80.20	36.27	0.14	–0.79	0.59	799	109	582
	9:00	–05.85	44.69	0.29	–0.65	0.70	839	115	705
	10:00	–48.29	52.09	0.41	–0.46	0.79	864	118	800
	11:00	–20.18	57.44	0.48	–0.24	0.84	877	120	859
	12:00	0.00	59.45	0.51	0.00	0.86	881	121	879
								1,532	8,476 *D* (Wh/m²/day)
									1,663 kWh/m²/year

L = 56°	Approx. Clear-Sky Irradiation (Wh/m^2)								
	AST	α_{sol}(°)	β_{sol} (°)	σ_s	σ_w	σ_z	I_b	I_d	I
Dec	8:40	–44.03	0.00	0.71	–0.70	0.00			
	9:00	–40.47	1.88	0.76	–0.65	0.03	16	2	2
	10:00	–27.50	6.57	0.88	–0.46	0.11	351	36	76
	11:00	–13.93	9.53	0.96	–0.24	0.17	514	53	138
	12:00	0.00	10.55	0.98	0.00	0.18	557	57	159
								239	593 D (Wh/m^2/day)
Jan/Nov	8:13	–51.64	0.00	0.62	–0.78	0.00			
	9:00	–41.72	4.77	0.74	–0.66	0.08	215	22	40
	10:00	–28.40	9.58	0.87	–0.47	0.17	508	53	138
	11:00	–14.40	12.64	0.95	–0.24	0.22	624	65	202
	12:00	0.00	13.69	0.97	0.00	0.24	655	68	223
								350	983 D (Wh/m^2/day)
Feb/Oct	7:11	–08.09	0.00	0.36	–0.93	0.00			
	8:00	–58.51	6.04	0.52	–0.85	0.11	291	31	62
	9:00	–45.20	12.63	0.69	–0.69	0.22	601	65	196
	10:00	–30.94	17.80	0.82	–0.49	0.31	727	78	301
	11:00	–15.76	21.12	0.90	–0.25	0.36	782	84	366
	12:00	0.00	22.28	0.93	0.00	0.38	798	86	388
								602	2,238 D (Wh/m^2/day)
Mar/Sep	0:00	–90.00	0.00	0.00	–1.00	0.00			
	7:00	–77.48	8.32	0.21	–0.97	0.14	389	45	101
	8:00	–64.42	16.24	0.41	–0.87	0.28	656	75	259
	9:00	–50.34	23.29	0.59	–0.71	0.40	773	89	395
	10:00	–34.85	28.97	0.72	–0.50	0.48	832	96	498
	11:00	–17.91	32.69	0.80	–0.26	0.54	860	99	563
	12:00	0.00	34.00	0.83	0.00	0.56	868	100	586
								907	4,218 D (Wh/m^2/day)
Apr/Aug	4:48	–111.31	0.00	–0.36	–0.93	0.00			
	5:00	–108.90	1.53	–0.32	–0.95	0.03	2	0	0
	0:00	–90.02	9.70	–0.11	–0.98	0.17	401	51	118
	7:00	–84.18	18.07	0.10	–0.95	0.31	640	81	280
	8:00	–70.98	26.25	0.29	–0.85	0.44	756	96	431
	9:00	–56.38	33.75	0.46	–0.69	0.56	819	104	559
	10:00	–39.72	39.99	0.59	–0.49	0.64	855	109	658
	11:00	–20.71	44.21	0.67	–0.25	0.70	873	111	719
	12:00	0.00	45.73	0.70	0.00	0.72	878	112	741
								1,215	6,272 D (Wh/m^2/day)
May/Jul	3:40	–128.36	0.00	–0.62	–0.78	0.00			
	4:00	–125.00	1.46	–0.58	–0.81	0.03	1	0	0
	5:00	–113.58	8.74	–0.40	–0.91	0.15	333	45	95
	0:00	–101.69	16.72	–0.19	–0.94	0.29	585	78	247
	7:00	–89.55	25.05	0.01	–0.91	0.42	716	96	399
	8:00	–76.52	33.36	0.19	–0.81	0.55	790	106	541
	9:00	–61.79	41.19	0.36	–0.66	0.66	835	112	662
	10:00	–44.38	47.89	0.48	–0.47	0.74	861	115	754
	11:00	–23.55	52.59	0.56	–0.24	0.79	875	117	812
	12:00	0.00	54.31	0.58	0.00	0.81	879	118	832
								1,457	7,852 D (Wh/m^2/day)
Jun	3:19	–135.37	0.00	–0.71	–0.70	0.00			
	4:00	–127.19	4.21	–0.60	–0.79	0.07	88	12	18
	5:00	–115.33	11.37	–0.42	–0.89	0.20	427	59	143
	0:00	–103.63	19.26	–0.22	–0.92	0.33	623	85	291
	7:00	–91.66	27.56	–0.03	–0.89	0.46	732	100	439
	8:00	–78.77	35.90	0.16	–0.79	0.59	797	109	576
	9:00	–64.08	43.84	0.32	–0.65	0.69	836	115	694
	10:00	–46.44	50.73	0.44	–0.46	0.77	860	118	784
	11:00	–24.87	55.63	0.51	–0.24	0.83	873	120	840
	12:00	0.00	57.45	0.54	0.00	0.84	877	120	859
								1,555	8,429 D (Wh/m^2/day)
									1,590 kWh/m^2/year

L = 58°	*Approx. Clear-Sky Irradiation (Wh/m²)*								
	AST	α_{sol}(°)	β_{sol} (°)	σ_s	σ_w	σ_z	I_b	I_d	I
Dec	8:55	–41.33	0.00	0.75	–0.66	0.00			
	9:00	–40.45	0.30	0.76	–0.65	0.01	0	0	0
	10:00	–27.41	4.79	0.88	–0.46	0.08	223	23	42
	11:00	–13.80	7.59	0.96	–0.24	0.13	414	43	97
	12:00	0.00	8.55	0.99	0.00	0.15	466	48	117
								179	395 *D* (Wh/m²/day)
Jan/Nov	8:25	–49.08	0.00	0.65	–0.76	0.00			
	9:00	–41.02	3.27	0.75	–0.66	0.06	99	10	16
	10:00	–28.25	7.82	0.87	–0.47	0.14	420	44	101
	11:00	–14.30	10.70	0.95	–0.24	0.19	555	58	161
	12:00	0.00	11.69	0.98	0.00	0.20	592	62	182
								286	738 *D* (Wh/m²/day)
Feb/Oct	7:17	–07.45	0.00	0.38	–0.92	0.00			
	8:00	–58.34	5.00	0.52	–0.85	0.09	218	23	42
	9:00	–44.90	11.22	0.69	–0.69	0.19	553	59	167
	10:00	–30.03	16.08	0.83	–0.49	0.28	692	74	266
	11:00	–15.57	19.20	0.91	–0.25	0.33	752	81	328
	12:00	0.00	20.28	0.94	0.00	0.35	770	83	349
								559	1,957 *D* (Wh/m²/day)
Mar/Sep	0:00	–90.00	0.00	0.00	–1.00	0.00			
	7:00	–77.20	7.88	0.22	–0.97	0.14	366	42	92
	8:00	–03.91	15.36	0.42	–0.87	0.26	636	73	242
	9:00	–49.70	22.01	0.60	–0.71	0.37	756	87	370
	10:00	–34.25	27.32	0.73	–0.50	0.46	817	94	469
	11:00	–17.53	30.79	0.82	–0.26	0.51	846	97	530
	12:00	0.00	32.00	0.85	0.00	0.53	855	98	551
								885	3,959 *D* (Wh/m²/day)
Apr/Aug	4:42	–112.55	0.00	–0.38	–0.92	0.00			
	5:00	–108.83	2.18	–0.32	–0.95	0.04	12	2	2
	0:00	–90.28	9.92	–0.11	–0.98	0.17	410	52	123
	7:00	–83.53	17.86	0.11	–0.95	0.31	636	81	276
	8:00	–70.07	25.58	0.31	–0.85	0.43	749	95	419
	9:00	–55.30	32.63	0.48	–0.69	0.54	812	103	541
	10:00	–38.08	38.44	0.61	–0.49	0.62	847	108	634
	11:00	–20.05	42.34	0.69	–0.25	0.67	865	110	693
	12:00	0.00	43.73	0.72	0.00	0.69	871	111	713
								1,211	6,085 *D* (Wh/m²/day)
May/Jul	3:34	–130.92	0.00	–0.65	–0.76	0.00			
	4:00	–125.01	2.63	–0.58	–0.81	0.05	21	3	4
	5:00	–113.28	9.54	–0.39	–0.91	0.17	368	49	110
	0:00	–101.10	17.12	–0.18	–0.94	0.29	593	80	254
	7:00	–88.01	25.02	0.02	–0.91	0.42	716	96	399
	8:00	–75.20	32.88	0.21	–0.81	0.54	787	105	533
	9:00	–00.29	40.22	0.38	–0.66	0.65	830	111	647
	10:00	–42.89	46.45	0.50	–0.47	0.72	856	115	735
	11:00	–22.50	50.75	0.58	–0.24	0.77	870	117	790
	12:00	0.00	52.31	0.61	0.00	0.79	874	117	809
								1,468	7,753 *D* (Wh/m²/day)
Jun	3:04	–138.07	0.00	–0.75	–0.66	0.00			
	4:00	–127.05	5.42	–0.60	–0.79	0.09	154	21	36
	5:00	–114.95	12.22	–0.41	–0.89	0.21	456	62	159
	0:00	–102.95	19.72	–0.21	–0.92	0.34	631	86	299
	7:00	–90.02	27.60	–0.01	–0.89	0.46	732	100	440
	8:00	–77.30	35.49	0.18	–0.79	0.58	794	109	570
	9:00	–02.39	42.94	0.34	–0.65	0.68	832	114	681
	10:00	–44.74	49.33	0.46	–0.46	0.76	856	117	766
	11:00	–23.71	53.81	0.54	–0.24	0.81	868	119	820
	12:00	0.00	55.45	0.57	0.00	0.82	872	120	838
								1,578	8,379 *D* (Wh/m²/day)
									1,517 kWh/m²/year

$L = 60°$	Approx. Clear-Sky Irradiation (Wh/m^2)								
	AST	α_{sol} (°)	β_{sol} (°)	σ_s	σ_w	σ_z	I_b	I_d	I
Dec	9:14	–37.26	0.00	0.80	–0.61	0.00			
	10:00	–27.34	3.02	0.89	–0.46	0.05	83	9	13
	11:00	–13.80	5.65	0.97	–0.24	0.10	287	30	58
	12:00	0.00	6.55	0.99	0.00	0.11	350	36	76
								112	217 *D* (Wh/m^2/day)
Jan/Nov	8:39	–46.04	0.00	0.69	–0.72	0.00			
	9:00	–41.57	1.78	0.75	–0.66	0.03	12	1	2
	10:00	–28.14	6.06	0.88	–0.47	0.11	310	32	65
	11:00	–14.22	8.76	0.96	–0.24	0.15	469	49	121
	12:00	0.00	9.69	0.99	0.00	0.17	513	54	140
								219	515 *D* (Wh/m^2/day)
Feb/Oct	7:24	–66.02	0.00	0.41	–0.91	0.00			
	8:00	–58.21	3.94	0.53	–0.85	0.07	139	15	24
	9:00	–44.64	9.80	0.70	–0.69	0.17	496	53	138
	10:00	–30.35	14.36	0.84	–0.49	0.25	650	70	231
	11:00	–15.39	17.27	0.92	–0.25	0.30	717	77	290
	12:00	0.00	18.28	0.95	0.00	0.31	736	79	310
								510	1,677 *D* (Wh/m^2/day)
Mar/Sep	6:00	–90.00	0.00	0.00	–1.00	0.00			
	7:00	–76.94	7.44	0.22	–0.97	0.13	342	39	84
	8:00	–63.43	14.48	0.43	–0.87	0.25	614	71	224
	9:00	–49.11	20.70	0.61	–0.71	0.35	738	85	346
	10:00	–33.69	25.66	0.75	–0.50	0.43	800	92	439
	11:00	–17.19	28.88	0.84	–0.26	0.48	831	96	497
	12:00	0.00	30.00	0.87	0.00	0.50	840	97	517
								861	3,694 *D* (Wh/m^2/day)
Apr/Aug	4:35	–113.98	0.00	–0.41	–0.91	0.00			
	5:00	–108.75	2.82	–0.32	–0.95	0.05	33	4	6
	6:00	–95.92	10.14	–0.10	–0.98	0.18	419	53	127
	7:00	–82.90	17.62	0.12	–0.95	0.30	632	80	271
	8:00	–69.18	24.88	0.32	–0.85	0.42	741	94	406
	9:00	–54.27	31.48	0.50	–0.69	0.52	803	102	521
	10:00	–37.73	36.87	0.63	–0.49	0.60	838	106	609
	11:00	–19.45	40.46	0.72	–0.25	0.65	857	109	665
	12:00	0.00	41.73	0.75	0.00	0.67	862	110	684
								1,208	5,895 *D* (Wh/m^2/day)
May/Jul	3:20	–133.96	0.00	–0.69	–0.72	0.00			
	4:00	–125.51	3.79	–0.58	–0.81	0.07	71	9	14
	5:00	–112.96	10.32	–0.38	–0.91	0.18	399	54	125
	6:00	–100.48	17.49	–0.17	–0.94	0.30	601	81	261
	7:00	–87.68	24.96	0.04	–0.91	0.42	715	96	398
	8:00	–74.02	32.35	0.23	–0.81	0.54	783	105	524
	9:00	–58.85	39.21	0.40	–0.66	0.63	825	111	632
	10:00	–41.51	44.96	0.53	–0.47	0.71	850	114	715
	11:00	–21.67	48.90	0.61	–0.24	0.75	864	116	767
	12:00	0.00	50.31	0.64	0.00	0.77	868	116	785
								1,486	7,657 *D* (Wh/m^2/day)
Jun	2:45	–142.74	0.00	–0.80	–0.61	0.00			
	3:00	–139.55	1.16	–0.76	–0.65	0.02	0	0	0
	4:00	–126.89	6.62	–0.60	–0.79	0.12	219	30	55
	5:00	–114.54	13.06	–0.40	–0.89	0.23	481	66	175
	6:00	–102.24	20.16	–0.20	–0.92	0.34	638	87	307
	7:00	–89.57	27.60	0.01	–0.89	0.46	733	100	440
	8:00	–75.99	35.03	0.20	–0.79	0.57	791	108	562
	9:00	–60.78	41.99	0.36	–0.65	0.67	828	113	668
	10:00	–43.16	47.89	0.49	–0.46	0.74	851	117	748
	11:00	–22.67	51.97	0.57	–0.24	0.79	863	118	798
	12:00	0.00	53.45	0.60	0.00	0.80	867	119	816
								1,600	8,323 *D* (Wh/m^2/day)
									1,446 kWh/m^2/year

$L = 62°$	Approx. Clear-Sky Irradiation (Wh/m^2)								
	AST	α_{sol} (°)	β_{sol} (°)	σ_s	σ_w	σ_z	I_b	I_d	I
Dec	9:38	–32.04	0.00	0.85	–0.53	0.00			
	10:00	–27.31	1.24	0.89	–0.46	0.02	2	0	0
	11:00	–13.77	3.71	0.97	–0.24	0.06	136	14	23
	12:00	0.00	4.55	1.00	0.00	0.08	204	21	37
								49	83 *D* (Wh/m^2/day)
Jan/Nov	8:56	–42.33	0.00	0.74	–0.67	0.00			
	9:00	–41.54	0.28	0.75	–0.66	0.00	0	0	0
	10:00	–28.05	4.29	0.88	–0.47	0.07	178	19	32
	11:00	–14.15	6.83	0.96	–0.24	0.12	361	38	81
	12:00	0.00	7.69	0.99	0.00	0.13	412	43	98
								156	323 *D* (Wh/m^2/day)
Feb/Oct	7:31	–64.35	0.00	0.43	–0.90	0.00			
	8:00	–58.11	2.89	0.53	–0.85	0.05	64	7	10
	9:00	–44.41	8.37	0.71	–0.69	0.15	429	46	109
	10:00	–30.11	12.63	0.84	–0.49	0.22	601	65	196
	11:00	–15.24	15.34	0.93	–0.25	0.26	675	73	251
	12:00	0.00	16.28	0.96	0.00	0.28	696	75	270
								455	1,401 *D* (Wh/m^2/day)
Mar/Sep	6:00	–90.00	0.00	0.00	–1.00	0.00			
	7:00	–76.69	6.98	0.23	–0.97	0.12	316	36	75
	8:00	–62.99	13.58	0.44	–0.87	0.23	589	68	206
	9:00	–48.56	19.39	0.62	–0.71	0.33	717	82	320
	10:00	–33.18	23.99	0.76	–0.50	0.41	782	90	408
	11:00	–16.88	26.97	0.85	–0.26	0.45	813	94	462
	12:00	0.00	28.00	0.88	0.00	0.47	823	95	481
								835	3,423 *D* (Wh/m^2/day)
Apr/Aug	4:28	–115.65	0.00	–0.43	–0.90	0.00			
	5:00	–108.65	3.47	–0.32	–0.95	0.06	64	8	12
	6:00	–95.57	10.34	–0.10	–0.98	0.18	426	54	131
	7:00	–82.27	17.36	0.13	–0.95	0.30	626	80	266
	8:00	–68.33	24.16	0.34	–0.85	0.41	733	93	393
	9:00	–53.31	30.30	0.52	–0.69	0.50	794	101	501
	10:00	–36.85	35.28	0.65	–0.49	0.58	829	105	584
	11:00	–18.91	38.57	0.74	–0.25	0.62	847	108	636
	12:00	0.00	39.73	0.77	0.00	0.64	853	108	654
								1,206	5,701 *D* (Wh/m^2/day)
May/Jul	3:03	–137.67	0.00	–0.74	–0.67	0.00			
	4:00	–125.39	4.95	–0.58	–0.81	0.09	134	18	30
	5:00	–112.61	11.10	–0.38	–0.91	0.19	428	57	140
	6:00	–99.86	17.85	–0.16	–0.94	0.31	608	81	268
	7:00	–86.75	24.86	0.05	–0.91	0.42	714	96	396
	8:00	–72.82	31.78	0.25	–0.81	0.53	779	104	515
	9:00	–57.49	38.15	0.42	–0.66	0.62	820	110	616
	10:00	–40.24	43.45	0.55	–0.47	0.69	844	113	694
	11:00	–20.86	47.03	0.64	–0.24	0.73	858	115	743
	12:00	0.00	48.31	0.67	0.00	0.75	862	116	759
								1,505	7,560 *D* (Wh/m^2/day)
Jun	2:21	–147.96	0.00	–0.85	–0.53	0.00			
	3:00	–139.50	2.68	–0.76	–0.65	0.05	21	3	4
	4:00	–126.68	7.82	–0.59	–0.79	0.14	280	38	77
	5:00	–114.10	13.88	–0.40	–0.89	0.24	505	69	190
	6:00	–101.51	20.57	–0.19	–0.92	0.35	645	88	315
	7:00	–88.52	27.57	0.02	–0.89	0.46	732	100	439
	8:00	–74.64	34.52	0.22	–0.79	0.57	788	108	554
	9:00	–59.25	40.99	0.39	–0.65	0.66	824	113	653
	10:00	–41.71	46.42	0.51	–0.46	0.72	846	116	729
	11:00	–21.74	50.12	0.60	–0.24	0.77	858	118	776
	12:00	0.00	51.45	0.62	0.00	0.78	862	118	792
								1,625	8,266 *D* (Wh/m^2/day)
									1,378 kWh/m^2/year

L = 64°	Approx. Clear-Sky Irradiation (Wh/m^2)								
	AST	α_{sol} (°)	β_{sol} (°)	σ_s	σ_w	σ_z	I_b	I_d	I
Dec	10:11	–24.80	0.00	0.91	–0.42	0.00			
	11:00	–13.74	1.76	0.97	–0.24	0.03	12	1	2
	12:00	0.00	2.55	1.00	0.00	0.04	51	5	7
								8	11 *D* (Wh/m^2/day)
Jan/Nov	9:17	–37.65	0.00	0.79	–0.61	0.00			
	10:00	–27.99	2.53	0.88	–0.47	0.04	47	5	7
	11:00	–14.10	4.89	0.97	–0.24	0.09	224	23	43
	12:00	0.00	5.69	1.00	0.00	0.10	284	30	58
								86	157 *D* (Wh/m^2/day)
Feb/Oct	7:40	–62.38	0.00	0.46	–0.89	0.00			
	8:00	–58.04	1.83	0.53	–0.85	0.03	12	1	2
	9:00	–44.22	6.94	0.71	–0.69	0.12	349	37	80
	10:00	–29.90	10.90	0.85	–0.49	0.19	541	58	160
	11:00	–15.10	13.41	0.94	–0.25	0.23	624	67	212
	12:00	0.00	14.28	0.97	0.00	0.25	648	70	229
								398	1,137 *D* (Wh/m^2/day)
Mar/Sep	6:00	–90.00	0.00	0.00	–1.00	0.00			
	7:00	–76.46	6.51	0.23	–0.97	0.11	288	33	66
	8:00	–62.57	12.66	0.45	–0.87	0.22	562	65	188
	9:00	–48.05	18.06	0.64	–0.71	0.31	693	80	295
	10:00	–32.72	22.31	0.78	–0.50	0.38	760	87	376
	11:00	–16.60	25.05	0.87	–0.26	0.42	794	91	427
	12:00	0.00	26.00	0.90	0.00	0.44	804	92	445
								805	3,148 *D* (Wh/m^2/day)
Apr/Aug	4:19	–117.62	0.00	–0.46	–0.89	0.00			
	5:00	–108.52	4.10	–0.32	–0.95	0.07	100	13	20
	6:00	–95.20	10.52	–0.09	–0.98	0.18	434	55	134
	7:00	–81.66	17.08	0.14	–0.95	0.29	621	79	261
	8:00	–67.52	23.41	0.35	–0.85	0.40	724	92	379
	9:00	–52.40	29.09	0.53	–0.69	0.49	784	100	480
	10:00	–36.03	33.67	0.67	–0.49	0.55	819	104	558
	11:00	–18.42	36.67	0.76	–0.25	0.60	837	106	606
	12:00	0.00	37.73	0.79	0.00	0.61	843	107	623
								1,204	5,501 *D* (Wh/m^2/day)
May/Jul	2:42	–142.35	0.00	–0.79	–0.61	0.00			
	3:00	–138.45	1.22	–0.75	–0.66	0.02	0	0	0
	4:00	–125.23	6.11	–0.57	–0.81	0.11	200	27	48
	5:00	–112.23	11.86	–0.37	–0.91	0.21	455	61	154
	6:00	–99.21	18.18	–0.15	–0.94	0.31	614	82	274
	7:00	–85.83	24.73	0.07	–0.91	0.42	712	95	394
	8:00	–71.65	31.17	0.27	–0.81	0.52	774	104	504
	9:00	–56.20	37.06	0.44	–0.66	0.60	814	109	599
	10:00	–39.06	41.91	0.58	–0.47	0.67	838	112	672
	11:00	–20.13	45.16	0.66	–0.24	0.71	851	114	718
	12:00	0.00	46.31	0.69	0.00	0.72	855	115	733
								1,524	7,460 *D* (Wh/m^2/day)
Jun	1:48	–155.20	0.00	–0.91	–0.42	0.00			
	2:00	–152.70	0.54	–0.89	–0.46	0.01	0	0	0
	3:00	–139.42	4.20	–0.76	–0.65	0.07	88	12	18
	4:00	–126.45	9.01	–0.59	–0.79	0.16	335	46	98
	5:00	–113.64	14.69	–0.39	–0.89	0.25	526	72	206
	6:00	–100.77	20.96	–0.17	–0.92	0.36	651	89	322
	7:00	–87.48	27.50	0.04	–0.89	0.46	732	100	438
	8:00	–73.34	33.97	0.24	–0.79	0.56	784	107	546
	9:00	–57.79	39.94	0.41	–0.65	0.64	819	112	638
	10:00	–40.37	44.91	0.54	–0.46	0.71	840	115	708
	11:00	–20.89	48.26	0.62	–0.24	0.75	852	117	753
	12:00	0.00	49.45	0.65	0.00	0.76	856	117	768
								1,659	8,221 *D* (Wh/m^2/day)
									1,314 kWh/m^2/year

L = 68°	Approx. Clear-Sky Irradiation (Wh/m²)								
	AST	α_{sol} (°)	β_{sol} (°)	σ_s	σ_w	σ_z	I_b	I_d	I
Jan/Nov	10:25	–22.10	0.00	0.93	–0.38	0.00			
	11:00	–14.05	1.01	0.97	–0.24	0.02	0	0	0
	12:00	0.00	1.69	1.00	0.00	0.03	10	1	1
								1	1 *D* (Wh/m²/day)
Feb/Oct	8:03	–57.15	0.00	0.54	–0.84	0.00			
	9:00	–43.96	4.07	0.72	–0.69	0.07	148	16	26
	10:00	–29.58	7.43	0.86	–0.49	0.13	377	41	89
	11:00	–14.89	9.55	0.95	–0.25	0.17	485	52	133
	12:00	0.00	10.28	0.98	0.00	0.18	516	55	148
								273	644 *D* (Wh/m²/day)
Mar/Sep	6:00	–90.00	0.00	0.00	–1.00	0.00			
	7:00	–76.05	5.56	0.24	–0.97	0.10	228	26	48
	8:00	–61.84	10.80	0.46	–0.87	0.19	497	57	150
	9:00	–47.16	15.36	0.66	–0.71	0.26	636	73	242
	10:00	–31.91	18.93	0.80	–0.50	0.32	709	82	311
	11:00	–16.12	21.21	0.90	–0.26	0.36	745	86	355
	12:00	0.00	22.00	0.93	0.00	0.37	756	87	370
								734	2,584 *D* (Wh/m²/day)
Apr/Aug	3:56	–122.85	0.00	–0.54	–0.84	0.00			
	4:00	–122.01	0.29	–0.53	–0.85	0.01	0	0	0
	5:00	–108.21	5.36	–0.31	–0.95	0.09	176	22	39
	6:00	–94.45	10.86	–0.08	–0.98	0.19	447	57	141
	7:00	–80.47	16.46	0.16	–0.95	0.28	607	77	249
	8:00	–65.99	21.83	0.38	–0.85	0.37	702	89	350
	9:00	–50.74	26.60	0.57	–0.69	0.45	760	97	437
	10:00	–34.58	30.40	0.71	–0.49	0.51	795	101	503
	11:00	–17.56	32.87	0.80	–0.25	0.54	813	103	545
	12:00	0.00	33.73	0.83	0.00	0.56	819	104	559
								1,196	5,086 *D* (Wh/m²/day)
May/Jul	1:34	–157.90	0.00	–0.93	–0.38	0.00			
	2:00	–152.03	1.01	–0.88	–0.47	0.02	0	0	0
	3:00	–138.32	4.21	–0.74	–0.66	0.07	93	12	19
	4:00	–124.81	8.40	–0.56	–0.81	0.15	318	43	89
	5:00	–111.40	13.35	–0.36	–0.91	0.23	501	67	183
	6:00	–97.89	18.77	–0.13	–0.94	0.32	626	84	285
	7:00	–84.01	24.38	0.10	–0.91	0.41	708	95	387
	8:00	–69.43	29.83	0.30	–0.81	0.50	763	102	482
	9:00	–53.83	34.77	0.48	–0.66	0.57	800	107	563
	10:00	–36.97	38.76	0.62	–0.47	0.63	823	110	625
	11:00	–18.88	41.39	0.71	–0.24	0.66	836	112	664
	12:00	0.00	42.31	0.74	0.00	0.67	840	113	678
								1,578	7,274 *D* (Wh/m²/day)
Jun	0:00	–180.00	1.45	–1.00	0.00	0.03	1	0	0
	1:00	–166.25	2.12	–0.97	–0.24	0.04	7	1	1
	2:00	–152.62	4.09	–0.89	–0.46	0.07	82	11	17
	3:00	–139.16	7.24	–0.75	–0.65	0.13	251	34	66
	4:00	–125.86	11.37	–0.57	–0.79	0.20	427	59	143
	5:00	–112.62	16.26	–0.37	–0.89	0.28	564	77	235
	6:00	–99.23	21.65	–0.15	–0.92	0.37	661	91	335
	7:00	–85.41	27.25	0.07	–0.89	0.46	729	100	434
	8:00	–70.83	32.74	0.28	–0.79	0.54	776	106	526
	9:00	–55.11	37.73	0.45	–0.65	0.61	807	111	605
	10:00	–37.98	41.80	0.59	–0.46	0.67	827	113	665
	11:00	–19.45	44.50	0.67	–0.24	0.70	839	115	703
	12:00	0.00	45.45	0.70	0.00	0.71	842	115	716
								1,752	8,173 *D* (Wh/m²/day)
									1,202 kWh/m²/year

L = 70°	*Approx. Clear-Sky Irradiation* (Wh/m^2)								
	AST	α_{sol} (°)	β_{sol} (°)	σ_s	σ_w	σ_z	I_b	I_d	I
Feb/Oct	8:19	–53.55	0.00	0.59	–0.80	0.00			
	9:00	–43.87	2.63	0.72	–0.69	0.05	48	5	7
	10:00	–29.47	5.68	0.87	–0.49	0.10	267	29	55
	11:00	–14.81	7.61	0.96	–0.25	0.13	388	42	93
	12:00	0.00	8.28	0.99	0.00	0.14	424	46	107
								197	418 *D* (Wh/m^2/day)
Mar/Sep	6:00	–90.00	0.00	0.00	–1.00	0.00			
	7:00	–75.87	5.08	0.24	–0.97	0.09	195	22	40
	8:00	–61.52	9.85	0.47	–0.87	0.17	459	53	131
	9:00	–46.78	14.00	0.66	–0.71	0.24	601	69	214
	10:00	–31.57	17.23	0.81	–0.50	0.30	677	78	278
	11:00	–15.92	19.29	0.91	–0.26	0.33	715	82	318
	12:00	0.00	20.00	0.94	0.00	0.34	727	84	332
								692	2,297 *D* (Wh/m^2/day)
Apr/Aug	3:40	–126.45	0.00	–0.59	–0.80	0.00			
	4:00	–121.98	1.35	–0.53	–0.85	0.02	1	0	0
	5:00	–108.02	5.99	–0.31	–0.95	0.10	213	27	49
	6:00	–94.06	11.01	–0.07	–0.98	0.19	452	57	144
	7:00	–79.89	16.12	0.17	–0.95	0.28	600	76	243
	8:00	–65.27	21.00	0.39	–0.85	0.36	690	88	335
	9:00	–49.99	25.33	0.58	–0.69	0.43	746	95	414
	10:00	–33.95	28.75	0.73	–0.49	0.48	781	99	475
	11:00	–17.19	30.96	0.82	–0.25	0.51	799	101	513
	12:00	0.00	31.73	0.85	0.00	0.53	805	102	525
								1,190	4,870 *D* (Wh/m^2/day)
May/Jul	0:00	–180.00	0.31	–1.00	0.00	0.01	0	0	0
	1:00	–165.95	0.93	–0.97	–0.24	0.02	0	0	0
	2:00	–152.00	2.77	–0.88	–0.47	0.05	26	3	5
	3:00	–138.21	5.70	–0.74	–0.66	0.10	177	24	41
	4:00	–124.55	9.54	–0.56	–0.81	0.17	368	49	110
	5:00	–110.95	14.07	–0.35	–0.91	0.24	521	70	197
	6:00	–97.21	19.03	–0.12	–0.94	0.33	630	84	290
	7:00	–83.11	24.15	0.11	–0.91	0.41	706	95	383
	8:00	–68.38	29.11	0.32	–0.81	0.49	757	101	470
	9:00	–52.74	33.57	0.50	–0.66	0.55	792	106	544
	10:00	–36.04	37.15	0.64	–0.47	0.60	814	109	601
	11:00	–18.33	39.49	0.73	–0.24	0.64	827	111	636
	12:00	0.00	40.31	0.76	0.00	0.65	831	111	649
								1,617	7,202 *D* (Wh/m^2/day)
Jun	0:00	–180.00	3.45	–1.00	0.00	0.06	50	7	10
	1:00	–166.23	4.06	–0.97	–0.24	0.07	80	11	17
	2:00	–152.54	5.87	–0.88	–0.46	0.10	179	24	43
	3:00	–138.98	8.75	–0.75	–0.65	0.15	324	44	94
	4:00	–125.52	12.54	–0.57	–0.79	0.22	466	64	165
	5:00	–112.07	17.02	–0.36	–0.89	0.29	580	80	249
	6:00	–98.44	21.96	–0.14	–0.92	0.37	666	91	340
	7:00	–84.39	27.08	0.09	–0.89	0.46	727	100	431
	8:00	–69.63	32.06	0.29	–0.79	0.53	771	106	515
	9:00	–53.88	36.57	0.47	–0.65	0.60	801	110	587
	10:00	–36.92	40.22	0.61	–0.46	0.65	820	112	642
	11:00	–18.82	42.61	0.70	–0.24	0.68	831	114	676
	12:00	0.00	43.45	0.73	0.00	0.69	834	114	688
								1,832	8,213 *D* (Wh/m^2/day)
									1,155 kWh/m^2/year

$L = 74°$	*Approx. Clear-Sky Irradiation (Wh/m²)*								
	AST	α_{sol} (°)	β_{sol} (°)	σ_s	σ_w	σ_z	I_b	I_d	I
Feb/Oct	9:05	–42.50	0.00	0.74	–0.68	0.00			
	10:00	–29.34	2.20	0.87	–0.49	0.04	26	3	4
	11:00	–14.71	3.75	0.97	–0.25	0.07	124	13	21
	12:00	0.00	4.27	1.00	0.00	0.07	164	18	30
								50	80 *D* (Wh/m²/day)
Mar/Sep	6:00	–90.00	0.00	0.00	–1.00	0.00			
	7:00	–75.56	4.09	0.25	–0.97	0.07	127	15	24
	8:00	–60.97	7.92	0.48	–0.87	0.14	368	42	93
	9:00	–46.13	11.24	0.68	–0.71	0.19	514	59	159
	10:00	–30.99	13.81	0.83	–0.50	0.24	596	69	211
	11:00	–15.58	15.44	0.93	–0.26	0.27	638	73	243
	12:00	0.00	16.00	0.96	0.00	0.28	651	75	254
								591	1,714 *D* (Wh/m²/day)
Apr/Aug	2:54	–137.50	0.00	–0.74	–0.68	0.00			
	3:00	–136.18	0.26	–0.72	–0.69	0.00	0	0	0
	4:00	–121.84	3.46	–0.53	–0.85	0.06	64	8	12
	5:00	–107.58	7.21	–0.30	–0.95	0.13	282	36	71
	6:00	–93.27	11.26	–0.06	–0.98	0.20	461	59	149
	7:00	–78.78	15.38	0.19	–0.95	0.27	583	74	228
	8:00	–63.94	19.29	0.41	–0.85	0.33	662	84	303
	9:00	–48.64	22.72	0.61	–0.69	0.39	715	91	367
	10:00	–32.82	25.41	0.76	–0.49	0.43	747	95	416
	11:00	–16.54	27.13	0.85	–0.25	0.46	765	97	446
	12:00	0.00	27.73	0.89	0.00	0.47	771	98	457
								1,185	4,440 *D* (Wh/m²/day)
May/Jul	0:00	180.00	4.31	–1.00	0.00	0.08	98	13	21
	1:00	–165.90	4.81	–0.97	–0.24	0.08	126	17	28
	2:00	–151.85	6.30	–0.88	–0.47	0.11	210	28	51
	3:00	–137.87	8.68	–0.73	–0.66	0.15	330	44	94
	4:00	–123.93	11.79	–0.55	–0.81	0.20	452	61	153
	5:00	–109.96	15.47	–0.33	–0.91	0.27	557	75	223
	6:00	–95.82	19.49	–0.10	–0.94	0.33	638	86	298
	7:00	–81.36	23.61	0.14	–0.91	0.40	699	94	374
	8:00	–66.39	27.57	0.36	–0.81	0.46	743	100	443
	9:00	–50.75	31.09	0.54	–0.66	0.52	774	104	503
	10:00	–34.39	33.88	0.69	–0.47	0.56	794	106	549
	11:00	–17.39	35.68	0.78	–0.24	0.58	805	108	578
	12:00	0.00	36.31	0.81	0.00	0.59	809	108	588
								1,764	7,197 *D* (Wh/m²/day)
Jun	0:00	180.00	7.45	–0.99	0.00	0.13	262	36	70
	1:00	–166.13	7.95	–0.96	–0.24	0.14	287	39	79
	2:00	–152.29	9.41	–0.87	–0.46	0.16	352	48	106
	3:00	–138.50	11.75	–0.73	–0.65	0.20	440	60	150
	4:00	–124.72	14.84	–0.55	–0.79	0.26	530	73	208
	5:00	–110.87	18.49	–0.34	–0.89	0.32	609	83	277
	6:00	–96.82	22.49	–0.11	–0.92	0.38	673	92	350
	7:00	–82.38	26.61	0.12	–0.89	0.45	723	99	423
	8:00	–67.37	30.60	0.33	–0.79	0.51	759	104	490
	9:00	–51.61	34.15	0.51	–0.65	0.56	785	108	548
	10:00	–35.04	36.98	0.65	–0.46	0.60	803	110	593
	11:00	–17.74	38.81	0.74	–0.24	0.63	813	111	621
	12:00	0.00	39.45	0.77	0.00	0.64	816	112	630
								2,004	8,391 *D* (Wh/m²/day)
									1,078 kWh/m²/year

$L = 78°$	Approx. Clear-Sky Irradiation (Wh/m^2)								
	AST	α sol (°)	β sol (°)	σ_s	σ_w	σ_z	I_b	I_d	I
Feb/Oct	11:10	–12.20	0.00	0.98	–0.21	0.00			
	12:00	0.00	0.27	1.00	0.00	0.00	0	0	0
								0	0 *D* (Wh/m^2/day)
Mar/Sep	6:00	–90.00	0.00	0.00	–1.00	0.00			
	7:00	–75.31	3.08	0.25	–0.97	0.05	62	7	10
	8:00	–60.55	5.97	0.49	–0.87	0.10	254	29	56
	9:00	–45.63	8.45	0.69	–0.71	0.15	395	45	104
	10:00	–30.55	10.37	0.85	–0.50	0.18	481	55	142
	11:00	–15.32	11.59	0.94	–0.26	0.20	526	61	166
	12:00	0.00	12.00	0.98	0.00	0.21	540	62	175
								457	1,130 *D* (Wh/m^2/day)
Apr/Aug	0:49	–167.80	0.00	–0.98	–0.21	0.00			
	1:00	–165.32	0.12	–0.97	–0.25	0.00	0	0	0
	2:00	–150.68	1.29	–0.87	–0.49	0.02	1	0	0
	3:00	–136.10	3.14	–0.72	–0.69	0.05	48	6	9
	4:00	–121.57	5.57	–0.52	–0.85	0.10	188	24	42
	5:00	–107.05	8.40	–0.29	–0.95	0.15	342	43	93
	6:00	–92.47	11.47	–0.04	–0.98	0.20	468	59	153
	7:00	–77.73	14.56	0.21	–0.95	0.25	562	71	213
	8:00	–62.76	17.49	0.44	–0.85	0.30	629	80	269
	9:00	–47.48	20.04	0.63	–0.69	0.34	675	86	317
	10:00	–31.88	22.03	0.79	–0.49	0.38	705	90	354
	11:00	–16.02	23.29	0.88	–0.25	0.40	722	92	377
	12:00	0.00	23.73	0.92	0.00	0.40	728	92	385
								1,195	4,039 *D* (Wh/m^2/day)
May/Jul	0:00	180.00	8.31	–0.99	0.00	0.14	313	42	87
	1:00	–165.79	8.69	–0.96	–0.24	0.15	331	44	94
	2:00	–151.58	9.82	–0.87	–0.47	0.17	380	51	116
	3:00	–137.39	11.63	–0.72	–0.66	0.20	447	60	150
	4:00	–123.17	14.00	–0.53	–0.81	0.24	519	70	195
	5:00	–108.87	16.80	–0.31	–0.91	0.29	587	79	248
	6:00	–94.40	19.85	–0.07	–0.94	0.34	644	86	305
	7:00	–79.66	22.95	0.17	–0.91	0.39	690	93	362
	8:00	–64.55	25.91	0.39	–0.81	0.44	726	97	414
	9:00	–49.00	28.51	0.58	–0.66	0.48	752	101	460
	10:00	–32.99	30.55	0.72	–0.47	0.51	769	103	494
	11:00	–16.61	31.86	0.81	–0.24	0.53	780	104	516
	12:00	0.00	32.31	0.85	0.00	0.53	783	105	523
								1,922	7,319 *D* (Wh/m^2/day)
Jun	0:00	180.00	11.45	–0.98	0.00	0.20	430	59	144
	1:00	–165.96	11.83	–0.95	–0.24	0.21	443	61	151
	2:00	–151.92	12.95	–0.86	–0.46	0.22	478	66	173
	3:00	–137.87	14.74	–0.72	–0.65	0.25	528	72	207
	4:00	–123.78	17.09	–0.53	–0.79	0.29	582	80	251
	5:00	–109.57	19.87	–0.31	–0.89	0.34	634	87	302
	6:00	–95.15	22.91	–0.08	–0.92	0.39	679	93	357
	7:00	–80.42	26.02	0.15	–0.89	0.44	716	98	412
	8:00	–65.27	28.99	0.37	–0.79	0.48	745	102	463
	9:00	–49.62	31.61	0.55	–0.65	0.52	767	105	507
	10:00	–33.45	33.67	0.69	–0.46	0.55	782	107	541
	11:00	–16.85	34.99	0.78	–0.24	0.57	791	108	562
	12:00	0.00	35.45	0.81	0.00	0.58	794	109	569
								2,125	8,566 *D* (Wh/m^2/day)
									1,026 kWh/m^2/year

L = 82°	*Approx. Clear-Sky Irradiation (Wh/m²)*								
	AST	α_{sol} *(°)*	β_{sol} *(°)*	σ_s	σ_w	σ_z	I_b	I_d	I
Mar/Sep	6:00	–90.00	0.00	0.00	–1.00	0.00			
	7:00	–75.14	2.06	0.26	–0.97	0.04	15	2	2
	8:00	–60.24	3.99	0.50	–0.87	0.07	120	14	22
	9:00	–45.28	5.65	0.70	–0.71	0.10	233	27	50
	10:00	–30.24	6.92	0.86	–0.50	0.12	313	36	74
	11:00	–15.14	7.73	0.96	–0.26	0.13	358	41	89
	12:00	0.00	8.00	0.99	0.00	0.14	372	43	95
								282	569 *D* (Wh/m²/day)
Apr/Aug	0:00	180.00	3.73	–1.00	0.00	0.06	78	10	15
	1:00	–165.28	3.99	–0.96	–0.25	0.07	93	12	18
	2:00	–150.58	4.77	–0.87	–0.49	0.08	140	18	29
	3:00	–135.88	6.02	–0.71	–0.69	0.10	215	27	50
	4:00	–121.18	7.65	–0.51	–0.85	0.13	305	39	79
	5:00	–106.45	9.55	–0.28	–0.95	0.17	394	50	116
	6:00	–91.65	11.61	–0.03	–0.98	0.20	473	60	155
	7:00	–76.75	13.68	0.22	–0.95	0.24	538	68	196
	8:00	–61.70	15.63	0.46	–0.85	0.27	588	75	233
	9:00	–46.49	17.31	0.66	–0.69	0.30	625	79	266
	10:00	–31.10	18.62	0.81	–0.49	0.32	651	83	290
	11:00	–15.59	19.44	0.91	–0.25	0.33	665	84	306
	12:00	0.00	19.73	0.94	0.00	0.34	670	85	311
								1,286	3,803 *D* (Wh/m²/day)
May/Jul	0:00	180.00	12.31	–0.98	0.00	0.21	469	63	163
	1:00	–165.60	12.57	–0.95	–0.24	0.22	478	64	168
	2:00	–151.19	13.34	–0.85	–0.47	0.23	501	67	183
	3:00	–136.75	14.56	–0.71	–0.66	0.25	534	72	206
	4:00	–122.26	16.17	–0.51	–0.81	0.28	573	77	236
	5:00	–107.68	18.05	–0.29	–0.91	0.31	612	82	272
	6:00	–92.95	20.10	–0.05	–0.94	0.34	648	87	310
	7:00	–78.03	22.18	0.19	–0.91	0.38	680	91	348
	8:00	–62.88	24.14	0.42	–0.81	0.41	705	95	383
	9:00	–47.47	25.85	0.61	–0.66	0.44	725	97	413
	10:00	–31.81	27.18	0.76	–0.47	0.46	739	99	437
	11:00	–15.96	28.02	0.85	–0.24	0.47	747	100	451
	12:00	0.00	28.31	0.88	0.00	0.47	750	100	456
								2,024	7,430 *D* (Wh/m²/day)
Jun	0:00	180.00	15.45	–0.96	0.00	0.27	545	75	220
	1:00	–165.72	15.71	–0.93	–0.24	0.27	551	76	225
	2:00	–151.42	16.47	–0.84	–0.46	0.28	569	78	239
	3:00	–137.09	17.69	–0.70	–0.65	0.30	594	81	262
	4:00	–122.68	19.28	–0.51	–0.79	0.33	624	85	291
	5:00	–108.15	21.16	–0.29	–0.89	0.36	654	90	326
	6:00	–93.45	23.21	–0.06	–0.92	0.39	683	94	363
	7:00	–78.53	25.29	0.18	–0.89	0.43	708	97	399
	8:00	–63.34	27.25	0.40	–0.79	0.46	729	100	434
	9:00	–47.86	28.97	0.59	–0.65	0.48	745	102	463
	10:00	–32.09	30.31	0.73	–0.46	0.50	757	104	486
	11:00	–16.11	31.16	0.82	–0.24	0.52	764	105	500
	12:00	0.00	31.45	0.85	0.00	0.52	766	105	505
								2,201	8,699 *D* (Wh/m²/day)
									988 kWh/m²/year

L = 86°	Approx. Clear-Sky Irradiation (Wh/m²)								
	AST	α_{sol} (°)	β_{sol} (°)	σ_s	σ_w	σ_z	I_b	I_d	I
Mar/Sep	6:00	–90.00	0.00	0.00	–1.00	0.00			
	7:00	–75.03	1.03	0.26	–0.97	0.02	0	0	0
	8:00	–60.06	2.00	0.50	–0.87	0.03	13	1	2
	9:00	–45.07	2.83	0.71	–0.71	0.05	48	5	8
	10:00	–30.06	3.46	0.86	–0.50	0.06	86	10	15
	11:00	–15.03	3.86	0.96	–0.26	0.07	112	13	20
	12:00	0.00	4.00	1.00	0.00	0.07	121	14	22
								73	113 *D* (Wh/m²/day)
Apr/Aug	0:00	180.00	7.73	–0.99	0.00	0.13	309	39	81
	1:00	–165.18	7.86	–0.96	–0.25	0.14	316	40	83
	2:00	–150.35	8.25	–0.86	–0.49	0.14	335	43	91
	3:00	–135.51	8.88	–0.70	–0.69	0.15	365	46	103
	4:00	–120.65	9.70	–0.50	–0.85	0.17	401	51	118
	5:00	–105.76	10.66	–0.27	–0.95	0.19	439	56	137
	6:00	–90.83	11.70	–0.01	–0.98	0.20	476	61	157
	7:00	–75.84	12.73	0.24	–0.95	0.22	510	65	177
	8:00	–60.78	13.70	0.47	–0.85	0.24	539	68	196
	9:00	–45.66	14.54	0.68	–0.69	0.25	561	71	212
	10:00	–30.48	15.18	0.83	–0.49	0.26	578	73	225
	11:00	–15.25	15.59	0.93	–0.25	0.27	588	75	232
	12:00	0.00	15.73	0.96	0.00	0.27	591	75	235
								1,412	3,780 *D* (Wh/m²/day)
May/Jul	0:00	180.00	16.31	–0.96	0.00	0.28	576	77	239
	1:00	–165.34	16.44	–0.93	–0.24	0.28	579	78	241
	2:00	–150.67	16.83	–0.83	–0.47	0.29	587	79	249
	3:00	–135.96	17.46	–0.69	–0.66	0.30	600	80	261
	4:00	–121.21	18.27	–0.49	–0.81	0.31	616	83	276
	5:00	–106.38	19.23	–0.27	–0.91	0.33	634	85	294
	6:00	–91.48	20.26	–0.02	–0.94	0.35	651	87	313
	7:00	–76.47	21.29	0.22	–0.91	0.36	667	89	332
	8:00	–61.36	22.27	0.44	–0.81	0.38	681	91	349
	9:00	–46.14	23.11	0.64	–0.66	0.39	692	93	365
	10:00	–30.82	23.76	0.79	–0.47	0.40	701	94	376
	11:00	–15.43	24.17	0.88	–0.24	0.41	706	95	384
	12:00	0.00	24.31	0.91	0.00	0.41	707	95	386
								2,079	7,501 *D* (Wh/m²/day)
Jun	0:00	180.00	19.45	–0.94	0.00	0.33	627	86	294
	1:00	–165.40	19.58	–0.91	–0.24	0.34	629	86	297
	2:00	–150.79	19.97	–0.82	–0.46	0.34	635	87	304
	3:00	–136.13	20.59	–0.67	–0.65	0.35	645	88	315
	4:00	–121.42	21.41	–0.49	–0.79	0.36	658	90	330
	5:00	–106.63	22.36	–0.26	–0.89	0.38	671	92	347
	6:00	–91.73	23.39	–0.03	–0.92	0.40	685	94	366
	7:00	–76.72	24.43	0.21	–0.89	0.41	698	96	384
	8:00	–61.59	25.40	0.43	–0.79	0.43	709	97	402
	9:00	–46.33	26.25	0.62	–0.65	0.44	719	98	416
	10:00	–30.95	26.90	0.76	–0.46	0.45	725	99	428
	11:00	–15.50	27.31	0.86	–0.24	0.46	730	100	435
	12:00	0.00	27.45	0.89	0.00	0.46	731	100	437
								2,242	8,780 *D* (Wh/m²/day)
									966 kWh/m²/year

L = 90°	*Approx. Clear-Sky Irradiation (Wh/m²)*								
	AST	α_{sol} (°)	β_{sol} (°)	σ_s	σ_w	σ_z	I_b	I_d	I
Mar/Sep	0:00	180.00	0.00	–1.00	0.00	0.00	0	0	0
	1:00	–165.00	0.00	–0.97	–0.26	0.00	0	0	0
	2:00	–150.00	0.00	–0.87	–0.50	0.00	0	0	0
	3:00	–135.00	0.00	–0.71	–0.71	0.00	0	0	0
	4:00	–120.00	0.00	–0.50	–0.87	0.00	0	0	0
	5:00	–105.00	0.00	–0.26	–0.97	0.00	0	0	0
	6:00	–90.00	0.00	0.00	–1.00	0.00			
	7:00	–75.00	0.00	0.26	–0.97	0.00	0	0	0
	8:00	–60.00	0.00	0.50	–0.87	0.00	0	0	0
	9:00	–45.00	0.00	0.71	–0.71	0.00	0	0	0
	10:00	–30.00	0.00	0.87	–0.50	0.00	0	0	0
	11:00	–15.00	0.00	0.97	–0.26	0.00	0	0	0
	12:00	0.00	0.00	1.00	0.00	0.00	0	0	0
								0	0 *D* (Wh/m²/day)
Apr/Aug	0:00	180.00	11.73	–0.98	0.00	0.20	477	61	158
	1:00	–165.00	11.73	–0.95	–0.25	0.20	477	61	158
	2:00	–150.00	11.73	–0.85	–0.49	0.20	477	61	158
	3:00	–135.00	11.73	–0.69	–0.69	0.20	477	61	158
	4:00	–120.00	11.73	–0.49	–0.85	0.20	477	61	158
	5:00	–105.00	11.73	–0.25	–0.95	0.20	477	61	158
	6:00	–90.00	11.73	0.00	–0.98	0.20	477	61	158
	7:00	–75.00	11.73	0.25	–0.95	0.20	477	61	158
	8:00	–60.00	11.73	0.49	–0.85	0.20	477	61	158
	9:00	–45.00	11.73	0.69	–0.69	0.20	477	61	158
	10:00	–30.00	11.73	0.85	–0.49	0.20	477	61	158
	11:00	–15.00	11.73	0.95	–0.25	0.20	477	61	158
	12:00	0.00	11.73	0.98	0.00	0.20	477	61	158
								1,455	3,784 *D* (Wh/m²/day)
May/Jul	0:00	180.00	20.31	–0.94	0.00	0.35	652	87	314
	1:00	–165.00	20.31	–0.91	–0.24	0.35	652	87	314
	2:00	–150.00	20.31	–0.81	–0.47	0.35	652	87	314
	3:00	–135.00	20.31	–0.66	–0.66	0.35	652	87	314
	4:00	–120.00	20.31	–0.47	–0.81	0.35	652	87	314
	5:00	–105.00	20.31	–0.24	–0.91	0.35	652	87	314
	6:00	–90.00	20.31	0.00	–0.94	0.35	652	87	314
	7:00	–75.00	20.31	0.24	–0.91	0.35	652	87	314
	8:00	–60.00	20.31	0.47	–0.81	0.35	652	87	314
	9:00	–45.00	20.31	0.66	–0.66	0.35	652	87	314
	10:00	–30.00	20.31	0.81	–0.47	0.35	652	87	314
	11:00	–15.00	20.31	0.91	–0.24	0.35	652	87	314
	12:00	0.00	20.31	0.94	0.00	0.35	652	87	314
								2,096	7,525 *D* (Wh/m²/day)
Jun	0:00	180.00	23.45	–0.92	0.00	0.40	686	94	367
	1:00	–165.00	23.45	–0.89	–0.24	0.40	686	94	367
	2:00	–150.00	23.45	–0.79	–0.46	0.40	686	94	367
	3:00	–135.00	23.45	–0.65	–0.65	0.40	686	94	367
	4:00	–120.00	23.45	–0.46	–0.79	0.40	686	94	367
	5:00	–105.00	23.45	–0.24	–0.89	0.40	686	94	367
	6:00	–90.00	23.45	0.00	–0.92	0.40	686	94	367
	7:00	–75.00	23.45	0.24	–0.89	0.40	686	94	367
	8:00	–60.00	23.45	0.46	–0.79	0.40	686	94	367
	9:00	–45.00	23.45	0.65	–0.65	0.40	686	94	367
	10:00	–30.00	23.45	0.79	–0.46	0.40	686	94	367
	11:00	–15.00	23.45	0.89	–0.24	0.40	686	94	367
	12:00	0.00	23.45	0.92	0.00	0.40	686	94	367
								2,256	8,807 *D* (Wh/m²/day)
									962 kWh/m²/year

APPENDIX D: SAMPLE STATISTICAL SUMMARY RADIATION FILES

The following tables present typical solar radiation data for several cities used as example locations in the text. The data were adapted from the statistical files included with EnergyPlus weather files.[1]

Austin, Texas, USA

WMO Station 722544
L = 30.3° N, *LON* = 97.8° W
UTC –6.0 Hours

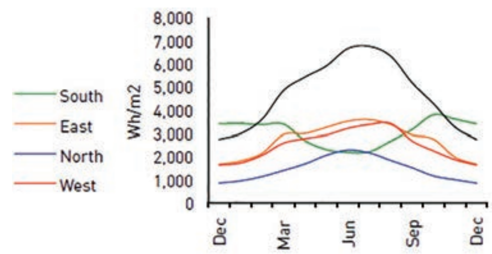

Monthly Statistics for Solar Radiation: Direct Normal, Diffuse, Global Horizontal [Wh/m²]

	Jan	*Feb*	*Mar*	*Apr*	*May*	*Jun*	*Jul*	*Aug*	*Sep*	*Oct*	*Nov*	*Dec*
Direct Average	3,622	3,840	4,907	4,533	4,464	5,523	6,093	5,900	4,783	5,012	3,982	3,609
Direct Maximum	8,826	9,442	10,196	10,227	8,565	9,939	10,250	9,294	9,385	8,046	8,275	8,374
Day of Month	24	23	20	6	24	7	22	27	26	14	11	8
Diffuse Average	1,320	1,565	1,847	2,232	2,608	2,534	2,311	2,191	2,012	1,483	1,363	1,182
Global Horizontal Average	3,016	3,627	4,850	5,403	5,914	6,666	6,760	6,353	5,228	4,300	3,341	2,790

Maximum Direct Normal Solar of 10,250 Wh/m² on Jul 22

Average Hourly Statistics for Direct Normal Solar Radiation [Wh/m^2]

	Jan	*Feb*	*Mar*	*Apr*	*May*	*Jun*	*Jul*	*Aug*	*Sep*	*Oct*	*Nov*	*Dec*
0:01–1:00	0	0	0	0	0	0	0	0	0	0	0	0
1:01–2:00	0	0	0	0	0	0	0	0	0	0	0	0
2:01–3:00	0	0	0	0	0	0	0	0	0	0	0	0
3:01–4:00	0	0	0	0	0	0	0	0	0	0	0	0
4:01–5:00	0	0	0	0	0	0	0	0	0	0	0	0
5:01–6:00	0	0	0	0	2	10	6	0	0	0	0	0
6:01–7:00	0	0	11	45	64	124	158	121	37	9	3	0
7:01–8:00	45	89	207	200	195	212	276	372	187	208	142	70
8:01–9:00	233	266	344	304	295	366	421	438	313	356	288	248
9:01–10:00	364	331	393	370	387	462	526	540	436	451	388	369
10:01–11:00	405	412	442	457	424	529	592	595	477	453	424	409
11:01–12:00	439	425	469	486	444	581	589	610	553	495	482	432
12:01–13:00	478	480	551	482	483	596	601	576	536	564	501	455
13:01–14:00	448	468	522	520	477	541	606	560	550	626	501	459
14:01–15:00	421	418	542	520	400	537	539	567	497	612	485	444
15:01–16:00	397	419	549	418	432	481	562	494	492	583	411	391
16:01–17:00	283	326	473	345	424	440	495	508	410	466	299	275
17:01–18:00	108	191	344	279	302	400	432	362	254	188	56	57
18:01–19:00	0	14	59	105	130	223	260	151	43	0	0	0
19:01–20:00	0	0	0	0	4	22	28	4	0	0	0	0
20:01–21:00	0	0	0	0	0	0	0	0	0	0	0	0
21:01–22:00	0	0	0	0	0	0	0	0	0	0	0	0
22:01–23:00	0	0	0	0	0	0	0	0	0	0	0	0
23:01–24:00	0	0	0	0	0	0	0	0	0	0	0	0
Max Hour	13	13	13	14	13	13	14	12	12	14	13	14
Min Hour	1	1	1	1	1	1	1	1	1	1	1	1

Kuwait City, Kuwait

WMO Station 405820
L = 29.2° N, LON = 48.0° E
UTC +3.0 Hours

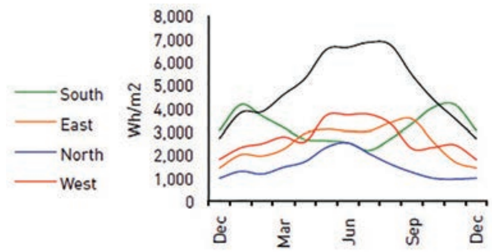

Monthly Statistics for Solar Radiation: Direct Normal, Diffuse, Global Horizontal [Wh/m²]

	Jan	*Feb*	*Mar*	*Apr*	*May*	*Jun*	*Jul*	*Aug*	*Sep*	*Oct*	*Nov*	*Dec*
Direct Average	4,261	4,258	4,091	4,080	4,680	4,289	6,130	6,904	6,244	5,695	4,805	2,859
Direct Maximum	8,072	8,641	8,292	9,391	7,818	6,981	8,931	8,110	8,300	7,977	6,905	6,057
Day of Month	16	26	22	8	6	1	9	7	11	20	12	5
Diffuse Average	1,818	1,573	2,013	2,319	3,021	3,292	2,195	1,672	1,390	1,106	1,200	1,454
Global Horizontal Average	3,961	4,259	5,047	5,960	7,097	7,416	7,259	7,063	6,213	4,971	4,093	2,951

Maximum Direct Normal Solar of 10,250 Wh/m² on Jul 22

Average Hourly Statistics for Direct Normal Solar Radiation [Wh/m²]

	Jan	*Feb*	*Mar*	*Apr*	*May*	*Jun*	*Jul*	*Aug*	*Sep*	*Oct*	*Nov*	*Dec*
0:01–1:00	0	0	0	0	0	0	0	0	0	0	0	0
1:01–2:00	0	0	0	0	0	0	0	0	0	0	0	0
2:01–3:00	0	0	0	0	0	0	0	0	0	0	0	0
3:01–4:00	0	0	0	0	0	0	0	0	0	0	0	0
4:01–5:00	0	0	0	0	0	0	0	0	0	0	0	0
5:01–6:00	0	0	0	0	10	3	0	0	0	0	0	0
6:01–7:00	0	14	77	14	154	104	119	44	1	0	0	0
7:01–8:00	174	208	232	113	370	349	408	316	21	197	325	152
8:01–9:00	360	371	356	219	461	433	583	525	266	442	505	254
9:01–10:00	436	479	454	306	474	472	672	645	481	565	608	336
10:01–11:00	511	508	511	435	512	508	720	720	587	632	649	388
11:01–12:00	585	516	515	504	529	510	709	756	689	682	670	376
12:01–13:00	625	550	471	498	493	486	646	749	722	689	609	386
13:01–14:00	565	515	452	429	480	453	593	756	726	693	560	371
14:01–15:00	444	480	393	477	425	385	553	709	710	625	489	314
15:01–16:00	374	370	329	436	374	296	453	642	663	570	312	221
16:01–17:00	188	214	220	349	253	193	343	528	586	427	78	56
17:01–18:00	0	33	81	221	126	87	222	370	478	173	1	4
18:01–19:00	0	0	0	79	20	10	99	141	276	0	0	0
19:01–20:00	0	0	0	0	0	0	10	3	38	0	0	0
20:01–21:00	0	0	0	0	0	0	0	0	0	0	0	0
21:01–22:00	0	0	0	0	0	0	0	0	0	0	0	0
22:01–23:00	0	0	0	0	0	0	0	0	0	0	0	0
23:01–24:00	0	0	0	0	0	0	0	0	0	0	0	0
Max Hour	13	13	12	12	12	12	11 *	12	14	14	12	11 *
Min Hour	1	1	1	1	1	1	1	1	1	1	1	1

Shanghai, China

WMO Station 583620
L = 31.4° N, LON = 121.4° E
UTC +8.0 Hours

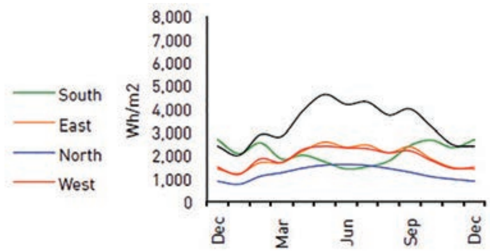

Monthly Statistics for Solar Radiation: Direct Normal, Diffuse, Global Horizontal [Wh/m²]

	Jan	*Feb*	*Mar*	*Apr*	*May*	*Jun*	*Jul*	*Aug*	*Sep*	*Oct*	*Nov*	*Dec*
Direct Average	1,994	2,545	1,555	2,765	3,849	3,594	3,648	2,563	3,546	2,915	2,057	2,503
Direct Maximum	5,693	6,581	5,763	8,280	8,265	8,909	8,700	7,839	7,478	6,344	5,281	5,103
Day of Month	27	21	30	22	27	2	25	17	17	26	6	31
Diffuse Average	1,110	1,617	1,951	2,074	1,880	1,753	1,764	1,993	1,752	1,521	1,458	1,306
Global Horizontal Average	2,025	3,064	2,873	4,039	4,709	4,347	4,372	3,802	4,246	3,366	2,493	2,457

Maximum Direct Normal Solar of 8,908 Wh/m² on Jun 2

Average Hourly Statistics for Direct Normal Solar Radiation [Wh/m²]

	Jan	*Feb*	*Mar*	*Apr*	*May*	*Jun*	*Jul*	*Aug*	*Sep*	*Oct*	*Nov*	*Dec*
0:01–1:00	0	0	0	0	0	0	0	0	0	0	0	0
1:01–2:00	0	0	0	0	0	0	0	0	0	0	0	0
2:01–3:00	0	0	0	0	0	0	0	0	0	0	0	0
3:01–4:00	0	0	0	0	0	0	0	0	0	0	0	0
4:01–5:00	0	0	0	0	0	0	0	0	0	0	0	0
5:01–6:00	0	0	0	0	4	41	7	0	0	0	0	0
6:01–7:00	0	0	49	142	165	192	150	133	60	0	0	0
7:01–8:00	78	198	143	172	224	237	227	155	186	134	72	47
8:01–9:00	104	213	117	198	255	304	270	153	282	163	128	236
9:01–10:00	216	254	107	222	288	280	249	186	299	301	217	251
10:01–11:00	259	195	131	278	337	318	334	268	326	346	257	313
11:01–12:00	226	283	179	260	363	309	315	259	328	434	290	338
12:01–13:00	230	260	119	256	355	277	309	215	385	318	211	282
13:01–14:00	211	330	164	295	399	216	304	280	346	291	230	337
14:01–15:00	240	275	141	268	335	353	342	219	355	327	278	274
15:01–16:00	202	272	123	278	378	271	301	202	373	364	258	281
16:01–17:00	227	187	181	160	359	307	339	184	341	226	115	143
17:01–18:00	0	79	100	236	306	292	280	272	265	12	0	0
18:01–19:00	0	0	0	0	82	196	221	37	0	0	0	0
19:01–20:00	0	0	0	0	0	0	0	0	0	0	0	0
20:01–21:00	0	0	0	0	0	0	0	0	0	0	0	0
21:01–22:00	0	0	0	0	0	0	0	0	0	0	0	0
22:01–23:00	0	0	0	0	0	0	0	0	0	0	0	0
23:01–24:00	0	0	0	0	0	0	0	0	0	0	0	0
Max Hour	11*	14	17*	14	14	15	15	14	13	12	12	12
Min Hour	1	1	1	1	1	1	1	1	1	1	1	1

Caracas, Venezuela

WMO Station 804150
L = 10.6° N, LON = 67.0° W
UTC –4.0 Hours

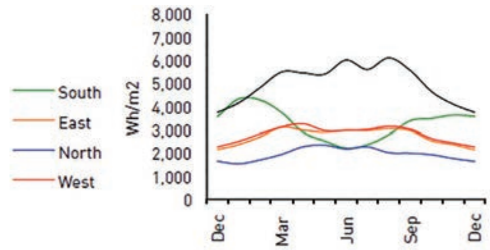

Monthly Statistics for Solar Radiation: Direct Normal, Diffuse, Global Horizontal [Wh/m²]

	Jan	*Feb*	*Mar*	*Apr*	*May*	*Jun*	*Jul*	*Aug*	*Sep*	*Oct*	*Nov*	*Dec*
Direct Average	4,046	4,330	4,316	2,913	2,497	3,937	3,117	4,352	3,868	2,803	2,775	2,679
Direct Maximum	6,895	7,684	7,673	4,616	6,775	7,834	6,047	7,005	7,038	6,389	6,347	6,127
Day of Month	30	24	11	25	28	15	21	25	15	5	13	18
Diffuse Average	2,255	2,450	2,797	3,445	3,482	2,855	3,206	2,769	2,889	2,928	2,725	2,551
Global Horizontal Average	5,015	5,560	5,944	5,541	5,349	5,848	5,505	6,161	5,883	5,086	4,666	4,359

Maximum Direct Normal Solar of 7,834 Wh/m² on Jun 15

Average Hourly Statistics for Direct Normal Solar Radiation [Wh/m²]

	Jan	*Feb*	*Mar*	*Apr*	*May*	*Jun*	*Jul*	*Aug*	*Sep*	*Oct*	*Nov*	*Dec*
0:01–1:00	0	0	0	0	0	0	0	0	0	0	0	0
1:01–2:00	0	0	0	0	0	0	0	0	0	0	0	0
2:01–3:00	0	0	0	0	0	0	0	0	0	0	0	0
3:01–4:00	0	0	0	0	0	0	0	0	0	0	0	0
4:01–5:00	0	0	0	0	0	0	0	0	0	0	0	0
5:01–6:00	0	0	0	0	0	0	0	0	0	0	0	0
6:01–7:00	0	0	0	4	6	1	0	0	0	0	0	0
7:01–8:00	25	49	171	171	124	133	141	154	143	65	73	26
8:01–9:00	258	300	345	380	257	336	315	353	333	227	240	203
9:01–10:00	459	480	453	353	275	411	341	453	410	321	318	315
10:01–11:00	544	529	419	333	233	376	311	477	414	356	341	342
11:01–12:00	585	555	485	310	294	463	312	520	473	409	388	387
12:01–13:00	545	551	503	265	276	460	310	506	462	404	370	379
13:01–14:00	446	503	468	210	254	458	296	491	448	324	318	326
14:01–15:00	430	485	434	212	232	412	313	482	434	308	309	295
15:01–16:00	407	422	406	238	205	369	311	425	389	243	273	258
16:01–17:00	277	317	362	263	205	314	284	337	281	140	146	138
17:01–18:00	68	141	271	175	136	204	183	154	82	6	0	10
18:01–19:00	0	0	0	0	0	0	0	0	0	0	0	0
19:01–20:00	0	0	0	0	0	0	0	0	0	0	0	0
20:01–21:00	0	0	0	0	0	0	0	0	0	0	0	0
21:01–22:00	0	0	0	0	0	0	0	0	0	0	0	0
22:01–23:00	0	0	0	0	0	0	0	0	0	0	0	0
23:01–24:00	0	0	0	0	0	0	0	0	0	0	0	0
Max Hour	12	12	13	9*	12	12	10*	12	12	12	12	12
Min Hour	1	1	1	1	1	1	1	1	1	1	1	1

London, England

WMO Station 037760
L = 51.2° N, *LON* = 0.2° W
UTC +0.0 Hours

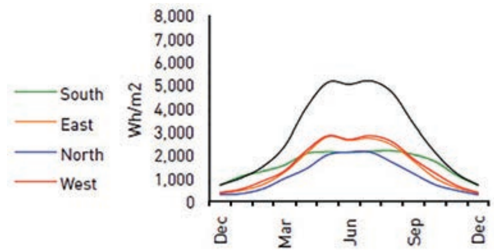

Monthly Statistics for Solar Radiation: Direct Normal, Diffuse, Global Horizontal [Wh/m²]

	Jan	*Feb*	*Mar*	*Apr*	*May*	*Jun*	*Jul*	*Aug*	*Sep*	*Oct*	*Nov*	*Dec*
Direct Average	1,024	1,222	1,309	2,785	3,441	2,730	3,118	3,203	2,306	1,775	928	527
Direct Maximum	3,685	5,093	5,861	7,890	8,645	8,690	8,255	7,766	6,904	5,817	3,911	2,100
Day of Month	19	21	2	24	30	28	20	4	6	1	5	4
Diffuse Average	461	780	1,492	1,983	2,680	2,954	2,885	2,337	1,732	1,011	692	423
Global Horizontal Average	710	1,194	2,116	3,637	4,911	4,906	5,020	4,351	2,973	1,748	969	549

Maximum Direct Normal Solar of 8,690 Wh/m² on Jun 28

Average Hourly Statistics for Direct Normal Solar Radiation [Wh/m²]

	Jan	*Feb*	*Mar*	*Apr*	*May*	*Jun*	*Jul*	*Aug*	*Sep*	*Oct*	*Nov*	*Dec*
0:01–1:00	0	0	0	0	0	0	0	0	0	0	0	0
1:01–2:00	0	0	0	0	0	0	0	0	0	0	0	0
2:01–3:00	0	0	0	0	0	0	0	0	0	0	0	0
3:01–4:00	0	0	0	0	0	0	0	0	0	0	0	0
4:01–5:00	0	0	0	0	0	0	0	0	0	0	0	0
5:01–6:00	0	0	0	3	60	31	40	5	0	0	0	0
6:01–7:00	0	0	0	52	159	82	110	104	26	0	0	0
7:01–8:00	0	0	34	138	225	129	182	177	120	64	5	0
8:01–9:00	17	65	77	225	273	170	244	251	168	156	40	5
9:01–10:00	71	155	140	254	289	241	258	289	218	222	121	48
10:01–11:00	166	195	156	309	299	291	300	312	264	256	167	78
11:01–12:00	196	202	147	306	317	340	318	318	278	288	166	117
12:01–13:00	184	182	215	314	306	306	317	313	280	256	158	137
13:01–14:00	200	159	189	325	319	256	329	376	268	204	149	97
14:01–15:00	136	144	145	312	346	263	305	371	270	182	101	44
15:01–16:00	54	102	112	272	303	237	262	330	240	126	21	0
16:01–17:00	0	18	76	192	280	185	222	240	148	22	0	0
17:01–18:00	0	0	18	84	212	144	166	105	25	0	0	0
18:01–19:00	0	0	0	1	57	56	65	12	0	0	0	0
19:01–20:00	0	0	0	0	0	0	0	0	0	0	0	0
20:01–21:00	0	0	0	0	0	0	0	0	0	0	0	0
21:01–22:00	0	0	0	0	0	0	0	0	0	0	0	0
22:01–23:00	0	0	0	0	0	0	0	0	0	0	0	0
23:01–24:00	0	0	0	0	0	0	0	0	0	0	0	0
Max Hour	14	12	13	14	15	12	14	14	13	12	11*	13
Min Hour	1	1	1	1	1	1	1	1	1	1	1	1

NOTE

1 "Weather Data," *EnergyPlus*, accessed March 5, 2016, https://energyplus.net/weather.

APPENDIX E: SOLAR PROTRACTOR COMPONENTS

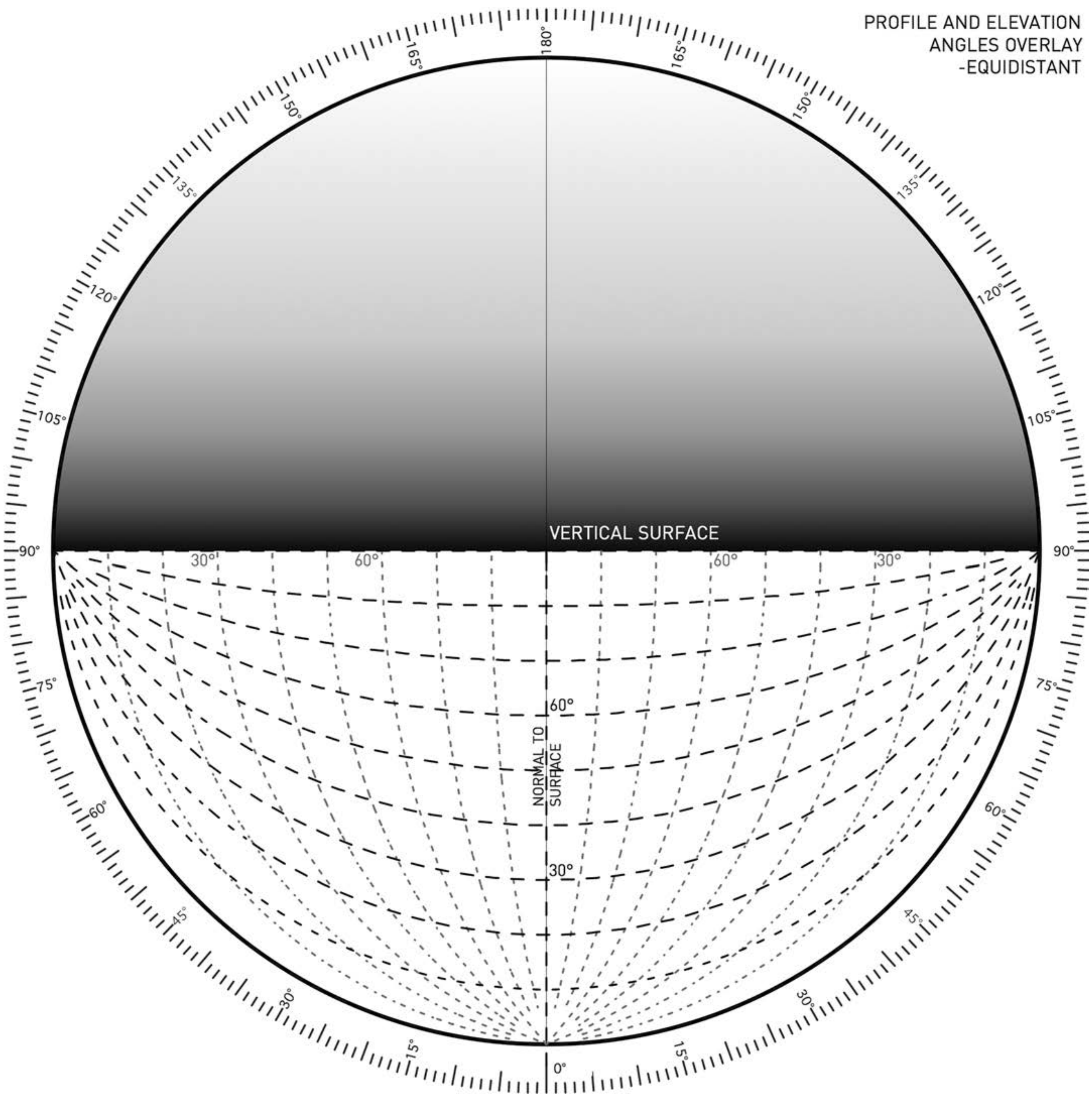

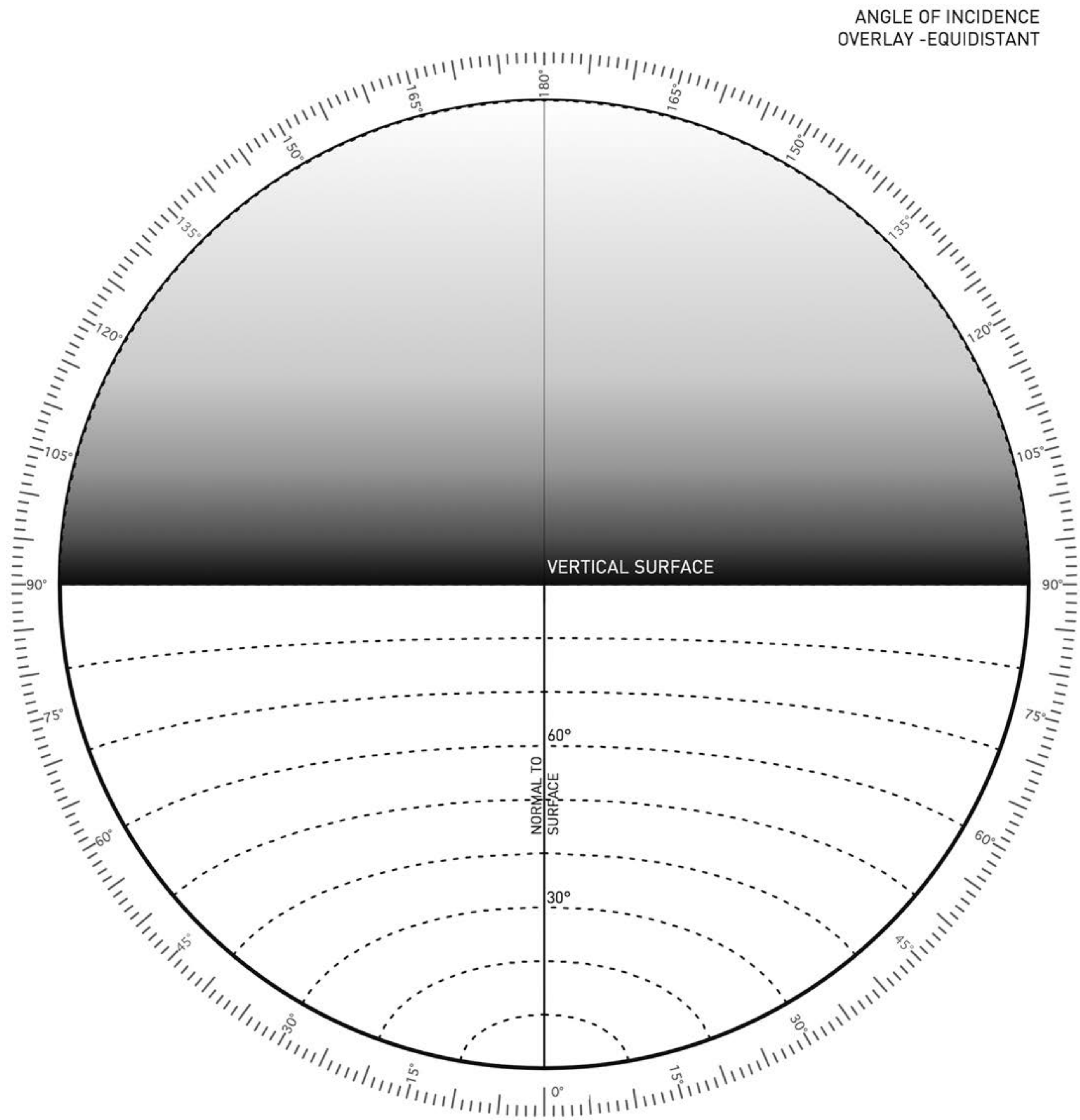
ANGLE OF INCIDENCE
OVERLAY -EQUIDISTANT
180°
165°
150°
135°
120°
105°
90°
75°
60°
45°
30°
15°
0°
VERTICAL SURFACE
NORMAL TO SURFACE
60°
30°

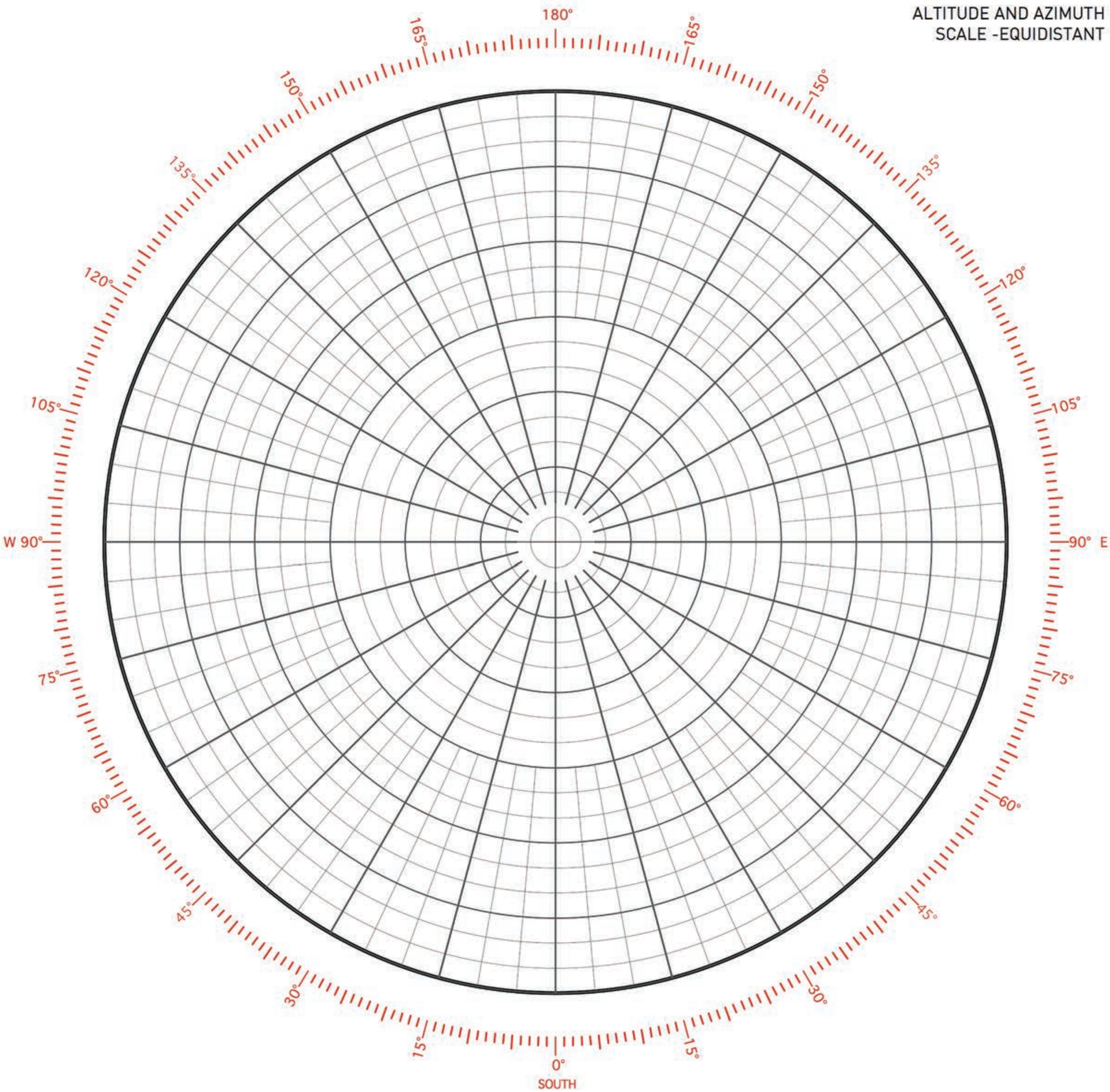
ALTITUDE AND AZIMUTH
SCALE -EQUIDISTANT
180°
165°
150°
135°
120°
105°
W 90°
75°
60°
45°
30°
15°
0°
SOUTH
90° E

EXAMPLE SUN PATH DIAGRAM- 30°N -EQUIDISTANT

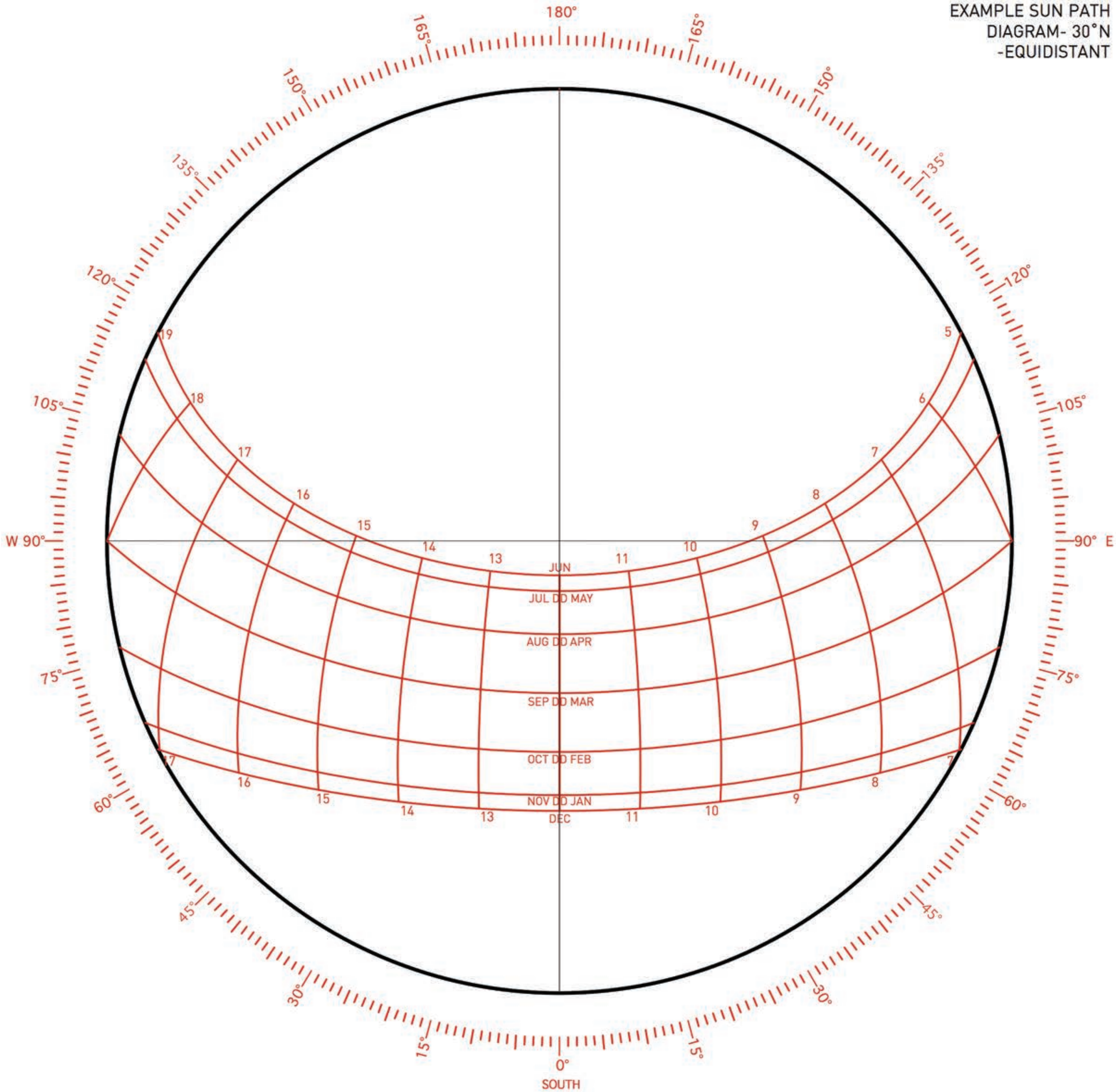

GLOSSARY

12-hour time The system of time-keeping most often used in the United States in which the 24 hours in a day are split into two 12-hour groups distinguished between a.m. and p.m. The abbreviation a.m. comes from Latin ante and post meridiem, literally before and after the sun transits the meridian of a given location. Because of the ambiguity of 12-hour time, we use *24-hour time*.

24-hour time The time-keeping convention in which hours are numbered sequentially 1–24 rather than distinguishing between a.m./p.m. Although 24-hour time is the most commonly used convention worldwide, the United States still primarily relies on 12-hour time. We will use 24-hour time because it eliminates the ambiguity of the 12-hour system. For example, 3:25 p.m. is 15:25 in 24-hour time.

agonic line A magnetic contour line where true north and magnetic north are aligned.

altitude The angle between the ground plane and a point or vector. The true altitude is that angle observed from a viewpoint perpendicular to the azimuth of the vector.

angle of incidence Absolute angle of a vector incident upon a surface relative to the surface's normal vector. Angle of incidence is independent of orientation.

anisotropic sky model Sky diffuse solar radiation models, which display luminance distributed unevenly across a sky dome.

Antarctic Circle The southern parallel of latitude (approx -66.55˚) at which the solar ray strikes the Earth tangent to its surface on either solstice. Within the Antarctic Circle, there are 24 hours of darkness on the June solstice.

antimeridian The meridian at 180˚ of longitude from the prime meridian (0˚) passing through Greenwich, England. When it is solar noon at the prime meridian, it is midnight at the antimeridian. The antimeridian passes through roughly the middle of the Pacific Ocean. Also see *International Date Line*.

aphelion The point in the Earth's orbit around the sun at which it is furthest from the sun, approximately 152.5 million kilometers.

apparent declination See *declination*.

Arctic Circle The northern parallel of latitude (approx 66.55˚) at which the solar ray strikes the Earth tangent to its surface on either solstice. Within the Arctic Circle, there is 24 hours of darkness on the December solstice.

area The true area of a surface as distinct from its projected area.

astrometry The field of astronomy dealing with the positions and motions of celestial bodies.

axial tilt The tilt of the Earth's rotational axis relative to a line perpendicular to the ecliptic plane. This angle is equal to the obliquity of the ecliptic.

azimuth Angle on the ground plane from some reference line to a point of interest. Our convention is that clockwise rotation is positive, counter-clockwise negative.

base reference direction Primary reference direction from which true azimuth angles are measured, notated as 0° azimuth. The base reference direction we use for solar calculations is due south. When using sun path and other analysis diagrams, it is useful to use the direction toward the equator as the reference direction (i.e., 0˚ = north in the southern hemisphere). To do so, subtract 180˚ from all calculated azimuths and plot the revised azimuth relative to the north direction.

British thermal unit The Btu is the standard IP unit of energy. It is the quantity of heat required to raise the temperature of one pound of water one degree Fahrenheit at standard atmospheric pressure. One Btu is approximately equivalent to the energy contained in a wooden match. One Btu could lift a one-pound weight 778 ft.

calendar date orbital angle Value used in calculating extraterrestrial solar radiation and the equation of time. Not to be used for sun position calculations.

Cartesian coordinates This coordinate system locates any point in space by specifying a distance in each of three dimensions (frequently denoted x, y, and z) from the origin point. While solar coordinates are usually given in the *spherical coordinate* system, for certain applications, it is useful to convert to Cartesian coordinates.

celestial sphere In astronomy and navigation, the celestial sphere is an imaginary sphere of arbitrarily large radius, concentric with the Earth and rotating upon the same axis. All objects in the sky can be modeled as projected upon the celestial sphere. Projected upward from Earth's equator and poles are the celestial equator and the celestial poles.

clear-sky radiation The amount of solar radiation a given location would receive under completely clear skies. May be estimated by calculations or measured.

conductance The rate at which heat is transferred by conduction through a surface.

Coordinated Universal Time UTC is the standard time used to coordinate clocks throughout the world. Although there are some subtle differences between UTC and Greenwich Mean Time (GMT), for most practical applications, the two are close enough to be considered interchangeable. UTC standard essentially superseded GMT and should be used whenever possible.

daytime Any time when the sun is above the horizon.

December solstice The precise point in time at which the Earth's rotational axis is at its minimum positive declination. At this time, the northern hemisphere experiences winter, as it is tilted away from the sun, resulting in less direct radiation and shorter days. The day of the December solstice is considered the beginning of winter. Sometimes called the winter solstice, for clarity, December solstice is now the preferred term because it is only the beginning of winter in the northern hemisphere.

decimal hours Time converted to hours and decimal fractions of an hour from hours, minutes, and seconds.

declination The apparent tilt of the Earth's rotational axis at a given time relative to the ecliptic pole. The apparent solar declination, generally referred to simply as declination, represents a change in the apparent tilt of the Earth on its axis relative to the sun and is responsible for the Earth's seasons. In astronomy, an angular distance between a reference line or plane and another line or plane, usually one that changes positions over time. See *magnetic declination*.

design day A representative day of each month at increments of 1/12 of the Earth's orbit around the sun. The solstices and equinoxes are included among these days. Design days roughly coincide with the 21st of each month, but do not necessarily actually fall on that day.

diagram A distorted drawing to make something easier to read, such as an equidistant projection.

diffuse insolation, ground reflected Both diffuse and direct radiation that has struck the ground and been reflected. Ground surfaces tend to be diffuse with the exception of water, which can be highly specular, especially at low sun angles. Twenty percent reflectance is commonly assumed for the ground in the absence of more specific information. In the case of a building located adjacent to a more reflective surface such as snow, ice, water, or white sand, it is important to adjust for the proper reflectance value because it can potentially make a substantial contribution to insolation in these situations.

diffuse radiation Solar radiation that arrives at a surface having been scattered by the atmosphere or other surfaces.

diffuse radiation, sky component The solar radiation scattered in the atmosphere before its arrival on a surface. Under clear-sky conditions, diffuse sky light is due mainly to Rayleigh scattering, while under overcast conditions, the diffusion occurs as sunlight passes through the clouds.

direct beam radiation Solar radiation arriving directly from the sun. This is the portion of the sun's radiation that passes through the atmosphere unobstructed and directly contacts a surface. It is measured normal to the beam and is also known as direct normal or beam normal radiation.

direction cosines Sometimes referred to as sigma values, these are Cartesian coordinates locating the sun's position on the sky dome. The individual direction cosines also indicate relative beam radiation for a surface facing one of the cardinal directions or the zenith.

ecliptic plane The plane on which the Earth and other planets orbit around the sun.

ecliptic pole The point where the imaginary line perpendicular to the ecliptic plane and passing through the center of the Earth intersects the celestial sphere.

effective absorptance of a room cavity The fraction of transmitted radiation that is absorbed within the room cavity. The radiation not absorbed is reflected back out through the windows.

elevation angle A profile angle measured along the line parallel to the surface in question. The elevation angle is often used to determine the required horizontal or vertical length of shading devices.

elevation shading angle The elevation angle of the solar ray on the building surface at the beginning or end of the shading period. The *ESA* determines how long a horizontal shading device must be to fully shade the window. To avoid excessive length of required shading, often, the time period during which shading is required is reduced to the period when the angle of incidence is low enough to be a concern.

ellipse In terms of 3D geometry, an ellipse is a projection of a circle viewed from a vantage point other than normal to its center point.

energy The ability to do work. Power applied over a defined timespan.

equation of time An equation used to calculate the difference between apparent solar time and local standard time at the local meridian each day.

equator The great circle around the Earth equidistant from the poles and perpendicular to the axis of rotation.

equatorial plane The plane on which the equator exists.

equinox The point in time at which the Earth's rotational axis is at 0° declination. If the sun was a point rather than a disc and there was no atmospheric refraction, all locations on Earth would experience precisely 12 hours of day and 12 hours of night on the day of the equinox. Because of these factors, however, the day with actual equal duration of day and night is offset from the equinox by several days.

extraterrestrial radiant flux Extraterrestrial radiation incident on the Earth normal to the solar ray.

geocentric A model of the universe placing the Earth at the center. This was the view of the ancients, disproven by Copernicus, Galileo, and Kepler in the early Renaissance. While the heliocentric model is a better representation of solar system mechanics, for the purposes of solar geometry applications in design, we use a geocentric model. This is because in design, we are concerned about how the sun will impact our building or site, thus we need to know where the sun is at any point in time relative to that point on Earth.

geodesy The branch of geography that studies the measurement and representation of the Earth. This includes geometry, positions, tides, gravitational field, and so on.

global radiation The total radiation incident on a horizontal plane at a given time. Global radiation includes direct, diffuse, and reflected components.

gnomon The shadow-casting element of a sundial or sundial-like structure.

great circle A circle inscribed on a sphere that traces the full circumference of that sphere.

ground plane An imaginary plane tangent to the surface of the Earth at the origin point extending outward to the surface of the sky dome. The ground plane is perceived as horizontal to an observer at the origin point. The zenith direction is always normal to the ground plane.

ground reflected radiation Solar radiation reflected from the ground. Modeled as diffuse.

ground view factor See *view*. The ground view factor is the ratio that describes a surface's exposure to the ground in front of it. This factor affects the quantity of diffuse ground reflected radiation that the surface receives.

heliocentric The model of the solar system placing the sun roughly at the center of the orbits of the planets.

horizontal exposure angle A surface-solar azimuth at the beginning or end of an exposure period. In order to maintain the desired window exposure, a shading device must not encroach beyond the *HEA*. The *HEA* springs off of the outside edges of the window to be exposed.

horizontal shading angle The surface-solar azimuth for the beginning or end of a shading period. The *HSA* springs from the opposite edge of the window; for example, the *HSA* for a fin on the right side of a window springs from the opposite (left) edge of that window.

hour One hour corresponds to 15° of rotation of the Earth on its axis.

hour angle The Earth rotates on its axis 15° each hour to complete one 360° revolution in 24 hours. The hour angle describes the Earth's position in this rotation at a given time. The hour angle is 0° at solar noon, negative in the morning, and positive in the afternoon.

insolation Solar energy incident upon a surface over a specified time period. If the period is one hour, the symbol *I* is used. For the period of a day, use symbol *D*.

International Date Line The politically defined boundary that separates one day from another. Locations west of the line are one day (24 hours) ahead of locations to the east. In geodesic terms, ideally, the International Date Line would correspond with the *antimeridian*, but agreements to adjust the location of the line to avoid the extreme inconvenience of two different dates bisecting one populated area have created jogs and offsets in the alignment of the line. The International Date Line jogs east around the coast of Russia and around several groups of islands in the South Pacific.

isotropic sky model The model of sky diffuse insolation that assumes it is uniformly distributed across the sky dome.

Julian date The Julian date (JD) is the interval of time in days and fractions of a day since January 1, 4713 B.C. Greenwich noon, Julian proleptic calendar. The Julian date is important in astronomical calculations. Solar geometry calculations for practical applications use *ordinal dates* rather than Julian dates.

June solstice The precise point in time at which the Earth's rotational axis is at its maximum positive declination. At this time, the northern hemisphere experiences summer, as it is tilted toward the sun, resulting in more direct radiation and longer days. The day of the June solstice is considered the beginning of summer. Sometimes called the summer solstice, for clarity, June solstice is now the preferred term because it is only the beginning of summer in the northern hemisphere.

latitude The measure of north-south position on the Earth, latitude is the angular distance from the equatorial plane to a point on the surface of the Earth. Latitude ranges from 0° at the equator to 90° at the North Pole and -90° at the South Pole. Lines of latitude are known as parallels.

lines of constant profile angle Usually used as an overlay, a drawing of lines of constant profile angle is an indispensible tool in the use of solar path diagrams. These lines show, relative to a given azimuth, a line upon which any point will have the same *profile angle* relative to that azimuth. This tool is used when drawing projections and designing shading devices.

local standard meridian The reference meridian located at the center of each idealized time zone representing one hour (15°) of the Earth's rotation. The prime meridian is the local standard meridian for UTC ±0.

local standard time The "clock time" in a particular location, not accounting for daylight saving time if it is in effect.

longitude The measure of east-west position on the Earth, longitude is the angular distance on the equatorial plane of a point's meridian from the prime meridian (0˚). Longitude ranges from +180˚ eastward to -180˚ westward. Determining accurate longitudinal positions was a very difficult navigational problem to solve.

longitude time adjustment An adjustment to apparent solar time that accounts for the longitudinal position of a place within its time zone.

magnetic declination The angle at any location between magnetic north and true north. Magnetic declination varies considerably from place to place and also changes as the magnetic pole moves.

magnetic north The direction of the Earth's magnetic pole toward which a compass needle will point. The magnetic pole is currently located in Canada and moves northwest at a rate of around 41 km/year. Magnetic north should not be confused with north or true north.

March equinox The March equinox is considered to be the beginning of spring in the northern hemisphere and fall in the southern hemisphere. Colloquially defined as the day of March 21, the precise date and time of the equinox varies from year to year. Sometimes called the vernal equinox, for clarity, March equinox is now the preferred term because it is only the beginning of spring in the northern hemisphere.

meridian An imaginary semi-circular line starting at one pole, passing through a point of interest, and ending at the other pole. All points on a meridian are at the same longitude. Often referred to as lines of longitude.

meridian of current solar noon The meridian of longitude where the hour angle is 0˚ and solar noon is occurring at a given point in time. This meridian is perpendicular to the terminator line and aligned with the center of the solar disc.

microclimate Climatic conditions in a localized area that differ from the prevailing climate of the area.

minor circle A circle inscribed on a sphere that traces something less than the full circumference of that sphere.

nighttime Any time when the sun is below the horizon.

normal Usually refers to a vector perpendicular to a surface.

normal direction cosine, sigma normal This value is a measure of the projected area of a surface viewed from the position of the sun. It is primarily used as a measure of *relative insolation*.

North Pole The point north of the equator (90˚) where the Earth's rotational axis intersects the surface of the Earth. At the North Pole, the sun rises and sets once per year, creating 24 hours of darkness on the winter side of the equinoxes and 24 hours of light on the summer side.

north, true north North is the direction toward the North Pole along a meridian. Also known as true north, it is important to distinguish from *magnetic north*.

nutation A rocking of the Earth's axis of rotation due to tidal forces.

obliquity of the ecliptic The angle (23.45˚) between the Earth's equatorial plane and the ecliptic plane.

offset The time at which the direct rays of the sun no longer strike a surface. Sometimes referred to as surface sunset.

onset The moment at which the direct rays of the sun first strike a surface. Sometimes referred to as surface sunrise.

orbit The elliptical path of one celestial body around another. Earth's orbit traces an ellipse around the sun with an eccentricity of 0.0167, making it very nearly circular.

orbital angle The angle describing the location of Earth in its orbit at any time. The March equinox is arbitrarily assigned an orbital angle of 0˚.

ordinal date A date specified with a day number resulting from the sequential numbering of days from January 1 through December 31. Generally, solar geometry calculations ignore the year number and use a non-leap year.

orientation The azimuth and altitude of a surface or object.

overshadowing diagram See *sky dome projection*.

parallel (of latitude) In geodesic terms, parallels are lines of constant latitude that encircle the Earth. The equator is a great circle while all other parallels are minor circles, except for the poles, at which 90˚ is a single point.

perihelion The point in the Earth's orbit around the sun at which it is closest to the sun, approximately 147.3 million km.

point of interest A point on an object viewed from the reference point. Its location relative to the reference point may be described with either polar or Cartesian coordinates.

poles The point where the Earth's rotational axis intersects the surface of the Earth. The poles occur at 90˚ north and south latitude.

positive azimuth Clockwise rotation from the reference direction.

power The rate at which work is performed.

precession A change in the orientation of the rotational axis. Earth's axis precesses over a very long period.

prime meridian The meridian passing through Greenwich, England, that, by convention, is defined as 0˚ longitude.

profile A side or sectional view.

profile angle The altitude of a vector or point relative to an arbitrary axis that may differ from the true azimuth of the vector. Most often, the profile angle is taken along the line perpendicular to a surface in question. A profile angle will always be greater than or equal to the true altitude of the vector. Also see *vertical shading angle*.

projected area The apparent area of a surface as viewed from some angle other than normal to the surface. Subscripts are applied to the projected area to indicate the cardinal direction of viewing angle. See also *surface normal vector components*.

projection A true geometrically constructed view of some object. A method of drawing something from another viewpoint.

radiation The transfer of energy by electromagnetic waves.

Rayleigh scattering The scattering of light by particles smaller than the wavelength of the radiation. The sky appears blue because this scattering is more pronounced at the shorter wavelengths of the visible spectrum. Conversely, the sun appears yellowish because the longer wavelengths have not been diffused as much.

reference axis A user-defined axis about which measurements are made.

reference point, origin The point of observation on Earth where the sky dome is placed.

relative beam radiation The ratio of the insolation received by a surface at a given time to the amount it would receive if the surface were aligned normal to the sun position at that time. Multiplying relative beam radiation by the surface area gives the projected area of the surface relative to the position of the sun.

relative diffuse radiation The ratio of diffuse radiation incident on a surface to the total available diffuse radiation at a given time.

shade The apparent darkness of an area out of direct view of the sun, usually in contrast to visible sunlight striking surfaces nearby.

shading mask A diagram expressing shading and exposure criteria or generalized shading performance on a sky dome projection.

shadow The projected shape of an object onto another along the ray of a light source.

shadow study An analysis of a site or proposed design showing how shadows are cast on significant dates.

sky dome An imaginary hemispherical dome centered on a *reference point* used to model solar and terrestrial geometry. Solar geometry works such that the sun's movement appears to trace a path across this dome. We can also project the positions of objects on the surface of the Earth onto the sky dome in order to compare their locations with the sun position at a given time. The sky dome includes all solar positions above the horizon (daytime). The concept could be extended to a sphere to model solar positions relative to the reference point when the sun is below the horizon. The sky dome is similar to the *celestial sphere* concept used in astrometry; however, the sky dome is centered on a reference point on Earth rather than the center of the Earth. The geometric differences relative to celestial geometry are, for our purposes, irrelevant; however, the differences for projections of objects located on the Earth's surface are important.

sky dome projection A projection onto the sky dome of the geometry of objects surrounding the reference point.

sky view factor See *view*. The sky view factor is the ratio that describes a surface's exposure to the sky. This factor affects the quantity of diffuse sky radiation that the surface receives.

solar altitude The true altitude of the sun's position at a point in time.

solar azimuth Angular distance on the ground plane from due south to the sun's position.

solar day The period from solar noon to solar noon.

solar declination See *declination*.

solar heat gain coefficient The fraction of incident solar heat transmitted through glazing. *SHGC* includes both direct transmission and the inward-flowing fraction of absorbed radiation. The solar heat gain coefficient is given at a normal angle of incidence and must be adjusted for other angles of incidence as well as for diffuse radiation.

solar irradiance (without subscript refers to global) Rate at which solar radiation is incident on a surface.

solar irradiation See *insolation*.

solar noon The time at which the sun transits (crosses) the meridian of a given location. On Earth, this translates to the time at which the sun is located precisely in the direction of the equator—south in the northern hemisphere, north in the southern hemisphere.

solar path band The strip of spherical grid across the sky dome created by the sun paths for design days and hours. The width of the solar path band is equal to two times the obliquity of the ecliptic (46.90˚). Changes in latitude of the reference point of the sky dome cause the solar path band to rotate across the sky dome, but the date and hour lines always maintain the same relationships to one another. Therefore, if one remembers that the latitude is equal to the zenith angle at solar noon on the equinox, one can mentally position the center of the solar path band at that angle and instantly visualize the approximate solar position for any date and time during the year.

solar radiation The electromagnetic radiation emitted by the sun.

solar ray The vector that connects the sun's position on the sky dome to the origin at a given time.

solar time, apparent solar time Solar time is the timekeeping convention where noon is always defined as the time at which the sun transits the local meridian and solar position is symmetrical at approximately noon. See also *solar noon*. Solar time varies from the time kept by clocks due to a number of factors. See also *local standard time*.

solar vector envelope (solar beam envelope) The imaginary surface modeled by the sweep of the solar ray throughout the course of a day. This envelope is conical on any day except the equinoxes, when it is flat. From the point of view of an observer looking across the origin of the sky dome toward the equator, the conical surface is concave in summer and convex in winter.

solar view Parallel line projection of a scene from the point of view of the sun.

solar year The time it takes for the Earth to complete one 360˚ orbit around the sun, or 365.24 days.

solstice The point in time when the Earth's rotational axis is at its maximum or minimum declination relative to the ecliptic pole.

South Pole The point south of the equator (-90˚) where the Earth's rotational axis intersects the surface of the Earth. At the South Pole, the sun rises and sets once per year, creating 24 hours of darkness on the winter side of the equinoxes and 24 hours of light on the summer side.

specular reflection Reflection such as that from a mirror where incoming rays are reflected at an angle equal to the angle of incidence. In most architectural applications, insolation due to specular reflection is not a major contributor with the most frequent exception being surfaces adjacent to mirrored glass fenestration.

spherical coordinates A coordinate system by which any point in space can be specified using angular coordinates (azimuth and altitude) and a radius. In solar geometry applications, the radius used is always a dimensionless unit of "1," locating all points on the sky dome. Therefore, in this context, only the azimuth and altitude need to be specified to locate any vector in space.

spiral solar path The actual path of the sun traces a spiral around the sky dome back and forth between the solstices when declination is at its maximum and minimum. In practice, the spiraling that occurs between morning and afternoon in a single day is negligible from an architectural perspective. Therefore, we model the path of the sun on a given day as an arc symmetrical at approximately noon instead of a segment of a spiral.

sun-path diagram A plan-view projection diagram showing the path of the sun on representative days of the year.

sunrise The moment in time at which the center of the solar disc transits from below to above the ground plane.

sunset The moment in time at which the center of the solar disc transits from above to below the ground plane.

surface azimuth, bearing Azimuth of a *surface's normal vector* relative to the base reference direction.

surface global insolation The total radiation incident on a surface of arbitrary orientation at a given time, including direct, diffuse, and reflected components.

surface normal altitude The altitude of a *surface normal vector*.

surface normal vector An imaginary line perpendicular to a surface extending outward usually from its center. Such a vector is modeled as if it begins at the origin and extends to the surface of the sky dome.

surface normal vector components Rectangular coordinates locating the end of a surface normal vector on the sky dome.

surface-solar azimuth Azimuth of the sun's position relative to the normal vector of a surface. Some sources refer to the surface-solar azimuth as the *horizontal shading angle*.

terminator line The line around the Earth that divides night from day. For our purposes, the terminator is the great circle around the Earth perpendicular to the solar ray. Assuming the sun's rays are parallel, they would be striking the surface of the Earth tangent at the terminator line. In fact, the terminator line is somewhat fuzzy and slightly more of the Earth is in daylight than darkness at any given time due to bending sunlight by the atmosphere.

tilt angle Angle of a surface plane upward from the ground plane. The tilt angle is equal to the zenith angle of the *surface normal*.

time zone In order to standardize time from place to place, time zones have been established to create regions where the time is uniform. This uniform time is known as *local standard time*. Idealized time zones representing one hour increments would occur every 15° of longitude. Such idealized time zones are represented by the *local standard meridian*. Socio-political decisions have established different boundaries for time zones with the result that any given time zone may have boundaries that vary greatly from the idealized 7.5° range on either side of the standard meridian. Time zones are designated by the number of hours they are offset from UTC, which is the time at the prime meridian. Example: Austin, Texas, is located in the time zone UTC -6. Therefore, when the UTC time is 14:00, it is 8:00 in Austin.

total solar irradiance Formerly referred to as the solar constant, *TSI* is the power of solar radiation incident upon the Earth's atmosphere normal to the sun at the mean sun-Earth distance of 1.495 x 10^{11} m. Estimates have varied over time, but 1,360 W/m^2 (431 Btu/ft^2 hr) is the currently accepted value. The power of radiation arriving at the surface of the Earth will in all cases be less than *TSI* due to atmospheric attenuation.

transit To cross.

transmittance The fraction of incident solar radiation transmitted through a transparent or translucent material at a given angle of incidence.

Tropic of Cancer The parallel of latitude at which the solar ray strikes the Earth normal to its surface on the June solstice when the Earth is at its maximum apparent declination.

Tropic of Capricorn The parallel of latitude at which the solar ray strikes the Earth normal to its surface on the December solstice when the Earth is at its minimum apparent declination.

U factor (U value) Conductance of an assembly including air films.

vector A line with a specific origin and endpoint describing a particular orientation in space. Solar and surface normal vectors are always described as originating at the reference point of the sky dome and terminating on the surface of the sky dome. Vector positions may be described with polar or Cartesian coordinates.

vertical exposure angle A profile angle used in shading design that represents the maximum elevation of the sun relative to a surface during the exposure period. In order to maintain the desired window exposure, a shading device must not encroach beyond the *VEA*.

vertical shading angle Also see *profile angle*. The profile angle of the solar ray relative to a building surface. This angle is the lowest elevation of the sun relative to a surface during the shading period. To meet the shading criteria, this angle, which springs from the sill of the window, must be obstructed by a shading device.

view In physical terms, a view is the unobstructed solid angular area by which one object is exposed to another.

visible transmittance The fraction of the total solar radiation in the visible spectrum transmitted by a fenestration product.

winter funnel The solid angular area within which nothing can encroach to maintain full exposure of a window in a desired period of time. The winter funnel is precisely defined by sweeping the solar vector cone for the exposure period around the perimeter of a window. The outermost envelope of this sweep is the winter funnel. The *VEA* and $HEA_{am/pm}$ are often used to create a simple approximation of the winter funnel.

zenith angle Angle of a vector from the vertical direction toward the ground plane.

zenith direction Straight up. The line from the center of the Earth, through the reference point, extending straight out into space.

INDEX

Note: Page numbers in italic indicate a figure and page numbers in bold indicate a table on the corresponding page.

absorptance: defined 202; effective cavity absorptance 202–203, **222**
air flow, shading and 179
Akhenaton 2
albedo 109, 201–202
Albers, Josef 208–209
altitude: defined 43; of a point 147; solar protractor overlay *272*; surface normal altitude 99; zenith and altitude angle relationship 44, **219**
Amarna art style, solar rays depicted in 2–3, *3*
analemma 30, *31*
Anasazi Indians 181
Ando, Tadao 126
angle of incidence: calculation of 101, **221**; glass transmittance at 200, *200*; shading design and 158–159, *158*, *159*; solar protractor overlay *159*, *271*
anisotropic sky factor 108, **221**
anisotropic sky model 107–108
Antarctic Circle 36, 40
antimeridian 18
aphelion **19**
apparent declination *see* declination
apparent solar time (AST): calculation of spherical coordinates from 45, *45*; conversion from local standard time 31, **219**; conversion to local time 34; defined 24–25; equation of time 30, *30*
arbitrarily tilted surfaces, calculation of offset for 102–103, **221**
architectural renderings 211
Arctic Circle 36, 40
Aristarchus 4
Aristotle 3–4, 39
astronomical units 11
azimuth: defined 43; determining 55; surface-solar azimuth 101, **221**; *see also* solar azimuth
balance point 156–157
Barcelona, Spain: Museum of Contemporary Art *154*; street layouts in 71, *71*, *72*
beam radiation 80; defined 103–104; on horizontal plane 106–107, **221**; relative 104–105, *106*; surface direct 105–106, **221**
bearing 99
Boubekri, Mohamed 207
building envelopes 182
building orientation, insolation and 119–121, *120*

calculated clear-sky radiation 91–95; global average amount of cloud cover *92*; global frequency of completely clear skies *91*; irradiance data for clear-sky calculations **93**
calendar date orbital angle: calculation of 30–31, **219**
calendar dates, conversion to ordinal dates 15
cardo 69
Carpenter, James 182
Cartesian coordinates *49*; calculation of relative beam radiation with 104–105, **221**; direction cosines 49–51, *50*; influence on architecture 71–72; Pythagorean check of 51; solar table for **51**
cavity absorptance 202–203, **222**
Cezanne, Paul 210
chromosphere *12*
circles: great 16, 41; minor 17, 41
city planning, sunlight and 68–73, *69*, *71*, *72*, *73*
clear day hourly direct beam insolation 93, **220**
clear day hourly sky diffuse insolation 94, **221**
clear-sky insolation trends *114–115*
clear-sky radiation: calculated 91; equations for 91–94, **220**; global average amount of cloud cover *92*; global clear-sky insolation trends *114–115*, 116; global frequency of completely clear skies *91*; illuminance diagrams for *185–197*; irradiance data for clear-sky calculations **93**; solar tables for **95**, **224–263**; total global horizontal insolation by latitude *93*; typical radiation values compared to 119, *119*
climate change data 82–83
Climate Consultant 84, 157, *158*
climate criteria 157, *158*
clock time 33–34
cloud cover 91–92, *92*, *185–197*; *see also* clear-sky radiation
color, light and 208–210
commodification of light 9–10
complex shadow-casting 131–132, *131*
composite shadow studies 135–137, *137*
conduction 199
convection 199
coordinated universal time (UTC) 26
Copernicus, Nicolaus 4
corona *12*
crepuscular rays 183
Cubism 210
cylindrical projections *63*, **220**; coordinates for 63–64; modified cylindrical projections 64–65, *64*, **220**

daily total insolation: calculation of 112–113, **113**, **222**; direct beam insolation 80, 106; ground reflected diffuse insolation 81; sky diffuse insolation 80
daily total radiation 78, 112–113, **113**, **222**
data collection for solar radiation 82
date lines 41

daylight autonomy 199
"daylight factor" 183, *184–198*
Daylighting, Architecture, and Health (Boubekri) 207
daylight savings time (DST) 33–34, **33**, **219**
days: apparent solar time 24–25; design days 16; hour angle 25–26, *25*, **219**; solar declination 34–36, *35*, **219**; terminator line 24, *24*; zenith angle 36–38, *36*, *37*, **219**; *see also* standard time
December solstice: shadow studies for 135–137, *137*
declination: calculation of 35–36, **219**; defined 34; at hour rise 49, **220**; at key dates *35*
decumanus 69
Descartes, René 5–6, *5*, 71
design days/months 16; *see also* solar position coordinate tables
detached shades 165
diagrams: illuminance diagrams *184–198*; *see also* sky dome projections; sun-path diagrams
diameter of sun **19**
dielectric properties of glass *158*
diffuse radiation 80, 107–109
diffuse sky insolation *see* sky diffuse insolation
diffuse solar gain through partially shaded windows 204, *205*
direct beam gain through partially shaded windows 204, *205*
direct beam insolation 80, 90, 96, 105–106, **220–221**
direct beam irradiance 80, **220**
direction cosines: calculation of 50, **220**; defined 49
distances **19**
Duvall, Robert 9, *9*

Eames, Charles 11
Eames, Ray 11
earth's orbit 12–13
Earth-sun relationship 23–24; geodesy 16–23, *16*, *20*, **21**, *22*; geometry 23–24, *23*; planetary orbits 12–16, **14**, *14*; sun characteristics 11–12, *11*, *12*; *see also* days
ecliptic plane 23, *23*
ecliptic pole 23, 35
Ecotect Analysis software 149
effective cavity absorptance 202–203, **222**
Einstein, Albert 6
electromagnetic spectrum 73
elevation angles: calculation of 128–130, *129*, **222**; solar protractor overlay *159*, *270*
elevation shading angle (ESA) 161
Eliasson, Olafur 211–212
ellipses: meridians 18; planetary orbits 5; profile and elevation angle curves 129; sky dome projections 142
energy: power versus 77
EnergyPlus Weather Data for Simulation 83–84, 88
epicycles 4
equation of time (ET) 30–32, *30*, **219**
equations, table of **219–222**
equator 16
equator-facing solar controls 166–170, *168*, *169*, *170*
equatorial plane 16
equidistant solar protractor *144*, *145*
equidistant sun-path diagrams 59–62, *59*, *61*, **220**
equinox: March 13, *14*, 16; September *14*; zenith angle at solar noon on 36, **219**
Eratosthenes 127
estimated hourly global horizontal insolation from daily total 90, **220**
estimated hourly sky diffuse insolation from daily value 86–87, **220**
estimate of hemispherical diffuse transmittance 201, **222**
ether 5–6
exposure angles 161, 164
exposure criteria: angle of incidence 158–159, *158*, *159*; balance point 156–157; climate 157, *158*; setting 159; *see also* shading
extraterrestrial radiant flux 75–76, **220**
extraterrestrial solar radiation *76*; extraterrestrial radiant flux 75–77, **220**; power versus energy 77–78, **77**
The Eyes of the Skin (Pallasmaa) 7

fascade glazing *see* glazing
fenestration: cavity absorptance 201–203, **222**; daylight autonomy 199; illuminance diagrams for *184–198*; light filtration 183; solar gain through shaded or partially shaded windows 204, *205*; solar gain through unshaded windows 201, **222**; solar heat gain coefficient (SHGC) 199–201, **222**; thermal qualities and 181–182; translucency 182–183; transparency 182
Fine Arts, use of light in 211–213
fins, vertical 164–165

Galilei, Galileo 4–5
genius loci 152
geocentric model 4, 39–40; *see also* sky dome concept; sun-path diagrams
geodesic grid 16–19, *16*
geodesy: geodesic grid 16–19, *16*; magnetic declination 19–23, *20*, **21**, *22*
geometry of Earth 23–24, *23*
glass *see* glazing
glazing 199–201; cavity absorptance 201–203; daylight autonomy 199; glass transmittance at arbitrary angle of incidence 200, *200*, **222**; illuminance diagrams for *184–198*; light filtration 183; solar gain through shaded or partially shaded windows 204, *205*; solar gain through unshaded windows 201, **222**; solar heat gain coefficient (SHGC) 199–201, **222**; thermal qualities and 181–182; translucency 182–183; transparency 182; *see also* fenestration; shading
global daily total statistical data 88–90, **89**
global horizontal insolation 111, **222**
global radiation 81
gnomon 24, 66
great circles 16, 41
Greenwich Mean Time (GMT) 26
ground reflected radiation: calculation of 109–111, **110**; defined 81
ground view factor: calculation of 111, **222**

health, daylight and 207–208
heliocentric model: historical perspective of 4–6, 39
heliodon 41, *42*
hemispherical diffuse transmittance, estimate of 201, **222**
Heschong, Lisa 181–182
historical perspectives on light: city planning 68–73; Egyptian depictions 2–3; geocentric model 4; heliocentric model 4–6; shadows 123–127, *124*, *125*; wave theory 6–7
historical weather data 83
Holl, Steven 212–213
Hong Kong, Walled City of Kowloon 8–9, *8*, *9*
hoods 165
Hopper, Edward 210–211
horizontal exposure angle (HEA) 164
horizontal overhangs: shading geometries 164, *164*; solar gain through 204, *205*
horizontal planes, beam radiation on 106–107, **221**
horizontal shading angle (HSA) 164
horizontal sun-path diagrams 53–59; reference points 55; spherical projections *54*, 55–59, *55*, *57*, *58*
hour angle: calculation of 26, 47, **219**; defined 25, *25*; relationship with local standard meridians *29*; at sunset 47, **219**

hour lines 41, 49, *52*, 53, 58
hourly beam insolation: direct beam insolation 80; from global horizontal and sky diffuse 90, **220**; on the horizontal 107, 221; on surface **221**
hourly diffuse solar gain through window 201, **222**
hourly direct beam solar gain through window 201, **222**
hourly fraction of global insolation 88, 90, **220**
hourly fraction of sky diffuse insolation 86–87, **220**
hourly global ratio coefficient A 88, **220**
hourly global ratio coefficient B 88, **220**
hourly ground reflected diffuse insolation 81
hourly horizontal beam insolation 107, **221**
hourly irradiation 77–78
hourly sky diffuse insolation 80, 108–109, **221**
hour rise, solar declination at 49, **220**
hours *see also* hour angle; hour lines
Huygens, Christian 6

illuminance diagrams *184–198*
incidence, angle of: calculation of 101, **221**; glass transmittance at 200, *200*; shading design and 158–159, *158*, *159*; solar protractor overlay *159*, *271*
insolation: building orientation and 119–121, *120*; clear day values 93–94, **220**; clear-sky trends *114–115*, 116; daily total 80–81, 106, 112–113, **113**, **222**; defined 74, 76–77; diffuse sky **221**; direct beam 80, 90, 105–106, **220–221**; estimating from solar radiation data 96; global 88–90, **220**; ground reflected 109–111, **110**, **222**; impact of shading on *176*, 177; local patterns 116–117, *117*; orientation and 119–121, *120*; power versus energy 77–78, **77**; sky diffuse 86, 94, 96, 108, **220–221**; solar tables for **224–263**; surface global 111–112, 173–177, **174–175**, **222**; *see also* solar radiation
instantaneous irradiance 77
International Date Line 27
International Style 208
irradiance *see* solar irradiance
irradiation *see* insolation
Islamic houses, structure of *70*
isotropic sky model 107–108

Jeanneret, Charles-Édouard *see* Le Corbusier

Kahn, Louis 124–125, *125*, 211
Kepler, Johannes 5
Kowloon, Walled City of 8–9, *8*, *9*
Kwan, Leung Ping 8–9
Kwinter, Sanford 212

Larsen, Henning 98
latitude: construction of *17*; defined 17; example of *18*; illuminance diagrams for *185–197*; shading strategies by 177–178
Le Corbusier 1, 212
Levins, Gail 210
Libby Owens Ford Glass Company 59
Light in Architecture (Vergés) 183
light perception theory 5–6
local insolation patterns 116–117, *117*
local standard meridians (LSM): calculation of 28, **219**; defined 26; relationship with hour angle *29*
local standard time (LST): apparent solar time calculation from 31–32, **219**; conversion from apparent solar time 34; conversion to daylight savings time 33, **33**; defined 26, 28; spherical coordinates calculation from 46, *46*
location of shadow on horizontal plane 132, **222**
Locke, John 152
loco-centric model *see* geocentric model
longitude: construction of *17*; defined 17; example of *18*; time adjustment 28–30, *29*, **219**
louvers 165
Ludlum, Robert 8–9

magnetic declination 19–23, *20*, **21**, *22*
magnetic north 19
Malton, Thomas *153*
March equinox 13, *14*, 16
Marden, Brice 209–210
masks *see* shading masks
mathematical symbols **216–217**
mean time 30
Mercator map 53
meridians: antimeridian 18; defined 17; prime 18; *see also* local standard meridians (LSM)
microclimates 134–135; solar site analysis 135–138, *136–137*; *see also* sky dome projections
Middle Eastern settlements 68–69, *69*, *70*
Mies van der Rohe, Ludwig 182
minimum solar shade geometry 160, *161*
minor circles 17, 41
"The Miracle in the Cave" (Saenredam) 123, *124*
modified cylindrical projections 64–65, *64*, **220**
Moonlight Towers 212
multi-sensory architecture 7
Museum of Contemporary Art Barcelona *154*

nadir 42, 61
National Renewable Energy Laboratory 88
National Solar Radiation Database Typical Meteorological Year 3 (TMY3) files 83
net solar gain 203, **222**
Newton, Isaac 6
north: magnetic 19; true 19–23
North Pole 13, 16–17
North Star 24
nutation 23

obliquity of the ecliptic 23
offset 101
onset 101
operable shading controls 165
orbital angle 13–16, *14*, **219**
orbits *see* planetary orbits
ordinal dates 13–15, **14**
orientation: insolation and 119–121, *120*
origin 43, 55
orthographic projections *see* spherical projections
overhangs: horizontal 164, *164*; solar gain through 204, *205*
overshadowing diagrams *see* sky dome projections

Pallasmaa, Juhani 7
parallels 17
Parthenon 124
perihelion **19**
phenomenology, light and 207–213
photoelectric effect 7
Pilkington Glass Company 59
Pilkington Sun Angle Calculator (PSAC) 143, *143*
planetary orbits: design days/months 16; earth's orbit 12–13; orbital angle 13–16, *14*, **219**; ordinal dates 13–15, **14**
Plank, Max 6
Plato 123
points: altitude or profile angles of 147, **222**; point of interest 17, 43
Polaris 24
poles 16
Pole Star 24
Pollock, Jackson 210
polycarbonate panels 183
Powers of Ten 11
precession 23
prime meridian 18
profile *see also* profile angles
profile angles: calculation of 128–130, *129*, *130*, **222**; of a point 147, **222**; solar protractor overlay *159*, *270*
projections: construction of *54*; cylindrical 63–64, *63*, **220**; defined

53; gnomonic 66; modified cylindrical 64–65, *64*, **220**; radial 53; spherical 55–59, *55*, *57*, *58*; stereographic 61–62, *61*, **220**; vertical equidistant 65, *65*
protractors, solar *see* solar protractors
Ptolemaic model 39
Ptolemy, Claudius 4
pyranometers 82
pyroheliometers 82
Pythagorean checks: of Cartesian coordinates 51, **220**; for normal vector components 100, **221**

quanta 6
quantum theory 6

radial projections 53
radiation *see* solar radiation
Rayeigh scattering 80
reduction of air flow, shading and 179
reference axis 142
reference points 55
reflectance, shading and 179
reflected radiation 81; albedo 202–203; ground reflected radiation 81, 109–111, **110**
relative beam radiation: calculation of 104–105, *106*, **221**; on the horizontal 106, **221**
The Republic (Plato) 123
ribbon windows 208
right ascension 34
"right to light" 9–10
Roman city layouts 69–71

Saenredam, Pieter 123, *124*
September equinox *14*
shade *see also* shading
shading: angle of incidence 158–159, *158*, *159*; balance point 156–157; climate 157, *158*; criteria for 156–159, *158*, *159*; design considerations for 179; elevation angles **222**; equator-facing solar controls 166–170, *168*, *169*, *170*; fenestration and 183; genius loci and 152, *153*, *154*; geometry of 155; impact on insolation of windows *176*, 177; by latitude 177–178; profile angles **222**; setting 159; shading device geometry 160–166, *161*, *162–163*, *164*; shadow coordinates **222**; solar gain through 204, *205*; solar vector envelope 155–156, *155*; strategies by latitude 177–178; surface insolation and solar gain analysis 173–177, **174–175**; windows of any orientation 171–173, *171*, *172*, *173*; winter funnels 159, *160*; *see also* shadows
shading and exposure angles 161, 164
shading device geometry: minimum solar shade geometry 160, *161*; shading and exposure angles 161, 164; shading geometries 164–166, *164*; shading masks 160–161, *162–163*, *167*, *171*
shading geometries 164–166, *164*
shading masks 160–161, *162–163*, *167*, *171*
shadows: complex shadow-casting 131–132, *131*; constructing 128; elevation angles 128–130, *129*; geometry of 127, *127*, *128*; historical perspectives on 123–127, *124*, *125*; profile angles 128–130, *129*, *130*; shadow coordinates 132–133; shadow studies 135–137, *137*; solar views and 128, *128*; *see also* shading
sigma values *see* direction cosines
sky diffuse insolation: cause of 80; clear day hourly 94, **221**; common scenarios 96; estimated hourly 86, **220**; hourly fraction of 86, **220**; on a surface 108, **221**
sky diffuse radiation: anisotropic sky model 107–108; isotropic sky model 107–108
sky dome concept 40–41, *41*; Cartesian coordinates 49–51, *49*, *50*, **51**; solar path band 41–43, *43*; spherical coordinates 43–47, *44*, *45*; sunrise 47–49; sunset 47–49
sky dome projections: construction of *141*, 145–149, *146*, **147**, *148*; geometry of 142; solar microclimate analysis with 149–151, *150*, *151*; Solar Pathfinder 139–142, *140*
sky sphere *see* sky dome concept
sky view factor: calculation of 107, **221**
Snell, Willebrord 5
Snell's Law 5
solar altitude 43
solar azimuth: calculation of 45, 48, **219**, **220**; defined 43; finding 55; at sunset 48, **220**
solar constant 75
solar declination: calculation of 35–36, **219**; defined 34; at hour rise 49, **220**; at key dates *35*
solar gain: analysis 173–177, **174–175**; cavity absorptance and 201–203; net solar gain 203, **222**; solar heat gain coefficient 199–201, **222**; through shaded or partially shaded windows 204, *205*; through unshaded windows 201, **222**
solar heat gain coefficient (SHGC) 199–201, **222**
solar irradiance 74
solar irradiation *see* insolation
solar microclimate *see* microclimates
solar noon: defined 24; zenith angle at 36, *37*, **219**
solar orbital angle 31, **219**
solar path band 41–43, *43*
Solar Pathfinder 139–142, *140*
solar position coordinate tables **224–263**
solar power 67–68
solar protractors 142–145; altitude and azimuth scale *272*; angle of incidence overlay *159*, *271*; equidistant solar protractor *144*, *145*; example sun path diagram *273*; Pilkington Sun Angle Calculator (PSAC) 143, *143*; profile and elevation angles overlay *159*, *270*
solar radiation: beam radiation 80, 103–107, *106*, **221**; daily total radiation 78, 112–113, **113**, **222**; defined 199; diffuse radiation 80, 107–109; estimating surface insolation with 96; extraterrestrial solar radiation 75–78, *76*, **77**, **220**; global radiation 81; ground reflected radiation 81, 109–111, **110**; perception of 81; properties of 73–75, *74*; relative beam radiation 104–105, 106, *106*, **221**; solar irradiance 74; spectrum of *75*; surface global radiation 111–112, **222**; terrestrial solar radiation 78–79, *78*, *79*; *see also* clear-sky radiation; insolation; solar gain; solar radiation data
solar radiation data: climate change data 82–83; collection of 82; global daily total statistical data 88–90, **89**; historical weather data 83; statistical summary data 84–88, **85**, *86*, *87*; weather data files 83–84; *see also* clear-sky radiation
Solar Radiation Data Manual (SRDM) 88
solar rays 43
solar site analysis 135; shadow studies 135–137, *137*; solar views 138, *138*
solar system models: heliocentric 4–6, 39; Ptolemaic 4; *see also* geocentric model
solar time *see* apparent solar time (AST)
solar vector 43
solar vector envelope 155–156, *155*
solar views 128, *128*, 138, *138*
solar year 12
solar zoning legislation 207–208
south direction cosine 50, **220**
south normal vector component 100, **221**
South Pole 16–17
spherical coordinates *44*; calculation of 43–47, *45*; solar table for *51*; surface-solar transformation using 101

spherical projections 55–59, *55*, *57*, *58*
spiral solar path 41, 43
standard time: clock time 33–34; coordinated universal time 26; daylight savings time 33–34, **33**, **219**; equation of time 30–32, *30*, *31*, **219**; International Date Line 27; local standard meridians 26, 28, *29*, **219**; longitude time adjustment 28–30, *29*, **219**; time zones 26–27, *27*; *see also* local standard time (LST)
.stat files 88
statistical summary radiation files 84–88, **85**, *86*, *87*, **264–269**
stereographic projections 61–62, *61*, **220**
structural steel 192
subscript symbols **217–218**
Sun Angle Calculator 59
sun characteristics 11–12, *11*, *12*
sun-path diagrams: contents of 52–53; declination at hour rise for 49; equidistant 59–61, *59*; example of *273*; horizontal 53–59, *54*; vertical 62–66; *see also* projections
sun position *see* spherical coordinates; sun-path diagrams
sunrise 47–49; *see also* onset
sunset 47–49; *see also* offset
surface altitude 99
surface azimuth 99
surface direct beam radiation 105–106, **221**
surface geometry: onset/offset 101–103; surface normal vectors 98–100, *99*; surface-solar transformation using spherical coordinates 101
surface global radiation 111–112, **222**
surface insolation 173–177, **174–175**; estimating from solar radiation data 96
surface normal vectors: calculation of 98–100, *99*
surface-solar azimuth: calculation of 101, **221**
surface-solar transformation using spherical coordinates 101
surface sunrise *see* onset
surface sunset *see* offset
surface tilt 99
sustainability, sunlight and 1
symbolic value of light 210–211
symbols: mathematical **216–217**; subscript **217–218**

terminator line 24, *24*
terrestrial solar radiation 78–79, *78*, *79*
thermal bridging 179
Thermal Delight in Architecture (Heschong) 181
thermal mass 179
Thubian 24
THX 1138 9–10, *9*
tilt angle 99
tilted surface facing equator, calculation of offset for 102, **221**
time zones (TZ) 26–27, *27*
topics, shading strategies for 178
total solar irradiance 75
transit of sun 24, 43
translucency 182–183
transmittance: hemispherical diffuse transmittance 201, **222**; transmittance value by angle of incidence 200, *200*, **222**; visible 199
transparency 182
transposition of sunposition to arbitrary surface-sigma X component 132, **222**
transposition of sunposition to arbitrary surface-sigma Y component 132, **222**
"Treatise on Perspective" (Malton) *153*
trees, as shading elements 165–166
true north 19–23
Turrell, James 211

ultraviolet (UV) rays 6
United States Department of Energy 83
unshaded windows, solar gain through 201
Upanishad, Taittiriya 67
UTC *see* coordinated universal time (UTC)

vertical equidistant projections 65, *65*
vertical exposure angle (VEA) 164
vertical fins 164–165
vertical shading angle (VSA) 161
vertical sun-path diagrams 62–63; cylindrical projections 63–64, *63*, **220**; gnomonic projections 66; modified cylindrical projections 64–65, *64*, **220**; solar protractors 142–145, *143*, *144*, *145*; vertical equidistant projections 65, *65*; Waldram diagrams 65
views: ground view factor 111, **222**; shading and 179
visible transmittance (VT) 199; *see also* transmittance
vitamin D 207–208

Waldman, Gary 2
Waldram diagrams 65
Walled City of Kowloon 8–9, *8*, *9*
wave theory 6–7
weather data files 83–84
Weather Project (Eliasson) 211–212
west direction cosine 50, **220**
west normal vector component 100, **221**
White Light (Pollock) 210
windows *see* fenestration; shading
winter funnels 159, *160*

X-coordinates: for cylindrical projections 63–64, **220**; for equidistant diagram 60, **220**; shadow coordinates 132, **222**; for stereographic projection 62, **220**

Y-coordinates: for cylindrical projections 63–64, **220**; for equidistant diagram 60, **220**; for modified cylindrical projections 64, **220**; shadow coordinates 132, **222**; for stereographic projection 62, **220**
year, solar 12

zenith 36
zenith angle **219**; altitude angle relationship and 44, **219**; at solar noon 36–38, *36*, *37*; at solar noon on equinox 36, **219**
zenith direction: zenith direction cosine 50, **220**
zenith normal vector component 100, **221**